Cloning and Analysis of the Microbisporicin Lantibiotic Gene Cluster from *Microbispora corallina*.

Lucy Clementine Foulston

2010

Thesis submitted to the University of East Anglia for the degree of Doctor of Philosophy

Acknowledgements

Firstly I would like to thank my supervisor Prof. Mervyn Bibb. His support, guidance, generosity and encouragement have been unwavering during the past three years even through the most difficult phases of the project. Thank you for giving me the opportunity to work with you on this fascinating project, to present my work internationally and to meet so many wonderful people along the way. Finally thank you for your continued support into the next stage of my career.

Many thanks to Prof. Mark Buttner for support during my PhD and for advice in my future career plans. I would like to thank Prof. Nick Brewin and my rotation supervisors. The utmost thanks to Sean O'Rourke, Andy Hesketh and Maureen Bibb for their day-to-day help and technical advice. Many thanks to Gerhard Saalbach, Mike Naldrett, Kim Findlay and Andrew Davis. I would like to acknowledge the invaluable help and friendship of many individuals in Molecular Microbiology; Govind Chandra, Jan Claesen, Jennifer Parker, Robert Bell, Emma Sherwood, Tung Le, Ngat Tran, Juan-Pablo Gomez Escribano, Peter Slavny, Jeremy Thornton and Marij Frederix. Thanks to everyone past and present in the Molecular Microbiology Department for making it such a wonderful place to work. Enormous thanks to all the ladies in the Chatt and Bateson media kitchens, Sue Riches and Karen Reding – for your help, kindness and for constantly keeping me entertained!

I would like to acknowledge the support of Prof. Flavia Marinelli and her research group at the University of Insubria for providing me with invaluable help and for hosting me during an insightful research trip to her lab. I would also like to give great thanks to my friend Letizia Marcone for her help, encouragement and I warmly thank Letizia and her family for their generosity in hosting me at their home during my stay in Italy.

I would like to thank Anne Edwards for giving me the opportunity at the age of 16 to work at the John Innes Centre and decide that one day I would undertake my PhD here, and for her continued support in making that goal achievable in the 10 years since. Thank you to the rest of my family for keeping a continual interest in my work. I would like to thank all my friends for their help but most importantly Briony for your constant friendship, reassurance and emotional support through some very challenging times!! Finally I would like to thank my parents for their continual love, support and guidance, and most importantly for helping me to learn MRS GREN and for not knowing why the sky is blue…..

Abstract

The increasing occurrence of antibiotic resistance, and frequently multi-drug resistance, in a wide range of bacterial pathogens has led to an urgent need for new antibiotics. Lantibiotics are ribosomally synthesised, post-translationally-modified peptide antibiotics with clinical potential. They are characterised by lanthionine and methyl lanthionine bridges between cysteine and dehydrated serine and threonine residues, respectively, giving lantibiotics their characteristic conformations and stability. The actinomycete *Microbispora corallina* produces a potent lantibiotic, microbisporicin. Microbisporicin shows a high degree of modification including chlorinated tryptophan, dihydroxyproline and aminovinyl-cysteine residues. The gene cluster responsible for the production of microbisporicin was identified by genome scanning and isolated from a *M. corallina* cosmid library. The microbisporicin gene cluster was initially investigated using bioinformatic methods which revealed a number of intriguing and novel features. Heterologous expression in *Nonomuraea* sp. ATCC 39727 confirmed that all of the genes required for microbisporicin biosynthesis were present in the cluster. Methods were developed for the genetic manipulation of *M. corallina*. Deletion analysis revealed novel insights into the biosynthesis of this unusual and potentially clinically useful lantibiotic, shedding new light on mechanisms of regulation and self-resistance. In particular, this study describes the first example of the involvement of a tryptophan halogenase in the modification of a ribosomally-synthesised peptide and the pathway-specific regulation of an antibiotic biosynthetic gene cluster by an ECF σ factor:anti-σ factor complex.

General Abbreviations

A	Adenine
Abu	Aminobutyrate
AviCys	S-[(*Z*)-2-aminovinyl]-D-cysteine
Apra	Apramycin
ATP	Adenosine-triphosphate
ADP	Adenosine-diphosphate
BLAST	Basic local alignment search tool
C	Cytosine
cAMP	Cyclic adenosine monophosphate
Carb	Carbenicillin
cDNA	Complementary DNA
C-terminal	Carboxy-terminal
Dha	2,3-didehydroalanine
Dhb	((Z)-2,3-didehydrobutyrine
DMSO	Dimethylsulfoxide
DNA	Deoxyribonucleic acid
DNA	Difco Nutrient Agar
DNAse	Deoxyribonuclease
dNTP	Deoxynucleoside triphosphate
EF	Elongation Factor
FAD	Flavin adenine dinucleotide
FMN	Flavin mononucleotide
G	Guanine
gDNA	Genomic DNA
HPLC	High Pressure Liquid Chromatography
Hyg	Hygromycin
Kan	Kanamycin

kDa	Kilodalton
lacZ	β-galactosidase
Lan	Lanthionine
lux	Luciferase
MALDI-ToF	Matrix-assisted laser desorption ionisation time-of-flight
MCS	Multiple-cloning site
MeLan	Methyl-lanthionine
MS	Mass spectrometry
Mw	Molecular Weight
Nal	Nalidixic acid
NAD	Nicotinamide adenine dinucleotide
N-terminal	Amino-terminal
OD	Optical Density
PCR	Polymerase Chain Reaction
qRT-PCR	Quantitative Reverse transcriptase Polymerase Chain Reaction
RNA	Ribonucleic acid
mRNA	Messenger RNA
rRNA	Ribosomal RNA
RNAse	Ribonuclease
RT-PCR	Reverse transcriptase Polymerase Chain Reaction
T	Thymine
UV	Ultraviolet

Contents

List of Tables and Figures

Chapter 1 - Introduction

Chapter 2 – Materials and Methods

Chapter 3 - Identification of the microbisporicin biosynthetic gene cluster

Chapter 1 – Introduction

1.1 Actinobacteria and Antibiotics

1.1.1 Actinobacteria and secondary metabolites

The Actinobacteria are a major phylum of Gram-positive bacteria (Figure 1.1) with genomes of high GC-content (65-75 mol% GC) (Miao *et al.* 2010). They are commonly found in the soil and the rhizosphere but have also been isolated from sea water and fresh water. Certain sub-groups of Actinobacteria have been extremely important in human health and medicine. Most notably the genus *Streptomyces* has been widely exploited for its production of antibacterial, antifungal, immunomodulatory and anti-cancer compounds (Table 1.1). Other groups are important human pathogens, in particular the *Mycobacteria*, including the causative agents of tuberculosis and leprosy (Miao *et al.* 2010).

Many of the classes of Actinobacteria exhibit multicellular mycelial growth and complex developmental processes including the formation of spores. This has been well studied in the model actinomycete family *Streptomycetaceae* and in particular in the model organism *Streptomyces coelicolor* A3(2) (Elliot *et al.* 2008). *S. coelicolor* grows as a vegetative mycelium likely on the surface of soil particles. Under growth-limiting conditions a cascade of developmental changes is initiated involving the formation of aerial mycelium and culminating in the production of chains of spores. Spores are highly tolerant of adverse environmental conditions and allow *Streptomyces* to disperse to growth-favourable areas where they germinate to establish a new mycelial colony (Elliot *et al.* 2008). This developmental transition in *S. coelicolor* coincides with the production of at least four secondary metabolites; actinorhodin, undecylprodigosin, methylenomycin and the calcium-dependent antibiotic (CDA) (Wright *et al.* 1976b; Wright *et al.* 1976a; Rudd *et al.* 1980; Lakey *et al.* 1983; Elliot *et al.* 2008). Secondary metabolites are small molecule products that are not essential for basic cell growth and primary metabolism. The genus *Streptomyces* is responsible for the production of a vast array of such secondary metabolites many of which have been exploited for their medicinal properties (Table 1.1) (Miao *et al.* 2010).

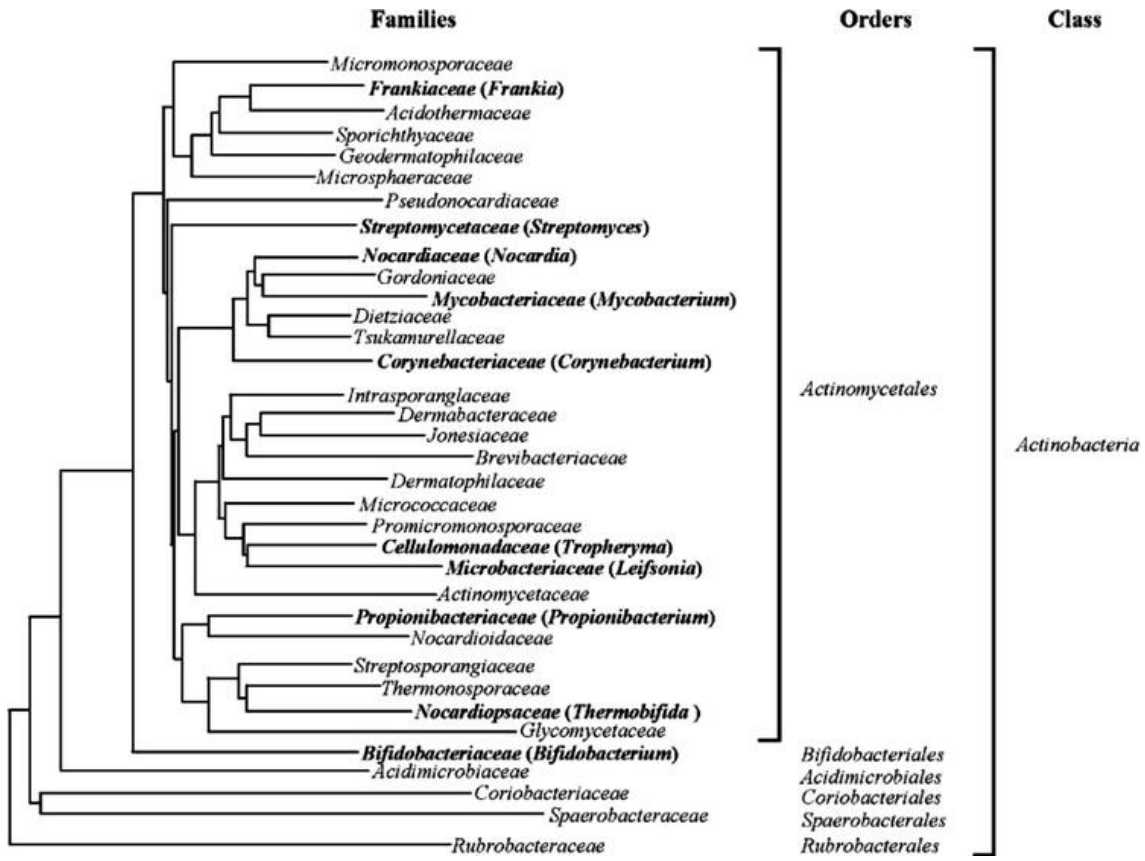

Figure 1.1 Phylogenetic tree of *Actinobacteria* based on 1,500 nucleotides of 16S rRNA. Families containing members subjected to complete genome sequencing at the time of writing are depicted in *bold*. Orders are indicated. Figure and legend reproduced from Miao and Davies 2010.

Table 1.1 Examples of secondary metabolites produced by the *Streptomyces* genus and their uses. Table adapted from Miao and Davies, 2010.

Producing organism	Compound	Application
Streptomyces aureofaciens	Tetracycline	Antibacterial
Streptomyces griseus	Streptomycin	Antibacterial
Streptomyces kanamyceticus	Kanamycin	Antibacterial
Streptomyces lactamdurans	Cefoxitin	Antibacterial
Streptomyces mediterranei	Rifamycin	Antibacterial
Streptomyces pristinaspiraelis	Pristinamycin	Antibacterial
Streptomyces roseosporus	Daptomycin	Antibacterial
Streptomyces spheroides	Novobiocin	Antibacterial
Streptomyces venezuelae	Chloramphenicol	Antibacterial
Streptomyces avermitilis	Ivermectin	Antihelminthic
Streptomyces clavuligerus	Clavulanic acid	ß-Lactamase inhibitor
Streptomyces hygroscopicus	Bialophos	Herbicide
Streptomyces hygroscopicus	Rapamycin	Immunosuppressive
Streptomyces noursei	Nystatin	Antifungal
Streptomyces verticillus	Bleomycin	Anticancer

A number of hypotheses have been put forward to explain why some bacteria produce secondary metabolites and what functions these compounds may have in their natural habitats. A widely held view is that the soil, as a complex microbial habitat, is an extremely competitive ecosystem that requires the production of antimicrobial compounds by different species to protect particular niches or resources (Yim *et al.* 2006; Hibbing *et al.* 2010). It thus follows that secondary metabolites are produced at the transition to the development of spores in most *Streptomyces* sp. since this will occur when resources and

nutrients become limiting and therefore competition is utmost. However, many secondary metabolites do not exhibit high levels of antimicrobial activity, and for those that do under laboratory conditions it is unknown whether a sufficient concentration would be produced in the soil to successfully act as a growth-inhibitor (Yim *et al.* 2006). Although some secondary metabolites might function in this role it is clear that many do not. A likely role for many secondary metabolites is in signalling and communication (Yim *et al.* 2006; Mlot 2009). Such signalling may occur within the same bacterial species (intraspecies) and result in developmental changes, for example A-factor; a small hormone molecule responsible for inducing development and the production of secondary metabolites in *Streptomyces griseus* (Ohnishi *et al.* 2005). Secondary metabolites may also mediate signals between bacterial species (interspecies) as a mechanism of competition or to promote a mutually beneficial outcome, such as the formation of multispecies biofilms (Linares *et al.* 2006; Straight *et al.* 2009). A final role for secondary metabolites is their contribution to mutualistic or pathogenic interactions with plants and animals. For example compounds produced by actinomycetes carried on insects, including ants and beetles, are used as antifungals by these animals (Scott *et al.* 2008; Oh *et al.* 2009). Another example is the secondary metabolite thaxtomin which is utilised by the plant pathogen *Streptomyces scabies* as a toxin (Loria *et al.* 2008).

1.1.2 Antibiotics

Secondary metabolites are defined as antibiotics if they exhibit appreciable growth inhibition or killing of target bacteria under laboratory conditions. The anti-bacterial activity of compounds produced by microbes was first appreciated in 1928 when Alexander Fleming identified penicillin (Newman *et al.* 2000). Subsequently during the Golden Age of antibiotic discovery in the 1940's and '50's, many such compounds were isolated and identified as drugs suitable for the treatment of a broad spectrum of bacterial infections (Newman *et al.* 2000). A large number of these compounds were isolated from *Streptomyces* sp., starting with streptomycin, identified by Selman Waksman in 1943 from *Streptomyces griseus* (Newman *et al.* 2000). Hundreds of antibiotics are now known and have revolutionised modern medicine (Newman *et al.* 2000).

The secondary metabolites produced by actinomycetes that possess antibiotic activity fall into several chemical classes. These molecules are typically synthesised by dedicated production lines of enzymes encoded by individual gene clusters. For example the

polyketide antibiotics typified by the macrolide erythromycin, produced by *Saccharopolyspora erythrea*, is biosynthesised by three large, multidomain proteins or polyketide synthases (PKS) (Cortes *et al.* 1990). Each of the modules on these proteins is responsible for the incorporation of a fatty acid unit into the final compound and they function in a processive manner (Donadio *et al.* 1991). Another important class of secondary metabolic enzymes are the non-ribosomal peptide synthetases (NRPS). Peptide-based natural products constitute a large and important class of antibiotics that include medically useful compounds such as the glycopeptide vancomycin and the lipopeptide daptomycin. NRPSs are large multidomain proteins which also function in a modular, processive way to generate the initial peptide chain. Unlike ribosomal peptides, NRPS-generated molecules can incorporate a range of non-proteinogenic amino acids giving them a vast array of chemical properties and structures (Lautru *et al.* 2004). Tailoring enzymes can further modify the structures of these compounds, adding for example sugar residues, methyl or hydroxyl groups (Walsh *et al.* 2001). Some secondary metabolites are synthesised by hybrid PKS and NRPS systems, for example the anti-tumour drug bleomycin from *Streptomyces verticillus* (Du *et al.* 2000). In addition, there are ribosomally-synthesised peptides, such as the unmodified bacteriocins, largely produced by other phyla of bacteria (Nes *et al.* 2000), and the highly-modified lantibiotics, produced by a range of Gram-positive bacteria including the actinomycetes (Guder *et al.* 2000; Widdick *et al.* 2003; Boakes *et al.* 2009).

The marked recent rise in the development of multi-antibiotic resistant bacterial pathogens has led to an urgent requirement for new classes of molecules with bactericidal activities. Gram-positive pathogens such as *Staphylococcus aureus, Streptococcus pneumoniae, Enterrococcus faecalis* and *Clostridium difficile* have rapidly increased in prevalence in recent years as hospital-acquired (nosocomial) infections. In 2006, 95% of clinical *S. aureus* isolates in the USA were resistant to penicillin (and other antibiotics of the β-lactam family excluding methicillin) and around 50% were also resistant to methicillin (MRSA) (Appelbaum 2006a). The number of deaths attributed to MRSA in the UK rose steadily until 2006 but has subsequently declined due to the introduction of new hygiene standards in hospitals[1]. The problem is compounded by the increase in vancomycin intermediate (VISA) and resistant strains (VRSA, 5 cases were reported up to 2006 in the USA) since vancomycin was previously the drug of "last-resort" against MRSA (Appelbaum 2006b). Previously, cases of MRSA were found predominantly in a hospital-

[1] Office for National Statistics (2010) MRSA deaths decrease for second year running

http://www.statistics.gov.uk/cci/nugget.asp?id=1067

based setting, particularly amongst older people or those with long-term health problems, such as diabetes. However, increasingly MRSA is being found as a community-based problem with nasal colonisation by MRSA as high as 7% of the population (Appelbaum 2006b; Appelbaum 2006a).

Other Gram-positive pathogens of concern are *Enterococci* and *Clostridium difficile*. *Enterococcus faecium* and *Enterococcus faecalis* are widely associated with multidrug resistant infections in hospital-settings, exhibiting resistance to most clinically used antibiotics (Woodford *et al.* 2009). Of particular importance is the increase in the resistance of *Enterococci* to aminoglycosides and glycopeptides, including vancomycin and teicoplanin. Furthermore, non-susceptibility of *Enterococci* to many of the newly introduced antibiotics has already been reported, for example to linezolid and tigecycline (Woodford *et al.* 2009).

Additional challenges are posed by Gram-negative pathogens, particularly *Escherichia coli*, *Klebsiella spp.*, *Pseudomonas aeruginosa*, *Acinetobacter baumannii* and *Neisseria gonorrhoeae* (Livermore 2009). The presence of the Gram-negative outer membrane provides an additional barrier to the penetration of antimicrobials and limits the number of compounds that can be used in the treatment of such infections. Furthermore there is a wide-spread accumulation of resistance determinants against the current treatment options including extended-spectrum β-lactamases and carbapenemases (Livermore 2009). Of particular concern is that very few new antibiotic compounds are available, or are likely to become available in the near future, for the treatment of resistant Gram negative infections (Livermore 2009).

1.2. Lantibiotics

Lantibiotics are ribosomally synthesised, post-translationally-modified peptide antibiotics. They are characterised by lanthionine and methyl lanthionine bridges between cysteine and dehydrated serine (2,3-didehydroalanine) and threonine ((*Z*)-2,3-didehydrobutyrine) residues, respectively, giving lantibiotics their characteristic conformations and stability (Figure 1.2A). Lantibiotics appear to be produced exclusively by Gram-positive bacteria (Chatterjee *et al.* 2005).

The first lantibiotic, nisin, was described over 40 years ago. It is produced by *Lactococcus lactis* and has been used extensively in the food industry (Chatterjee *et al.* 2005). A large number of lantibiotics (more than 50) have been described, mostly made by low GC

Gram-positive bacterial genera, such as *Lactococci*, *Bacilli* and *Staphylococci*. The gene clusters responsible for the production of nisin and many other lantibiotics have been determined (section 1.2.1). A number of lantibiotics have also been isolated from actinomycetes, including cinnamycin and the related duramycins (Widdick *et al.* 2003), actagardine (Boakes *et al.* 2009), planosporicin (Castiglione *et al.* 2007) and microbisporicin (Castiglione *et al.* 2008) (section 1.2.2).

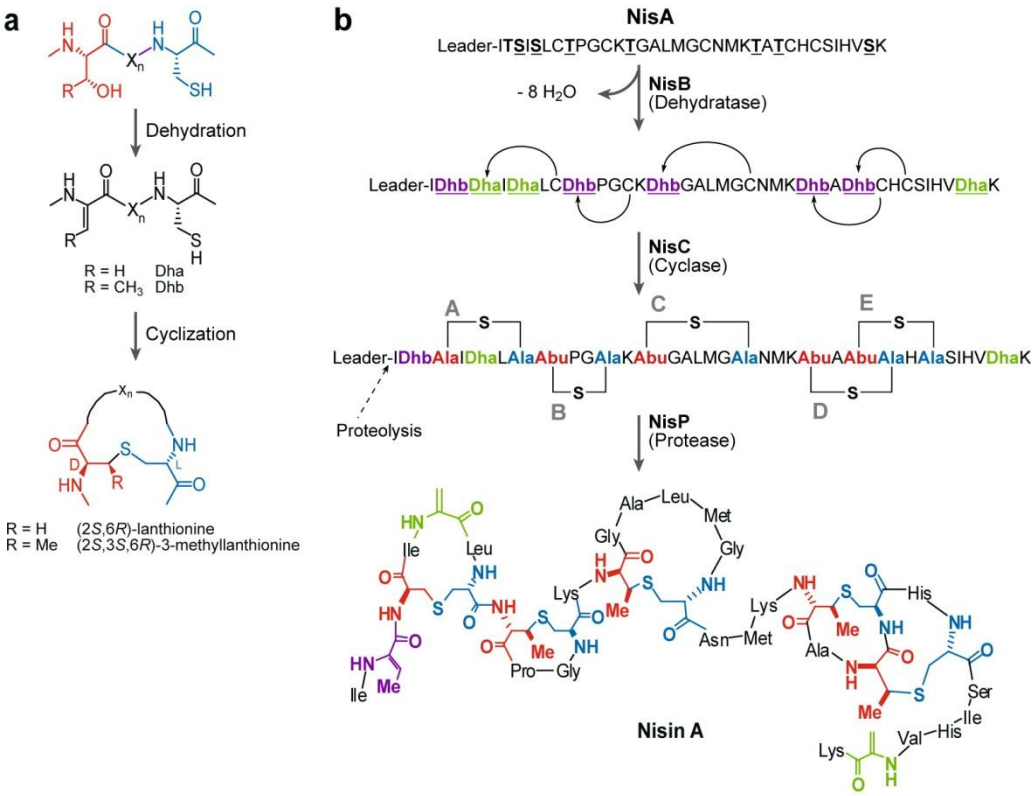

Figure 1.2 a) Installation of lanthionine (Lan) or methyllanthionine (MeLan) residues into lantibiotic prepropeptides. A serine or threonine residue (Red) is dehydrated to yield didehydroalanine (Dha) or didehydrobutyrine (Dhb) respectively. A Lan or MeLan bridge results from the cyclisation of these residues with the side chain of cysteine (blue). **b)** The posttranslational maturation process of nisin as described in the text. For Lan and MeLan structures, the segments derived from Ser/Thr are in red and those derived from Cys are in blue. Figures reproduced from Willey and van der Donk 2007.

Lantibiotics are encoded by a structural gene (*lanA*) whose product is post-translationally modified by enzymes that include dehydratases, cyclases and leader peptidases (Figure 1.2B). Additional proteins are required for export of the lantibiotic and for host resistance (section 1.2.3). The genes encoding these proteins are found in clusters, and are co-expressed.

Lantibiotics typically have anti-bacterial activity against Gram-positive bacteria and are often ineffective against Gram-negatives. The lantibiotics described to date exhibit a range of mechanisms of anti-microbial and other activities (section 1.2.4). Unlike PKS and NRPS synthesised antibiotics, lantibiotics are highly amenable to genetic manipulation. Since the precursor peptide of the final product is genetically encoded, in principle each amino acid can be replaced with the other 19 natural amino acids and the resulting variants tested for improved pharmacokinetic properties (Appleyard *et al.* 2009; Boakes *et al.* 2009).

1.2.1 Lantibiotics from low GC Gram-positive Bacteria

Several schemes have been proposed to classify the lantibiotics that have been characterised to date, mainly on the basis of their structural features but more recently on the enzymes utilised for peptide maturation (Willey *et al.* 2007). The most widely used naming scheme, used in this work, is based on three classes; types AI, AII and B (Chatterjee *et al.* 2005). The type A lantibiotics typically exhibit a more elongated structure whereas type B are more globular (Figure 1.3) (Chatterjee *et al.* 2005). The type AI lantibiotics, typified by nisin, are modified by two enzymes that separately dehydrate serine and threonine residues in the peptide (LanB) and subsequently catalyse the nucleophilic attack of a cysteine on one of these dehydrated residues (LanC) to generate a lanthionine bridge (Figure 1.2B). By contrast both types AII and B utilise a bi-functional enzyme (LanM) which is capable of catalysing both these reactions (Chatterjee *et al.* 2005). The type AII lantibiotics are exemplified by lacticin 481 and the type B by mersacidin (Figure 1.3).

As is the case for the majority of secondary metabolites characterised to date, the genes involved in lantibiotic biosynthesis are found clustered together on the chromosome (e.g. subtilin) or on plasmids, phages and transposons (e.g. nisin) (Chatterjee *et al.* 2005). The reason why secondary metabolite genes are clustered is not clear but it might allow closely coordinated gene expression. It may also be a consequence of horizontal transfer of useful groups of genes between species. The gene clusters encoding several

lantibiotics from low GC Gram-positive bacteria have been characterised (Figure 1.4). They typically consist of the precursor peptide (prepropeptide) encoding gene, generically named *lanA*, the genes encoding the lanthionine bridge introducing enzymes *lanBC* or *lanM*, a dedicated export protein *lanT*, and often a dedicated leader peptidase *lanP*. The genes involved in regulation of biosynthesis typically encode a two-component histidine sensor kinase-response regulator system named *lanRK*. Self-resistance is often mediated by one or two systems, an ABC transporter encoded by *lanFEG* and/or a lipoprotein encoded by *lanI* (Chatterjee *et al.* 2005).

Thus far, nisin is the only lantibiotic to be used commercially. Nisin has been used as an additive to prevent the growth of pathogenic microbes in food products (Willey *et al.* 2007). Clinical applications have been suggested for other low GC lantibiotics, in particular mersacidin for the treatment of MRSA (Appleyard *et al.* 2009) and mutacin 1140 for the treatment of dental caries (Hillman 2002).

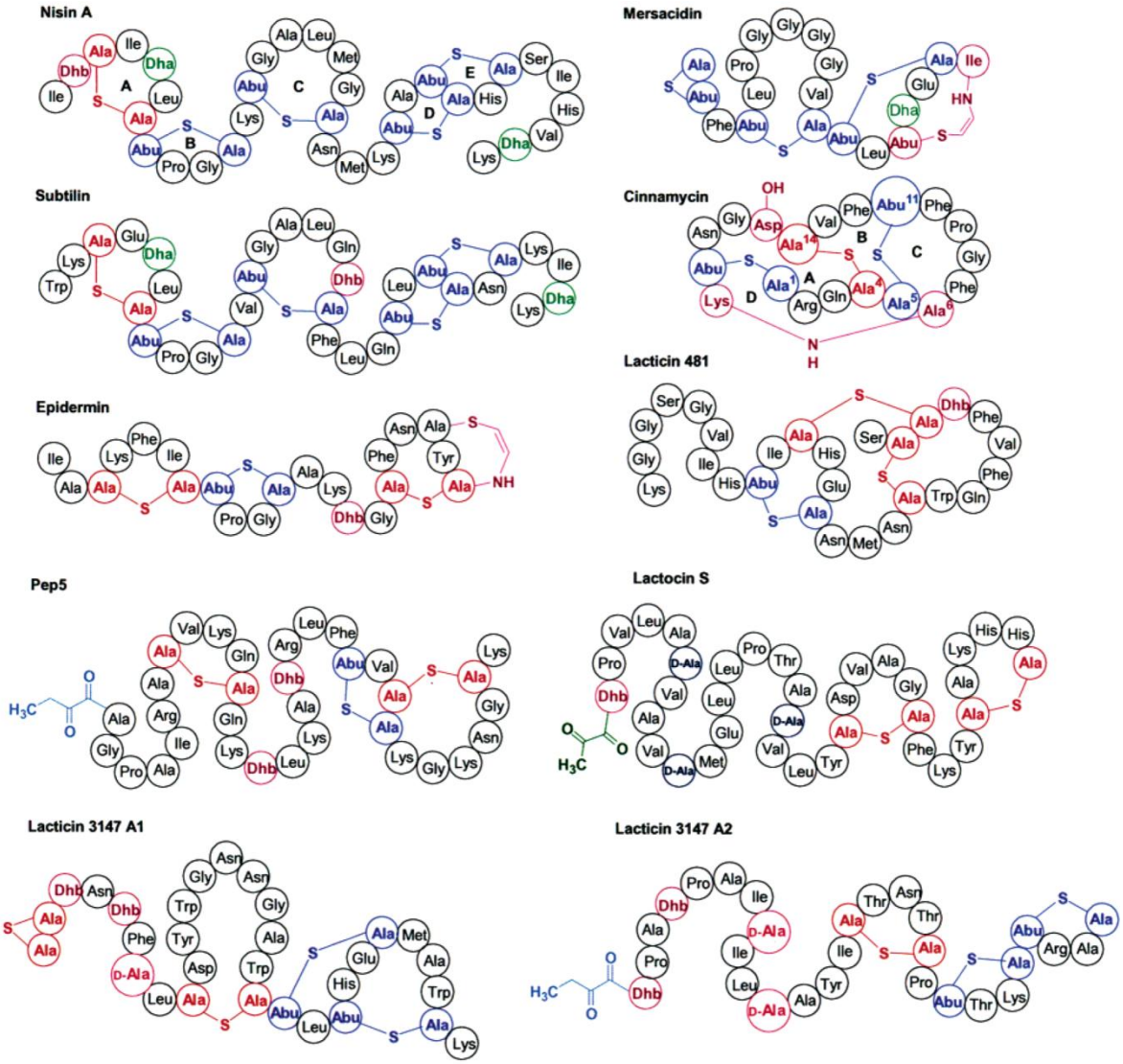

Figure 1.3 A selection of lantibiotic structures, representing the three classes of lantibiotics described in the text. Type AI; nisin, subtilin, epidermin and Pep5, Type AII; lacticin 481and lactocin S, Type B; mersacidin and cinnamycin. Also shown is the two-component lantibiotic lacticin 3147. Dha, 2,3-didehydroalanine; Dhb, (Z)-2,3-didehydrobutyrine and Abu, aminobutyrate. Image reproduced from Chatterjee *et al.* 2005.

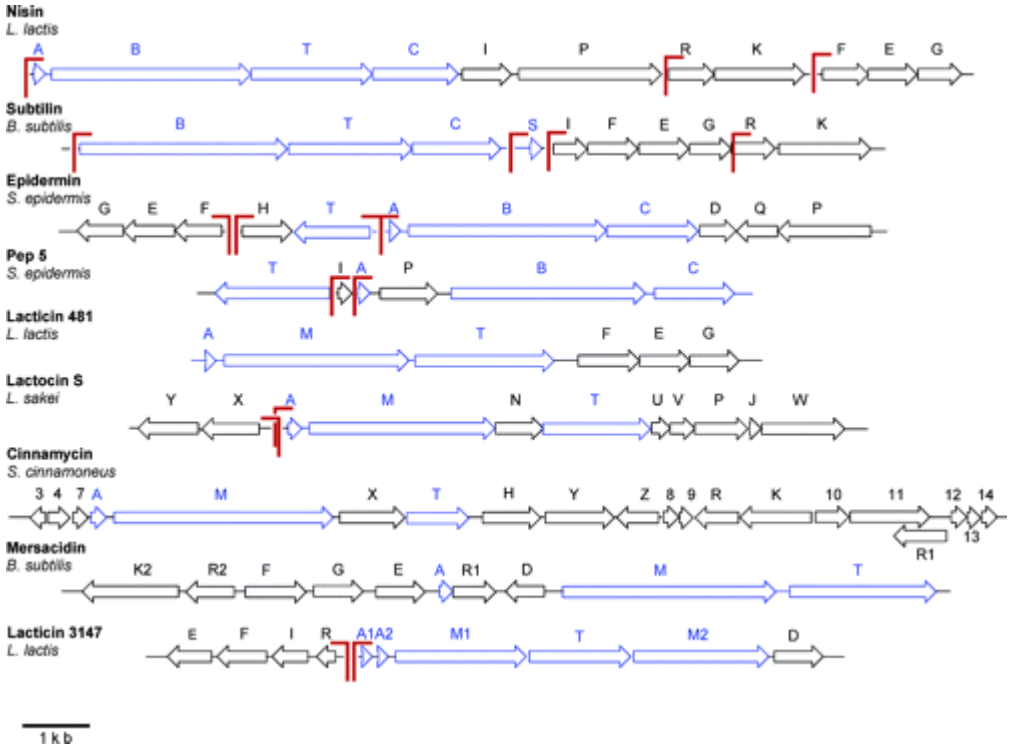

Figure 1.4 A selection of known lantibiotic gene clusters. Genes in blue are represented in all the displayed gene clusters. Red lines indicate the positions of known promoter sites. Gene functions are described in the text. Image reproduced from Chatterjee *et al.* 2005.

1.2.2 Lantibiotics from Actinomycetes

Unlike the large number of compounds isolated from low GC Gram-positive bacteria, only a handful of compounds have been isolated to date from actinomycetes and subsequently shown to be lanthionine-containing peptides. SapB was identified from *S. coelicolor* and shown to be involved in the formation of aerial mycelium during *Streptomyces* development (Kodani *et al.* 2004; Kodani *et al.* 2005). SapB, like the lantibiotics, is generated from a prepropeptide via the introduction of lanthionine bridges and the gene cluster involved in its production has been identified (Kodani *et al.* 2004). SapB does not however possess significant antibacterial activity and has been proposed to form a separate class of lanthionine-containing peptides (Willey *et al.* 2007).

Cinnamycin, a type B lantibiotic, was isolated from *Streptomyces cinnamoneus* and the gene cluster has been identified (Widdick *et al.* 2003). The related duramycin compounds are structurally very similar to cinnamycin and also produced by actinomycetes. Cinnamycin has a globular structure and contains two unusual lantibiotic modifications; a lysinoalanine bridge and hydroxylated aspartate (Figure 1.5). Cinnamycin biosynthesis is encoded by one of the largest lantibiotic gene clusters described to date, consisting of 17 ORFs (Figure 1.6) (Widdick *et al.* 2003). Several genes of unknown function were identified in the gene cluster (Widdick *et al.* 2003) and a novel lantibiotic modifying enzyme was identified, likely involved in aspartate hydroxylation (O'Rourke and Bibb, unpublished). Furthermore, unusual mechanisms of producer self-resistance and regulation were identified (O'Rourke and Bibb, unpublished).

Actagardine, deoxyactagardine B (DAB) and michiganin A are related type B lantibiotics isolated from the actinomycetes *Actinoplanes garbadenensis*, *Actinoplanes liguriae* and *Clavibacter michiganensis,* respectively (Figure 1.5). The structures of all three molecules are highly similar and resemble mersacidin (Holtsmark *et al.* 2006; Boakes *et al.* 2009; Boakes *et al.* 2010). The gene clusters for actagardine and DAB are very similar, (the DAB cluster contains one additional ORF) (Figure 1.6) (Boakes *et al.* 2009; Boakes *et al.* 2010), and share features with that of cinnamycin, such as *garTH*, *ligTH* and *cinTH,* each encoding two-component ABC transporters likely to have a role in lantibiotic export (Widdick *et al.* 2003; Boakes *et al.* 2009; Boakes *et al.* 2010). None of the three type B actinomycete lantibiotic gene clusters encodes a dedicated leader peptidase (LanP) (Widdick *et al.* 2003; Boakes *et al.* 2009; Boakes *et al.* 2010). Actagardine and DAB show anti-bacterial activity against a range of Gram-positive bacteria and actagardine has been the subject of optimisation via variant generation (Boakes *et al.* 2009; Boakes *et al.* 2010).

Cypemycin was isolated from *Streptomyces* sp. OH-4156 and contains dehydrated threonine residues ((Z)-2,3-didehydrobutyrine) also found in lantibiotics (Komiyama *et al.* 1993). Cypemycin does not contain any lanthionine bridges but does contain several unusual modifications; N-dimethylalanine, allo-isoleucine and [(Z)-2-aminovinyl]cysteine (Figure 1.5) (Minami *et al.* 1994). Subsequent elucidation of the biosynthetic gene cluster of cypemycin revealed that it belongs to a novel family of peptide antibiotics (Claesen *et al.*). The gene cluster for cypemycin biosynthesis thus shows no similarity to that of other actinomycete lantibiotics characterised to date (Claesen *et al.*).

A final member of the actinomycete lantibiotic group was isolated from *Planomonospora* sp., a member of the rare actinomycete family the *Streptosporangiaceae*. Planosporicin was initially thought to be similar in structure to the type B lantibiotics mersacidin and actagardine (Castiglione *et al.* 2007), but a recent revision led to its reassignment as a type AI lantibiotic (Figure 1.5) (Maffioli *et al.* 2009). Planosporicin shows bacteriocidal activity against a wide range of Gram-positive pathogens (Castiglione *et al.* 2007), and blocks cell wall formation in target bacteria by inhibiting peptidoglycan biosynthesis (Castiglione *et al.* 2007).

The rapid increase in the availability of genome sequence data has allowed the identification of a number of potential lantibiotic gene clusters from actinomycetes, including *S. coelicolor* (M. Bibb, personal communication), for which the mature products have not yet been identified. A gene cluster from *Streptomyces venezuelae* was shown to encode a lantibiotic-like peptide and an unusual modification enzyme (lyase) involved in lanthionine bridge formation that was named VenL (Goto *et al.* 2010). Homologs were identified in other gene clusters with the potential to produce lanthionine-containing peptides (Goto *et al.* 2010). The product of the gene cluster, venezuelin, was produced *in vitro* and possessed a globular structure similar to type B lantibiotics; however no antibiotic activity could be detected from the small amount of available compound (Goto *et al.* 2010).

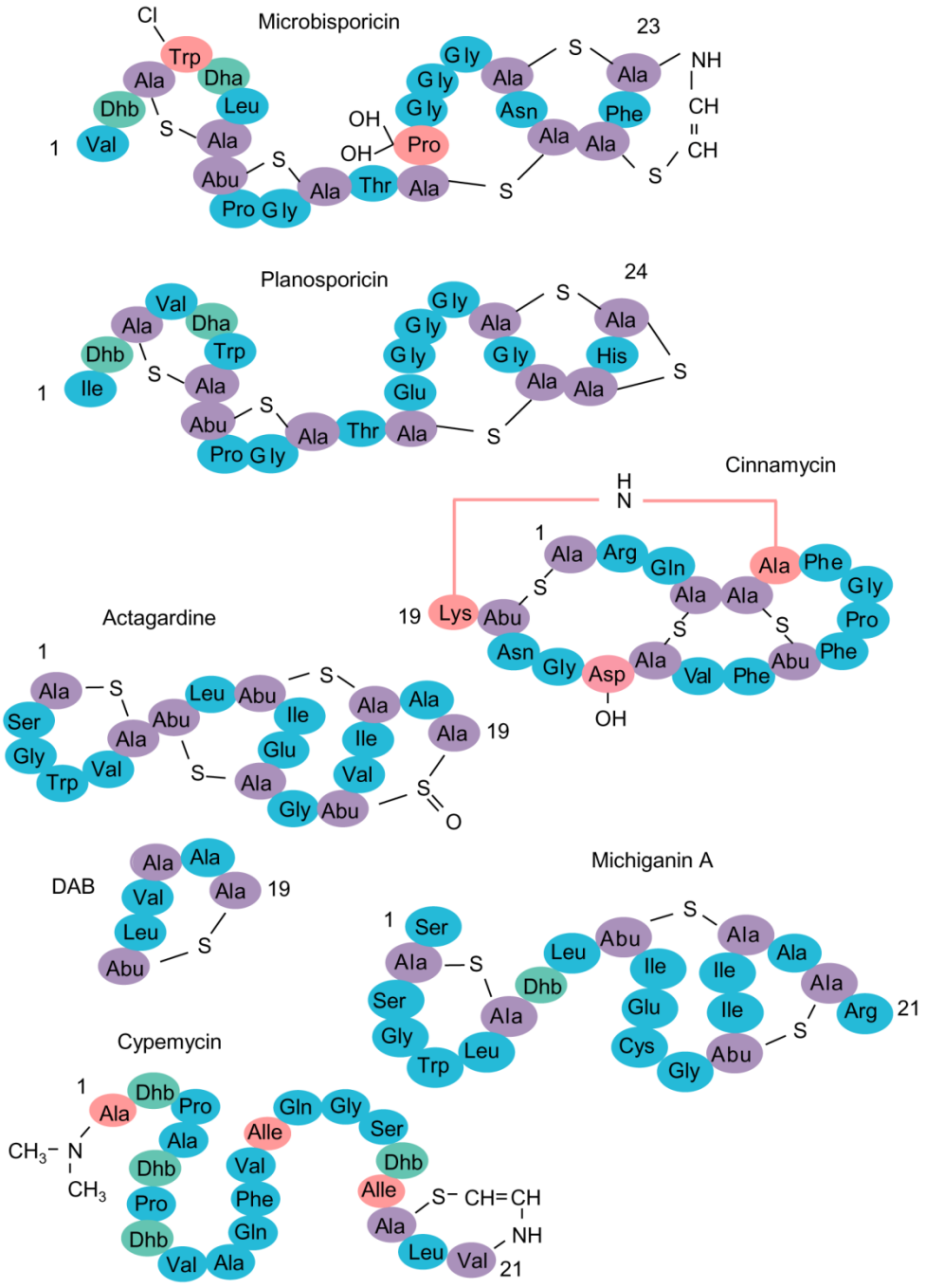

Figure 1.5 The structures of known actinomycete lantibiotics as described in the text. The number of amino acids in the mature peptide is given. Unmodified residues are in blue, residues participating in lanthionine bridges or AviCys residues are in purple, Dha and Dhb are in green and specially modified residues are in pink. Deoxyactagardine B (DAB; residues 14-19 shown below actagardine) differs from actagardine only at positions 15 and 16, which are Leu and Val, respectively, and in having a lanthionine bridge in place of the oxidised lanthionine bridge of actagardine.

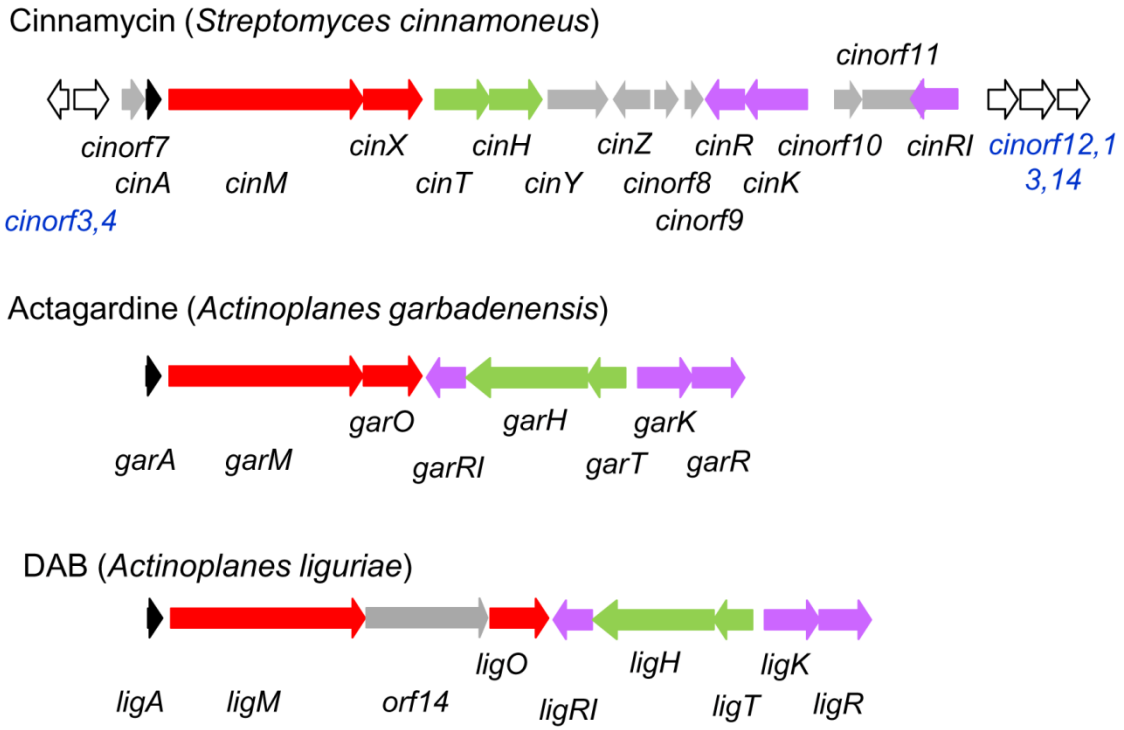

Figure 1.6 The known lantibiotic biosynthetic gene clusters from actinomycetes. Shown are genes encoding the prepropeptide (black), modification enzymes (red), two-component ABC export systems (green), putative regulators (purple), genes of unknown function (grey) and flanking genes (white) (Widdick *et al.* 2003, Boakes *et al.* 2009; Boakes *et al.* 2010).

1.2.3 Lantibiotic Biosynthesis

The pathways for lantibiotic biosynthesis are unique to each molecule and producing species, and regulation and self-resistance mechanisms, in particular, vary widely. Trends and similarities will be reviewed in this section. The most well-studied lantibiotic to date is nisin but certain aspects of nisin biosynthesis (summarised in Figure 1.7) differ from that of other type AI lantibiotics and will be noted with reference to other characterised gene clusters. The main focus will be on the type AI lantibiotics, but differences with other lantibiotic types will be highlighted.

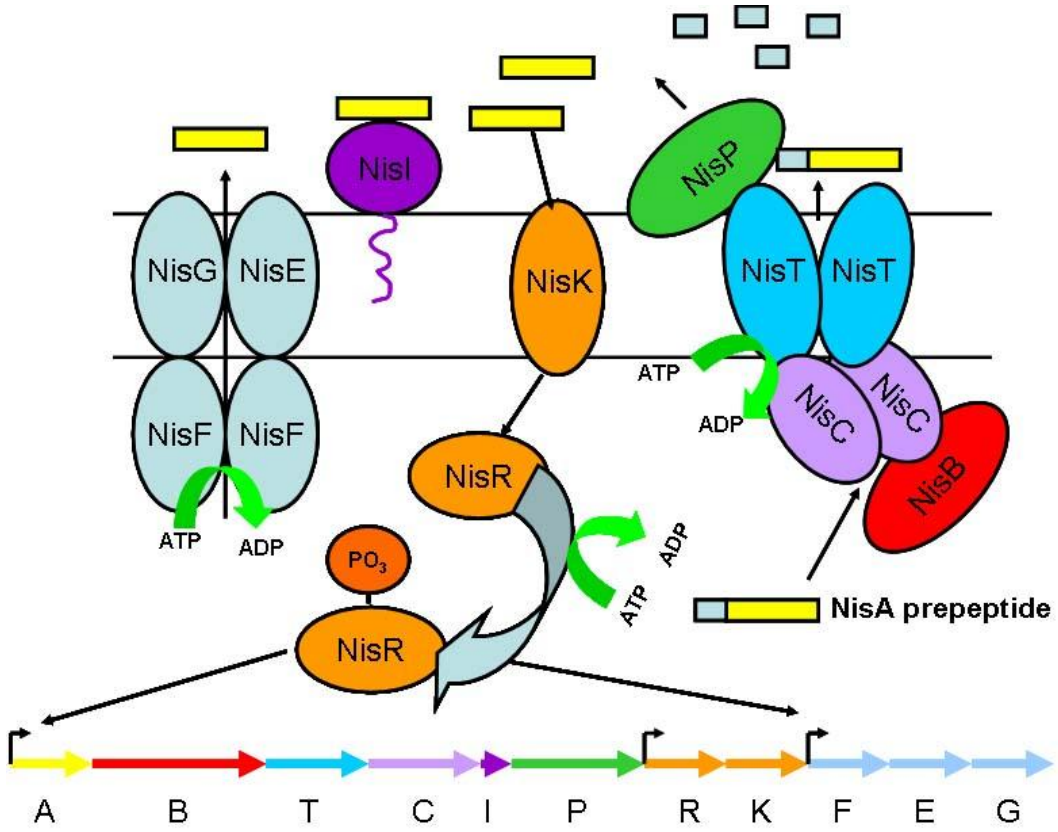

Figure 1.7 A summary of the regulation, biosynthesis and self-immunity mechanisms responsible for nisin production. Extracellular nisin at low concentration induces the NisRK two-component regulatory system which initiates transcription of the biosynthetic genes and subsequent nisin production with modification by NisB and NisC. Pre-nisin is exported by NisT and the leader peptide removed by NisP. Host immunity is conveyed by NisI and NisFEG. Adapted from Patton and van der Donk (2005).

1.2.3.1 Prepropeptide and leader peptide

The *lanA* gene encodes a precursor peptide (prepropeptide) that includes the future mature peptide sequence (propeptide) at its C-terminus and an N-terminal leader peptide. Conserved sequences within the leader peptides of characterised lantibiotics define two classes (Chatterjee *et al.* 2005). Lantibiotics modified by LanBC enzymes (type AI) typically have a conserved FNLD motif in the leader peptide (e.g. nisin, Figure 1.8). Mutation of the FNLD motif of the nisin prepropeptide prevented secretion or intracellular accumulation of mature nisin or its precursors, suggesting a fundamental role for this motif in nisin maturation and secretion (van der Meer *et al.* 1993). This was not the case for Pep5, where the lantibiotic was correctly processed after mutation of Phe^{19} (to Ser) or Glu^{16} (to Lys) in the FNLEI motif, although the yield of final compound decreased by 2-fold compared to the wild type control (Neis *et al.* 1997). Lantibiotics modified by LanM (types AII and B) typically have a “GG” or “GA” cleavage site and contain multiple Asp and Glu residues in the leader peptide (Figure 1.8) (Chatterjee *et al.* 2005). Replacement of the double Gly motif in mutacin II resulted in complete loss of lantibiotic activity (Chen *et al.* 2001). In contrast, cinnamycin has an AXA motif preceding the site of signal peptidase cleavage reminiscent of that used by the sec secretory pathway (Figure 1.8) (Widdick *et al.* 2003).

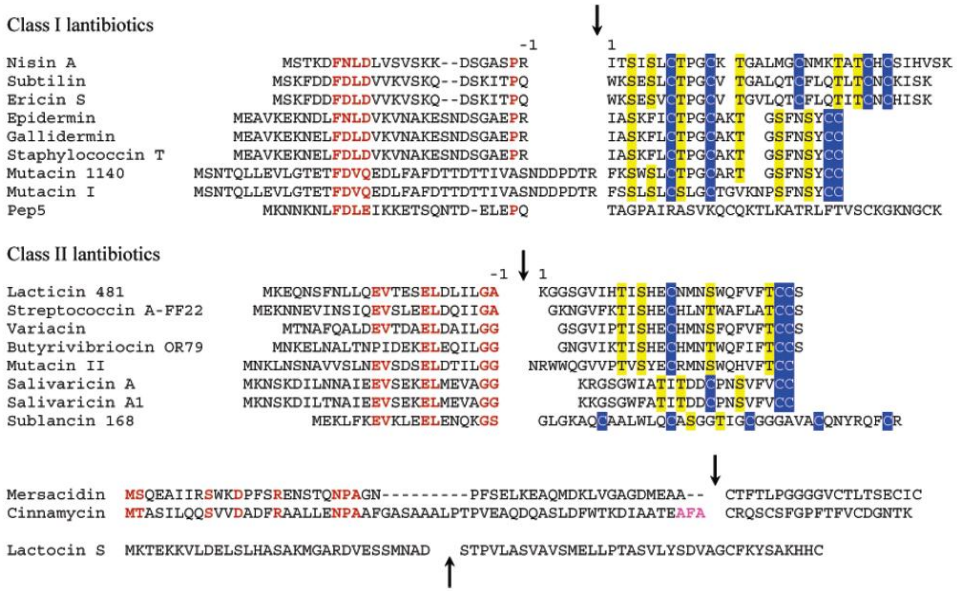

Figure 1.8 Alignments of the prepropeptide sequences of representative lantibiotics displaying the conserved leader peptide motifs, in red, as described in the text. Conserved serine/threonine and cysteine residues in the propeptide that are involved in lanthionine bridge formation are shown in yellow and blue, respectively. Leader peptide cleavage sites are marked with a black arrow. Image reproduced from Chatterjee *et al.* 2005.

The leader peptide appears to specify transport of the substrate by the NisT transporter since a number of non-lantibiotic peptides fused to the *nis*A leader sequence could be secreted from *L. lactis* and secretion was dependent upon the co-expression of NisT (Kuipers *et al.* 2004). Thus the leader peptide appears to define correct secretion of mature lantibiotics. A second function of the leader peptide is likely to be as a protective mechanism for the host cell, such that lantibiotics are kept in an inactive state until secreted. Lantibiotics with the leader sequence attached show little or no anti-bacterial activity (van der Meer *et al.* 1994; Li *et al.* 2006a). Initial studies with nisin chimeras with subtilin leader sequences suggested that the leader sequence may specify further processing by the LanBC or LanM enzymes (Chakicherla *et al.* 1995). However, studies with other chimeras suggest that this may not be the case for all lantibiotics (Kuipers *et al.* 1993b; Levengood *et al.* 2007). In particular EpiD, which forms the amino-vinyl cysteine modification in epidermin (section 1.2.3.2), does not require the leader peptide for activity (Kupke *et al.* 1995). The leader peptide has also been suggested to contribute to the directionality of lanthionine bridge-formation (Levengood *et al.* 2007; Lee *et al.* 2009; Oman *et al.* 2010).

The leader peptide cleavage sites of type AI lantibiotics show particular conservation at positions -1, -2 and -4, which are commonly arginine/glutamine, proline and alanine/isoleucine, respectively (Figure 1.8) (Chatterjee *et al.* 2005). Site-directed mutation of the -2 position of the nisin leader indicated only a minor role for this residue in nisin leader processing (van der Meer *et al.* 1994). By contrast, leader peptide removal from pre-nisin was strongly dependent on the presence of arginine at -1 and alanine at -4 (van der Meer *et al.* 1994). This was likely a specific property of the NisP leader peptidase since *in vitro* cleavage of the modified leader resulted in active nisin, suggesting that these residues do not influence nisin propeptide maturation (van der Meer *et al.* 1994).

1.2.3.2 Post-translational Modifications

LanB Dehydratase

Studies of LanB activity have been severely hindered by the inability to reconstitute enzyme activity *in vitro* (Xie *et al.* 2002; Chatterjee *et al.* 2005). In addition there are no known homologs of LanB proteins that might shed light on their mechanism of action. LanB orthologs on average share only around 30% amino acid sequence identity, which is thought to reflect the large differences in substrate sequence and structure between different lantibiotics (Chatterjee *et al.* 2005). In a *nisC* mutant, but not a *nisBC* double mutant, a dehydrated pre-peptide could be recovered, providing evidence that NisB is responsible for this activity (Koponen *et al.* 2002). Successful synthesis of nisin using an *in vitro* transcription/translation system required the presence of the *nisB* transcript (Cheng *et al.* 2007). *nisB* is essential for high level accumulation of pre-nisin in *L. lactis* cells, suggesting instability of the prepropeptide in its absence (van den Berg van Saparoea *et al.* 2008). NisB does not contain any predicted transmembrane regions but localises at the cell membrane, along with NisC and NisT, suggesting the formation of a multimeric functional complex (Siegers *et al.* 1996). Models for LanB enzymatic activity have been largely extrapolated from data on LanM bifunctional enzymes (see below). NisB exhibits relatively low substrate specificity and was shown to dehydrate non-lantibiotic peptides expressed in *L. lactis* when the NisA leader peptide was fused to them (Kluskens *et al.* 2005; Rink *et al.* 2005).

LanC Cyclase

A great deal more information is available about LanC than LanB enzymes, since *in vitro* reconstitution of LanC function was demonstrated (Li *et al.* 2006a). A particularly well-studied example is NisC, which carries out the cyclisation reaction of nisin. *In vitro,* NisC was able to cyclise a dehydrated pre-nisin substrate isolated from *L. lactis* Δ*nisC.* This activity was not seen when the leader peptide was first cleaved from the substrate, suggesting a requirement of the nisin leader peptide for NisC activity (Li *et al.* 2006a). The crystal structure of NisC was solved to 2.5Å resolution allowing a thorough investigation of its mechanism of action. Conserved histidine and cysteine residues at the active site coordinate a zinc ion, activating the attacking thiolate group for nucleophilic attack on the dehydrated Dha or Dhb substrate (Figure 1.9). The structure also suggests a possible binding site for the leader sequence of prenisin (Li *et al.* 2006a). The importance of the active site residues and coordination of zinc was further demonstrated by site directed mutagenesis. However, Arg^{280}, which had previously been postulated as important for cyclisation, was shown not to be essential for cyclisation, which correlates with the

absence of this residue in the LanM enzymes, while Trp^{283} was postulated to be important for protein stability since the mutant protein was prone to precipitation (Li *et al.* 2007).

The substrate specificity of LanC enzymes is quite low. EpiC, encoded by the epidermin biosynthetic gene cluster, could complement a SpaC (subtilin) deletion mutant (Helfrich *et al.* 2007). Furthermore, alanine replacement mutagenesis in SpaC has identified residues essential for enzyme activity. This indicated conservation of catalytic residues between NisC and SpaC, with the most important being those involved in zinc coordination (Helfrich *et al.* 2007). NisC is predicted to form a complex with NisB and NisT at the membrane (Siegers *et al.* 1996). Recent evidence from *in vitro* synthesis of nisin suggests, however, that membrane association is not essential for nisin biosynthesis (Cheng *et al.* 2007).

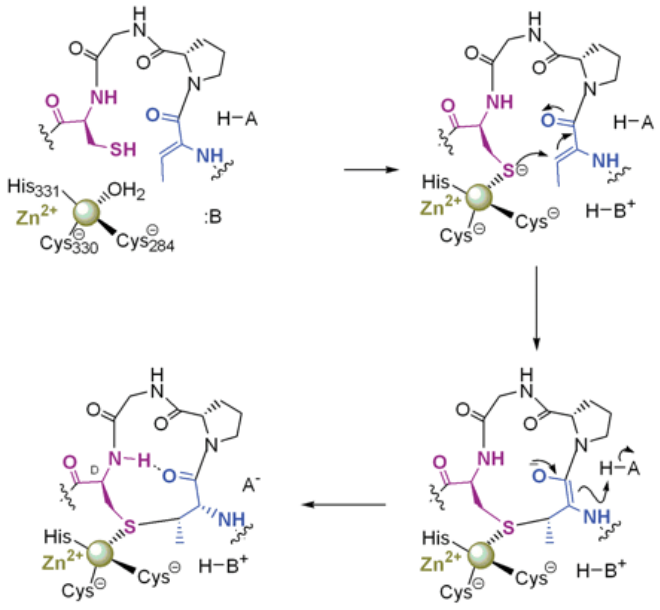

Figure 1.9 The proposed mechanism for the formation of a lanthionine bridge in nisin by NisC. A zinc atom is coordinated by two cysteine residues, a histidine residue and water at the active site of NisC. Upon substrate binding the water molecule is displaced by the sulphur atom of a cysteine in the nisin prepropeptide. The sulphur atom is deprotonated via the interaction with zinc which lowers its $pK_{a.}$ This allows a nucleophilic attack upon the carbon-carbon double bond of Dhb (or Dha) in the prepropeptide to yield an enolate intermediate which is subsequently protonated. Image reproduced from Li *et al.* 2006.

LanM Bi-functional dehydratase/cyclase

LanM enzymes are bi-functional, carrying out both the dehydration and cyclisation reactions for type AII and type B lantibiotics. The C-termini of LanM enzymes share around 20-27% identity with LanC proteins, but there is conversely no homology between LanM and LanB proteins. This suggests that *lanM* genes did not result from a fusion of *lanB* and *lanC* (Chatterjee, 2005). A well-studied example is LctM, which dehydrates and cyclises the appropriate residues during the biosynthesis of lacticin 481 by *Lactococcus lactis*. The *in vitro* biosynthesis of lacticin 481 confirmed the dual activity of LctM in the presence of ATP and Mg^{2+}. EDTA abolished activity suggesting that zinc is important for catalysis, as in the case of NisC (Xie *et al.* 2004). Consistent with this, mutations that remove the putative zinc coordinating ligands of LctM prevent cyclisation but not dehydration (Paul *et al.* 2007). This also indicates that the cyclisation and dehydration activities of LanM enzymes can be uncoupled. Only residues 10-24 of the leader peptide were necessary for LctM activity (Xie *et al.* 2004). Attempts at crystallisation of LctM have so far been unsuccessful but a recent report has shed some light on the catalytic mechanism of dehydration through the use of site-directed mutagenesis (You *et al.* 2007). LctM was shown to have low substrate specificity and could dehydrate non-lantibiotic peptides attached to the LctA leader peptide (You *et al.* 2009). Mutant forms of LctM could function as general serine/threonine kinases, potentially shedding light on the evolution of LanM enzymes from this widely distributed class of proteins (You *et al.* 2009).

LanL Bi-functional dehydratase/cyclase

A third class of lanthionine bridge-forming enzymes was recently described (Goto *et al.* 2010). These enzymes, typified by the initially identified member, VenL, from *S. venezualae* consist of three domains; a phosphoserine/threonine lyase domain, a kinase domain and a LanC-like cyclase domain. The N-terminal Ser/Thr kinase and lyase domains were involved in dehydratase activity of the protein. This class of enzymes appears to be widespread in sequenced genomes from the current database (Goto *et al.* 2010).

LanD Decarboxylase

LanD enzymes are involved in the conversion of C-terminal cysteine to an S-[(*Z*)-2-aminovinyl]-D-cysteine (AviCys) modification. Specifically LanD enzymes are flavoproteins which decarboxylate the C-terminal cysteine of the peptide chain to yield an enethiol intermediate which subsequently forms an AviCys bridge via cyclisation with a didehydroalanine or didehydrobutyrine in the chain, possibly catalysed by LanC (Figure

1.10) (Chatterjee *et al.* 2005). EpiD involved in epidermin biosynthesis is a well-studied example for which the crystal structure is also available (Blaesse *et al.* 2000; Chatterjee *et al.* 2005). EpiD and MrsD (mersacidin) are members of the homooligomeric flavin-containing cysteine decarboxylase (HFCD) superfamily (Blaesse *et al.* 2003). EpiD function does not require a leader peptide. The substrate specificity of EpiD was investigated using peptide libraries. EpiD displays relatively low substrate specificity with only the C-terminal cysteine being an absolute requirement although the nature of all three residues at the C-terminus could affect enzyme activity and not all substrate changes were tolerated. Furthermore the three C-terminal residues alone were not sufficient for enzyme activity which required a minimum of a tetrapeptide substrate (for weak activity). Based on these findings a consensus amino acid sequence for the C-terminus of an EpiD substrate was suggested; (V/I/L/(M)/F/**Y**/W)-(A/S/V/T/**C**/(I/L))-**C** (Kupke *et al.* 1995). Structural studies of EpiD and MrsD provided insights into the catalytic mechanism of the enzymes, which require FMN or FAD (MrsD only) for functionality (Blaesse *et al.* 2000; Blaesse *et al.* 2003).

The exact function of this C-terminal modification in the lantibiotics which possess it, epidermin, mersacidin and mutacin III, is not clear. EpiD is essential for epidermin bioactivity in *Staphlococcus epidermis* but it is not known whether the presence of the modification contributes to bioactivity directly or to the stability/production efficiency of the molecule (Augustin *et al.* 1992). Although the essentiality of *mrsD* for mersacidin biosynthesis has not been directly addressed, during experiments to generate mersacidin variants, alterations at Ile19 (next to the decarboxylated cysteine residues) were, unlike those at many other sites, not well-tolerated (the respective molecules being absent or produced at very low yields), suggesting that cysteine decarboxylation may be essential for mersacidin biosynthesis (Appleyard *et al.* 2009).

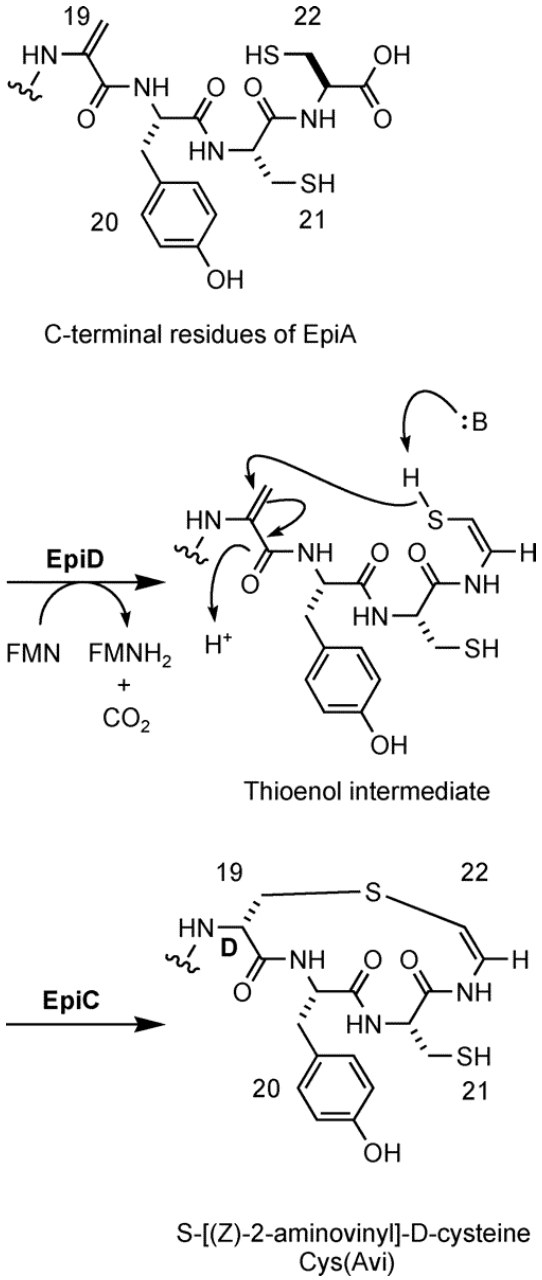

Figure 1.10 The proposed mechanism for the formation of S-[(*Z*)-2-aminovinyl]-D-cysteine (AviCys) in the epidermin prepropeptide EpiA, catalysed by EpiD and EpiC. EpiD decarboxylates the C-terminal cysteine at position 22 of the prepropeptide, in a flavin-dependent manner, to yield an enethiol intermediate. The enethiol intermediate subsequently forms an AviCys bridge via cyclisation with Dha at position 19, most likely in a reaction catalysed by EpiC. Image reproduced from Chatterjee *et al.* 2005.

Other Post-Translational Modifications

Several other post-translational modifications of lantibiotics, in addition to the introduction of lanthionine bridges and AviCys residues, have been reported. These tailoring modifications likely influence the specific properties of the final compound, as is the case for polyketide and non-ribosomal peptide antibiotics (Walsh *et al.* 2001). N-terminal modifications have been described, presumably providing protection from aminopeptidase activity, and are proposed to be introduced subsequent to leader peptide removal (Chatterjee *et al.* 2005). This suggests either that the leader peptide is removed intracellularly (as was shown for Pep5 (de Vos *et al.* 1995)) or the tailoring enzymes work outside the cell membrane, perhaps in concert with leader peptide removal. Examples include the 2-oxobutyryl and 2-oxopropionyl groups in Pep5 and epilancin K7 (Chatterjee *et al.* 2005). Formation of a lysinoalanine bridge in cinnamycin also likely protects the N-terminus of the molecule and creates a highly globular structure. Lysinoalanine is unique to cinnamycin, as is the introduction of hydroxyaspartate (Widdick *et al.* 2003). Both lactocin S and lacticin 3147 have a D-alanine in place of the genetically encoded L-serine, which is thought to result from a stereospecific hydrogenation of dehydroalanine (Chatterjee *et al.* 2005). Finally, the modified peptide antibiotic cypemycin possesses dimethylalanine at the N-terminus and also contains two allo-isoleucines (Minami *et al.* 1994).

1.2.3.3 Export and Leader-peptide removal

Following biosynthesis the lantibiotic is exported from the cell. This may be concomittant with or prior to leader peptide removal. In some cases the leader peptide is removed intracellularly (de Vos *et al.* 1995). Lantibiotic export is mediated by the ABC-transporter family of proteins which can be roughly divided into three classes.

The LanT proteins are members of the single-component ABC-family of ATP-dependent transporters in which the membrane domain is fused to the ATP-binding domain (Young *et al.* 1999). LanT proteins encoded by type AI lantibiotic gene clusters from low GC Gram-positive bacteria, typified by the export protein for nisin, NisT, consist of a large hydrophobic region, which forms six membrane-spanning helices, and a cytoplasmic ATP-binding domain (Figure 1.11) (Chatterjee *et al.* 2005; Lubelski *et al.* 2008). It is likely that two NisT monomers come together to form the complete ABC transporter. NisT interacts, at the cytoplasmic side of the cell membrane, with NisC and is likely to be involved in a complex for nisin modification and transport, also involving NisB ((Siegers *et al.* 1996; van den Berg van Saparoea *et al.* 2008). However, NisT is not essential for nisin biosynthesis *in vitro* (Cheng *et al.* 2007). In the absence of NisT, pre-nisin accumulates in the

cytoplasm (Qiao *et al.* 1996; van den Berg van Saparoea *et al.* 2008). Substrates do not need to be modified by the biosynthetic enzymes to be secreted by NisT (van den Berg van Saparoea *et al.* 2008). NisT shows broad specificity range and could transport non-lantibiotic protein substrates which were fused to the pre-nisin leader peptide (Kuipers *et al.* 2004). Pre-nisin leader peptide cleavage is not coupled to export (van den Berg van Saparoea *et al.* 2008). The LanT proteins GdmT (gallidermin), PepT (Pep5), NisT and SpaT (subtilin) show very little N-terminal similarity, though their hydrophobicity profiles are similar, but the C-terminal ATP-binding domains share identities of 20-31%. GdmT (and EpiT) requires GdmH (or EpiH), a predicted hydrophobic protein lacking sequence similarity to other proteins in the database, for full transport capability (Peschel *et al.* 1997; Hille *et al.* 2001).

The type AII and B lantibiotics from low GC Gram-positive bacteria use a related LanT transporter which similarly consists of a fused membrane-spanning domain and ATP-binding domain; however they are extended at the N-terminus by the inclusion of a protease domain (Chatterjee *et al.* 2005; Furgerson Ihnken *et al.* 2008). Both the ATP-binding and protease domains are predicted to be located in the cytoplasm, based on findings for the related transporter LcnC of the bacteriocin lactococcin A (Figure 1.11) (Franke *et al.* 1999). This protease fulfils the role of the separate LanP proteases of type AI lantibiotic gene clusters and in the case of LctT was identified to be a member of the cysteine protease family (Furgerson Ihnken *et al.* 2008). These proteases typically recognise the double glycine cleavage motif conserved in the leader peptides of type AII and B lantibiotics (Furgerson Ihnken *et al.* 2008).

The actinomycete lantibiotics characterised to date appear to use an alternative export system which instead consists of a two-component ABC transporter with separate membrane-spanning permease and ATP-binding domain proteins (Figure 1.11). These transporters are reminiscent of the multidrug export protein family (Young *et al.* 1999). CinTH of the cinnamycin biosynthetic gene cluster, postulated to export cinnamycin, have sequence homology with the daunorubicin resistance proteins DrrA and DrrB found in many actinomycetes (Kaur 1997; Widdick *et al.* 2003). The actagardine and deoxyactagardine B gene clusters both encode two-component ABC transporters postulated to have a role in lantibiotic export (Boakes *et al.* 2009; Boakes *et al.* 2010). Although these proteins have little sequence homology to CinTH, they share the same two-component arrangement. Interestingly GarH and LigH (permease component) are significantly extended at the N-terminus compared to CinH suggesting the possible presence of an integral protease domain; however, no such domain could be detected through sequence comparisons (Boakes *et al.* 2009; Boakes *et al.* 2010).

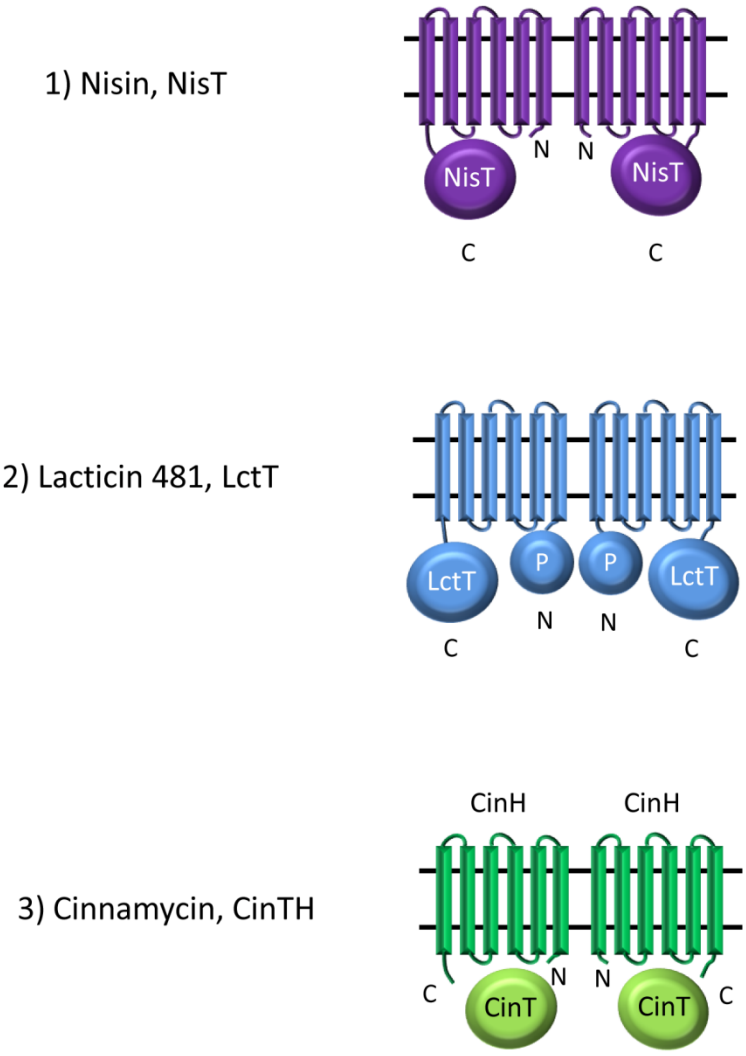

Figure 1.11 A summary of the three types of lantibiotic export ABC-transporters as described in the text. P indicates the presence of a protease domain. N and C indicate the N and C-termini of the proteins, respectively. ATP-binding domains are represented as ovals and permease domains by their transmembrane spanning helices.

As discussed the LanT proteins exporting type AII and B lantibiotics have an N-terminal protease which cleaves the leader peptide (Altena *et al.* 2000; Chatterjee *et al.* 2005; Furgerson Ihnken *et al.* 2008). In the type AI lantibiotics from low GC Gram positive bacteria this activity is supplied by a separate protease, LanP. NisP belongs to the subtilisin family of proteases and is likely exported from the cell due to the presence of a Sec-signal at its N-terminus (van der Meer *et al.* 1993). Pre-nisin is made in the absence of NisP, which is not required for its biosynthesis or transport from the cell (Qiao *et al.* 1996; Kuipers *et al.* 2004; van den Berg van Saparoea *et al.* 2008). NisP displays sequence specificity for leader peptide cleavage and was not able to cleave a subtilin leader-nisin chimera peptide *in vivo* (Kuipers *et al.* 1993b). In epidermin biosynthesis, the protease EpiP is a point of post-translational control of epidermin production. Regulated via the quorum sensing *agr* system in an undefined way, EpiP activity altered with cell-density, such that active mature epidermin should only be produced at high cell density (Kies *et al.* 2003).

Several lantibiotic gene clusters do not encode a dedicated LanP protease but appear to rely on non-specific proteases for leader peptide cleavage (Chatterjee *et al.* 2005). Subtilin was processed by at least three extracellular proteases of *B. subtilis in vivo* (Corvey *et al.* 2003). Haloduracin, a two-component lantibiotic produced by *Bacillus halodurans*, was similarly processed by extracellular proteases in the culture supernatant of the natural producer, however it is not clear whether HalT may also play a role in leader peptide processing (McClerren *et al.* 2006; Lawton *et al.* 2007). Finally the actinomycete lantibiotics do not have clear candidate protease enzymes encoded within their biosynthetic gene clusters and are also likely processed by extracellular proteases (Widdick *et al.* 2003; Gartemann *et al.* 2008; Boakes *et al.* 2009; Boakes *et al.* 2010). Cinnamycin and actagardine were successfully expressed in the heterologous host *S. lividans* suggesting that the general protease involved in their maturation is also likely to be present in this species (Widdick *et al.* 2003; Boakes *et al.* 2009).

1.2.3.4 Producer Self-Resistance

Lantibiotic producing host strains require mechanisms of self-protection. In the nisin biosynthetic gene cluster this is provided by the *lanI* and *lanFEG* genes (Siegers *et al.* 1995). The LanI protein, NisI, is a lipoprotein, anchored to the cell membrane, which acts to block nisin activity by interacting with the lantibiotic before it can bind to its target substrate lipid II or interact with the membrane to form pores (see also section 1.2.4) (Figure 1.7) (Qiao *et al.* 1995; Stein *et al.* 2003). NisI specifically binds to nisin and did not bind to or give immunity against subtilin (Stein *et al.* 2003). The immunity function of the nisin cluster was initially thought to be regulated along with the biosynthetic genes, via nisin autoregulation (see below). Recently a NisI specific promoter has been identified internal to the *nisABTCIP* operon which allows NisI expression prior to nisin biosynthesis (Li *et al.* 2006b). NisI truncation experiments have revealed the C-terminal region to be of particular importance for NisI activity and in conferring specificity of a hybrid SpaI-NisI protein towards nisin (Takala *et al.* 2006).

A number of lantibiotic clusters have only LanI genes as an immunity mechanism and do not have LanFEG homologs (described below). Examples include Pep5, cytolysin, epicidin and lactocin S (Chatterjee *et al.* 2005). These LanI proteins are integral membrane proteins rather than lipoproteins and do not share sequence homology with NisI and SpaI. PepI localises to the cell wall-membrane interface, with the N-terminus of the protein regulating its own export and the C-terminus conferring immunity (Hoffmann *et al.* 2004).

A further example in which a small protein confers increased resistance to a lantibiotic is the Nukacin ISK-1 NukH protein (Aso *et al.* 2004; Aso *et al.* 2005). This small protein is predicted to have three transmembrane domains and two external loops (Okuda *et al.* 2005). It localises to the cell membrane when expressed heterologously in *Lactococcus lactis* and interacts with Nukacin ISK-1 via its C-terminus. It is thought that NukH binds Nukacin ISK-1 at the membrane and directs it to the ABC-complex of NukFEG (Okuda *et al.* 2008).

In the case of nisin, full protection for producer cells seems to be conferred only when both LanFEG (NisFEG) and LanI (NisI) are present. The effect appears to be additive since each system alone only confers 5-20% of the full immunity level (Ra *et al.* 1999). The *nisFEG* genes lie downstream of the nisin biosynthetic cluster and form a separate operon, transcribed from a promoter upstream of *nisF* (Siegers *et al.* 1995). The NisFEG proteins constitute an ABC-transporter; NisF is an ATP-binding domain protein and NisE and NisG are the membrane-spanning proteins of the transporter (Figure 1.7). It is likely that two NisF proteins interact with a heterodimer of NisEG, on the basis of structural similarity to the maltose and histidine transport systems (Chatterjee *et al.* 2005). Heterologous expression of NisFEG in *B. subtilis* decreased the levels of cell associated nisin suggesting that the function of the transporter is to export nisin away from the producer cell surface and prevent nisin interaction with its target lipid II (Stein *et al.* 2003). The ATP-binding domain LanF proteins involved in lantibiotic resistance differ from other ATP-binding domain proteins in the conserved Q-loop, which is replaced by an E-loop (Okuda *et al.* 2010). This may have functional significance for the exported substrates and define these proteins as a separate class (Okuda *et al.* 2010).

The epidermin gene cluster does not have a *nisI* homolog but does have *lanFEG* genes, which appear to constitute the complete immunity system for epidermin (Peschel *et al.* 1996). EpiFEG constitute an ABC transporter that has been shown to export gallidermin in an ATP-dependent manner (Otto *et al.* 1998). The *epiFEG* genes form an operon, the expression of which is regulated along with the biosynthetic and transport genes, by EpiQ. The presence of *epiFEG* is required for wild type levels of epidermin biosynthesis in a heterologous host (Peschel *et al.* 1996). EpiH and its close relative GmdH are also involved in the immunity mechanisms for epidermin and gallidermin, respectively. GmdH and EpiH do not have homologs in other lantibiotic clusters but do have similarity to other proteins of unknown function in a range of bacteria (Peschel *et al.* 1997; Hille *et al.* 2001). Like epidermin, a number of lantibiotic clusters encode *lanFEG* homologs but do not possess *lanI* genes; examples include mersacidin, lacticin 481 and macedocin (Rince *et al.* 1997; Altena *et al.* 2000; Papadelli *et al.* 2007).

1.2.3.5 Regulation

The regulatory mechanisms employed by different lantibiotic gene clusters appear to vary widely. This likely reflects the wide range of input signals which induce lantibiotic biosynthesis in different producing organisms. Many lantibiotics regulate their own expression in a cell-density dependent manner but often this is integrated with other external signals, such as developmental cues, pH and cell stress responses (Stein *et al.* 2002; Kies *et al.* 2003; Hindre *et al.* 2004). The regulation of lantibiotic biosynthetic genes occurs most commonly via a two-component system (Figure 1.7) (Chatterjee *et al.* 2005).

The nisin regulatory system has been extensively studied and is similar to that of subtilin (Stein *et al.* 2002). Induction of expression of the nisin biosynthetic gene cluster in a *nisA* mutant is dependent on the presence of exogenously added nisin in a dose-dependent manner (Kuipers *et al.* 1995). The first 11 residues of nisin, including the A and B rings, were sufficient for the induction of *nis* gene transcription (Kuipers *et al.* 1995). Additionally, an in-frame deletion of the nisin biosynthetic gene *nisB* prevented self-induction suggesting that the structure of the molecule, introduced by the lanthionine bridges, is important for induction (Kuipers *et al.* 1995). Induction of *nis* gene expression in response to nisin is dependent on the presence of *nisRK* (Engelke *et al.* 1994; Kuipers *et al.* 1995). The membrane embedded NisK histidine kinase likely “senses” the presence of nisin at the membrane, either directly or indirectly (Kuipers *et al.* 1995). This induces histidine kinase autophosphorylation. Phosphotransfer to the response regulator NisR likely induces the ability to interact with operator sequences preceding *nisA* and *nisF* in the gene cluster (de Ruyter *et al.* 1996). Over-expression of NisR alone is capable of stimulating *nis* gene transcription (van der Meer *et al.* 1993). This activates transcription of *nisABTCIP* and *nisFEG* (de Ruyter *et al.* 1996). *nisR and nisK* are by contrast constitutively expressed from a separate *nisR* promoter (de Ruyter *et al.* 1996). This raises the question of how host cells protect themselves if immunity mechanisms are initiated only at the same time as biosynthesis. Recently a separate *nisI* promoter was identified internal to the operon that can activate *nisI* expression without *nisA* activation (Li *et al.* 2006b), and which presumably serves this protective role. This promoter exhibits weak constitutive activity, possibly induced by DNA curvature effects (Li *et al.* 2006b).

The SpaRK system in *B. subtilis* operates in a similar way to NisRK and both NisK and SpaK can phosphorylate NisR. Moreover, NisK-SpaK chimeras are functional, with the N-terminus providing specificity for the inducer (Kleerebezem *et al.* 1997; Kleerebezem *et al.* 2001). Subtilin production by *B. subitilis* is also positively influenced by the developmental sigma factor SigH, which is regulated in a density dependent manner, and negatively by

AbrB, a transition state regulator of late-growth gene transcription, which may act via SigH (Stein *et al.* 2002).

A number of lantibiotic gene clusters deviate from this mode of regulation and do not use classical two-component systems. Epidermin production is linked to the quorum sensing (*agr*) system, however a direct transcriptional effect was ruled out. *agr* regulates, by an unknown mechanism, the activity of the EpiP protease, preventing it from removing the leader peptide of the epidermin prepeptide and thus keeping it in an inactive state until cell density reaches an appropriate level (Kies *et al.* 2003). A single regulatory protein EpiQ is encoded with the epidermin cluster and is essential for epidermin biosynthesis. EpiQ is a response regulator but no cognate histidine kinase is encoded within the cluster. EpiQ activates transcription of the other epidermin biosynthetic genes, however there is no knowledge of how EpiQ itself is regulated and epidermin biosynthesis appears to be independent of the external epidermin concentration (Peschel *et al.* 1993; Kies *et al.* 2003).

The mersacidin biosynthetic gene cluster encodes a histidine kinase and two response regulators (Altena *et al.* 2000). The orphan response regulator encoded by *mrsR1* was required for mersacidin production and thus likely regulates transcription of *mrsA* and the biosynthetic genes, although its cognate histidine kinase is unknown (Guder *et al.* 2002; Schmitz *et al.* 2006). MrsK2/R2 act as a two-component regulatory system for the immunity genes *mrsFEG* (Guder *et al.* 2002). Like nisin and subtilin, mersacidin acts as its own autoinducer (although mersacidin is required at higher concentrations) (Schmitz *et al.* 2006). When induced by mersacidin, a Δ*mrsK2/R2* mutant fails to transcribe the *mrsA* prepropeptide gene. This initially seems at odds with the earlier findings but might be explained by a fail-safe mechanism that prevents mersacidin production in the absence of immunity gene transcription and if the role of MrsK2/MrsR2 is to coordinate biosynthesis and resistance (Schmitz *et al.* 2006). Unlike subtilin biosynthesis, sigma factor SigH does not influence mersacidin biosynthesis in *Bacillus* sp. (Schmitz *et al.* 2006). The possibility that MrsR1 is not part of a conventional two-component system is supported by the finding of several other orphan regulators encoded by lantibiotic gene clusters, such as EpiQ, MutR, LasX and ltnR (described below).

The mutacin II gene cluster encodes the regulator MutR which is required for mutacin II biosynthesis and appears to regulate the *mutA* and *mutR* promoters. MutR is a member of the Rgg family of transcriptional regulators (Qi *et al.* 1999a). Lacticin 3147 biosynthesis has similarly been found not to involve a two-component system. The negative regulator LtnR, one of a few found in lantibiotic gene clusters, regulates its own transcription, and

that of the immunity genes, in a negative feedback loop. The biosynthetic gene operon appears to be constitutive in this case, with a transcriptional attenuator downstream of *ltnA* maintaining the appropriate stoichiometric ratio of the prepropeptide with the biosynthetic enzymes (McAuliffe *et al.* 2001). The LasX protein expressed from the lactocin S cluster acts as both a positive and negative regulator. LasX up-regulates transcription of the biosynthetic genes whilst down-regulating its own transcription in order to maintain a steady state. LasX, like MutR, belongs to the Rgg family and its binding site has been identified but the signal regulating LasX is unknown (Rawlinson *et al.* 2002; Rawlinson *et al.* 2005).

1.2.4 Modes of Lantibiotic Action

Many lantibiotics function by binding to Lipid II, the precursor for peptidoglycan biosynthesis. The peptidoglycan layer is a cross-linked network of amino sugars and tetrapeptides that provides structural integrity to the cell, preventing the lysis that might otherwise result from high internal osmotic pressure. The formation of peptidoglycan during bacterial cell wall biosynthesis is a cyclical process that alternates between the inner and outer leaflet of the cell membrane and involves a polyisoprenoid carrier molecule (Figure 1.12). The undecaprenylphosphate carrier on the inner leaflet of the membrane is attached, via a UDP intermediate, to *N*-acetylmuramic acid (MurNAc)-pentapeptide (most commonly L-Ala-D–γ-Glu-L-Lys-D-Ala-D-Ala) by MraY. This is followed by the addition of *N*-acetylglucosamine (GlcNAc) from UDP-*N*-acetylglucosamine by MurG to form Lipid II. Lipid II is transported from the inner leaflet to the outer leaflet by an unknown process, likely a specialised protein translocator. Penicillin-binding proteins in the outer leaflet of the membrane catalyse the transfer of the pentapeptidyldisaccharide from the carrier molecule to the growing peptidoglycan chain by transglycosylation. Subsequently transpeptidase activity induces peptide chain cross-linking to provide structural rigidity to the resulting peptidoglycan.

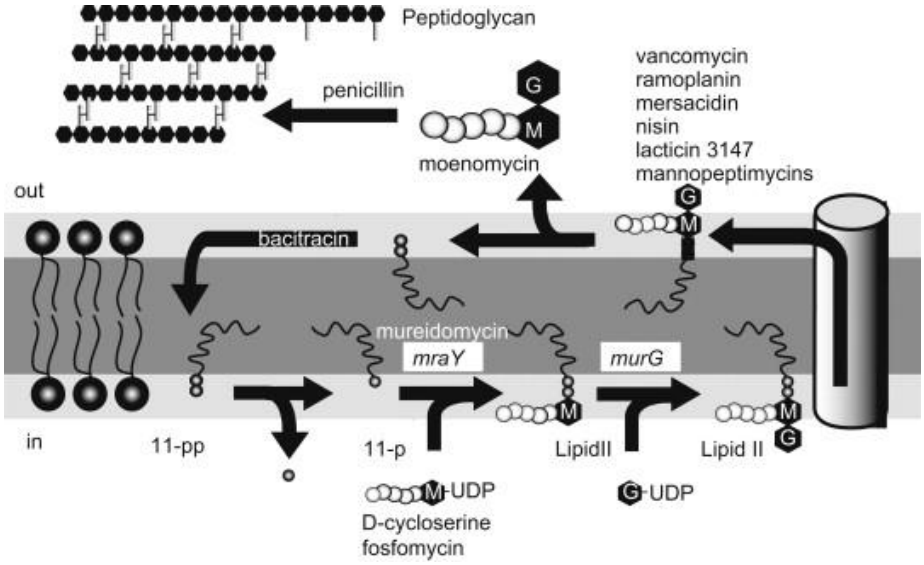

Figure 1.12 Summary of the events of the peptidoglycan biosynthetic cycle in the cell membrane of a Gram-positive bacterium as described in the text. Antibiotics which act at specific points in the cycle are indicated. 11-pp, undecaprenylphosphate carrier; the pentapeptide is represented by five spheres; M, *N*-acetylmuramic acid (MurNAc); G, *N*-acetylglucosamine (GlcNAc). Image reproduced from de Kruijff *et al.* 2008.

The universal nature of peptidoglycan biosynthesis in bacteria, and the importance of the cell wall for bacterial viability, renders cell wall biosynthesis a particularly suitable target for antibiotic activity. For example, vancomycin targets the C-terminal two residues of the pentapeptide of Lipid II and penicillin interacts with the penicillin-binding proteins to prevent transglycosylation (Figure 1.12) (de Kruijff *et al.* 2008). Several lantibiotics also target Lipid II, inhibiting peptidoglycan biosynthesis, weakening the cell wall and inducing cell lysis.

Nisin exhibits two mechanisms of cell killing, the formation of membrane pores which leads to osmotic shock and cell lysis, and the inhibition of cell wall biosynthesis preventing cell division and increasing the risk of cell lysis due to internal osmotic pressures (Bauer *et al.* 2005; Breukink *et al.* 2006). These mechanisms are both mediated by the ability of nisin to bind to Lipid II (Breukink *et al.* 2006). The complex of nisin with Lipid II has been extensively studied; rings A and B of nisin form a cage for the pyrophosphate moiety of Lipid II. The cage is formed by the backbone of the nisin peptide chain rather than being mediated by specific side chains (Figure 1.13) (Hsu *et al.* 2004). The backbone amides form five hydrogen bonds to the pyrophosphate (Hsu *et al.* 2004). Binding to lipid II is a crucial step in membrane pore formation, recruiting nisin monomers to the membrane and

allowing them to oligomerise to form pores (Hasper *et al.* 2004). Lipid II plays a key role in pore formation with four molecules per pore complex along with eight of nisin. The pores are extremely stable and not disrupted by mild detergents (Hasper *et al.* 2004). The hinge region between rings C/D of nisin is critical for pore formation, allowing insertion of nisin molecules across the bilayer membrane where they are stabilised by interaction with lipid II (Hasper *et al.* 2004).

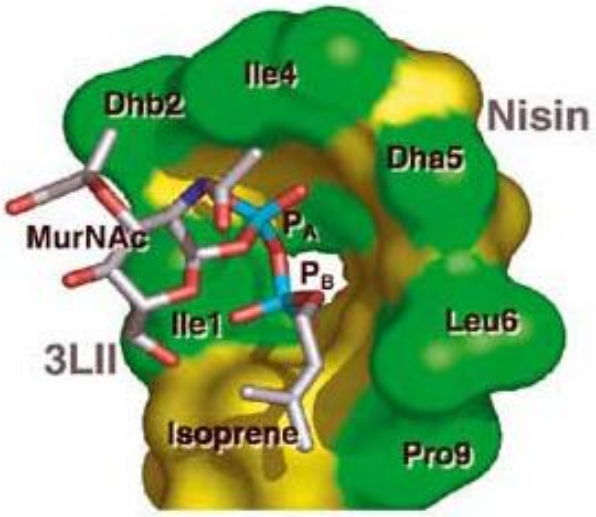

Figure 1.13 The N-terminal part of nisin (residues 1−12 shown in van der Waals surface with backbone and side chain atoms in yellow and green, respectively) encages the pyrophosphate moiety of 3LII (a variant of Lipid II with a shortened prenyl tail of three isoprene units instead of 11 in the full-length structure). The side chains (green) of nisin are labeled. Carbon, nitrogen, oxygen and phosphorus atoms of 3LII are white, blue, red and cyan, respectively. Image and legend reproduced from Hsu *et al.* 2004.

Mutational analysis of nisin revealed that alterations in the hinge region prevent the formation of membrane pores but do not affect the bacteriocidal activity of nisin (Hasper *et al.* 2004). Furthermore, several type AI lantibiotics with the conserved A and B rings required for interaction with Lipid II do not form membrane pores and are bacteriocidal (Bonelli *et al.* 2006; Hasper *et al.* 2006). This indicated the involvement of a second Lipid II-mediated activity. In *Bacillus* sp. nisin altered the normal distribution of Lipid II in the cell membrane, mobilising it away from sites where Lipid II accumulates in the absence of nisin, such as at the cell division septum (Hasper *et al.* 2006). This was also the case in susceptible *L. lactis*. This indicates that nisin is capable of sequestering Lipid II away from sites of cell wall synthesis and thus prevents peptidoglycan biosynthesis and weakens the cell wall (Hasper *et al.* 2006). This mechanism of action is likely common to type AI

lantibiotics, many of which may also lack the cell permeabilising activity of nisin (Hasper *et al.* 2006).

Epidermin and gallidermin share a high degree of homology with the A and B rings of nisin but do not share C-terminal homology and are much shorter (30 Å in length compared to 50 Å for nisin). Both lantibiotics can bind Lipid II but are too short to form pores except for in the thinnest membranes *in vitro* (Bonelli *et al.* 2006). Although able to form pores in a few target species (e.g. *Micrococcus flavus*), in others (e.g. *Lactococcus* sp.) pore formation appeared to contribute very little to the activity of gallidermin, contrasting with that of nisin (Bonelli *et al.* 2006). Gallidermin and epidermin have 10-20 times the bacteriocidal activity of nisin against *L. lactis* despite the absence of detectable pore formation suggesting that they may have a more efficient mechanism of inhibiting cell wall biosynthesis, possibly through increased Lipid II affinity. Lys^{4} was suggested to be important for this since it would increase the positive charge and promote the pyrophosphate interaction (Bonelli *et al.* 2006; Rink *et al.* 2007).

Mersacidin, a type B lantibiotic without structural similarity to nisin, similarly does not create membrane pores but does inhibit cell wall biosynthesis. It has a highly flexible $Ala^{12}Abu^{13}$ region and flexible glycine rich region which appear to be important for its mechanism of action (Hsu *et al.* 2003). Glu^{17} might be involved in the Lipid II interaction and its removal inactivates mersacidin (Hsu *et al.* 2003). Plantaricin C has a structure intermediate between nisin and mersacidin, and it too does not form pores, except in the most susceptible species, but is a potent inhibitor of cell wall synthesis (Wiedemann *et al.* 2006). Mutacin III and mutacin 1140 share considerable similarity to nisin particularly at the N-termini. Mutacin 1140 however did not appear to form transmembrane pores in a susceptible *Streptococcus* sp. but did interact with Lipid II (Smith *et al.* 2008).

Nisin and subtilin, in addition to cell killing activity, also inhibit spore outgrowth in *B. subtilis*. Replacement of the conserved dehydroalanine residue at position 5 with alanine prevented this activity in both molecules (Liu *et al.* 1992; Chan *et al.* 1996). However substitution with phenylalanine at this position in nisin enhanced activity (Rink *et al.* 2007).

Finally, other modes of lantibiotic action have also been described. An example is the type B lantibiotic cinnamycin which binds to phosphatidylethanolamine in the membrane and thus disrupts membrane morphology and stability (Makino *et al.* 2003).

1.3 Microbisporicin

1.3.1 Background

The *Streptosporangiaceae* family are a relatively under-studied group of the actinomycetes. These bacteria are rarely isolated in the environment and are often slow growing (Lazzarini *et al.* 2000). However literature surveys suggest that this group could be a rich source of antimicrobials (Lazzarini *et al.* 2000). This family includes the genera *Microbispora*, *Nonomuraea*, *Planomonospora*, *Planobispora* and *Streptosporangium,* all of which have been described to produce interesting secondary metabolites (Lazzarini *et al.* 2000; Sosio *et al.* 2003; Beltrametti *et al.* 2007; Castiglione *et al.* 2007; Castiglione *et al.* 2008).

Members of the genus *Microbispora* (Nonomura *et al.* 1957) were named for the observed production of pairs of spores on aerial mycelia. A number of *Microbispora* species (with the most prevalent species being *M. rosea*) have been described to date and several reported to produce secondary metabolites (Ivanova *et al.* 2007; Okujo *et al.* 2007). Additionally, a thermophilic strain of *M. rosea* was reported to degrade synthetic polymers, such as the biodegradable plastics polyethylene succinate (PES) and polyhydroxybutyrate (PHB), and could be utilised for bioremediation (Hoang *et al.* 2007).

A new species of *Microbispora* was isolated in Thailand in 1999 and was named *Microbispora corallina* (Nakajima *et al.* 1999). These bacteria were found to grow as mycelium and to produce pairs of spores under certain growth conditions (Nakajima *et al.* 1999). The type strain for this species DSM 44682 (DF-32 or JCM10267) and a second isolate DSM 44681 (DF28 or JCM 10266) were characterised as members of the *Microbispora* genus on the basis of 16s rDNA similarity and chemotaxonomic properties (Figure 1.14) (Nakajima *et al.* 1999).

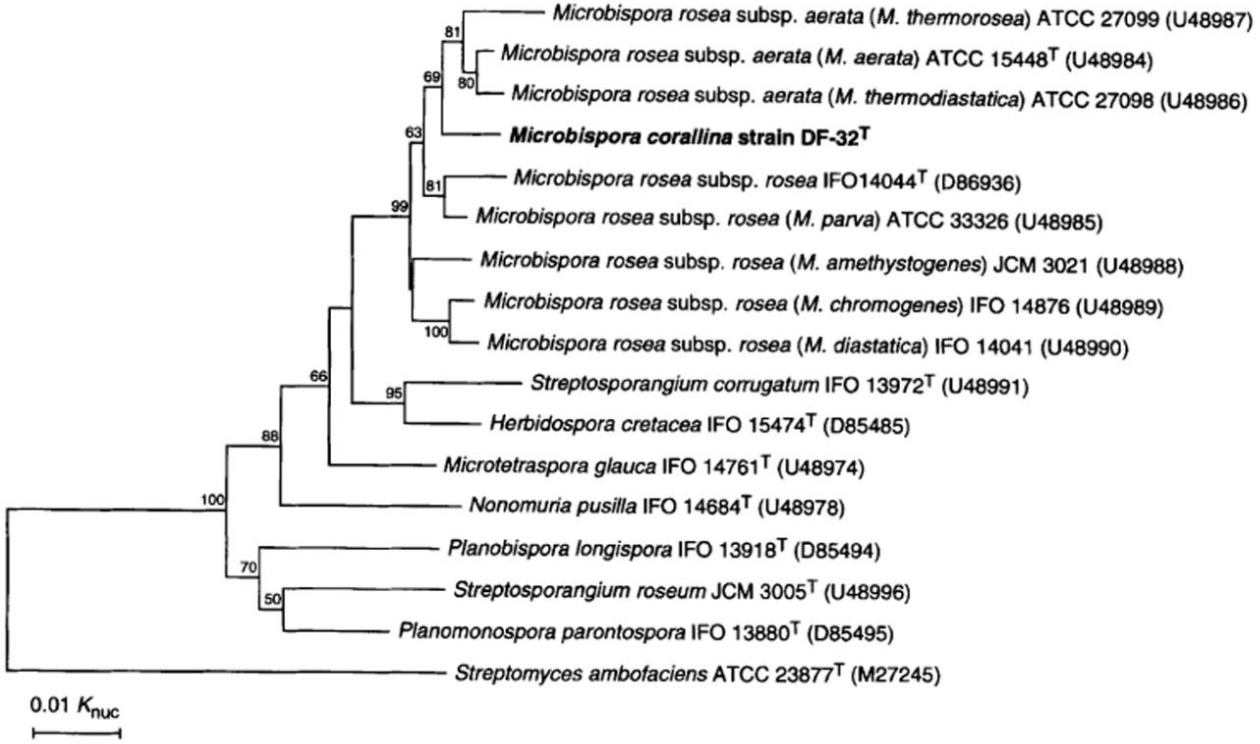

Figure 1.14 Phylogenetic tree showing the relationship between *Microbispora corallina* type strain DF32^T to other members of the *Microbispora* genus, to other *Streptosporangiaceae* family members, including *Planomonospora*, *Nonomuraea*, *Herbidospora* and *Streptosporangium*, and to *Streptomyces ambofaciens*. The numbers on the branches indicate the percentage bootstrap values of 1000 replicates (greater than 50%). The scientific names in parentheses are the originally proposed names of the strains; the numbers in parentheses are the GenBank/EMBL/DDBJ database accession numbers. Image and legend partially reproduced from Nakajima *et al.* 1999.

A novel strain of *M. corallina*, NRRL 30420, was reported in a patent from the pharmaceutical company Essential Therapeutics in 2003 to produce two potent bactericidal lantibiotic compounds (Lee 2003). This strain of *M. corallina* was isolated from the soil around the roots of a Peanut plant (*Arachis hipogea*) in West Java, Indonesia and was found to share 16s rDNA sequence similarity with DSM 44682 (Lee 2003). It was not reported whether this strain produced pairs of spores under the culture conditions used (Lee 2003). The physical properties and molecular weights of the two isolated compounds, MF-BA-1768$_{\alpha1}$ and MF-BA-1768$_{\beta1}$, were determined but structural information was not reported (Lee 2003). The two compounds had potent activity against a wide range of Gram-positive pathogens including MRSA and VRE. Furthermore, the two compounds showed MICs comparable to the clinically-useful antibiotic vancomycin against MRSA (Lee 2003).

In 2005 a second pharmaceutical company, Vicuron Pharmaceuticals, reported the production of two lantibiotic compounds from a new strain of *Microbispora* ATCC PTA-5024 (Lazzarini *et al.* 2005). There are no details of the isolation of this strain but on the basis of 16s rDNA sequence similarity it was determined to be a member of the *M. corallina* species, sharing over 97.5% (the cut-off for strains belonging to the same species) nucleotide sequence identity with DSM 44682 and NRRL 30420 (Lazzarini *et al.* 2005). However, the authors note that NRRL 30420 and ATCC PTA-5024 are certainly different strains of the same species (Lazzarini *et al.* 2005). The two compounds described, 107891 factor A1 and factor A2, had different physical properties and molecular weights from MF-BA-1768$_{\alpha1}$ and MF-BA-1768$_{\beta1}$ (Table 1.2). The structures of the two compounds were reported and were found to be identical except for the addition of either one (A2) or two (A1) hydroxyl groups onto a proline residue in the peptide and are thus likely derived from the same prepropeptide (Lazzarini *et al.* 2005). The complex of the two compounds was renamed microbisporicin to reflect this (Castiglione *et al.* 2008). Microbisporicin was reported to contain three lanthionine and one methyl-lanthione bridges and thus belongs to the lantibiotic class of antibiotics (Lazzarini *et al.* 2005; Castiglione *et al.* 2008). Microbisporicin additionally has an *S*-[(*Z*)-2-aminovinyl]-D-cysteine at the C-terminal end and two novel modifications are found in its structure; a 5-chlorotryptophan at position 4 and a 3,4-dihydroxyproline (A1) or 4-hydroxyproline (A2) at position 14 (Figure 1.15) (Lazzarini *et al.* 2005; Castiglione *et al.* 2008).

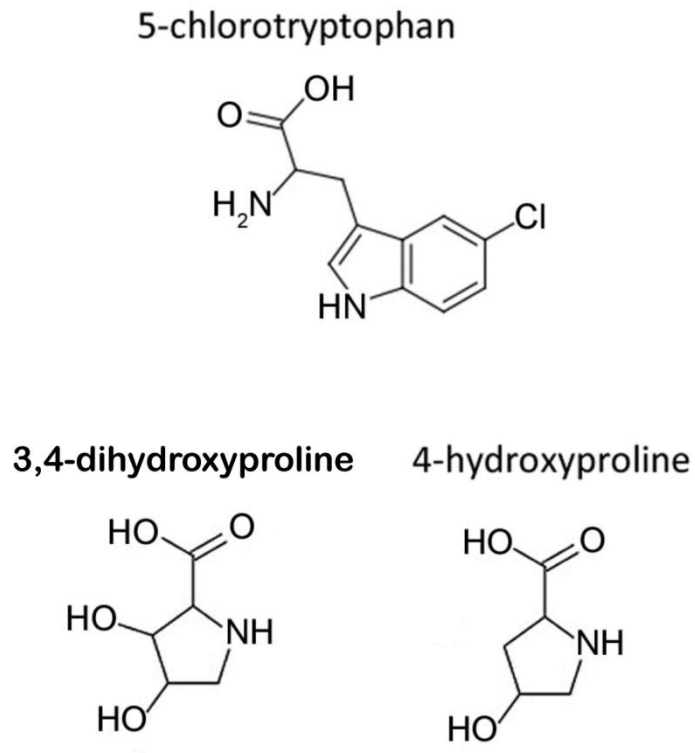

Figure 1.15 The chemical structures of the unusual modifications found in microbisporicin; 5-chlorotryptophan, 3,4-dihydroxyproline (107891 A1) and 4-hydroxyproline (107891 A2).

Table 1.2 A comparison of the four reported lantibiotic compounds produced by *Microbispora corallina*. The molecular weights (Mw) reported for each compound are given (Lee 2003, Lazzarini *et al.* 2005). The minimum inhibitory concentration for each compound (in µg/ml) against the indicated test organism is given as determined and reported by Lazzarini *et al.* 2005.

Compound	Mw	MIC (µg/ml)				
		1400 *Staphylococcus aureus* cl. isol. Met R	568 *Enterrococcus faecium* cl. isol.	*569 Enterrococcus faecium* cl. isol. VanA	559 *Enterrococcus faecalis* cl. isol.	560 *Enterrococcus faecalis* cl. isol. Van A
MF-BA-1768$_{\alpha 1}$	2214.88	0.13	4	4	4	4
MF-BA-1768$_{\beta 1}$	2180.81	0.5	16	8	8	8
107891 A1	2246.71	0.13	1	1	1	0.5
107891 A2	2230.71	0.13	2	2	2	1

1.3.2 Activity of Microbisporicin as an Antibiotic

Microbisporicin showed a similar activity profile to MF-BA-1768$_{\alpha 1}$ and MF-BA-1768$_{\beta 1}$, displaying anti-bacterial activity against a range of bacterial pathogens including both Gram-positive and some Gram-negative species (Table 1.3) (Lazzarini *et al.* 2005; Castiglione *et al.* 2008). Of particular interest is its efficacy with regard to methicillin-resistant and vancomycin-intermediate resistant strains of *Staphylococcus aureus.* The efficacy and toxicity of microbisporicin was also determined by injection into mice infected with clinical isolates of MRSA (Lazzarini *et al.* 2005; Castiglione *et al.* 2008). Microbisporicin was found to selectively inhibit peptidoglycan synthesis in *Staphylococcus aureus* and *Bacillus megaterium* (Castiglione *et al.* 2008).

Comparison of the biological activity of the four identified lantibiotic compounds from *M. corallina* suggested slight differences in the efficacy of each against certain bacterial species but that on the whole they displayed a similar efficacy profile (Table 1.2) (Lazzarini *et al.* 2005). Microbisporicin activity was also compared to that of the known lantibiotics planosporicin, actagardine (from actinomycetes), mersacidin and nisin (Table 1.3) (Castiglione *et al.* 2008). Microbisporcin displayed higher potency against all target bacteria tested except L-form *Staphylococcus aureus* (which do not have a cell wall and are thus largely unaffected by Lipid II interacting lantibiotics) and against *E. coli* and *Candida albicans*, against which lantibiotics are generally ineffective.

Table 1.3 Minimum inhibitory concentrations (in µg/ml) for microbisporicin (107891 complex), planosporicin, actagardine, mersacidin and nisin against a range of target pathogens as indicated. ATCC, American Type Culture Collection; met-r, methicillin-resistant; MRSA, methicillin-resistant *Staphylococcus aureus*; n.d., not determined; VanA, vancomycin-resistant; VISA, vancomycin-intermediate-resistant *Staphylococcus aureus*. Reproduced from Castiglione *et al.* 2008.

MIC (µg/ml)	Microbisporicin	Planosporicin	Actagardine	Mersacidin	Nisin
L100 *Staphylococcus aureus* ATCC6538P	≤0.13	2	32	4	0.5
L3751 *Staphylococcus aureus* L form	>128	>128	>128	64	16
L819 *Staphylococcus aureus* Smith ATCC19636	≤0.13	16	32	4	2
L1400 *Staphylococcus aureus* MRSA	≤0.13	16	16	8	2
L613 *Staphylococcus aureus* MRSA	≤0.13	32	16	64	8
L3798 *Staphylococcus aureus* VISA	2	128	128	128	32
L3797 *Staphylococcus aureus* VISA met-r	2	>128	>128	128	8
L3798 *Staphylococcus epidermidis* ATCC12228	≤0.13	32	128	16	2
L1729 *Staphylococcus haemolyticus* met-r	8	>128	>128	8	4

MIC (µg/ml)	Microbisporicin	Planosporicin	Actagardine	Mersacidin	Nisin
L49 *Streptococcus pyogenes*	≤0.13	0.5	2	n.d.	n.d.
L44 *Streptococcus pneumoniae*	≤0.13	4	32	4	0.25
L559 *Enterococcus faecalis*	1	16	32	32	4
L560 *Enterococcus faecalis* Van A	0.5	64	128	64	4
LA533 *Enterococcus faecalis* Van A	1	128	16	32	4
L568 *Enterococcus faecium*	2	64	64	64	2
L569 *Enterococcus faecium* Van A	1	128	128	64	2
LB518 *Enterococcus faecium* Van A	2	>128	>128	128	1
L884 *Lactobacillus garviae*	≤0.13	4	4	16	n.d.
L148 *Lactobacillus delbrueckii* ATCC04797	4	16	>128	>128	>128
L3607 *Clostridium perfringens* ATCC13124	≤0.125	≤0.25	4	8	≤0.13
L4018 *Clostridium difficile*	≤0.125	1	4	8	≤0.13
L4043 *Clostridium butyricum*	≤0.125	n.d.	n.d.	n.d.	n.d.
Propionibacterium granulosum ATCC25564	0.03	n.d.	n.d.	n.d.	n.d.

MIC (µg/ml)	Microbisporicin	Planosporicin	Actagardine	Mersacidin	Nisin
L1329 *Propionibacterium acnes*	0.5	n.d.	n.d.	n.d.	n.d.
Propionibacterium limphophylum ATCC27250	0.015	n.d.	n.d.	n.d.	n.d.
L970 *Haemophilus influenzae* ATCC19418	32	>128	>128	>128	>128
L76 *Moraxella catarrhalis* ATCC8176	0.25	1	32	2	1
L1613 *Neisseria meningitidis* ATCC13090	0.5	>128	>128	>128	8
L997 *Neisseria gonorrhoeae*	0.25	>128	>128	>128	4
L47 *Escherichia coli*	>128	>128	>128	n.d.	>128
L145 *Candida albicans*	>128	>128	>128	n.d.	>128

The heightened effectiveness of microbisporicin against some Gram-negative species, including *Haemophilus influenzae*, *Neisseria* sp. and *Moraxella catharrhalis*, compared to the other tested lantibiotics suggests that it could have a novel mechanism of action (Table 1.3) (Castiglione *et al.* 2008). These organisms are known opportunistic human pathogens and include the causative agents of meningococcal septicaemia and gonorrhoea. Furthermore, there has been an increased prevalence of antibiotic resistance in these bacteria in recent years (Livermore 2009). A report by the Health Protection Agency in 2008 reported a 28% incidence of ciprofloxacin resistance in cases of *N. gonorhaea* in England and Wales, and warned of likely future treatment difficulties with third-generation cephlosporins (the currently approved oral treatment); "the future emergence of gonococcal strains resistant to all current treatment options is therefore a real possibility, which would have major public health implications"[2].

[2] Health Protection Agency, June 2009, GRASP 2008 Report: Trends in Antimicrobial Resistant Gonorrhoea
http://www.hpa.org.uk/web/HPAweb&HPAwebStandard/HPAweb_C/1245914959952

Microbisporicin, under the commercial name NAI-107, is currently in late preclinical-phase trials[3] and has demonstrated superior efficacy in animal models of multi-drug resistant infections compared to the drugs-of-last resort, linezolid and vancomycin (Jabes *et al.* 2009b). Interestingly, no microbisporicin resistant mutants were observed during these studies (Jabes *et al.* 2009a).

1.3.3 Structure of Microbisporicin

The N-terminal 11 residues of microbisporicin are identical to those of nisin except for valine at position 1 and chlorinated tryptophan at position 4, which are both isoleucine in nisin. These 11 residues form the A and B loops of nisin involved in binding Lipid II (Hsu *et al.* 2004) and are partially conserved in a number of other lantibiotics, including subtilin, epidermin and mutacin-III (Figure 1.16) (Qi *et al.* 1999b; Willey *et al.* 2007). Interestingly, mutacin-III and mutacin 1140 have tryptophan at position 4 (Qi *et al.* 1999b; Smith *et al.* 2000).

In addition to sharing N-terminal homology, epidermin and microbisporicin also have C-terminal similarity (Figure 1.16). Both have amino-vinyl-cysteine modifications and large aromatic amino acids between the residues forming this modification; phenylalanine in microbisporicin and tyrosine in epidermin. Microbisporicin also shares similarity with the recently revised structure of planosporicin from *Planomonospora* sp. (Figure 1.6) (Castiglione *et al.* 2007; Maffioli *et al.* 2009). This is the only known actinomycete-derived lantibiotic to which microbisporicin seems to have any similarity. The evidence suggests that microbisporicin falls within the type AI lantibiotic group.

A moderate similarity is also found with the type B lantibiotic mersacidin. Mersacidin has a highly flexible Ala^{12}Abu^{13} region and flexible glycine rich region which appear to be important for its mechanism of action (Hsu *et al.* 2003). The run of glycine residues that form the B ring of mersacidin are partially conserved in the C ring of microbisporicin, where the hydroxy-proline residue is also found (Figure 1.16).

[3] http://www.naicons.com/

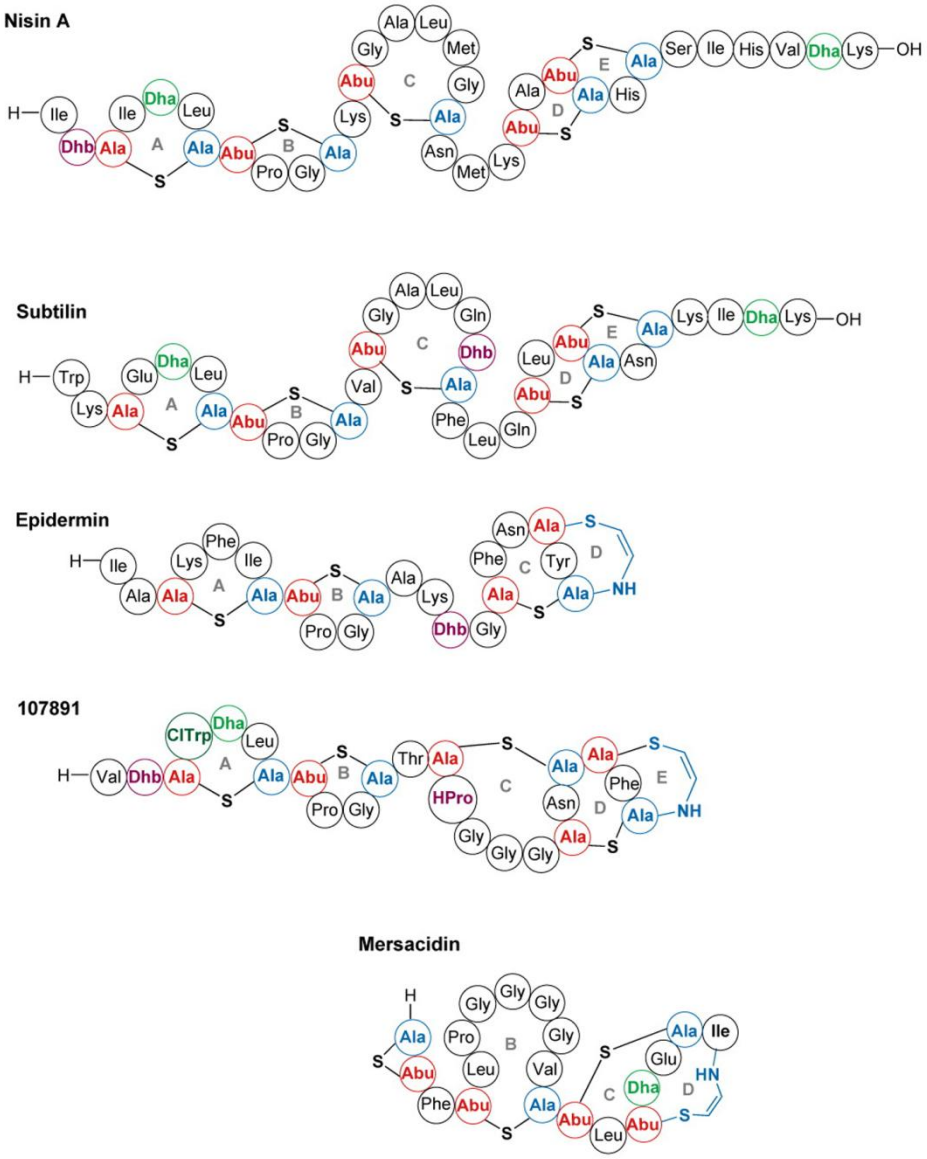

Figure 1.16 A comparison of several known lantibiotic structures with that of microbisporicin (107891) as described in the text. Dha; 2,3-didehydroalanine, Dhb; (Z)-2,3-didehydrobutyrine, Abu; aminobutyrate, ClTrp; 5-chlorotryptophan and HPro; 3,4-dihydroxyproline. Images reproduced from Willey and van der Donk, 2007.

The incorporation of chlorine at the carbon-5 position of the indole ring of tryptophan-4 in microbisporicin is a novel modification among lantibiotics (Figure 1.15). However, the incorporation of halides into biological molecules is common with nearly 4000 so far reported, including the production of organohalides by over 50 *Streptomyces* species (Gribble 2003). The organohalide group occurs in several antibacterial compounds, including vancomycin, where incorporation of chlorine enhances anti-bacterial activity and substrate binding (Harris *et al.* 1985; Ohi *et al.* 1987; Malabarba *et al.* 1989).

The dihydroxyproline modification at position 14 of microbisporicin (Figure 1.15) is similarly unique amongst characterised lantibiotics as well as being rare in other bacterial peptides. Proline hydroxylation of ribosomally synthesised peptides in bacteria is a rare occurrence and has only been described for the formation of bacterial collagen in *Bacillus anthracis* (Culpepper *et al.* 2010). This reaction was catalysed by a prolyl-4-hydroxylase enzyme that is related to those found in vertebrates and for which the structure has been solved (Culpepper *et al.* 2010). A wide variety of naturally occurring hydroxyproline analogs are known, many of which are found in actinomycetes and particularly in small-molecule anti-bacterial and anti-cancer drugs, for example in telomycin (*Streptomyces sp.*) and AO 341B (*S. candidus*) (Mauger 1996). Hydroxyproline is also integral to vertebrate collagen function, in which it stabilises the triple helix structure through extensive interstrand hydrogen bonding (Berg 2002), and is found in several proteins in plant cell walls. Dihydroxyproline specifically however has not, as yet, been found in actinomycetes (Mauger 1996). *2,3-cis*-3,4-*trans*-dihydroxy-L-proline was first identified in the cell walls of diatoms (Nakajima *et al.* 1969) and other diastereomers are found in Mefp1, an adhesive protein of the mussel *Mytilus edulis* and in virotoxins from *Amanita virosa* (Mauger 1996). The exact function of dihydroxyproline in these compounds is yet to be determined.

The masses for the four reported lantibiotic-like compounds produced by *M. corallina* strains are 2180.81 Da (MF-BA-1768$_{\beta1}$), 2214.880 Da (MF-BA-1768$_{\alpha1}$) (Lee 2003), 2230.71 Da (107891 A2) and 2246.71 Da (107891 A1) (Lazzarini *et al.* 2005; Castiglione *et al.* 2008). The known structures of 107891 A1 and A2 (Lazzarini *et al.* 2005; Castiglione *et al.* 2008) and the mass differences between these compounds and MF-BA-1768$_{\alpha1}$ and MF-BA-1768$_{\beta1}$ suggest that they are closely related. This is also suggested by the similar activity profiles of the four compounds. MF-BA-1768$_{\alpha1}$ is 16 Da lighter than 107891 A2, which suggests the loss of one oxygen atom. This could result from the loss of the remaining hydroxyl group on Pro^{14} which would then be replaced by a proton (Figure 1.17). MF-BA-1768$_{\beta1}$ is 34 Da lighter than MF-BA-1768$_{\alpha1}$. This could result from the loss of the chlorine atom on Trp^{4} which would then be replaced by a proton (Figure 1.17).

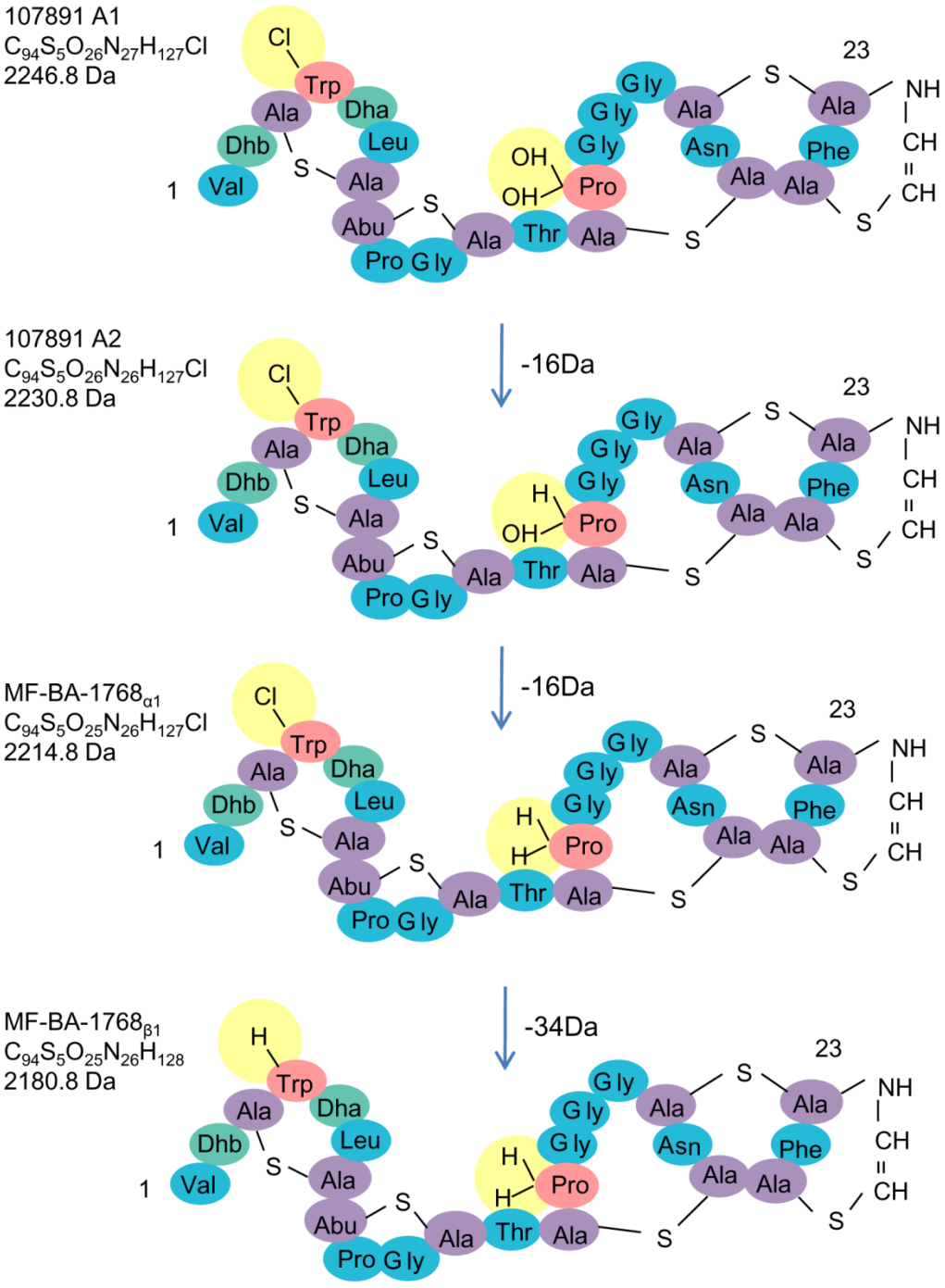

Figure 1.17 A comparison of the known structures of 107891 A1 and A2 (Lazzarini *et al.* 2005; Castiglione *et al.* 2008) and the predicted structures for MF-BA-1768$_{\alpha 1}$ and MF-BA-1768$_{\beta 1}$ (Lee 2003) as described in the text. For each compound the theoretical molecular formulae and mass (in Daltons) is given. The expected mass difference resulting from the loss of each modification is shown.

1.4 Aims

The aim of this work is to characterise the genetic basis for the biosynthesis of microbisporicin by *M. corallina*. The identification and characterisation of the genes responsible for microbisporicin biosynthesis, and the development of methods for the genetic manipulation of the pathway, could allow knowledge-based increases in strain productivity and the generation of variants with potentially improved pharmacological properties. This has already been demonstrated for a number of lantibiotics including nisin, mersacidin and actagardine (Rink *et al.* 2007; Appleyard *et al.* 2009; Boakes *et al.* 2009).

Few examples of actinomycete lantibiotic gene clusters exist. Those that do (cinnamycin and actagardine) belong to type B lantibiotics (Widdick *et al.* 2003; Boakes *et al.* 2009). Microbisporicin is a member of the type AI lantibiotics and thus it will be interesting to determine whether any similarities exist within the microbisporicin gene cluster to the other actinomycete lantibiotics or to the characterised type AI gene clusters from low GC Gram-positive bacteria.

The novel modifications of 5-chlorotryptophan and 3,4-dihydroxyproline are likely to require unusual enzyme activities that are probably encoded within the microbisporicin biosynthetic gene cluster. All the known examples of hydroxyproline and chlorinated tryptophan have been described for small molecule antibiotics (Mauger 1996; Gribble 2003). It will be interesting to see how these enzymatic modifications are applied to the alteration of a ribosomally-synthesised peptide molecule and how site-specificity is mediated. It will also be interesting to investigate the necessity of these modifications for lantibiotic activity.

Finally it is likely that unique mechanisms of regulation and producer immunity will exist in *M. corallina*. Understanding these processes will allow improvements in strain productivity and help to overcome a significant hurdle in the commercial production of microbisporicin, which is the low natural yield from *M. corallina* (Castiglione *et al.* 2008). Elucidation of the function of each of the genes of the microbisporicin gene cluster and the minimal gene set required for the biosynthesis of microbisporicin could be most easily assessed through the use of a heterologous host. *Streptomyces* sp. have been used routinely as heterologous hosts for secondary metabolite gene clusters and for the lantibiotics cinnamycin and actagardine (Widdick *et al.* 2003; Boakes *et al.* 2009). Successful heterologous production in a more amenable/tractable host organism may provide a convenient route for the commercial production of microbisporicin and novel variants.

1.5 Summary of Main Objectives

- To identify the gene cluster encoding the novel lantibiotic microbisporicin produced by *Microbispora corallina* by genome scanning (using sequence information from the rapid sequencing power of Solexa (Illumina) and 454 (Roche)) or via other methods e.g. hybridisation screening, heterologous expression and bioassay, and/or cloning for linked resistance genes.
- To make gene knockouts (including in-frame deletions) within the gene cluster to define the minimal gene set and establish individual gene functions.
- Determine similarities/differences to other lantibiotic gene clusters.
- To characterise the functions of the biosynthetic enzymes involved in novel peptide modifications (i.e. formation of 5-chlorotryptophan, 3,4-dihydroxyproline and S-[(*Z*)-2-amino-vinyl]-D-cysteine).
- To define the mechanisms regulating expression of the gene cluster.
- To define host immunity mechanisms.

Chapter 2 - Materials and Methods

2.1 Bacterial strains and plasmids

Table 2.1 *E. coli* strains used and constructed in this study.

Strain	Genotype	Antibiotic resistance	Reference
DH5α	*recA1 endA1 gyrA96 thi-1 hsdR17 supE44 relA1 lac*	None	(Sambrook *et al.* 2001)
ET12567	*dam13::*Tn*9 dcm6 hsdM hsdR recF143 zjj201::*Tn*10 galK galT22 ara14 lacY1 xyl5 leuB6 thi*l *ton*A31 *rpL*136 *his*G4 *tsx*78 *mtl*i *glnV*44 F^-	Chl, Tet	(MacNeil *et al.* 1992)
BW25113	Δ(*araD-araB*)*567* Δ*lacZ4787*(::*rrnB-4*) *lacIp-4000*(lacI^Q) λ^- *rpoS369*(Am) *rph-1* Δ(*rhaD-rhaB*)568 *hsdR514*	None	(Datsenko *et al.* 2000)
DH5α/BT340	As DH5α with pCP20 (*FLP*+, *λ* ci857+, λ P_R Rep^{ts}, Ap^R, Cm^R)	Chl	(Cherepanov *et al.* 1995; Datsenko *et al.* 2000)
S17-1	*recA*1 *pro thi hsdR* RP4-2-Tc::Mu-Km::Tn7	Thio, Str, Sp	(Simon *et al.* 1983)
BTH101	F^- *cya-99 araD139 galE15 galK16 rpsL1* (Str^r) *hsdR2 mcrA1 mcrB1*	Str	(Ladant *et al.* 1999)
XL1-Blue	*rec*A1, *end*A1, *gyr*A96, *thi*-1, *hsd*R17(r_K-, m_K+), *sup*E44, *rel*A1, *lac*, [F', *proAB*, *lac*I^{q}ZΔM15::Tn10(tet^r)]	Nal	(Sambrook *et al.* 2001)

Table 2.2 *Streptomyces* strains used in this study:

Species	Strain	Genotype	Source/ Reference
Streptomyces coelicolor	M145	SCP1$^-$ SCP2$^-$	(Redenbach *et al.* 1996)
Streptomyces coelicolor	M1146	M145 Δ*act* Δ*red* Δ*cpk* Δ*cda*	(Gomez-Escribano *et al.* 2010)
Streptomyces coelicolor	M1155	M1146 *rpsL* (A262G C271T) selected as exconjugants resistant to 5 ug/ml streptomycin (clone 7)	(Gomez-Escribano *et al.* 2010)
Streptomyces coelicolor	M1156	M1146 *rpsL* (A262G) selected as exconjugants resistant to 5 ug/ml streptomycin (clone 8)	(Gomez-Escribano *et al.* 2010)
Streptomyces lividans	TK24	Str-6 SLP2$^-$ SLP3$^-$	(Kieser *et al.* 2000)
Streptomyces venezualae	ATCC10712		Prof. Mervyn Bibb, The John Innes Centre
Streptomyces fungicidicus			Prof. Greg Challis, Uni. Of Warwick
Streptomyces albus			Prof. Greg Challis, Uni. Of Warwick

Table 2.3 Other Actinomycetes used in this study

Species	Strain	Genotype	Source/ Reference
Microbispora corallina	NRRL 30420		(Lee 2003)/NRRL culture collection
Microbispora corallina	DSM 44681		(Nakajima *et al.* 1999)/DSMZ culture collection
Microbispora corallina	DSM 44682		(Nakajima *et al.* 1999)/DSMZ culture collection
Nonomuraea sp.	ATCC39727		Prof. Flavia Marinelli, University of Insubria, Italy
Micrococcus luteus	ATCC4698		Novacta Biosciences

Table 2.4 *Microbispora corallina* strains constructed in this study

Background Strain	Strain No.	Genotype
NRRL30420	M1126	*attB*::pSET152
NRRL30420	M1127	Δ*mibA::aac(3)*IV
NRRL30420	M1128	Δ*mibD:: aac(3)*IV
NRRL30420	M1129	Δ*mibTU:: aac(3)*IV
NRRL30420	M1130	Δ*mibV:: aac(3)*IV
NRRL30420	M1131	Δ*mibEF:: aac(3)*IV
NRRL30420	M1132	Δ*mibH:: aac(3)*IV
NRRL30420	M1133	Δ*mibN:: aac(3)*IV
NRRL30420	M1134	Δ*downstream:: aac(3)*IV
NRRL30420	M1135	Δ*mibX:: aac(3)*IV
NRRL30420	M1136	Δ*mibZ-mibR:: aac(3)*IV
NRRL30420	M1138	*attB:*pIJ10706
DSM 44682	M1139	*attB*::pSET152

Table 2.5 Plasmids and cosmids used and constructed in this study

Plasmid Name	Description	Selection Markers	Reference/Origin
pSuperCos1	Cosmid library vector – pUC*ori cos*	Carb Kan	Stratagene
pIJ10702	*attP int* (ΦC31) *ori*T pUC*ori* (pMJCOS1)	Carb Apra	Yanai ,*et al.* 2006
pSET152	*attP int* (ΦC31) *ori*T pUC*ori*	Apra	Bierman, *et al.* 1992
pIJ10706	pSET152-Hyg	Hyg	O'Rourke, S, unpublished
pRT802	*attP int* (ΦBT1) *ori*T pUC*ori*	Kan	Gregory, *et al.* 2003
pGEM©-T easy	Commercial TA cloning vector	Carb	Promega
pIJ773	PCR targeting cassette vector: P1-FRT-*aac3*(IV)-oriT-FRT-P2	Apra	Gust, *et al.* 2003
pIJ778	PCR targeting cassette vector: P1-FRT-*aadA*-oriT-FRT-P2	Sp Str	Gust, *et al.* 2003
pIJ12121	SuperCos1 1H11	Carb Kan	This study
pIJ12122	SuperCos1 3E5	Carb Kan	This study
pIJ12123	SuperCos1 3K13	Carb Kan	This study
pIJ12124	SuperCos1 4G2	Carb Kan	This study
pIJ12125	SuperCos1 5A7	Carb Kan	This study
pIJ12126	SuperCos1 7C22	Carb Kan	This study
pIJ12127	pIJ10702 1H11	Carb Apra	This study
pIJ12128	pIJ10702 3E5	Carb Apra	This study

Plasmid Name	Description	Selection Markers	Reference/Origin
pIJ12129	pIJ10702 3K13	Carb Apra	This study
pIJ12130	pIJ10702 4G2	Carb Apra	This study
pIJ12131	pIJ10702 5A7	Carb Apra	This study
pIJ12132	pIJ10702 7C22	Carb Apra	This study
pIJ10705	pGEMT-easy-Tc^R-ermE*-RBS(EF-Tu)	Carb Tet	O'Rourke, S, unpublished
pIJ12363	pIJ12131 Tc^R-*ermE**-RBS(EF-Tu)-*mibA*	Carb Apra Tet	This study
pIJ12364	pIJ12131 Tc^R-*ermE**-RBS(EF-Tu)-*mibE*	Carb Apra Tet	This study
pIJ12365	pIJ12131 Tc^R-ermE*-RBS(EF-Tu)-*mibX*	Carb Apra Tet	This study
pIJ12363::*scar*	pIJ12131 *ermE**-RBS(EF-Tu)-*mibA* ΔTc^R	Carb Apra	This study
pIJ12366	pIJ12131 *ermE**-*mibA* ΔTc^R *ermE**-*mibE*::Tc^R	Carb Apra Tet	This study
pIJ12131 Δ*mibA::aadA*	pIJ12131 Δ*mibA ::aadA* (pIJ778)	Carb Apra Sp Str	This study
pIJ12131 Δ*mibA::scar*	pIJ12131 Δ*mibA::scar*	Carb Apra	This study
pIJ12131 Δ*mibX::aadA*	pIJ12131 Δ*mibX::aadA*	Carb Apra Sp Str	This study
pIJ12131 Δ*mibX::scar*	pIJ12131 Δ*mibX::scar*	Carb Apra	This study
pIJ12131 Δ*mibW::aadA*	pIJ12131 Δ*mibW::aadA*	Carb Apra Sp Str	This study
pIJ12131 Δ*mibW::scar*	pIJ12131 Δ*mibW::scar*	Carb Apra	This study
pIJ12131 Δ*mibXW::aadA*	pIJ12131 Δ*mibXW::aadA*	Carb Apra Sp Str	This study
pIJ12131 Δ*mibXW::scar*	pIJ12131 Δ*mibXW::scar*	Carb Apra	This study

Plasmid Name	Description	Selection Markers	Reference/Origin
pIJ12131 Δ*mibD::aadA*	pIJ12131 Δ*mibD::aadA*	Carb Apra Sp Str	This study
pIJ12131 Δ*mibD*::scar	pIJ12131 Δ*mibD*::scar	Carb Apra	This study
pIJ12131 Δ*mibTU::aadA*	pIJ12131 Δ*mibTU::aadA*	Carb Apra Sp Str	This study
pIJ12131 Δ*mibTU::scar*	pIJ12131 Δ*mibTU::scar*	Carb Apra	This study
pIJ12131 Δ*mibV::aadA*	pIJ12131 Δ*mibV::aadA*	Carb Apra Sp Str	This study
pIJ12131 Δ*mibV::scar*	pIJ12131 Δ*mibV::scar*	Carb Apra	This study
pIJ12131 Δ*mibEF*::*aadA*	pIJ12131 Δ*mibEF*::*aadA*	Carb Apra Sp Str	This study
pIJ12131 Δ*mibEF*::scar	pIJ12131 Δ*mibEF*::scar	Carb Apra	This study
pIJ12131 Δ*mibH*::*aadA*	pIJ12131 Δ*mibH*::*aadA*	Carb Apra Sp Str	This study
pIJ12131 Δ*mibH*::scar	pIJ12131 Δ*mibH*::scar	Carb Apra	This study
pIJ12131 Δ*mibN*::*aadA*	pIJ12131 Δ*mibN*::*aadA*	Carb Apra Sp Str	This study
pIJ12131 Δ*mibN*::scar	pIJ12131 Δ*mibN*::scar	Carb Apra	This study
pIJ12131 Δ*mibZ-mibR*::*aadA*	pIJ12131 Δ*mibZ-mibR*::*aadA*	Carb Apra Sp Str	This study
pIJ12131 Δ*mibZ-mibR::scar*	pIJ12131 Δ*mibZ-mibR::scar*	Carb Apra	This study
pIJ12125 Δ*downstream* 7kb:: scar	pIJ12125 Δ*downstream* 7kb scar	Carb Kan	This study
pIJ12131 Δ*downstream* 7kb::scar	pIJ12131 Δ*downstream* 7kb scar	Carb Apra	This study
pIJ12125 Δ*mibA::aac(3)IV*	pIJ12125 Δ*mibA::aac(3)*IV (pIJ773)	Carb Apra Kan	This study

Plasmid Name	Description	Selection Markers	Reference/Origin
pIJ12125 Δ*mibD*::aac(3)IV	pIJ12125 Δ*mibD::aac(3)*IV (pIJ773)	Carb Apra Kan	This study
pIJ12125 Δ*mibTU::aac(3)IV*	pIJ12125 Δ*mibTU::aac(3)*IV (pIJ773)	Carb Apra Kan	This study
pIJ12125 Δ*mibV::aac(3)IV*	pIJ12125 Δ*mibV::aac(3)*IV (pIJ773)	Carb Apra Kan	This study
pIJ12125 Δ*mibEF::aac(3)IV*	pIJ12125 Δ*mibEF::aac(3)*IV (pIJ773)	Carb Apra Kan	This study
pIJ12125 Δ*mibH::aac(3)IV*	pIJ12125 Δ*mibH::aac(3)*IV (pIJ773)	Carb Apra Kan	This study
pIJ12125 Δ*mibN::aac(3)IV*	pIJ12125 Δ*mibN::aac(3)*IV (pIJ773)	Carb Apra Kan	This study
pIJ12125 Δ*downstream 7kb::aac(3)IV*	pIJ12125 Δ*downstream::aac(3)*IV (pIJ773)	Carb Apra Kan	This study
pIJ12125 Δ*mibZ-mibR::aac(3)IV*	pIJ12125 Δ*mibZ-mibR*::*aac(3)*IV (pIJ773)	Carb Apra Kan	This study
pIJ12125 Δ*mibX::aac(3)IV*	pIJ12125 Δ*mibX*::*aac(3)*IV (pIJ773)	Carb Apra Kan	This study
pIJ12125 Δ*mibW::aac(3)IV*	pIJ12125 Δ*mibW*::*aac(3)*IV (pIJ773)	Carb Apra Kan	This study
pIJ12125 Δds*::scar ΔmibTU::aac(3)IV*	pIJ12125 Δds*::scar ΔmibTU::aac(3)IV* (pIJ773)	Carb Apra Kan	This study
pIJ12125 Δds*::scar ΔmibW::aac(3)IV*	pIJ12125 Δds*::scar ΔmibW::aac(3)IV* (pIJ773)	Carb Apra Kan	This study
pIJ12126 Δ*mibZ-mibR::aac(3)IV*	pIJ12126 Δ*mibZ-mibR*::*aac(3)*IV (pIJ773)	Carb Apra Kan	This study
pIJ12138	pIJ10706-P_{mibA}-*mibA*	Hyg	This study
pIJ12139	pIJ10706-P_{mibA}-*Nde*I-*Xba*I	Hyg	This study
pIJ12140	pIJ10706-P_{mibE}-*Nde*I-*Xba*I	Hyg	This study

Plasmid Name	Description	Selection Markers	Reference/Origin
pIJ12139-*mibD*	pIJ12139-P_{mibA}-*Nde*I-RBS-*mibD-Xba*I	Hyg	This study
pIJ12139-*mibV*	pIJ12139-P_{mibA}-*Nde*I-RBS-*mibV-Xba*I	Hyg	This study
pIJ12140-*mibEF*	pIJ12140-P_{mibE}-*Nde*I-RBS-*mibEF-Xba*I	Hyg	This study
pIJ12140-*mibE*	pIJ12140-P_{mibE}-*Nde*I-RBS-*mibE-Xba*I	Hyg	This study
pIJ12140-*mibF*	pIJ12140-P_{mibE}-*Nde*I-RBS-*mibF-Xba*I	Hyg	This study
pIJ12140-*mibH*	pIJ12140-P_{mibE}-*Nde*I-RBS-*mibH-Xba*I	Hyg	This study
pIJ12140-*mibS*	pIJ12140-P_{mibE}-*Nde*I-RBS-*mibS-Xba*I	Hyg	This study
pIJ12140-*mibHS*	pIJ12140-P_{mibE}-*Nde*I-RBS-*mibHS-Xba*I	Hyg	This study
pIJ5972	pSET152 -TTA free *luxAB* (Reporter plasmid)	Apra	Aigle, *et al.* 2000, M. Paget pers. comm..
pIJ12341	pIJ5972-*EcoR*I-*mibX*-P_{mibA}-*Bam*HI	Apra	This study
pIJ12342	pIJ5972-*EcoR*I-P_{mibA}-*Bam*HI	Apra	This study
pIJ12343	pIJ5972-*EcoR*I-P_{mibX}-*mibX-Bam*HI	Apra	This study
pIJ12344	pIJ5972-*EcoR*I-P_{mibX}-*Bam*HI	Apra	This study
XP458	(pT25) *cyaA*' MCS (*Bam*HI *Kpn*I) *ori* p15A	Chl	Karimova*, et al.* 1998
XP461	pT25-zip (leucine zipper in *Kpn*I site)	Chl	Karimova, *et al.* 1998
pUT18	MCS cyaA' T18	Carb	Euromedex
pUT18-zip	pUT18-zip (leucine zipper from XP461 in *Kpn*I site)	Carb	This study

Plasmid Name	Description	Selection Markers	Reference/Origin
pUT18C	cyaA' T18 MCS	Carb	Euromedex
pUT18C-zip	pUT18C-zip (leucine zipper from XP461 in *Kpn*I site)	Carb	This study
pIJ12367	pUT18-*mibX*	Carb	This study
pIJ12368	pUT18C-*mibX*	Carb	This study
pIJ12369	XP458 (pT25)-*mibW* (full-length)	Chl	This study
pIJ12370	XP458 (pT25)-*mibW* (N-terminus)	Chl	This study
pIJ12371	XP458 (pT25)-*mibW* (C-terminus)	Chl	This study
pIJ12349	pIJ10706-P_{mibX}-*mibX*	Hyg	This study
pIJ12350	pIJ10706-P_{mibX}-*mibXW*	Hyg	This study
pIJ12362	pIJ10706-P_{mibA}-*mibABCD*	Hyg	This study

2.2 Oligonucleotides used in this study

Table 2.6 General Primers

Primer Name	Sequence (5'-3')	Application/Target
LF001F	CTCACCGAGCCGATCACAG	*mibC*_12864_3259 contig
LF001R	GTCGTCGGTCATCGTCCAG	*mibC*_12864_3259 contig
LF002F	CTGGACGATGACCGACGAC	*mibC*_12864_3259 contig
LF002R	CAGCAGCGCGGTGAC	*mibC*_12864_3259 contig
LF003F	GTTACCACGAGGCGTTCC	*mibB*_9864 contig
LF003R	TGTCGTCGAGGAGTTCGAG	*mibB*_9864 contig
LF004F	GCACGACCAGGGAAAGG	*mibD*_9897 contig
LF004R	CCACATCACCGGGTTCATC	*mibD*_9897 contig
LF005F	ATTCTGGTGAGCCTGCTTCC	*mibH*_4619 contig
LF005R	GTCGTGTACGGCTTGAGATGG	*mibH* _4619 contig
LF006F	CGAGTCCGCCGACATCC	*mibH* _ 5675 contig
LF006R	GGTAGGCGAAGGGCAGG	*mibH* _ 5675 contig
LF007F	GGACACGCCGTTCTGG	*mibH* _4619 contig
LF007R	GGTGGTGAACAGGCTGC	*mibH* _4619 contig
LF008F	AGGACGGCTGTCAGGTC	*mibB*_1562 contig
LF008R	GCACGCTTCGCTCTCG	*mibB*_1562 contig
LF009F	CAACCTGGAACGTCTCTGC	*mibB*
LF009R	TCGTACTCGGGGTCGTACTG	*mibB*
LF010F	ACCTGGCATGACCACAGTC	*mibB*
LF011F	CTGACATCCTGGAGACC	*mibA*

Primer Name	Sequence (5'-3')	Application/Target
LF012R	AGCAACTCCGTGGATACCAG	*mibE*
LF013F	GCAATGCCCGCTGACATCC	*mibA*
LF013R	GTGAGGCCAGCTCCACG	*mibA-mibB* intergenic sequence
LF014R	GGTCGTTGAGAGCGTAGGTC	Lipoprotein (5A7 and 4G2)
LF015F	CCTACTGGCTTGGCCTGAG	Cytochrome P450 (5A7)
LF016F	GATCAGCCAGGGATGACGTAG	TetR regulator (4G2)
End_F	ACATTTCCCCGAAAAGTGC	Cosmid End-sequencing
End_R	GCCTCGTGATACGCCTAT	Cosmid End-sequencing
pSET152F	TCGCCATTCAGGCTGC	Flanking pSET152 MCS
pSET152R	CTCATTAGGCACCCCAGG	Flanking pSET152 MCS
LF041F2	TGGGATGAAGCGTGTGTAAGG	pIJ12126 insert end-sequencing
LF041F3	CCTGCTCACACAGAAGGTCG	pIJ12126 insert end-sequencing
LF041F4	ATCAGCGACGACGAGGT	pIJ12126 insert end-sequencing
LF041R	CAGTCGGCGTAGAAGTCCTC	pIJ12126 insert end-sequencing
LF041R2	GCATGAGTGAGAACGACGAG	pIJ12126 insert end-sequencing
LF044F	CGAAGATCCCGTCGATGATGT	Putative ΦC31 attachment site in *M. corallina*
LF044R	CGTTCATCCACATGGACCAGA	Putative ΦC31 attachment site in *M. corallina*
LF045F	GAAGCGGTTTTCGGGAGTAGT	ΦC31 attachment site in pSET152
LF045R	CACAACCCCTTGTGTCATGTC	ΦC31 attachment site in pSET152
LF046F	GCTAACTAGTAGTTCCTTCGTCACC	Flanking pRT802 MCS
LF046R	CCGGCTCGTATGTTGTGTG	Flanking pRT802 MCS
LF081F	TGATGATGGCGAGGATCTTGT	Genes downstream from *mibN* internal
LF081R	TACGTGCGGAGCACTCTT	Genes downstream from *mibN* internal
Dbv5_F	GTGACCCTGACCTTGTCACC	*dbv5*

Primer Name	Sequence (5'-3')	Application/Target
Dbv5_R	CTCACTGCTGGTCGGTATCA	*dbv5*

Table 2.7 Cloning Primers

Primer Name	Sequence (5'-3')	Application/Target
LF035_3	TATTAGGATCCTCAGCAGCAGAAGCTGCAG	*Bam*HI-*mibA*
LF078F	TATTAGGATCCTTCGTACAGCATGCGAAGCG	*Bam*HI-P_{mibA}
LF078R	AAATCTAGACATATGCTCGCTCCTTTCCG	*Xba*I-*Nde*I-P_{mibA}
LF082F	TTTGATATCCGCACGCGTCGTGCCG	*EcoR*V-P_{mibE}
LF082R	AAATCTAGACATATGCGAGGGGGAGTCGGTC	*Xba*I-*Nde*I-P_{mibE}
LF083F	GGATATCATATGAGGAGAGCCAGACCAT	*Nde*I-*mibD*
LF083R2	AATCTAGATCATGCCAAGGCCTCC	*Xba*I-*mibD*
LF084F	ATATAACATATGGGGAGGTGACCGGC	*Nde*I-*mibV*
LF084R	AATCTAGAAACGGGTCACGCATCGG	*Xba*I-*mibV*
LF085F	ATTATACATATGCGGATCCGGAGCGG	*Nde*I-*pspV*
LF085R	AATCTAGAACCGCATCCGGTGCG	*Xba*I-*pspV*
LF086F	GGATATCATATGGAGGTCTGACATGGCC	*Nde*I-*mibF*
LF086R	GGATCTAGACAGGTCATCTCACTGCGG	*Xba*I-*mibF*
LF087F	ATATATCATATGGCGGCCCTGGTAT	*Nde*I-*mibE*
LF087R	GGTCTAGATGTCAGACCTCCTTCCG	*Xba*I-*mibE*
LF088F	ATATATCATATGTAAGGACGATCGGGAACATGG	*Nde*I-*mibH*
LF088R	AATCTAGATCGTCATCTCAGGCCGG	*Xba*I-*mibH*
LF105F	ATATATCATATGTAAGGCCGGCCTGAGATGAC	*Nde*I-*mibS*

Primer Name	Sequence (5'-3')	Application/Target
LF105R	AATCTAGAAGCTGCTCGGCGTTCAC	*Xba*I-*mibS*
LF089F	TGTGGAATTGTGAGCGGATAAC	complementation constructs verification
LF089R	GTTTTCCCAGTCACGACGTT	complementation constructs verification
LF089F2	AATCTTGTCCGAACGAACACC	verification of pIJ12139 constructs
LF089F3	ATGCAGATGAACGACCATGAC	verification of pIJ12140 constructs
LF096F	TTTTGAATTCTCATCTATCACCAGTCCGCCC	*Eco*RI-*mibX*-P_{mibA}
LF096F2	TATAGAATTCCATGAGGACGGCATCCTCG	*Eco*RI-P_{mibA}
LF096R	CCCGGATCCTGCTCGCTCCTTTCCGGT	*Bam*HI-P_{mibA}
LF097F	TTTTGAATTCTGCTCGCTCCTTTCCGGT	*Eco*RI-P_{mibx}-*mibX*
LF097R	TTTTTTGGATCCTCATCTATCACCAGTCCGCCC	*Bam*H*I*I-*mibX*
LF097R2	TTTTTGGATCCGGCATCCTCGGACACCTC	*Bam*H*I*I-P_{mibX}
LF098F	AACTGCTGCACACGTTCGTA	P_{mibXA} internal
LF098R	GGTTCGATGAATGGCAGGAATG	P_{mibXA} internal
LF101F	TTTTTGGATCCCATGAGACGCGTGGCCGAC	*Bam*HI-*mibX* (BACTH)
LF101R	AATATAGGTACCCGTCTATCACCAGTCCGCCCC	*Kpn*I-(no stop)-*mibX* (BACTH)
LF101R2	ATATATGGTACCTCATCTATCACCAGTCCGCCC	*KpnI*-(stop)-*mibX* (BACTH)
LF102F	TTTTTTTGGATCCCGTGATAGATGACGAGGATCAGGACGC	*Bam*HI-*mibW* (BACTH)
LF102R	TTTTTGGTACCTCAGCCGTCCGACCCGG	*Kpn*I-*mibW* (BACTH)
LF103F	TTATATAGGATCCCATGCCGCGGTCGCTCG	*Bam*HI-*mibW-C* (BACTH)
LF103R	AATATAGGTACCTCACCGCGGCATCAGCC	*Kpn*I-*mibW-N* (BACTH)
LF104F	CGCCGGATGTACTGGAAAC	Flanking pUT18C MCS
LF104R	AGCAGACAAGCCCGTCA	Flanking pUT18C MCS

Table 2.8 Mutant Primers

Primer Name	Sequence (5'-3')	Application/Target
LF017F	CCGGAATCTTGTCCGAACGAACACCGGAAAGGAGCGAGCAATTTAAATCGCCGGCTTCCATT	*mibA-ermE**
LF017R	CGGTCTCGGAAGTCCGGGTCTCCAGGATGTCAGCGGGCATATGGGGCCTCCTGTTCTA	*mibA-ermE**
LF018F	GGCGCCCGGCGGGACCGCCGGCCCGACCGACTCCCCCTCGATTTAAATCGCCGGCTTCCATT	*mibE-ermE**
LF018R	AACGCAGTCTGAGCAACTCCGTGGATACCAGGGCCGCCATATGGGGCCTCCTGTTCTA	*mibE-ermE**
LF019F	ACCGGAGCTCTCCGCGGAGGTGTCCGAGGATGCCGTCCTCATTTAAATCGCCGGCTTCCATT	*mibX-ermE**
LF019F	GCGAAGCGCCACCTCCTCGCCGTCGGCCACGCGTCTCATATGGGGCCTCCTGTTCTA	*mibX-ermE**
LF020F	ACGAAAGGGCCTCGTGATAC	Tc^R internal primer
LF021R	GTTCGTACAGCATGCGAAGC	*mibX* internal primer
LF022F	AATCTTGTCCGAACGAACACCGGAAAGGAGCGAGCAATGATTCCGGGGATCCGTCGACC	Δ*mibA*
LF022R	CCGGGCTGGTTACAGCCCCTGTTGTCTGCGGTTATGTCATGTAGGCTGGAGCTGCTTC	Δ*mibA*
LF023F	TCCGTCCTCGTTTCTGTCATTC	Δ*mibA* verification
LF023R2	CTCCCCTTCGCCAAAGC	Δ*mibA* verification
LF031F	GAGCTCTCCGCGGAGGTGTCCGAGGATGCCGTCCTCATGATTCCGGGGATCCGTCGACC	Δ*mibX*
LF037R	GCCGTCAGGGCGTCCTGATCCTCGTCATCTATCACCAGTTGTAGGCTGGAGCTGCTTC	Δ*mibX*
LF032F	GTCCTCGGTCTCGGAAGTC	Δ*mibX* verification
LF032R	GAGCAGCAGCACCACC	Δ*mibX* verification
LF038F	CAAATCCGAAAGGGGGGCGGACTGGTGATAGATGACGAGATTCCGGGGATCCGTCGACC	Δ*mibW*
LF038R	CGCGTAGCAGGCCCCAGAACCCGCCCCCCGCTCCCGTCATGTAGGCTGGAGCTGCTTC	Δ*mibW*
LF039F	CGCGAGGTGCTCGTG	Δ*mibW* verification
LF039R	GGATGGTGACGTGGTTTCG	Δ*mibW* verification
LF049F	TGTGTTGACGCCCCGACCCATCAGGAGAGCCAGACCATGATTCCGGGGATCCGTCGACC	Δ*mibD*

Primer Name	Sequence (5'-3')	Application/Target
LF049R	TGAGCTCGAACGCCGGGACCGTCATGCCAAGGCCTCCGCTGTAGGCTGGAGCTGCTTC	Δ*mibD*
LF050F	CGTGGAGGCCGTGGAGGCCGCGGAGGCCTTGGCATGACGATTCCGGGGATCCGTCGACC	Δ*mibTU* (*mibT*)
LF051R	CCGGTCGTCGTCGCGGTGGTCACCGGCCGGTCACCTCCCTGTAGGCTGGAGCTGCTTC	Δ*mibTU* (*mibU*)
LF052F	CGGCGCTGCGACTGCGGGTGGGGAGGTGACCGGCCGGTGATTCCGGGGATCCGTCGACC	Δ*mibV*
LF052R	GGCACGACGCGTGCGAGGGCCCCGGTCAGCAACGGGTCATGTAGGCTGGAGCTGCTTC	Δ*mibV*
LF053F	CCCGGCGGGACCGCCGGCCCGACCGACTCCCCCTCGATGATTCCGGGGATCCGTCGACC	Δ*mibEF (mibE)*
LF054R	CCATGTTCCCGATCGTCCTTCCGTTCGTGGTTCAGGTCATGTAGGCTGGAGCTGCTTC	Δ*mibEF (mibF)*
LF055F	ATGACCTGAACCACGAACGGAAGGACGATCGGGAACATGATTCCGGGGATCCGTCGACC	Δ*mibH*
LF055R	GTTCGACGGCATGGGCGACCGTGGTGCCGGTCGTCATCTTGTAGGCTGGAGCTGCTTC	Δ*mibH*
LF057F	GTGAACGCCGAGCAGCTCACCGGTGTGGTCATCGCCGATATTCCGGGGATCCGTCGACC	Δ*mibN*
LF057R	TCGACGGCGGGACCGCCTGACGACCGCGCGCTCCTGTCATGTAGGCTGGAGCTGCTTC	Δ*mibN*
LF058F	CCAGCGACACCGGGAGGGACATCGGGCACACCGCGGGTGATTCCGGGGATCCGTCGACC	Δ*mibR*
LF058R	ATGTCACACCGGCCGCGTCATCGAACCGCGTAGCCCTCATGTAGGCTGGAGCTGCTTC	Δ*mibR*
LF061F	GGCCGTGGCTCGGATCTGGACGGAGCGTTACCGGTGAACATTCCGGGGATCCGTCGACC	Δ*mibZ*
LF065F	AGTCGCGCAGGGCGTCCCGGTCGAGGGCGCCCAGGTTCTATTCCGGGGATCCGTCGACC	Δ7kb region downsteam from *mibN*
LF065R	CCGGCAGGGCCGCGCACAGCGTGACGACGCCGGCCGCGGTGTAGGCTGGAGCTGCTTC	Δ7kb region downsteam from *mibN*
LF068F	CCCGACCCATCAGGAGAG	*ΔmibD* verification
LF068R	ACCGTCAGGTCGCTGAG	Δ*mibD* verification
LF069F	CGATCGTCGAGGGTCTGG	Δ*mibTU* verification
LF070R	CGGCAGATGATGAGGAGTTC	Δ*mibTU* verification
LF071F	GCTCAATCCGATGATGTACGC	Δ*mibV* verification
LF071R	CTCGCCTTCCAGCTTCTC	Δ*mibV* verification
LF072F	GATGCAGATGAACGACCATGAC	Δ*mibEF* verification

Primer Name	Sequence (5'-3')	Application/Target
LF073R	GCCAGGGTGTTGCTCTC	Δ*mibEF* verification
LF074F	GACCTCGAACAGGGCTTTTTC	Δ*mibH* verification
LF074R	GTGACACTGCAGACCGAAC	Δ*mibH* verification
LF075F	GTGGTCTTCGGCCAAGTG	Δ*mibN* verification
LF075R	GGTGTAGGCAAGACGACGA	Δ*mibN* verification
LF076F	CGATACCCACGGTGTCCTAC	Δ*mibZ-R* verification
LF076R	GAAACCACGTCACCATCCATG	Δ*mibZ-R* verification
LF077F	GAGCTGATCGTGCTCAATGTG	Δ*ds* verification
LF077R	GTCCCACTTCATCTCGTTGC	Δ*ds* verification

Table 2.9 RT-PCR primers

Primer Name	Sequence (5'-3')	Application/Target
LF024F	TCCTCGTGGAGTTGGAGAAG	*mibX*
LF024R	CCAAGTATTACGGCCACCTG	*mibX*
LF025F	CGCTGACATCCTGGAGAC	*mibA*
LF025R	GCACAGCGACCAGCTC	*mibA*
LF026F	GAGCACGACCAGGGAAAG	*mibD*
LF026R	GAACGTGATCGGGCAGTC	*mibD*
LF027F	ATCCACGGAGTTGCTCAGAC	*mibE*
LF027R	GCTGAAGGTCTCCCAGAGG	*mibE*
LF028F	ACCATCTCGGCTACGTGTT	*mibH*
LF028R	GAAGCAGGCTCACCAGAATC	*mibH*

Primer Name	Sequence (5'-3')	Application/Target
LF029F	GGAACGCTTCGGGCTG	*mibT*
LF029R	GAGGTCGTCCCATACGGTC	*mibT*
LF030F	GCTCGTCGTGGCCCAC	*mibU*
LF030R	CGCCGAACTCGCGGTC	*mibU*
LF042F	GTCGTGCAGTTGTTCAGCTC	*mibW*
LF042R	GAGAGCGCGAGGTCGATT	*mibW*
LF043F	GTTGTCGAACGCTCTGGTG	*mibO*
LF043R	CGCCCAATATCTCAGGACCTC	*mibO*
LF080F	GGTGCCCTGGATGCTGG	*mibN*
LF080R	GCCGAACACCGGATGCAG	*mibN*
LF106F	ACTTCTGGACCTCGATGACCTTC	*hrdB* (NRRL30420)
LF106R	GGTCGAGGTGATCAACAAGCTG	*hrdB* (NRRL30420)
LF107F	TCGCCCAGCGGGTCATCGAC	*mibV*
LF107R	AGAGCCGTACGACCGGCCAG	*mibV*
LF108F	CCGACGTTGTACGGGATACTC	*orf1*
LF108R	CAGTTGTCCCGGTAGGTCAG	*orf1*
LF109F	CGATACCCACGGTGTCCTAC	*mibY*
LF109R	CCAGCACGACGAGTATGTTCA	*mibY*
LF110F	GAGCAGCAAGCAGGACATC	*mibQ*
LF110R	GGTCGTTGAGAGCGTAGGTC	*mibQ*
LF111F	ACGCGATCTGTACCGAAGTTACG	*mibR*
LF111R	GAGAAGGTGGGTCGACAGC	*mibR*

2.3 Culture media and antibiotics

2.3.1 Antibiotics

Table 2.10 Concentration of antibiotics used in this study

Antibiotic	Concentration in media (µg/ml)
Carbenicillin (Carb)	100
Kanamycin (Kan)	50
Chloramphenicol (Chl)	25
Apramycin (Apra)	50
Hygromycin (Hyg)	40
Nalidixic acid (Nal)	20
Spectinomycin (Sp)	50 (*E. coli*) 200 (*Streptomyces* sp.)
Streptomycin (Str)	50 (*E. coli*) 10 (*Streptomyces* sp.)
Tetracycline (Tet)	10

2.3.2 Solid Media

Unless stated otherwise, the media used for the culturing of *Streptomyces coelicolor* and *E. coli* were prepared as previously described (Kieser *et al.* 2000; Sambrook *et al.* 2001).

Table 2.11 Solid media used in this study

Medium	Composition		Instructions for preparation
L-Agar	Agar	10 g	The ingredients, except agar, were dissolved, in the distilled water and 200 ml aliquots were dispensed into 250 ml Erlenmeyer flasks containing 2 *g* agar. The flasks were closed and autoclaved.
	Difco Bacto tryptone	10 g	
	NaCl	5 g	
	Glucose	1 g	
	Distilled water	Up to 1000 ml	

Medium	Composition		Instructions for preparation
LB-Agar	Agar Difco Bacto tryptone Yeast extract NaCl Distilled Water	15g 10g 5g 10g Up to 1000 ml	The ingredients, except agar, were dissolved, in the distilled water and pH altered to 7.5 with NaOH 200 ml aliquots were dispensed into 250 ml Erlenmeyer flasks containing 2 *g* agar. The flasks were closed and autoclaved.
Difco nutrient agar (DNA)	Difco Nutrient Agar Distilled water	4.6 g 200 ml	Difco Nutrient Agar was placed in each 250 ml Erlenmeyer flask and distilled water was added. The flasks were closed and autoclaved.
Soft Nutrient Agar (SNA)	Difco Nutrient Broth Powder Difco Bacto Agar Distilled water	8 g 5g Up to 1000 ml	The ingredients, except agar, were dissolved, in the distilled water and 200 ml aliquots were dispensed into 250 ml Erlenmeyer flasks containing 2 *g* agar. The flasks were closed and autoclaved.
MacConkey/Maltose Medium	MacConkey Agar (Difco) Distilled water	40g Up to 1000 ml	MacConkey Agar was placed in each 250 ml Erlenmeyer flask and distilled water was added. The flasks were closed and autoclaved. After autoclaving maltose solution (20% in water) was added to 1% w/v.

Medium	Composition		Instructions for preparation
Mannitol soya flour medium (SFM or MS)	Agar Mannitol Soya Flour Tap water	20 g 20 g 20 g Up to 1000 ml	The mannitol was dissolved in the water and 200 ml aliquots poured into 250 ml Erlenmeyer flasks each containing 2 *g* agar and 2 *g* soya flour. The flasks were closed and autoclaved twice (115 °C/15min), with gentle shaking between the two runs.
Minimal medium for *Streptomyces* (MM)	L-asparagine K_2HPO_4 $MgSO_4.7H_2O$ $FeSO_4.7H_2O$ Lab M Agar De-ionised water 10 % Mannitol	0.5 g 0.5 g 0.2 g 0.01 g 10 g Up to 1000 ml 20 ml	The ingredients except agar were dissolved and the pH adjusted to 7.0 -7.2. 200 ml aliquots were dispensed into 250 ml Erlenmeyer flasks containing 2 *g* Lab M agar. The flasks were closed and autoclaved. Before use the medium was re-melted and 20 ml 10 % mannitol (or another carbon source) added.
Oatbran Medium (OBM)	Porridge Oats Lab M Agar Tap Water	40g 20g To 1000ml	The ingredients were mixed and dispensed into 250 ml Erlenmeyer flasks. The flasks were closed and autoclaved twice (115 °C/15min), with gentle shaking between the two runs.

Medium	Composition		Instructions for preparation
V0.1 (Marcone *et al.* 2010b)	Agar (SIGMA) Soluble starch (DIFCO) Dextrose Meat extract Yeast extract Triptose dH_2O	15 2.4 0.1 0.3 0.5 0.5 To 1000ml	The ingredients were dissolved, in the distilled water and the pH adjusted to pH7.2. 200 ml aliquots were dispensed into 250 ml Erlenmeyer flasks. The flasks were closed and autoclaved.
M3 (Marcone *et al.* 2010b)	The base for M3 is identical to V0.1. After autoclaving the following is added to molten V0.1 80g/L sucrose, 3.5g/L proline, 50mM $CaCl_2$ and 10mM $MgCl_2$. The molten medium is filter sterilized using a Vacuum Filter/Storage Bottle System, 0.22µm Pore 19.6cm² PES Membrane (Corning).		
VM0.1 (Marcone *et al.* 2010b)	Low Melting Point Agar (SIGMA) Soluble starch (DIFCO) Dextrose Meat extract Yeast extract Triptose dH_2O	4 2.4 0.1 0.3 0.5 0.5 To 1000ml	The ingredients were dissolved, in the distilled water and the pH adjusted to pH7.2. 200 ml aliquots were dispensed into 250 ml Erlenmeyer flasks. The flasks were closed and autoclaved.
VMS0.1 (Marcone *et al.* 2010b)	The base for VMS0.1 is identical to VM0.1. After autoclaving the following is added to molten V0.1 103g/L sucrose and 3.5g/L proline. The molten medium is filter sterilized using a Vacuum Filter/Storage Bottle System, 0.22µm Pore 19.6cm² PES Membrane (Corning).		

2.3.3 Liquid Media

Unless stated otherwise, the media used for the culturing of *Streptomyces coelicolor* and *E. coli* were prepared as previously described (Kieser *et al.* 2000; Sambrook *et al.* 2001).

Table 2.12 Liquid media used in this study

Medium	Composition		Instructions for preparation
L (Lennox)-Broth	Difco Bacto tryptone Difco yeast extract NaCl Glucose Distilled water	10 g 5 g 5 g 1 g Up to 1000 ml	The ingredients were dissolved, in the distilled water and aliquots were dispensed into universals or 250ml flasks and autoclaved.
LB (Luria-Bertani)-broth	Difco Bacto tryptone Difco yeast extract NaCl Distilled water	10g 5g 10g Up to 1000 ml	The ingredients were dissolved, in the distilled water and pH adjusted to 7. Aliquots were dispensed into universals or 250ml flasks and autoclaved.
SOB (minus Mg)	Tryptone Yeast extract NaCl Distilled water	20 g 5 g 0.5 g Up to 950 ml	After dissolving the solutes in water, 10 ml 250 mM KCl was added and the pH was adjusted to pH 7 with 5 N NaOH. The volume was then made up to 1000 ml with deionised water and autoclaved.
SOC			SOC medium is identical to SOB medium except that after autoclaving, 20 ml of sterile 1 M solution of glucose and 5 ml of sterile 2 M $MgCl_2$ were added.
2 X YT medium	Difco Bacto tryptone Difco yeast extract NaCl Distilled water	16 g 10 g 5 g Up to 1000 ml	The ingredients were dissolved, in the distilled water and 10 ml aliquots were dispensed into universals and autoclaved.
V (Marcone *et al.* 2010b)	Soluble starch (DIFCO) Dextrose Meat extract Yeast extract Triptose dH_2O	24 1 3 5 5 To 1000ml	The ingredients were dissolved in the distilled water and the pH adjusted to pH7.2. 200 ml aliquots were dispensed into 250 ml Erlenmeyer flasks. The flasks were closed and autoclaved.
VSP (Marcone *et al.* 2010b)			VSP is identical to V except for the addition of sucrose to a final concentration of 50g/L and of L-proline to 0.5g/L after autoclaving.

Medium	Composition		Instructions for preparation
VSPA	Agar Soluble starch (DIFCO) Dextrose Meat extract Yeast extract Triptose dH_2O	1 24 1 3 5 5 To 1000ml	The ingredients were dissolved in the distilled water and the pH adjusted to pH7.2. 200 ml aliquots were dispensed into 250 ml Erlenmeyer flasks. The flasks were closed and autoclaved. After autoclaving sucrose was added to a final concentration of 50g/L and L-proline to 0.5g/L
VM (Marcone *et al.* 2010b)			VM is identical to V except for the addition of sucrose to a final concentration of 103g/L and of L-proline to 3.5g/L after autoclaving.
Streptosporangium Medium (SM)	Soluble starch (DIFCO) Glycerol Tryptone Bacteriological Peptone Yeast extract NaCl $CaCO_3$ Tap Water	10 10 2.5 5 2 1 3 To 1000ml	The ingredients were dissolved in the distilled water and the pH adjusted to pH7.3. 200 ml aliquots were dispensed into 250 ml Erlenmeyer flasks. The flasks were closed and autoclaved.

2.4 Solutions and buffers

Table 2.13 Solutions and buffers used in this study

Solution/buffer	Compostion and instructions for preparation	
Cosmid isolation solution I	Glucose Tris-HCl (pH 8) EDTA	50 mM 25 mM 10 mM
Cosmid isolation solution II	NaOH SDS	0.2 M 1 %
Cosmid isolation solution III	Sodium acetate (pH 5.5) Acetic acid	3 M

Solution/buffer	Compostion and instructions for preparation	
Cosmid Library Probing Hybridisation Buffer	SSC	6x
	Denhardt's Solution	1x
	SDS	0.5%
	Denatured calf thymus DNA	50µg/ml
Cosmid Library Probing Wash Buffer	SSC	0.1x
	SDS	1%
DNA loading buffer	Bromophenol blue	0.125 % (w/v)
	Xylene- cyanol blue	0.125 % (w/v)
	Glycerol	62.5 % (v/v)
	SDS	0.625 % (w/v)
Elution Buffer	Tris-Cl	10 mM
		pH 8.5
Lysis Buffer for β-galactosidase assay	Z-Buffer	100ml
	β-mercaptoethanol	270µl
	10% SDS	50µl
P (protoplast) Buffer	Sucrose	128.75g/L
	K2S04	0.313g/L
	MgCl2.6H20	2.53 g/L
	Trace Element Solution	0.25% (v/v)
	KH2PO4	0.005%
	CaCl2.2H2O	0.368%
	TES buffer (pH7.2)	0.573%
SET buffer	NaCl	75mM
	Tris-HCl (pH 8)	20 mM
	EDTA (pH 8)	25 mM
Southern blotting denaturation solution	NaOH	500 mM
	NaCl	1.5 M

Solution/buffer	Compostion and instructions for preparation	
Southern blotting neutralisation solution	NaCl	3 M
	Tris-HCl (pH 7.5)	500 mM
Southern blotting blocking reagent stock solution	Blocking reagent was dissolved in maleic acid buffer to a final concentration of 10% (w/v) with shaking and heating.	
Southern blotting maleic acid buffer	Maleic acid	0.1 M
	NaCl	0.15 M
	Adjust to pH 7.5 with concentrated NaOH	
Southern blotting detection buffer	Tris-HCl (pH 9.5)	100 mM
	NaCl	100 mM
Southern hybridisation buffer	SSC	5 x
	N-lauroylsarcosine	0.1 %
	SDS	0.2 %
	Blocking reagent	1 %
20xSSC	Sodium Citrate	300mM
	NaCl	3M
TBE buffer	Tris base	89mM
	Boric Acid	89mM
	EDTA (pH8.0)	2mM
TAE buffer	Tris	40 mM
	Acetic acid	1.142 %
	EDTA	1 mM
TES Buffer	Tris-HCl (pH 8)	10 mM
	EDTA	1 mM
	NaCl	1 M

Solution/buffer	Compostion and instructions for preparation	
Trace Elements for P Buffer	$ZnCl_2$	40 mg/L
	$FeCl_3.6H_2O$	200 mg/L
	$CuCl_2.2H_2O$	10 mg/L
	$MnCl_2.4H_2O$	10 mg/L
	$Na_2B_4O_7.10H_2O$	10 mg/L
	$(NH_4)_6Mo_7O_{24}.4H_2O$.	10 mg/L
Z-Buffer	Na_2HPO_4	0.06M
	NaH_2PO_4-$2H_20$	0.04M
	KCl	0.01M
	$MgSO_4$-$7H_20$	0.001M

2.5 General Molecular Biology Methods

2.5.1 Plasmid Isolation

Qiagen miniprep kits were used according to the manufacturer's instructions. Briefly, 5 ml of an overnight LB culture harbouring the plasmid of interest were centrifuged at 3000 x *g* for 10 min. The cell pellet was then resuspended and underwent alkaline lysis. The lysate was then neutralised and centrifuged in a microcentrifuge at 16000 x *g* to remove cell debris and precipitated protein. The supernatant was then applied to a silica membrane mounted in a microcentrifuge tube where it was washed under high salt and ethanolic buffer conditions during which time the DNA remains bound to the column. DNA was eluted from the column in ultrapure water or elution buffer. Plasmid DNA was routinely stored at -20°C.

2.5.2 Cosmid Isolation

Cosmid isolation from *E. coli* was carried out by alkaline lysis as described by Sambrook *et al.* (2001). The cell pellet from 1.5 ml of culture was resuspended by vortexing in 100 µl solution I. 200 µl solution II were added and the tubes inverted ten times. A volume of 150 µl solution III was then added and mixed in by inverting the tube five times. The tube was then centrifuged at 16000 x *g* in a microcentrifuge for 5 min at room temperature. The supernatant was mixed with 400 µl phenol/chloroform, vortexed briefly to mix and then centrifuged at 16000 x *g* in a micro centrifuge for 5 min. The upper phase was then transferred to a 1.5 ml tube, 600 µl of ice cold isopropanol were added and DNA precipitation was achieved by placing the tube on ice for 10 min followed by centrifuging at 16000 x *g* in a micro centrifuge for 5 min. The pellet was washed with 1 ml 70% ethanol and centrifuged at 1600 0 x *g* in a microcentrifuge. The pellet was dried by leaving the tube open for 5 min at room temperature prior to resuspension in 30 µl elution buffer.

2.5.3 Agarose gel electrophoresis

1% agarose gels were prepared with TBE buffer with 0.5 µg/ml ethidium bromide. Agarose gel electrophoresis was carried out in 1% TBE buffer at 100 V until completion. Hyperladder I (Bioline), 1 kb ladder (NEB) or 100 bp ladder (NEB) were used to provide size markers as indicated in figure legends.

2.5.4 Pulsed-Field Gel Electrophoresis

Pulsed-field gel electrophoresis (PFGE) was carried out using CHEF DR II pulse field gel apparatus with cooling module (Bio-Rad) to maintain the buffer at a constant temperature.

The apparatus was used as per manufacturer's instructions. 0.5% TBE buffer was circulated through the electrophoresis tank (at 0.75 L/min) and pre-cooled to 14 °C. A 1% TBE gel was cast in the standard casting frame supplied (14 x 13 cm). Approximately 1-2 mm of MidRange PFG Marker I embedded in 1% agarose (NEB) was introduced into the first well of the cast gel and the well sealed with molten agarose. The gel was immersed in the buffer in the electrophoresis tank and the samples loaded into the appropriate wells (in a volume of 20 µl in 1x loading dye). Electrophoresis was carried out for 14 h at 14°C, 6 V/cm with an initial switch time of 1 s and a final switch time of 25 s.

2.5.5 DNA extraction from an agarose gel

DNA fragments separated in agarose gels were excised from the gel using a clean scalpel and purified using the Qiaquick™ gel extraction kit (Qiagen), following the manufacturer's instructions. Briefly, the agarose gel slice containing the DNA fragment of interest was dissolved in a neutral pH, high salt buffer provided with the kit and applied to a silica gel membrane mounted in a microcentrifuge tube. The column was washed and the DNA fragment was eluted in elution buffer.

2.5.6 DNA digestion with restriction enzymes

Restriction enzyme digestion of cosmids, plasmids or genomic DNA was carried out according to the enzyme manufacturer's instructions. In the case of double digests, an appropriate buffer was selected after consulting the manufacturer's literature (Roche or NEB). The reaction volume was usually 20 µl for analytical digests and 50-100 µl for preparative digests. Digests were typically carried out for 1 h at 37°C.

2.5.7 Ligation

Ligation of DNA fragments was carried out using LigaFast T4 DNA ligase and buffer (Promega) following manufacturer's instructions. Typically 50-100 ng of restriction-digested, gel-purified vector were used in a 1:3 molar ratio with the restriction-digested, gel-purifed insert fragment. For blunt-end ligations, vector ends were typically treated with Fast Alkaline Phosphatase (Fermentas) at 37°C for 20 min. Ligations were typically carried out at room temperature for 15 min for cohesive ends and 1 h for blunt ends. Typically, chemically competent *E. coli* DH5α were transformed with 3 µl of a ligation reaction.

2.5.8 Preparation and transformation of electro-competent *E. coli*

The desired *E. coli* strain was grown overnight at 37 or 30°C in 5 ml L broth (Luria-Bertani medium; Sambrook *et al*., 1998) containing the appropriate antibiotic for selection. 1% of this overnight culture was used to inoculate an appropriate growth medium (typically L broth or SOB) and grown at 37 or 30°C with shaking at 250 rpm to an OD_{600} of ~ 0.4. The cells were recovered by centrifugation at 3000 x *g* for 5 min at 4°C in a Sorvall GS3 rotor. The medium was decanted and the pellet resuspended by gentle mixing in 10 ml ice-cold 10 % glycerol. Centrifugation was repeated as above and the pellet resuspended in 5 ml ice-cold 10 % glycerol. Centrifugation was repeated as above and the pellet resuspended in ~ 100 µl ice-cold 10 % glycerol. 50 µl of this cell suspension were typically mixed with ~ 100 ng of cosmid DNA. Electroporation was carried out in a 0.2 cm ice-cold electroporation cuvette using a BioRad GenePulser II set to: 200 Ω, 25 µF and 2.5 kV. The time constant was typically 4.5 – 4.9 ms. 1 ml ice cold SOC medium was immediately added to the shocked cells. The cells were incubated with shaking at 250 rpm for 1 h at 37 or 30°C. Typically 100 µl and 900 µl of the transformation were spread onto L agar containing the appropriate selection (or DNA agar in the case of hygromycin selection). Plates were incubated overnight at 37 or 30°C.

2.5.9 Transformation of chemically-competent *E. coli*

Chemically-competent *E. coli* DH5α (Invitrogen) were transformed with DNA according to manufacturer's instructions. Briefly, cells were thawed on ice for 15 min. A 50 µl aliquot of cells was used for each transformation. Cells were mixed gently with a maximum of 100 ng DNA. Cells were incubated on ice for 30 min before heat shocking at 42°C for 20-40 s before resting on ice for 2 min.

2.5.10 Southern blot hybridization

4 µg of genomic DNA were digested with the appropriate restriction enzyme in a volume of 50 µl at 37°C overnight. Digestion was confirmed by separating 400 ng of the digested DNA fragments on a 1% TBE agarose gel by electrophoresis. The remaining digested DNA was loaded into one lane of a 1% TAE agarose gel (20 cm by 20 cm). Gel electrophoresis was carried out in 1% TAE buffer at 30 V for 16-18 h. The inclusion of 5 ng of 1 kb DNA ladder (Invitrogen) was used to determine the size of the bands on the developed Southern blot. The gel was stained with ethidium bromide both prior to Southern blotting and after capillary transfer to confirm good separation of DNA fragments and efficient transfer to the membrane. The gel was rinsed in distilled water and soaked twice, with shaking, for 15 min in denaturation buffer at room temperature. The gel was

washed in distilled water and soaked twice, with shaking, for 15 min in neutralisation buffer at room temperature. DNA was transferred to a nylon membrane (Amersham Pharmacia Hybond™-N) using capillary transfer. 20 x SSC was poured into a plastic tray and a glass plate was placed across it. A sheet of Whatman 3MM paper was soaked in 20 x SSC and placed on the plate so that the ends of the paper were in contact with the buffer in the tray. The treated and neutralised agarose gel was placed on the paper pad. A piece of nylon membrane cut to the size of the gel was placed on top of the gel, followed by three pieces of Whatman 3MM paper of the same size, stacks of paper towels, a glass plate and finally a weight. The DNA was allowed to transfer overnight at room temperature by capillary action. After transfer, the filter was removed and the transferred DNA was permanently fixed to the membrane by UV crosslinking in a Stratagene UV Stratalinker™ 2400. The membranes were used immediately for detection with DIG labelled DNA probes as outlines below.

For generation of the DIG labelled DNA probes DNA was labelled with Digoxigenin-11-dUTP using the random primed DNA labelling method. 2.5 µg of cosmid DNA were partially digested with *Sau3*AI (Roche) for 15 min at 37°C. The partially digested cosmid was purified using a Qiagen PCR purification kit according to the manufacturer's instructions and was eluted from the column in 12 µl of elution buffer. 1 µg of cosmid DNA template (or 1 kb ladder (Invitrogen) for the ladder probe) was used in a labelling reaction. 1 µg DNA template was diluted in H_2O for a total volume of 16 µl. The DNA template was heat-denatured in a boiling water bath for 10 min, and quickly chilled on ice. 2 µl of Hexanucleotide mixture (10x) and 2 µl dNTP labelling mixture (10x) were added to the tube (on ice). 1 µl Klenow enzyme was added for a final concentration of 100 U/ml and mixed. The reaction mixture was incubated at 37°C for 16 hours. The probe was purified using a Qiagen PCR purification kit according to the manufacturer's instructions to remove unincorporated label and enzyme. The probe was eluted from the column in 30 µl of water.

For hybridisation of the DNA probes with membrane-bound DNA the membrane was placed in a hybridisation tube containing 20 ml prehybridization solution per 100 cm^2 of membrane surface area. Prehybridization was carried out at 67°C for at least 2 h. The DIG-labelled probe DNA was denatured by heating in a boiling water bath for 10 min and chilling directly on ice. After discarding the prehybridization solution, the hybridisation solution containing the DIG-labelled cosmid and ladder probes (25 ng/ml and 10 ng/ml respectively) was added. Hybridisation was carried out overnight at 67°C. The hybridisation solution was discarded and the membrane was washed twice, 15 min per

wash, in 50 ml of (preheated) 0.5 x SSC, 0.1% SDS at 67^{o}C. This was followed by three washes, 20 min per wash with 50 ml of (preheated) 0.1 x SSC, 0.1% SDS at 67°C.

For detection of the membrane-bound DIG-labelled probe, the membrane was transferred to a freshly washed dish and equilibrated in washing buffer for 1 min (at room temperature). The membrane was blocked by gently agitating in 30 ml of blocking solution for 60 min at room temperature. The blocking solution was discarded and replaced with 30 ml of blocking solution containing the anti-digoxigenin antibody-conjugate diluted 1:10,000. The membrane was incubated for 30 min at room temperature with gentle agitation. The antibody solution was discarded and the membrane was washed twice, 15 min per wash in washing buffer and then equilibrated for 2 min in 30 ml of detection buffer. The membrane was placed between two sheets of plastic and 0.5-1 ml of CPD-star chemiluminescent substrate was added to the membrane (per 100 cm^2 of surface area) ensuring the chemiluminescent substrate was dispersed evenly across the surface of the membrane. The membrane was incubated for 5 min at room temperature. The membrane was then sealed in cling film. For detection of the chemiluminescent signal, the membrane was exposed to X-ray film for 5 min, adjusting the exposure time to allow for optimisation of the signal.

2.6 General PCR and Sanger sequencing

Polymerase chain reaction was typically carried out using a BioRad DNA Engine Thermal Cycler. The conditions typically used for different applications are listed below. In general primers were designed to have an annealing temperature between 55 and 60°C such that the annealing temperature used for most applications was 56°C. The use of 5% DMSO in PCR reactions facilitates the amplification of high G+C content templates at these temperatures. PCR tubes were a strip of 8 thin-walled 0.2 ml tubes with domed-caps (Thermo Scientific).

2.6.1 General Analytical PCR

Component	Amount/Concentration	Volume (µl)	Final Concentration
Template DNA	1-10 ng	x	
Forward Primer	10 µM	1	0.4 µM
Reverse Primer	10 µM	1	0.4 µM
dNTPs	40 mM (10 mM each)	0.25	400 µM (100 µM each)
Taq Buffer (Roche)	10x	2.5	1x
DMSO	100%	1.25	5%
Taq (Roche)	5 U/µl	0.25	1.25 U
dH_2O		to 25	

95°C 1 min

95°C 45 s
56-60°C 30 s
72°C 0.5-3 min
} x 25 cycles

72 °C 10 min

2.6.2 High-Fidelity Amplification for Cloning Applications

The following reactions were scaled up to 50 or 100 µl to increase product yield as necessary for the application:

Component	Amount/Concentration	Volume (µl)	Final Concentration
Template DNA	100 ng/µl	0.25	1 ng/µl
Forward Primer	100 µM	0.25	1 µM
Reverse Primer	100 µM	0.25	1 µM
dNTPs	40 mM (10 mM each)	0.5	800 µM (100 µM each)
Expand HiFi Buffer 2 (Roche)	10x	2.5	1x
DMSO	100%	1.25	5%
Expand HiFi Taq (Roche)	3.5 U/µl	0.5	1.75 U
dH_2O		to 25	

94°C 2 min

94°C 45 s
56-60°C 45 s
72°C 0.5-3 min
} x 25 cycles

72 °C 10 min

2.6.3 Colony PCR in *E. coli*

The PCR reaction mix was as in 2.6.1. Colonies of *E. coli* were picked from agar plates using a sterile yellow Gilson pipette tip (Starlabs) and streaked on to a fresh L agar plate containing the appropriate antibiotic for selection before introducing directly into a PCR tube containing the appropriate PCR mix. Samples were mixed with a Gilson pipette set at 20 µl four times to remove cell debris from the tip before placing the reaction tubes into the thermal cycler. Cycling conditions were:

95°C 10 min

95°C 45 s
56-60°C 30 s
72°C 0.5-3 min
} x 30 cycles

72°C 10 min

2.6.4 Colony PCR in *Streptomyces sp.*

Streptomyces single colonies were patched on to DNA media containing 1% glucose. Plates were incubated at 30ºC overnight (20-24 h). *Streptomyces* mycelium was scraped from the plates using a sterile toothpick and introduced into 50 µl 100% DMSO in a 1.5 ml Eppendorf tube. The tube was shaken vigorously for 30-45 min and then briefly centrifuged to pellet cell debris. 2.5 µl of the supernatant were used as the template in the reaction as shown below. Control DNA samples were diluted 1 µl into 1.5 µl DMSO and were used in the same way.

Component	Volume (µl)
Forward Primer (10µM)	2
Reverse Primer (10µM)	2
dNTPs (40mM)	0.5
10x Taq Buffer (Roche)	5
DMSO (100%) + template	2.5
Taq Polymerase (Roche)	0.5
H_2O	to 50

95°C 10min

94°C 45s
56-60°C 30s
72°C 1min
} x 30 cycles

72°C 10min

2.6.5 Colony PCR in *M. corallina* and *Nonomuraea*

Single colonies were patched on to MV0.1 media. Plates were incubated at 30ºC for 5-7 days. Mycelium was scraped from the plates using a sterile toothpick and introduced into 50 µl 100% DMSO in a 1.5 ml Eppendorf tube containing 2 glass beads. The tube was shaken vigorously for 2 hours and then briefly centrifuged to pellet cell debris and beads. 2.5 µl of the supernatant were used as the template as described in 2.6.4.

2.6.6 Purification of PCR products

The QIAquick™ PCR purification kit (Qiagen) was used to remove unincorporated primers, dNTPs and enzymes from completed PCR reactions following manufacturer's instructions. One tenth of the PCR reaction mixture was submitted to agarose gel electrophoresis. The remaining PCR mixture was diluted 5 times in the manufacturer's high salt buffer and applied to a silica gel membrane mounted in a microcentrifuge tube. The PCR products were washed free of primers, dNTPs and enzymes and the DNA fragment was eluted in elution buffer.

2.6.7 Sanger sequencing using Big Dye v3.1

Typically purified PCR products or vectors purified by mini-prep (Qiagen) were labeled with ABI BigDye® 3.1 dye-terminator reaction mix (Applied Biosystems) according to manufacturer's instructions. The manufacturer's instructions were consulted for the appropriate amount of DNA to use for the particular template in question, based on the nature of the product and its length. Big Dye labeling was carried out as detailed below. Reactions were subsequently submitted to the John Innes Genome Centre Sequencing Service for ABI Sanger Sequencing. The resulting sequence chromatogram files were analysed using VectorNTI ContigExpress software.

Component	Volume (µl)
Template	x
Primer (3.2 µM)	1
ABI BigDye® 3.1 dye-terminator reaction mix	1
5x BigDye® 3.1 Reaction Buffer	1.5
H_20	to 10

96°C 1 min

96°C 10 s
50°C 5 s
60°C 4 min
} x 25 cycles

2.7 Growth conditions

2.7.1 Growth and storage of *E. coli*

E. coli strains were typically grown on L agar with antibiotic selection as appropriate or in L broth with shaking at 250 rpm at 30 or 37°C. For long-term storage strains were grown over-night in L medium and cells resuspended in 20% glycerol and stored at -20°C or -80°C.

2.7.2 Growth and Storage of *Micrococcus luteus*

Micrococcus luteus ATCC4698 was typically grown in L broth with shaking at 250 rpm or on L agar at 30 or 37°C. For long-term storage, strains were grown over-night in L medium and cells resuspended in 20% glycerol and stored at -20°C or -80°C.

2.7.3 Growth and storage of *Streptomyces*

Streptomyces strains were grown and manipulated as described in (Kieser *et al.* 2000). Growth media were as stated in the text. For manipulation of *Streptomyces* (e.g. ex-conjugants), SFM agar medium was used with the appropriate antibiotic selection. For the preparation of spore stocks for long-term storage, *Streptomyces* was grown on SFM or OBM (with selection as appropriate; OBM was used for *S. lividans* strains that sporulated poorly on SFM) at 30°C for up to 7 days until grey (*S. lividans and S. coelicolor*) or green (*S. venezualae*). Spores were collected in approximately 2 ml 20% glycerol using a sterile cotton pad through which spores were filtered by collecting with a 2 ml syringe and transferring to a 2 ml cryotube. Spore stocks were stored at -20°C. Spore stocks were titred by making serial dilutions in water and plating on SFM. Resulting colonies were counted from at least three dilutions and averaged.

2.7.4 Growth and storage of *M. corallina*

M. corallina NRRL 30420 was obtained from the NRRL culture collection and *M. corallina* DSM 44681 and DSM 44682 were obtained from the DSMZ culture collection. *M. corallina* strains were grown on V0.1 agar medium at 30°C. For liquid culture, *M. corallina* was typically inoculated 1 in 10 into VSPA medium in a 25-100 ml flask containing 3-6 glass beads (2 mm diameter) and incubated with shaking at 230 rpm at 30°C. The inclusion of 0.1% agar in VSPA aids dispersed growth (Kieser *et al.* 2000). The inclusion of 0.05% Antifoam 289 (Sigma) in *M. corallina* liquid cultures prevented foaming. For long-term storage, culture broth containing mycelium was dispensed into 2 ml cryotubes and stored at -20°C (medium-term storage/working cell bank) or -80°C (long-term storage/master cell bank).

2.7.5 Growth and storage of *Nonomuraea* ATCC39727

Nonomuraea ATCC39727 was a kind gift from Flavia Marinelli (Università dell'Insubria). *Nonomuraea* ATCC39727 was grown on V0.1 agar medium at 30°C. For liquid culture *Nonomuraea* ATCC39727 was typically inoculated 1 in 10 into VSP medium in a 25-100 ml flask containing 3-6 glass beads (2 mm diameter) and incubated with shaking at 230 rpm at 30°C. The inclusion of 0.05% Antifoam 289 (Sigma) in *Nonomuraea* liquid cultures prevented foaming. For long-term storage, culture broth containing mycelium was dispensed into 2 ml cryotubes and stored at -20°C (medium-term storage/working cell bank) or -80°C (long-term storage/master cell bank).

2.7.6 *M. corallina* growth curve

The growth rate of *M. corallina* was assessed in VSPA by measuring optical density at OD_{450}, with VSPA as a blank. 1 ml of *M. corallina* mycelium from a working stock stored at -20°C was used to inoculate 10 ml VSPA in a 25 ml flask containing three glass beads. The culture was grown for 24-48 h at 30°C with shaking at 230 rpm. 100 µl of the resulting mycelium was diluted in 1 ml VSPA and the optical density at OD_{450} assessed. Three 100 ml flasks containing 25 ml VSPA and 10 glass beads were inoculated to a starting OD_{450} of 0.1-0.2. The flasks were incubated at 30°C with shaking at 230 rpm. Samples were removed at appropriate time intervals to measure the OD_{450} (using a 1 in 10 dilution when OD_{450}>1.5).

2.8 Isolation of genomic DNA

2.8.1 *M. corallina*

2.8.1.1 High-Molecular Weight genomic DNA

Microbispora corallina NRRL 30420 mycelium was harvested by centrifugation after 48 h growth in liquid culture and washed with 10 ml 10.3% sucrose to remove traces of medium. The pellet was resuspended in 20 ml SET buffer followed by dispersion in a hand-held glass-homogeniser. The pH of the solution was adjusted to pH8 with 1 N NaOH. Lysozyme (Sigma) was added to a final concentration of 20 mg/ml and the tube incubated at 37°C for 30 h, adding fresh lysozyme at intervals (approximately 50 mg every 8-12 h). After 24 h incubation, 100 µg ribonuclease A was added and the incubation continued at 37°C. After 28 h, 12 mg proteinase K was added and the incubation continued at 37°C. After 30 h incubation, SDS was added to a final concentration of 1% and the solution mixed by inversion, followed by an overnight incubation at 55°C. 8 ml 5M NaCl was added and the DNA extracted with 8 ml phenol-chloroform-isoamylalcohol pH8 using gentle hand mixing. The phenol and aqueous phases were separated by centrifugation at 3000 *x g* for 10 min. The aqueous phase was removed to a fresh 15 ml tube. The DNA was precipitated with ice-cold isopropanol. DNA was spooled from tubes using a sealed glass Pasteur pipette and washed in 70% ethanol. The DNA was air-dried and resuspended in elution buffer. gDNA was stored at 4°C.

2.8.1.2 Small-scale genomic DNA extraction

Microbispora corallina NRRL 30420 mycelium was harvested from 5 ml culture by centrifugation after 48 h growth in liquid culture and washed with 10 ml 10.3% sucrose to remove traces of medium. The pellet was resuspended in 5 ml SET buffer followed by dispersion in a hand-held glass-homogeniser if the mycelium was not well-dispersed. The pH of the solution was adjusted to pH8 with 1 N NaOH. Lysozyme (Sigma) was added to a final concentration of 20 mg/ml and the tube incubated at 37°C for 30 h, adding fresh lysozyme at intervals (approximately 50 mg every 8-12 h). After 24 h incubation, 25 µg ribonuclease A was added and the incubation continued at 37°C. After 28 h, 3 mg proteinase K was added and the incubation continued at 37°C. After 30 h incubation, SDS was added to a final concentration of 1% and the solution mixed by inversion followed by an overnight incubation at 55°C. 2 ml 5 M NaCl were added. The DNA was extracted with 4 ml phenol-chloroform-isoamylalcohol pH8 with vortexing to mix thoroughly and centrifugation at 3000 *x g* for 10 min. The aqueous phase was removed to a fresh 15 ml

tube and 4 ml chloroform added. The tube was vortexed to mix thoroughly and centrifuged at 3000 *x g* for 10 min. The aqueous phase was removed to a fresh 15ml tube. The DNA was precipitated with 0.6 volumes of ice-cold isopropanol. DNA was spooled from tubes using a sealed glass Pasteur pipette and washed in 70% ethanol. The DNA was air-dried and resuspended in elution buffer. gDNA was stored at 4°C (concentrated samples) and at a concentration of 10 ng/µl at -20°C.

2.8.2 *Nonomuraea*

Nonomuraea mycelium was harvested from 5 ml of culture by centrifugation after 48 h growth in liquid culture and washed with 10 ml 10.3% sucrose to remove traces of medium. The pellet was resuspended in 5 ml SET buffer. The pH of the solution was adjusted to pH8 with 1 N NaOH. Lysozyme (Sigma) was added to a final concentration of 10 mg/ml and the tube incubated at 37°C for 24 h, adding fresh lysozyme at intervals (approximately 50 mg every 8-12 h). After 16 h incubation 25 µg ribonuclease A was added and the incubation continued at 37°C. After 20 h, 3 mg proteinase K was added and the incubation continued at 37°C. After 24 h incubation, SDS was added to a final concentration of 1% and the solution mixed by inversion followed by an overnight incubation at 55°C. 2 ml 5 M NaCl were added and mixed well. The DNA was extracted with 4 ml phenol-chloroform-isoamylalcohol pH8 with vortexing to mix thoroughly and centrifugation at 3000 *x g* for 10 min. The aqueous phase was removed to a fresh 15 ml tube and 4 ml chloroform added. The tube was vortexed to mix thoroughly and centrifuged at 3000 *x g* for 10 min. The aqueous phase was removed to a fresh 15 ml tube. The DNA was precipitated with 0.6 volumes ice-cold isopropanol. DNA was spooled from tubes using a sealed glass Pasteur pipette and washed in 70% ethanol. The DNA was air-dried and resuspended in elution buffer. gDNA was stored at 4°C (concentrated samples) and at a concentration of 10 ng/µl at -20°C.

2.8.3 Streptomyces

Approximately 10 µl spores were inoculated into 10 ml SOC in a glass Universal containing a spring for mixing. The culture was incubated at 30°C for 24-36 h. The mycelium was harvested and resuspended in 2.5 ml of SET containing 10 mg/ml lysozyme and 25 µg Rnase A. The mycelium was incubated at 37°C for 2 h. 30 µl of proteinase K (20 mg/ml) were added and incubation continued for a further 30 min. SDS

was added to a final concentration of 1% and mixed by inversion before incubating at 55°C for 15 min. The DNA was extracted with 1 ml phenol-chloroform-isoamylalcohol pH8 with vortexing to mix thoroughly and centrifugation at 3000 *x g* for 10 min. The aqueous phase was removed to a fresh tube. The DNA was precipitated with 0.3 M sodium acetate and 1 volume ice-cold isopropanol. DNA was pelleted by centrifugation for 3 min at 16000 *x g* and washed in 70% ethanol. The DNA was air-dried and resuspended in elution buffer. gDNA was stored at 4°C (concentrated samples) and at a concentration of 10 ng/µl at -20°C.

2.9 Solexa and 454 sequencing and analysis

Genomic DNA isolated from *M. corallina* NRRL 30420 was sequenced using Solexa sequencing technology (Illumina) by Dr. Eric Kemen and Dr. David Studholme (The Sainsbury Laboratory). The method used was as described in (Farrer *et al.* 2009). In total, 7 lanes of data were collected totaling 881 Mb of sequence. Sequence reads were assembled using Velvet 0.6 (Zerbino *et al.* 2008). Three separate data assemblies were made in total. Summary statistics for one of the data assemblies were:

Number of contigs = 14395

Mean length of contig= 204 nt

Median length of contig = 163 nt

Total sum of contig lengths = 2.93 Mb

Longest contig = 4436 nt

Genomic DNA isolated from *M. corallina* NRRL 30420 was sequenced using 454 sequencing technology (Cogenics). One lane of 454 sequencing yielded 28Mb of sequence data. Sequence reads were assembled using Newbler assembly software. Summary statistics for the data assembly were:

Large Contig Metrics

Number of Contigs = 3027

Number of Bases = 3383376

Average Contig Size = 1117 nt

N50 Contig Size = 1219 nt

Largest Contig Size = 8913 nt

Q40PlusBases = 2984663, 88.22%

Q39MinusBases = 398713, 11.78%

All Contig Metrics

Number of Contigs = 7580

Number of Bases = 4642930

The assembled contig sequences from each method were used to construct a database searchable by BLAST by Dr. Govind Chandra using the formatdb from the BLAST suite of programs version 2.2.18 (NCBI; (Altschul *et al.* 1990)).

2.10 Cosmid Library Preparation

2.10.1 Hydroshearing gDNA

20 µg of high molecular weight *M. corallina* gDNA in a volume of 140 µl was heated to 60ºC for 1 min. The DNA was loaded into a HydroShear® machine (GeneMachines) and sheared at speed code 40 for 5 cycles following manufacturer's instructions. 1 µg of the hydrosheared DNA was retained for analysis by pulsed-field gel electrophoresis. The remaining DNA was end-repaired.

2.10.2 End-Repair of Hydrosheared gDNA

Hydrosheared DNA (10 µg)	x µl
5 xT4 DNA polymerase buffer (Invitrogen)	40 µl
40 mM total dNTP mix (10mM each)	5 µl
10 mM ATP	20 µl
T4 DNA polymerase (Invitrogen; 5 U/µl)	8 µl
T4 polynucleotide kinase (USB; 3 U/µl)	4 µl
H_2O	to 200 µl

The reaction was incubated at room temperature for 45 min. The volume was adjusted to 700 µl final with elution buffer. DNA was extracted with 700 µl phenol-chloroform-isoamylalcohol (pH8) with mixing by inversion for 5 min and centrifugation at 16000 *x g* for 5 min. The aqueous phase was removed to a fresh tube and the extraction repeated with 400 µl chloroform. The DNA was precipitated with 0.3 M sodium acetate and two volumes of 100% ethanol at -20°C for 30 min. The DNA was pelleted by centrifugation and washed in 70% ethanol. The pellet was air-dried before resuspending overnight in 10 µl of elution buffer at 4°C. The DNA was checked by PFGE.

2.10.3 Preparation of pSupercos1 vector and ligation with insert DNA

10 µg SuperCosI vector (Stratagene) was linearised with 9 U/µg *Xba*I (Roche) in a total volume of 100 µl with 1 x buffer H at 37ºC for 1 h. The digestion was checked by separating 1 µl (100 ng) DNA on a 0.8% TBE agarose gel by electrophoresis. Complete digestion was indicated by a linear SuperCosI band at 7.9 kb. The vector DNA was purified from the remaining reaction with the Qiagen PCR purification kit. The DNA was eluted twice in 25 µl elution buffer and 25 µl dH_2O (warmed to 60 ºC) at 60 ºC for 5 min. The purified *Xba*I-digested DNA was treated with 30 U calf intestinal alkaline phosphatase (Cambio), in 100 ul total reaction volume with 1xCIAP buffer for 1 h at 37 ºC. The DNA was purified with the Qiagen PCR kit and eluted twice in 25 µl elution buffer and 25 µl dH_2O (warmed to 60ºC) at 60ºC for 5 min. The DNA was digested with 10 U/µg *Zra*I (NEB) in 100 µl total volume with 1 x buffer 1 at 37ºC for 1 h. The DNA was purified with the Qiagen PCR kit and eluted with 10 µl elution buffer and 10 µl dH_2O (warmed to 60ºC). The generation of fragments of the expected sizes of 1245 and 6695bp was checked by separating 2 µl of the treated DNA and 200 ng of uncut control DNA on a 0.8% TBE agarose gel by electrophoresis.

Ligation was carried out as follows:

Component	Sample	Negative Control
Insert DNA end-repaired	2.5 µg	2.5 µg
pSuperCosI blunt ended	1 µg	1 µg
10 x T4 ligase buffer (Promega)	2 µl	2 µl
T4 DNA ligase 3U/µl (Promega)	1 µl	-
H_2O	to 20 µl	to 20 µl

Reactions were incubated at 4ºC overnight.

2.10.4 Phage packaging

4 µl of each ligation reaction were packaged into λ-phage using the Stratagene GigaPack III Gold Packaging Extract and following the manufacturer's instructions. Briefly, packaging extracts were removed from -80°C storage to dry ice. Extracts were rapidly thawed and 4 µl of each ligation reaction added. The extract was gently mixed and incubated at room temperature for 2 h. 500 µl SM buffer were added followed by 20 µl chloroform. Packaged phage were stored at 4°C and used within 1 month.

2.10.5 Phage titration

Escherichia coli XL-I Blue (Stratagene) was streaked from a glycerol stock at -20°C on to LB agar and was grown at 37ºC overnight. A single colony from this plate was used to inoculate 10 ml LB broth which was grown at 37ºC overnight. 1 ml of this culture was used to inoculate 50 ml LB broth containing 10 mM $MgSO_4$ and 0.2% maltose. This culture was grown at 37ºC for 2.5 h. Cells were recovered by centrifugation and diluted to an OD_{600} of 0.5 in 10 mM $MgSO_4$. Packaged phage were diluted in SM buffer. Transfections of *E. coli* cells with 1 µl of undiluted, 1/10, 1/50 and 1/100 (made up to a total volume of 25 µl with SM buffer) dilutions of phage were carried out by mixing 25 µl cells with 25 µl each dilution and incubating cells at room temperature for 30 min. 200 µl LB broth were added to each tube and incubated at 37°C for 1 h with shaking gently every 15 min. The entire transfection reaction was plated out on LB agar containing 100 µg/ml carbenicillin and incubated overnight at 37°C. The resulting colonies were counted to give the phage titre per µl of phage extract used. The resulting clones were picked into 5 ml LB broth and grown at 37ºC overnight. 1.5 ml of each culture were used for the preparation of cosmid DNA which was then verified by restriction digest. Since the packaged extract initially gave only 4 colonies per µl of undiluted extract, the packaging reaction was repeated with a further 4 µl of the ligation. The two extracts were pooled before transfection to construct the final cosmid library.

2.10.6 Phage Transfection of *E. coli* to construct cosmid library

This was carried out as described for phage titration except that transfection was scaled to use 1 ml *E. coli* cells (at OD_{600} 0.5) in 10 mM $MgSO_4$ with 1 ml of the pooled packaged phage extracts (made up with SM buffer). 8 ml LB broth was added and 1.4 ml of the transfection mix plated out on each of 7 Vented QTrays (240 x 240 x 20 mm) containing 200 ml LB agar with 100 µg/ml carbenicillin to give an estimated plating density of 500-800 colonies per plate. Plates were incubated inverted overnight at 37°C.

2.10.7 Library Picking and Transfer to Membrane

3072 colonies were picked using Q-Bot (Genetix) into 8x384 well archive plates containing freezing broth (LB and glycerol) and 100 µg/ml carbenicillin. Two copies of the archive plates were replicated. All copies of the library were stored at -80ºC. The entire library was spotted two-fold onto nylon membrane in a double off-set pattern. The clones on the membrane were grown on LB agar overnight and baked on to the membrane at 80ºC. The membrane was stored at -20ºC.

2.10.8 Probe preparation and library hybridization

The probe was amplified from *M. corallina* gDNA by PCR using the primers LF001F and LF004R. The 1250 bp PCR product was separated by electrophoresis on a 1% TBE agarose gel and was purified by gel extraction. 25 ng of the purified DNA fragment was diluted to a final volume of 50 µl in TE. The DNA was denatured at 95-100ºC for 5 min and snap-cooled on ice for 5 min before centrifuging briefly. The DNA was added to a tube containing Rediprime II random prime labelling reaction mix (Amersham), to which was then added 5 µl ^{32}P-αdCTP. The reaction was incubated at 37ºC for 1 h and the reaction stopped by adding 5 µl 0.2 M EDTA.

The membrane containing the cosmid library clones was prepared by soaking for 2-3 h at 42^{o}C in 5 x SSC, 0.5% SDS, 1 mM EDTA pH8. All bacterial debris was scraped off using a paper towel and the membrane rinsed twice in 2 x SSC.

The membrane was placed into a large hybridization tube containing 50 ml of hybridization buffer warmed to 60ºC and was pre-hybridised for 2-4 h at 65ºC in a Techne oven. The pre-hybridization solution was replaced with 20 ml of fresh hybridization buffer to which was added 30 µl of the labelled probe. The filter was hybridized at 65^{o}C in a Techne oven overnight. The hybridization solution was removed and the filter washed three times in 50 ml of pre-warmed wash buffer at 65ºC. The filter was wrapped in Clingfilm and exposed to a phosphorimager plate for 5 h. The plate was visualised using a phosphoimager (Fuji). Alignment of the membrane with the grid pattern of the 386 well plates along with the double off-set pattern of the spots allowed the location of the positive clones to be identified. Positive clones were selected from the library and grown on LB agar containing 100 µg/ml carbenicillin.

2.11 Cosmid sequencing and sequence analysis

Cosmids 5A7 and 4G2 were sequenced using Sanger sequencing by the Cambridge University DNA Sequencing Service. Cosmid end-sequencing was carried out as described in 2.6.7 using the primers End_F and End_R (approximately 600 base pairs of sequence per end). The complete cosmid sequences were annotated with the putative open-reading frames which were characterised by searches for homology using NCBI Blast. The sequence annotation was carried out using Artemis (Sanger Centre, Cambridge). Open-reading frames were called on the basis of the GC content and start sites (ATG or GTG) were further adjusted taking into account the presence of ribosome binding sites approximately 6-10 nucleotides upstream of the start site and based around the sequence GGAGG ((Kieser *et al.* 2000)).

2.12 PCR targeting of cosmids

In general, the strategy is carried out with minor modifications to that described in REDIRECT© technology: PCR-targeting system in *Streptomyces coelicolor* by Gust *et al*., (2002).

2.12.1 Construction of integrative cosmids

E. coli BW25113/pIJ790 containing the SuperCos1 cosmid to be targeted was grown in 10 ml L broth containing 50 µg/ml carbenicillin, 50 µg/ml kanamycin and 25 µg/ml chloramphenicol overnight at 30°C with shaking at 250 rpm. 10 ml SOB (minus Mg) containing carbenicillin, kanamycin, chloramphenicol and 10 mM L-arabinose was inoculated 1 in 20 with this overnight culture which was incubated with shaking at 30°C for 90 min. An additional 100 µl 1 M L-arabinose were added and incubation continued at 30°C for an additional 60 min (until OD_{600} ~0.6). Electrocompetent cells were generated from the induced culture as described in 2.5.8. 50 µl of the cell suspension were mixed with ~100 ng gel purified 5247 bp *SspI* fragment derived from pIJ10702 (pMJCOS1). Electroporation was carried out as 2.5.8. Typically 500 µl aliquots of the transformation mix were plated onto two plates of L agar containing 50 µg/ml apramycin and 100 µg/ml carbenicillin and incubated overnight at 37°C.

After overnight incubation, colonies were scraped from one transformation plate in 1 ml H_2O and the cosmid DNA purified using a variation of the standard cosmid preparation protocol (2.5.2). Briefly, cells were pelleted by centrifugation and resuspended by vortexing in 200 µl solution I. 400 µl solution II were added and the tubes inverted ten

times. A volume of 300 µl solution III was then added and mixed in by inverting the tube five times. The tube was then centrifuged at 16000 *x g* in a microcentrifuge for 10 min at room temperature. The supernatant was transferred to a 2 ml tube, 1 ml of ice cold isopropanol was added and DNA precipitation was achieved by placing the tube on ice for 10 min followed by centrifuging at 16000 *x g* in a micro centrifuge for 5 min. The pellet was washed with 1 ml 70 % ethanol and centrifuged at 16000 *x g* in a microcentrifuge. The pellet was dried by leaving the tube open for 5-10 min at room temperature prior to resuspension in 100 µl elution buffer. 1 µl of the resulting cosmid DNA was used to transform 50 µl chemically competent *E. coli* DH5α (as 2.5.9). Typically 100 µl and 900 µl of the transformation were plated on to L agar containing 50 ug/ml apramycin and 100 µg/ml carbenicillin and incubated overnight at 37°C. Resulting transformants were picked into 5 ml L broth containing 50 µg/ml apramycin and 100 µg/ml carbenicillin and grown overnight at 37°C. Cosmid DNA was prepared from these overnight cultures following the standard cosmid preparation protocol (2.5.2). Cosmid DNA that had been successfully targeted with the pIJ10702 *Ssp*I fragment was confirmed by a *NotI* restriction digest, which yields a diagnostic band-shift of 6807bp → 8682bp. Digest with *Bam*HI was used to confirm the identity of the cosmid.

2.12.2 Construction of mutant cosmids by gene replacement

The mutation of a specific cosmid by gene replacement was carried out in *E. coli* BW25113/pIJ790 containing the cosmid to be targeted essentially as described in 2.12.1. The gene replacement cassette was amplified by high-fidelity PCR from the appropriate vector (e.g. pIJ773 or pIJ778) using primers designed to anneal to the universal primer binding sites (of 19 and 20 bp) which flank these cassettes and having 39 nt extensions homologous to the sequence flanking the gene to be replaced. Primer sequences were designed such that gene replacement would not affect the expression of downstream open-reading frames by ensuring that all start codons and ribosome-binding sites were left intact. For all primer sequences used for gene replacement see Table 2.8. PCR was carried out as follows:

Component	Amount/Concentration	Volume (µl)	Final Concentration
Template DNA	100 ng/µl	0.5	
Forward Primer	100 µM	0.5	1 µM
Reverse Primer	100 µM	0.5	1 µM
dNTPs	40 mM (10mM each)	1	800 µM (100 µM each)
Expand HiFi Buffer 2 (Roche)	10x	5	1x
DMSO	100%	2.5	5%
Expand HiFi Taq (Roche)	2.5 U/µl	1	2.5 U
dH_2O		to 50	

94°C 2min

94°C 45s
50°C 45s
72°C 90s
} x 10 cycles

94°C 45s
55°C 45s
72°C 90s
} x 15 cycles

72 °C 5 min

The PCR reaction was treated with 1 µl *Dpn*I (NEB; 20U/µl) for 1 h at 37°C (to remove template DNA). The PCR-amplified template was purified using the Qiagen PCR purification kit and eluted in 12 µl elution buffer (heated to 55-60°C). 1 µl of the purified cassette was analysed on a 1% TBE agarose gel by electrophoresis to check the size and quality of the cassette DNA. 1 µl (approximately 100 ng) of the purified cassette DNA was used to transform *E. coli* BW25113/pIJ790 containing the cosmid, and prepared as described in 2.12.1. Transformants were selected on L agar containing the antibiotic for which resistance is conferred by the introduced cassette. Manipulated cosmids were transferred to *E. coli* DH5α as described in 2.12.1 and the correct targeting of the cosmid confirmed by PCR, using primers flanking the cassette insertion (see Table 2.8). The resulting confirmation PCR products were purified by gel extraction or by using a PCR purification kit and the integrity of the cassette and the correct replacement of the gene in question confirmed by sequencing as per 2.6.7. To confirm that no other gross rearrangements had occurred in the targeted cosmids, targeted and wild type cosmids were subjected to restriction digest analysis (usually with *Not*I) and fragments compared by separating on a 1% TBE agarose gel by electrophoresis. The restriction digest patterns were compared to those from *in silico* digests of the respective wild type and mutant cosmids (using VectorNTI; Invitrogen).

2.12.3 Insertion of the *ermE** constitutive promoter

This was carried out as described for the generation of gene replacement mutant cosmids except that PCR primers for cassette amplification were designed to anneal to the region flanking the Tc^R-*ermE**- EF-Tu ribosome binding site (*Streptomyces ramocissimus tuf1*) cassette in pIJ10705 with 5' 39 nt extensions homologous to the sequence flanking the region where the cassette would be inserted (Bibb *et al.* 1994; van Wezel *et al.* 2000; O'Rourke unpublished). Each *ermE** cassette was designed to be introduced adjacent to the start codon of the gene to be over-expressed, primer F having the sequence upstream of the start codon of that gene and primer R having the sequence downstream (and inclusive of) the start codon. The sequences of the primers used for the construction of these constructs are listed in Table 2.8. 10 µg/ml tetracycline was used for the selection of transformants carrying the targeted cosmid. Targeted cosmids were confirmed as described in 2.12.2.

2.12.4 FLP-mediated recombination to generate scar mutants

E. coli DH5α/BT340 was grown in 10 ml L broth containing 25 µg/ml chloramphenicol overnight at 30°C with shaking at 250 rpm. 10 ml L broth containing chloramphenicol were inoculated 1 in 20 with this overnight culture and incubated with shaking at 30°C for 3-4 h until OD_{600} ~0.6. Electrocompetent cells were generated from the induced culture as described in 2.5.8. 50 µl of the cell suspension were mixed with ~100 ng cosmid containing the FRT-flanked cassette to be removed. Electroporation was carried out as 2.5.8. Typically 100 µl and 900 µl aliquots of the transformation mix were plated onto L agar containing 25 ug/ml chloramphenicol and the selection encoded by the cassette in the cosmid and incubated for 2 days at 30°C. Approximately eight single colonies were picked and streaked on to L agar without antibiotics and incubated at 42°C overnight to promote FLP-recombination. Single colonies from these plates were picked and streaked first on to L agar containing the antibiotic selection for the cassette used for the mutagenesis (apramycin or spectinomycin/streptomycin) and then on to L agar containing selection for the backbone of the cosmid (carbenicillin and kanamycin for Supercos or carbenicillin and apramycin for pIJ10702). The plates were incubated at 37°C overnight and compared to identify clones sensitive to the selection for the cassette used for mutagenesis but resistant to the selection for the cosmid backbone. Four to eight such clones were selected and the removal of the cassette confirmed by PCR using flanking primers and the PCR products checked by Sanger sequencing.

2.13 Bioassay methods

2.13.1 Solid bioassay

The indicator organism was *Micrococcus luteus* ATCC4698. 50 µl of a glycerol stock were streaked onto L agar plates and incubated for 2 days at 30ºC. A single colony was used to inoculate L broth which was grown overnight at 30ºC with shaking. This culture was diluted 1 in 25 into 50 ml L broth and grown at 30ºC with shaking until an OD of 0.4-0.6 was reached. This culture was diluted 1 in 10 into molten soft nutrient agar at 50ºC and approximately 10 ml used to overlay each 25 ml plate containing the growing producer organism. The plates were incubated at 30ºC until halos were visible, usually overnight.

2.13.2 Liquid bioassay

The indicator organism was *Micrococcus luteus* ATCC4698. 50 µl of a glycerol stock was streaked onto L agar plates and incubated for 2 days at 30ºC. A single colony was used to inoculate L broth which was grown overnight at 30ºC with shaking. This culture was diluted 1 in 25 into 50 ml L broth and grown at 30ºC with shaking until an OD of 0.4-0.6 was reached. This culture was diluted 1 in 10 into molten L agar at 50ºC and approximately 20 ml poured into 90 mm standard Petri dishes or approximately 40 ml into 100 mm square Petri dishes. 40 µl samples of spent culture supernatant and controls were applied to sterile antibiotic assay discs and allowed to dry. These were then placed onto plates containing the target organism and the plates incubated at 30ºC until halos were visible, usually overnight.

2.13.3 *M. corallina* microbisporicin resistance assay

For co-culture experiments, *M. corallina* was grown in a patch across one side of a V0.1 agar plate for 11 d at 30°C. The test organism was then streaked perpendicular to each of the patches and its growth monitored for several days. For well diffusion assays, square petri dishes (10x10 cm) with 25 compartments (Sterilin) were prepared with 2 ml V0.1 per compartment. The test organism was applied to the agar at the appropriate time point and spread to allow confluent growth. The plates were incubated at 30°C for the required time period. At the zero time point, 200 µl yellow pipette tips (StarLabs) were used to generate wells of fixed diameter in the agar. The tip was inverted using sterile forceps and stamped into the centre of the agar well. The narrow end of the tip was covered with a gloved finger to generate a seal such that removal of the tip from the agar also removed the agar plug, which was discarded. 40-50 µl of test supernatant was added to each well. Liquid was

allowed to diffuse into the agar for several hours before the plates were inverted. Plates were further incubated at 30°C and the growth of mycelium monitored daily.

2.14 Matrix-Assisted Laser-Desorption Ionisation Time of Flight Mass Spectrometry (MALDI-ToF)

Culture supernatants were diluted 1 in 5 with 5% formic acid. The diluted sample (ca. 0.8 µl) was spotted onto a PAC plate (Prespotted AnchorChipTM MALDI target plate, Bruker Daltonics, Bremen, Germany) and the spots washed briefly with 8 µl 5% formic acid according to the manufacturer. After drying, the samples were analysed by MALDI-TOF on a Bruker Ultraflex TOF/TOF. The instrument was calibrated using the prespotted standards (ca. 200 laser shots). Samples were analysed using a laser power of approx. 25% and spectra were summed from ca. 20 x 20 laser shots. The accuracy of MALDI-ToF MS was 20-50 ppm. Analysis of mass spectrometry data and figure preparation was carried out using FlexAnalysis software (Bruker Daltonics, Bremen, Germany).

2.15 Extraction Methods for microbisporicin

2.15.1 Concentration with Diaion HP20 bead matrix

Diaion HP20 polystyrene resin (Mitsubishi Chemical Co.) was prepared by washing in 100% methanol for 5 min followed by water for 5 min and added to the supernatant from which microbisporicin was to be recovered at 2.3% v/v. Tubes containing supernatant and resin were incubated overnight at room temperature on a vertical rotating mixer. Samples were subjected to centrifugation at 3000 *x g* for 10 min to pellet the matrix. The bulk of the supernatant was carefully removed with a pipette without disrupting the resin and was stored for later analysis. The resin was washed once in methanol:distilled water (2:3) and the wash fraction stored for later analysis. The resin was eluted once in 1 ml methanol:water-saturated butanol:water (9:1:1) for 30 min at room temperature on a vertical rotating mixer. The eluant was stored for later analysis. The elution was repeated for 2 h at room temperature on a vertical rotating mixer. 40 µl samples were tested for bioactivity by applying to antibiotic assay discs. Some eluant samples were concentrated by drying under vacuum and samples resuspended in 5% formic acid for MALDI-ToF mass spectrometry.

2.15.2 Analytical High-Pressure Liquid Chromatography

Analytical HPLC for microbisporicin compounds was carried out as recommended by Professor Flavia Marinelli (Universita del'Insubria; personal communication). 50 ml of culture was separated into supernatant and mycelial pellet by centrifugation at 3000 *x g* for 10 min. The supernatant was prepared by acidifing to pH3 with 50% formic acid and methanol added to 1:1 before analyzing by HPLC. The mycelium was prepared by extracting the mycelial pellets with 2.5 ml 100% methanol on a vertical rotating wheel for 20 min. The mycelium was subsequently removed by centrifugation and discarded. The supernatant was analysed by HPLC.

HPLC was carried out on a C18 4.6x250 mm column (Waters) maintained at 50°C. Phase A was 90% ammonium formate (2% v/v) and 10% HPLC-grade acetonitrile. Phase B was 30% ammonium formate (2% v/v) and 70% HPLC-grade acetonitrile. The HPLC column was equilibrated over-night to 65% phase A and 35% phase B. A 40 µl injection of supernatant or methanol-extracted mycelium was loaded on to the column. The elution gradient was phase B from 35% to 90% in 30 min with a flow rate of 1 ml/min. UV spectroscopy data were collected at 268 nm. HPLC fractions were collected from 100 µl injections using an auto-collector set to collect fractions with a UV 268 nm absorbance above 3 mAu in a maximum volume of 800 µl per vial.

2.16 Microscopy

2.16.1 Phase-contrast microscopy

Samples were placed on 76x26 mm glass slides (VWR international) and covered with a glass cover slip (18x18 mm; VWR international). Slides were typically observed at 400 times magnification with a Photomicroscope II in phase-contrast mode (Zeiss).

2.16.2 Cryo-Scanning Electron Microscopy

High-resolution SEM was carried out by Kim Findlay at the John Innes Centre using a Zeiss Supra 55 VP FEG SEM with a Gatan Alto 2500 cryo system at an accelerating voltage of 3 kV.

2.17 Shotgun Library

2.17.1 Cloning strategy

High molecular weight genomic DNA was isolated from *M. corallina* NRRL 30420 and 5 µg were digested with *Bam*HI (10 U) at 37°C in a volume 50 µl. 10 µl samples were removed at 0, 1, 5, and 20 min after enzyme addition and added to 15 µl 0.5 M EDTA and immediately frozen in liquid nitrogen. The digested DNA in each sample was separated on a 1% TBE agarose gel by electrophoresis. The DNA was digested to below the required size range (5-10 kb) so the process was repeated, taking samples at 0, 1, 2, 3, 4 and 5 min. A digestion time of 2-3 min was identified as appropriate for the required size range of DNA. The preparative digest was carried out using 5 µg of DNA which was digested with 10 U *Bam*HI in a volume of 50 µl for 2.5 min at 37°C. 75 µl of 0.5M EDTA were added to stop the reaction and the sample frozen in liquid nitrogen. The digested fragments were separated on a 0.8% TBE agarose gel. The lanes containing the ladder DNA on either side of the gel were removed, stained in TBE containing 0.5 µg/ml ethidium bromide and visualized with UV. The size region from 5-10 kb of genomic DNA was marked with a scalpel. The gel slices were rearranged and the marked ladder sections used as a guide to remove the gel segment containing fragmented NRRL 30420 DNA of that size range (without having to directly expose this DNA to ethidium bromide and UV light which could damage the DNA). The DNA from this gel slice was purified using a Qiagen gel extraction kit and eluted in 100 µl elution buffer giving a final concentration of 19 ng/µl. Approximately 100 ng was analysed by gel electrophoresis and the DNA had a size range of 3-8 kb with an estimated mean size of 5-6 kb.

pRT802 (Gregory *et al.* 2003) integrates specifically at the *Streptomyces* ΦBT1 attachment site and carries the kanamycin resistance marker. 5 µg pRT802 were digested with 50 U *Bam*HI at 37°C for 2 h. The digested vector was purified using a Qiagen gel extraction kit and eluted in 50 µl elution buffer. The vector was treated with 60 U calf intestinal alkaline phosphatase for 1 h at 37°C and purified using a Qiagen PCR purification kit. The cut vector was checked by gel electrophoresis on a 0.8% TBE agarose gel and had the expected linear size of 5700 bp. The partially digested NRRL 30420 genomic DNA was ligated in a 3 to 1 ratio with 100 ng of the prepared pRT802 vector. A vector-only control ligation indicated that approximately 1 in 60 transformants in the library would carry the vector alone. Library efficient *E. coli* DH5α cells were transformed with the ligation reaction to yield approximately 2500 kanamycin-resistant clones. With an average insert size of 6 kb and with an estimated 1/60 clones carrying the

vector alone, this library give an approximate 2.5-3 fold genome coverage (assuming a genome size of 5 Mb). The *E. coli* clones were pooled and plasmid DNA purified by alkaline lysis (see cosmid isolation section 2.5.2). The isolated DNA was checked by PCR using primers corresponding to *mib* genes.

E. coli S17-1 (Simon *et al.* 1983) was transformed with 100 ng of the isolated library DNA in four independent transformation reactions. Approximately 3600 kanamycin resistant clones were scraped from the plates in 1 ml L broth and inoculated into 110 ml L broth containing 50 µg/ml kanamycin. The culture was grown for 3 h until at an OD_{600} of 0.6. Cells from 100 ml of this culture were stored in 20% glycerol at -20°C. Cells from 10 ml of culture were washed twice in L broth by centrifugation at 3000 *x g* for 10 min. Cells were resuspended in 500 µl L broth. *S. lividans* TK24 pIJ12131 spores were prepared for conjugation as section 2.18.1 and were mixed with the S17-1 library cells. Ex-conjugants were selected with 50 µg/ml kanamycin, 10 µg/ml apramycin (to ensure pIJ12131 is maintained) and 25 µg/ml nalidixic acid (to kill the S17-1 *E. coli* donor). Three independent conjugations (from separate cultures of S17-1) were carried out to generate the final *Streptomyces* library.

2.17.2 Library construction and screening

In total, approximately 3000 ex-conjugants were picked and patched on SFM containing 50 µg/ml kanamycin, 10 µg/ml apramycin and 25 µg/ml nalidixic acid with 30 patches per plate. All plates were grown at 30°C for 4 d until spore pigment was visible. All plates were replicated on to V0.1 agar using velvet squares (Kieser *et al.* 2000). SFM library plates were stored at 4°C. V0.1 agar plates were incubated at 30°C for 4 days and were overlaid with *M. luteus* in soft nutrient agar (see section 2.13.1). Plates were incubated overnight at 30°C. Clones identified producing zones of inhibition in the lawn of *M. luteus* growth were identified from the SFM library plates and re-tested by bioassay on V0.1 agar medium.

2.18 Conjugation methods

2.18.1 Streptomyces

E. coli ET12567/pUZ8002 containing the *oriT*-containing plasmid to be transferred was grown overnight in 5 ml L broth with plasmid selection and 50 µg/ml kanamycin and 25 µg/ml chloramphenicol at 37°C with shaking at 250 rpm. 100 µl of this overnight culture were inoculated into 10 ml L broth with antibiotic selection and grown at 37°C with shaking at 250 rpm until the culture reached an OD_{600} of 0.4. The cells were washed twice with 10

ml of L broth, with centrifugation at 3000 *x g* for 10 min, to remove antibiotics and finally resuspended in 1 ml of L broth. For each conjugation, 10 µl (approximately 10^8) *Streptomyces* spores were added to 500 µl 2 × YT broth. Spores were heat shocked at 50°C for 10 min and allowed to cool (except *S. venezualae*). 0.5 ml of the *E. coli* cell suspension was mixed with the spores. 100 µl, 10 µl and 1 µl of the mixture were plated out on to SFM agar medium containing 10 mM $MgCl_2$. The plates were incubated at 30°C for 16-20 h. Each plate was overlaid with 1 ml water containing 0.5 mg nalidixic acid (to kill *E. coli* donor cells) and antibiotic selection for the plasmid as appropriate (as detailed in (Kieser *et al.* 2000)). Incubation was continued at 30°C. Single ex-conjugants were picked after 3-5 days growth and streaked on to SFM containing naladixic acid (25 µg/ml) and the plasmid selection.

2.18.2 *M. corallina*

M. corallina mycelium was harvested from 48 h old cultures by centrifugation at 3000 *x g* for 10 min and washed twice in ice cold 20% glycerol. The mycelial pellet was resuspended in approximately half the original volume ice-cold 20% glycerol. Mycelial samples were used immediately or were stored at -80°C and thawed on ice prior to conjugation. *E. coli* ET12567 pUZ8002 carrying the *oriT*-containing plasmid to be transferred were prepared for conjugation as described in 2.17.1 (Kieser *et al.* 2000). 0.5 ml of mycelium was mixed with 0.5 ml of *E. coli* for each conjugation. 100 µl of the mixture were plated on to V0.1 agar medium containing 10 mM $MgCl_2$. The plates were incubated at 30°C for 16-20 h. Each plate was overlaid with 1 ml water containing 0.5 mg nalidixic acid and the appropriate selection for the plasmid (typically 1.25 mg apramycin or hygromycin). One plate from each conjugation was overlaid with 1 ml water containing 0.5 mg nalidixic acid only as a control. Incubation was continued at 30°C. Single ex-conjugants were picked after 14 days (small integrative constructs) or 3-5 weeks (homologous recombination with cosmids) growth.

2.18.3 *Nonomuraea*

Nonomuraea mycelium was harvested from 24 h old cultures by centrifugation at 3000 *x g* for 10 min and washed twice in ice cold 20% glycerol. The mycelial pellet was resuspended in approximately half the original volume ice-cold 20% glycerol. Mycelial samples were used immediately or stored at -80°C and thawed on ice prior to conjugation. Conjugation with *E. coli* ET12567 pUZ8002 was carried out as described in 2.17.2.

2.19 *M. corallina* Protoplasts

M. corallina protoplasts were produced and regenerated according to (Marcone *et al.* 2010b). Protoplast transformation was carried out as (Marcone *et al.* 2010c). Protoplast generation and transformation were carried out with the assistance of Dr. G.L. Marcone (Universita del'Insubria) and Dr. F. Beltrametti (Actygea, Gerenzano, Italy).

2.19.1 Protoplast production

M. corallina was grown for 48 h in VM medium. Mycelium was harvested by centrifugation at 3000 *x g* for 10 min and washed once in P buffer and resuspended in an equal volume of P buffer. Lysozyme and mutanolysin (Sigma) were dissolved in P buffer at final concentrations of 5 mg/ml and 0.018 mg/ml, respectively. Cell wall digestion was carried out at 30°C with gentle shaking at 150 rpm for 24 h. Protoplasts were removed from residual mycelium clumps by thoroughly pipetting up and down. Protoplasts were separated from residual hyphal fragments by filtration through glass wool. Protoplasts were pelleted by centrifugation at 16000 x *g* at 4°C, washed once in P buffer and were finally re-suspended in 1 ml P buffer. Formation of protoplasts was followed by microscopic observation and protoplasts were counted by using a Petroff-Hausser counting chamber and a Zeiss phase-contrast microscope at 400x.

2.19.2 Protoplast regeneration

Protoplasts were diluted in P buffer (undiluted, 10^{-2}, 10^{-4} and 10^{-6}) and protoplasts present in each dilution counted using a Petroff-Hausser counting chamber (counted in five different squares and averaged) and a Zeiss phase-contrast microscope at 400x. 100 µl of each dilution were placed on to M3 agar medium and 4 ml molten VMS0.1 at 37°C added and mixed with the protoplasts to spread them evenly over the plate surface. Plates were allowed to dry on a level surface. To check for hyphal contamination, this was repeated on a plate of V0.1 medium, which does not support the growth of protoplasts (hypotonic medium). V0.1 plates were overlaid with VM0.1 at 37°C.

2.19.3 Protoplast transformation

Plasmid or cosmid DNA was isolated from *E. coli* DH5α or ET12567/pUZ8002 (see chapter 7) and resuspended at a concentration of 1 µg/µl. 1 µg of DNA was resuspended in 20 µl of distilled water for each transformation and 20 µl Lipofectamine™ 2000 (Invitrogen) added. Protoplasts were pelleted by centrifugation at 16000 x *g* for 2 min and gently resuspended in 100 µl P buffer. The DNA and lipofectamine mixture was added to the protoplasts and gently mixed. Tubes were incubated at room temperature for 2 min.

Protoplasts were pelleted by centrifugation at 16000 x *g* for 2 min and gently resuspended in 500 µl P buffer. Protoplasts were allowed to regenerate as described in 2.19.2 for 48 h. Plates were further overlaid with 8 ml VMS0.1 containing 800 mg/L apramycin (a final concentration of 50 µg/ml) and allowed to dry on a level surface. Incubation was continued at 30°C for several weeks before colonies were visible. Putative transformants were picked and streaked on V0.1 containing apramycin.

2.20 Generation of mutants by homologous recombination in *M. corallina*

The region of cosmid pIJ12125 encoding the gene to be deleted was replaced with the apramycin^R-oriT cassette amplified by high-fidelity PCR from pIJ773 using the appropriate primer pair (Table 2.8) as described in 2.12.2. The successful mutation of the cosmid to pIJ12125 Δ*ORF*::Apra^R-oriT was confirmed by PCR using the appropriate verification primer pair (Table 2.8) along with restriction digest to confirm the integrity of the rest of the cosmid. The mutant cosmid was transferred to *E. coli* ET12567 pUZ8002 and the resulting strain used to transfer the cosmid to *M. corallina* NRRL 30420 mycelium by conjugation. Ex-conjugants were selected on V0.1 containing 50 µg/ml apramycin. These were typically sub-cultured in VSPA containing 25 µg/ml apramycin for 6 days at 30°C to promote double-crossover recombination events. Mycelium from this culture was cultured to obtained single colonies on V0.1 containing 50 µg/ml apramycin. Single colonies were assayed for growth on V0.1 containing 50 µg/ml kanamycin. Clones sensitive to kanamycin (indicating a double-crossover recombination event) were selected and sub-cultured in VSPA containing 50 µg/ml apramycin for 6 days at 30°C from which mycelium was stored as a master cell bank at -80°C. A further sub-culture in VSPA containing 25 µg/ml apramycin was grown at 30°C for 48 h for preparation of genomic DNA which was analyzed by PCR using the appropriate verification primer pair. The absence of the wild type gene was also confirmed using gene internal primers. The genotype of the clones was further confirmed by Southern hybridisation analysis.

2.21 Complementation of Mutant Phenotypes

Complementation of mutant phenotypes was carried out via the introduction of the deleted open-reading frame *in trans* with expression from the native promoter of the open-reading frame in question. The vector was pIJ10706, a variant of pSET152, which contains the hygromycin resistance marker and integrates at the ΦC31 integration site in *M. corallina*.

To complement the deletion of *mibA*, the region between *mibX* and *mibA* (P_{mibA}) and the open-reading frame of *mibA* were amplified by high-fidelity PCR using primers LF078F and LF035_3. The resulting fragment was cloned into the *Bam*HI site of pIJ10706 to create pIJ12138. The genes *mibABCD* were removed from the construct pIJ12125 Δ*mibTU*::*aac(3)*IV by digestion with *Spe*I and *Xba*I yielding a 6155 bp product which was gel purified. This fragment was cloned into pIJ1239 (see below) cut with *Spe*I and *Xba*I to generate pIJ12362, in which P_{mibA} is upstream of *mibABCD* as in the native gene cluster (due to cloning in the unique *Spe*I site in P_{mibA}).

To complement the other deletion mutants two vectors, pIJ12139 and pIJ12140, were generated based on pIJ10706, which was modified to contain either the intergenic region between *mibX* and *mibA* (P_{mibA}; pIJ12139) or between *mibV* and *mibE* (P_{mibE}; pIJ12140). These regions were amplified by high-fidelity PCR using primers LF078F and LF078R, and LF082F and LF082R, respectively. These primers were designed to allow introduction of the fragment into pIJ10706 using *Bam*HI/*Xba*I or *Eco*RV/*Xba*I, respectively, as well as introducing a unique *Nde*I site. The respective open-reading frame and its cognate putative ribosome-binding site (GGAGG lying 9-12 bp upstream from the start codon (Kieser *et al.* 2000)) were amplified from pIJ12125 by high-fidelity PCR using the appropriate primer pair (Table 2.7). Primers were designed to allow the ORF to be cloned into the unique *Nde*I and *Xba*I sites in pIJ12139 and pIJ12140 such that they lay downstream of the respective promoter region. The inclusion of a stop codon in the region directly downstream of the ATG sequence of the *Nde*I site in each forward primer prevented the formation of spurious read-through proteins from this introduced start site.

To complement the deletion of the *mibX* (which is in the opposite orientation compared to the rest of the gene cluster apart from *mibW*) two PCR products were amplified by high-fidelity PCR using primers LF097F and LF097R or LF97F and LF102R. These fragments contain, respectively, the intergenic region between *mibX* and *mibA* (in the inverse orientation P_{mibX}) followed by *mibX* alone or *mibXW*. The fragments were blunt-end cloned into the *Eco*RV site of pIJ10706 to generate pIJ12349 and pIJ12350, respectively.

All constructs were confirmed by Sanger sequencing. The resulting constructs, along with the empty vector controls (promoter only), were mobilised into the respective mutant strain via conjugation from *E. coli* ET12567 pUZ8002 as described in section 2.17.2.

2.22 RNA methods

2.22.1 Isolation of RNA from *S. lividans*

S. lividans spores (10^9) were inoculated into 10 ml V medium in universal tubes containing baffles, with lids taped loosely for aeration, and were grown for 26 h at 30°C with shaking at 250 rpm. 1 ml culture was harvested, mixed with 2 ml RNAprotect solution (Qiagen), vortexed for 5 s and allowed to stand for 5 min at room temperature. Mycelium was collected by centrifugation at 3000 x *g* for 10 min and the supernatant removed. Mycelial pellets were stored at -80°C for up to 2 weeks before the extraction of RNA.

Mycelial pellets were resuspended in 200 µl TE buffer containing 15 mg/ml lysozyme. Tubes were incubated at room temperature for 1 h. 700 µl of pre-cooled RLT buffer (containing 10 µl per ml β-mercaptoethanol; Qiagen) were added. Mycelium was sonicated on ice for 3 cycles of 5 s on and 5 s off at an amplitude of 5 microns. The resulting lysate was cleared by phenol chloroform-isoamylalcohol pH8 extraction. The aqueous phase was removed to a 2 ml tube and 700 µl chloroform added. The tube was vortexed to mix thoroughly and centrifuged at 16000 x *g* for 5 min. The aqueous phase was removed to an RNase-free 2 ml tube and 440 µl 100% ethanol added. The solution was mixed well and was applied to an RNeasy mini column (Qiagen). The RNA was purified following the manufacturer's instructions and by performing an on-column DNaseI digestion. RNA was eluted from the column twice with 30 µl of RNase-free distilled water. RNA was stored at -80°C.

2.22.2 Isolation of RNA from *M. corallina*

M. corallina strains were grown in VSPA medium as pre-cultures for 48-72 h. Mycelial density was estimated by optical density at 450 nm and cultures were inoculated to a starting OD_{450} of 0.1-0.2. 2.5-5 ml culture were harvested at the appropriate time points and stored using RNAprotect solution (Qiagen) following the manufacturer's instructions. Mycelial pellets were resuspended in 10 mM Tris-HCl pH8.0. 250 µl of resuspended mycelium were added to 700 µl of pre-cooled RLT buffer (containing 10 µl per ml β-mercaptoethanol; Qiagen) in 2 ml tubes containing approximately 300 mg 0.1 mm diameter silica beads (Biospec Products Inc.). Mycelium was lysed in a FastPrep machine (Thermo Scientific) at speed 6.5 for 30 s. The resulting lysate was cleared by successive phenol chloroform-isoamylalcohol pH8 extractions. The cleared lysate was applied to an RNeasy mini column (Qiagen) and RNA purified following the manufacturer's instructions

and by performing an on-column DNaseI digestion. RNA was eluted from the column twice with 30 µl of RNase-free distilled water. RNA was stored at -80°C.

2.22.3 DNase1 treatment of RNA

To ensure RNA samples were free from genomic DNA contamination prior to RT-PCR approximately 10 µg purifed RNA were further treated with 20 U RNase-free DNaseI (Promega) in a volume of 100 µl at 37°C for 1 h. The RNA was re-purified using the RNeasy mini kit (Qiagen) and following manufacturer's instructions for RNA clean-up. To confirm the absence of DNA in RNA samples, standard PCR was carried out using 1 µl RNA as a template with Taq polymerase, the primers LF027F and LF027R, with 30 cycles. 10 ng NRRL 30420 gDNA were used as a positive control.

2.22.4 Confirming RNA quality

2.22.4.1 Checking for DNA contamination

To confirm the absence of DNA in RNA samples, standard PCR was carried out using 150-300 ng RNA as a template with Taq polymerase, the primers LF027F and LF027R, with 30 cycles. 10 ng NRRL 30420gDNA were used as a positive control.

2.22.4.2 Checking concentration and quality using Nanodrop

The quantity and quality of RNA was initially determined using Nanodrop (Thermo scientific). For pure RNA a 260/280 ratio between 1.9 and 2.3 was expected and a 260/230 ratio preferably greater than 1.8 (ideally greater than 260/280).

2.22.4.3 Checking concentration and quality using agarose gel electrophoresis

RNA was checked using a 1% TBE agarose gel prepared RNase-free and containing 2 g/L sodium iodoacetate and 0.5 µg/ml ethidium bromide. Approximately 750 ng RNA were separated on the gel by electrophoresis. Typically 23S and 16S bands were visible and often 5S and aggregates.

2.22.4.4 Checking concentration and quality using Bioanalyser

The quantity and quality of RNA was determined using the Experion Bioanalyser (Bio-Rad) following manufacturer's instructions.

2.22.5 One-step reverse transcriptase PCR

One-step reverse transcriptase PCR was carried out using the One-step RT-PCR kit (Qiagen) following manufacturer's instructions and using primers as listed in Table 2.9. RNA samples were thawed on ice and 0.5 µg RNA was made up to 5 µl with RNase-free water. The following master mix was set-up:

Component	Volume (µl)
5x one step RT-PCR buffer (Qiagen)	10
Rnase-free dNTP mix (40 mM ; Qiagen)	2
5xQ-solution (Qiagen)	10
Primer A (10 µM)	3
Primer B (10 µM)	3
One-step RT-PCR Enzyme Mix (Qiagen)	2
Rnase free H_20	to 45

45 µl master mix were aliquoted into each PCR tube (0.5 ml individual tubes; RNase-free; Thermo Scientific). 5 µl RNA template were added to the respective tubes. Each 50 µl reaction mixture was split into 2x25 µl in 0.5 ml tubes. Samples for reverse transcriptase treatment (RT samples) were placed into a PCR machine and incubated at 50ºC for 30 min. Samples acting as controls for the presence of gDNA (No RT samples) were kept on ice until the PCR machine reached 95ºC (see below).

50ºC 30 min (Reverse Transcriptase)

95ºC 15 min (Inactivation of RT enzyme and hot-start for polymerase)

94ºC 1 min
56ºC 1 min } 35 cycles
72ºC 1 min

72ºC 10 min

2.22.6 Two-step reverse transcriptase PCR

1 µg RNA was converted to cDNA using Superscript III 1st strand synthesis Supermix (Invitrogen) following manufacturer's instructions. Reactions were carried out as follows:

Component	Volume (µl)
2x Reaction Mix (Invitrogen)	10
Superscript III 1st strand RT enzyme mix (Invitrogen)	2
Template RNA (1 µg)	x
Rnase-free dH_2O	to 20

25°C 10 min

42°C 120 min

50°C 30 min

55°C 30 min

85°C 5 min

1 µl RNase H (Invitrogen) was added to each reaction with incubation at 37°C for 20 min. cDNA from the reverse transcriptase reaction was diluted 1 in 10 in H_2O and was determined by nanodrop to contain approximately 60-70 ng cDNA per reaction. PCRs were carried out using the primers in Table 2.9 and following the protocol for standard PCR with Taq polymerase (section 2.6.1) using 30 cycles of amplification and annealing temperatures of 56°C or 58°C depending on the primer pair. The PCR products were checked by analysing 12.5 µl of the PCR on a 2% TBE agarose gel by electrophoresis. As an internal control, a homolog (91% nucleotide identity) of *S. coelicolor hrdB* was identified from the 454 contig database and used to design primers LF106F and LF106R (Table 2.9).

2.23 Bacterial-2-hybrid analysis in *E. coli*

2.23.1 Cloning strategy

XP458 (pT25) contains a multiple-cloning site (MCS) preceded by a fragment of the gene *cya* encoding half of the catalytic domain (T25) of CyaA from *Bordetella pertussis* (Karimova *et al.* 1998). XP461 is XP458 containing the leucine zipper fragment. These vectors were obtained from Marij Frederix (John Innes Centre). The other half of the protein (T18) is encoded in pUT18 and is preceded by a MCS. pUT18C is similar to

pUT18 except that the MCS follows the *cya* gene allowing the formation of C-terminal rather than N-terminal fusion. These vectors were obtained from Richard Little (John Innes Centre). The leucine zipper fragment from XP461 was removed by *Kpn*I digestion and was cloned into the *Kpn*I site present in both pUT18 and pUT18C to generate positive control plasmids pUT18-zip and pUT18C-zip.

mibX was amplified by high-fidelity PCR from pIJ12125 using the primers (Table 2.7) LF101F and LF101R (no stop codon included) and LF101F and LF101R2 (stop codon included), which introduce *Bam*HI and *Kpn*I sites into the resulting PCR products. The PCR products were gel purified and digested with *Bam*HI and *Kpn*I. The resulting inserts were ligated into pUT18 and pUT18C cut with *Bam*HI and *Kpn*I, respectively, to generate pIJ12367 and pIJ12368. *mibW* was amplified by high-fidelity PCR from pIJ12125 using three primer sets; LF102F and LF102R (full-length *mibW*), LF102F and LF103R (5' 219 nt of *mibW*) and LF103F and LF102R (3' 549 nt of *mibW*), which introduce *Bam*HI and *Kpn*I sites into the resulting PCR products. The PCR products were gel purified and digested with *Bam*HI and *Kpn*I. The resulting inserts were ligated into XP458 (pT25) cut with *Bam*HI and *Kpn*I to generate pIJ12369, pIJ12370 and pIJ12371 respectively. All constructs were confirmed by Sanger sequencing.

2.23.2 Visualisation of phenotypes on MacConkey/Maltose agar

E. coli BTH101 was streaked from a glycerol stock on LB agar containing 100 µg/ml streptomycin, 0.1 mM IPTG and 40 µg/ml X-gal and incubated overnight at 37°C. A white colony was selected and inoculated into 5 ml LB and grown overnight at 37°C. This culture was used to inoculate LB 1 in 50 and was grown for 3 h at 37°C until at an OD_{600} of 0.4-0.6. Electrocompetent cells were made from this culture as described in 2.5.8. 50 µl aliquots of electrocompetent cells were transformed with 25 ng DNA of each of a pair of constructs for which an interaction was to be measured. In most cases the control interactions used were a positive control (leucine zipper containing plasmids) and negative controls (empty vector plasmids with each test plasmid and with each other). 100 µl and 900 µl of each transformation reaction were plated out on MacConkey/Maltose medium containing 0.5 mM IPTG, 25 µg/ml chloramphenicol and 100 µg/ml carbenicillin. Plates were incubated at 30°C for several days until the colour of colonies had developed fully.

2.23.3 Quantification of interactions using β-galactosidase assay

The quantification of β-galactosidase activity was carried out as described in (Slavny *et al.* 2010). Two clones from each interaction plate were selected and inoculated into 5 ml LB

containing 25 µg/ml chloramphenicol and 100 µg/ml carbenicillin and were grown at 30°C for 9 h. 100 µl of these cultures were inoculated into 7 ml LB containing 0.5 mM IPTG, 1% glucose, 25 µg/ml chloramphenicol and 100 µg/ml carbenicillin in plastic Universals (7 ml total volume). These were grown for 16 h at 30°C and then placed on ice. To each reaction test tube was added 970 µl lysis buffer followed by 30 µl of the appropriate overnight culture. 20 µl chloroform were added to each tube and the tubes vortexed for 10 s to mix. Tubes were incubated at 30°C for 10 min until the solution was clear. The OD_{600} of the overnight cultures was measured by transferring 300 µl of each culture to each well of a 96-well microtiter plate with 300 µl LB as a blank. The OD_{600} measurement was carried out using a PowerWave 340 plate reader (BioTek). The test tubes were kept at 30°C and 200 µl 4 mg/ml O-Nitrophenyl β–D-Galactopuyranoside added to the first tube and the time was recorded. When a yellow colour appeared 500 µl of 1 M Na_2CO_3 was added and the time recorded. The tube was placed on ice and the total reaction time calculated. This was repeated for all samples. 300 µl of each sample were transferred to each well of a 96-well microtiter plate and the OD_{420} and OD_{550} measured for each using 200 µl lysis buffer and 100 µl Na_2CO_3 as a blank. The measurements were carried out using a PowerWave 340 plate reader (BioTek).

The β-galactosidase activity (in Miller Units) of each sample was calculated as:

$$= \frac{1000 \times f}{t \times V \times OD_{600}}$$

where $f = OD_{420} - (1.75 \times OD_{550})$

t = total reaction time (min)

v = the volume of culture added (0.03 ml)

The average activity was calculated from the two clones of each strain and the value for each clone used to generate error bars.

2.24 Luciferase assays

The intergenic region between *mibX* and *mibA,* with and without the *mibX* open-reading frame, was amplified by PCR using upstream primers carrying an *Eco*RI site and downstream primers carrying a *Bam*HI site in two orientations (see Figure 7.37) The primers used were LF096F and LF096R (pIJ12341), LF096F2 and LF096R (pIJ12342), LF097F and LF097R (pIJ12343) and LF097F and LF097R2 (pIJ12344) (Table 2.7). The

resulting PCR fragments were cloned into *Eco*RI-*Bam*HI-cut pIJ5972, an integrative, *Streptomyces* promoter-probe plasmid based on TTA codon-free derivatives of the *luxAB* reporter genes (Le *et al.* 2009). The resulting constructs along with pIJ5972 were transferred by conjugation into *S. coelicolor* M1146 (Gomez-Escribano *et al.* 2010). Plasmid-containing strains were grown on Difco Nutrient Agar in single wells of a 25-well plate (10 cmx10 cm; Sterilin) for 2 days. Each well was inoculated with approximately 5×10^6 spores. Plates were exposed to filter paper impregnated with n-decanal for 5 min and luciferase activities were observed using a NightOwl camera (Berthold) equipped with WinLight software (Berthold) using a 1 min exposure time.

Chapter 3 - Identification and Sequence Determination of the Microbisporicin Biosynthetic Gene Cluster

3.1 Introduction

The initial aim of the project was the identification and characterisation of the microbisporicin gene cluster from the producer strain *Microbispora corallina* NRRL 30420. As a prelude to the identification of the gene cluster for microbisporicin production, this chapter will also describe our attempts to characterise the available strains of *M. corallina*.

As mentioned in chapter 1 the species *Microbispora corallina* (Nakajima *et al.* 1999) is currently represented by four strains: DSM 44681 (DF-28; JCM 10266), DSM 44682 (DF-32^T; JCM 10267) (Nakajima *et al.* 1999), NRRL 30420 (Lee 2003) and ATCC PTA 5024 (Lazzarini *et al.* 2005). Strains DSM 44681 (DF-28) and DSM 44682 (DF-32^T) were the first described members of this unusual species and were isolated from a deciduous dipterocarp forest in Thailand (Nakajima *et al.* 1999). To date no anti-bacterial activities or lantibiotic-like compounds have been described for these two strains. NRRL 30420 was isolated from the soil roots of *Arachis hipogea* (Peanut plant) in Indonesia and reported to make the compounds MF-BA-1768$_{\alpha 1}$ and MF-BA-1768$_{\beta 1}$ (Lee 2003). The location of the isolation of ATCC PTA 5024 is not clear but it was reported to make compounds 107891 A1 and A2 (Lazzarini *et al.* 2005). These compounds were asserted to be of different molecular origin to MF-BA-1768$_{\alpha 1}$ and MF-BA-1768$_{\beta 1}$ based on physico-chemical properties (Lazzarini *et al.* 2005). One aim for the initial characterisation of NRRL 30420 was to determine whether this assertion was correct and whether two different lantibiotics (resulting from two separate biosynthetic gene clusters) are produced by the two *M. corallina* strains.

NRRL 30420 and ATCC PTA 5024 were identified as *M. corallina* species on the basis of 16s DNA sequence similarity to DSM 44681 (DF-28) and DSM 44682 (DF-32^T). The strains NRRL 30420, DSM 44681 and DSM 44682 were acquired from the respective culture collections. ATCC PTA 5024 was unavailable for this work and thus any

comparisons made with this strain are based on the details provided by (Lazzarini *et al.* 2005).

A number of methods have been conventionally applied to the identification of biosynthetic gene clusters in actinomycetes, however they can often be time-consuming or carry other disadvantages. For example, a mutant of a producer strain blocked in the production of the compound, with the assumption that the mutation lies within the biosynthetic gene cluster of interest, can be used to screen for complementing fragments of the wild type genome allowing the identification of biosynthetic genes within the cluster (Rhodes *et al.* 1981). However, this approach relies on the availability of such a mutant and requires that methods have been established for genetically manipulating the strain of interest. This was not the case for *M. corallina* in which no such mutant was available and for which there were no methods for genetic manipulation of the strain. Other approaches, such as cloning linked resistance genes or directly cloning the biosynthetic gene cluster, require a suitable heterologous expression host and assume that the genes will be appropriately expressed in this host. They require large-scale screening and an appropriate screen for resistance or bioactivity, respectively. Furthermore, this method assumes that the resistance genes will be closely linked to the biosynthetic genes, which is not always the case (Birmingham *et al.* 1986). Another approach is to generate a cosmid or BAC library which is then screened using a degenerate probe (Zhao *et al.* 2006). This relies on having sufficient information about the gene cluster as well as about the codon usage of the organism. Since *M. corallina* is a rare actinomycete which has not previously been studied in any molecular detail, and microbisporicin is the first example of a type AI lantibiotic from an actinomycete, it would not be easy to design such degenerate probes with any degree of confidence. Furthermore, degenerate probes can often give non-specific or negative results, as was the case in the detection of the cypemycin lantibiotic gene cluster (Jan Claesen, personal communication). These conventional methods, although useful under certain circumstances, were not well-suited to identifying the microbisporicin gene cluster from *M. corallina* and so a novel method of genome scanning was applied which will be described in this chapter. Briefly, this involves using new rapid genome sequencing technologies such as Solexa (Illumina) and 454 (Roche) to identify genes likely to be part of the biosynthetic gene cluster. This information can then be used to design specific probes to identify cosmids containing the gene cluster from a cosmid library. Both Solexa and 454 sequencing technologies were available at the John Innes Centre (JIC) at the outset of this study and consequently both methods were used for the identification of the microbisporicin gene cluster to compare the usefulness of the two sequencing technologies for genome scanning in actinomycetes.

3.2 *M. corallina*

3.2.1 Description of growth

Microbispora corallina NRRL 30420 was found to grow as bald mycelium with a red/orange/brown colouring on the standard agar growth medium selected for this work; medium V0.1 (Marcone *et al.* 2010b) (Figure 3.1B). The production of white/pink aerial mycelium was occasionally observed after very long periods of incubation (10-14 days) on V0.1 but was often observed when NRRL 30420 was grown on oatbran agar medium (Figure 3.1A). *Microbispora corallina* DSM 44681 and DSM 44682 were also found to grow as mainly bald mycelium on V0.1 but aerial mycelium formation was more routinely observed. As described in 3.2.2, these strains were found to produce pairs of spores on aerial mycelium when grown on oatbran agar medium. All of the *M. corallina* strains grew slowly on agar media, taking 7-14 days to produce workable colonies (1-3mm diameter).

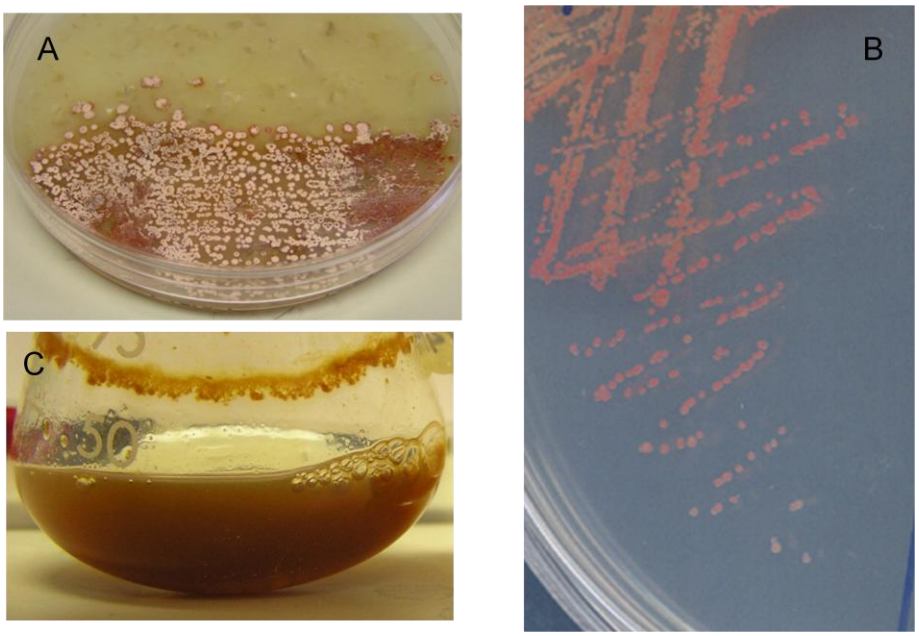

Figure 3.1 Growth of *M. corallina* NRRL 30420 on different media. A; oatbran agar medium, B; V0.1 agar medium, C; VSPA liquid medium with four glass beads and shaking at 230rpm. All cultures were grown at 30^{o}C.

An analysis of the growth rate of *M. corallina* NRRL 30420 in liquid culture was carried out by measuring the optical density of the culture at 450nm. In the standard VSPA liquid medium used for this study, *M. corallina* NRRL 30420 grew in a dispersed manner when cultured in the presence of glass beads (Figure 3.1C). *M. corallina* NRRL 30420 entered exponential growth phase after approximately 8-12 hours. Exponential growth continued for up to about 72 hours post-inoculation (about 60 hours in total) (Figure 3.2).

Microbisporicin production was assayed at each time point by bioassay of culture supernatant against *Micrococcus luteus*. Under the conditions used, production of microbisporicin was first detected 46-48 hours post-inoculation and appeared to peak at the entrance to stationary phase at 72 hours post-inoculation (Figure 3.2). Bioactivity was still detectable 14 days post-inoculation (the latest time point sampled) suggesting that microbisporicin is stable in the culture supernatant after a prolonged period in stationary phase.

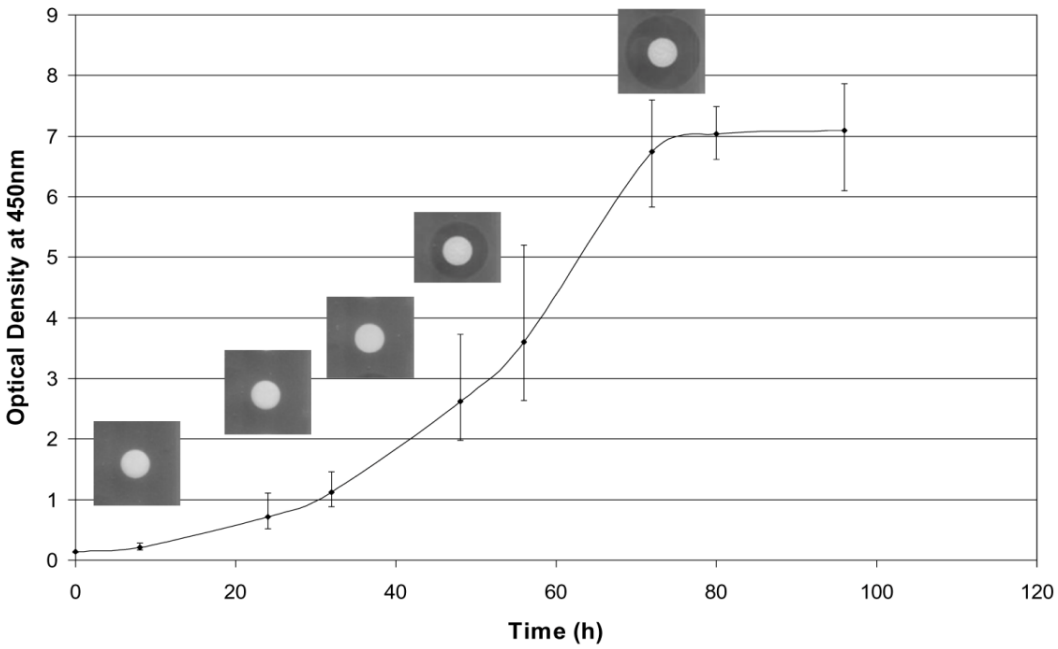

Figure 3.2 Analysis of growth rate and microbisporicin production in *M. corallina* NRRL 30420 grown in VSPA with four glass beads. The growth curve shows the average optical density measured at 450nm of three independent cultures for each time point shown. Error bars indicate the variability between cultures. Inlaid are typical images of bioassays against *M. luteus* using supernatants collected at the respective time points.

3.2.2 Scanning Electron Microscopy

Scanning electron microscopy was carried out (by Kim Findlay, JIC) to investigate the colony structure and sporulation state of each strain. In the case of NRRL 30420, aerial hyphae were found and in a few instances potential immature spores were identified (on oatbran medium); however mature spores were not found for this strain under the conditions used (Figure 3.3 C&D). Pairs of spores attached to aerial hyphae were found for DSM 44681 and DSM 44682 grown on oatbran medium (Figure 3.3 A&B).

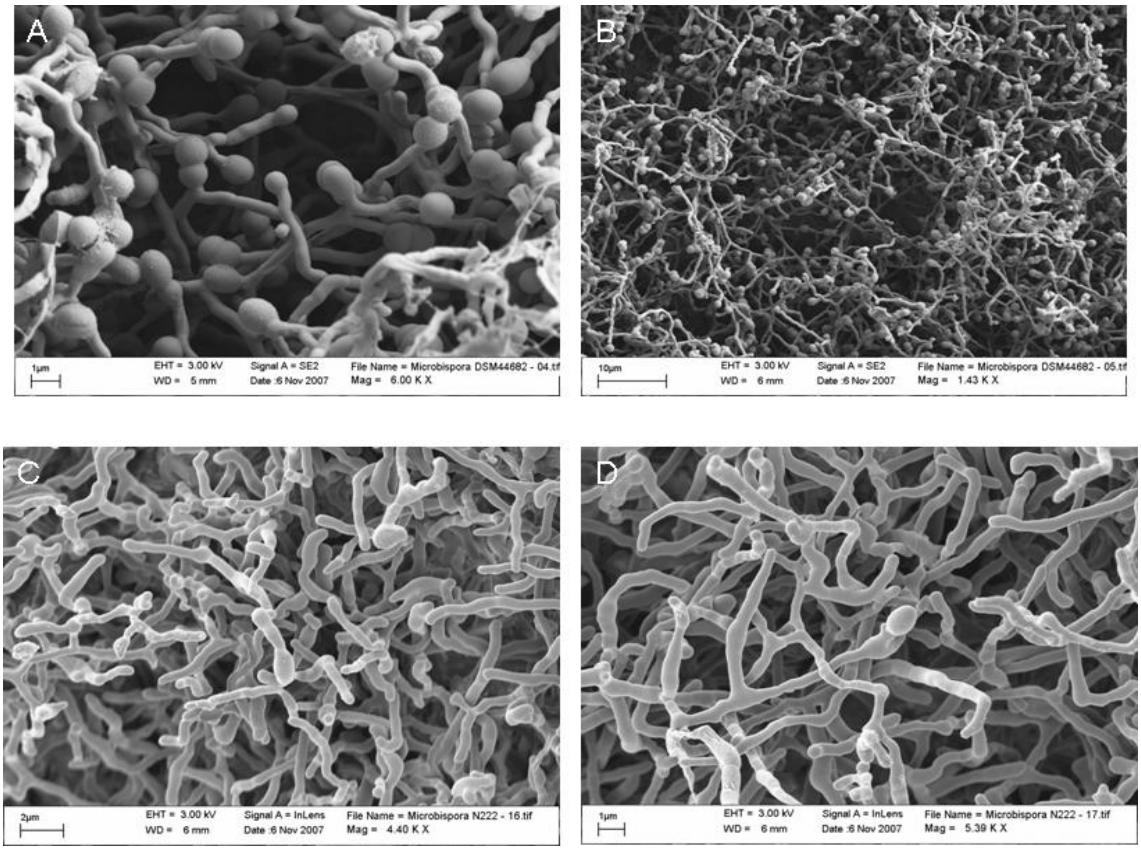

Figure 3.3 Example images from scanning electron microscopic analysis of *M. corallina* strains grown on oatbran medium. Scale is given in the bottom left corner of each image. **A;** DSM 44682 colony at 6K x magnification showing spores and aerial hyphae; **B;** DSM 44682 colony at 1.43K x magnification showing spores and aerial hyphae; **C;** NRRL 30420 colony at 4.4K x magnification showing aerial hyphae; **D;** NRRL 30420 colony at 5.3K x magnification with a possible immature spore at the centre of the image. Scanning electron microscopy carried out by Kim Findlay (JIC).

3.2.3 Production conditions for microbisporicin and description of MALDI-ToF mass spectrometry results

Production of a bioactive compound by *M. corallina* NRRL 30420 could be detected when the strain was grown on solid or in liquid media. *M. corallina* NRRL 30420 grown on V0.1 for 5 days was overlaid with the target organism *M. luteus* in soft nutrient agar and the plates incubated at 30°C over-night. Large zones of inhibition of growth of *M. luteus* were clearly observed around the growing producer organism (Figure 3.4). When the producing organism was grown for 6 days or more, growth of the target organism was completely absent from bioassay plates indicating the potency of this compound for Gram-positive organisms (data not shown). By contrast, neither *M. corallina* DSM 44681 or DSM 44682 were capable of producing a bioactive compound that could inhibit the growth of *M. luteus* under the same conditions and even when strains were grown for up to 14 days before applying the target organism (Figure 3.5).

Figure 3.4 *M. corallina* NRRL 30420 was tested for production of antibacterial compounds in a plate bioassay against the target organism *M. luteus*. *M. corallina* was grown for 5 days on V0.1 medium, followed by overlay with *M. luteus* in soft nutrent agar. The plate was incubated overnight at 30°C.

Production of a bioactive compound by NRRL 30420 was also assayed in the liquid growth medium VSPA by sampling the supernatant after 7 days fermentation and applying it to an antibiotic assay disc placed on a lawn of *M. luteus* (Figure 3.6 inset). The supernatant was subjected to MALDI-ToF mass spectrometry in the range of 0-4000 Da to identify compounds that could be responsible for the bioactivity (MALDI-TOF carried out by Dr. Gerhard Saalbach and Dr. Mike Naldrett (JIC proteomics)) (Figure 3.6).

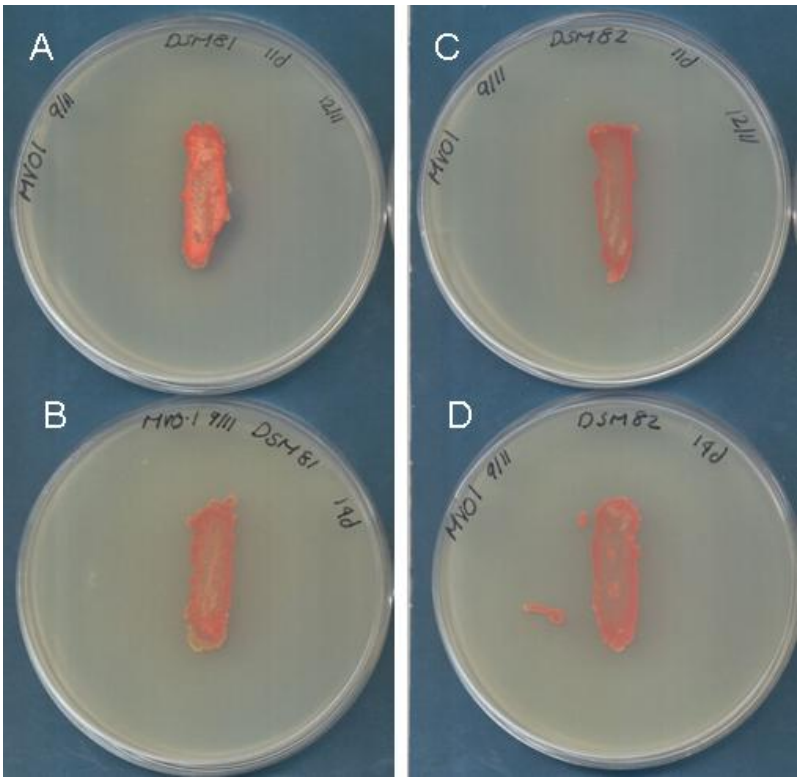

Figure 3.5 DSM 44681 (A & B) and DSM 44682 (C & D) were tested for production of antibacterial compounds in a plate bioassay against the target organism *M. luteus*. The *M. corallina* strains were grown for 11 (A&C) or 14 (B&D) days on V0.1 medium, followed by an overlay with *M. luteus* in soft nutrent agar. The plates were incubated overnight at 30°C.

The reported masses for the four reported lantibiotic-like compounds produced by *M. corallina* strains (hereafter collectively called microbisporicin) are 2180.81 Da (MF-BA-1768$_{\beta1}$), 2214.880 Da (MF-BA-1768$_{\alpha1}$) (Lee 2003), 2230.71 Da (107891 A2) and 2246.71 Da (107891 A1) (Lazzarini *et al.* 2005; Castiglione *et al.* 2008) (Table 3.1). As discussed in Chapter 1 the known structures of 107891 A1 and A2 (Lazzarini *et al.* 2005; Castiglione *et al.* 2008) and the mass differences between these compounds and MF-BA-1768$_{\alpha1}$ and MF-BA-1768$_{\beta1}$ led us to the hypothesis that MF-BA-1768$_{\alpha1}$ represents a non-hydroxylated form of microbisporicin while MF-BA-1768$_{\beta1}$ represents a non-hydroxylated and non-chlorinated form (Figure 1.17). Since all four masses have been described previously as being produced by closely related (over 97% 16s rDNA identity) *M. corallina* strains (Lee 2003; Lazzarini *et al.* 2005), we hypothesise that microbisporicin results from a single prepropeptide produced by a single biosynthetic gene cluster (which is highly similar in both *M. corallina* producer strains) and that the composition of the microbisporicin complex varies with the culture conditions used. This is contrary to the previous assertion that NRRL 30420 and ATCC-PTA-5024 are responsible for producing two separate lantibiotics (Lazzarini *et al.* 2005).

A number of compounds with masses in the region of 2215 to 2300 were detected in the supernatant of NRRL 30420 grown for 7 days in VSPA liquid medium that were not identified in a medium only control (Figure 3.6). Samples for MALDI-ToF mass

spectrometry were acidified prior to application on the matrix-containing plate such that in all cases the ions identified represent the protonated form of the compound (i.e. $[M+H^+]$). However it is also common to see the sodium or potassium adducts of the compound, which are 23 and 39 Da heavier than the expected molecular weight of the compound, respectively. The observed spectrum consists of multiple peaks, the m/z ions of which can be attributed to the protonated and sodium/potassium adducts of MF-BA-17681$_{\alpha 1}$, 107891 A1 and A2 (Table 3.1 and Figure 3.6). However, several larger ions were also detected with incremental mass increases of 16 Da that are likely caused by oxidation of the lanthionine bridges in microbisporicin (Wilson-Stanford *et al.* 2009). This has previously been observed for MALDI-ToF spectra of the lantibiotic actagardine (Robert Bell, personal communication). The mass change associated with hydroxylation of proline to convert MF-BA-17681$_{\alpha 1}$ into 107891 A2 and then A1 is the same as that due to the oxidation of the lanthionine bridges and thus it is not possible to be sure, using this technique, that 107891 A2 and A1 are actually produced under these fermentation conditions. The only one of the four previously reported variants that was not detected at all under these conditions was MF-BA-1768$_{\beta 1}$ (Figure 3.6). MF-BA-1768$_{\beta 1}$ is expected to be the non-chlorinated form of microbisporicin, suggesting that only the fully chlorinated form of the compound is produced under the culture conditions used in these experiments.

s

Table 3.1 The predicted masses of variants of microbisporicin. The theoretical molecular formulae of each compound (determined from the known structures of 107891 A1 and A2 and predicted for MF-BA-1768$_{\alpha 1}$ and MF-BA-1768$_{\beta 1}$) are given along with the theoretical (determined from the molecular formulae) and reported molecular weights in Daltons (Lee 2003; Lazzarini *et al.* 2005). The expected m/z peaks for the protonated [M+H$^+$], sodium [M+Na$^+$] and potassium [M+K$^+$] adducts of each compound are shown. For simplicity only masses resulting from the oxidation of a single lanthionine bridge (with 1 O) are shown (see text).

	Theoretical Molecular Formula	Theoretical Mw	Reported Mw	[M+H+]	with 1 O	[M+Na+]	with 1 O	[M+K+]	with 1 O
MF-BA-1768$_{\beta 1}$	C94S5O25N26H128	2180.82	2180.81	2181.81	2197.81	2203.81	2219.81	2219.81	2235.81
MF-BA-1768$_{\alpha 1}$	C94S5O25N26H127Cl	2214.78	2214.88	2215.85	2231.85	2237.84	2253.83	2253.83	2269.83
107891-A2	C94S5O26N26H127Cl	2230.77	2230.71	2231.85	2247.85	2253.83	2269.83	2269.83	2285.81
107891-A1	C94S5O27N26H127Cl	2246.77	2246.71	2247.85	2263.83	2269.83	2285.81	2285.81	2301.79

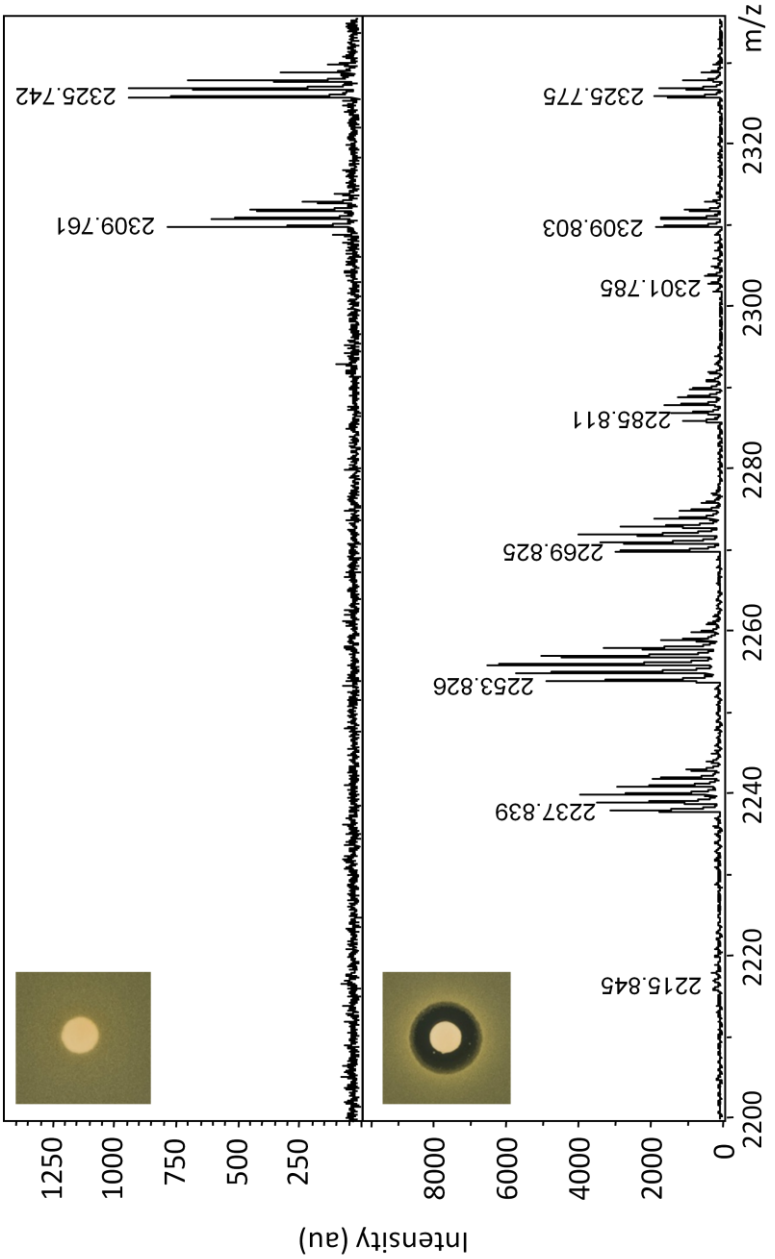

Figure 3.6 An example of a MALDI mass spectrometry analysis of a VSPA medium only control (top panel) and of the supernatant from NRRL 30420 grown for 7 days in VSPA and found to give anti-bacterial activity against *M. luteus* (inset). Samples are acidified prior to MALDI so all m/zs represent the molecular weight +1 Da. Peak splitting occurs due to the presence of isotopes of atoms within the compound. The monoisotopic m/z is given above the peak. The expected identities of the lowest m/z isotopomeric ion within each peak envelope are shown in Table 3.1.

3.3 Solexa Sequence data

In total seven lanes of Solexa sequence data were acquired from gDNA prepared from *M. corallina* NRRL 30420. The generation of the Solexa sequence data used in this study (1G Genome Analyser, Illumina) was based on read lengths of 36 nucleotides which were assembled using Velvet (Zerbino *et al.* 2008). The sequence was assembled by Dr. David Studholme (The Sainsbury Laboratory) as three separate batches of contigs (3/9/07, 6/9/07 and 2/11/07) using different amounts of data and parameters, which altered the length of the contigs and the quality of the sequence (Figure 3.7). The contigs generated for *M. corallina* gDNA were on average quite small (204 nucleotides) which suggests that the bioinformatic software may have had difficulties in assembling high GC content sequence. This is also reflected in the overall GC content of the assembled data, which is only 67.82 mol%GC, significantly less than the overall GC content of individual reads (72 mol%GC). Despite the small contig sizes in this data set it was possible to use the data to search for the microbisporicin biosynthetic gene cluster.

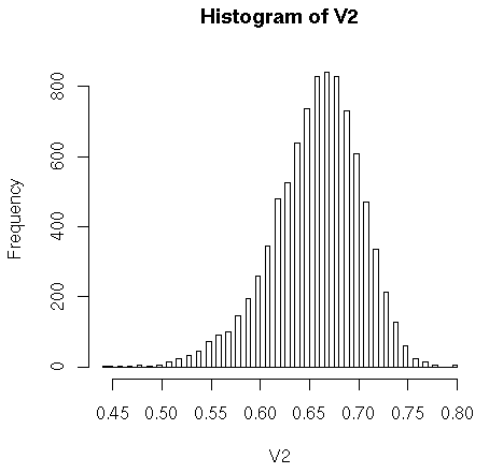

Figure 3.7 Summary of 6/9/07 Solexa data assembly. The left panel shows a histogram of the GC content for the assembled contigs giving a mean GC content of 67.82%. The right panel gives summary statistics for the data assembly including the total number of assembled contigs and information about contig lengths.

3.3.1 Solexa Sequence BLAST Results

The assembled contigs for the three separate data sets were used to construct a database that could be interrogated for homologs of known lantibiotic biosynthetic genes using an NCBI-type BLAST algorithm (Altschul *et al.* 1990) with either a nucleotide (BlastN) or amino acid (tBlastN) input (databases constructed by Dr. Govind Chandra (JIC)). Targets for BLAST searches were selected from lantibiotic biosynthetic genes from known clusters in other bacteria, such as homologs in *Streptomyces coelicolor* (SCO6929; uncharacterised *lanC* homolog) or genes from well-studied clusters such as the subtilin biosynthetic gene cluster from *Bacillus subtilis*. Based on structural similarities, microbisporicin was predicted to fall into the type A(I) lantibiotic family (Lee 2003; Lazzarini *et al.* 2005; Castiglione *et al.* 2008) that possess LanB and LanC enzymes for lanthionine bridge formation (Chatterjee *et al.* 2005). LanB and LanC enzymes are reasonably well conserved between type A(I) clusters (typically around 30% amino acid sequence identity) (Chatterjee *et al.* 2005) making them appropriate search inputs for identifying lantibiotic gene clusters. Furthermore, microbisporicin contains the *S*-[(*Z*)-2-aminovinyl]-D-cysteine modification known in other lantibiotics to be catalysed by a flavoprotein LanD enzyme (Kupke *et al.* 1992; Majer *et al.* 2002). These enzymes are well-conserved in the epidermin and mersacidin gene clusters in which they have been characterised (Chatterjee *et al.* 2005). Finally, the incorporation of chlorine at tryptophan-4 in microbisporicin suggests the involvement of a member of the FAD-dependent tryptophan halogenase class of enzymes typified by PrnA (*Pseudomonas fluorescens*) (Keller *et al.* 2000) and PyrH (*Streptomyces rugosporus*) (Zehner *et al.* 2005). Due to the infrequent occurrence of such enzymes in bacterial genomes (all identified members of this class are associated with secondary metabolite synthesis (van Pee *et al.* 2006)), they are also good targets for BLAST searches. Other components of characterised lantibiotic gene clusters, such as ABC transporters and regulatory proteins, are not optimal for BLAST searches since they show high levels of homology to other members of these families that are not associated with lantibiotic gene clusters and that are abundant in bacterial genomes.

Through analysis of the three data sets, a number of contigs were identified containing homologs of the target genes and proteins discussed above. Two contigs showed overlapping sequence and were manually assembled. The identified genes were homologs of *lanC* ((contig_12864 3/9/07) and (contig_3259 6/9/07)), *lanB* (contig_9864 6/9/07) and *lanD* (contig_9897 6/9/07) genes (Figure 3.9). Two contigs were identified

with homology to the tryptophan halogenase PyrH ((contig_4619 6/9/07) and (contig_5675 6/6/07)). Using the expected unmodified sequence for the precursor peptide of microbisporicin (VTSWSLCTPGCTSPGGGSNCSFCC; inferred from the final modified structure (Lazzarini *et al.* 2005; Castiglione *et al.* 2008) as a BLAST search input did not yield any contigs potentially containing the prepropeptide encoding gene *mibA*.

3.3.2 Southern Blot Linkage Analysis

Due to the small size of the identified contigs it was not possible with this information alone to confidently conclude that the identified open-reading frames were genetically-linked and therefore likely to be part of a gene cluster. To determine whether this might be the case, Southern blot hybrisation analysis was carried out. NRRL 30420 gDNA was digested with the restriction enzymes *Bam*HI, *Pst*I and *Bgl*II, and subjected to Southern blot hybridisation using probes LF001 (contig_12864 3/9/07), LF002 (contig_3259 6/9/07), LF004 (contig_9897 6/9/07) and LF006 (contig_5675 6/6/07) generated by PCR amplification from an *M. corallina* gDNA template (using the primer pairs of the same numbers; see Figures 3.9 and 3.12 for primer binding sites and Chapter 2 for oligonucleotide sequences). Linkage with the homolog of *lanB* (contig_9864 6/9/0) was not examined as the available contig sequence was too short to amplify a specific probe. Primers LF005F and LF005R designed from the sequence of one contig ((contig_4619 6/9/07) containing a gene putatively encoding a tryptophan halogenase homolog failed to amplify a product by PCR using NRRL 30420 gDNA as a template; this was later found to be due to contig misassembly (see 3.4.1).

The Southern blot hybridisation analysis indicated a close genetic linkage between the two *lanC* contigs and the *lanD* contig but not with the tryptophan halogenase homolog (Figure 3.8). The two *lanC* probes (LF001 and LF002) and the *lanD* probe (LF004) all hybridised to *Bam*HI fragments of apparently the same size, suggesting that the genes were genetically linked and thus likely to be part of a lantibiotic gene cluster. Similarly, the 3' *lan*C probe (LF002) and the *lanD* probe (LF004) both hybridised to *Pst*I fragments of similar size, again suggesting that that may be physically linked. However the 5' part of *lanC* appears on a different *Pst*I fragment (explained by a *Pst*I site within contig_12864, 3' of the binding site for probe LF001).

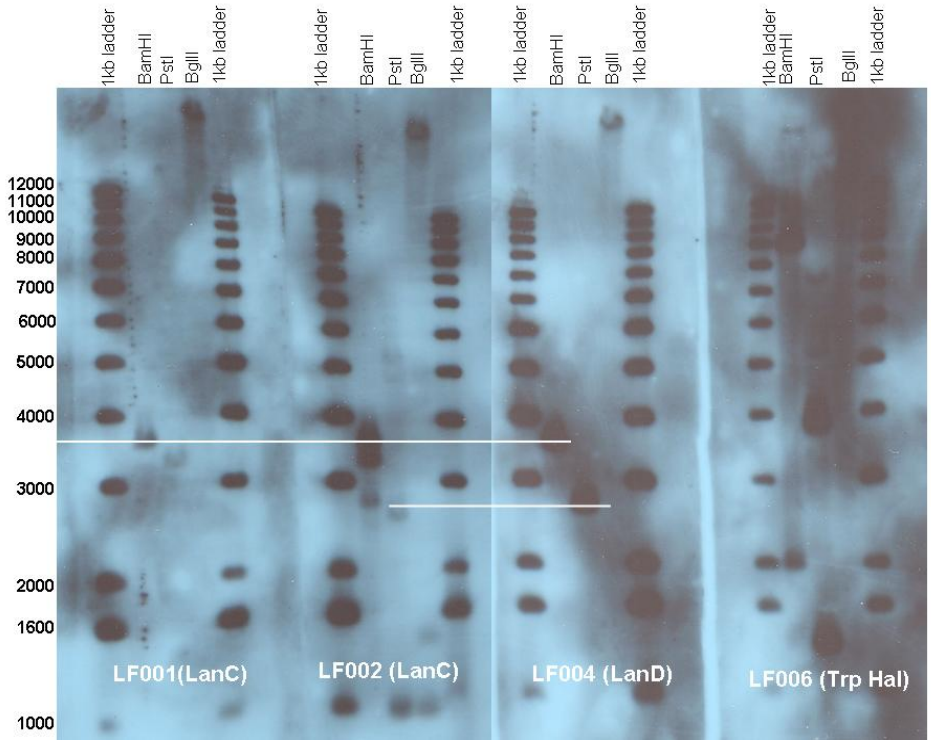

Figure 3.8 Southern blot hybridisation to identify linkage between Solexa contigs. NRRL 30420 gDNA was separately digested with the restriction enzymes *Bam*HI, *Pst*I and *Bgl*II as indicated on the top row and the resulting fragments separated on a 1% agarose gel. DNA was transferred to a nylon membrane by Southern transfer and each blot was probed with a different DIG-labelled PCR product probe, as indicated at the bottom of each blot; LF001 and LF002 are probes from each of the two *lanC* contigs, LF004 is from the *lanD* contig and LF006 from the tryptophan halogenase contig. The molecular weights of the size markers (Invitrogen 1kb ladder) are given on the far left. Bands believed to be shared between probes are indicated by a white line.

3.3.3 Details inferred from linking PCRs

Since a genetic linkage between *lanC* and *lanD* was suggested by Southern blot hybridisation, a PCR linkage strategy was attempted in which pairs of primers complementary to the ends of each identified contig were designed and used to "link" the contigs by PCR. Where PCR products were detected, these products were extracted, purified and submitted for Sanger sequencing (JIC Genome Centre Sequencing Service) to confirm their origin and determine any intermediate sequence. This method not only yielded useful information about gene orientation and linkage, it also unexpectedly yielded a new gene homolog downstream of *lanD* due to non-specific binding of one primer (LF001R). This new (but incomplete) open reading frame had homology to *lanT* genes in other clusters, particularly *cinT* from the cinnamycin gene cluster. LanT proteins are usually involved in lantibiotic transport across the cell membrane of the producing organism. The identification of further *lanB* sequence was aided by an additional contig found to lie within this gene (contig_1562 2/11/07; 220bp) (Figure 3.9). The two contigs were linked to the rest of the cluster by PCR (Figure 3.9) although the *lanB* open-reading frame remained incomplete at the N-terminus. The complete assembly spanned approximately 4.9kb (Figure 3.9).

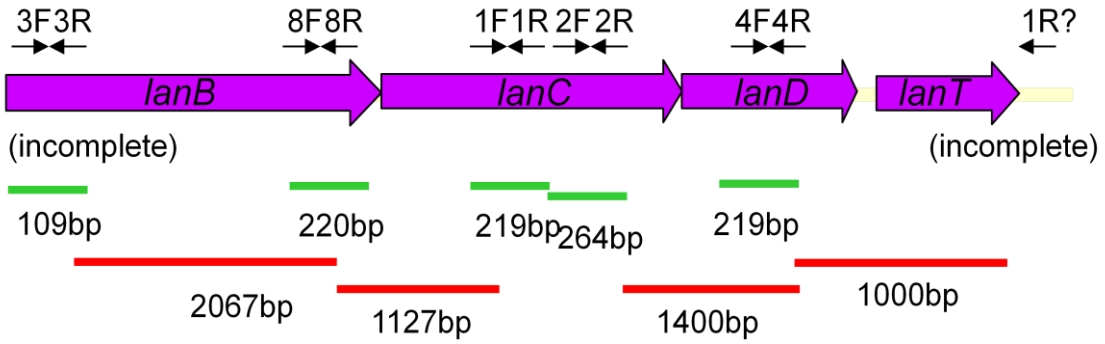

Figure 3.9 The lantibiotic gene cluster as determined from Solexa data by a combination of BLAST searches, manual assembly and linking PCR. Purple arrows indicate potential open-reading frames for genes in the cluster. Solexa contigs with homology to known lantibiotic genes are shown as green lines with their sizes indicated. Bridging PCR products are shown in red with sizes. The positions of the primers (LF00xX) used for the linking PCR reactions are given above the assembly. The 1000bp product was created by the fortuitous non-specific binding of one primer (LF001R) within *lanT*.

3.4 454 sequencing

M. corallina NRRL 30420 gDNA was also subjected to one quarter of a run of 454 sequencing (Cogenics/Roche) (Figure 3.10). This allowed a comparison to be made between the two rapid sequencing methods with respect to an actinomycete genome. 454 sequencing utilises longer read lengths (200-400bp) than Solexa, making the process of contig assembly more reliable. In particular it was noted that 454 sequencing gave larger contigs overall (average 1117bp) compared to Solexa (Figure 3.10). This yielded some very important findings about the microbisporicin cluster as described below.

Number of Contigs = 3027

Number of Bases = 3383376

Average Contig Size = 1117 bp

Largest Contig Size = 8913 bp

Average mol% GC = 70 %

Figure 3.10 Summary of data assembly from one quarter run of 454 sequencing with *M. corallina* NRRL 30420 gDNA (large contigs (>500 bp) only).

3.4.1 454 Sequence BLAST Results

As with the Solexa data sets, the assembled 454 contigs were used to construct a database that could be interrogated for homologs of known lantibiotic biosynthetic genes using an NCBI-type BLAST algorithm (Altschul *et al.* 1990) with either a nucleotide (BlastN) or amino acid (tBlastN) input (databases constructed by Dr. Govind Chandra (JIC)). Initially the 454 sequence data were used to confirm what had already been deduced about the microbisporicin cluster. The 454 data was however also able to extend the known data, for example the known sequence for *lanT* was extended by ~200bp. A number of new open reading frames were identified with homology to lantibiotic genes including *lanA*, *lanE* and *lanF*.

The inferred prepeptide sequence of MibA (VTSWSLCTPGCTSPGGGSNCSFCC; inferred from the final modified structure (Lazzarini *et al.* 2005; Castiglione *et al.* 2008)

was used as a tBLASTN input, identifying a contig (contig01839) that contained an identical sequence when translated *in silico*. The complete *mibA* open-reading frame was determined from this contig sequence. The start of a possible open reading frame was found downstream of *lan*A but insufficient sequence was available to determine its identity with confidence although *lanB* was a likely candidate. PCR was carried out to show that a primer designed within the *lanA* gene (LF011F) could be linked to a primer lying within the previously identified *lanB* gene (from Solexa data) (LF003R), giving a product of approximately 1500bp (Figure 3.11).

Upstream of *mibA*, an ECF sigma factor encoding gene was found in the opposite orientation, which may or may not be part of the biosynthetic cluster (Figure 3.11). However it was interesting to note that a conserved ECF sigma factor gene was found upstream of and in the same orientation as *lanA* in the putative *Planomonospora* lantibiotic biosynthetic gene cluster (Andrew Hesketh, personal communication) and so could have significance. Additionally sigma factor H is a known regulator of subtilin biosynthesis in *B. subtilis* (Stein *et al.* 2002).

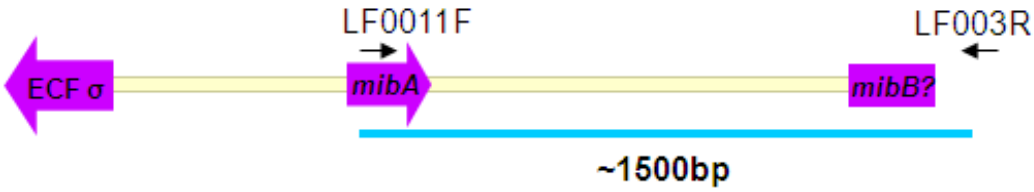

Figure 3.11 The genetic context of *mibA* revealed by the sequence of contig_01839. A gene encoding an ECF sigma factor family member (ECF σ) lies upstream and in an inverted orientation. *lanB* (*mibB*) was thought to lie downstream of *mibA* and the two sequences were linked by PCR amplification using the primers shown, giving a 1500 bp product.

Contigs were found in the 454 data that extended the tryptophan halogenase gene sequence identified in the Solexa data. The data provided the complete open reading frame for this gene and also indicated that the earlier identified second contig (4619 6/9/07), which could not be amplified by PCR, was caused by an assembly error in the Solexa data. The contig (contig00667) containing the 5' part of the tryptophan halogenase gene (*lanH*) contained other open reading frames, the sequences of which were homologs of *lanE* and *lanF* type genes in other lantibiotic clusters (Figure 3.12). The entire open reading frames of these genes appear to be present. LanE and LanF proteins are involved

in producer self-immunity to the lantibiotic in other systems by acting as membrane transport complexes, usually with a LanG component, although this was not found in this data. *lanE* (LF012R) was linked by PCR to *lanD* (LF004F), identified in the Solexa data, generating a PCR product of approximately 3500-4000bp and suggesting that the two potential cluster sequences might be genetically linked in the genome, however the identity of this product was not confirmed by sequencing (Figure 3.12).

A further open reading frame was identified in contig_07347 that appears to contain the 3' end of *lanH* and downstream sequence including an incomplete open-reading frame to which the halogenase gene appears to be translationally coupled (Figure 3.12). The product of this gene (*lanS*) shares homology with flavin reductase proteins.

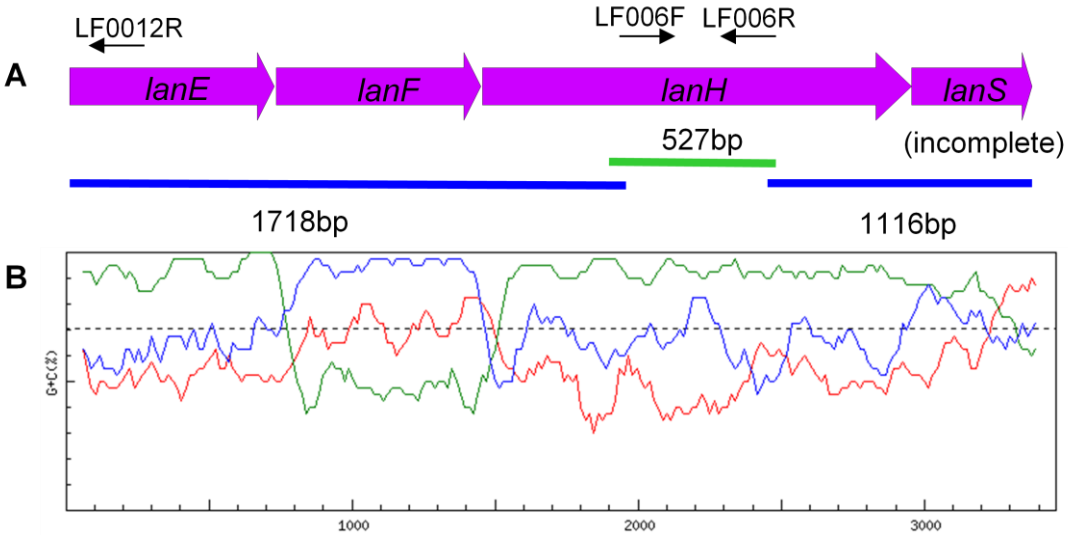

Figure 3.12 A; Organisation of *lanE*, *lanF*, *lanH* and *lanS* in the putative microbisporicin gene cluster and primers used for linking PCR reactions (arrows). The Solexa contig_5675 with homology to tryptophan halogenase genes is shown as a green line with its size indicated. 454 contigs (contig_00667 (1718bp) and contig_07347 (1116bp)) are shown in blue with their sizes. **B;** Frameplot (Bibb *et al.*, 1984; Ishikawa and Hotta, 1999) of the assembled contig sequences, showing the presence of the open reading frames illustrated above.

3.5 Cosmid Library Preparation

A cosmid library was generated using genomic DNA from *M. corallina* NRRL 30420. As described in chapter 2, an unconventional approach was taken in the construction of the cosmid library. Problems in purification of high molecular weight genomic DNA from *M. corallina*, likely due to the lengthy cell wall digestion steps found to be required for lysis of *M. corallina*, resulted in partial *Sau*3AI digests yielding fragments that were too small for cosmid library construction. Therefore an alternative mechanism for preparing gDNA fragments of the correct size was designed as described in detail in the following sections.

3.5.1 gDNA preparation to yield approximately 40kb fragments

gDNA was purified from *M. corallina* NRRL 30420 as described in chapter 2 and sized by pulsed field gel electrophoresis; the maximum size was estimated to be about 120kb (Figure 3.13a). To create a cosmid library using the SuperCosI vector (Stratagene), *Sau*3AI digests of this DNA were carried out. However, even at enzyme concentrations of 0.005U/µg gDNA, the DNA was digested to sizes smaller than the required 32-50kb optimal for phage packaging (data not shown). Instead, an alternative approach was initiated. This involved the use of Hydroshear (Genomic Solutions) to fragment the gDNA via mechanical shearing. Optimisation of shearing speed and number of shearing cycles resulted in DNA within the size range useful for cosmid library generation (Figure 3.13b).

Mechanical shearing of DNA can result in staggered broken ends and the removal of 5' phosphate groups. To improve the efficiency of subsequent blunt-end ligation, the DNA ends were filled-in using T4 polymerase and 5' phosphates reintroduced with T4 polynucleotide kinase (Figure 3.14).

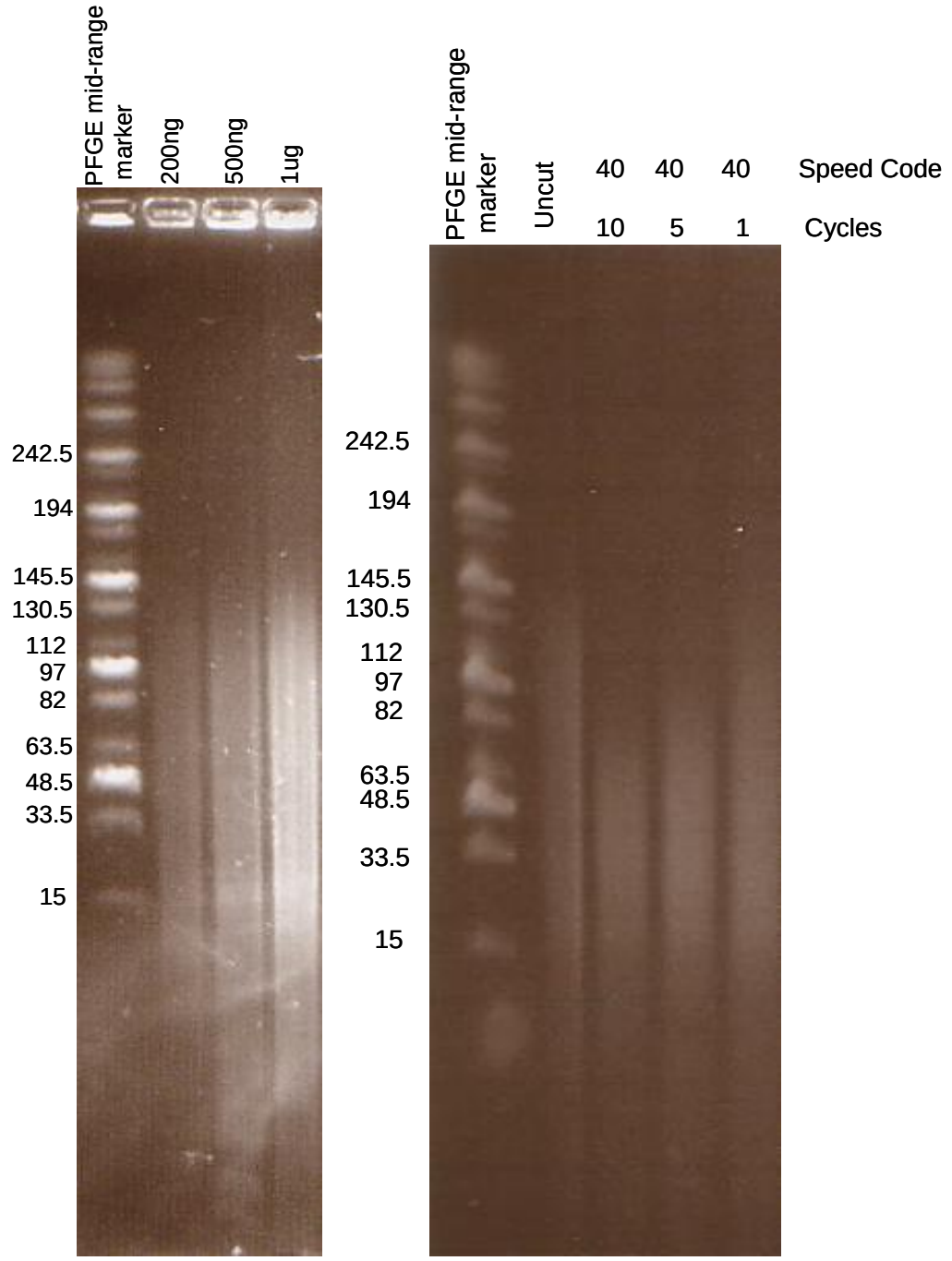

Figure 3.13 NRRL 30420 gDNA sized by pulsed-field gel electrophoresis A; 200, 500 and 1000 ng of NRRL 30420 gDNA run on a 1% agarose gel at 6 V with initial switch 1s and final switch 25 s for 18 h at 14ºC. B; 1 µg gDNA digested at each of the different hydroshear settings is shown. 5 cycles at a speed code of 40 appears to give DNA fragments within the correct size range (30-60 kb). The PFGE mid-range marker (NEB; in kb) was used to size the gDNA on both gels.

3.5.2 Cosmid library generation

The cosmid library was generated as described in Chapter 2. The Supercos1 vector was prepared for blunt-end ligation by first linearising with *Xba*I (a requirement for phage packaging) and the ends dephosphorylated (to prevent non-productive ligation of the two subsequent vector fragments and recircularisation of the vector); finally the vector was digested with the blunt-end cutter *Zra*I to yield two fragments (Figure 3.14). These fragments were ligated to the blunt-ended *M. corallina* gDNA. The resulting product was packaged into phage lambda heads and introduced into *E. coli* XL1 Blue by transfection. The final library consisted of 3072 clones of *E. coli* each carrying a cosmid with an insert size of 35-50 kb giving an estimated genome coverage of 20-30 fold (assuming a genome size of 5 Mb, estimated from the total unique sequence from Solexa and 454 sequence reads). The cosmid library was transferred to a nylon membrane with each cosmid spotted twice in a characteristic duplex pattern.

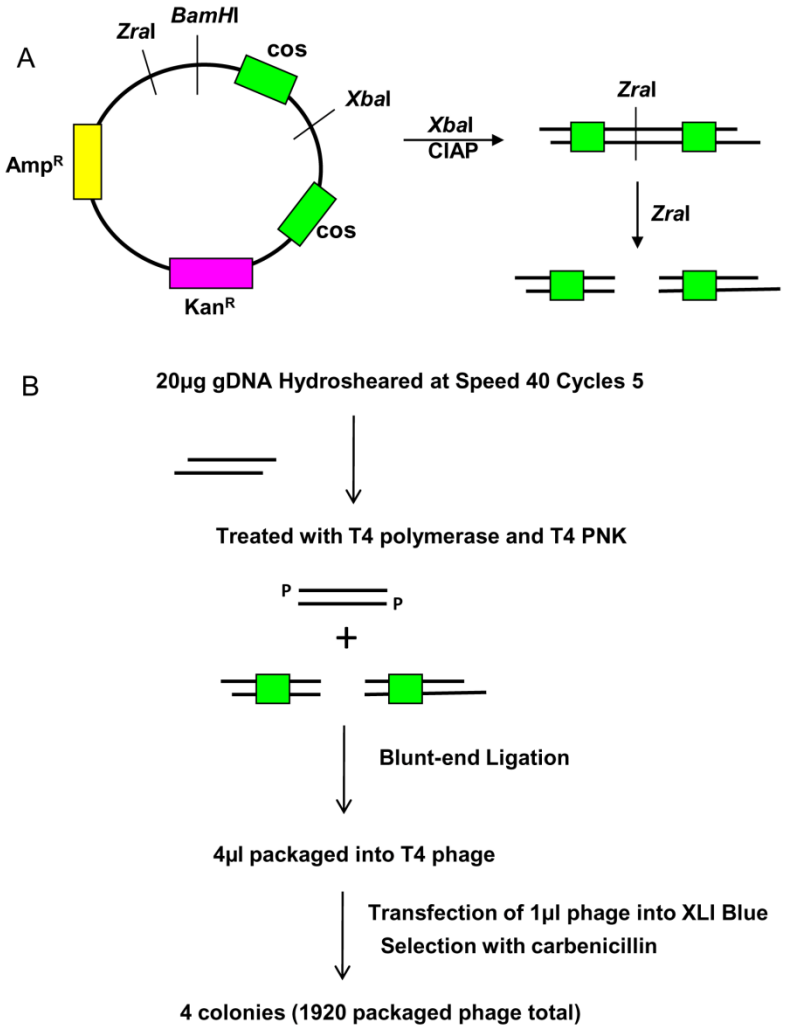

Figure 13.14 Strategy for cosmid library generation. **A;** The method designed to prepare the SuperCosI vector for blunt-ended cloning. The vector was first linearised with *Xba*I and the cleaved ends dephosphorylated with calf intestinal alkaline phosphatase (CIAP). The linear vector was treated with the blunt-end cutter *Zra*I to yield fragments of 6695bp and 1245bp with a phage cos1 site in each fragment (green boxes).

B; 20µg of NRRL 30420 genomic DNA was hydrosheared at a speed code of 40 for 5 cycles to yield mechanically sheared DNA. 10 µg was treated with T4 polymerase and T4 polynucleotide kinase (PNK). 2.5 µg was ligated to 1 µg of the SuperCosI vector prepared as described in A. 4 µl of each ligation was packaged into λ-phage heads using the Gigapack III Gold packaging extract (Stratagene). To titre the cosmid library, 1 µl of phage was introduced into *E. coli* XL1 Blue MR cells by transfection with selection on carbenicillin (100 µg/ml). The number of resulting colonies and the estimated total number of packaged phage in the extract (assuming 100% transfection efficiency) is given.

3.5.3 Probe preparation and cosmid library probing

Using one of the larger contigs identified by genome scanning and verified in both the Solexa and 454 data sets, the primers LF001F and LF004R were designed to amplify an approximately 1250bp probe from the *lanC-lanD* region using *M. corallina* gDNA as a template. The resulting PCR product was randomly labelled with ^{32}P-αdCTP. This probe was hybridised to the *M. corallina* cosmid library and hybridisation visualised as described in Chapter 2. This resulted in the observation of six clear double-spots (Figure 3.15). Double-spot hybridisation (i.e. probe bound to the same cosmid in both copies of the library) was indicative of specific hybridisation, rather than a membrane or hybridisation artefact.

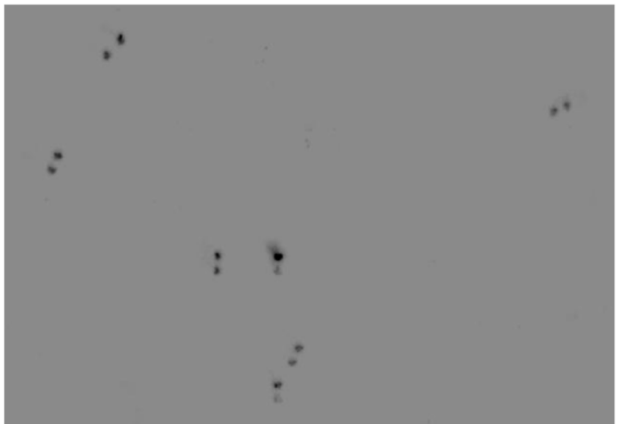

Figure 3.15 *M. corallina* NRRL 30420 double-spotted cosmid library hybridised to ^{32}P-labelled probe generated by PCR from *M. corallina* gDNA using primers LF001F and LF004R. Probe hybridisation positions were visualised by exposing the membrane to a phosphoimager plate for 5h before detection with a phosphoimager (Fuji).

3.6 Cosmids isolated from the library

3.6.1 PCR and digest confirmation

The six identified clones were identified and sampled from the library (1H11, 3E5, 3K13, 4G2, 5A7 and 7C22). The cosmids were purified and five were confirmed by PCR to contain parts of the microbisporicin gene cluster identified by genome scanning (*lanA*, *lanB*, *lanC*, *lanD* and the tryptophan halogenase gene). One cosmid (3K13) lacked the tryptophan halogenase gene and was not characterised further. Restriction digest mapping of the five remaining cosmids using *BamH*I and *Pst*I indicated conserved bands presumably resulting from the shared gene cluster (Figure 3.16).

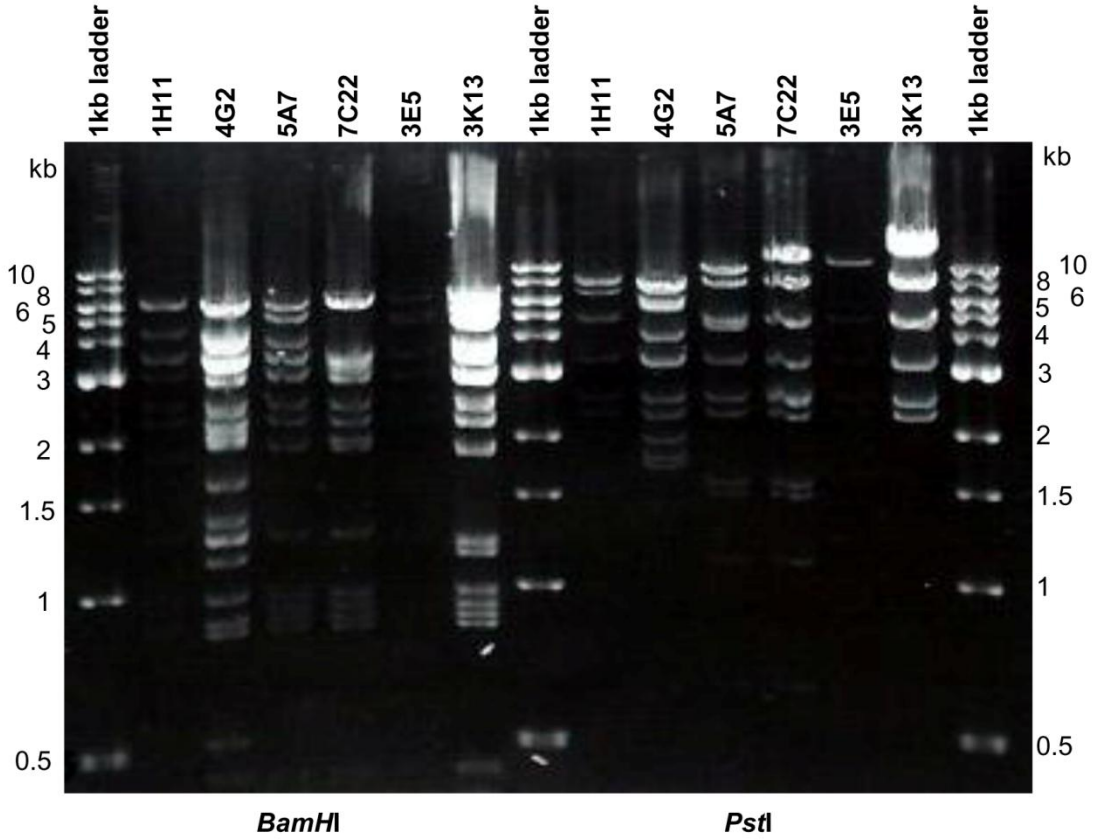

Figure 3.16 Digests of the six cosmids identified as containing parts of the microbisporicin gene cluster by cosmid library hybridisation. Each cosmid was purified from *E. coli* and 500ng-1µg digested with either *Bam*HI (left panel) or *Pst*I (right panel). The resulting fragments from each digested cosmid were separated on a 1% TBE agarose gel by electrophoresis. The name of each cosmid is given above the appropriate lane. The marker is the 1kb ladder (NEB).

3.6.2 Two cosmids completely sequenced

Cosmids 5A7 and 4G2 were chosen to be completely sequenced (because they showed the largest number of differences in the restriction digests in 3.6.1) using Sanger sequencing at the DNA sequencing facility at Cambridge University. The complete sequences of 4G2 and 5A7 revealed inconsistencies in the sequence upstream of the putative microbisporicin cluster (Figure 3.17). An ORF possibly encoding a member of the lipoprotein family was common to both sequences as was all the downstream sequence. However in the region upstream of this ORF, there was a putative cytochrome P450 in 5A7 but a TetR-like regulator in 4G2.

```
5A7     TCGAGGAGGTCCTGAGATATTGGGCGCCAACCCAGCACCAGGGCCGTACCCTCACCGCTG 919
4G2     GGGCGTGATCGGCGTGATGCTGGGCATGATCACAGCCCCCT--TTGGACGGGCGCACCCA 908
          * *         * ***  *****   * * **** **      * **   * *  *

5A7     CTGTGCGCCTGCACGGCCGGCTGCTCCCGGCCGGAGCACACGTGCTGCTGCTGACCGGAT 979
4G2     CCAC-CACGCCCACCGCCG-CCACCACCACATCCACCACCGCCGCCAGCG-TGACCAGCG 965
        *    * *   *** **** *  *  **      * ***    **    * ***** *

5A7     CGGCGGGC-AGGGACGAGCGCGCCTACCCCGACCCGGACGTCTTCGACATCGGCAGGTTC 1038
4G2     CACAGGCCCGGGGACGAGCGCGCCTACCCCGACCCGGACGTCTTCGACATCGGCAGGTTC 1025
        *   ** *  **************************************************

5A7     CACCCCGACCGGCGTCCCAGCACCGCGCTCGGGTTCGGTCTCGGCGCGCACTTCTGCCTG 1098
4G2     CACCCCGACCGGCGTCCCAGCACCGCGCTCGGGTTCGGTCTCGGCGCGCACTTCTGCCTG 1085
        ************************************************************
```

Figure 3.17 An alignment (constructed using ClustalW) to show the region of divergence between the sequences of cosmids 4G2 and 5A7.

To determine which cosmid encoded the true microbisporicin gene cluster sequence, PCR analysis was carried out. A PCR primer was designed within the shared sequence between the two cosmids (LF014R) and one primer was designed in each of the divergent parts of the sequences (LF015F in 5A7 and LF016F in 4G2). DNA of the two cosmids and *M. corallina* genomic DNA were used as templates for PCR analysis. Only LF015F and LF014R gave the expected PCR product from both the cosmid (5A7) and gDNA templates, although a weak non-specific product of incorrect size was derived from 4G2 with these primers (Figure 3.18). With LF014R and LF016F, the only band amplified was from the 4G2 template indicating that these two regions are not closely linked in the NRRL 30420 genome (Figure 3.18). Overall this analysis indicates that cosmid 5A7 has the correct sequence whereas 4G2 was likely formed by the joining of two non-contiguous segments of DNA (Figure 3.18).

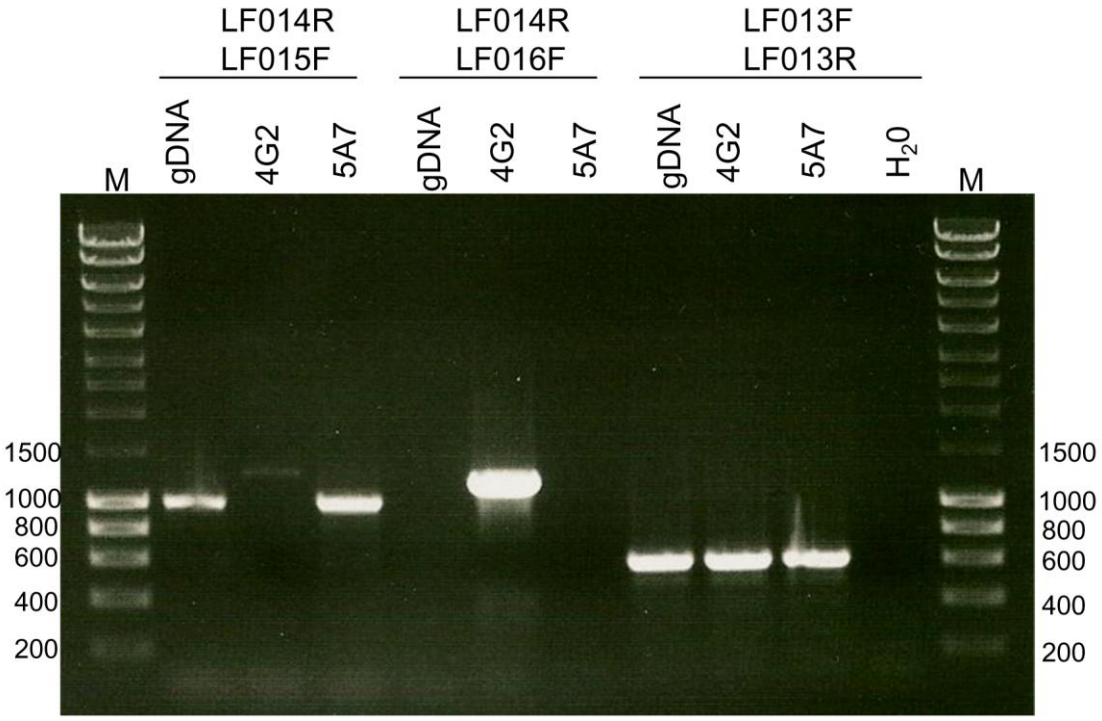

Figure 3.18 PCR analysis to determine whether 4G2 or 5A7 has the correct sequence. PCR analysis was carried out with primers designed within the shared sequence between the two cosmids (LF014R) and one in each of the divergent parts of the sequences (LF015F in 5A7 (expected to give a product of 998bp) and LF016F in 4G2 (expected to give a product of 1145bp)). The two cosmids and *M. corallina* genomic DNA (gDNA) were used as templates for the PCR analysis. The primers LF013F and LF013R, designed within the mibA-mibB region of the gene cluster serve as a positive control. Only LF015F and LF014R gave a PCR product of the expected size from both the cosmid (5A7) and from gDNA indicating that this cosmid had the correct sequence. The marker (M) is hyperladder (Bioline) and the sizes are shown in bp on both sides of the gel.

3.6.3 End-sequencing

All five cosmids were end-sequenced using the primers End_F and End_R (Table 2.6; approximately 600 base pairs of sequence per end). The resulting end-sequences along with the digest patterns (described in 3.6.1) and the complete sequence of cosmid 5A7 (described in 3.6.2) were used to generate an approximate map of each cosmid with respect to the known sequence of the gene cluster (Figure 3.19). The end-sequences of the cosmids 1H11, 3E5 and 7C22 indicated that all three had one end which matched the sequence in 5A7 downstream of the putative microbisporicin gene cluster. The other end of these cosmids did not map within the known sequence of 5A7 although restriction digest analysis of these cosmids suggests that they may have more upstream sequence than 5A7 (Figure 3.19).

3.6.4 Cosmid 5A7 annotation

The annotation of the complete 5A7 cosmid sequence was carried out using Artemis software (Sanger Centre, Cambridge (Rutherford *et al.* 2000)) and the GC-frame plot tool (with a typical window size of 50-120bp). Due to the high GC content of actinomycete genomes there is a marked difference in the GC content of the three nucleotide positions within codons which results, on average, in intermediate:low:high GC content at the first, second and third codon positions, respectively (Bibb *et al.* 1984). The GC-frameplot tool allows the user to follow the GC content at each of three positions within a moving window of nucleotide triplets. It is then possible to determine where open-reading frames are situated by identifying regions with such a GC distribution (Figure 3.20). This information can also be used to determine the direction of the open-reading frame. Open-reading frames in cosmid 5A7 were called on this basis and start sites (ATG or GTG) were further adjusted by taking into account the presence of putative ribosome binding sites (based around the sequence GGAGG) approximately 9-12 nucleotides upstream of the translation start codon (Kieser *et al.* 2000). A number of open-reading frames overlapped, indicative of translational coupling. This is often associated with proteins which function co-ordinately or in a 1:1 stoichometry, and is common in gene clusters. Putative open-reading frames were submitted to NCBI protein-protein BLAST analysis (blastP) to identify homologous proteins in the protein database (Altschul *et al.* 1990). The putative functions of the encoded proteins were determined on the basis of the BLAST output.

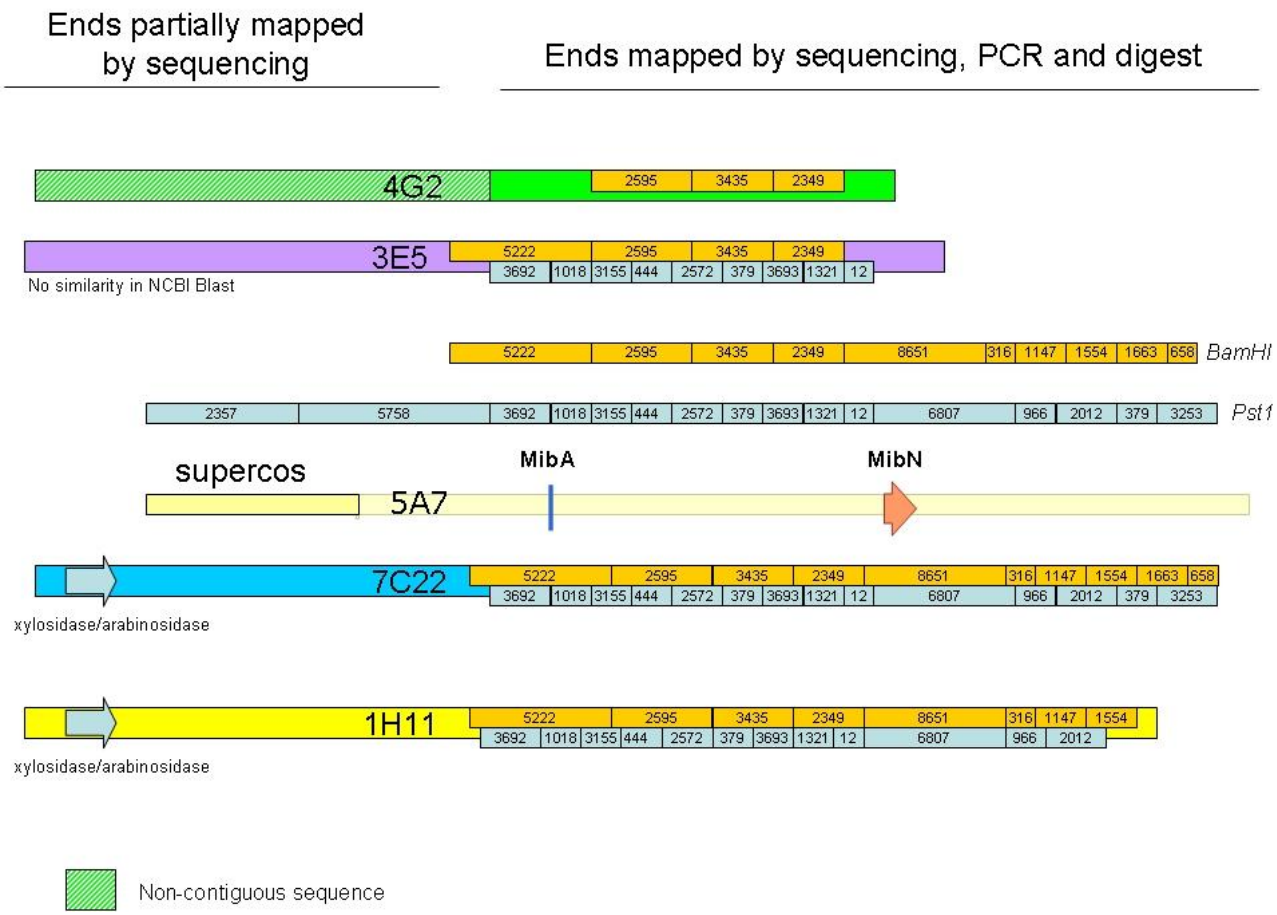

Figure 3.19 A graphical representation of the 5 cosmids containing all or part of the microbisporicin gene cluster. Cosmid 5A7 was completely sequenced and is shown as a reference sequence. 4G2 was also completely sequenced but differs from 5A7 in the upstream sequence. PCR analysis revealed that this region of 4G2 contains non-contiguous sequence (hatched). The end-sequences of the other three cosmids all map, at one end, within the sequence of 5A7 (downsteam of the *mib* gene cluster). This was confirmed by restriction mapping with *Bam*HI (fragments in orange) and *Pst*I (in blue). The other end of each of these cosmids could not be mapped within the known sequence and may extend beyond it as shown.

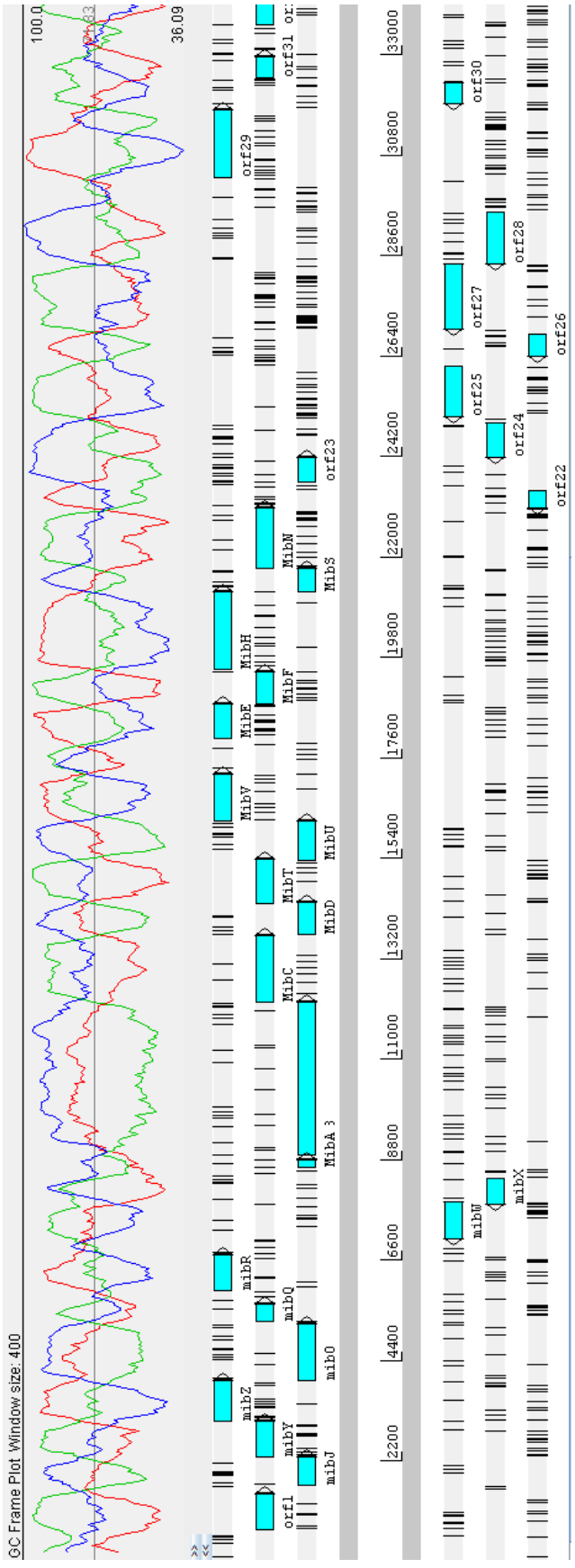

Figure 3.20 The annotated sequence of cosmid 5A7 displayed in Artemis (Sanger Centre, Cambridge) and showing the GC frameplot (window size 400) indication of ORF positions. The GC frameplot was used to estimate the positions and directions of ORFs. Start codons were annotated accordingly and were adjusted to accommodate the positions of putative ribosome binding sites 9-12 nucleotides upstream of the start codon.

3.7 Discussion

3.7.1 Discussion

The initial characterisation of the available *M. corallina* strains has revealed a number of interesting features and in particular striking differences. Production of a bioactive compound was found for strain NRRL 30420 and culture supernatant revealed ions associated with the known variants described for microbisporicin (Lee 2003; Lazzarini *et al.* 2005). This provided strong evidence that this strain of *M. corallina* was capable of producing the compound of interest under the culture conditions selected for this study. By comparison strains DSM 44681 and DSM 44682 were not found to produce any bioactive compounds, suggesting that these strains may not have the genetic capacity to biosynthesise microbisporicin. This will be discussed in further detail in chapter 4.

The ability of NRRL 30420 to generate spores was not described in detail in previous studies (Lee 2003). Under the conditions used in this study, significant levels of sporulation by NRRL 30420 were not observed, the strain growing as vegetative mycelium on agar culture media. Interestingly, spore formation could be observed with DSM 44681 and DSM 44682. The generation of such spores was described previously for these two strains and provided the name for the genus - *Microbispora* (Nakajima *et al.* 1999). Despite the reported high level of similarity in 16s rRNA gene sequences between NRRL 30420 and these “type” strains (Lee 2003), there appear to be fundamental differences both in terms of development and microbisporicin production.

Analysis of bioactive supernatant from NRRL 30420 by MALDI-ToF mass spectrometry revealed a spectrum of peaks that could be attributed to microbisporicins. However, due to the formation of oxidised variants (likely caused by lanthionine bridge oxidations) it has not been possible to deduce whether this strain (previously only described to produce MF-BA-1768$_{\beta 1}$ and MF-BA-1768$_{\alpha 1}$ (Lee 2003)) is also capable of producing the molecules 107891 A1 and A2 (Lazzarini *et al.* 2005). However, our interpretation of the mass differences between the four compounds and our further analysis of the microbisporicin gene cluster (as described in chapter 4) leads us to the conclusion that the previously described masses for lantibiotics produced by *M. corallina* strains result from the differential modification of one prepropeptide product and can thus be collectively referred to as microbisporicin, despite earlier assertions that these were in fact different products (Lazzarini *et al.* 2005).

This chapter describes how the novel method of genome scanning has been successfully applied to the identification of the microbisporicin gene cluster from *M. corallina*. Other

more conventional methods might have been employed, but are likely to have been more time-consuming and possibly unsuccessful (particularly those involving heterologous expression, as discussed in chapter 5). The genome scanning approach has furthermore provided information about other features of the *M. corallina* genome, such as the presence of other secondary metabolite gene clusters, which could be explored in future, and of integration sites, such as the ΦC31 integration site, observed in many actinomycetes (Combes *et al.* 2002), which might be used for later genetic manipulation of this species.

For this initial attempt at using genome scanning to identify an actinomycete biosynthetic gene cluster, both the rapid genome sequencing technologies of Solexa and 454 were utilised. This has allowed a rough comparison of these two methods in relation to their utility for genome scanning. On average, Solexa sequencing yielded shorter contigs and several inaccuracies were found in contig assembly when later compared to 454 sequence data. In relation to the microbisporicin gene cluster, the 454 data provided more information about the cluster and much more confidence that the correct gene cluster had been identified without the need to employ other techniques, such as Southern blot hybridisation analysis and PCR linkage, as was the case with Solexa sequencing. A retrospective analysis of the two datasets, using 4943bp of the microbisporicin gene cluster including *lanB*, *lanC* and *lanD* (initially indentified as the best targets for BLAST searches), indicates that 17 Solexa contigs (all of approximately 200bp in length) map to this region with a total coverage of 55%, from an assembly of 2.6Mb from a total of 881Mb of sequence data. By contrast seven 454 contigs provide 70% overall coverage of this region, from 4.6Mb of assembled sequence resulting from only 28Mb of total sequence. On the whole, although more economical, Solexa sequencing was found to be less useful than 454 sequencing for genome scanning in this particular case.

The *M. corallina* cosmid library had an estimated genome coverage of about 25-30 fold (i.e. 3072 clones x (40 kb – 50 kb insert) / 5 Mb). Based on the estimated 5Mb genome size of *M. corallina* and an expected minimal cosmid insert size of 40 kb, the probability (to 99% probability) of identifying cosmids within the library containing the 1250bp sequence used to probe for the microbisporicin gene cluster (=LN(1-0.99)/LN(1-(40000-1250)/5E6)) is 1 in 592 cosmids. In a cosmid library of 3072 clones, this equates to 5-6 clones, which is exactly the number identified by library hybridisation. This can be extended to estimate the probability of finding a cosmid containing the entire microbisporicin gene cluster (by estimating the gene cluster size as 20kb; =LN(1-0.99)/LN(1-(40000-20000)/5E6), which is 1 in 1149 or 2-3 clones in the total library. This matches well with the results presented here since 5A7, 1H11, 3E5 and 7C22 are

expected to contain the complete gene cluster (although it is only possible to be confident about 5A7; Figure 3.19). The microbisporicin gene cluster was successfully identified in the cosmid 5A7 and will be described in detail in Chapter 4.

3.7.2 Summary Points

- Growth of *M. corallina* strains NRRL 30420, DSM 44681 and DSM 44682 was characterised on agar media. NRRL 30420 grew without appreciable sporulation, whereas DSM 44681 and DSM 44682 produced pairs of spores on aerial mycelium.
- On V0.1 agar medium, *M. corallina* NRRL 30420 produced a compound that inhibited the growth of *M. luteus.* By contrast, DSM 44681 and DSM 44682 did not.
- *M. corallina* NRRL 30420 grew in a dispersed manner in liquid medium VSPA with defined growth and antibiotic production phases.
- *M. corallina* NRRL 30420 grown in VSPA produced compounds with masses corresponding to the microbisporicin complex, including three of the four previously described compounds.
- A genome scanning approach was used to identify the microbisporicin gene cluster from an *M. corallina* NRRL 30420 cosmid library.
- Comparison of the Solexa and 454 rapid sequencing technologies indicated that 454 sequencing was of greater use when identifying the microbisporicin gene cluster.
- Cosmid 5A7 was completely sequenced and annotated with open-reading frames, many of which are part of the microbisporicin gene cluster and will be described in Chapter 4.

Chapter 4 – The Microbisporicin Gene Cluster

4.1 Introduction

To provide a better understanding of microbisporicin biosynthesis, bioinformatic analysis of the microbisporicin (*mib*) gene cluster was carried out. This chapter describes the characteristics of the DNA fragment cloned in cosmid 5A7 (hereafter referred to as pIJ12125; GenBank accession HM536998) and in particular of those genes thought to be part of the *mib* gene cluster.

Annotation of the cloned insert of pIJ12125 (which contained 33 complete open-reading frames) was carried out as described in Chapter 3 and provided useful insights into the likely extent of the gene cluster within the 36668bp insert (Figure 4.1). *mibA,* encoding the microbisporicin prepropeptide (identified in Chapter 3), is located approximately 8.5 kb from one end of the cosmid insert (Figure 4.1). The region upstream of *mibA* contains the first open-reading frame (ORF) in the cosmid insert, *orf1,* as well as genes putatively assigned to the *mib* gene cluster (*mibJ* to *mibX*). The region downstream of *mibA* extends for approximately 15kb to the final ORF putatively assigned to the *mib* gene cluster, *mibN,* and is then followed by a further 12 ORFs that appear to be associated with primary metabolic functions and which were consequently not assigned to the *mib* gene cluster (Table 4.1).

In Chapter 3, *M. corallina* strains DSM 44681 and DSM 44682 failed to produce microbisporicin under the culture conditions used. The possibility that these strains do not contain a microbisporicin gene cluster is assessed in section 4.7.

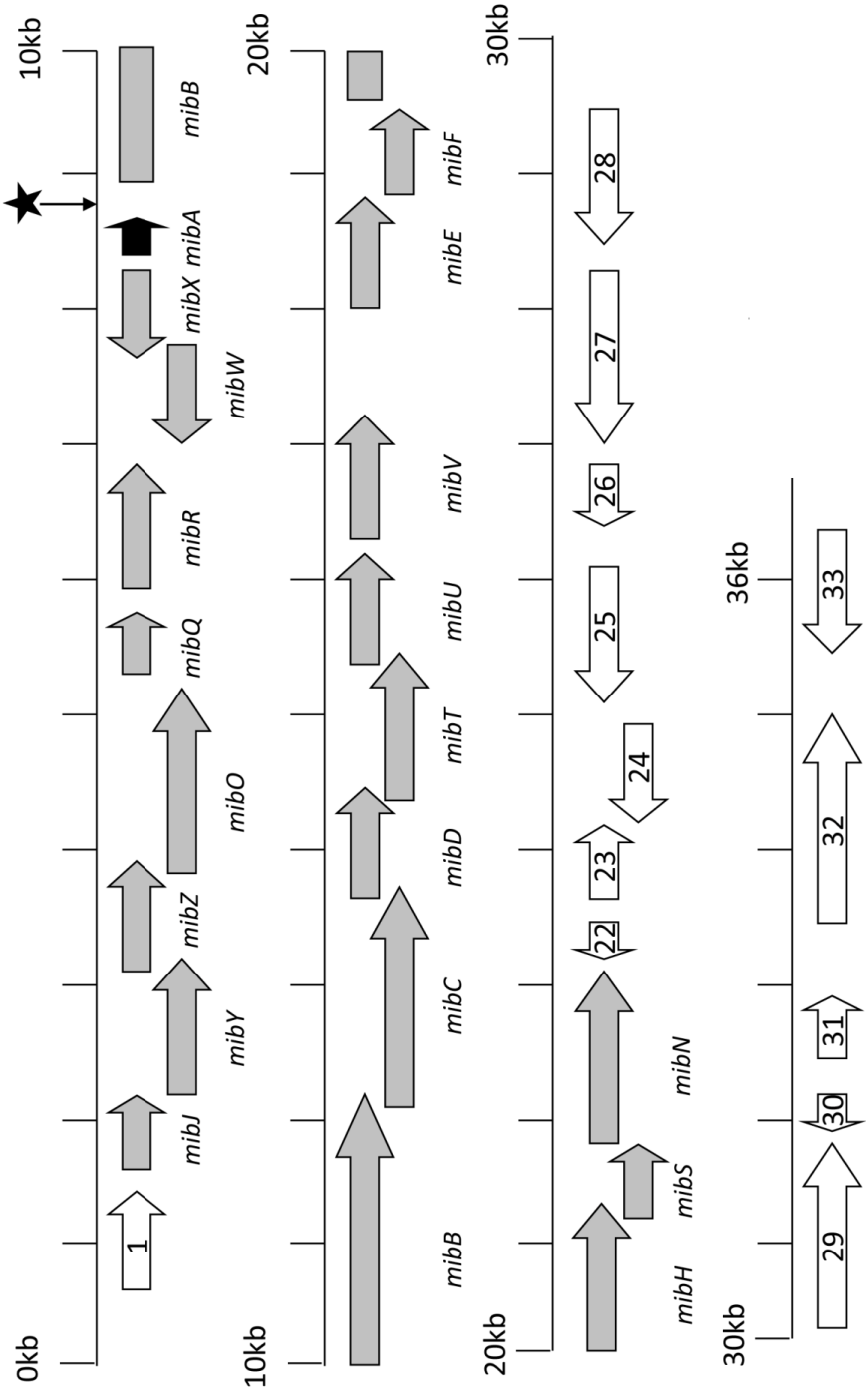

Figure 4.1 The microbisporicin gene cluster. Each gene is shown to scale with its position in pIJ12125 marked in kb. *mib* genes are shown in grey. The prepropeptide encoded by *mibA* is shown in black. Other genes on the cosmid are shown in white and are numbered. A black star denotes the position of predicted RNA secondary structure.

Table 4.1 The open-reading frames identified in pIJ12125. Open-reading frames are numbered as shown in Figure 4.1. The nearest homolog and percentage identity with that sequence was determined by a NCBI Blast search (Altschul *et al.* 1990) against the non-redundant protein database (as of 21st February 2010) using the predicted amino acid sequence in each case.

Open-reading frame Number	Proposed function	Length (aa)	Nearest Homolog	% Identity (across x amino acids)
1	XRE-family transcriptional regulator	254	ZP_05000646.1 DNA-binding protein [Streptomyces sp. Mg1]	51% (227)
2	MibJ (Unknown)	210	YP_001508288.1 hypothetical protein Franean1_3993 [Frankia sp. EAN1pec]	33% (183)
3	MibY (ABC permease)	258	YP_001508289.1 hypothetical protein Franean1_3994 [Frankia sp. EAN1pec]	31% (215)
4	MibZ (ABC transporter ATP-binding sub-unit)	300	YP_003181816.1 ABC transporter related [Eggerthella lenta DSM 2243]	59% (266)
5	MibO (Cytochrome P450)	414	ZP_06235262.1 cytochrome P450 [Frankia sp. EuI1c]	40% (415)
6	MibQ (Putative lipoprotein)	129	YP_002322870.1 hypothetical protein Blon_1406 [Bifidobacterium longum subsp. infantis ATCC 15697]	37% (138)
7	MibR (Transcriptional regulator)	260	ZP_06397847.1 response regulator receiver protein [Micromonospora sp. L5]	29% (161)
8	MibW (putative anti-sigma factor)	255	YP_003336912.1 hypothetical protein Sros_1171 [Streptosporangium roseum DSM 43021]	29% (174)
9	MibX (ECF sigma factor)	181	YP_003336913.1 RNA polymerase, sigma-24 subunit, ECF subfamily [Streptosporangium roseum DSM 43021]	49% (164)
10	MibA (microbisporicin prepropeptide)	57	gb|ACW83043.1 structural protein 97518 preproprotein [Planomonospora sp. DSM14920]	67% (46)

Open-reading frame Number	Proposed function	Length (aa)	Nearest Homolog	% Identity (across x amino acids)
11	MibB (dehydratase)	1115	YP_177053.1 lantibiotic biosynthesis protein [Bacillus clausii KSM-K16]	28% (1056)
12	MibC (cyclase)	485	ZP_06162154.1 conserved hypothetical protein [Actinomyces sp. oral taxon 848 str. F0332]	41% (474)
13	MibD (flavoprotein)	227	ZP_06162155.1 phosphopantothenoylcysteine decarboxylase/phosphopantothenate--cysteine ligase [Actinomyces sp. oral taxon 848 str. F0332]	44% (168)
14	MibT (ABC transporter ATP-binding sub-unit)	316	ZP_04485817.1 daunorubicin resistance ABC transporter ATP-binding subunit [Stackebrandtia nassauensis DSM 44728]	43% (309)
15	MibU (ABC permease)	290	YP_003320386.1 ABC-2 type transporter [Sphaerobacter thermophilus DSM 20745]	37% (222)
16	MibV (unknown)	334	ZP_04334065.1 hypothetical protein NdasDRAFT_3165 [Nocardiopsis dassonvillei subsp. dassonvillei DSM 43111]	36% (320)
17	MibE (ABC permease)	249	ZP_03293380.1 hypothetical protein CLOHIR_01328 [Clostridium hiranonis DSM 13275]	23% (256)
18	MibF (ABC transporter ATP-binding sub-unit)	236	ZP_05336621.1 ABC transporter related protein [Thermoanaerobacterium thermosaccharolyticum DSM 571]	47% (225)
19	MibH (FAD-dependent tryptophan halogenase)	568	NP_968288.1 tryptophan halogenase [Bdellovibrio bacteriovorus HD100]	39% (519)
20	MibS (flavin reductase)	178	gb|ABV56599.1 KtzS [Kutzneria sp. 744]	55% (154)
21	MibN (Na^+/H^+ antiporter)	434	gb|AAK81829.1 integral membrane ion antiporter [Streptomyces lavendulae]	61% (416)

Open-reading frame Number	Proposed function	Length (aa)	Nearest Homolog	% Identity (across x amino acids)
22	Unknown	118	YP_001793177.1 hypothetical protein Lcho_4161 [Leptothrix cholodnii SP-6]	32% (114)
23	Pyramidine reductase	184	YP_003324478.1 bifunctional deaminase-reductase domain protein [Thermobaculum terrenum ATCC BAA-798]	50% (183)
24	Unknown	236	YP_001108055.1 hypothetical protein SACE_5947 [Saccharopolyspora erythraea NRRL 2338]	45% (232)
25	Oxidoreductase domain protein	362	YP_001363208.1 oxidoreductase domain protein [Kineococcus radiotolerans SRS30216]	63% (353)
26	Glyoxalase/bleomycin resistance protein/dioxygenase	151	YP_824593.1 glyoxalase/bleomycin resistance protein/dioxygenase [Solibacter usitatus Ellin6076]	33% (122)
27	Esterase, PHB depolymerase family	460	ZP_06397018.1 esterase, PHB depolymerase family [Micromonospora sp. L5]	60% (433)
28	Xylanase	368	ZP_04606278.1 xylanase [Micromonospora sp. ATCC 39149]	79% (223)
29	Beta-1,4-xylanase	495	YP_003115119.1 glycoside hydrolase family 10 [Catenulispora acidiphila DSM 44928]	60% (479)
30	MarR-type regulator	148	YP_003342264.1 hypothetical protein Sros_6813 [Streptosporangium roseum DSM 43021]	60% (143)
31	Unknown	150	ZP_03168892.1 hypothetical protein RUMLAC_02595 [Ruminococcus lactaris ATCC 29176]	25% (133)
32	Secreted endo-1,4-beta-xylanase	480	ZP_05528201.1 secreted endo-1,4-beta-xylanase [Streptomyces lividans TK24]	59% (438)
33	Prephenate dehydratase	280	YP_003380192.1 Prephenate dehydratase [Kribbella flavida DSM 17836]	65% (274)

4.2 MibA

MibA is the 57-amino acid prepropeptide of microbisporicin, with a leader sequence extending from residues 1 to 33. Alignment of the putative leader peptide with those of other type A(I) lantibiotics, such as nisin, subtilin and epidermin, revealed a possibly conserved "FNLD" motif (LDLD in microbisporicin, Figure 4.2) potentially involved in lantibiotic processing (van der Meer *et al.* 1994). The MibA cleavage site also resembles those of other type AI lantibiotics (Figure 4.2), with proline at the -2 position and alanine at -4 (van der Meer *et al.* 1994). Mutation of Pro^{-2} in pre-nisin had a minimal affect on leader peptide processing whereas the Ala^{-4} to Asp variant of pre-nisin was not cleaved by the leader peptidase NisP *in vivo* but could be cleaved by trypsin *in vitro* (van der Meer *et al.* 1994). Mutation of the -1 arginine residue of nisin to glutamine resulted in decreased leader peptide processing (van der Meer *et al.* 1994). This residue is not conserved in microbisporicin, where it is alanine. This may suggest that the protease involved in cleaving microbisporicin is significantly different from that involved in leader peptide removal in the other type A (I) lantibiotics. The leader peptide of MibA is longer than those of nisin, subtilin and epidermin and shows only low levels of overall conservation (e.g. 20% amino acid identity with EpiA).

```
NisA    ----------MST-KDFNLDL-VSVSK-KDSGASPR 23
SpaS    ----------MSKFDDFDLDV-VKVSK-QDSKITPQ 24
EpiA    -----MEA-VKEKNDLFNLDVKVNAKESNDSGAEPR 30
MibA    MPADILETRTSETEDLLDLDLSIGVEE---ITAGPA 33
                    .. . ::**: : ..:     . *
```

Figure 4.2 An alignment (constructed using ClustalW (Chenna *et al.* 2003)) of the MibA leader peptide with those of example type A(I) lantibiotics (NisA (nisin), SpaS (subtilin), EpiA (epidermin)). The partially conserved FNLD motif is shown in light blue. A putative conserved cleavage site is shown in green.

The propeptide sequence of MibA agrees with the published NMR structure of microbisporicin (Figure 4.3) (Lazzarini *et al.* 2005; Castiglione *et al.* 2008). All serine residues and all but one threonine residue of the propeptide are dehydrated by a LanB enzyme to yield dehydroalanine and dehydrobutyrine, respectively. Each dehydrated residue is then subject to nucleophilic attack by the thiol group of a cysteine residue in the peptide chain, catalysed by LanC, resulting in the formation of lanthionine bridges. Only two dehydrated residues, a dehydroalanine and dehydrobutyrine, are not incorporated into lanthionine bridges. The C-terminal cysteine residue of the propeptide is decarboxylated

by a LanD enzyme to yield another free thiol group which forms a bridge with a dehydroalanine, yielding *S*-[(*Z*)-2-aminovinyl]-D-cysteine. The tryptophan residue at position 4 of the propeptide is chlorinated and the proline at position 14 is hydroxlated.

mibA appears to lie at the start of an operon that contains modification and export genes. A 247bp gap lies between the 5' end of *mibA* and the preceding oppositely transcribed gene *mibX,* and presumably contains the *mibA* promoter, while 117bp of non-coding sequence between *mibA* and *mibB* might reflect the presence of a transcriptional attenuator. Indeed, an RNA secondary structure (ΔG= -123 kJ mol^{-1}) was predicted for region 8820-8854bp using Clone Manager [4] (Figure 4.1). Such structures occur in other lantibiotic gene clusters and are thought to maintain an appropriate stoichiometry between the prepropeptide and the modification enzymes (McAuliffe *et al.* 2001).

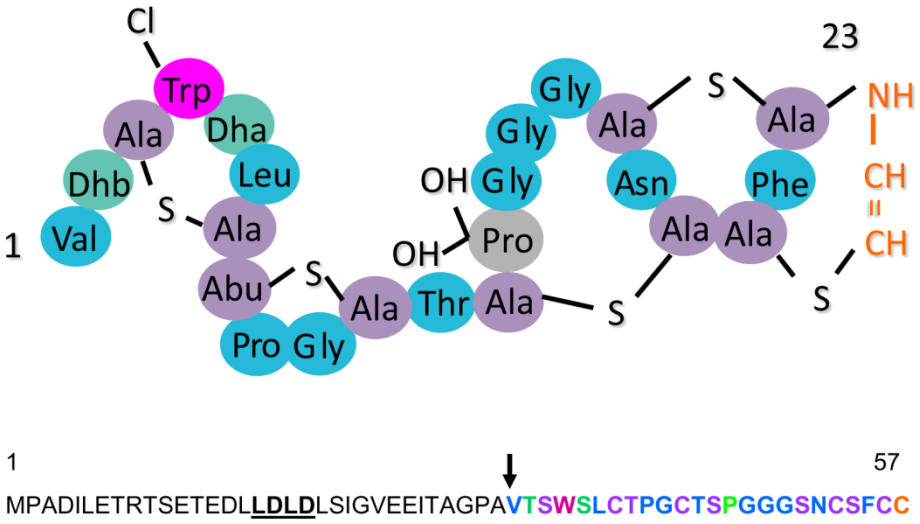

Figure 4.3 The relationship between the MibA prepropeptide and modified microbisporicin. The structure of microbisporicin as determined by NMR (Lazzarini *et al.* 2005) colour-coded to show the introduced modifications; unmodified residues (blue) dehydrated residues (green) dehydrated and cyclised residues (purple), chlorinated tryptophan (pink), hydroxylated proline (grey) and the *S*-[(*Z*)-2-aminovinyl]-D-cysteine formed from decarboxylated cysteine (orange). Below is the MibA prepropeptide sequence with the leader peptide in black and propeptide colour-coded (as above) with the positions of the modifications to occur. The underlined bold LDLD motif is the conserved "FNLD" motif of the type A(I) lantibiotics. An arrow represents the putative cleavage site of the prepropeptide.

[4] Clone manager, Scientific & Educational Software. (2001).

4.3 Biosynthetic and Modification Enzymes

4.3.1 MibB

MibB is a homolog of lantibiotic dehydratases (LanBs). Closest relatives are LanB-like proteins from currently uncharacterised lantibiotic gene clusters from *Bacillus clausii* (28% amino acid identity) and from actinomycetes such as *Actinomyces* oral taxon 848 str. F0332 (31% amino acid identity), *Streptomyces noursei* and *Streptomyces griseus* (both with 34% amino acid identity). This relatively low level of identity to other MibB proteins is characteristic of this enzyme family, members of which typically share amino acid identities of less than 30% (Chatterjee *et al.* 2005). MibB also has homologs amongst the well-studied type A(I) lantibiotic biosynthetic gene clusters including SpaB (subtilin; 24% amino acid sequence identity), EpiB (epidermin) and MutB (mutacin III). By comparison to the LanB enzymes in other lantibiotic gene clusters (Koponen *et al.* 2002), MibB is likely to dehydrate serine and threonine residues in the prepropeptide to yield didehydroalanine and didehydrobutyrine, respectively.

4.3.2 MibC

MibC shows homology to lantibiotic cyclases (LanCs). Closest relatives are LanC-like proteins from currently uncharacterised lantibiotic gene clusters from *Bacillus clausii* (32% amino acid identity) and from actinomycetes such as *Actinomyces* oral taxon 848 (41% amino acid identity) and *Streptomyces coelicolor* (SCO0270; 33% amino acid identity). Other close homologs include SpaC (subtilin; 33% amino acid identity), NisC (nisin) and MutC (mutacin III). LanC enzymes involved in the biosynthesis of lantibiotics such as subtilin and nisin are responsible for forming (methyl-)lanthionine bridges (Koponen *et al.* 2002; Li *et al.* 2006a; Cheng *et al.* 2007; Helfrich *et al.* 2007). Conserved histidine and cysteine residues within the active site of NisC coordinate a zinc ion involved in catalysis (Li *et al.* 2007). These residues are conserved in MibC (Figure 4.4) suggesting that this is a LanC-type cyclase involved in the introduction of lanthionine bridges into microbisporicin.

```
MibC   MTTVGRTSCGVTSDRHPARFLRGSAARRAARLVRLVAERLADPDAVAGIAARPG--NSVP 58
SpaC   -------------------MERGTVSRIEVEIVKEMARQISNYDKVLEIVNQKDNFRSIG 41
NisC   ---------------------------------MRIMMNKKNIKRNVEKIIAQWD-ERTRK 27
                                        :: : .:      *  *  : .  .:

MibC   VNGLSMWSPATLSHGFPGIAVFYAELGRIDP--AWSAFAHRHLRAAAAAVET--APSGGL 114
SpaC   EVPLIPWKSTALSHGIPGICMLYGELHAHFPEEGWDDIGHQYLSILVNEIKEKGLHTPSM 101
NisC   NKENFDFGELTLSTGLPGIILMLAELKNKDNSKIYQKKIDNYIEYIVSKLSTYGLLTGSL 87
             :   :** *:*** :: .**        :.   ..::   .  :.     : .:

MibC   FAGPASLLAAAQSCAGPAGHYRGLRRKLTAWLAADHAGRLAVARDRPGPGVAWTDYDVVH 174
SpaC   FSGAAGIGLAAICLSQRFTYYNGLISSINEYLAETVPQLLTEFDQRQ---VCMSDYDVIE 158
NisC   YSGAAGIALSILHLREDDEKYKNLLDSLNRYIEYFVIEKIEGFNLEN---ITPPDYDVIE 144
       ::*.*.:  :          *..*  .:. ::       :     .    :  .****:.

MibC   GLSGTTRLLLDAACDPDDETAAVASGAVTDTLRHLVRLTEPITVDGHEVPGWWVPSHLQP 234
SpaC   GVSGIANYLLLFQED------KAMGDLLIDILKYLVRLTEDIIVDGEKVPGWHIPSQHQF 212
NisC   GLSGILSYLLLINDE----------QYDDLKILIINFLSNLTKENKGLISLYIKSENQM 193
       *:**    **    :             *    ::.: . :  :.. : .  : *. *

MibC   VEQDRRDYPRGDLNLGLAHGAAGPLSVLATATLHGMEVPGQREAVARLAEWLLGWTMTDD 294
SpaC   TDIEKKAYPYGNFNMGLAHGIPGPICVLSSALIQGIKVKGQERAIEKMANFLLEFSEKEQ 272
NisC   SQSESEMYPLGCLNMGLAHGLAGAGCILAYAHIKGYSNEASLSALQKIIFIYEKFELEIK 253
        : : . ** * :*:***** .*. .:*: * ::* .  ..  *: ::      :    .

MibC   TGAYWPCRISWDEQIAAVRPDAS-FTRTAWCYGAPGVCAALHRAGLALGVTEWREVAVTA 353
SpaC   DSLFWKGIISFEEYQYGSPPNAVNFSRDAWCYGRPGVCLALVKAGKALQNTELINIGVQN 332
NisC   NQFLWKDGLVADELKKEKVIREASFIRDAWCYGGPGISLLYLYGGLALDNDYFVDKAEKI 313
           *   :  :*          * * ***** **:.     .* **      : .

MibC   LLDGLRRDRSAWRVDGSTVCHGYAGLLQVLSRVGAESGDPRLLDGCLDVARMVLGEADES 413
SpaC   LRYTISDIR---GIFSPTICHGYSGIGQILLAVNLLTGQEYFKEELQEIKQKIMSYYDKD 389
NisC   LESAMQRKLG---IDSYMICHGYSGLIEICSLFKRLLN------------TKKFDSYIEE 358
       *   :        : .  :****:*: ::   .    .              :.   :.

MibC   APFVFPHLVPDSPDGWRNATGYLPLDGAGLLEGAAGVACALLSVIPPSSLCGTDPAPERA 473
SpaC   YIFGFHNYESMEGD------EAVPLQYVGLLDGAVGVGLGVLNMELGS------------ 431
NisC   FNVNSEQILEEYGD----------ESGTGFLEGISGCILVLSKFEYSIN----------- 397
         .   :      *           . .*:*:*  *    : ..

MibC   DLPPWDRCLALC---------- 485
SpaC   -KTDWTKALLI----------- 441
NisC   -FTYWRQALLLFDDFLKGGKRK 418
         . * :.* :
```

Figure 4.4 An alignment (constructed using ClustalW (Chenna *et al.* 2003)) of MibC with other members of the LanC class of enzymes (NisC (nisin) and SpaC (subtilin)). Conserved residues are highlighted; zinc-coordinating residues from NisC (light blue; Li *et al.* 2006), essential catalytic residues in NisC and SpaC (yellow, Li *et al.* 2006; Helfrich *et al.* 2007), other conserved active site residues (green, Li *et al.* 2006) and prepropeptide binding residues in NisC (pink, Li *et al.* 2006).

4.3.3 MibD

MibD is homologous to flavoproteins, specifically those involved in *S*-[(*Z*)-2-aminovinyl]-D-cysteine formation, such as MrsD (mersacidin; 37% amino acid identity) and MutD (mutacin III; 32% amino acid identity). It also has homologs in uncharacterised lantibiotic gene clusters, including one in *Bacillus clausii* (34% amino acid identity) and one in *Actinomyces* oral taxon 848 (44% amino acid identity). LanD enzymes from the epidermin (EpiD) and mersacidin (MrsD) clusters have been studied extensively *in vitro* (Kupke *et al.* 1992; Kupke *et al.* 1994; Majer *et al.* 2002). These enzymes decarboxylate the C-terminal cysteine of the peptide chain to yield a free thiol group that subsequently forms a lanthionine bridge via cyclisation with a dehydrated serine or threonine residue located towards the C-terminus of the propeptide, a reaction likely catalysed by LanC (Kupke *et al.* 1994; Kupke *et al.* 1995; Majer *et al.* 2002).

Many of the motifs and residues identified to have importance in the catalysis of EpiD and MrsD are conserved in MibD (Figure 4.5) (Blaesse *et al.* 2000; Blaesse *et al.* 2003). The substrate specificity of MibD may be similar to that of EpiD. EpiD favours a large hydrophobic amino acid three residues from the end of the peptide (Schmid *et al.* 2002); in EpiA this is a tyrosine, while in MibA it is a phenylalanine. Phenylalanine at this position is tolerated by EpiD (Kupke *et al.* 1995). While EpiD utilises FMN as a flavin-cofactor, MrsD uses FAD. Despite the availability of structures for both enzymes, it is not clear which residues determine the choice of cofactor (Blaesse *et al.* 2003) and thus it is not possible, on the basis of sequence alone, to determine whether MibD utilises FAD or FMN.

MibD is presumably involved in formation of the *S*-[(*Z*)-2-aminovinyl]-D-cysteine moiety at the C-terminus of microbisporicin (Lazzarini *et al.* 2005; Castiglione *et al.* 2008). The exact function of this modification in lantibiotics that contain it has been largely unexplored. An *epiD* mutant of *Staphlococcus epidermis* failed to produce a biologically active compound, however it was not clear whether this was due to the complete absence of epidermin biosynthesis or due to the production of an inactive molecule (Augustin *et al.* 1992). Thus it is unclear whether this C-terminal modification contributes to lantibiotic mode of action or stability.

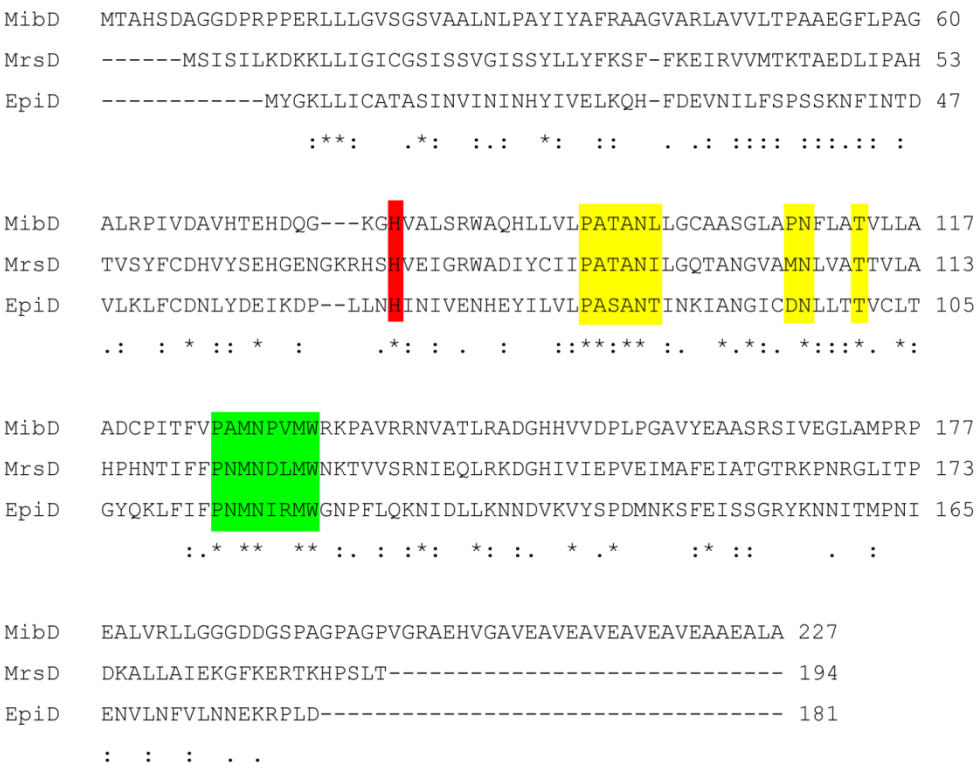

Figure 4.5 An alignment (constructed using ClustalW (Chenna *et al.* 2003)) of MibD with other characterised members of the LanD class of enzymes (MrsD (mersacidin) and EpiD (epidermin)). Conserved residues are highlighted; the His^{67} active site base in EpiD (red), the PASANT motif and other FMN-binding residues of EpiD (yellow), the PXMNXXMW motif of EpiD also involved in FMN-binding (green) (Blaesse *et al.* 2000).

4.3.4 MibHS

Chlorination of tryptophan in microbisporicin is a unique lantibiotic modification. Based on the involvement of FAD-dependent tryptophan halogenases in the biosynthesis of many other classes of antibiotics, this enzyme family appeared to be a good candidate to fulfil this role in microbisporicin. As described in Chapter 3, a gene, *mibH,* encoding a member of this family of proteins was found towards the end of the *mib* gene cluster along with a downstream and translationally-coupled gene *mibS* (Figure 4.1).

MibH shares homology with members of the FAD-dependent tryptophan halogenase family typified by PrnA from *Pseudomonas fluorescens* (31% amino acid identity), which converts free tryptophan to 7-chlorotryptophan during pyrrolnitrin biosynthesis (Keller *et al.* 2000). Other MibH homologs include an uncharacterised tryptophan halogenase from *Bdellovibrio bacteriovorus* HD100 (39% amino acid identity), a tryptophan 5-halogenase (PyrH) involved in pyrroindomycin B biosynthesis in *S. rugosporus* (36% amino acid identity (Zehner *et al.* 2005)) and KtzR involved in kutznerides biosynthesis in *Kutzneria* sp. 744 (34% amino acid identity (Fujimori *et al.* 2007; Heemstra *et al.* 2008)).

Members of the flavin-dependent tryptophan halogenase family have been identified in gene clusters associated with biosynthesis of a wide variety of secondary metabolites, many from actinomycetes, including; *Streptomyces rugosporus, Streptomyces venezuelae* (chloroamphenicol), *Streptomyces roseochromogenes* (chlorobiocin) and *Streptomyces viridochromogenes* (avilamycin) (Murphy 2006). PyrH from *S. rugosporus* was the first member of this class found to incorporate chlorine at carbon-5 in tryptophan (Zehner *et al.* 2005). This is the same regioselective reaction that would be expected to occur in microbisporicin biosynthesis (Lazzarini *et al.* 2005).

Chlorination of secondary metabolites has been reported to improve anti-bacterial activity (Harris *et al.* 1985; Ohi *et al.* 1987; Malabarba *et al.* 1989). Flavin-dependent halogenases could therefore be used in an attempt to produce novel compounds with enhanced antibiotic activity. This has already been partially addressed in a proof of principle experiment in which halogenated indolocarbazole derivatives were created through the introduction of *pyrH* into the indolocarbazole gene cluster followed by expression in a heterologous host, although compounds with higher anti-tumor activities were not produced through this approach (Sanchez *et al.* 2005).

The crystal structure of PrnA was solved to 1.95Å and, through the use of crystals containing FAD, tryptophan or chlorotryptophan, shed light on the catalytic mechanism of the enzyme (Dong *et al.* 2005). The enzyme behaves as a dimer with each monomer

consisting of a FAD-binding domain and substrate binding domain (Dong *et al.* 2005). $FADH_2$ reacts with molecular oxygen to create a peroxide moiety linked to the FAD ring (Dong *et al.* 2005). Chlorine, held in the protein by interaction with Thr^{348} and Gly^{349}, attacks the peroxide to yield HOCl (Dong *et al.* 2005). Since this site is some 10Å away from the site of the bound substrate, the authors postulate that the HOCl is conducted down a tunnel to the substrate which is held, by the enzyme, in an orientation that promotes the regioselective addition of chlorine to carbon-7 of the substrate. Lys^{79} and Glu^{346} are predicted to activate the chlorine and promote its electrophilicity in this reaction, whilst Glu^{346} also stabilises the resulting Wheland intermediate (Dong *et al.* 2005; Flecks *et al.* 2008).

MibH contains several amino acid sequence motifs that are conserved in the flavin-dependent tryptophan halogenase family and that are important for the catalytic mechanism of PrnA (Dong *et al.* 2005; Flecks *et al.* 2008). This includes the GxGxxG motif located near the N-terminus involved in binding the flavin co-substrate in PrnA (Dong *et al.* 2005) and WxWxIP thought to be involved in preventing mono-oxygenase activity in that enzyme (Dong *et al.* 2005) (Figure 4.6). In addition, a number of residues involved in the catalytic mechanism of PrnA and found to be essential for enzyme functionality (Dong *et al.* 2005; Flecks *et al.* 2008), are conserved in MibH (Figure 4.6). These conserved features clearly suggest that MibH is a true member of the flavin-dependent halogenase family. However, MibH shares relatively low amino acid sequence identity across the whole protein sequence with other flavin-dependent halogenases, e.g. 24% and 31% with PrnA and PyrH, respectively, while the two enzymes share 41% identity with each other (determined from full length protein sequences aligned using ClustalW (Chenna *et al.* 2003) rather than by NCBI BLAST (Altschul *et al.* 1990) used for earlier stated identities). This might reflect differences in the type of substrate; while PrnA and PyrH act on free tryptophan (Dong *et al.* 2005; Zehner *et al.* 2005), MibH presumably acts post-translationally on a potentially structured peptide. This could require significant adaptation within the substrate binding pocket of the enzyme.

For many of the flavin-dependent halogenases that have been identified, the substrates are unknown and most are unlikely to use free tryptophan due to the structurally different nature of the compounds involved (van Pee *et al.* 2006). These enzymes are more likely to act upon the coenzyme A derivative of the substrate or on substrates bound to peptidyl carrier proteins (van Pee *et al.* 2006). For example, ChlA, a flavin-dependent halogenase isolated from the amoeba *Dictyostelium*, was reported to directly catalyse the *in vitro* chlorination of the core polyketide substrate (2,4,6-trihydroxyphenyl)-1-hexan-1-one (THPH) (Neumann *et al.* 2010). PltA, involved in biosynthesis of the hybrid polyketide/non-

ribosomal peptide molecule pyoluteorin in *P. fluorescens*, chlorinates a pyrrole ring in the molecule only when the substrate is bound via a thioester link to the PltL carrier protein *in vitro* (Dorrestein *et al.* 2005). The CndH enzyme in the chondrochloren biosynthetic pathway of the myxobacterium *Chondromyces crocatus* acts on a tyrosine substrate bound to a peptidyl carrier protein (Buedenbender *et al.* 2008). Perhaps not surprisingly, this results in structural differences between CndH and PrnA, with the former possessing a more extensive solvent exposed substrate binding surface (Buedenbender *et al.* 2008). Although some amino acid motifs are conserved, the active site base Glu^{346} is not conserved in CndH and this function is proposed to be supplied by the peptidyl carrier protein (Buedenbender *et al.* 2008). A similarly large substrate binding surface might be expected for MibH although it shares very little sequence similarity with CndH.

In the case of PrnA, $FADH_2$ is provided to the enzyme by a partner flavin reductase that uses NADH for the reduction of FAD (Keller *et al.* 2000). However, PrnA could also accept $FADH_2$ from a non-specific flavin reductase from *E. coli* (Hammer *et al.* 1997), and even chemically-reduced FAD could be utilised by the enzyme (Unversucht *et al.* 2005). Some flavin-dependent halogenases, such as RebH (Sanchez *et al.* 2002), and many mono-oxygenases are encoded by genes that lie near or next to a gene encoding a partner flavin reductase, suggesting co-regulation and the requirement for a 1:1 stoichometry between the enzyme products (Louie *et al.* 2003). RebH was found to interact quite tightly with its cognate flavin reductase RebF (Yeh *et al.* 2005).

mibS lies downstream of *mibH* and the two genes are likely to be translationally coupled. MibS shows a high degree of homology with members of the flavin reductase family of proteins. The closest homolog of MibS is KtzS from the kutznerides biosynthetic gene cluster of the actinomycete *Kutzneria* sp. 744 (55% amino acid identity). Kutznerides are hexadepsipeptides with antimicrobial activity manufactured by an NRPS system (Fujimori *et al.* 2007). MibH is also a homolog of KtzR from the same biosynthetic gene cluster (Fujimori *et al.* 2007; Heemstra *et al.* 2008). An *in vitro* analysis of KtsR activity as a tryptophan-6-halogenase indicated that KtzS could function to provide $FADH_2$ for the reaction (Heemstra *et al.* 2008). MibS therefore likely functions to provide $FADH_2$ to MibH to facilitate the chlorination of microbisporicin. It is not clear whether the two proteins physically interact but translational coupling indicates that they are likely to be required in a 1:1 stoichometry.

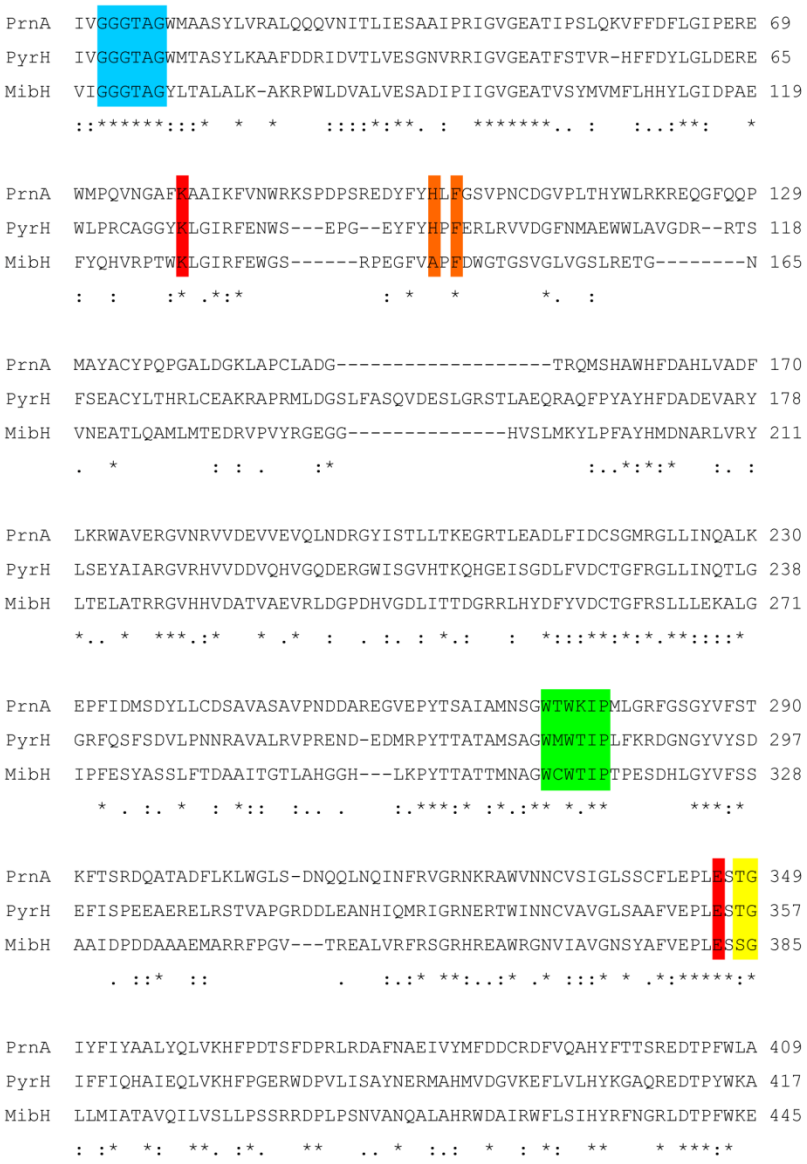

Figure 4.6 A section of an alignment (constructed using ClustalW (Chenna *et al.* 2003)) of MibH with other characterised members of the flavin-dependent class of tryptophan halogenase enzymes (PrnA (pyrollnitrin) and PyrH (pyrroindomycin B)). Conserved residues are highlighted; the GxGxxG motif involved in flavin co-factor binding in PrnA (blue), the WxWxIP motif of PrnA (green), residues involved in binding Cl^- (yellow), Lys^{79} and Glu^{346} involved in the interaction with the reaction intermediate HOCl (red) and residues involved in binding the tryptophan substrate of PrnA (orange) (Dong, *et al.* 2005; Flecks, *et al.* 2008).

4.3.5 MibO

Hydroxylation of proline-14 of microbisporicin is another unique lantibiotic modification. As discussed in Chapter 1, proline hydroxylation of ribosomally synthesised peptides in bacteria has only been described to date in the formation of bacterial collagen in *Bacillus anthracis* , catalysed by a prolyl-4-hydroxylase enzyme (Culpepper *et al.* 2010). This type of enzyme was therefore initially thought to be a candidate for the enzyme catalysing proline hydroxylation in microbisporicin, which would also be expected to occur on a ribosomally-synthesised peptide. However, no such candidate gene was identified in pIJ12125. However, a cytochrome P450 was identified and named MibO.

MibO is a 414 amino acid protein, the closest homologs of which are uncharacterised cytochrome P450 family members from *Frankia* EuI1C (FraEuI1cDRAFT_1316; 40% amino acid identity over 415 amino acids) and *Frankia* EAN1pec (Franean1_4324; 39% amino acid identity over 425 amino acids). MibO also shares a high degree of homology with other cytochrome P450 proteins from other actinomycetes, including CYP130 from *Mycobacterium tuberculosis* H37Rv (34% end-to-end amino acid sequence identity; (Ouellet *et al.* 2008)) and StaP involved in staurosporine biosynthesis in *Streptomyces sp.* TP-AO274 (30% end-to-end amino acid sequence identity; (Makino *et al.* 2007)). Alignment of the amino acid sequence of MibO with those of these structurally characterised members of the cytochrome P450 family indicates that MibO contains a number of conserved motifs including FGHGxHxCLG known to be involved in heme binding (van Wageningen *et al.* 1998) (Figure 4.7).

Cytochrome P450 enzymes typically function as mono-oxygenases, binding dioxygen at a haem iron centre and introducing a single oxygen atom into an organic substrate with production of a molecule of water (McLean *et al.* 2005). Electrons are supplied by NAD(P)H via a redox partner, such as flavodoxin or ferredoxin (McLean *et al.* 2005). *Streptomyces* cytochrome P450 enzymes are often involved in polyketide (e.g. erythromycin) (Chun *et al.* 2006) or non-ribosomal-peptide biosynthesis (e.g. β-hydroxylation in novobiocin biosynthesis) (Walsh *et al.* 2001). There are currently no reports of a bacterial cytochrome P450 enzyme utilising a ribosomally-synthesised peptide as a substrate. Given the position of *mibO* within the microbisporicin gene cluster, it seems likely that MibO is responsible for the unique di-hydroxylation of proline-14 of microbisporicin. However the mechanism by which this occurs and the substrate selectivity involved will be of interest for future study. It is also of interest to note that this enzyme would apparently be capable of hydroxylating two carbon centres within the same amino acid. This is highly unusual in bacterial cytochrome P450s described to date (Prof.

D. Lamb, personal communication). Some plant cytochrome P450 enzymes involved in isoprenoid and sesquiterpene (artemisinin) biosynthesis have been shown to act on multiple carbon centres within one substrate and thus there is precedent for this kind of catalytic mechanism (Ro *et al.* 2005; Covello *et al.* 2007). There are examples of bacterial cytochrome P450s which can produce multiple products from a single substrate through substrate hydroxylatation and release from the active site followed by the binding of another substrate molecule which is then hydroxylated in a different position, producing an array of products (Furuya *et al.* 2010). Furthermore an enzyme has been described which doubly hydroxylates the same carbon centre to produce a keto group during albaflavenone biosynthesis in *S. coelicolor* (Zhao *et al.* 2008).

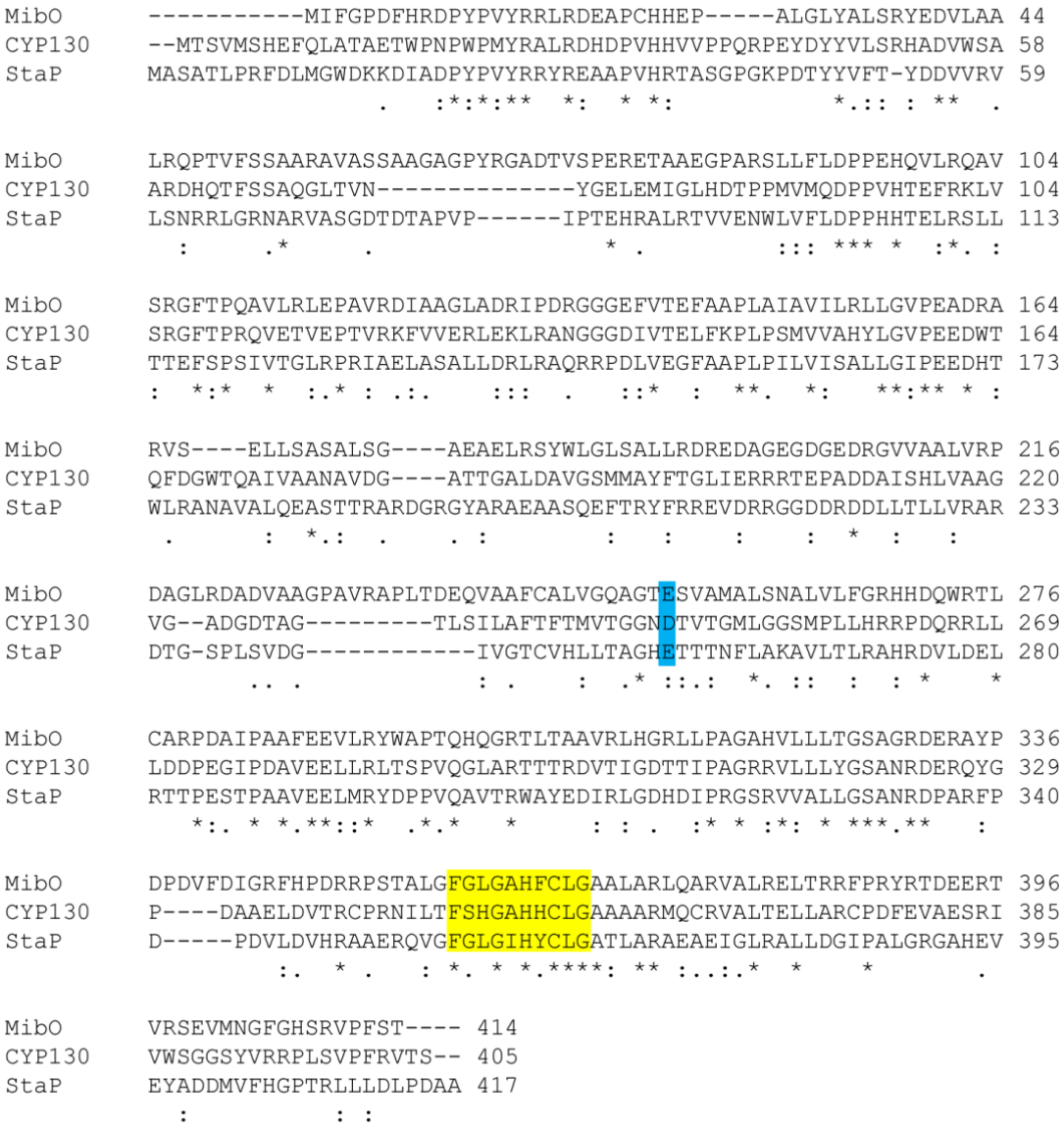

Figure 4.7 A section of an alignment (constructed using ClustalW (Chenna *et al.* 2003)) of MibO with other characterised members of the cytochrome P450 class of enzymes from actinomycetes i.e. CYP130 (*Mycobacterium tuberculosis* H37Rv) and StaP (*Streptomyces sp.* TP-AO274). Highlighted are the conserved negatively charged catalytic residue of CYP130 (blue) (Ouellet *et al.* 2008) and the heme binding motif FGHGxHxCLG (yellow) (van Wageningen *et al.* 1998).

4.4 Export and Resistance

The *mib* gene cluster (Figure 4.1) contains genes encoding three putative two-component ABC transporters (MibTU, MibEF and MibYZ) and a putative sodium/proton antiporter, MibN. Transport proteins in other lantibiotic and antibiotic gene clusters have been variously attributed to roles that include compound export, producer organism self-resistance and regulation. The possible functions of the transporters encoded by the *mib* gene cluster are discussed in the following sections.

4.4.1 MibTU

mibT encodes a 316 amino acid protein with homology to members of the ATP-binding cassette family of proteins. *mibU* encodes a 290 amino acid protein with homology to members of the ABC-transporter permease family of proteins. *mibT* and *mibU* appear to be translationally-coupled suggesting that the encoded proteins function together with a 1:1 stoichometry. Based on other two-component ABC transport systems, it seems likely that the proteins would work as a T_2U_2 unit (Young *et al.* 1999). MibTU share similarity with CinTH of the cinnamycin biosynthetic gene cluster (Widdick *et al.* 2003). Both MibT and CinT have motifs conserved in ATP-binding cassette proteins (such as Walker A, Walker B, Signature (also known as LSGGQ motif) and H-loop amino acid motifs; Figure 4.8). The lower level of similarity between the permease proteins, MibU and CinH, compared to the ATP-binding domains (30% between MibU and CinH, 46% between MibT and CinT) may reflect differences between the two predicted substrates; whereas cinnamycin is a globular type B lantibiotic, microbisporicin is a more elongated type A(I) lantibiotic. No putative peptidase domain was identified in MibU.

As discussed in Chapter 1 the CinTH/MibTU class of lantibiotic transporters differs from those for export of type A(I), A(II) and B lantibiotics in low-GC organisms. This class of putative lantibiotic export ABC-transporters may be specific to actinomycete lantibiotic gene clusters. Both MibTU and CinTH show significant homology to the daunorubicin-resistance ABC transport proteins DrrA (43% amino acid sequence identity with MibT) and DrrB (26% amino acid sequence identity with MibU) of *Streptomyces peucetius*, the producer of daunorubicin (Kaur 1997). This suggests a general function for these ABC-transporters in the export of secondary metabolites. MibTU are likely to function in the export of microbisporicin from *M. corallina*.

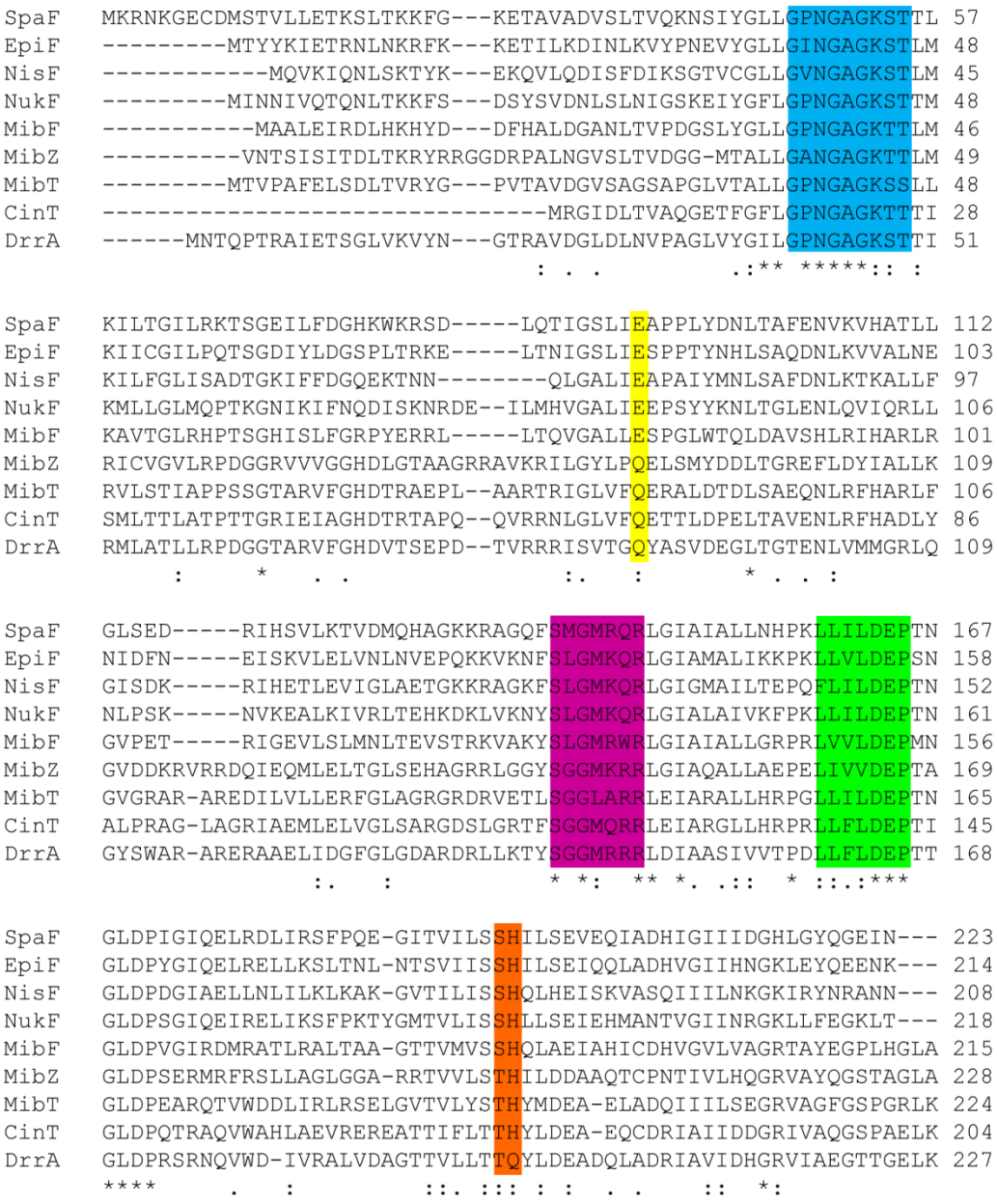

Figure 4.8 Lantibiotic ATP-binding domain proteins. A section of an alignment (constructed using ClustalW (Chenna *et al.* 2003)) of MibF, MibT and MibZ amino acid sequences with those of ATP-binding domain proteins of other lantibiotic LanF proteins (SpaF, subtilin, EpiF, epidermin, NisF, nisin, NukF, nukacin-ISK-1), CinT (cinnamycin) and the daunorubicin export ATP-binding protein DrrA from *Streptomyces peuciticus*. Highlighted are the Walker A motif (blue), E/Q loop (yellow; see text), Signature motif (pink), Walker B motif (green) and H-loop (orange) (Okuda *et al.*, 2010).

4.4.2 MibEF

mibE encodes a 249 amino acid protein with homology to members of the ABC-transporter permease family of proteins. *mibF* encodes a 236 amino acid protein with homology to members of the ATP-binding cassette family of proteins. Based on homology to the LanE and LanF proteins encoded by other type A (I) lantibiotic gene clusters, such as subtilin (SpaEF), epidermin (EpiEF) and mutacin (MutEF), it is likely that MibE and MibF function co-ordinately, with MibF acting as an ATP-binding cassette and MibE as a membrane embedded permease unit. LanE and LanF, usually also in concert with LanG, are involved in conferring resistance to the lantibiotic made by many producing strains (Klein *et al.* 1994; Peschel *et al.* 1996). LanF proteins are the ATP-binding component of the these transporters with a LanE and LanG heterodimer forming the permease structure in the membrane (Draper *et al.* 2008). In some cases, such as mersacidin, LanFEG appear to be the only requirement for self-resistance (Guder *et al.* 2002).

A gene encoding a homolog of the LanG proteins was not identified in the microbisporicin gene cluster suggesting that MibEF alone may be capable of forming the transporter. This would likely be through the formation of a MibE homodimeric permease. This is not without precedent as the absence of a LanG component has also been reported for the lacticin 3147 gene cluster where, although a *lanI* gene is present (secondary system of immunity), the *lanEF* genes are required for full immunity (Draper *et al.* 2009). Similarly the bovicin HJ50 biosynthetic gene cluster does not appear to encode a LanG component (Liu *et al.* 2009). Furthermore it was reported that although inactivation of NisE or NisF renders a nisin-producing strain of *Lactococcus lactis* more sensitive to exogenously applied nisin, this was not the case when NisG was inactivated when there was a much more subtle enhancement in sensitivity (Siegers *et al.* 1995). This suggests that NisEF alone are capable of providing nearly wildtype levels of resistance to nisin. This was not however the case for subtilin where SpaG was found to be essential for resistance in *Bacillus subtilis* (Klein *et al.* 1994). Taken together the evidence suggests that LanG might be dispensible for the formation of an ABC-transporter capable of providing resistance against some lantibiotics.

ABC-transporters typically have a transmembrane-spanning permease component that consists of a total of 12 α-helices, with 6 α-helices per monomer (Young *et al.* 1999). MibE is predicted to have 6 transmembrane helices consistent with the formation of a dimeric permease unit that traverses the membrane. MibF has motifs characteristic of an ATP-binding cassette protein (including Walker A, Walker B, Signature and H-loop amino acid motifs; Figure 4.8) and shares homology with LanF proteins. LanF proteins possess a

conserved E-loop in place of the Q-loop found in the ATP-binding proteins of other classes of ABC transporters (Okuda *et al.* 2010). E85 in the E-loop of NukF is essential for resistance to nukacin_ISK-1 in *Staphylococcus warneri* ISK-1 but is not required for ATPase activity (Okuda *et al.* 2010). When E85 in NukF was replaced with Q as in other ATP-binding proteins and Q88 in DrrA (daunorubicin transporter) was replaced with E as in the LanF proteins, both proteins retained transport activity although not to wildtype levels (Rao *et al.* 2008; Okuda *et al.* 2010). This suggests a functional difference between the two groups of ABC transporters (Okuda *et al.* 2010). Interestingly, by aligning the sequences of MibF and MibT with proteins of both classes of ABC-transporter (Figure 4.8 and 4.9) it is possible to deduce that MibF falls clearly into the LanF group with a conserved E-loop whereas MibT is more similar to DrrA with a Q-loop. Based on models of LanFEG proteins, it is assumed that MibEF would function to provide producer immunity by actively transporting the antibiotic compound away from its lipid II target within the membrane (Otto *et al.* 1998; Stein *et al.* 2003).

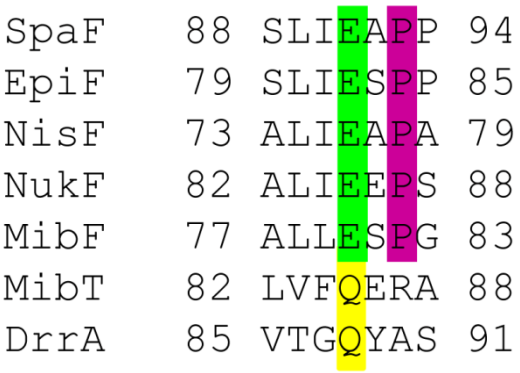

Figure 4.9 A section of an alignment (constructed using ClustalW (Chenna *et al.* 2003)) of MibF and MibT ATP-binding domain proteins with other lantibiotic LanF proteins (SpaF, subtilin, EpiF, epidermin, NisF, nisin, NukF, nukacin-ISK-1) and the daunorubicin export ATP-binding protein DrrA from *Streptomyces peuciticus*. The alignment shows the region of LanF proteins reported to contain the E-loop in lantibiotic immunity systems (green box) rather than the canonical Q-loop of other ABC systems (yellow box) (Okuda *et al.*, 2010). A proline residue also conserved in the LanF proteins is highlighted in pink although the significance of this residue is not known (Okuda *et al.*, 2010). The alignment was constructed based on a larger alignment from Okuda *et al.*, 2010.

4.4.3 MibYZ

mibY encodes a 258 amino acid protein with homology to members of the ABC-transporter permease family of proteins. *mibZ* encodes a 300 amino acid protein with homology to members of the ATP-binding cassette family of proteins and has motifs that are conserved within this protein family (Figure 4.8). Like MibT, MibZ falls into the Q-loop sub-class of this group of proteins (Okuda *et al.* 2010) suggesting that this ABC transporter, unlike MibF, is not involved in lantibiotic immunity.

Close homologs of these two proteins are encoded by pairs of genes in other actinomycete genomes including *Frankia* EAN1pec (Franean1_3994 with 31% amino acid identity to MibY and Franean1_3995 with 54% amino acid identity to MibZ), *Streptosporangium roseum* (Sros_1169 with 28% amino acid identity to MibY and Sros_1168 with 55% amino acid identity to MibZ) and *Actinomyces* oral taxon 848 (ZP_06162160.1 with 29% amino acid identity to MibY and ZP_06162161.1 with 56% amino acid identity to MibZ). Interestingly, *mibJ*, *mibW* and *mibX* are also conserved in an operon with the *mibYZ* homologs of these strains (Figure 4.10). Furthermore, although these genes are not located near a lantibiotic gene cluster in *Frankia* EAN1pec and *Streptosporangium roseum,* those in *Actinomyces* oral taxon 848 are located with a group of genes with very high levels of homology to *mibA*, *mibB*, *mibC* and *mibD* (see also section 4.3; Figure 4.10). This actinomycete likely produces a very similar lantibiotic to microbisporicin (discussed in detail in section 4.8). This also suggests that *mibXWYZJ* may be important for lantibiotic biosynthesis in *M. corallina*.

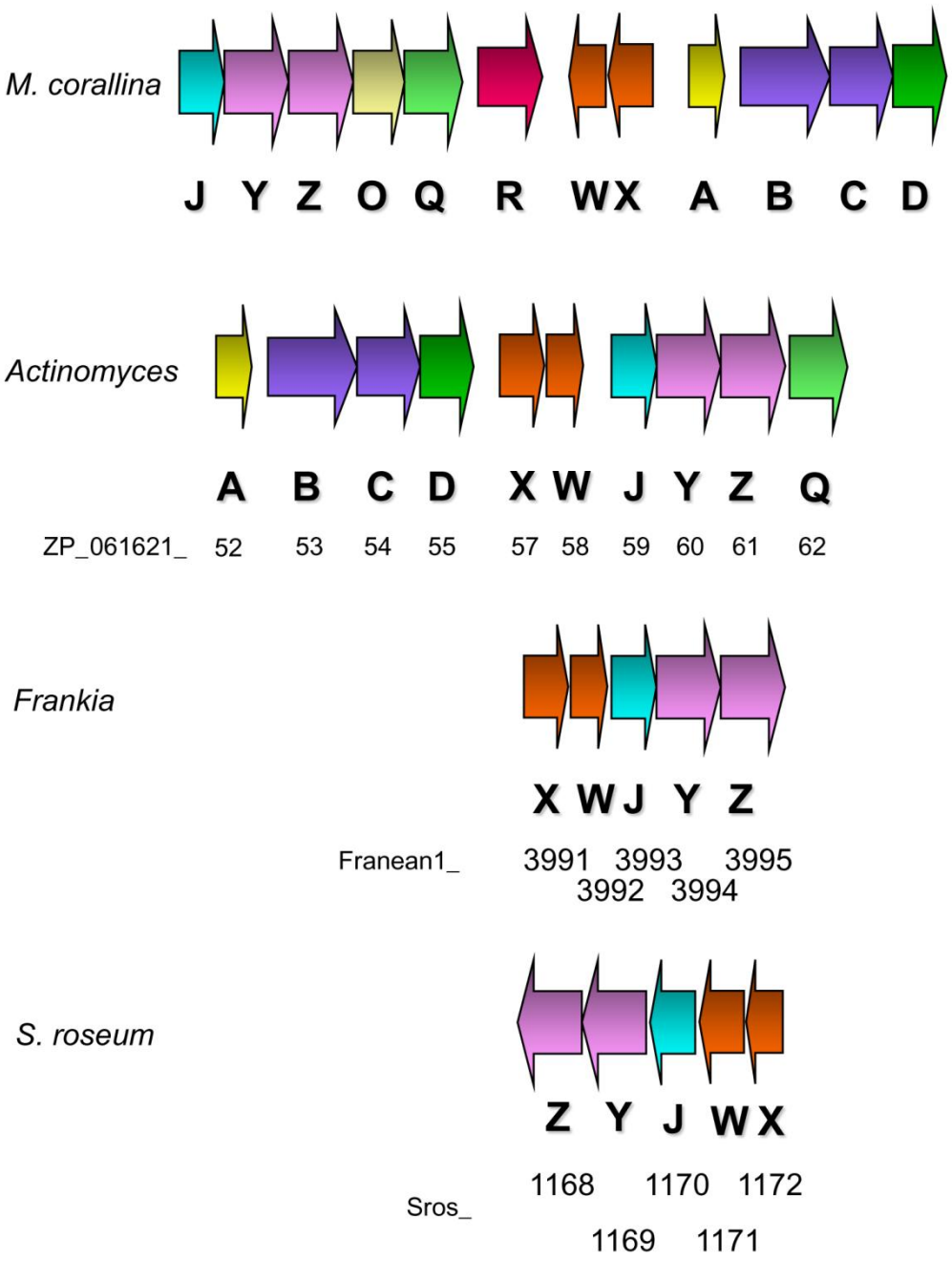

Figure 4.10 A schematic showing the syntenous arrangement of the homologs of *mibX*, *mibW*, *mibJ*, *mibY* and *mibZ* in the actinomycetes listed. Also shown are the homologs of *mibA*, *mibB*, *mibC, mibD* and *mibQ* in *Actinomyces* oral taxon 848. Genes are colour coded and labelled with the names of the respective genes from the *mib* cluster. In each case, the locus tags or gene names are given below.

4.4.4 MibN

MibN encodes a 434 amino acid protein with homology to members of the sodium/proton antiporter family, particularly those associated with non-ribosomal-peptide synthetase (NRPS) and glycopeptide biosynthetic gene clusters, such as ComF (complestatin; *Streptomyces lavendulae;* 61% amino acid identity), ForY (fortimicin; *Micromonospora olivasterospora*; 47% amino acid identity), NapR2 (napyradiomycin; *Streptomyces aculeolatus*; 44% amino acid identity) and StaN (A47934; *Streptomyces toyocaensis*; 43% amino acid identity). The function of these proteins has not been investigated in detail but roles have been postulated in compound export and producer self-resistance (Dairi *et al.* 1992; Chiu *et al.* 2001; Pootoolal *et al.* 2002; Winter *et al.* 2007).

A feature common to all of the above apart from the fortimicin gene cluster is the presence of a gene encoding a flavin-dependent halogenase. Unlike MibH, these enzymes, although belonging to the flavin-dependent group, do not use tryptophan as a substrate (Chiu *et al.* 2001; Pootoolal *et al.* 2002; Winter *et al.* 2007). These proteins are quite similar to each other but have very low similarity (<20%) with MibH. However, in all of these proteins the GxGxxG motif is conserved, consistent with binding a flavin molecule (Dong *et al.* 2005). Several other NRPS/glycopeptide gene clusters also contain genes encoding a halogenase and a sodium/proton antiporter, including the dalbavancin/A40926 (*Nonomuraea sp.*) gene cluster (Sosio *et al.* 2003). The pyrrolnitrin gene cluster of *Pseudomonas fluorescens* consists of four genes (*prnA,B,C* and *D*, with *prnA* encoding a flavin dependent tryptophan halogenase) that were sufficient for pyrrolnitrin production in a heterologous host (Hammer *et al.* 1997). However, it is interesting to note that in the genome sequence of *Pseudomonas fluorescens Pf-5* the genes adjacent to this cluster include a sodium/proton antiporter (PFL_3608; with 29% similarity to MibN) and a flavin reductase (PFL_3609; with 27% similarity to MibS). One possible conclusion from the co-occurrence of the halogenase and antiporter genes within the same gene clusters (though not usually translationally coupled) is that they function together, however there are currently no reports of a requirement for ion transport as part of the halogenase mechanism. Alternatively, since the halogenase MibH does not appear to show high levels of similarity to the halogenases in these other gene clusters, MibH and MibN may not have co-evolved. The two genes may have been acquired by *M. corallina* via horizontal transfer from an NRPS gene cluster, after which only the halogenase has adapted to use a different substrate (the MibA prepropeptide) while MibN has no role in microbisporicin production.

MibN is predicted to contain 11 transmembrane helices (TMHs), consistent with a membrane embedded transport protein. Although classified as a sodium (or potassium)/proton antiporter by sequence homology, it is possible that the transporter is able to export other substrates and it may have a resistance function. Interestingly, in *Bacillus subtilis* a sodium/proton antiporter, TetA(L), with 14 predicted TMHs, exports tetracycline in exchange for proton influx as part of a tetracycline resistance mechanism, as well as acting as a sodium/proton exchanger (Cheng *et al.* 1996a; Cheng *et al.* 1996b; Cheng *et al.* 1996c). TetA(L) may play a major role in ion homeostasis as well as having a protective role against tetracycline (Cheng *et al.* 1996a; Cheng *et al.* 1996b; Cheng *et al.* 1996c), and it is possible that many bacterial antiporter proteins play dual roles in both cellular physiology and drug efflux (Krulwich *et al.* 2005). However, it should be noted that there is no sequence similarity between TetA(L) and MibN.

A third possible role for this protein is in regulation. Recently a system was described in *B. subtilis* in which the movement (in this case leakage out of the cell) of potassium ions is sensed by a histidine kinase protein leading to the induction of a signalling cascade that results in biofilm formation (Lopez *et al.* 2008). This raises the possibility that many ion fluxes across membranes could have a hitherto unrecognised regulatory function. An ion antiporter could play a role in altering ion concentrations that would subsequently induce a regulatory response. Interestingly, the recent heterologous over-expression of a sodium/proton antiporter (SCO7832) from *S. coelicolor* in *Streptomyces lividans* increased actinorhodin biosynthesis and in *Streptomyces* sp. CK4412 induced tautomycetin biosynthesis (Park *et al.* 2009). Increased levels of tautomycin biosynthesis were shown to coincide with increases in expression of the biosynthetic gene cluster and not to increased export of the compound from the mycelium (Park *et al.* 2009).

4.5 Regulation

4.5.1 MibXW

MibX belongs to the extracytoplasmic function (ECF) family of σ factors, sharing 49% and 43% amino acid identity with putative ECF σ factors from *Streptosporangium roseum* DSM43021 (Sros_1172) and *Frankia* sp. EAN1pec (Franean1_3991), respectively. MibX also shares 27% identity with CnrH, an experimentally-verified ECF sigma factor regulating cobalt and nickel resistance in *Cupriavidus metallidurans* CH34 (previously *Ralstonia metallidurans* CH34) (Tibazarwa *et al.* 2000). A recent report grouped ECF sigma factors by sequence comparison into 40 distinct groups (Staron *et al.* 2009). Although MibX was not part of this analysis, close homologs of MibX from *Bradyrhizobium*

BTAi1 (BBta_3011; 37% amino acid sequence identity), *Mesorhizobium loti* MAFF303099 (mll5118; 34% identity) and *Rhodopseudomonas palustris* TIE-1 (Rpal_2022; 35% identity) were grouped into class 33 (Staron *et al.* 2009). No members of this group have been investigated experimentally and so far appear restricted to the Proteobacteria (Staron *et al.* 2009).

The ECF sigma factors are a sub-group of RNA polymerase sigma factors that respond to extracellular signals (e.g. membrane stress) by influencing transcription initiation through recruitment of RNA polymerase core enzyme at relevant promoter sequences (Paget *et al.* 2002). These sigma factors fall into the wider group of the σ^{70} family. The ECF sigma factors were originally described in *S. coelicolor* (σ^{E}) (Lonetto *et al.* 1994) but have subsequently been identified in a wide variety of Gram-positive and Gram-negative bacteria (Paget *et al.* 2002). In several bacteria, especially those undergoing complex development, the ECF sigma factors represent the largest group of sigma factors, for example 51 of a total of 65 sigma factors in *S. coelicolor* (Paget *et al.* 2002). In general ECF sigma factors are involved in responses to stress (such as cell envelope or oxidative stress), iron or other metal uptake, development and virulence regulation (Staron *et al.* 2009). ECF sigma factors often have pleiotropic effects with large regulons (Paget *et al.* 2002).

ECF sigma factors differ from other σ^{70} proteins in having only the σ_2 and σ_4 regions conserved for DNA binding and interaction with RNA polymerase (Lonetto *et al.* 1994), respectively. Furthermore, an alternative consensus motif is found at many ECF-dependent promoters compared to that of the σ^{70} proteins, characterised by an “AAC” motif at the -35 region and “CGT” nucleotides clustered at the -10 region (Helmann 2002; Lane *et al.* 2006). Many ECF sigma factors auto-regulate their own expression (Staron *et al.* 2009).

ECF sigma factor activity is regulated by a number of mechanisms including at the level of transcription (e.g. *S. coelicolor* σ^{E}) or by the protoeolytic processing of a pro-σ-factor (e.g. *S. coelicolor* BldN) (Paget *et al.* 2002). However, in the majority of characterised ECF sigma factors a second protein, usually coexpressed, is involved in regulating ECF sigma factor activity. The anti-σ-factor is able to sequester the σ-factor away from its promoter binding sites thus preventing transcription initiation until the receipt of a specific signal (Staron *et al.* 2009). This signal would likely be sensed by the anti-σ-factor, or a protein regulating it in some way, leading to the release of the σ-factor and subsequent expression of the regulated genes. This release can be mediated via a conformational

change (for example in *S. coelicolor* σ^R regulation by RsrA (Paget *et al.* 2002) or via proteolytic degradation (Heinrich *et al.* 2009a).

Proteolytic degradation of an anti-sigma factor as a mechanism for ECF sigma factor release has been well studied for RsiW, the anti-sigma factor regulating σ^W in *B. subtilis*. Here the signal for ECF sigma factor release is cell envelope stress (CES) induced by antibiotics such as vancomycin or by alkaline shock (Cao *et al.* 2002b). The membrane embedded RsiW binds to σ^W in the absence of such signals but upon CES RsiW undergoes a two-step regulated intramembrane proteolysis (RIP) that releases the cytoplasmic domain of RsiW along with the bound σ-factor (Schobel *et al.* 2004). It is thought that the protease carrying out the first cleavage of RsiW, PrsW, is the point of regulation and likely responds to the membrane signals (Ellermeier *et al.* 2006). Critical residues in the extracytoplasmic loops of this protein, which may have a role in this mechanism, have been identified (Ellermeier *et al.* 2006). More recently an ABC transporter EcsAB was found to play a role in regulating the activity of the second protease, RasP (Schobel *et al.* 2004), although the mechanism of this is unknown (Heinrich *et al.* 2008). EcsAB has interestingly been grouped with antibiotic resistance efflux transporters (Heinrich *et al.* 2008) and contains an E-loop rather than the standard Q-loop of other ABC transporters (discussed in section 4.4.2). The soluble N-terminal fragment of RsiW is subsequently degraded by a cytoplasmic ClpP proteolytic complex releasing the active σ-factor (Zellmeier *et al.* 2006). Sequence similarity between anti-σ-factor genes is often very low, however some features are conserved, such as the location of the gene near (if not downstream of and translationally coupled to) the cognate ECF σ-factor gene. The anti-sigma factor domain (ASD) is also conserved in an estimated 33% of anti-sigma factors and includes the highly conserved HxxxCxxC motif in the ZAS family of anti-σ-factors (38% of ASD-containing anti-sigma factors (Campbell *et al.* 2007; Jordan *et al.* 2008)). The ASD was identified through structure-based studies of *Rhodobacter sphaerorides* ChrR and *E. coli* RseA, which share homology in the N-terminal 1-81 and 1-90 amino acids, respectively (Campbell *et al.* 2007). Many of these residues were found to be involved in contacting the cognate ECF sigma factor (Campbell *et al.* 2007). In contrast, the C-terminal domains of these proteins share very little homology (Campbell *et al.* 2007).

mibW, downstream of and apparently translationally coupled to *mibX*, encodes a protein with low levels of similarity to genes lying downstream of homologs of *mibX*; MibW homologs occur in *S. roseum* DSM43021 (Sros_1171), *Actinomyces* oral taxon 848 (ZP_06162158) and *Frankia* sp. EAN1pec (Franean1_3992), sharing 20%, 21% and 18% identity with MibW, respectively (Figure 4.10). More convincingly, the proteins from

Actinomyces and *Frankia* share with MibW a predicted structure of six transmembrane helices with a cytoplasmic N-terminal region (73 amino acids long in MibW) (TMHMM v.2 (Kall *et al.* 2007); Figure 4.11 and 4.12). Sros_1171 by contrast is predicted to form five transmembrane helices with a large cytoplasmic loop between helices 1 and 2, and a N-terminal extension outside the cell (TMHMM v.2 (Kall *et al.* 2007); Figure 4.11). The class of ECF sigma factors (class 33) into which close homologs of MibX group (discussed above) was noted to contain characteristic membrane-anchored anti-σ factors (Staron *et al.* 2009). An alignment of the amino acid sequences of MibW with the *Actinomyces* and *Frankia* proteins indicates some conserved residues, particularly arginines in the N-terminal region and residues predicted to project from the internal loops at the ends of the transmembrane helices (Figure 4.12). These residues might be involved in interacting with the ECF sigma factors. There was no obvious homology with the ASD consensus of some other anti-sigma factors (Campbell *et al.* 2007). A number of conserved proline residues are also present that are likely to introduce kinks into the transmembrane helices (Figure 4.12).

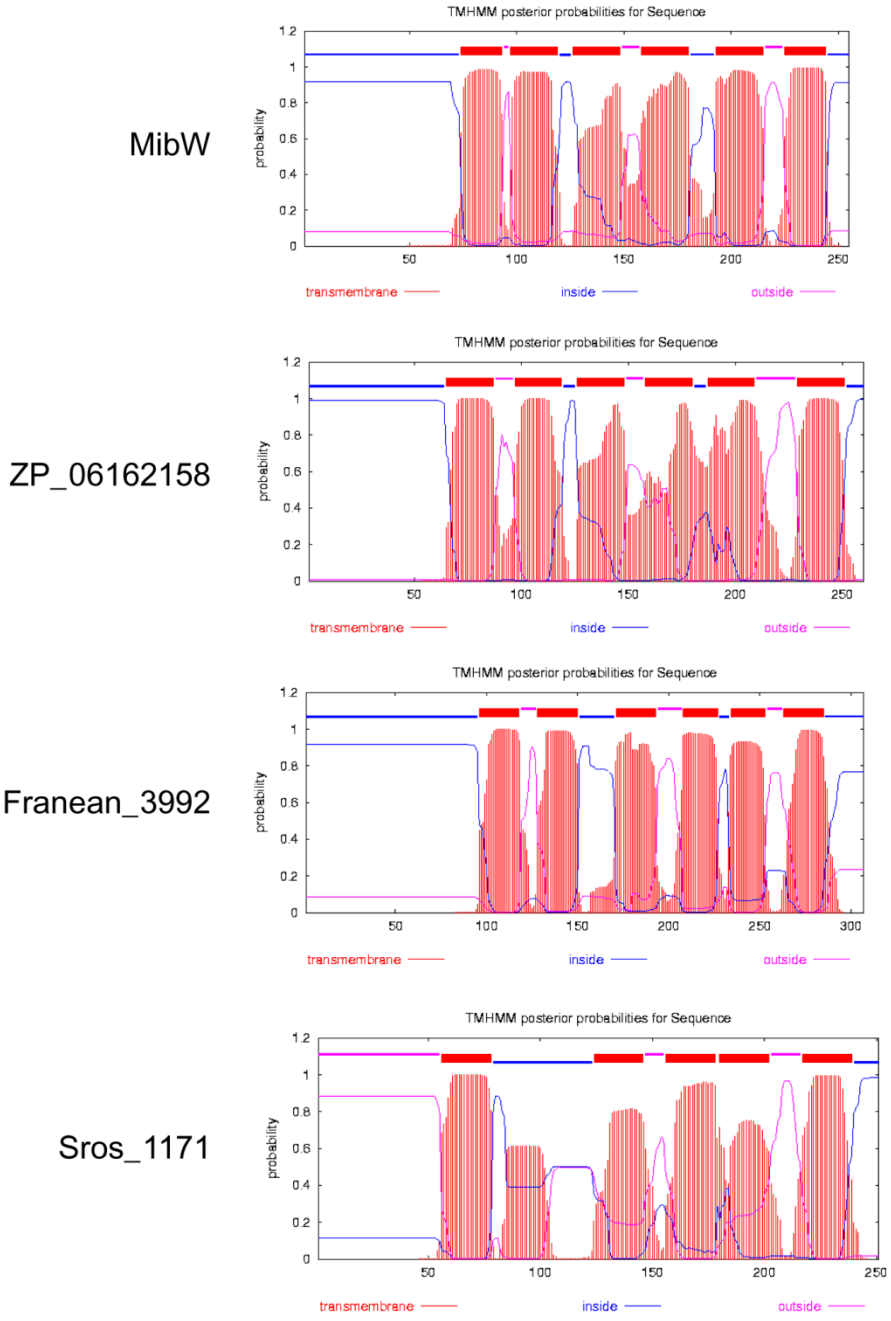

Figure 4.11 A schematic showing the predicted arrangements of the transmembrane helices of MibW and its homologs ZP_06162158 (*Actinomyces* oral taxon 848), Franean_3992 (*Frankia* EAN1pec) and Sros_1171 (*Streptosporangium roseum*). Predictions were made using the full length protein sequences submitted to TMHMM v.2 (Kall *et al.* 2007). Transmembrane helices are shown in red, inside loops in blue and outside loops in pink.

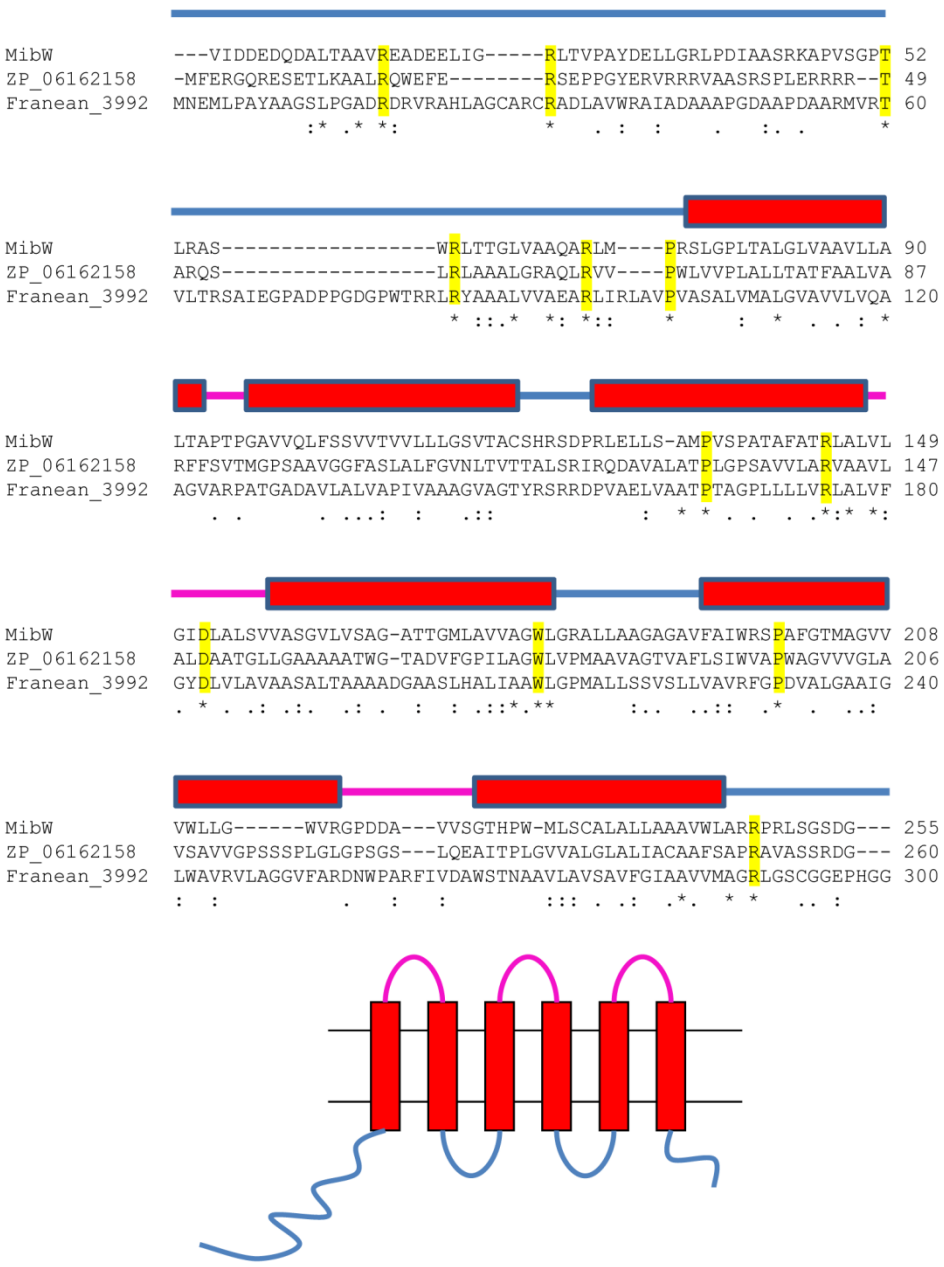

Figure 4.12 A schematic showing an alignment (constructed using ClustalW (Chenna *et al.* 2003)) of the amino acid sequence of MibW with its homologs ZP_06162158 (*Actinomyces* oral taxon 848) and Franean_3992 (*Frankia* EAN1pec). The arrangement of helices and loops in MibW is modelled above the alignment. Predictions were made using the full length protein sequences submitted to TMHMMv.2 (Kall *et al.* 2007). Transmembrane helices are shown in red, inside loops in blue and outside loops in pink. Conserved charged and polar residues, prolines and tryptophan are highlighted in yellow.

The proximity of these *mibW* homologs to the *mibX* homologs suggests that they may function as anti-σ factors to suppress cognate ECF sigma factor activity. The predicted structure of these proteins suggests that this is likely to be mediated by sequestration of the ECF sigma factor at the cell membrane. Release of the ECF sigma factor is likely to be mediated by regulated intramembrane proteolysis or by the receipt of a specific signal at the cell membrane inducing a conformational change in the anti-sigma factor. By analogy to RsiW in *B. subtilis,* a proteolytic mechanism would involve at least one protease acting within the cell membrane and possibly an ABC-transporter like EcsAB (Heinrich *et al.* 2008). These functions could be provided by *mibJ* (section 4.6.1), *mibY* and *mibZ* (section 4.4.3), homologs of which are genetically linked to *mibXW* homologs in other species suggesting a functional linkage (Figure 4.10).

The position of *mibXW* within the microbisporicin gene cluster, and also of their homologs in *Actinomyces* oral taxon 848 within a gene cluster likely to encode a similar lantibiotic (Figure 4.10 and section 4.8), suggests that the encoded proteins play a role in regulating lantibiotic production. This may not be surprising given the roles ECF sigma factors play in regulating the expression of genes associated with cell envelope stress (which would be expected to be induced by the action of microbisporicin inhibiting cell wall biosynthesis) and antibiotic-induced stress. For example, the σ^W regulon in *B. subtilis*, which includes genes involved in antimicrobial resistance, was induced by antibiotics that inhibit cell wall biosynthesis (Cao *et al.* 2002b; Butcher *et al.* 2006). However, due to the wide range of compounds that induced σ^W activity, the authors concluded that this response is more likely to be mediated by general cell envelope stress than by the interaction of a specific antibiotic with the anti-sigma factor RsiW (or one of the proteins regulating its proteolysis) (Cao *et al.* 2002b). The σ^X regulon of *B. subtilis* was similarly found to include genes involved in providing protection against antimicrobial peptides such as nisin by affecting cell envelope properties (Cao *et al.* 2004). Furthermore, the bacitracin resistance gene *bcrC* was reported to be regulated by both σ^X and σ^M (Cao *et al.* 2002a) but this is again most likely mediated through sensing cell envelope stress (Rietkotter *et al.* 2008). Finally, biosynthesis of sublancin, a type A(II) lantibiotic produced by *B. subtilis* strains that are lysogenic for the SPβ bacteriophage, was reported to be dependent on both σ^X and, to a lesser extent, σ^M. However this effect is mediated in an indirect manner though the up-regulation of the transition state regulator Abh which induces the sublancin biosynthetic operon (Luo *et al.* 2009).

Given their location within the *mib* cluster, MibXW would be predicted to be pathway-specific regulators of microbisporicin biosynthesis. ECF sigma factors are typically pleiotropic regulators with large unlinked regulons, however some examples exist of

pathway-specific regulation. One of the early examples of an ECF sigma factor was CarQ from *Myxococcus xanthus*, which is involved in the regulation of light-induced carotenogenesis (Browning *et al.* 2003). However the full regulon of CarQ has not been explored and could include other genes and operons. Nickel and cobalt resistance in *Cupriavidus metallidurans* CH34 is mediated by a single operon *cnrYHXCBAT* that encodes the efflux pump CnrCBA (Grass *et al.* 2000; Grass *et al.* 2005). *cnrH* encodes an ECF-sigma factor (which shares homology with MibX as described above), while *cnrX and cnrY* encode its cognate anti-sigma factor complex (CnrX senses nickel at the cell surface and CnrY, a transmembrane protein, interacts with CnrH in the cytoplasm) (Grass *et al.* 2000). These proteins are responsible for regulating expression of the *cnr* operon in response to nickel (Grass *et al.* 2000). There are also examples where sigma factor genes are linked to antibiotic gene clusters. For example, a new class of sigma-70 factor (group 5), which is related to ECF sigma factors but with distinct features, was identified in *Clostridium* species where members often regulate the expression of linked toxin genes and in one case the expression of a bacteriocin (Dupuy *et al.* 2006). A recent report has described the presence of an ECF sigma factor gene *dhpO*, within the dehydrophos biosynthetic gene cluster of *Streptomyces luridus*, the product of which shares 25% amino acid sequence identity with MibX (Circello *et al.* 2010). However, there is no indication of the presence of an anti-sigma factor gene in the *dhp* cluster and no phenotype was reported for the inactivation of *dhpO* when the mutant cluster is expressed in a heterologous host, suggesting that it is not essential for dehydrophos biosynthesis (Circello *et al.* 2010).

MibX encodes an ECF sigma factor likely involved in regulating the expression of genes in the *mib* cluster and its activity is likely to be controlled by the putative anti-sigma factor MibW. MibW would sequester MibX at the cell membrane, away from its promoter targets until receipt of a specific signal. This as-yet-unknown signal would induce the release of the ECF sigma factor allowing it to interact with promoters in the *mib* gene cluster.

4.5.2 MibR

mibR encodes a hypothetical protein of 260 amino acids that has very little end-to-end homology with any proteins in the current NCBI database. MibR possesses a helix-turn-helix domain found in the LuxR family of regulatory proteins between amino acids 173 to 214 (Pfam; (Finn *et al.* 2008)). The closest homolog of MibR is a response regulator receiver domain protein from *Micromonospora* sp. L5 (29% amino acid identity across a 161 amino acid alignment). Other protein homologs mainly show similarity only within the

putative helix-turn-helix domain of the protein. A homolog in *S. coelicolor* (SCO5455; 35% identity across 125 amino acids) is encoded by a gene located in an operon with a putative sensor kinase, an integral membrane protein and ATP-binding domain protein (StrepDB). MibR is a candidate transcriptional regulator of the microbisporicin gene cluster.

4.6 Genes of unknown function

4.6.1 MibJ

mibJ encodes a 210 amino acid protein with very few homologs in the current NCBI database. Homologs of MibJ are proteins of *Frankia* EAN 1pec (Franean1_3993; 33% amino acid identity over 183 amino acids) and *Streptosporangium roseum* (Sros_1170; 37% identity over 94 amino acids) that are clustered with homologs of *mibYZWX,* as described previously (Figure 4.10). Through low homology to MibJ, it was also possible to identify further homologs of this group of genes in the *Gordonibacter pamelaeae* 7-10-1-bT draft genome sequence (GPA_30300 to GPA_30370). This organism is also an actinomycete (within the *Coriobacteridae* sub-class). The conservation of *mibX, mibW, mibY, mibZ and mibJ* in such an array of actinomycete genomes (*Frankia* EAN1pec, *Streptosporangium roseum*, *Actinomyces* oral taxon 848 (ZP_06162159 shows very low overall sequence similarity to MibJ but contains conserved elements as described below), *Eggertella lenta* DSM 2243 (*Coriobacteridae*; Elen_1454–Elen_1458), and *Bifidobacterium longum* subsp. infantis ATCC 15697 (*Actinobacteridae*; Blon_1401-Blon_1405)) strongly suggests a functional linkage between these proteins. MibJ is likely to be involved in the mechanism of ECF sigma factor regulation but the exact function of this protein is unknown.

MibJ is predicted to contain four transmembrane helices suggesting a membrane-embedded location in the cell. Franean1_3993 and Sros_1170 (which share higher sequence similarity to each other than to MibJ) are both predicted to form five transmembrane helices (TMHMM v2 (Kall *et al.* 2007); Figure 4.13). An internally projected loop is predicted in all three proteins between residues 66-90 (MibJ numbering) and includes a number of conserved charged and polar residues including aspartates/glutamates, glutamine, threonine and arginines (Figure 4.13). Despite low overall (<20%) amino acid sequence homology between MibJ and ZP_06162159 (*Actinomyces* oral taxon 848), this protein is predicted by TMHMM v2 (Kall *et al.* 2007) to contain six TMHs with the same conserved cytoplasmic loop (between amino acids 68-86). Alignment of MibJ with all of the possible MibJ homologs from actinomycetes

containing the *mibXWYZJ* genes indicates that many of the residues described above are conserved within this putative loop region (Figure 4.14). These residues are likely to be functionally important and given the high number of charged and polar residues they could play a catalytic role or be involved in a protein-protein interaction.

```
Franean_3993    MRPLTLWRYEARRAGWAALLGPP-IAVALGVSAALVNALPG-DATTARILLGALEMAVPL 58
Sros_1170       MKPLDLWSHEIRRAGPAAMLAPPALVVLIALLAAFGTRLGSREGNTAWFLLGAVETGIPL 60
MibJ            MVSVELWRHEVRRCGLVALVTPLAVVASTTLLSALAG-----GGMHDFLAVWLPAALLPL 55
                * .: ** :* **.* .*:: *  :..   : :*:        .    : :      :**

Franean_3993    AAGVGCASLVGRDPAVELQLAAPTPYRVTLLRRMAVTLGWAAVVAGLTAAVLIATGWWGR 118
Sros_1170       LTGTAAASLIGRDRAVELQLTLPTGYRSTLLRRLAVTAGWSCLCALAASALLTVTGWWDL 120
MibJ            VAGVCAVGVVSREVMPELQATFPTPYPVTVRRRLRLLI----VAVGAGVVVLAVS----- 106
                 :*. ...::.*:   *** : ** *  *: **: :      : .    .:* .:

Franean_3993    WPANHGPFAGQLTWAAPTVGLGAVGFAAGAVFRSPAAAGALVSTLWTFQQLFADLVQQHL 178
Sros_1170       MPGVPGGLTGQLTWLSPMLWLSALGLLAAVALRSASAAAAVVGAVWVFGQVFHGVLQANP 180
MibJ            --AATG------AGHDPVTGQGASGPVLSSLFS-AASSAAFSLLLIGMGAYAAAGRTRNR 157
                  .  *      :   *    .* *   .  :  .:::.*.   :  :          :

Franean_3993    PGRLLYLFATTRGAVPGDWTRNRLALLGAAATLVALALVVLARSERLIGEEEE 231
Sros_1170       VSRSLALFATTYGTPPGEWLPNRLTLLSTAPLFLAAAWLLLGAAERTLGGETE 233
MibJ            GGPASALVMTAWLAKLLVLDRIPLPPAAVAVAFAAAGVWSMVRGSTRAGGEAV 210
                 .    *. *:  :         *.  ..*  : * .   :  ..   * *
```

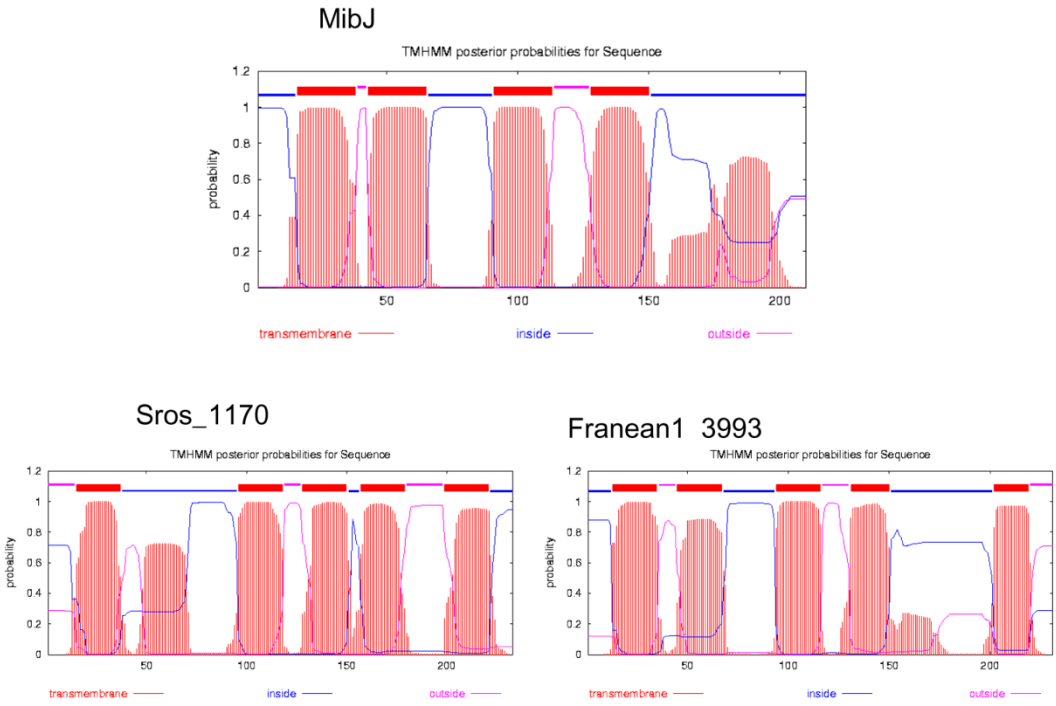

Figure 4.13 A schematic showing an alignment (constructed using ClustalW (Chenna *et al.* 2003)) of the amino acid sequences of MibJ and its homologs Franean_3993 (*Frankia* EAN1pec) and Sros_1170 (*Streptosporangium roseum*). Below are shown the predicted arrangements of the transmembrane helices of the same proteins. Predictions were made using the full length protein sequences submitted to TMHMM v.2 (Kall *et al.* 2007). Transmembrane helices are shown in red, inside loops in blue and outside loops in pink. Above the alignment a blue line indicates the position of a conserved internally positioned loop predicted in all three proteins (MibJ; amino acids 66-90, Sros_1170; amino acids 38-95, Franean_3993 amino acids 68-93). Conserved proline, charged and polar residues in this loop are highlighted in yellow.

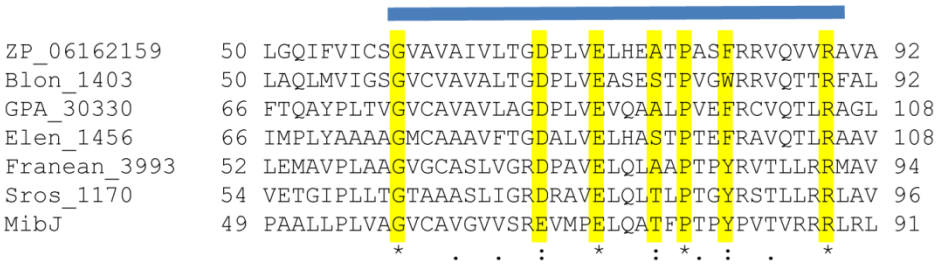

Figure 4.14 A section from an alignment (constructed using ClustalW (Chenna *et al.* 2003)) of the amino acid sequences of MibJ and its close homologs Franean_3993 (*Frankia* EAN1pec) and Sros_1170 (*Streptosporangium roseum*) along with proteins from other actinomycetes which are weak homologs of MibJ; ZP_06162159 (*Actinomyces* oral taxon 848), Elen_1456 (*Eggertella lenta* DSM 2243), Blon_1403 (*Bifidobacterium longum* subsp. infantis ATCC 15697) and GPA_30330 (*Gordonibacter pamelaeae*). The region shown is predicted to contain a cytoplasmic loop in MibJ (and several of its homologs; see text) indicated by the blue line above the alignment. Residues that are conserved or partially conserved between the sequences are highlighted with yellow boxes.

4.6.2 MibQ

mibQ encodes a hypothetical protein of 129 amino acids. MibQ shows homology to proteins from *Actinomyces* oral taxon 848 (ZP_06162162; 38% identity over 91 amino acids) and from *Bifidobacterium longum* subsp. infantis ATCC 15697 (Blon_1406; 37% amino acid sequence identity end-to-end), the genes for which are located with the *mibXWYZJ* homologs of these organisms (sections 4.4.3, 4.5.1 and 4.6.1) (Figure 4.10). Alignment of these three protein sequences suggested that the *Actinomyces* homolog might be missing amino acids at the N-terminus. The open-reading frame encoding ZP_06162162 as indentified in the draft genome sequence by Glimmer2 was reannotated to include a further 43 amino acids at the N-terminus which placed the start codon very close to a putative ribosome-binding site (Kieser *et al.* 2000). The alignment of the resulting protein sequence (ZP_06162162*) with those of MibQ and Blon_1406 indicates a number of conserved residues (Figure 4.15a).

MibQ has a predicted signal peptide sequence with a predicted cleavage site at amino acids 30-31(SignalP 3.0; (Emanuelsson *et al.* 2007)) and contains a conserved lipobox motif LAGC (Sutcliffe *et al.* 2002; Hutchings *et al.* 2009). This motif is also predicted by the tool lipoP (Juncker *et al.* 2003). The lipobox motif (L_{-3}-[A/S/T]$_{-2}$-[G/A]-$_{-1}$-C_{+1}) in the signal peptide of lipoproteins allows them to be anchored in the cell membrane by covalent N-terminal lipidation (Sutcliffe *et al.* 2002; Hutchings *et al.* 2009). Alignment of the predicted signal peptide regions of the three proteins described above (MibQ, ZP_06162162 and Blon1406) revealed conservation of this motif (Figure 4.15b). Analysis of the amino acid sequence of MibQ using Pfam (Finn *et al.* 2008) indicates that it may share motifs with other lipoproteins, such as the sporulation lipoprotein YhcN/YlaJ from *B. subtilis.* Lipoproteins in Gram-positive bacteria are involved in a range of functions including sensing, substrate recognition and cell envelope homeostasis (Hutchings *et al.* 2009).

CseA is a lipoprotein involved in negatively regulating the ECF sigma factor σ^E in *S. coelicolor* (Hutchings *et al.* 2006). The lipobox motif of MibQ and its homologs is conserved with that of CseA, although CseA shares only 19% amino acid sequence identity with MibQ (Figure 4.15b). The exact mechanism by which CseA functions is not clear but the implication of a lipoprotein regulating activation of an ECF sigma factor suggests that this could be the role of MibQ. This is supported by the conservation of *mibQ* homologs near the homologs of *mibXW* in at least three actinomycetes.

A

```
Blon_1406       MTN-TTHAIQTITATG--------LAAIMALGLTACMD----GIEHPENYPTNGSKKITA 47
ZP_06162162*    MKQKNTVERENIAKRGASSRAPRRIRGVIAAGLLGAMGLSGCGMLHPEDYPTDTAKLPKA 60
MibQ            MTN---TTRARLSGAG---------LLAAALLLAGCTG---GGRADPAHRSP--VPLPSP 43
                *.:        ::  *            *  * .. .    *  .* . ..      ..

Blon_1406       TSNPQDISADQLGHTWPLTVDHGTVSCTHNSKGDPVMRFTAPDGTQYALNQTSDNKDLPD 107
ZP_06162162*    TSNPAKISKATFRHSWNLTVDHGTVYCKLNSAGDPILYFTAPNGTEYALNSVTGNGGRPN 120
MibQ            TSSKQDISEANLAYLWPLTVDHGTIECLPSDN----AVFVAPDGTTYALNDRAEKAGHPP 99
                **.  .**   : : * *******: *  ..      *.**:** ****. : : . *

Blon_1406       INQLLADGK-----STGTLTSFAFTVCDVK 132
ZP_06162162*    IED-IADG------SVGPIRSFAFSVCDVK 143
MibQ            ITPIRAKGSGGGYISLGALLSTTLNLCGKG 129
                *    *.*      * *.: * ::.:*.
```

B

```
MibQ              15 LAAALLLAGCTGGGR 29
CseA              28 VALGVSLAGCGTGGT 42
ZP_06162162*      27 LLGAMGLSGCGMLHP 40
Blon_1406         18 AIMALGLTACMDGIE 31
                        .: *:.*
                           LAGC
Lipobox Consensus Residues:  SA
                             T
```

Figure 4.15 A; An alignment (constructed using ClustalW (Chenna *et al.* 2003)) of the amino acid sequences of MibQ and its homologs ZP_06162162 (*Actinomyces* oral taxon 848; the start codon was adjusted compared to the reported amino acid sequence from the NCBI database as indicated by a *, see text for details) and Blon_1406 (*Bifidobacterium longum* subsp. infantis ATCC 15697). **B;** A section from an alignment of the predicted signal peptide regions of the same proteins with that from CseA (*S. coelicolor*) showing the conserved lipobox motif L_{-3}-[A/S/T]$_{-2}$-[G/A]-$_{-1}$-C_{+1} (Sutcliffe and Harrington 2002) highlighted in yellow.

A number of lantibiotic clusters, including those of the type A(I) group, contain genes encoding LanI proteins. NisI is a lipoprotein (containing a signal peptide and lipobox motif LSGC). Post-translational removal of the first 19 amino acids of NisI allows the addition of palmitic acid at the conserved cysteine of the lipobox motif, anchoring the protein to the cell membrane where it acts to block nisin activity by binding the lantibiotic before it can bind to the cellular target lipid II (Qiao *et al.* 1995; Stein *et al.* 2003). There is very little sequence similarity between LanI proteins presumably reflecting differences in the bound lantibiotic target (Draper *et al.* 2008). There is no indication of any sequence similarity between MibQ and either NisI or SpaI except for the lipobox motif which is present in the N-terminal region of all three proteins. An alternative function of MibQ could therefore be as an auxiliary self-resistance mechanism for *M. corallina* through the interaction with microbisporicin at the cell envelope to prevent interaction with the presumed cellular target Lipid II.

4.6.3 MibV

mibV encodes a 334 amino acid hypothetical protein with very few homologs in the current non-redundant protein database. MibV shows low similarity (<30% amino acid sequence identity) to hypothetical proteins in a number of *Streptomyces* species, including *S. coelicolor*, *S. griseus*, *S. venezuelae* and *S. ambofaciens,* as well as to *Bacillus amyloliquefaciens*, *Burkholderia ubonensis* and *Saccharopolyspora erythraea*. The closest homolog (NdasDRAFT_3165; 36% amino acid identity) of MibV is found in a recently completed genome sequence of the actinomycete *Nocardiopsis dassonvillei*. In this organism the homolog of *mibV* is located next to genes that appear to belong to an uncharacterised lantibiotic gene cluster. The *lanA* gene from this cluster was predicted to encode a prepropeptide falling within the type A(I) class (it has the “FNLD” motif) but with otherwise only low similarity to MibA. Homologs of MibV do not indicate any potential function but association with a lantibiotic gene cluster in another organism suggests that this protein might have a novel role in lantibiotic biosynthesis.

4.7 Microbisporicin-like lantibiotics from other bacteria

The identification of genes homologous to those of the *mib* cluster in other bacteria suggests that microbisporicin may belong to a larger family of lantibiotics. The biosynthetic enzymes encoded by *mibB*, *mibC* and *mibD* have homologs in both *Bacillus clausii* KSM-K16 and *Actinomyces* oral taxon 848 (section 4.3). This observation prompted a more detailed examination of the genome sequences of these organisms in the neighbouring regions of these genes.

In the *B. clausii* genome a possible *lanA* gene had not been identified by the genome annotation software. However by analysing this region (*B. clausii* KSM-K16 369440-3707200) in Artemis (Rutherford *et al.* 2000) it was possible to identify a putative *lanA* gene from 3706154-3706766. The *lanA* gene encodes a putative prepropeptide with significant homology to MibA (34% end-to-end amino acid sequence identity; Figure 4.16) and using the known structure of microbisporicin as a guide it was possible to predict the structure of the mature putative lantibiotic, which was named clausin (Figure 4.17). This molecule was also isolated from another strain of *B. clausii* and the predicted structure confirmed (Bouhss *et al.* 2009; Bressollier *et al.* 2009). This strain of *B. clausii* was isolated from a probiotic solution of multi-antibioitic resistant *Bacillus* spores used in the treatment of intestinal disorders, marketed as Enterogermina© by Sanofi-Aventis (Bressollier *et al.* 2009). Clausin has recently been reported to interact with lipid precursors Lipid I and Lipid II of cell wall biosynthesis through binding to the pyrophosphate moiety within the membrane (Bouhss *et al.* 2009). Apart from the homology to *mibA, B, C* and *D*, there is no other similarity between the two gene clusters and the *B. clausii* cluster otherwise shares more similarity with those of the low GC Gram-positive type A (I) clusters, as would be expected for a *Bacillus* species e.g. a LanT-like export protein and a two-component histidine kinase-response regulator pair presumably involved in regulation. Although not possessing the chlorinated tryptophan of microbisporicin at position 4 (where valine is incorporated) or the dihydroxylated proline at position 14 (where there is a threonine), clausin appears to have a similar C-terminal structure and a highly conserved MibD homolog suggests that an *S*-[(*Z*)-2-aminovinyl]-D-cysteine will be present in the mature compound (Figure 4.17). Clausin is likely to have largely the same lanthionine bridge structure as microbisporicin, although it is shorter by two amino acids (Figure 4.17). A very similar compound and gene cluster was also identified through a homolog of *mibB* in the genome sequence of *Bacillus mycoides* DSM 2048.

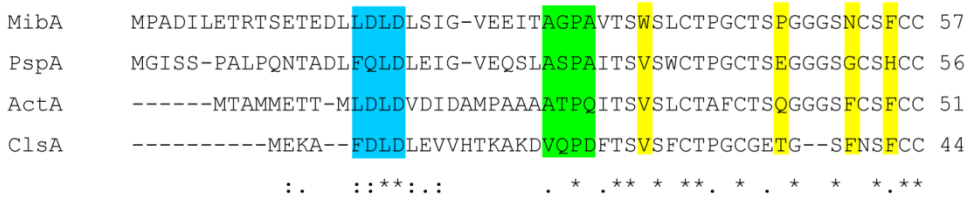

Figure 4.16 An alignment (constructed using ClustalW (Chenna *et al.* 2003)) of the MibA prepropeptide with those of planosporicin (PspA), actoracin (ActA) and clausin (ClsA). The partially conserved FNLD motif is shown in light blue. A putative conserved cleavage site is shown in green. Residues that appear to vary highly in this group of lantibiotics are highlighted in yellow.

A lantibiotic gene cluster with a great deal of similarity to the *mib* cluster was identified in nucleotide region 154000-170000 of the *Actinomyces* oral taxon 848 draft genome sequence (Figure 4.10). In this cluster, not only were the biosynthetic genes *mibB*, *mibC* and *mibD* highly conserved (section 4.3) but also *mibXWJYZ* (sections 4.4, 4.5 and 4.6) (Figure 4.10). The *Actinomyces* prepropeptide (LanA) shares 49% amino acid similarity (end-to-end) with MibA (Figure 4.16) and modelling this peptide using the microbisporicin structure suggests that it is likely to possess even greater similarity to microbisporicin than clausin (Figure 4.17). This putative lantibiotic was named actoracin. As with clausin, although the residues for chlorination and hydroxylation are not present (tryptophan and proline are replaced by valine and glutamine, respectively), actoracin is likely to have the C-terminal *S*-[(*Z*)-2-aminovinyl]-D-cysteine modification (Figure 4.17). The genome of *Actinomyces* oral taxon 848 strain F0332 was sequenced as part of the human microbiome project (http://nihroadmap.nih.gov/hmp/) after isolation from the human oral cavity. Many actinomycetes of the *Actinomyces* genera are commensals and some are also pathogens, for example *Actinomyces israelii.* Due to the large number of bacteria co-habiting in the human mouth it is conceivable that actoracin could be an anti-microbial used by *Actinomyces* for competition. However it is curious that within the actoracin gene cluster there is no homolog of the *mibTU* export genes, or genes that could be involved in self-resistance, although it is possible that the homologs of MibYZ could have this role or these functions could be provided by other genes in the genome. The absence of self-resistance genes might however imply that this compound has a signalling function rather than acting as an anti-microbial.

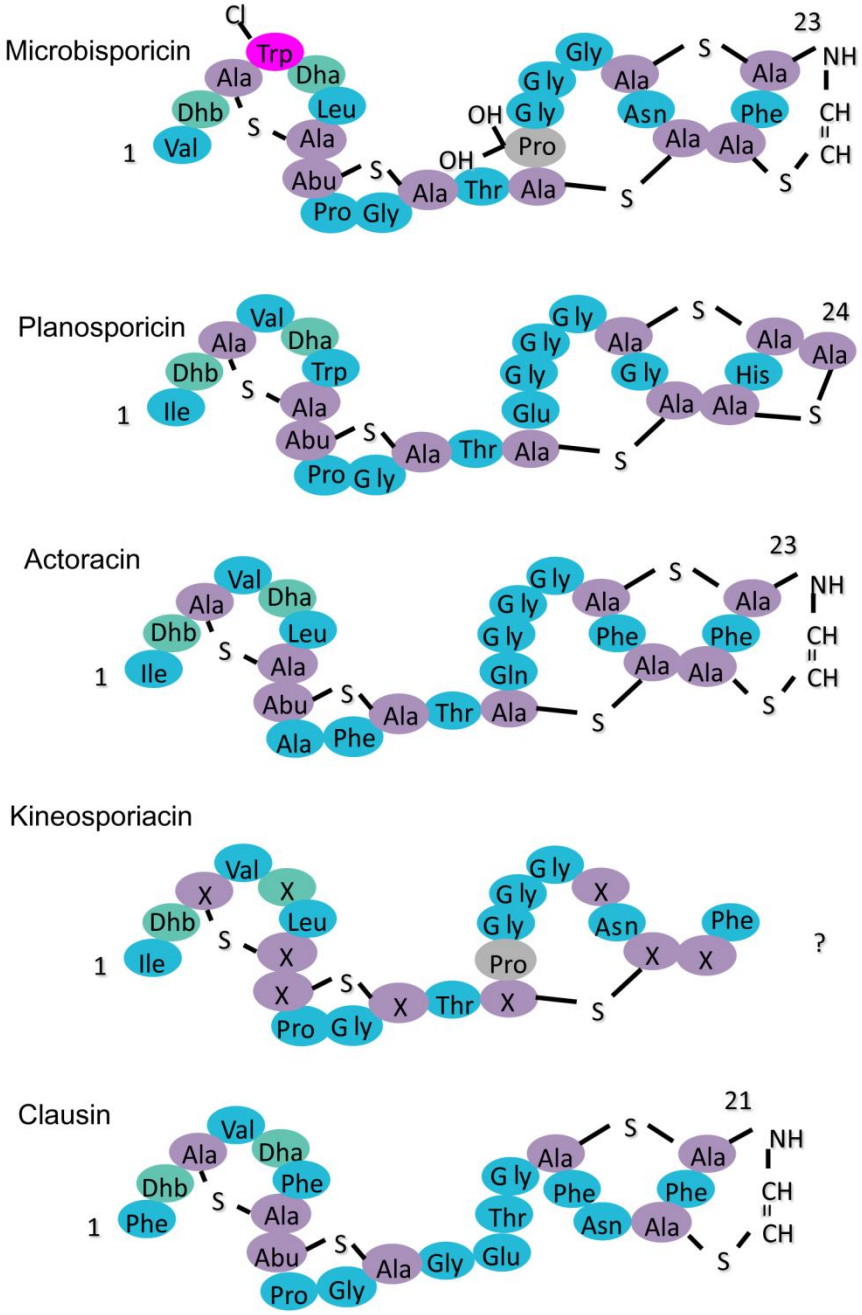

Figure 4.17 A comparison of microbisporicin-like lantibiotic structures. The microbisporicin and planosporicin structures are as reported (Castiglione *et al.* 2008; Maffioli *et al.* 2009). The structures of actoracin (*Actinomyces*), kineosporiacin (*Kineosporia* sp.) and clausin (*B. clausii*) were modelled on microbisporicin as described in the text. Residues are; unmodified (blue), dehydrated (green) dehydrated and cyclised residues (purple), chlorinated tryptophan (pink) and (putative) hydroxylated proline (grey).

Another potential member of the microbisporicin-like lantibiotic family was identified from *Kineosporia* sp. and a patent (in Japanese) was filed for this compound (Shimizu *et al.* 2004). *Kineosporia* is an actinomycete of the *Kineosporiaceae* family. These authors report that Edman sequencing was blocked after the first residue, probably due to the incorporation of lanthionine bridges in the molecule (Shimizu *et al.* 2004). Instead they used a chemical-derivitisation method which makes the peptide accessible to Edman sequenicing (Meyer *et al.* 1994). However this method does not allow the discrimination of cysteine, serine and threonine incorporated into lanthionine bridges and dehydrated serine and threonine residues and therefore only the partial amino acid sequence of the mature compound was reported (Shimizu *et al.* 2004). Since the genome sequence for this species of *Kineosporia* (or any *Kineosporia* sp.) is not available, it is not possible to look for sequence similarities with the *mib* gene cluster. The structure of the mature molecule, termed here kineosporiacin, was predicted from the partial sequence available (Shimizu *et al.* 2004) and the structure of microbisporicin (Figure 4.17). The proline residue at position 14 in microbisporicin is conserved in kineosporiacin, suggesting that it too could be hydroxylated. A phenylalanine at the C-terminus of this molecule suggests that a *S*-[(*Z*)-2-aminovinyl]-D-cysteine modification similar to that of microbisporicin might be present in the mature molecule and could not be detected by the methods used by these authors.

The final lantibiotic with reported similarity to microbisporicin is planosporicin from *Planomonospora* sp., an actinomycete in the same family as *M. corallina* (Castiglione *et al.* 2007; Maffioli *et al.* 2009). Planosporicin shares a number of similarities with microbisporicin, although interestingly, like clausin and actoracin, it is not modified by chlorination or hydroxylation and does not contain a *S*-[(*Z*)-2-aminovinyl]-D-cysteine at the C-terminus (Figure 4.17). Instead, planosporicin has a lanthionine bridge at the C-terminus, the reason for which is not clear. The planosporicin prepropeptide was identified as part of the structural revision of this molecule (structural protein 97518 preproprotein from *Planomonospora* sp. DSM 14920; (Maffioli *et al.* 2009)) (Figure 4.16).

This analysis indicates that microbisporicin appears to be a member of a larger group of lantibiotics (many of which are produced by rare actinomycetes) which share structural and sequence features that presumably contribute to a specific mode of action. It is interesting to speculate on how these gene clusters have evolved in such diverse species (in actinomycetes and *Bacillus* sp.) and whether the arrival at this final structure is due to convergent evolution selecting a particularly effective anti-microbial action. The conservation of the biosynthetic enzymes in the clausin, actoracin and microbisporicin gene clusters may be a product of horizontal transfer or of convergent evolution.

4.8 The absence of the microbisporicin gene cluster in *M. corallina* DSM 44681 and DSM 44682

The lack of microbisporicin production by *M. corallina* strains DSM 44681 and DSM 44682 was described in Chapter 3. To investigate whether this reflected the absence of the microbisporicin gene cluster from these strains or the presence of a silent gene cluster, PCR-based and Southern blot hybridisation strategies were employed using genes from the *mib* gene cluster as probes.

PCR primers (LFnnnR/F) were designed for the following regions of the *mib* cluster: *mibA* (*mibA* plus downstream intergenic sequence - LF013F and LF013R yielding a 592bp product), *mibC* 5' (LF001F and LF001R yielding a 249bp product), *mibC* 3' (LF002F and LF002R yielding a 202 bp product), *mibD* (LF004F and LF004R yielding a 184 bp product) and *mibH* (LF006F and LF006R yielding a 344 bp product). These primers were used to amplify these regions from control NRRL 30420 gDNA and from DSM 44681 and DSM 44682 gDNA samples (Figure 4.18). In each case a band of the correct size was amplified from the NRRL 30402 gDNA control. Although with some primer pairs (namely those for *mibA* and *mibH*) non-specific bands were amplified from the DSM 44681 and DSM 44862 template gDNA, no bands of the expected sizes were obtained (Figure 4.18). One of the putative *mibA* amplicons from the DSM 44682 gDNA sample (about 470 bp in size compared to the expected 592 bp) was excised, purified by gel extraction and the resulting PCR fragment sequenced. The sequence bore no similarity to *mibA* and appeared to have originated by fortuitous amplification of part of a histidine kinase gene.

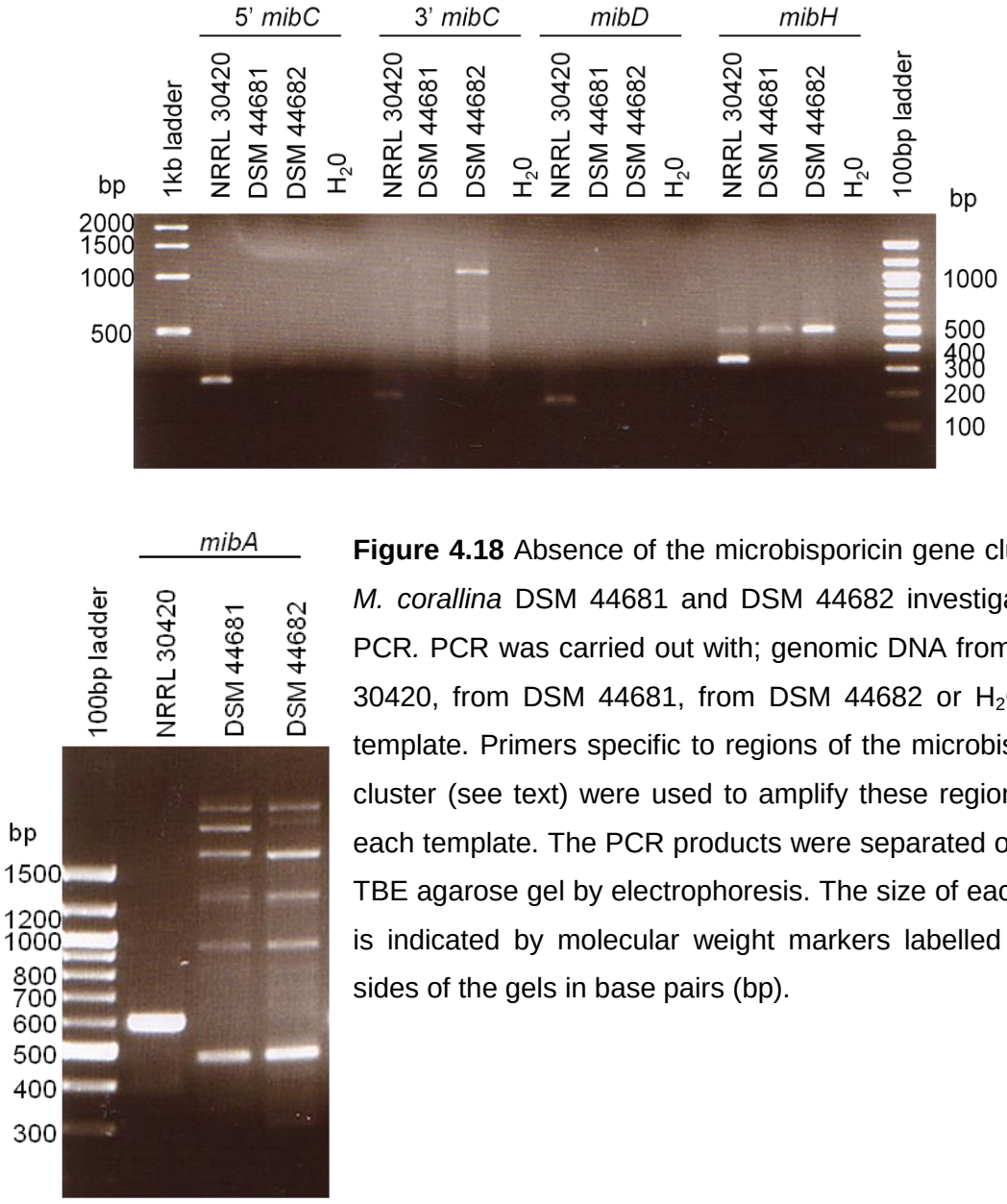

Figure 4.18 Absence of the microbisporicin gene cluster in *M. corallina* DSM 44681 and DSM 44682 investigated by PCR. PCR was carried out with; genomic DNA from NRRL 30420, from DSM 44681, from DSM 44682 or H_2O as a template. Primers specific to regions of the microbisporicin cluster (see text) were used to amplify these regions from each template. The PCR products were separated on a 1% TBE agarose gel by electrophoresis. The size of each band is indicated by molecular weight markers labelled on the sides of the gels in base pairs (bp).

These results were supported by Southern blot hybridisation using digoxigenin-labelled probes designed to bind to *mibA* (*mibA* plus the downstream region between *mibA* and *mibB*; generated by PCR amplification using primers LF013F and LF013R) and *mibD* (generated by PCR amplification using primers LF004F and LF004R). Genomic DNA extracted from NRRL 30420, DSM 44681, DSM 44682 and from *Streptomyces lividans* TK24 (as a negative control) was digested with *Bam*HI and subjected to Southern blot hybridisation with each of the two probes. Both probes bound with very high signal strength to the digested NRRL 30420 gDNA but both also bound non-specifically (at very high molecular weight) within gDNA from *S. lividans* (Figure 4.19). Only the *mibA* probe bound with low signal strength to gDNA from DSM 44681 and DSM 44682 (same fragment size in both samples, and slightly larger than that from NRRL 30420), although this might be expected given the PCR results. This probe also hybridised to other genomic fragments in the NRRL 30420, DSM 44681 and DSM 44682 genomic DNA samples suggesting that it is not a good marker for the *mib* gene cluster. In contrast, the *mibD* probe gave just one hybridising band with NRRL 30420 gDNA and did not hybridise at all with DSM 44681 or DSM 44682 gDNA (Figure 4.19).

The combined evidence from the PCR and Southern blot analyses suggests that the non-microbisporicin producing strains of *M. corallina* do not possess a gene cluster with high levels of similarity to the microbisporicin cluster from NRRL 30420.

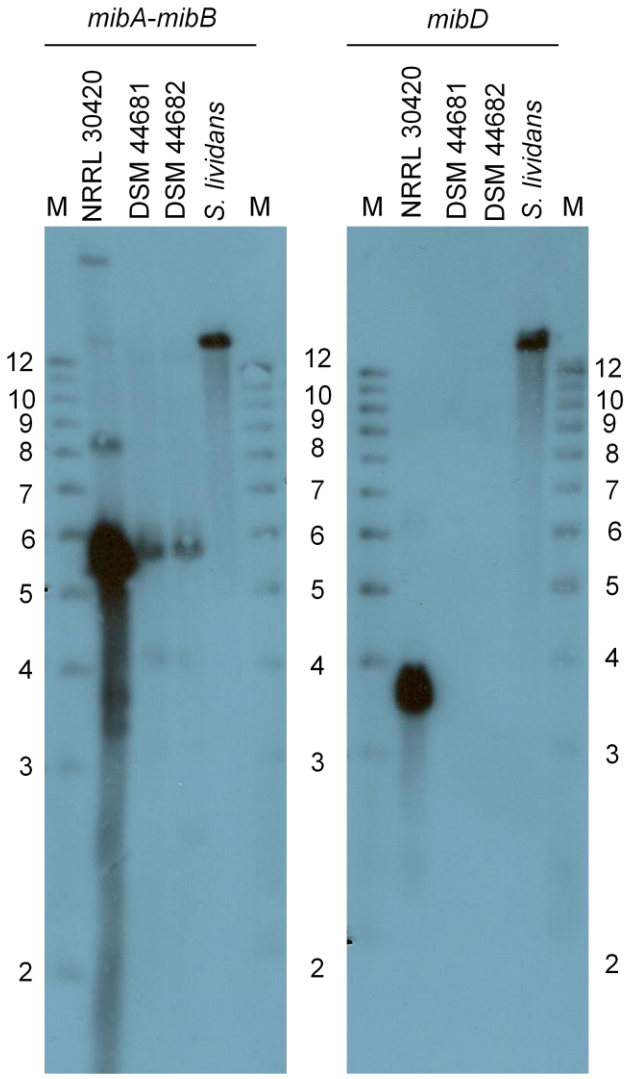

Figure 4.19 Southern blot hybridisation to determine whether the *mibA* and *mibD* regions of the *mib* gene cluster are present in DSM 44681 and DSM 44682. *M. corallina* NRRL 30420, DSM 44681, DSM 44682 and *Streptomyces lividans* TK24 gDNA was digested with the restriction enzyme *Bam*HI and the resulting fragments separated on a 1% agarose gel. DNA was transferred to a nylon membrane by Southern transfer and each blot was probed with a different DIG-labelled PCR product probe, as indicated at the top of each blot; *mibA-mibB* (*mibA* plus downstream region between *mibA* and *mibB*; generated by PCR amplification using the primers LF013F and LF013R) and *mibD* (generated by PCR amplification using the primers LF004F and LF004R). The molecular weights of each marker band (M; Invitrogen 1 kb ladder) are given on the sides of each blot (in kb).

4.9 Discussion and Summary Points

4.9.1 Discussion

Bioinformatic analysis of the microbisporicin gene cluster revealed a number of interesting features. The biosynthetic enzymes of the cluster, MibB, MibC and MibD, although largely unremarkable as classic members of their protein families, which have been well characterised in other lantibiotic gene clusters, revealed a family of microbisporicin-like lantibiotics with predicted shared sequence and structural features. These uncharacterised lantibiotics could have potential uses as anti-microbials and could be of interest for further study.

The chlorination of tryptophan and the hydroxylation of proline are post-translational modifications unique to microbisporicin. Interestingly both modifications appear to be carried out by enzymes belonging to families involved in the tailoring reactions of other secondary metabolites, including non-ribosomally synthesised peptides and polyketides. Deletion of these genes from the microbisporicin gene cluster will reveal whether these enzymes really are responsible for the attributed modifications and will indicate the contribution of each modification towards anti-microbial activity and microbisporicin's mechanism of action. Future structural studies of both of these enzymes will shed light on the mechanisms of these reactions and how substrate specificity is achieved.

The microbisporicin gene cluster is unique in containing four putative transport systems. Although the putative functions of MibTU and MibEF, in export and resistance, respectively, could be predicted based on sequence homology, these predictions require confirmation by mutational analysis. Similarly, the functions (if any) of MibYZ and MibN in microbisporicin biosynthesis require experimental analysis.

The mechanism by which the expression of the genes of the microbisporicin gene cluster is regulated is an intriguing question. Typical regulators associated with lantibiotic gene clusters are two-component systems such as NisRK (Chatterjee *et al.* 2005). Low levels of nisin (produced through low level expression of the prepropeptide and biosynthetic genes) induce this system likely through an interaction with NisK at the cell membrane leading to NisR activation by phosphorylation. Phosphorylated NisR then activates high level expression of the nisin gene cluster to generate high level production (see also Chapter 1; (Kuipers *et al.* 1995; de Ruyter *et al.* 1996)). This system appears to be largely shared by other low GC Gram-positive type A(I) lantibiotic gene clusters (Stein *et al.* 2002; Schmitz *et al.* 2006). This suggests that in many cases low level production of the compound itself induces expression of the gene cluster. In the microbisporicin gene cluster there is no two-

component system but instead an ECF sigma factor:anti-sigma factor pair, MibXW. These proteins could function in an analogous way to the NisRK system. Low levels of microbisporicin would induce cell envelope stress which would be sensed by MibW or alternatively MibW could bind directly to microbisporicin. This would somehow cause the release of bound MibX; possibilities such as a conformational change or intramembrane proteolysis were discussed in this chapter. MibX would then act as an activator of gene expression in the *mib* cluster. How other proteins encoded in this part of the gene cluster, including the transcriptional regulator MibR, would fit into this scheme remains to be determined. A number of strategies to test this model can be postulated. Initially a deletional analysis of this part of the gene cluster will yield information on whether any of these proteins are important for microbisporicin production and *mib* gene expression. The predicted interaction between MibX and MibW could also be investigated, as could possible interactions between MibW and MibJ.

A number of characterised lantibiotic gene clusters encode a dedicated extracellular protease (LanP) which removes the cognate leader peptide (Altena *et al.* 2000; Chatterjee *et al.* 2005). An enzyme responsible for leader peptide cleavage to generate mature microbisporicin has not been identified although it is possible that one of the genes of unknown function (*mibJ*, *mibQ* and *mibV*) could have this role. The subtilin, actagardine and cinnamycin gene clusters similarly do not appear to contain genes encoding a dedicated LanP-type enzyme but instead appear to rely on non-specific proteases for leader peptide cleavage (Widdick *et al.* 2003; Chatterjee *et al.* 2005; Boakes *et al.* 2009). When expressed in the heterologous host *S. lividans* mature cinnamycin is produced suggesting that a general protease in *Streptomyces* is able to fulfil this role (Widdick *et al.* 2003). This was found to be the case for full maturation of haloduracin (Cooper *et al.* 2008).

4.9.2 Summary Points

- MibA is the prepropeptide of microbisporicin.
- MibB is likely to dehydrate serine and threonine residues in the prepropeptide to yield didehydroalanine and didehydrobutyrine, respectively.
- MibC is likely to be involved in forming the (methyl-)lanthionine bridges of microbisporicin.
- MibD is presumably involved in formation of the *S*-[(*Z*)-2-aminovinyl]-D-cysteine moiety at the C-terminus of microbisporicin.
- MibH and MibS are a flavin-dependent tryptophan halogenase and flavin reductase, respectively, that likely act co-ordinately to chlorinate tryptophan at position 4 of microbisporicin.
- MibO is a cytochrome P450 that may be responsible for hydroxylation of proline-14 of microbisporicin.
- MibTU are a two-component ABC transporter likely involved in microbisporicin secretion.
- MibEF are a two-component ABC transporter likely involved in resistance of *M. corallina* to microbisporicin.
- MibYZ are a two-component ABC transporter of unknown function.
- *mibY and mibZ* appear to be translationally coupled, and encode proteins with most homology to the products of gene clusters in other actinomycetes that include homologs of *mibX, mibW and mibJ*.
- MibN is a putative sodium/proton antiporter of unknown function.
- MibX is an ECF σ-factor homolog and MibW likely acts as an anti-σ factor to suppress MibX activity.
- MibR possesses a helix-turn-helix domain found in the LuxR family of regulatory proteins.
- MibJ is a hypothetical protein with predicted transmembrane helices.

- *mibJ,* appears to encode a protein with most homology to the products of gene clusters in other actinomycetes that include homologs of *mibX,mibW, mibY and mibZ*.
- MibQ shows similarity to lipoproteins, with a predicted signal peptide sequence containing a conserved lipobox motif LAGC.
- MibV is a hypothetical protein with the closest homolog in the actinomycete *Nocardiopsis dassonvillei* and apparently part of an uncharacterised lantibiotic gene cluster.
- Microbisporicin is a member of a previously unrecognised group of lantibiotics with similar sequence and structural features.
- The microbisporicin gene cluster does not appear to be present in *M. corallina* strains DSM 44681 and DSM 44682.

Chapter 5 - Heterologous expression of the microbisporicin gene cluster in *Streptomyces*

5.1 Introduction

In chapter 4 the bioinformatic analysis of the microbisporicin gene cluster was described, highlighting a number of intriguing features. In order to explore these in more detail it would be prudent to undertake a deletional analysis by inactivating genes within the cluster and exploring the effect on compound production and strain self-resistance. By expanding the understanding of microbisporicin biosynthesis it is also possible that avenues for improving compound yield might be identified. Ideally such an analysis would be undertaken in the producing organism, however this is not an option if the strain in question is genetically intractable. As described in previous chapters, *M. corallina* is a slow growing actinomycete which does not sporulate efficiently under laboratory conditions. Furthermore, there are no examples available in the literature where any species of *Microbispora* has been genetically manipulated. In fact there are few reports of transformation methods for members of the *Streptosporangiaceae* family (Stinchi *et al.* 2003; Beltrametti *et al.* 2007). Thus the use of a genetically tractable heterologous host for the further analysis of the microbisporicin gene cluster was an attractive possibility.

Streptomyces sp. have been used as heterologous hosts for secondary metabolite gene clusters for a wide range of compounds including polyketides, non-ribosomal peptides and terpenoids (Zhang *et al.* 2008). *Streptomyces* sp. often grow more vigorously than the natural hosts of these clusters and many tools have been developed for their genetic manipulation (Kieser *et al.* 2000). In particular transformation is rapidly accomplished through the use of conjugation with *E. coli* (Kieser *et al.* 2000). *Streptomyces lividans*, *Streptomyces coelicolor* and *Streptomyces venezuelae* have been used routinely as heterologous hosts (Zhang *et al.* 2008).

Several lantibiotic gene clusters from the low GC Gram-positive bacteria have been expressed successfully in heterologous hosts. For example, the nukacin-ISK1 biosynthetic gene cluster from *Staphlococcus warneri* ISK1 was expressed in *Lactococcus lactis* by utilising the nisin-inducible regulatory system (NICE) (Aso *et al.* 2004). The gene cluster

for Epicidin 280 from *Staphylococcus epidermidis* BN 280 was expressed in *Staphylococcus carnosus* TM 300 (Heidrich *et al.* 1998), and that for Bovicin HJ50 was expressed in *Lactococcus lactis* (Liu *et al.* 2009). The transposon containing the nisin gene cluster was transferred into *Enterococcus* sp. but produced low levels of the lantibiotic when gene expression was induced with exogenously applied nisin (nisin is an inducer of its own synthesis) (Li *et al.* 2002). However other attempts have not been successful, particularly between genera. For example, mobilisation of the complete nisin gene cluster into *Bacillus subtilis* 168 failed to result in the production of the active lantibiotic even after induction with exogenous nisin. Transcription of the nisin genes was apparent and a possible pre-nisin was detected by Western blot analysis, leading the authors to speculate that the precursor peptide was not correctly processed in *B. subtilis* (Yuksel *et al.* 2007).

Heterologous expression has also been achieved for two actinomycete lantibiotics. Cinnamycin from *Streptomyces cinnamoneus* was produced in *S. lividans* 1326 through the mobilisation of the entire gene cluster into the ΦC31 phage integration site (Widdick *et al.* 2003). Actagardine produced by *Actinoplanes garbadinensis*, despite being from a genus not closely related to *Streptomyces*, was also produced in *S. lividans* 1326 using the same approach (Boakes *et al.* 2009). Actagardine has also been produced in *S. lividans* TK24 and *S. coelicolor* M1146 (Bell, R *et al.* unpublished). Based admittedly on a limited amount of data, these precedents suggested that *Streptomyces* species are suitable hosts for the heterologous expression of actinomycete lantibiotic gene clusters.

This chapter will describe the mobilisation of the microbisporicin gene cluster into the heterologous host *S. lividans* TK24 and characterisation of the resulting strains. The aim was to express the microbisporicin gene cluster in this host and then to carry out a deletion analysis of the functions of individual genes. As described in this chapter, initial attempts to produce microbisporicin in *S. lividans* were unsuccessful and so a number of approaches were taken to promote synthesis of the compound. These are described briefly below. Finally, an analysis of the expression of the genes of the microbisporicin gene cluster in *S. lividans* was undertaken and the results are also discussed.

5.2 Heterologous Expression of the *mib* gene cluster in *S. lividans*

5.2.1. Mobilisation of cosmids containing the *mib* gene cluster into *S. lividans*

As described in chapter 4 the complete *mib* gene cluster appears to be present within the DNA insert of cosmid pIJ12125. As described in chapter 3, cosmids pIJ12121 (1H11), pIJ12122 (3E5) and pIJ12126 (7C22) are also highly likely to contain the complete *mib* cluster. To maximise the chances of observing heterologous expression of microbisporicin and to avoid the possibility that one cosmid might contain a mutation that could prevent production, all four cosmids were mobilised into *S. lividans*. To achieve this, the Supercos backbone of the cosmids had to be altered to allow; firstly, integration of the cosmids at the ΦC31 attachment site in the *S. lividans* chromosome (Bierman *et al.* 1992), secondly, the transfer of the cosmids from *E. coli* to *S. lividans* by conjugation, and finally selection of the integration event in *S. lividans*. These features are all present in the vector pIJ10702 (also called pMJCOS1 (Yanai *et al.* 2006)) which contains the ΦC31 *attP* attachment site and integrase (Bierman *et al.* 1992), an *E. coli* origin of transfer (oriT; (Kieser *et al.* 2000)) and the *aac(3)*IV gene encoding apramycin resistance (Kieser *et al.* 2000). This vector shares sequence identity with Supercos in the regions flanking these features (Figure 5.1). This allows the replacement of the kanamycin resistance marker of Supercos cosmids with these elements by homologous recombination in a strain of *E. coli* (BW25113/pIJ790) that contains the arabinose-inducible λ RED recombination system, as described in detail in chapter 2 (Gust *et al.* 2003). Cosmids pIJ12121, pIJ12122, pIJ12125 and pIJ12126 were converted in this manner into their respective pIJ10702 variants, pIJ12127, pIJ12128, pIJ12131 and pIJ12132, respectively. These constructs were analysed by restriction digests to confirm that no gross rearrangements had taken place. The cosmids were mobilised into *S. lividans* TK24 by conjugation from the *E. coli* donor strain ET12567/pUZ8002 and ex-conjugants selected with 50 µg/ml apramycin (Kieser *et al.* 2000). Introduction of pIJ12131 into four independent clones of *S. lividans* was confirmed by PCR amplification of representative genes from the *mib* cluster (Figure 5.2).

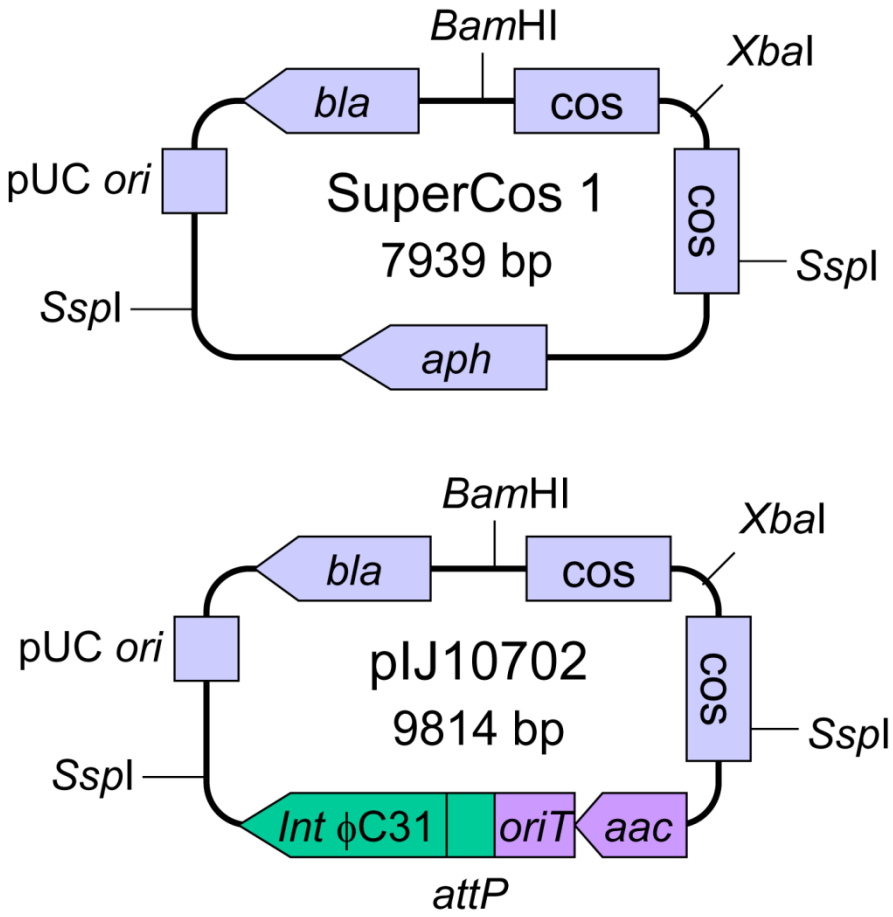

Figure 5.1 Vector maps of Supercos1 (Stratagene) and pIJ10702 (pMJCOS1; Yanai, *et al.* 2006). The region between the *Ssp*I sites of pIJ10702 contains a region of conserved sequence with Supercos1, flanking the ΦC31 integrase (*Int*) and attachment (*attP*) sites, the origin of transfer (*oriT*) and apramycin resistance marker (*aac(3)IV*). This region is used to replace the region between *Ssp*I sites in Supercos1 cosmids that contains the kanamycin resistance marker (*aph*). Also shown are the *cos* sites utilised for phage packaging during cosmid library construction, the origin of plasmid replication in *E. coli* (pUC *ori*) and the carbenicillin resistance marker (*bla*). Cosmid inserts would typically be cloned into the *BamH*I site but for the *M. corallina* cosmid library are in an adjacent *Zra*I site (not shown; see chapter 3). The size of each vector (before the *cos* site re-ligation that occurs during cosmid library construction, leaving just one *cos* site in the final cosmids) is given in base pairs.

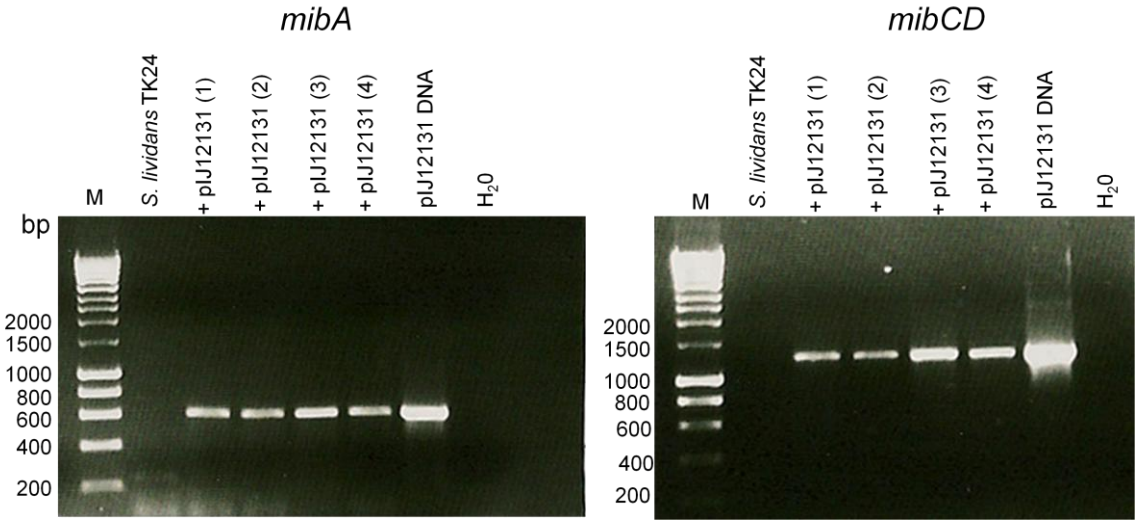

Figure 5.2 Confirmation of the presence of pIJ12131 in *S. lividans* by PCR amplification of *mibA* (LF013F and LF013R; 592 bp) and *mibCD* (LF001F and LF004R; 1250 bp) from the *mib gene* cluster. Colony PCR was carried out using mycelium from *S. lividans* TK24 wild type and four clones into which the pIJ12131 cosmid was mobilised and which were resistant to apramycin. pIJ12131 DNA was used as a positive control. PCR amplified fragments were separated on a 1% agarose gel by electrophoresis. The marker (M) is hyperladder (Bioline) and sizes are given at the side of each gel in base pairs.

5.2.2. Attempts to detect heterologous production in *S. lividans*

The production of microbisporicin in *S. lividans* was assessed through culture on both agar media and under liquid fermentation conditions. *S. lividans* clones containing each of the four cosmids and containing the vector pIJ10702 alone were grown on V0.1 agar medium for 7 days before overlaying with the target organism *Micrococcus luteus*. No zones of inhibition were observed around any of the clones containing the vector alone or the four cosmids, although an antibiotic disc loaded with supernatant from a 7d culture of *M. corallina* NRRL 340420 grown in VSPA produced a clear zone of inhibition (Figure 5.3). This suggests that *S. lividans* containing the *mib* gene cluster is unable to produce a bioactive compound on V0.1 agar.

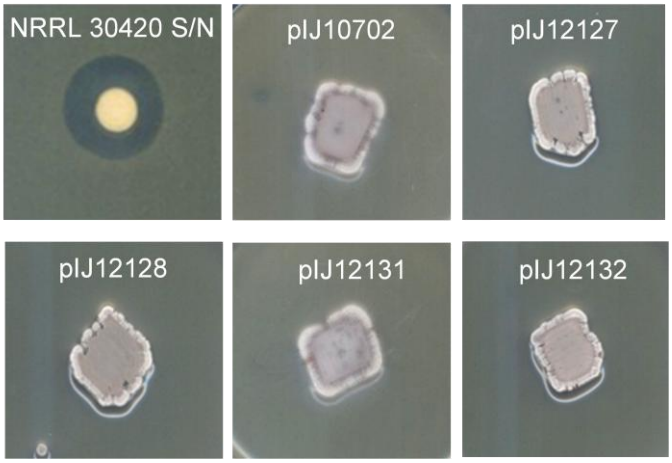

Figure 5.3 Bioassay to assess whether *S. lividans* containing the *mib* gene cluster can produce microbisporicin. *S. lividans* containing the vector pIJ10702 alone and one representative clone containing each of the four cosmids thought to contain the *mib* cluster were grown for 7 days on V0.1 agar before being overlaid with *M. luteus* in SNA. A plate of V0.1 overlaid with *M. luteus* in SNA was used as a positive control by placing an antibiotic assay disc containing 40 µl of *M. corallina* NRRL 30420 supernatant (S/N; from a culture grown for 7 days in VSPA) on to it. Plates were incubated at 30°C overnight before observing zones of inhibition.

S. lividans pIJ10702 and the clones containing the four cosmids were grown for three days in medium V (note that medium VSPA differs from medium V only by the addition of 5% sucrose, 0.5% proline and 0.1% agar, dispersive agents for the growth of *M. corallina* that are not required for the growth of *S. lividans*; microbisporicin is produced at similar levels when *M. corallina* is grown in medium V or VSPA) and supernatants assessed for

bioactive compounds by applying to antibiotic assay discs placed on a lawn of *M. luteus*. No zones of inhibition were observed around any of the discs containing supernatants from *S. lividans* containing the vector alone or any of the four cosmids, although an antibiotic disc loaded with supernatant from a 7 d culture of *M. corallina* NRRL 30420 grown in VSPA produced a clear zone of inhibition (Figure 5.4). This suggests that *S. lividans* containing the *mib* gene cluster is unable to produce a bioactive compound in medium V. To confirm that microbisporicin was not being produced at levels too low to have demonstrable bioactivity against *M. luteus*, the supernatants were subjected to MALDI-ToF mass spectrometry. This analysis did not reveal any compounds yielding m/z peaks associated with microbisporicin (data not shown).

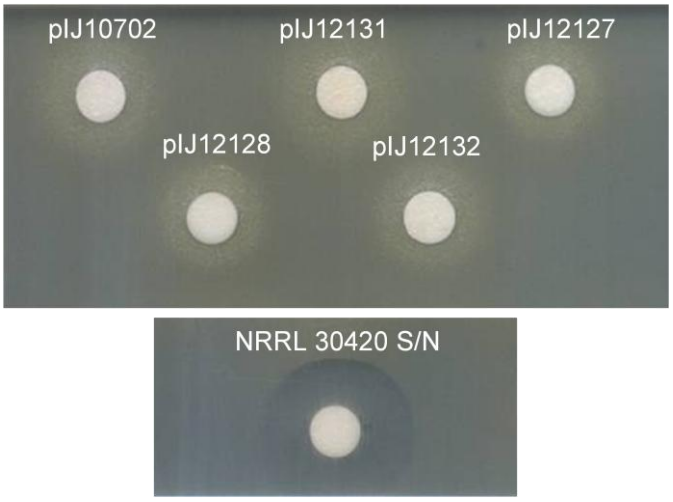

Figure 5.4 Bioassay to assess whether *S. lividans* containing the *mib* gene cluster can produce microbisporicin in liquid culture. *S. lividans* containing the vector pIJ10702 alone and one representative clone containing each of the four cosmids thought to contain the *mib* cluster were grown for 3 days in medium V. Supernatants were separated by centrifugation. Supernatant from a culture of *M. corallina* NRRL 30420 grown for 7 days in VSPA was used as a control. Antibiotic assay discs were each loaded with 40 µl supernatant, allowed to dry and were placed on to a plate of L agar containing *M. luteus*. Plates were incubated at 30°C overnight before observing zones of inhibition. All discs were applied to the same "lawn" of *M. luteus;* these images were cropped from a larger image of that plate.

To concentrate any microbisporicin potentially present in the supernatants, those derived from *S. lividans* pIJ10702 and *S. lividans* pIJ12131 (using the *M. corallina* supernatant as a control) were extracted with a polystyrene hydrophobic resin (Diaion HP20, see chapter 2 for details) and any bound compounds eluted with methanol:butanol:water (9:1:1) (Lazzarini *et al.* 2005; Castiglione *et al.* 2008). These eluted fractions were concentrated

by drying, resuspended in 5% formic acid and subjected to MALDI-ToF mass spectrometry. Although this method was found to highly concentrate and partially purify microbisporicin from the *M. corallina* NRRL 30420 supernatant, there was no indication of any m/zs associated with microbisporicin from either *S. lividans* supernatant sample (data not shown).

S. lividans pIJ10702 and pIJ12131 were grown for 24 h and 48 h in medium V and *M. corallina* NRRL 30420 was grown for 7 days in VSPA. The mycelial pellets were separated from the supernatant fractions. Pellets of mycelium were extracted with 100% methanol. Supernatants were adjusted to pH 3 with 50% formic acid and methanol added to 50% final v/v. HPLC analysis of these extracts was carried out on a C18 waters column as described in chapter 2. In a methanol extract of *M. corallina* NRRL 30420 pellet and in supernatant from the same culture it was possible to see two peaks eluting with retention times of 10.6 minutes and 11.6 minutes. These fractions were collected and were found to have bioactivity against *M. luteus,* and when investigated by MALDI-ToF mass spectrometry contained m/z peaks associated with variants of microbisporicin. Separate HPLC peaks might be expected for the different variants of microbisporicin due to their different chemical properties. It was previously observed that MF-BA-1768α_1, MF-BA-1768β_1, 107891 A1 and 107891 A2 have different retention times under certain HPLC conditions (Lazzarini *et al.* 2005). However under the conditions used here the three observed microbisporicin variants (giving m/z peaks of 2215.7 (MF-BA-1768α_1), 2231.7 (107891 A2) and 2247.7 (107891 A1) by MALDI-ToF) were identified in both HPLC peaks that were collected. The ratios of the three variants were seen to differ between the two peaks but all three were identified in both samples (Figure 5.5). This indicates that this HPLC method is not optimal for the separation of the variants of microbisporicin. These peaks were not observed in methanol-extracted mycelial pellets or supernatants from *S. lividans* pIJ10702 or *S. lividans* pIJ12131 grown for 24 or 48 h.

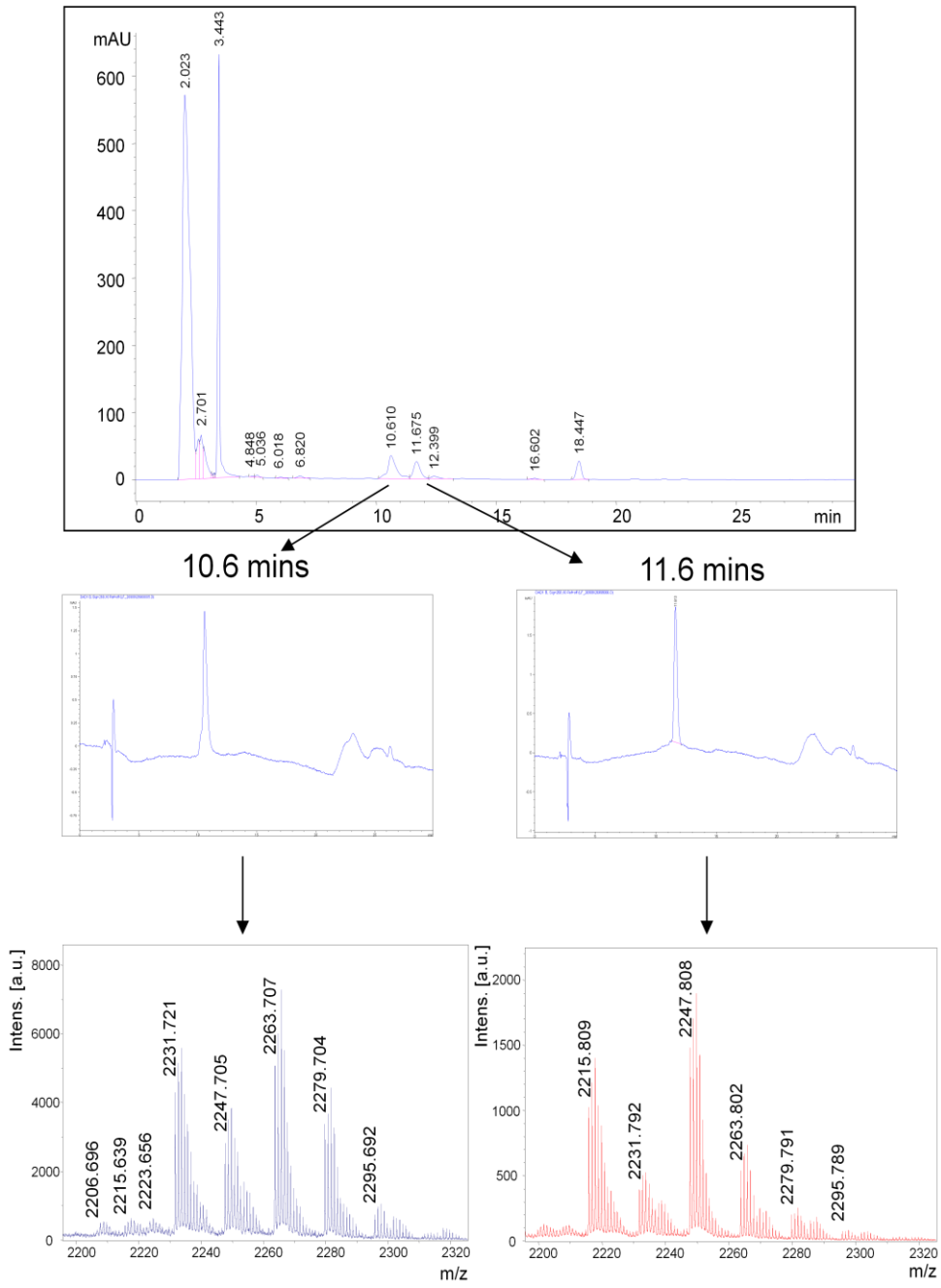

Figure 5.5 HPLC analysis of methanol-extracted *M. corallina* NRRL 30420 mycelium. The expected retention time for microbisporcin under these conditions is approximately 10-17 minutes (Flavia Marinelli, pers. comm.). The peaks at approximately 2-6 minutes and 18 minutes were observed in a medium only control HPLC run (data not shown). Two peaks at 10.6 and 11.6 minutes (top and middle panels) were collected and analysed by MALDI-ToF mass spectrometry (lower panels). Intensity is given on the y-axis in arbitrary units (au) and the mass/charge ratio (m/z) on the x-axis. [M+H$^+$] ions are labelled.

5.2.3 Attempts to stimulate microbisporicin production in *S. lividans*

The initial conditions tested for heterologous production failed to yield bioactivity or ions associated with the production of microbisporicin. This could be due to the culture conditions used, which were based on those used for production of the compound in *M. corallina* and which may not be suitable for production in *S. lividans*. Furthermore, a number of treatments have been reported that stimulate the production of secondary metabolites in *Streptomyces,* for example, the addition of N-acetylglucosamine or ATP (Li *et al.* 2008; Rigali *et al.* 2008). Finally, since the production of some lantibiotics is auto-inducible (Kuipers *et al.* 1995; Stein *et al.* 2002), this could also be the case for microbisporicin. If insufficient compound is produced to trigger the auto-induction mechanism, then high level compound production would not be observed; this was the case when nisin was expressed in *Enterrococcus* (Li *et al.* 2002). Consequently, attempts were made to stimulate microbisporicin production in *S. lividans* by altering the culture conditions. For these experiments, only *S. lividans* containing the sequenced cosmid pIJ12131 was used.

S. lividans pIJ12131 was grown on a wide range of actinomycete agar media including GYM, RARE-3, ISP4, AF/MS, D/Seed Veg, M8, Medium A, Medium B, Medium C, V6 and INA-5 for 7 days. The plates were overlaid with *M. luteus* in SNA. Zones of inhibition were observed on GYM, RARE-3 and V6. However when the control strain *S. lividans* pIJ10702 was grown on these media, similar zones of inhibition were visible, indicating the production of an antibiotic compound by *S. lividans* itself.

Production of actinorhodins and prodiginines by *S. coelicolor* and *S. lividans* is enhanced by the inclusion of 10 µM ATP in a complex medium (Li *et al.* 2008). *S. lividans* pIJ10702, *S. lividans* pIJ12131 and *M. corallina* NRRL 30420 were grown on V0.1 supplemented with 10 µM ATP for 7 days. Plates were overlaid with *M. luteus* in SNA. *M. corallina* NRRL 30420 gave a large, very clearly defined zone of inhibition whereas both *S. lividans* strains showed only faint poorly defined halos that were likely caused by actinorhodins or prodiginines. Similarly, 50 mM N-acetylglucosamine stimulates antibiotic production in *S. coelicolor* when used in a minimal medium, probably by triggering a starvation response (Rigali *et al.* 2008). *S. lividans* pIJ10702 and *S. lividans* pIJ12131 were grown on minimal media supplemented with 25 mM mannitol with and without 50 mM N-acetylglucosamine for 4 days before overlaying with *M. luteus*. Neither condition was found to stimulate the production of bioactive compounds from these strains.

Finally as discussed microbisporicin might be an inducer for the expression of the genes within the gene cluster in an auto-regulatory manner. Therefore exogenously supplied

microbisporicin might be able to induce the production of microbisporicin in a heterologous host. Purified microbisporicin compound was not available for this study and so supernatant from a 7 d culture of *M. corallina* NRRL 30420 grown in VSPA, and found to give bioactivity against *M. luteus* and to contain ions associated with microbisporicin by MALDI-ToF, was used. Since the concentration of microbisporicin in this supernatant was not known, an assay was set-up in which the *S. lividans* strain or *M. corallina* control strain was grown in a line away from a well in the agar plate for 24 hours. The NRRL 30420 supernatant or media only (as a control) was introduced into the wells such that by diffusion a concentration gradient of the compound away from the well would be established and the plates further incubated for 6 days. The plates were overlaid with *M. luteus* in SNA and the formation of zones of inhibition observed. Although zones of inhibition were observed as normal with NRRL 30420 grown on the plates, plates containing *S. lividans* strains did not give zones of inhibition when grown in the presence of the NRRL 30420 supernatant, suggesting that lack of auto-induction was not limiting the detection of microbisporicin production in the heterologous host.

5.2.4 Promoter Region Manipulation in pIJ12131

The methods used in an attempt to induce heterologous expression of the microbisporicin gene cluster in *S. lividans* TK24 had been unsuccessful. To obviate the possible necessity for induction of *mib* gene expression in *S. lividans*, pIJ12131 was modified to include the constitutive *ermE** promoter upstream of the putative operons of the *mib* cluster (Bibb *et al.* 1994). The *ermE** promoter was separately introduced upstream of the operons beginning with *mibA* (biosynthetic and export genes; pIJ12363), *mibE* (resistance genes; pIJ12364) and *mibX* (possible regulation mechanism; pIJ12365) as well as before both *mibA* and *mibE* operons in one cosmid (pIJ12366) (Figure 5.6). The resulting constructs were mobilised into *S. lividans* TK24 by conjugation from *E. coli* ET12567/pUZ8002 and the exconjugants assayed for the production of bioactive compounds on V0.1 agar and by culturing in medium V. Furthermore, supernatants from liquid grown cultures were submitted for MALDI-ToF analysis. These studies did not reveal the production of a bioactive compound or ions associated with the microbisporicin complex.

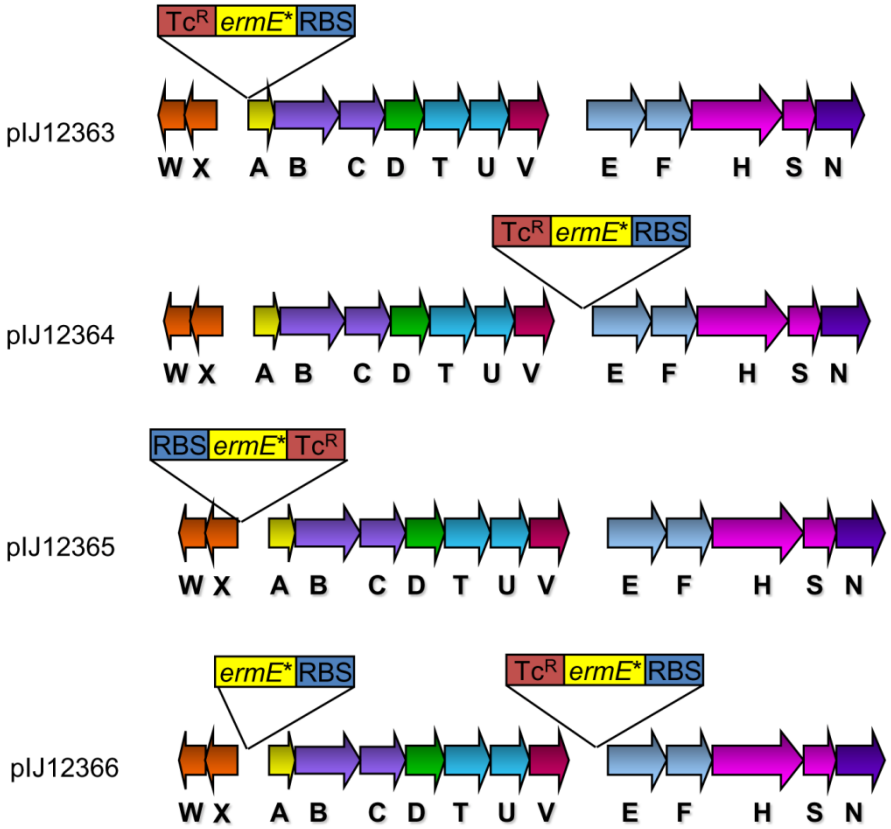

Figure 5.6 Insertion of the constitutive *ermE** promoter in the *mib* gene cluster of pIJ12131. The *ermE** cassette consists of a tetracycline resistance marker (Tc^R), the *ermE** promoter (Bibb, *et al.* 1994) and the EF-Tu ribosome-binding site (RBS) from *S. coelicolor* (van Wezel, *et al*. 2000). The cassette was introduced upstream of operons of the *mib* gene cluster in pIJ12131 as indicated by λ-RED mediated recombination in *E. coli* BW25113/pIJ790 (Gust *et al.,* 2003). To generate pIJ12366, the tetracycline resistance cassette in pIJ12363 was removed by FLP-recombinase, using the flanking FRT sites, in *E. coli* DH5α/BT340 (Gust *et al.,* 2003). The *ermE** cassette was then introduced upstream of *mibE* as shown.

5.2.5 Inactivation of *mib* cluster genes

The mechanism of regulation of the *mib* gene cluster was thought to be via the ECF sigma factor:anti-sigma factor pair *mibXW*, but the exact mechanism by which this occurred was not clear. However, it seemed reasonable to assume that if regulation of the ECF sigma factor MibX by its anti-sigma factor MibW could be relieved, then expression of the *mib* gene cluster might be activated. *mibX* and *mibW* were individually inactivated as well as both genes together and *mibA* as a control. The open-reading frames were replaced with the pIJ778 cassette that contains the *aadA* gene (providing resistance to spectinomycin and streptomycin) flanked by FRT sites (Figure 5.7). The open-reading frames were replaced in such a way as to leave intact any downstream open-reading frames in order to prevent polar effects. After gene replacement the *aadA* cassette was removed by FLP-mediated recombination in *E. coli* DH5α/BT340 to leave an 81-base pair scar (Gust *et al.* 2003). The resulting cosmids were mobilised into *S. lividans* TK24 by conjugation from *E. coli* ET12567/pUZ8002. Four clones of each strain were analysed for the production of bioactive compounds on V0.1 agar medium but no zones of inhibition were observed in a lawn of *M. luteus*. Similarly no bioactive compound was detected in culture supernatants of *S. lividans* strains grown for four days in medium V (Figure 5.8).

Figure 5.7 The pIJ778 cassette used to inactivate the *mibX*, *mibW and mibA* genes of the *mib* cluster in pIJ12131. P1 and P2 represent the conserved primer sites used in all PCR targetting cassettes, FRT sites are for site-specific FLP-mediated recombination, oriT is the origin of transfer and *aadA* encodes the adenyltransferase involved in streptomycin/spectinomycin resistance (Gust, *et al.* 2003).

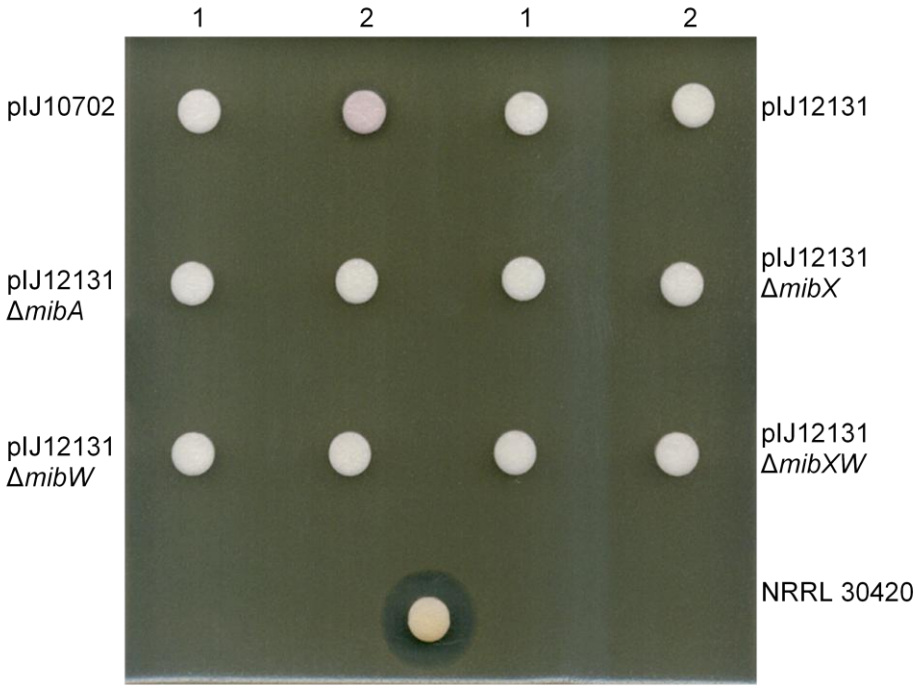

Figure 5.8 A representative bioassay of supernatants from *S. lividans* TK24 carrying pIJ12131 with various *mib* genes inactivated. Two clones of each strain were grown for four days in medium V and 40 µl supernatant applied to antibiotic assay discs on a lawn of the indicator strain *M. luteus*. 40 µl supernatant from a 7 day culture in VSPA of NRRL 30420 was used as a positive control. The plate was incubated overnight at 30°C before zones of inhibition were recorded.

5.2.6 Other *Streptomycete* hosts

S. lividans TK24 could be unique among streptomycetes in its inability to synthesise microbisporicin from the *mib* cluster of pIJ12131. Other streptomycetes have been used successfully as heterologous hosts in the past, for example *S. coelicolor* (Tang *et al.* 2000), *S. venezuelae* (Mervyn Bibb, personal communication), *S. fungicidicus* (Lautru *et al.* 2005) and *S. albus* (Wendt-Pienkowski *et al.* 2005). Furthermore, a superhost strain of *S. coelicolor* M145 (M1146) has recently been created with the four main secondary metabolite gene clusters inactivated, thus removing carbon sinks to promote the production of metabolites from heterologous clusters (Gomez-Escribano *et al.*, unpublished). A variant of this strain contains either a single (M1156) or double (M1155) site mutation in the *rpsL* gene of *S. coelicolor*. These mutations are selected by resistance to streptomycin and have been reported to increase the production of secondary metabolites (Hu *et al.* 2001). The vector pIJ10702 and the cosmid pIJ12131 (containing the *mib* gene cluster) were introduced into each of the above *Streptomyces* hosts by conjugation from *E. coli* ET12567/pUZ8002. The resulting strains were assayed for the production of bioactive compounds on V0.1 agar medium and in medium V. Several strains gave faint zones of inhibition when grown on agar medium and overlaid with *M. luteus* in SNA but these were always seen in both the vector only control strain and that containing the *mib* cluster, suggesting that these activities were due to the production of other compounds under these conditions or to the production of extracellular enzymes. When the strains were grown in medium V and supernatants applied to antibiotic assay discs on a lawn of *M. luteus,* only supernatant from *S. fungicidicus* gave appreciable zones of inhibition but this was seen for both the control strain and that carrying the *mib* cluster (Figure 5.9). These supernatants were investigated by MALDI-ToF mass spectrometry but were not found to produce any ions associated with the production of microbisporicin. This analysis indicates that all of the *Streptomyces* heterologous hosts used were incapable of producing microbisporicin from the genes of the cosmid pIJ12131.

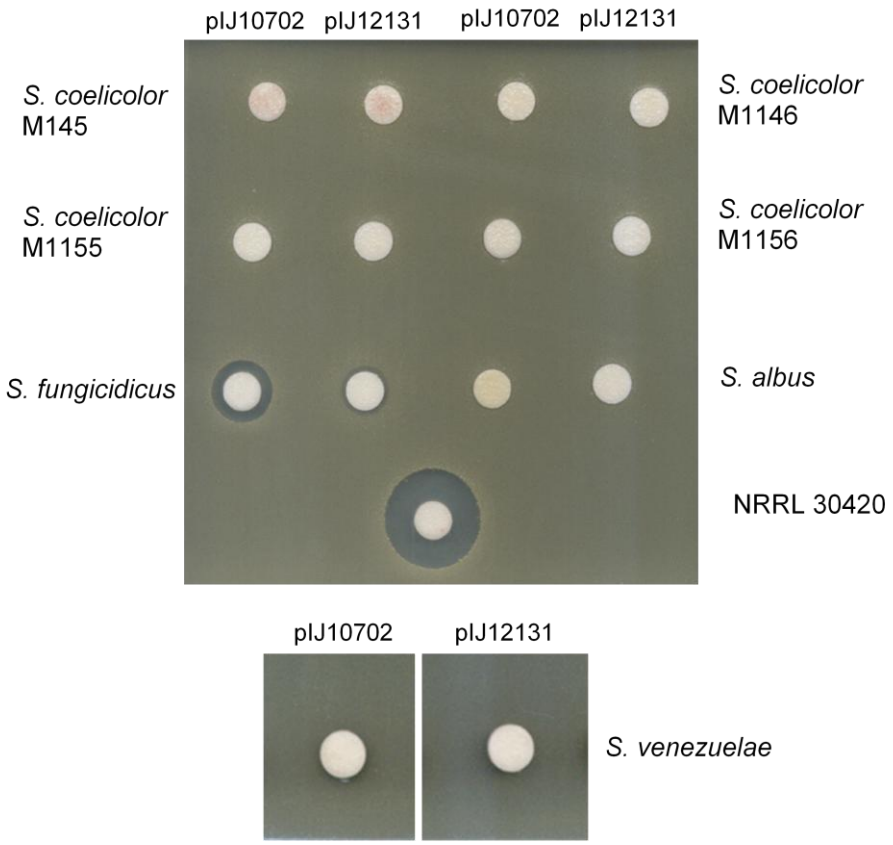

Figure 5.9 Representative bioassays of supernatants from different *Streptomyces* sp. carrying either pIJ10702 or pIJ12131. Strains were grown for three days in medium V and 40 µl supernatant applied to antibiotic assay discs on a lawn of the indicator strain *M. luteus*. 40 µl supernatant from a 7 day culture of NRRL 30420 was used as a positive control. The plates were incubated overnight at 30°C before zones of inhibition were recorded. The images of the bioassay of *S. venezuelae* supernatants were cropped from a larger image of a single plate of *M. luteus*.

5.3. Analysis of gene expression in *S. lividans* containing the *mib* cluster

The production of mature, active microbisporicin was not detected in any of the *Streptomyces* hosts containing pIJ12131. It had also not been possible to induce production of the compound in *S. lividans* TK24 using various approaches, including attempts to manipulate the regulatory mechanisms of the *mib* cluster. To assess at what level the block to microbisporicin production was occurring, transcription of several of the *mib* genes was assessed in the heterologous host *S. lividans* using Reverse-Transcriptase PCR (RT-PCR).

RNA was extracted from *S. lividans* pIJ10702 and pIJ12131 after 24 h growth in medium V and from *M. corallina* NRRL 30420 after 7 days growth in medium V. RT-PCR was carried out with the One-Step RT-PCR kit (Qiagen) using primers corresponding to internal regions of the selected *mib* genes (for primer sequences see chapter 2). Transcripts were amplified for all genes tested in RNA samples from both *M. corallina* and *S. lividans* pIJ12131, but not from *S. lividans* pIJ10702 (Figure 5.10 shows the data obtained for *mibA*; Table 5.1).

This analysis was also carried out with RNA extracted from strains constitutively expressing operons of the *mib* cluster after insertion of the *ermE** promoter in pIJ12131 (section 5.2.4; Figure 5.10, top panel) and *S. lividans* carrying pIJ12131 in which *mib* genes had been inactivated (section 5.2.5; Figure 5.10, bottom panel). All the transcripts amplified from the wild type cosmid were also amplified when the *ermE** promoter was introduced into the *mib* cluster but since RT-PCR is not quantitative it was not possible to deduce whether the introduction of these promoters had led to elevated levels of *mib* gene expression (Figure 5.10, top panel; Table 5.1). When gene expression was interrogated in the gene inactivation strains, the results confirmed that these genes had been successfully inactivated (no transcript for the inactivated gene) without polar effects on the downstream genes (for example, the *mibW* transcript was still apparent in the Δ*mibX* strain) (Figure 5.10, bottom panel; Table 5.1). However, inactivation of these genes had no effect on expression of transcripts from other genes in the *mib* cluster, suggesting that the ECF sigma factor MibX and the anti-sigma factor MibW may not be functional in *S. lividans*.

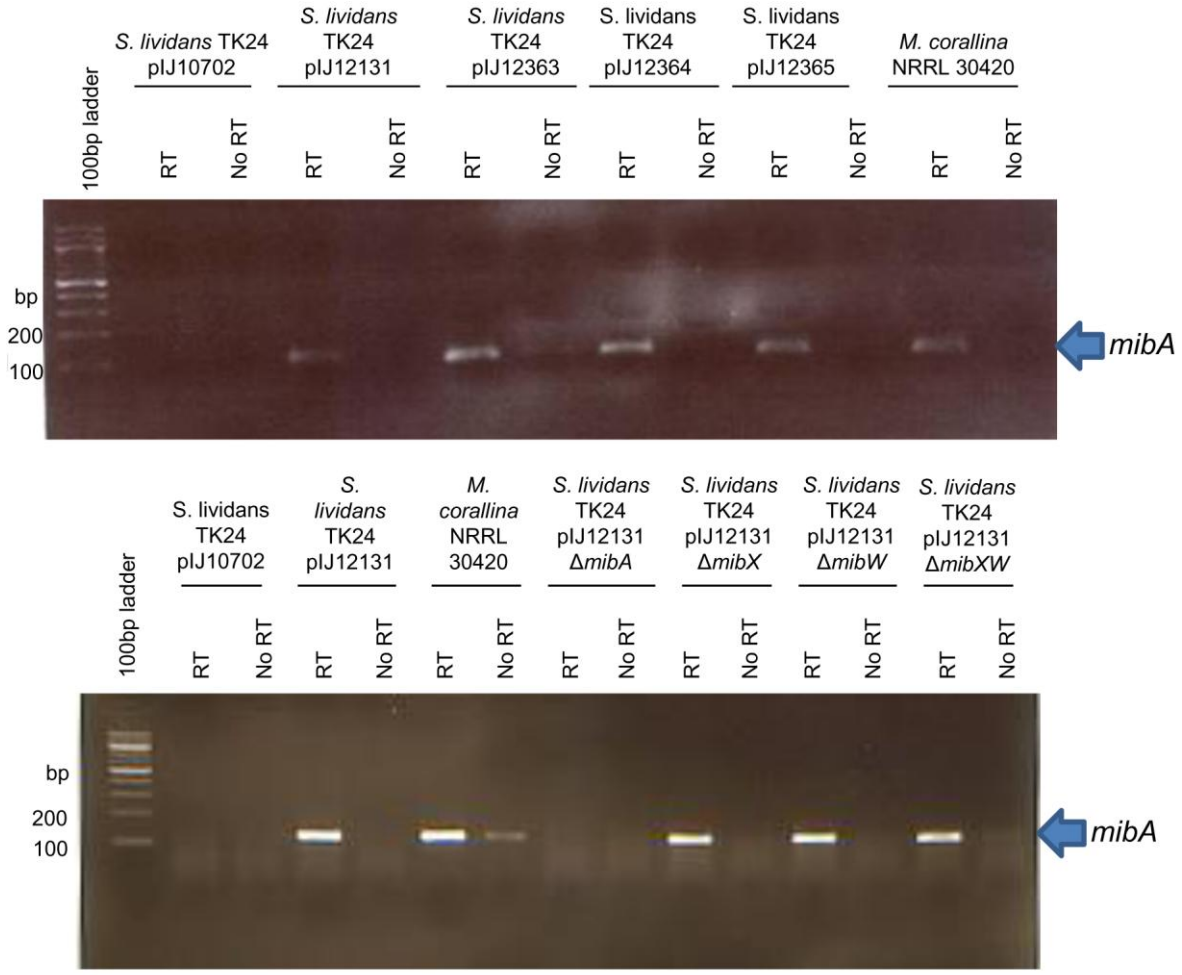

Figure 5.10 Analysis of transcription of genes of the *mib* gene cluster in *S. lividans* by RT-PCR. RNA was extracted from the strains shown after 24 h (*S. lividans*) or 7 days (*M. corallina*) growth in medium V. RNA was subjected to one-step RT-PCR (Qiagen) using primers specific to genes of the *mib* cluster (data shown here is for *mibA* amplified with LF025F and LF025R). The amplified *mibA* transcript is indicated with a blue arrow. The top panel shows the result using RNA extracted from pIJ12131 with the *ermE** constitutive promoter introduced. The lower panel shows the result using RNA extracted from deletion mutants in pIJ12131. Each reaction was carried out in the absence (no RT) or presence (RT) of reverse transcriptase as a control for the contamination of RNA with genomic DNA. PCR products were separated on a 1% TBE agarose gel by electrophoresis. The marker is the 100 bp ladder (NEB) and sizes are given in base pairs on the side of each gel image.

Table 5.1 Summary of the analysis of *mib* gene expression in *S. lividans.* Primer pairs for each transcript are as given in chapter 2. The presence of an amplification product for the respective transcript is indicated with a "plus" sign (+) and the absence with a negative sign (-). Reactions not carried out for a particular sample are given as not done (nd).

Transcript	NRRL 30420	*S. lividans* pIJ10702	*S. lividans* pIJ12131	*S. lividans* pIJ12363	*S. lividans* pIJ12364	*S. lividans* pIJ12365	*S. lividans* pIJ12131 Δ*mibA*	*S. lividans* pIJ12131 Δ*mibX*	*S. lividans* pIJ12131 Δ*mibW*	*S. lividans* pIJ12131 Δ*mibXW*
16s rRNA	+	+	+	nd	nd	nd	+	+	+	+
mibO	+	-	+	nd	nd	nd	+	+	+	+
mibW	+	-	+	nd	nd	nd	+	+	-	-
mibX	+	-	+	+	+	+	+	-	+	-
mibA	+	-	+	+	+	+	-	+	+	+
mibD	+	-	+	+	+	+	+	+	+	+
mibT	+	-	+	+	+	+	nd	nd	nd	nd
mibU	+	-	+	+	+	+	nd	nd	nd	nd
mibE	+	-	+	+	+	+	+	+	+	+
mibH	+	-	+	+	+	+	nd	nd	nd	nd

One caveat with these results is that because the number of cycles used for RT-PCR was high (35), amplification is likely to have reached saturation levels such that even basal levels of transcription might be detectable. It is therefore possible that the level of expression of the *mib* gene cluster in *S. lividans* is simply too low for detectable production of microbisporicin. For similar reasons, it is not possible to conclude whether deletion of *mibA*, *mibX* and *mibW* had any quantitative effect on *mib* gene expression in the heterologous host. For this reason it would be desirable to repeat these experiments with quantitative RT-PCR. Due to time constraints this was not carried out in this study.

5.4 Shotgun library

The lack of production of microbisporicin in heterologous streptomycete hosts might be due to the absence of factors essential for biosynthesis that are encoded within the *M. corallina* genome and that are not present within the four cosmids. To test whether the lack of heterologous production might be complemented by genes from the natural producer, a shotgun library was generated. *M. corallina* genomic DNA was partially digested with *Bam*HI to a size range of 3-8 kb. These fragments were cloned into pRT802 (Gregory *et al.* 2003) to generate a greater than two-fold coverage shotgun library in *E. coli*. The clones were then introduced into *S. lividans* pIJ12131 by conjugation from ET12567/pUZ8002 where pRT802 integrates in a second phage attachment site of *Streptomyces* (ΦBT1 (Gregory *et al.* 2003)). Approximately 3000 ex-conjugants were selected with 50µg/ml kanamycin and patched on V0.1 agar medium. Plates were overlaid with *M. luteus* after at least 4 days of growth and monitored for the presence of zones of growth inhibition around the patches. Any putative producer clones were re-patched from library plates and checked again by bioassay. Only 6 clones were identified as giving clear reproducible zones of clearing in *M. luteus* growth and all 6 were visually identified to be over-producers of the actinorhodin and/or undecylprodigiosin antibiotics of *S. lividans,* giving strong blue/purple pigmentation compared to the wild type (Figure 5.11). B3, B7 and B21 were grown in V medium for four days. The supernatants were tested by bioassay and MALDI-TOF. None of the clones produced bioactive compounds that could give zones of inhibition in a lawn of *M.luteus* and no compounds of ions associated with the production of microbisporicin could be detected by MALDI-ToF mass spectrometry.

The clones identified by this analysis that have higher than wild type levels of bioactivity against *M. luteus* have likely resulted from the introduction of a DNA fragment from the

genome of *M. corallina* encoding a protein capable of enhancing secondary metabolism in *S. lividans*. However, none of the cloned fragments appear to be capable of activating microbisporicin biosynthesis. However, this does not rule out the necessity for other factors in microbisporicin biosynthesis since the required protein(s) may not have been represented in the library or may be encoded by multiple loci at different locations in the *M. corallina* genome.

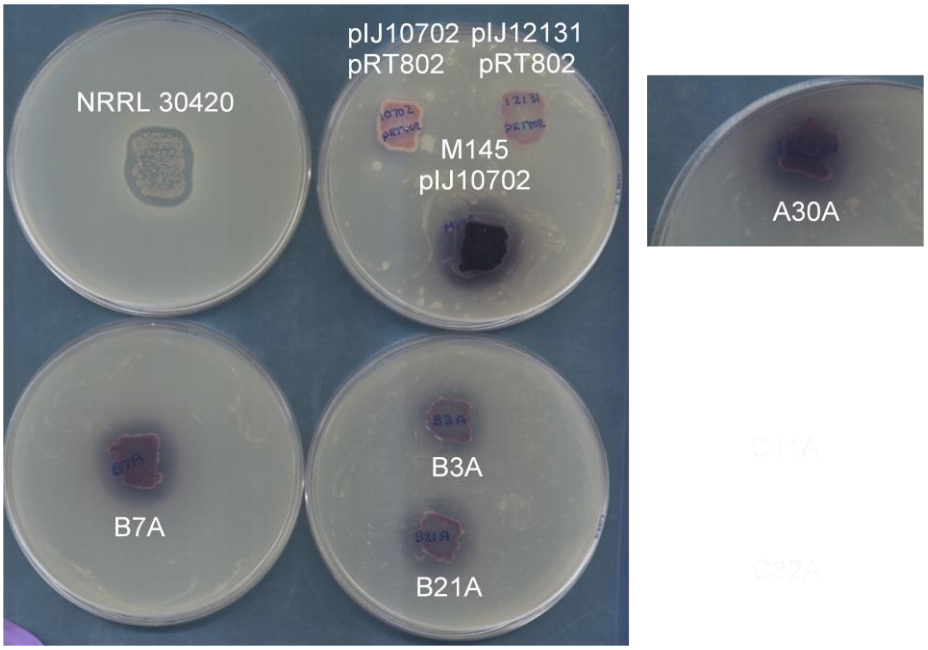

Figure 5.11 The clones identified from the shotgun cloning library as producing a bioactive compound capable of generating zones of clearing in an overlay of *M. luteus*. All patches were grown for 4 days before overlay with *M. luteus* in SNA. *M. corallina* NRRL 30420 was grown as a positive control (giving only a small zone of inhibition after just 4 days growth). Negative controls are *S. lividans* TK24 pIJ10702 pRT802 and *S. lividans* TK24 pIJ12131 pRT802. *S. coelicolor* M145 pIJ10702 was grown as a control for the production of actinorhodins and prodiginines. The clones A30A, B3A, B7A, B21A, were isolated from the shotgun library as producing bioactive compounds. Plates were incubated overnight at 30°C before visualising zones of inhibition.

5.6 Discussion and Summary Points

5.6.1 Discussion

Heterologous expression of the *mib* gene cluster, thought to be contained within the inserts of the cosmids pIJ12127, pIJ12128, pIJ12131 and pIJ12132, does not result in the production of microbisporicin in *Streptomyces* sp. As described in this chapter, a number of approaches were taken to promote heterologous expression and to understand the basis for the lack of production in *Streptomyces*. Due to time constraints not all possible approaches could be carried out to the fullest extent and the results that were acquired are unable to explain why heterologous expression in *Streptomyces* failed. As described in section 5.1, *Streptomyces* species have been used successfully as heterologous hosts for a wide range of secondary metabolite gene clusters, including two lantibiotic gene clusters. However, it is quite likely that when heterologous expression has failed, the result is not reported.

Many hypotheses explaining the lack of production in *Streptomyces* can be postulated. The biosynthesis of lantibiotics is quite complex, involving multiple proteins potentially in different cellular locations. A problem with just one of these components could completely prevent the biosynthesis of the active compound. For example, the lack of production of nisin in *B. subtilis* was attributed to the inability of NisP to correctly remove the leader peptide of pre-nisin (Yuksel *et al.* 2007) and low levels of production in *Enterococcus* to inefficient signal transduction through NisRK in the heterologous host (Li *et al.* 2002). A number of genes in the *mib* cluster encode proteins so far found to be unique to microbisporicin biosynthesis and it is possible that these proteins cannot function appropriately in a heterologous host.

The regulation of *mib* gene expression is likely to be complex and different from those lantibiotics studied to date. Regulation is likely to be very finely balanced with many inputs affecting gene expression. Thus although transcription could be detected from *mib* genes in *S. lividans* the relative levels of each transcript or the timing of induction could be extremely important for microbisporicin biosynthesis. The transcripts amplified from *S. lividans* by RT-PCR may represent a low basal level of transcription involved in an auto-induction mechanism (Kuipers *et al.* 1995; Stein *et al.* 2002; Schmitz *et al.* 2006). If the auto-induction fails at a subsequent step, then high level biosynthesis would not be seen. Low levels of microbisporicin outside the cells may not be appropriately perceived in *S. lividans*; for example proteins may not fold correctly within the cell membrane or microbisporicin may not be able to reach the cell membrane.

Even if auto-induction is not involved in the production of microbisporicin, induction of biosynthesis is likely to be closely tied to development and physiological stimuli. This was also found to be the case for many other lantibiotics. For example, although the genes of the subtilin gene cluster require a signal through the pathway-specific two-component system, SpaRK, for transcription, induction is also regulated with the development of cells by the transition state regulator AbrB via sigma factor H (Stein *et al.* 2002). Epidermin biosynthesis is regulated at least in part by global regulators of cell stress responses and of biofilm formation through the *agr* quorum sensing system (Kies *et al.* 2003) and extracellular pH regulates lacticin 481 production in *Lactococcus lactis* (Hindre *et al.* 2004). Introduction of the *ermE** constitutive promoter of *Streptomyces* might have been able to bypass some of these physiological or developmental inputs, but this was not found to be the case. Possibly the operons up-regulated by this approach were not the only ones needed for expression. Furthermore, if a fine-balance of transcripts/proteins is required for microbisporicin biosynthesis, introducing constitutive promoters may have had a detrimental rather than positive effect.

One characterised physiological difference between *Streptomyces* and other actinomycetes, including *M. corallina*, is cell wall composition. The composition of peptidoglycan in Gram-positive bacteria is found to vary widely, particularly in the amino acids of the pentapeptide linkage. *Streptomyces* sp. are quite unique in utilising the *LL*-form of 2,6-diaminopimelic acid (Dpm) at position 3 of the peptide linkage whereas *M. corallina* and many other rare actinomycetes utilise the *meso*-form of this amino acid (Lechevalier *et al.* 1970). Furthermore, *Streptomyces* sp. make the cross-linkage via a glycine residue whereas *M. corallina* appears to use a direct linkage from alanine to *meso*-Dpm (Schleifer *et al.* 1972). The exact effect of these differences on cell wall properties is not clear (Vollmer *et al.* 2008) but physiological differences such as this could prevent the appropriate perception of signals inducing microbisporicin production.

Although some level of transcription of the *mib* genes was observed in *S. lividans*, microbisporicin production could also be subject to post-transcriptional regulation. This was reported for epidermin biosynthesis, where peptide maturation via EpiP-mediated leader peptide removal provides a second level of regulation of production (Kies *et al.* 2003). Disparities between the time of biosynthetic-gene induction and the onset of production of mutacin II was also postulated to be due to post-transcriptional regulation (Qi *et al.* 1999a). Failure of such a mechanism to operate in *Streptomyces* species could also explain the observed lack of heterologous production.

Alternatively, *S. lividans* may not be able to utilise the native mechanism of self-resistance encoded by the *mib* gene cluster. As discussed in chapter 4 this is likely to be mediated via MibEF, an ABC transporter. These proteins may not be able to fold correctly within the cell membrane of their heterologous host or their expression may not be induced at appropriate levels to confer resistance. In the absence of resistance it is highly likely that, to prevent cell suicide, a mechanism of feedback regulation would be in place to prevent microbisporicin biosynthesis, processing or export.

The reason(s) why *Streptomyces* species are unable to produce microbisporicin cannot be resolved from the results presented in this chapter. As more details of the biosynthetic, regulatory and resistance mechanisms involved in microbisporicin production are revealed, it will hopefully be possible to determine why this is the case and perhaps to find a successful solution.

5.6.2 Summary Points

- Cosmids containing the *mib* gene cluster were mobilised into *S. lividans* TK24 but microbisporicin production was not detected.
- Microbisporicin production in *S. lividans* could not be induced by changing growth conditions or by the addition of external inducers.
- *ermE** driven expression of *mibX*, *mibA* and *mibE* in a modified version of pIJ12131 did not activate microbisporicin production in *S. lividans*.
- Inactivation of *mibX*, *mibW* and *mibXW* did not induce production of microbisporicin in *S. lividans*.
- Microbisporicin was not produced when the *mib* cluster was introduced into other *Streptomycete* heterologous hosts.
- Transcription of genes of the *mib* cluster was detected in *S. lividans*.
- A shotgun library of *M. corallina* DNA was constructed but did not complement the lack of microbisporicin production in *S. lividans*.
- *Streptomyces* is not suitable a heterologous genus for the genetic analysis of the *mib* gene cluster.

Chapter 6 - Heterologous Expression of the *mib* gene cluster in *Nonomuraea*

6.1 Introduction

As discussed in chapter 5, heterologous expression of the *mib* gene cluster in *Streptomyces* sp. was not successful. The considerable taxonomic distance between *Streptomyces* and *M. corallina* may result in physiological differences that prevented heterologous production of microbisporicin. Attempting to express the *mib* cluster in a more closely related genus might overcome this barrier. The *Streptosporangiaceae* family to which *M. corallina* belongs is a little studied group of actinomycetes (often referred to as rare actinomycetes). Members of this group include the genera *Herbidospora*, *Microtetraspora*, *Nonomuraea*, *Planomonospora*, *Planobispora*, *Planotetraspora* and *Streptosporangium*. Although a number of interesting secondary metabolites are made by this family, only two members have been genetically-manipulated. *Planobispora rosea*, the producer of the thiazoylpeptide antibiotic GE2270, was manipulated by protoplast fusion (Beltrametti *et al.* 2007). *Nonomuraea* ATCC39727, the producer of the glycopeptide antibiotic A40926, was genetically manipulated by conjugation from *E. coli* to generate an insertion mutation in the A40926 gene cluster (Sosio *et al.* 2003; Stinchi *et al.* 2003). Although the introduction of large DNA molecules, such as cosmids, into this strain had not been reported, *Nonomuraea* sp. appeared to be a potentially suitable strain to use when attempting to heterologously express the *mib* gene cluster. Furthermore, collaboration with the group of Professor Flavia Marinelli at the University of Insubria, Italy provided accessibility to the strain and protocols for its growth and manipulation. In collaboration with a visiting student from Professor Marinelli's group, Dr. Georgia Letizia Marcone, we set out to develop a method for transferring cosmids into *Nonomuraea* ATCC39727 with the ultimate aim of generating mutations within the A40926 gene cluster (as reported in (Marcone *et al.* 2010a)) and utilising *Nonomuraea* as a heterologous host for the *mib* gene cluster. Cosmid transfer was achieved using a modified version of conjugation protocols previously reported for actinomycete mycelium (Kieser *et al.* 2000; Sosio *et al.* 2003; Stinchi *et al.* 2003; Marcone *et al.* 2010c).

6.2. Heterologous Expression of the *mib* gene cluster in *Nonomuraea* ATCC39727

The integrative cosmid pIJ12131 containing the *mib* gene cluster (see chapter 5) and the vector control pIJ10702 were transferred into *Nonomuraea* sp. ATCC39727 mycelium by conjugation from *E. coli* ET12567/pUZ8002 (Marcone *et al.* 2010c). These constructs were expected to integrate into the *Nonomuraea* chromosome at the ΦC31 *attB* site (Stinchi *et al.* 2003). Ex-conjugants were selected on V0.1 containing 50 µg/ml apramycin and 25 µg/ml nalidixic acid. Transfer of pIJ10702 (a vector of approximately 10 kb) was efficient, yielding approximately $4x10^{-4}$ ex-conjugants per *Nonomuraea* sp. ATCC39727 CFU (based on typically using $5x10^{6}$ CFU *Nonomuraea* per conjugation as per (Marcone *et al.* 2010c)). In contrast, transfer of pIJ12131 (greater than 43 kb) was about 100 fold less efficient, yielding approximately $4x10^{-6}$ ex-conjugants per *Nonomuraea* sp. ATCC39727 CFU. This presumably reflects a decrease in the efficiency of conjugal transfer as the size of the plasmid increases (Flett *et al.* 1997).

Since conjugation was carried out using mycelial fragments it was important to ensure that the resulting recipient strains were homogeneous. Introduction of the construct carrying the resistance marker into a multi-nucleoid mycelial compartment could allow genomes not carrying the resistance gene to survive and propagate even in the presence of selection. Early characterisation of strains carrying pIJ12131 suggested that some clones were mixed mycelial populations that segregated in the absence of selection. Growing strains for several rounds of re-streaking under selective conditions should eventually lead to pure cultures. Thus, clones resulting from each conjugation were subjected to three rounds of growth as single colonies on V0.1 containing 50 µg/ml apramycin before analysis.

Nonomuraea sp. ATCC39727 derivatives containing pIJ10702 or pIJ12131 were grown in VSP and genomic DNA was purified. This was used to confirm the presence of the *mib* cluster in four independent clones of *Nonomuraea* pIJ12131 by PCR amplifying the *mibA, mibD and mibH* genes (Figure 6.1). These strains were confirmed as *Nonomuraea* sp. ATCC39727 derivatives by amplifying a gene, *dbv5,* from the A40926 gene cluster (using primers Dbv5F and Dbv5R). Contamination with *M. corallina* was ruled out by failing to amplify the *M. corallina* ΦC31 *attB* site (using primers LF044F and LF044R; see chapter 7) (Figure 6.1).

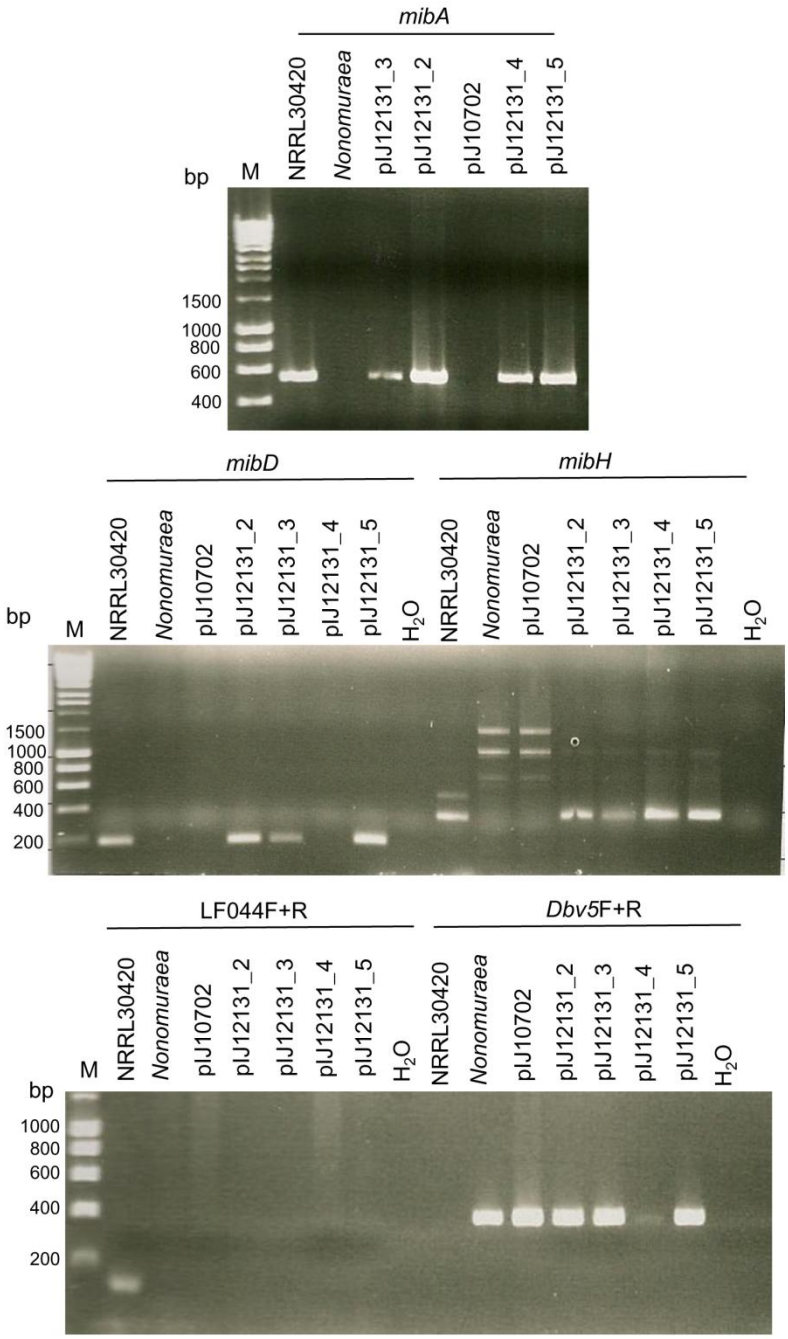

Figure 6.1 PCR confirmation of the integration of the *mib* cluster in *Nonomuraea* pIJ12131 by PCR amplification of *mibA* (LF023F and LF023R2; 545 bp), *mibD* (LF004F and LF004R; 189 bp) and *mibH* (LF006F and LF006R; 344 bp) genes from the *mib gene* cluster and of the ΦC31 *attB* site from *M. corallina* (LF044F and LF044R; 120 bp) and *dbv5* from the A40926 gene cluster of *Nonomuraea* (Dbv5F and Dbv5R; 375 bp). Template DNA was 10 ng genomic DNA extracted from the respective strain or water as a control. PCR amplified fragments were separated on a 1% agarose gel by electrophoresis. The marker (M) is Hyperladder (Bioline) and sizes are given at the side of each gel in base pairs.

These strains were grown in parallel with *Nonomuraea* ATCC39727 and *M. corallina* NRRL 30420 in VSP medium for 3, 5 and 7 days. Supernatants from these cultures were tested for bioactivity against *M.luteus*. Both *Nonomuraea* wild type and pIJ10702 supernatants produced small faint zones of inhibition in a lawn of *M. luteus* (Figure 6.2). This is probably due to the production of A40926 or some uncharacterised secondary metabolite of *Nonomuraea*. However, two clones of *Nonomuraea* pIJ12131 (clones 2 and 5) produced a compound that gave large sharp zones of inhibition with much more clearly defined edges (Figure 6.2). These zones of inhibition were similar to those seen with the *M. corallina* NRRL 30420 supernatant. The two remaining clones of *Nonomuraea* pIJ12131 (clones 3 and 4) gave faint zones of inhibition, particularly noticeable after 5 and 7 days of cultivation, that were more similar to those produced by the vector only and wild type *Nonomuraea* controls.

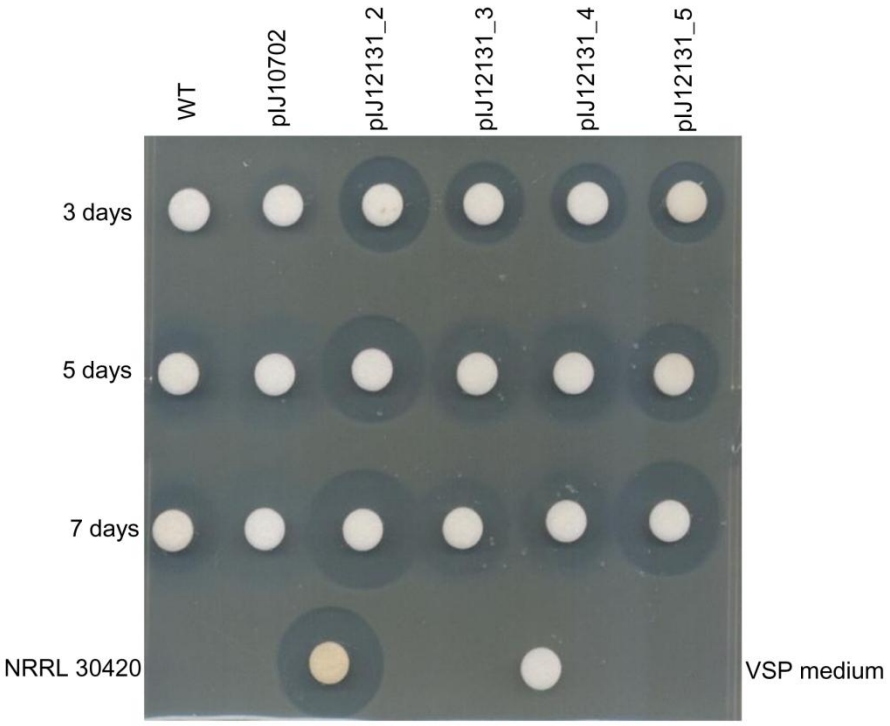

Figure 6.2 Heterologous expression of the microbisporicin gene cluster in *Nonomuraea* sp. ATCC39727. *Nonomuraea* wild type (WT), pIJ10702 and pIJ12131 clones 2-5 were grown in VSP medium. Supernatant samples were taken at 3, 5 and 7 days of fermentation and tested for bioactivity by applying 40 µl supernatant to antibiotic assay discs which were then applied to a lawn of *M. luteus*. Control discs contain supernatant from *M. corallina* NRRL 30420 grown for 7 days in VSP or VSP medium only. The plate was incubated overnight at 30°C before zones of inhibition were visualised.

The collected supernatants were analysed by for MALDI-ToF mass spectrometry. The *Nonomuraea* wild type and pIJ10702 supernatants did not produce any ions associated with described microbisporicin variants (Figure 6.3). All four *Nonomuraea* pIJ12131 clones and *M. corallina* NRRL 30420 supernatants produced ions associated with variants of microbisporicin (Figure 6.3, see also Table 3.1). As well as the appearance of ions for the three described microbisporicin variants (and their sodium/potassium adducts and oxidation products; see chapter 3) a small amount of non-chlorinated microbisporicin was also observed (peaks at m/z 2203.8 and 2219.8; Figure 6.3). This suggests that halogenation does not occur as efficiently in *Nonomuraea* as in *M. corallina.* Additionally, ions with m/zs larger than those previously described were noted in *Nonomuraea* pIJ12131 supernatants compared to the vector control (Figure 6.4). These ions were also found in supernatants of *M. corallina* NRRL 30420 grown under these conditions but had not previously been associated with microbisporicin (Figure 6.4). These ions are 225 Da larger than the spectrum of peaks associated with the microbisporicin variants (Figure 6.5). 225 Da is the mass difference expected if the three C-terminal residues of the leader peptide (GPA) are left intact (Tables 6.1 and 6.2). These compounds are likely to be microbisporicin variants since they have the same characteristic isotope pattern associated with the incorporation of chlorine in microbisporicin (see chapter 7). This suggests that under some conditions there might be two leader peptide cleavage sites for the MibA leader peptide. Whether these “GPA” variants of microbisporicin are active is not known. The fact that these appear in *Nonomuraea* suggests that the proteases associated with the two different cleavage positions are conserved in *Nonomuraea*.

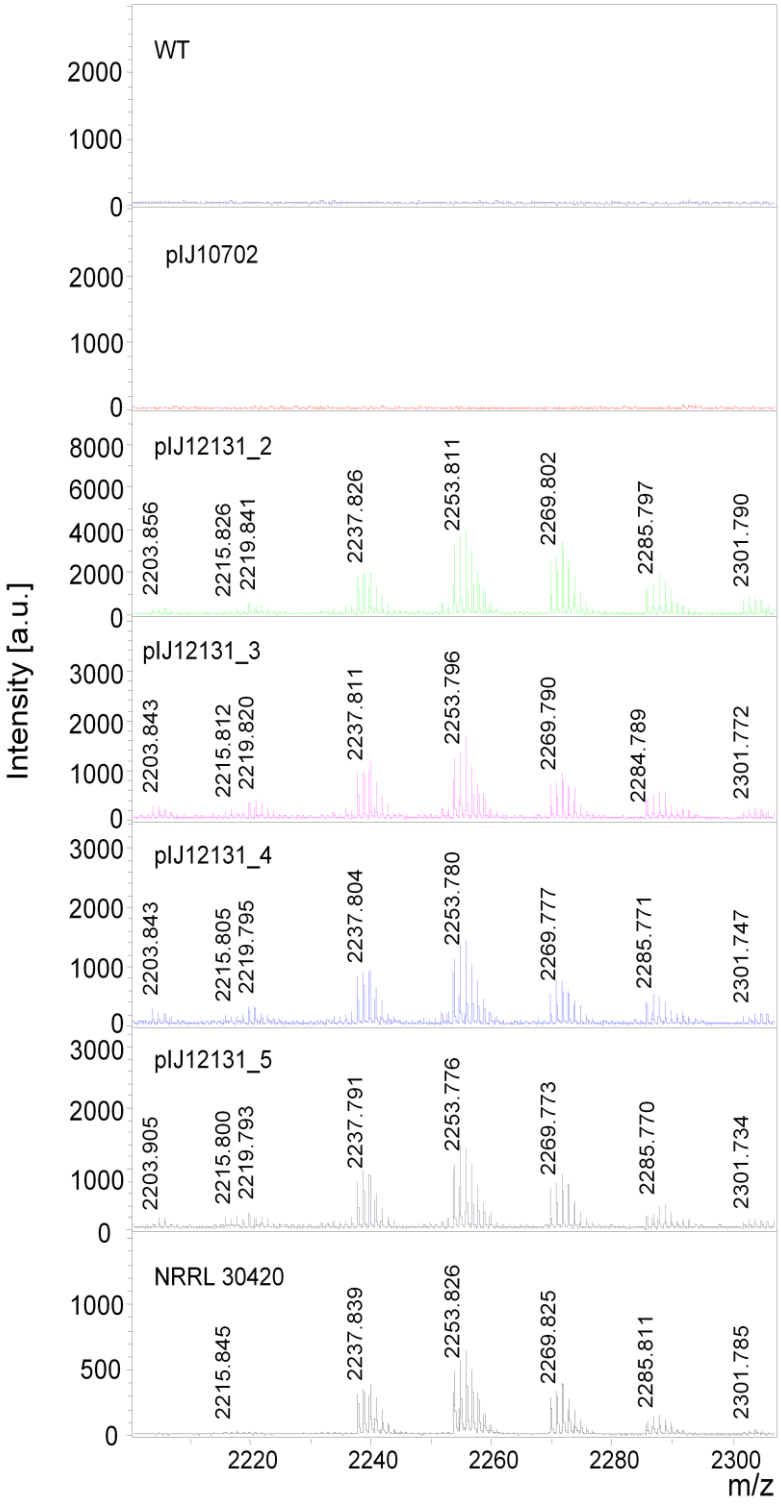

Figure 6.3 Heterologous production of microbisporicin in *Nonomuraea* ATCC39727. *Nonomuraea* wild type (WT), pIJ10702 and pIJ12131 clones 2-5 were grown in VSP medium. Supernatant samples were taken at 7 days of fermentation and investigated by MALDI-ToF mass spectrometry. A control spectrum from supernatant of *M. corallina* NRRL 30420 grown for 7 days is shown.

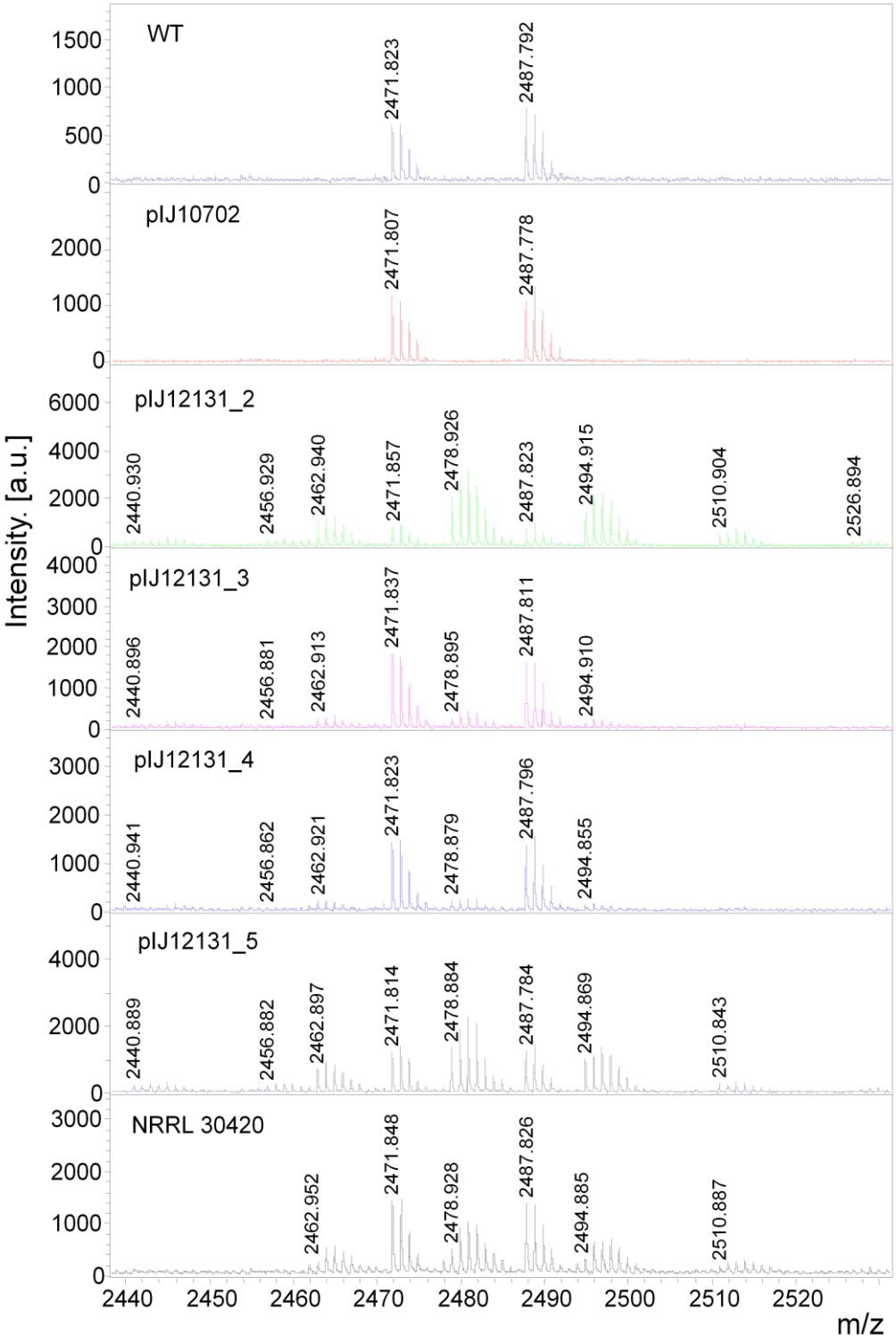

Figure 6.4 Heterologous production of microbisporicin in *Nonomuraea* ATCC39727. *Nonomuraea* wild type (WT), pIJ10702 and pIJ12131 clones 2-5 were grown in VSP medium. Supernatant samples were taken at 7 days of fermentation and investigated by MALDI-ToF mass spectrometry. A control spectrum from supernatant of *M. corallina* NRRL 30420 grown for 7 days is shown. Peaks at m/z 2471.8 and 2487.8 are media components and act as internal standards.

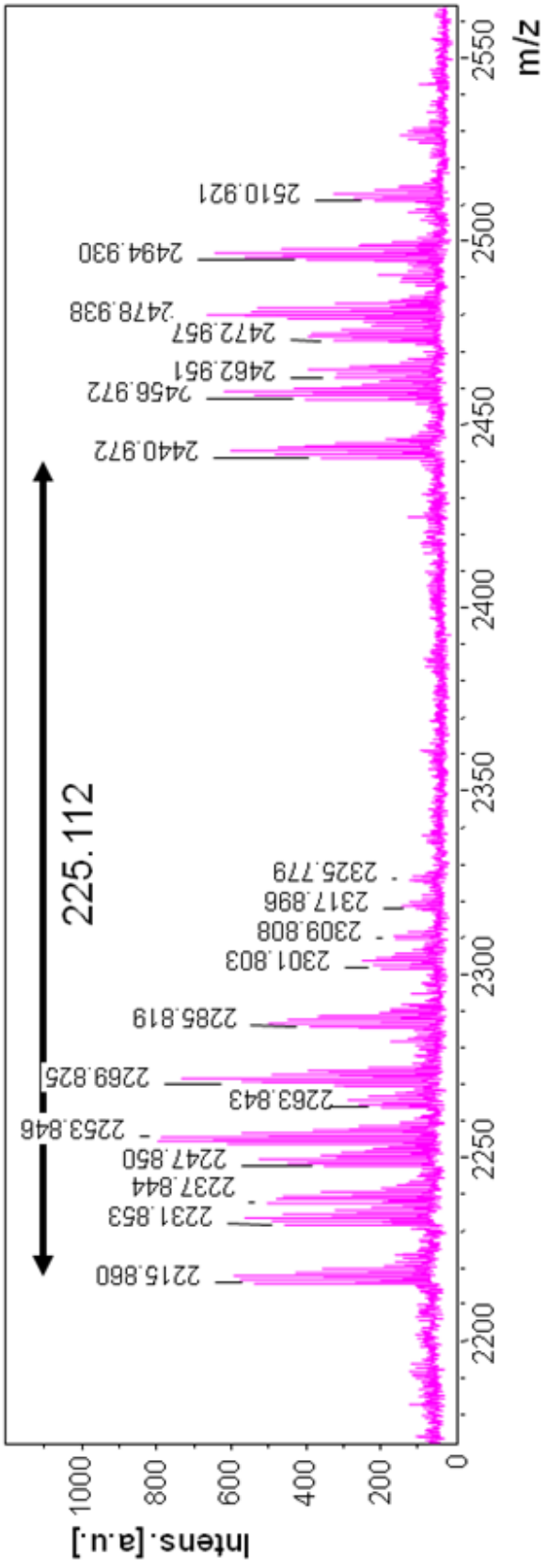

Figure 6.5 "GPA" variants of microbisporicin. An example mass spectrum showing a group of masses 225 Da heavier than those associated with microbisporicin, identified in *Nonomuraea* pIJ12131 clone supernatants and in *M. corallina* NRRL30420 supernatants. 225 Da is the mass difference associated with the extension of mature microbisporicin with three residues from the leader peptide; GPA (see also Table 6.1 and 6.2).

Table 6.1 The theoretical masses of the microbisporicin propeptide with the leader peptide removed between Ala-4 and Gly-3 or between Ala-1 and Val+1. The difference in the mass is 225.112 Da. The resulting mass of the modified compound is calculated as shown.

Amino acid sequence	GPAVTSWSLCTPGCTSPGGGSNCSFCC	VTSWSLCTPGCTSPGGGSNCSFCC	Mass Difference
Theoretical Monoisotopic Mass (Da)	2577.995	2352. 883	225.112
Each dehydration (7 in total) leads to mass decrease of 18Da (-126 Da)	2451.995	2226.883	225.112
C-terminal cysteine decarboxylation (loss of CO_2 with the gain of 2 protons) leads to mass loss of 46 Da (MF-BA-1768β_1)	2405.995	2180.883	225.112
Formation of 5-chlorotryptophan leads to mass increase of 34 Da (gain of ^{35}Cl with loss of one proton) (MF-BA-1768α_1)	2439.995	2214.883	225.112

Table 6.2 The expected masses of the four modified microbisporicin variants with "GPA" extensions at the N-terminus. Masses calculated from the theoretical modified compounds in Table 6.1. m/z peaks identified in spectra from supernatants from *Nonomuraea* pIJ12131 and *M. corallina* NRRL 30420 are highlighted in blue.

	MW (Da)	[M+H+]	with 1 O	[M+Na+]	with 1 O	[M+K+]	with 1 O	with 2 O
MF-BA-1768β-GPA	2405.995	2406.995	2422.995	2428.995	2444.995	2444.995	2460.995	2476.995
MF-BA-1768α-GPA	2439.995	2440.995	2456.995	2462.995	2478.995	2478.995	2494.995	2510.995
107891-A2-GPA	2455.995	2456.995	2472.995	2478.995	2494.995	2494.995	2510.995	2526.995
107891-A1-GPA	2471.995	2472.995	2488.995	2494.995	2510.995	2510.995	2526.995	2542.995

The data demonstrated that microbisporicin could be biosynthesised by *Nonomuraea* carrying the *mib* gene cluster in pIJ12131. This confirms that pIJ12131 contains all of the genes required for microbisporicin biosynthesis in a heterologous host. However, the phenotypes of the four clones thought to contain the *mib* cluster (by selection on apramycin and PCR amplification of *mib* genes) were quantitatively different. The production of ions associated with microbisporcin could be detected by MALDI-ToF mass spectrometry from all four clones; however only two showed reproducibly high levels of bioactivity against *M. luteus* (clones 2 and 5; Figure 6.6). This could have reflected a mixed population of genomes in strains 3 and 4 (with some genomes carrying the construct and others not). Further purification of these strains through rounds of single colony growth in the presence of selection failed to produce phenotypes similar to those of clones 2 and 5. Alternatively, the cosmids in these strains may have acquired a mutation that suppressed microbisporicin production, or strains 2 and 5 may have acquired a mutation in the genome or in the *mib* gene cluster that increased microbisporicin production. The copy number of the introduced cosmid could also be an important factor; pIJ12131 may have integrated multiple times into the genome of strains 2 and 5, thus increasing expression levels. The introduction of tandem copies of some integrating vectors has been described previously (Combes *et al.* 2002). Subsequent non-selective growth of the strains would be expected to resolve the tandem insertions but the phenotypes of strains 2 and 5 appeared to be stable. Finally, it is possible that the epigenetic context of the integrated cosmid could play a role. Expression from the *mib* gene cluster could be suppressed in strains 3 and 4 by incorporation into higher-order chromatin structure (McArthur *et al.* 2006).

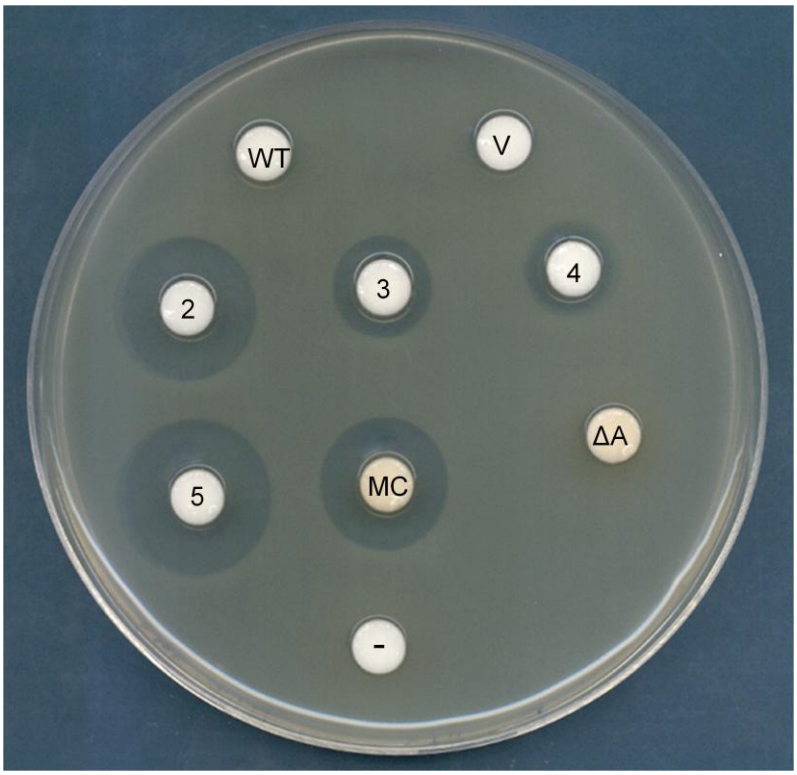

Figure 6.6 Heterologous production of microbisporicin in *Nonomuraea* ATCC39727. *Nonomuraea* wild type (WT), pIJ10702 (V) and pIJ12131 clones 2-5 were grown in medium V. Supernatant samples were taken at 7 days of fermentation and tested for bioactivity by applying 40 µl supernatant to antibiotic assay discs which were then applied to a lawn of *M. luteus*. Control discs contain supernatant from *M. corallina* NRRL 30420 wild type (MC) or Δ*mibA* mutant (ΔA; see chapter 7) grown for 7 days in VSPA and VSP medium only (-). The plate was incubated overnight at 30°C before zones of inhibition were visualised. For unknown reasons background activity from A40926 production was largely suppressed in this analysis.

6.3 Deletional analysis of the *mib* gene cluster in *Nonomuraea* ATCC39727

A series of in-frame gene deletions were generated in pIJ12131. Using the pIJ778 cassette employed to knock-out *mibA*, *mibX*, *mibW* and *mibXW* (chapter 5) the following additional genes were replaced; *mibZ-mibR*, *mibD*, *mibTU*, *mibV*, *mibEF*, *mibH* and *mibN.* The cassette was subsequently removed by FLP-mediated recombination to leave an 81bp scar. The 11 mutant cosmids described above were transferred into *Nonomuraea* ATCC39727 by conjugation from *E.coli* ET12567/pUZ8002. As with the wild type cosmid, transfer of the mutant cosmids was very inefficient. Often conjugations had to be repeated three or four times to obtain at least one clone of each mutant. As described for the wild type cosmid, the resulting ex-conjugants were cultured as single colonies for three successive rounds of growth on V0.1 containing 50 µg/ml apramycin. All strains were confirmed to contain representative genes of the *mib* cluster and the specific deletion in that cosmid by PCR analysis using genomic DNA extracted from the clones.

All strains were grown for 7 days in VSP media and supernatants tested for bioactivity against *M. luteus* (Figure 6.7). Supernatants were also investigated for the production of ions associated with microbisporicin by MALDI-ToF mass spectrometry. The results of this analysis were not very clear, due at least in part to the production of other bioactive compounds by *Nonomuraea,* as discussed in section 6.2. The only clones giving clear, defined zones of inhibition similar to those seen for NRRL 30420 or *Nonomuraea* pIJ12131_2 supernatants were Δ*mibXW*_1 (but not clone 2), Δ*mibTU*_1 (but not clone 2), Δ*mibV*_1 (but not clone 2) and Δ*mibN*_2 (but not clone 3). The lack of reproducibility between clones of strains carrying the same mutant cosmid (confirmed by PCR analysis) suggests a similar effect is occurring as that described in section 6.2 for different clones of the wild type cosmid. Upon MALDI-ToF mass spectrometry, the only supernatants revealing ions associated with microbisporicin were Δ*mibV*_1 and Δ*mibN*_2 despite the detection of bioactivity from two other clones (Δ*mibXW*_1 and Δ*mibTU*_1). In the supernatant of *Nonomuraea* pIJ12131 Δ*mibV*_1, only m/z peaks larger than those typically associated with microbisporicin were observed (the so-called “GPA” variants) (Figure 6.8). These masses were different from those seen in NRRL 30420 or *Nonomuraea* pIJ12131_2 supernatants: only GPA variants corresponding to the non-chlorinated form of microbisporicin were observed (the non-chlorinated form is 34 Da lighter than chlorinated microbisporicin due to the loss of chlorine-35 and the gain of one proton in its place; Tables 6.1 and 6.2). This suggests that *mibV* might be involved in the chlorination of microbisporicin. It is not clear why only the GPA variants were detected in this sample. Perhaps they were present in a higher concentration in this sample (an effect

of an acquired mutation on correct leader peptide processing?) or ionised more readily in the MALDI-ToF analysis. In the supernatant of *Nonomuraea* pIJ12131 Δ*mibN*_2, m/z peaks for both wild type microbisporicin and wild type GPA variants were detected (again the GPA variants were observed with higher intensity; Figure 6.8). Thus inactivation of *mibN* had no effect on microbisporicin biosynthesis in the heterologous host.

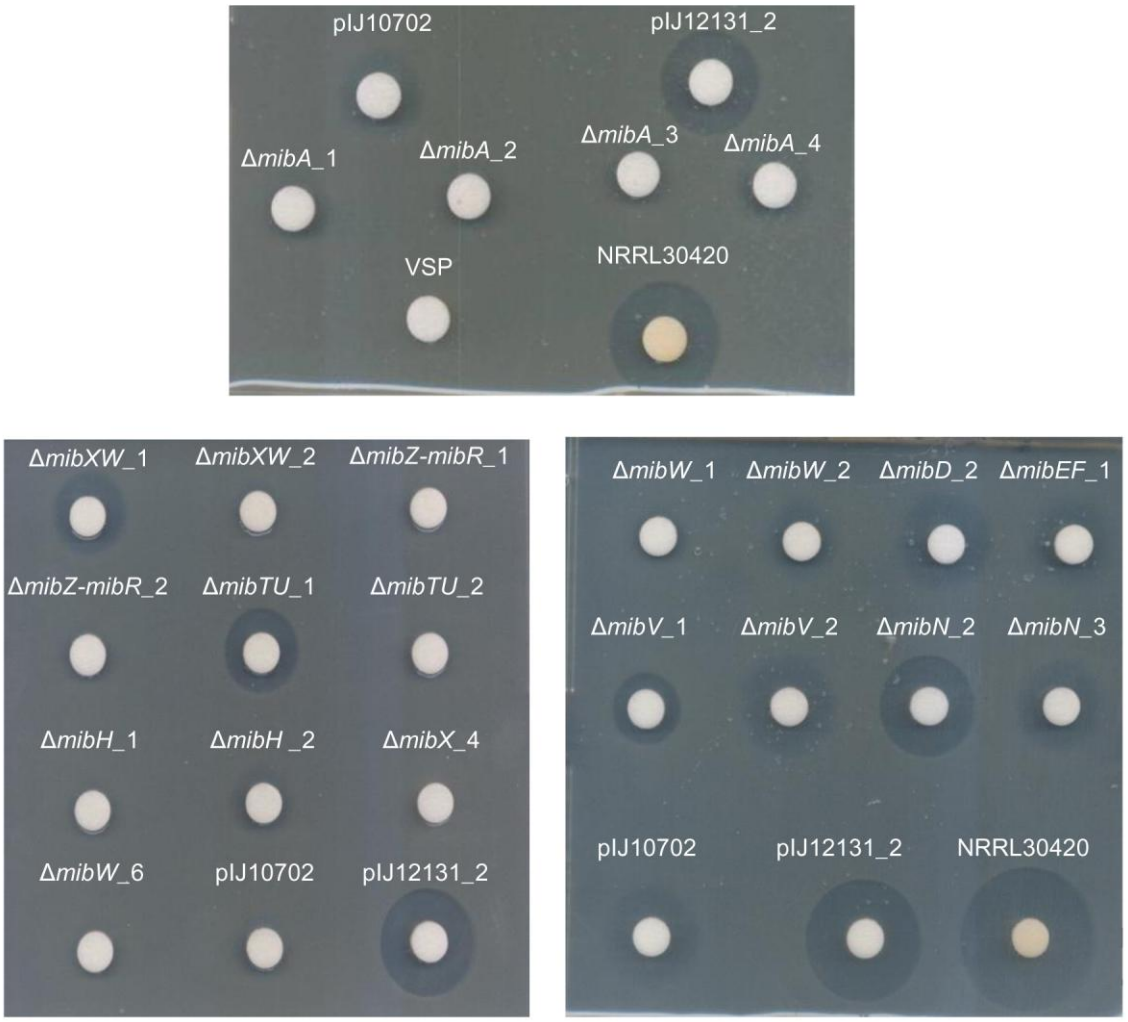

Figure 6.7 Heterologous production of microbisporicin from gene inactivation mutants of pIJ12131 in *Nonomuraea* ATCC39727. *Nonomuraea* strains were grown in VSP. Supernatant samples were taken at 7 days of fermentation and tested for bioactivity by applying 40 µl supernatant to antibiotic assay discs which were then applied to a lawn of *M. luteus*. Control discs contain supernatant from *M. corallina* NRRL 30420 wild type grown for 7 days in VSPA. The plate was incubated overnight at 30°C before zones of inhibition were visualised.

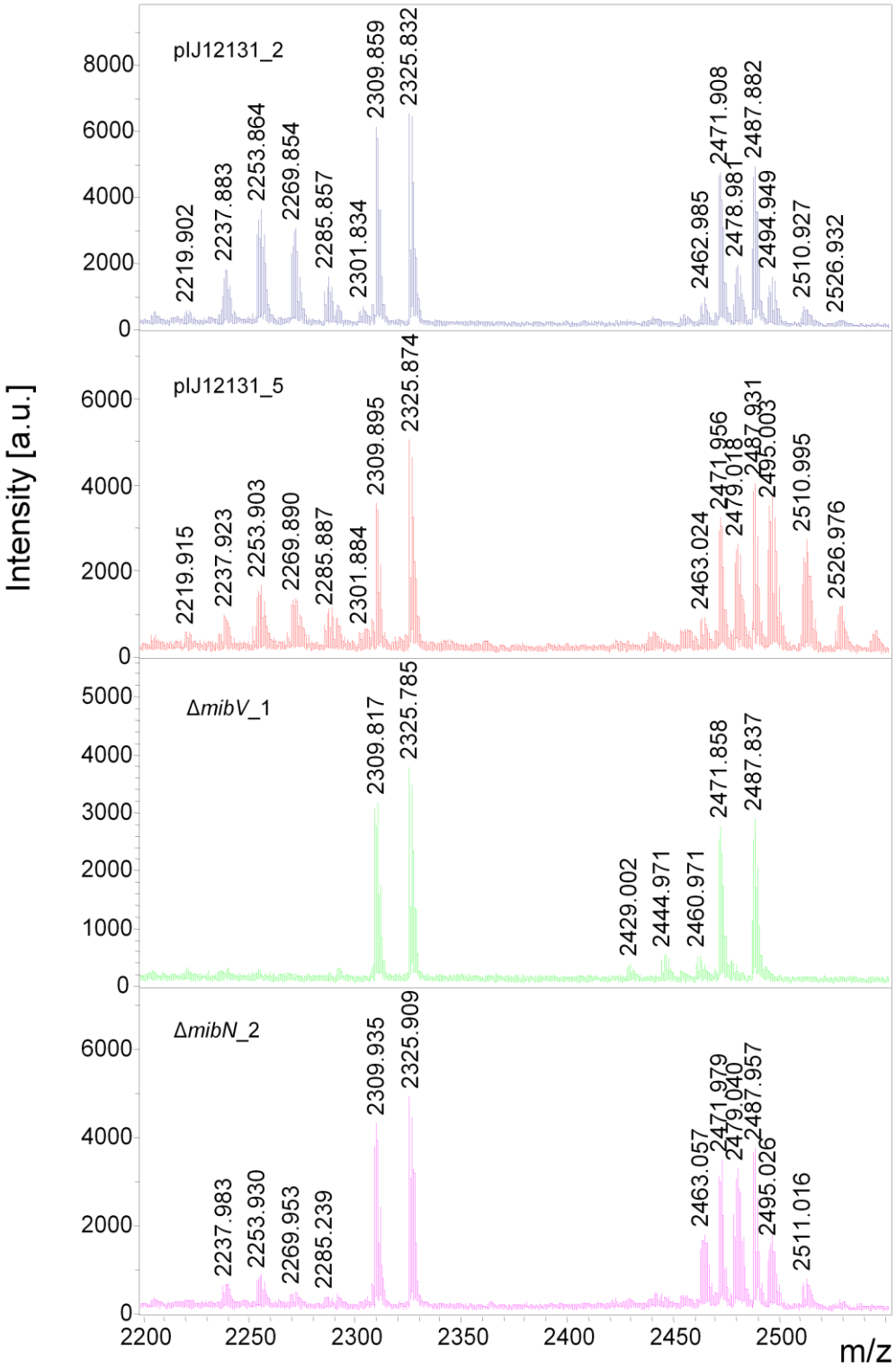

Figure 6.8 Heterologous production of microbisporicin from gene inactivation mutants of pIJ12131 in *Nonomuraea* ATCC39727. MALDI-ToF mass spectra for *Nonomuraea* pIJ12131_2, pIJ12131_5, pIJ12131 Δ*mibV*_1 and pIJ12131 Δ*mibN*_2.

Results for the other mutant cosmids in *Nonomuraea* were largely unclear. As described above, there were discrepancies between the bioassay and MALDI-ToF results, as well as between clones of the same mutants. This suggests that heterologous expression in *Nonomuraea* can produce both false-positive and false-negative results. The reasons for this may be similar to those proposed to explain the differences in phenotypes between clones containing the wild type cosmid (section 6.2). To try to find conditions where results would be more consistent, a different growth medium for *Nonomuraea* was used. Parallel studies of the planosporicin biosynthetic gene cluster in *Nonomuraea* by Emma Sherwood had revealed that a growth medium termed Streptosporangium Medium (SM; (Roes *et al.* 2008)) could be used reproducibly for the production of secondary metabolites in this strain. A number of the generated mutant strains were grown in this medium for 3-5 days and supernatant removed to test for bioactivity and for the presence of microbisporicin by MALDI-ToF mass spectrometry. This medium enhanced A40926 (and/or other bioactive compound) production, making the bioassay results difficult to interpret. However, MALDI-ToF analysis of the supernatants proved more reliable. *Nonomuraea* pIJ10702 supernatant, although giving bioactivity against *M. luteus*, was not found to produce ions associated with the production of microbisporicin. As when cultured in VSP, *Nonomuraea* pIJ12131 grown in SM produced both chlorinated and non-chlorinated forms of microbisporicin (figure 6.9). Larger “GPA” variants were found in this medium than in V or VSP, possibly suggesting that different proteases are active under different culture conditions in *Nonomuraea* (Figure 6.10). The exact molecular nature of these new variants could not be predicted on the basis of mass difference. These observations indicate that culture conditions can play an important role in the form of the final compound produced, although how this is mediated is not clear. Alternatively these m/z peaks may represent an unrelated secondary metabolite from *Nonomuraea,* the expression of which is induced by the production of microbisporicin. As described previously, *Nonomuraea* pIJ12131 Δ*mibV*_1 was found to make only the non-chlorinated form of microbisporicin and *Nonomuraea* pIJ12131 Δ*mibN*_2 was found to also make wild type microbisporicin (Figure 6.9). *Nonomuraea* pIJ12131 Δ*mibTU*_1 and 2 clones both produced wild type microbisporicin (Figure 6.11). Despite giving faint zones of inhibition in a lawn of *M. luteus*, supernatants from *Nonomuraea* pIJ12131 with deletions in *mibA*, *mibX*, *mibW*, *mibXW* and *mibZ-mibR* did not produce ions attributable to microbisporicin.

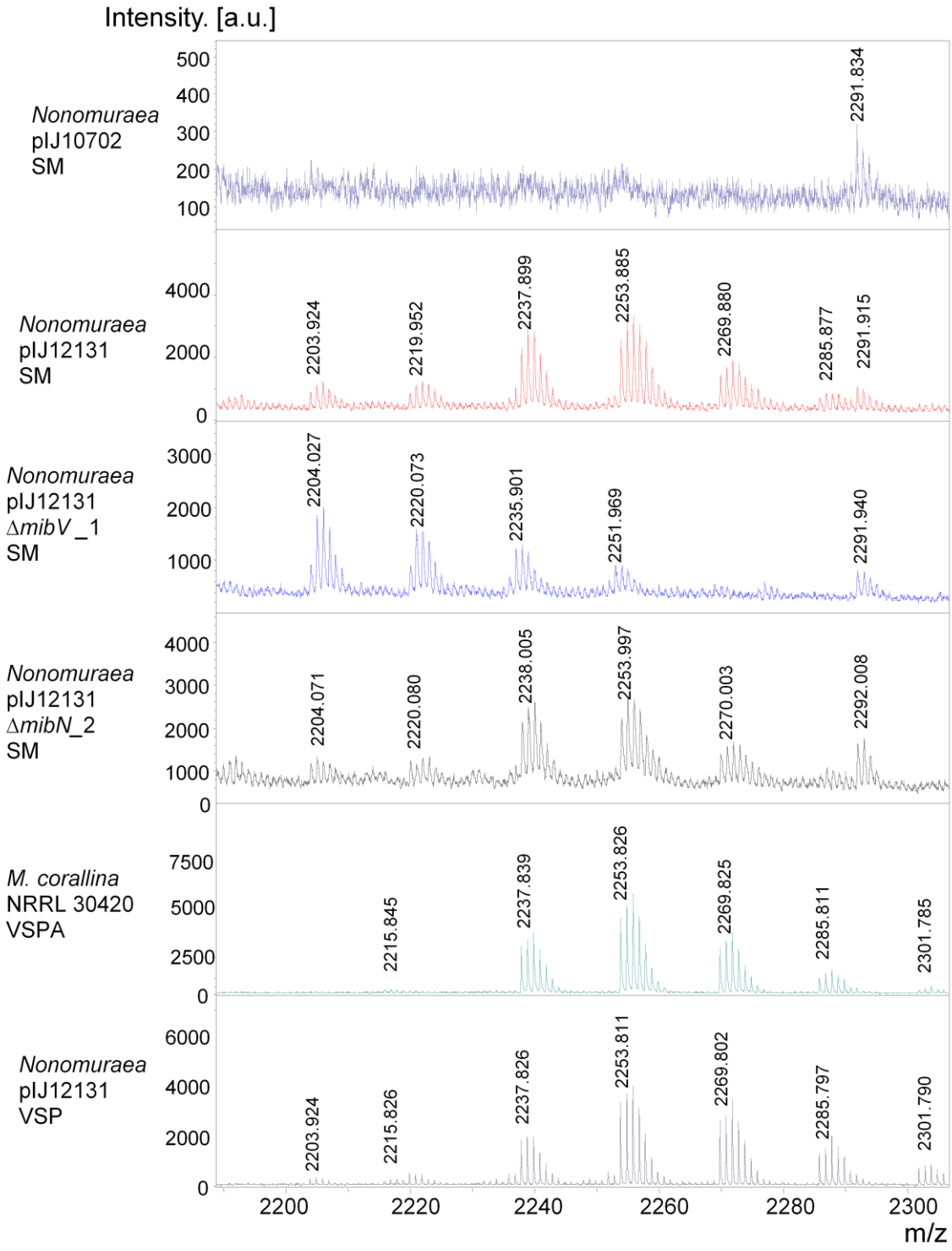

Figure 6.9 Heterologous production of microbisporicin from gene inactivation mutants of pIJ12131 in *Nonomuraea* sp. ATCC39727. *Nonomuraea* strains were grown in SM. Supernatant samples were taken at 5 days of fermentation and investigated with MALDI-ToF mass spectrometry.

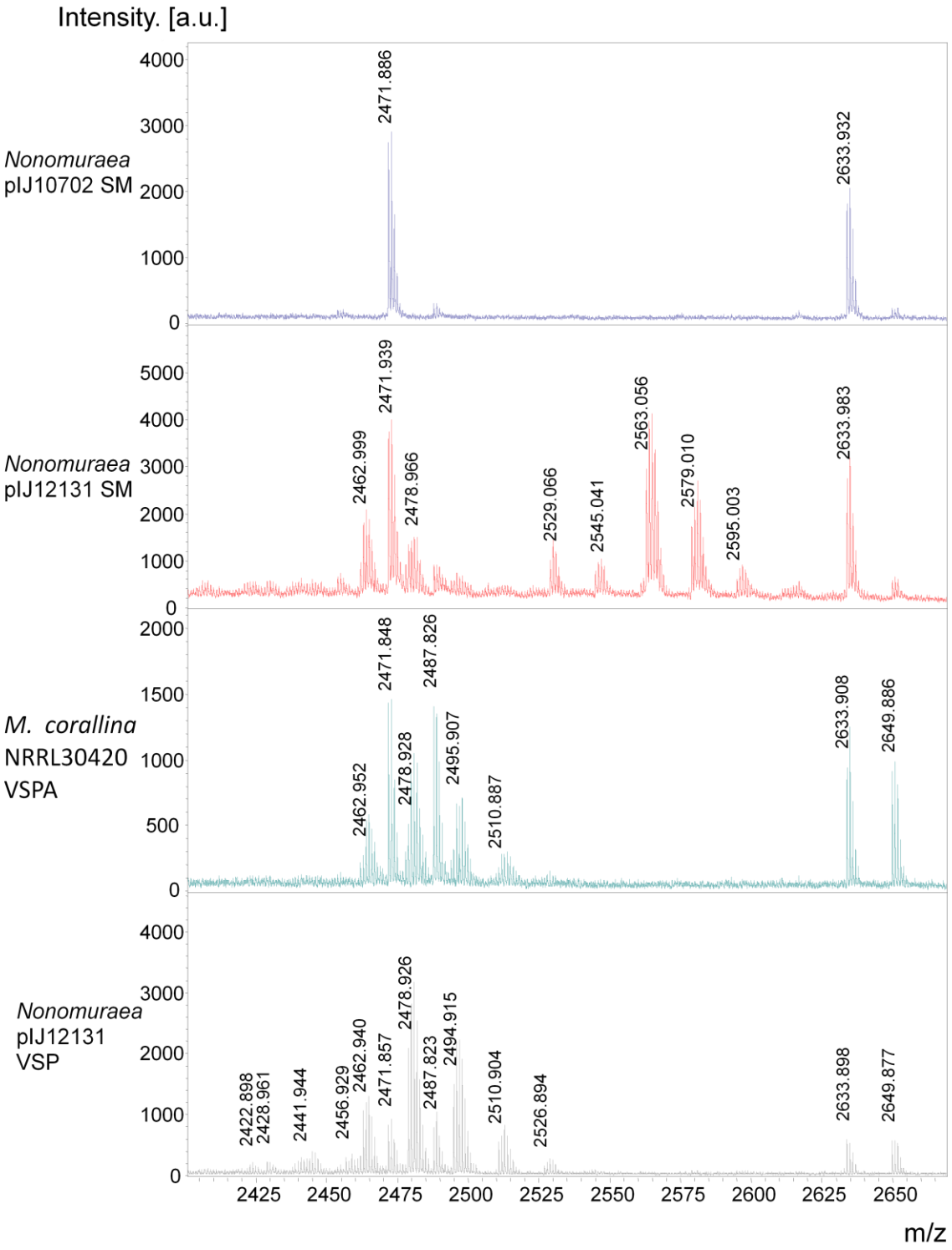

Figure 6.10 Heterologous production of microbisporicin in *Nonomuraea* sp. ATCC39727 pIJ12131 and NRRL 30420 under different growth conditions. *S*trains were grown in SM or VSP. Supernatant samples were investigated with MALDI-ToF mass spectrometry.

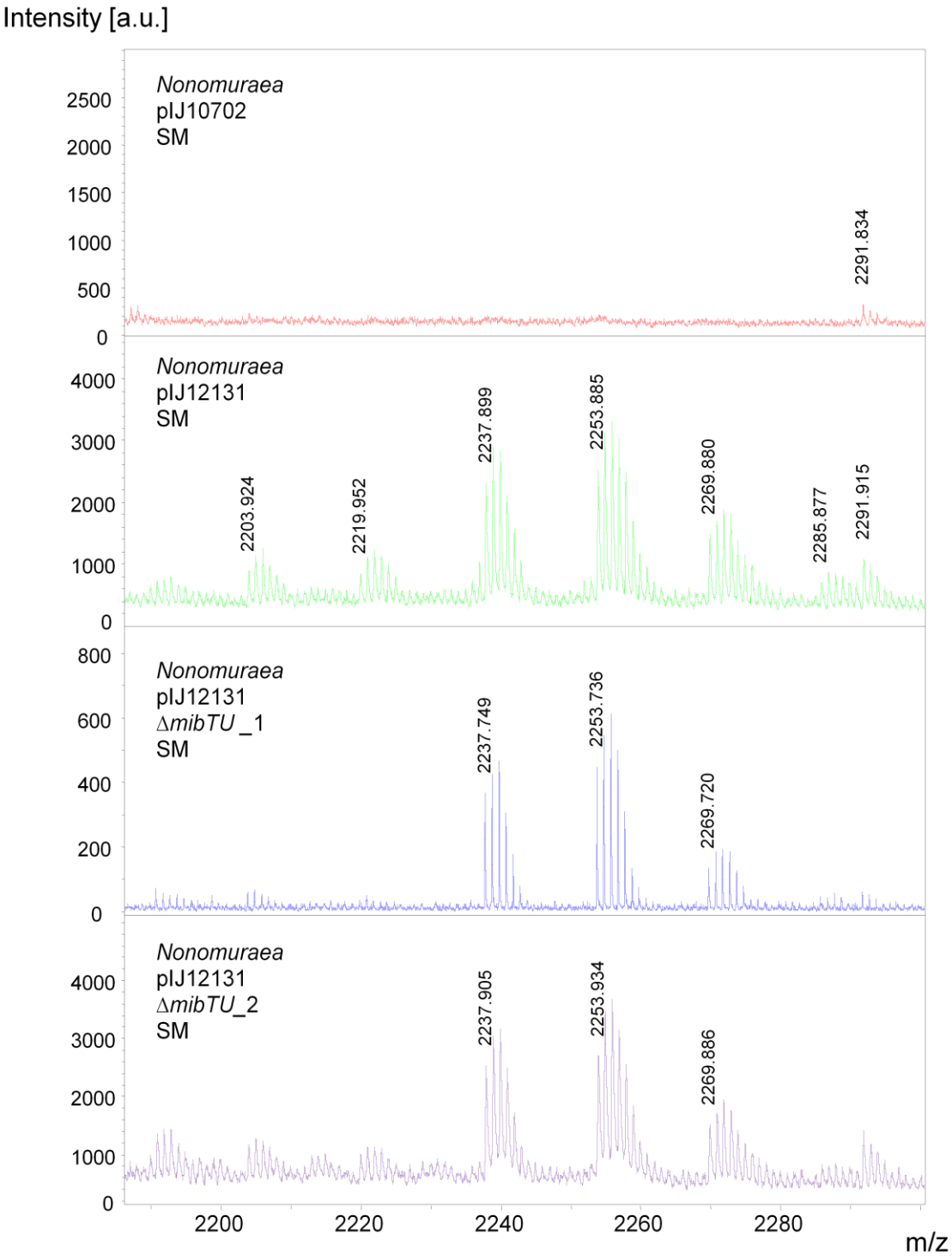

Figure 6.11 Heterologous production of microbisporicin from gene inactivation mutants (Δ*mibTU*) of pIJ12131 in *Nonomuraea* sp. ATCC39727. *Nonomuraea* strains were grown in SM. Supernatant samples were taken at 5 days of fermentation and investigated with MALDI-ToF mass spectrometry.

6.4 Discussion and Summary Points

6.4.1 Discussion

Nonomuraea sp. ATCC39727 is capable of generating and exporting mature, active microbisporicin from the *mib* gene cluster in pIJ12131, and could presumably be used to express antibiotic gene clusters from other members of the *Streptosporangiaceae* family. Heterologous expression indicated that the genes encoded within the insert of pIJ12131 include the minimal gene set required for the production of microbisporicin.

Inactivation of *mib* genes in *Nonomuraea* failed to yield convincing and reproducible evidence for their function in microbisporicin biosynthesis. However, inactivation of *mib* genes in *M. corallina* NRRL 30420 (described in chapter 7) supports the phenotypes that were observed for some of the *Nonomuraea* pIJ12131 mutant cosmids; MibV is involved in chlorination of microbisporicin, and MibN and MibTU are not essential for microbisporicin biosynthesis. In a heterologous host there is always some doubt surrounding mutant phenotypes. In the light of clearer results for mutants of the natural host, experiments with the mutant cosmids in *Nonomuraea* were discontinued. In *Nonomuraea*, a particular problem with heterologous expression is that compound production varied even between clones containing the same construct. This can make it difficult to be confident of the phenotypes observed, particularly those in which the compound is not produced at all since these may represent false negative results. Also, as a producer of at least one bioactive secondary metabolite, *Nonomuraea* is not an ideal host for activity screening. Although culture supernatants can be screened by MALDI-ToF mass spectrometry, this could become expensive when multiple clones of each mutant are assessed using a variety of culture conditions.

As discussed in section 6.2 there are numerous reasons why the phenotypes of *Nonomuraea* carrying the *mib* gene cluster could vary between clones. The most likely explanation is probably one of copy-number, either through a mixed genome population or through tandem insertion of the construct. This appears to be a particular problem when using mycelium, instead of spores, for the movement of vectors by conjugation from *E. coli*. Spore germination usually results in only one or two mycelial compartments that are available for conjugation with *E. coli* and this presumably helps to ensure a homogeneous population since all or almost all of the genomes within the mycelium will carry the construct. This is not an option with *Nonomuraea* ATCC39727, which does not sporulate under laboratory conditions (G. L. Marcone, personal communication).

6.4.2 Summary Points

- pIJ12131 was mobilised into *Nonomuraea* ATCC39727.
- Microbisporicin was produced in an active, exported form in *Nonomuraea* ATCC39727 pIJ12131.
- Gene inactivation studies were carried out on genes of the *mib* cluster in *Nonomuraea*.
- MibV appears to be involved in chlorination of tryptophan in microbisporicin biosynthesis in *Nonomuraea*.
- MibN and MibTU are not essential for microbisporicin biosynthesis in *Nonomuraea*.
- *Nonomuraea* is not an optimal host for gene inactivation studies of heterologous gene clusters: it can produce false-positive and false-negative results, it produces another bioactive molecule, and the transfer of cosmids by conjugation from *E. coli* is inefficient

Chapter 7 – Microbisporicin Gene Cluster Analysis in *M. corallina.*

7.1 Introduction

The problems encountered in the heterologous production of microbisporicin in both *Streptomyces* and *Nonomuraea* (Chapter 5 and 6) prompted a re-examination of the feasibility of carrying out gene cluster analysis in the natural host *M. corallina*. In the analysis of the cinnamycin and actagardine gene clusters in the heterologous host St*reptomyce*s *lividans* some genes were found not to be essential for biosynthesis and thus further analysis was carried out to determine whether this was also the case in the natural producer (O'Rourke, S, unpublished; Bell, R, unpublished). Finally, developing tools for the direct genetic manipulation of *M. corallina* presents an opportunity for future improvement of this strain. As discussed in chapter 6 very few members of the *Streptosporangiaceae* family have been genetically manipulated and some of the developed tools could be transferrable to other species within this group, many of which produce interesting and potentially useful secondary metabolites.

M. corallina poses a number of difficulties when contemplating genetic manipulation. NRRL 30420 was found to produce very few spores under laboratory conditions and was much more effectively cultured and stored as mycelium. This can present problems for the generation of clonal populations for example when constructing mutants. This issue was also encountered with *Nonomuraea* as described in chapter 6. *M. corallina* also grows quite slowly compared to other actinomycetes used in the laboratory, particularly on solid growth media (7-14 days) and when transferred from solid to liquid culture (requiring at least 6 days incubation to establish sufficient mycelial biomass). Finally, as mentioned above, there were no previous reports of the genetic manipulation of *M. corallina* or many representatives from the family to which it belongs. Although methods for protoplast formation and regeneration have been developed recently (Marcone *et al.* 2010b) protoplast transformation had not been achieved.

The aim of this chapter was to develop methods and tools for the genetic manipulation of *M. corallina*. Initially the aim was to mobilise a small vector developed for use in *Streptomyces* into *M. corallina* as a proof-of-principle and to optimise the procedure. Following this a method for the mobilisation of larger DNA constructs such as cosmids

would be developed to allow the formation of gene inactivation mutants via homologous recombination. Success at this stage would rely on the intrinsic homologous recombination efficiency of the strain (since the PCR targeting approach was developed based on the recombination efficiency of *Streptomyces*) and the ability to isolate double-crossover recombination events in *M. corallina* to yield clonal populations. The ultimate aim was to generate a succession of mutants inactivated in different genes from the *mib* cluster and to analyse the phenotypes of these mutants.

7.2. Methods to manipulate *M. corallina*

7.2.1 Selectable Markers

A number of selectable markers will be required for the genetic manipulation of *M. corallina*. Obvious choices would be those routinely used in *Streptomyces* sp. such as apramycin, kanamycin, spectinomycin/streptomycin and hygromycin resistance. To determine whether *M. corallina* was naturally resistant to these antibiotics (as is the case for *Nonomuraea*, which is naturally highly resistant to hygromycin, G.L. Marcone personal communication) and the minimum inhibitory concentration for each, NRRL 30420 was grown on V0.1 agar medium containing a range of concentrations of these compounds. Concentrations selected typically ranged from 0 to double the concentration used to select for resistance in *Streptomyces* on SFM. Concentration ranges were then narrowed in a second experiment (for an example, see Figure 7.1). *M. corallina* NRRL 30420 was sensitive to apramycin, hygromycin and kanamycin at concentrations of 3 µg/ml, 5 µg/ml and 1 µg/ml, respectively. *M. corallina* NRRL 30420 was sensitive to 25 µg/ml spectinomycin with 100 µg/ml streptomycin. These antibiotics were thus deemed to be suitable for selection of DNA introduced into *M. corallina*. DSM 44681 and DSM 44682 were similarly found to be sensitive to apramycin and hygromycin using the same method (other antibiotics not tested). *M. corallina* strains grew in the presence of 50 µg/ml nalidixic acid (an antibiotic to which actinomycetes are normally resistant but which kills other bacteria such as *E. coli*).

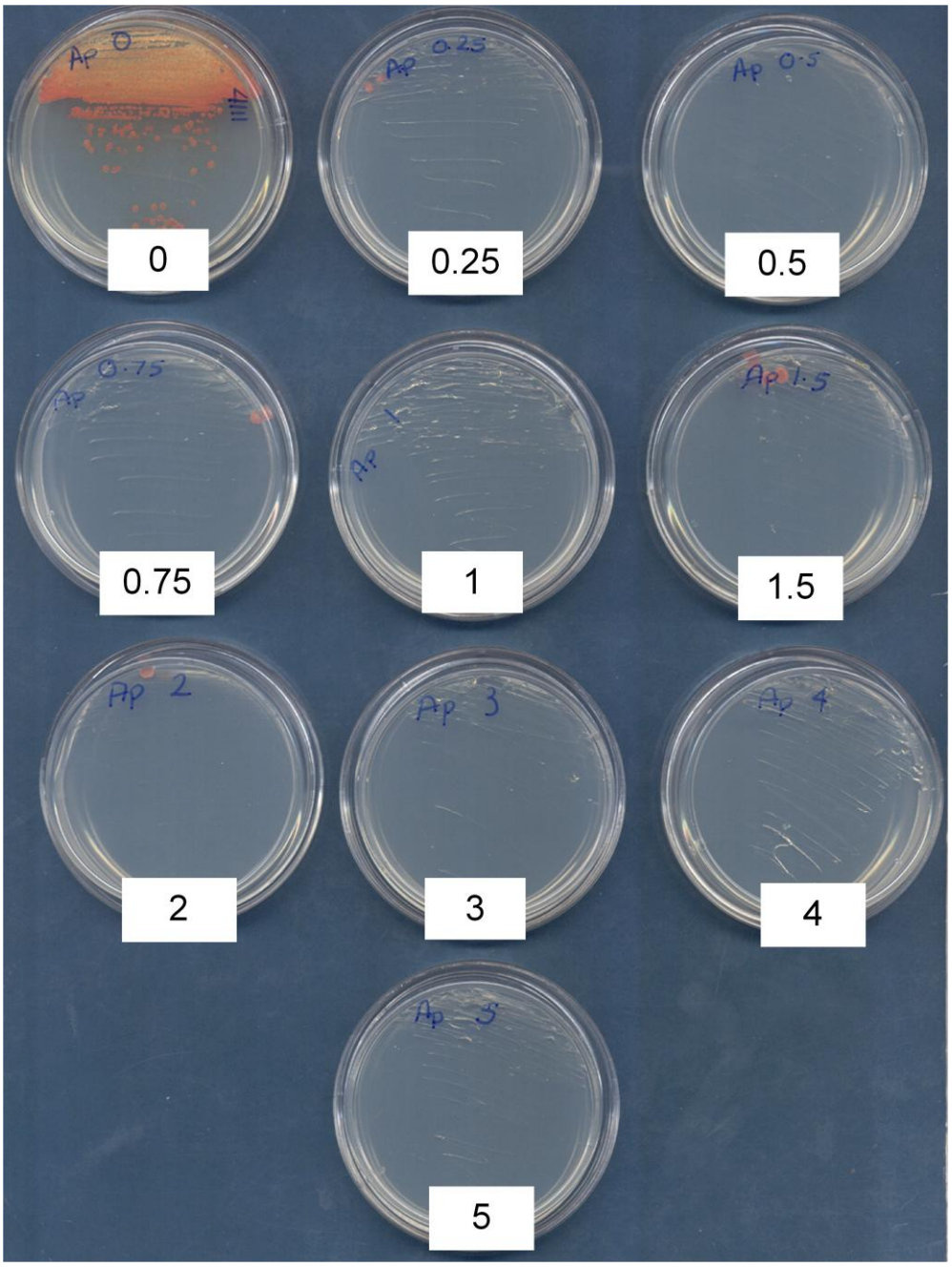

Figure 7.1 The determination of the minimum concentration of apramycin for inhibition of the growth of *M. corallina* NRRL30420. Plates were prepared containing 10 ml V0.1 and the indicated concentration of apramycin (in µg/ml). NRRL 30420 was streaked from a mycelial stock on to each plate. Plates were incubated for 12 d at 30°C.

7.2.3 Analysis of the ΦC31 attachment site in *M. corallina*

The ΦC31 phage attachment site identified in a wide variety of *Streptomyces* sp. and other actinomycetes has been extremely useful for the stable chromosomal incorporation of plasmids and phages (Kieser *et al.* 2000). The integration of vectors carrying the *attP* site into the *attB* site of streptomycete genomes has been well-studied (Combes *et al.* 2002). The *attB* site of *S. coelicolor* is 34 bp in length and although there is variation in the sequence of this site in other *Streptomyces* sp., a central TT pair surrounded by GC nucleotides is conserved (Combes *et al.* 2002). The *attB* site of *S. coelicolor* lies within an open-reading frame SCO3798 (StrepDB – *Streptomyces* annotation server (Bentley *et al.* 2002)). The *M. corallina* 454 contig database was searched using the nucleotide sequence of this open-reading frame as a BLASTN input. This analysis identified contig00075 (88% identity across 314 nucleotides). Within the aligned sequences a highly conserved region was noted which contained the consensus *attB* site of *S. coelicolor* (91% identity across 47 nucleotides; Figure 7.2A). PCR primers LF044F and LF044R were designed flanking the putative *attB* site in *M. corallina* and used to amplify a product of the expected 120 bp from *M. corallina* gDNA, indicating that this sequence is present in the genome and is not an artefact caused by the mis-assembly of the contigs in the 454 database (Figure 7.2B).

A

```
S.coel    CGGTGCGGGTGCCAGGGCGTGCCCTTGGGCTCCCCGGGCGCGTACTC
M.cora    CGGTGCGGGTGCCACGGCGTGCCCTTGGGCTCGCCCGGGGCGTACTC
          ********** ********** ** ** ********
```

B

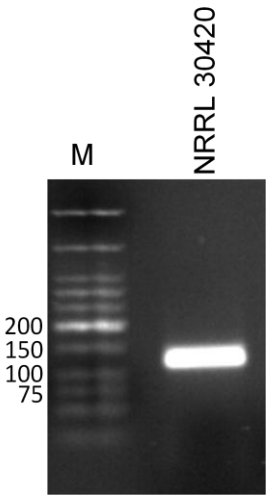

Figure 7.2 A An alignment of the *phi*C31 phage attachment site (*attB*) from *S. coelicolor* (*S. coel.*) (Combes, 2002) with the putative *attB* site from *M. corallina* NRRL 30420 (*M. cora*), identified through a homology search of the 454 contig database. The site of phage insertion (TT) is highlighted in bold. **B** A PCR carried out using the primers LF044F and LF044R with NRRL 30420 gDNA as a template. These primers were expected to amplify a 120 bp product across the putative ΦC31 *attB* site in the *M. corallina* genome. The PCR product was subjected to gel electrophoresis on a 2% TBE agarose gel. The marker (M) is the low Mw marker (NEB) and sizes are shown on the left of the gel image in bp.

7.2.3 Generation and Transformation of *M. corallina* protoplasts

The groups of Flavia Marinelli (Università dell'Insubria, Varese, Italy) and Fabrizio Beltrametti (Actygea, Gerenzano, Italy) had shown that protoplasts can be made and regenerated from a number of rare actinomycetes, including members of the *Streptosporangiaceae* family, such as *M. corallina* NRRL 30420, although transformation had not been attempted (Marcone *et al.* 2010b). In collaboration with these groups, protoplasts were generated from the three available strains of *M. corallina* and transformation attempted with pSET152 isolated from either a strain of methylating *E. coli* (DH5α) or a non-methylating strain (ET12567 pUZ8002); attempted transformation in the absence of DNA was used to assess the efficacy of selection and as a control for spontaneous resistant mutants. Plates were overlaid with a soft agar medium containing apramycin at a final concentration of 50 µg/ml. After 3 weeks growth at 30°C colonies were visible on plates of DSM 44682 and NRRL 30420 transformed with non-methylated pSET152 (Figure 7.3A). There were no colonies on plates transformed with methylated DNA or with the no DNA control, suggesting that the colonies were not spontaneous resistant mutants and that *M. corallina* likely possesses a methylation-specific restriction system, as is the case for many actinomycete species (MacNeil 1988; Kieser *et al.* 2000).

Putative transformants were streaked onto agar containing 50 µg/ml apramycin and transformation with pSET152 confirmed by colony PCR using primers amplifying a 319 bp region from the multiple cloning region of pSET152. A product of the expected size was observed in most of the transformant clones but not from wild type genomic DNA samples of the parent strains (Figure 7.3B). The identity of transformants of each strain was confirmed by colony PCR using primers which amplified a region of the *mibA* open-reading frame from genomic DNA of NRRL 30420 transformants, but not from that of DSM 44682 transformants; the latter strain is not thought to contain the microbisporicin gene cluster (chapter 3). Clones of the microbisporicin producer strain NRRL 30420 containing pSET152 retained bioactivity and microbisporicin was detected by MALDI-ToF analysis.

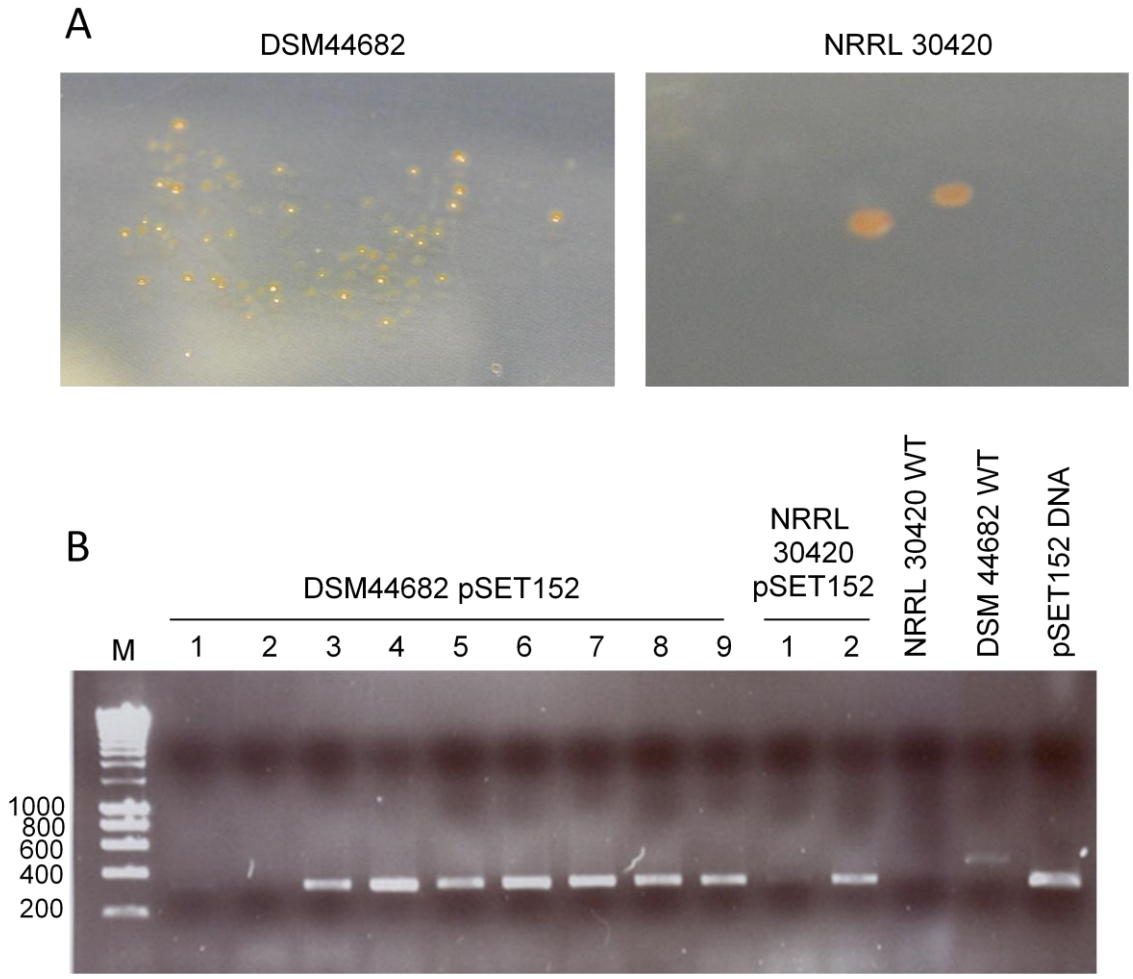

Figure 7.3

A Images of *M. corallina* DSM 44682 and NRRL 30420 clones originating from regenerated protoplasts transformed with pSET152 DNA.

B A colony PCR carried out using the primers pSET152F and pSET152R with clones of DSM 44682 pSET152 and NRRL 30420 pSET152. NRRL 30420 and DSM 44682 gDNA and pSET152 plasmid DNA were used as controls. These primers were expected to amplify a 319 bp product across the MCS in pSET152 The PCR product was separated by gel electrophoresis on a 1% TBE agarose gel. The marker (M) is hyperladder (Bioline) and sizes are shown on the left of the gel image in bp.

Since pSET152 could be introduced into these strains by transformation, and is an integrating and not freely replicating plasmid, *M. corallina* must contain a functional ΦC31 *attB* attachment site. To determine whether this is the same site as that identified in the 454 sequencing data, primers were designed to allow amplification across the boundaries of integration between the assumed ΦC31 *attB* site in the *M. corallina* genome and the *attP* site in pSET152 (Figure 7.4A). Primers LF045F and LF045R flank the *attP* site in pSET152, and primers LF044F and LF044R flank the putative *M. corallina attB* site. Integration of pSET152 into the putative *M. corallina attB* site would allow amplification of PCR products of 118 bp and 94 bp size using primer pairs LF044F and LF045R, and LF045F and LF044R, respectively (Figure 7.4A). Such amplification products were observed when gDNA from NRRL 30420 pSET152 was used as template, but not when wild type gDNA was used (Figure 7.4B). Thus the identified *attB* site is at least one site at which pSET152 can integrate in *M. corallina* (although there could be additional sites not detectable with this method). This indicates that vectors integrating at the ΦC31 attachment site are suitable for use in *M. corallina*.

Although the initial protoplast transformations with pSET152 were successful, further attempts at protoplast generation and transformation with other vectors, including cosmid transformation mediated by homologous recombination, were unsuccessful. Furthermore, protoplast generation and transformation had been extremely slow and inefficient (only two clones from NRRL 30420) suggesting that transformation with constructs significantly larger than pSET152 (approximately 7 kb) would be difficult (Kieser *et al.* 2000). For these reasons, an alternative method for introducing DNA into *M. corallina* was investigated.

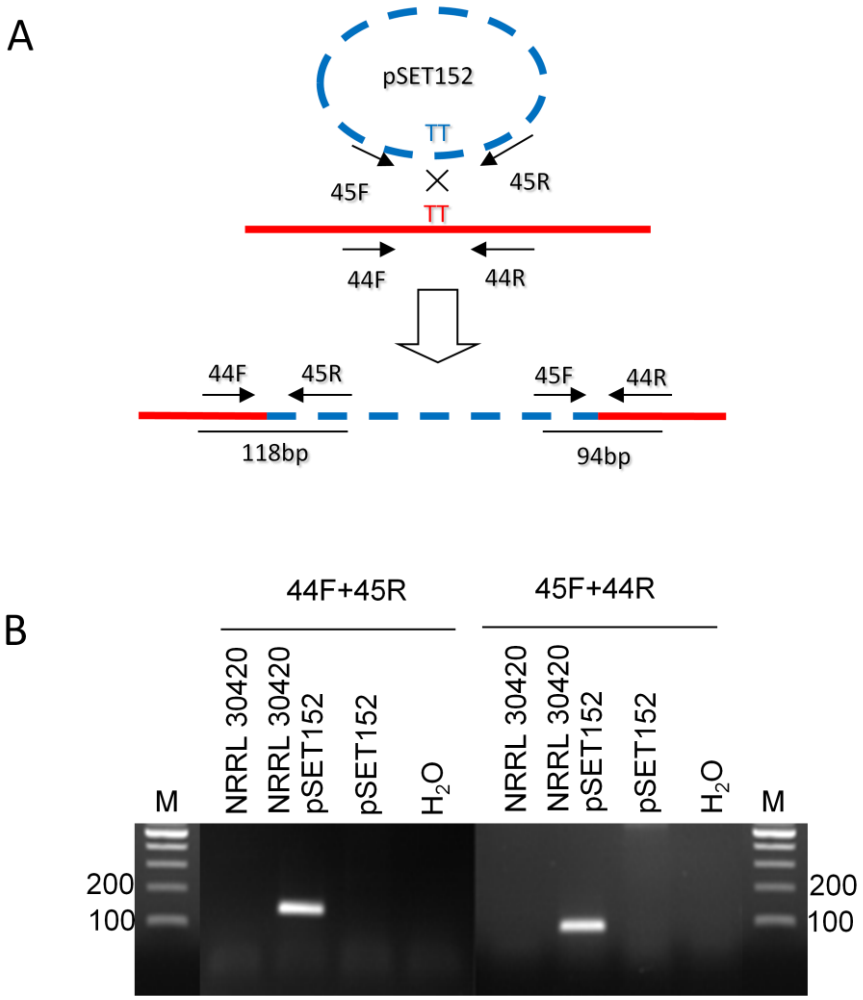

Figure 7.4 A A schematic showing the proposed mechanism of insertion of the integrating plasmid pSET152 (hatched blue line) in the putative *attB* site of *M. corallina* NRRL 30420 (red line). The approximate binding sites of primers LF044F (44F) and LF044R (44R), which were designed to flank the putative *attB* site from *M. corallina* NRRL 30420, and of LF045F (45F) and LF045R (45R), which were designed to flank the putative *attB* site from pSET152, are shown as labelled black arrows. The white arrow represents the integration event with the lower figure indicating the proposed resulting integration in the *M. corallina* NRRL 30420 genome. Sizes (in bp) given represent the expected PCR products from these primer pairs. **B** A PCR analysis of genomic DNA from a clone of *M. corallina* NRRL 30420 after integration of pSET152 compared to *M. corallina* NRRL 30420 wild type genomic DNA, pSET152 plasmid DNA and H_2O. The primer pairs used in each case are shown above. The marker (M) was the 100 bp ladder (NEB). Sizes are shown on the left of each gel.

7.2.4 Conjugation from *E. coli* ET12567/pUZ8002

Conjugation of vectors from *E. coli* ET12567/pUZ8002 is now the routine method used to introduce DNA into *Streptomyces* (Flett *et al.* 1997; Kieser *et al.* 2000). *E. coli* ET12567/pUZ8002 is a Dam-methylase deficient host that allows the transfer of unmethylated DNA into *Streptomyces* (Flett *et al.* 1997). Methylated DNA could not be used to transform *M. corallina* protoplasts (7.2.3) suggesting that, like *Streptomyces*, *M. corallina* possesses a methylation-selective restriction system (MacNeil 1988). *E. coli* ET12567/pUZ8002 is therefore an appropriate strain to use for conjugation with *M. corallina*. For *E. coli-Streptomyces* conjugations, freshly germinating spores are routinely used as a recipient host. This ensures that the conjugation event occurs when only one or a few mycelial compartments are present in the recipient and helps to promote clonally pure ex-conjugants (as discussed in chapter 6). For non-sporulating mutants of *Streptomyces* (such as the bald mutants), a method of conjugation from *E. coli* into mycelium was developed (Kieser *et al.* 2000). This method of conjugation was adapted for use in *M. corallina* and *Nonomuraea* (as discussed in chapter 6), two actinomycetes that sporulate inefficiently, if at all, under laboratory conditions.

M. corallina DSM 44682 grows well in liquid culture, giving more vigorous and dispersed growth than NRRL 30420. For this reason this strain was used to develop a method of conjugation between *E. coli* and *Microbispora* mycelium. Initially mycelial fragments were collected at mid to late exponential phase (after 48 h of growth) and washed in glycerol before being mixed with *E. coli* ET12567/pUZ8002 carrying pSET152 (Kieser *et al.* 2000). The appropriate growth medium for ex-conjugants of *Microbispora* was not known, but the addition of 10 mM $MgCl_2$ into growth media was known to promote conjugation between *Streptomyces* and *E. coli* (Kieser *et al.* 2000). SFM is used routinely for the growth of *Streptomyces* ex-conjugants but may not have been a suitable growth medium for *M. corallina*. Consequently, initially both SFM and V0.1 agar media containing 10 mM $MgCl_2$ were tested. Conjugation mixtures were plated out on these media and incubated for 20 h at 30°C. Plates were then overlaid with 1 ml water containing antibiotics to give a final concentration of either 25 µg/ml nalidixic acid alone (to kill the *E. coli* donor) or 25 µg/ml nalidixic acid and 50 µg/ml apramycin (to select for transconjugants). Single colonies were visible on V0.1 plus 10 mM $MgCl_2$ after approximately 10-14 days growth at 30°C in the presence of 50 µg/ml apramycin and 25 µg/ml nalidixic acid (Figure 7.5). Plates overlaid with nalidixic acid only gave lawns of *M. corallina* (Figure 7.5). No colonies were visible on SFM containing $MgCl_2$ in the presence of apramycin suggesting that this is not a suitable

medium for selection of *M. corallina* ex-conjugants (Figure 7.5). These results were found to be reproducible in a further experiment; furthermore, when *E. coli* ET12567/pUZ8002 lacking a conjugative plasmid was used in the mating, no apramycin resistant colonies were observed after 21 days of incubation (Figure 7.5). This suggests that the colonies identified from conjugation with *E. coli* carrying pSET152 were due to transfer of the plasmid (carrying the apramycin resistance marker) and not due to the spontaneous occurrence of apramycin resistant mutants. The DSM 44682 colonies obtained from the conjugation with *E. coli* ET12567/ pUZ8002 pSET152 were subsequently shown to contain pSET152. PCR using genomic DNA isolated from four of these clones was carried out and a band was amplified from the multiple cloning site of pSET152 (Figure 7.6). These initial experiments indicated that it was possible to transfer a small, integrating plasmid from the donor *E. coli* strain ET12567/pUZ8002 into *M. corallina* DSM 44682. Furthermore this method was more efficient and reliable than protoplast transformation, and was much more straightforward and rapid.

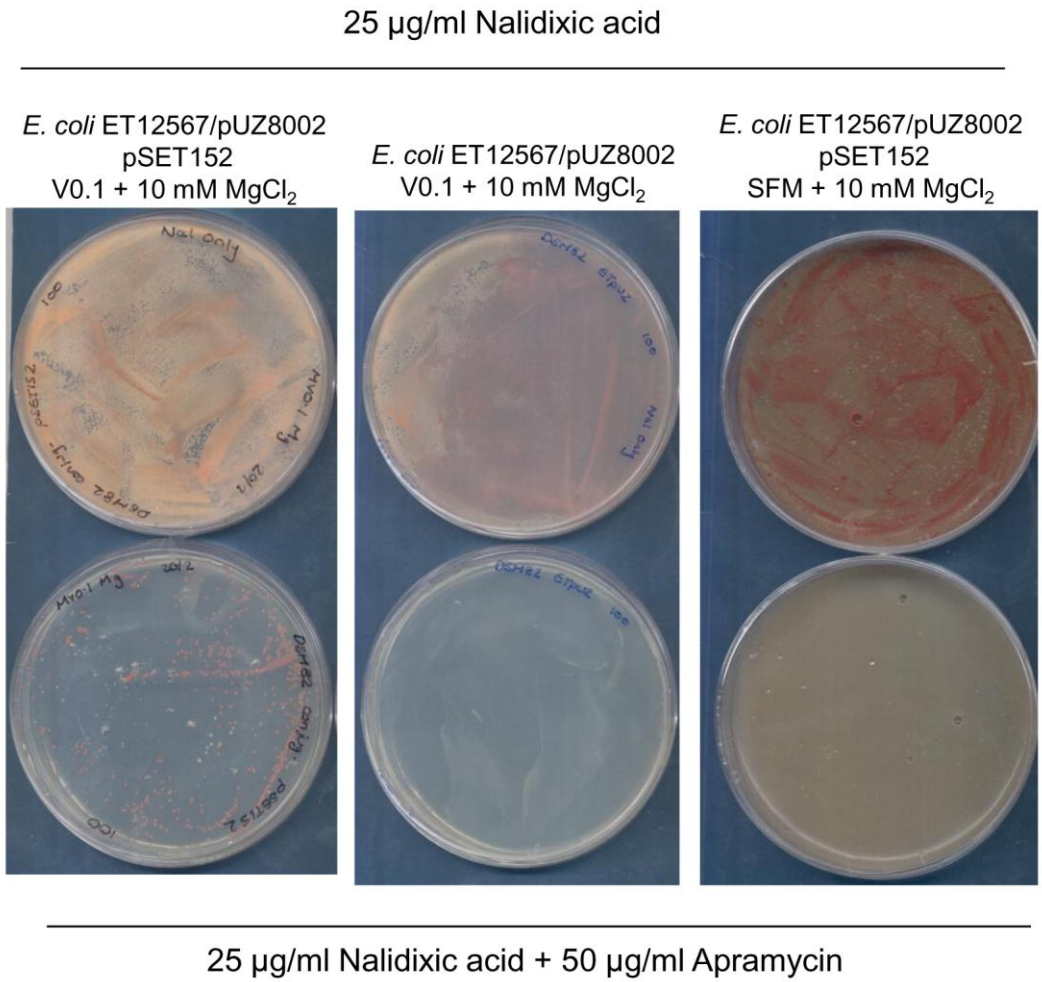

Figure 7.5 The outcome of conjugations between *E. coli* ET12567/pUZ8002 strains and *M. corallina* DSM 44682. The indicated *E. coli* strain was mixed with mycelial fragments of DSM 44682 and 100 µl plated on the solid growth medium shown. Plates were incubated for 20 h at 30°C. Plates were then overlaid with 1 ml water containing antibiotics to give a final concentration of either 25 µg/ml nalidixic acid alone (top row) or 25 µg/ml nalidixic acid and 50 µg/ml apramycin (bottom row). Plates were incubated at 30°C for 21 days before these images were taken.

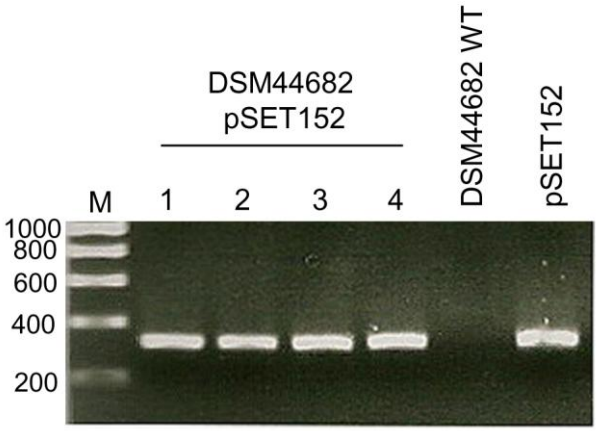

Figure 7.6 Agarose gel electrophoresis analysis of PCR carried out using the primers pSET152F and pSET152R. Templates were genomic DNA isolated from four putative clones of DSM 44682 pSET152 derived from conjugation with *E. coli* ET12567/pUZ8002 pSET152, DSM 44682 wild type and pSET152 plasmid DNA. The expected size of the band amplified across the MCS of pSET152 by these primers is 319 bp. The marker (M) was hyperladder (Bioline). Sizes are shown on the left of the gel.

Conjugation from *E. coli* was next assessed for NRRL 30420. By isolating mycelial fragments from a well-dispersed culture at mid-exponential growth, pSET152 could be successfully transferred from *E. coli* ET12567/pUZ8002 into NRRL 30420 yielding apramycin resistant clones. However in order to manipulate *M. corallina* it would be necessary to transfer larger vectors such as cosmids and to determine whether homologous recombination would occur at a high enough efficiency to allow gene replacement. To test this, pIJ12125 was manipulated in *E. coli* to replace the *mibA* gene with the apramycin resistance cassette from pIJ773 by λ RED recombination. This construct was mobilised into NRRL 30420 mycelial fragments by transfer from *E. coli* ET12567/pUZ8002. Plates were then overlaid with water containing antibiotics to give a final concentration of either 25 µg/ml nalidixic acid alone or 25 µg/ml nalidixic acid and 50 µg/ml apramycin. After approximately 3 weeks growth at 30°C, the plates overlaid with nalidixic acid only had a lawn of *M. corallina* but those also overlaid with apramycin had some single colonies. Seven of these colonies grew when streaked on V0.1 agar medium containing 50 µg/ml apramycin. Mycelium from the seven putative ex-conjugants was assessed by colony PCR using primers LF023F and LF023R2 that flank *mibA* in the NRRL 30420 genome. If the wild type gene had been replaced by the apramycin cassette a band shift would be expected for the amplified product from 545 bp to 1776 bp. This was

observed in four out of seven clones with two of the remaining clones amplifying both bands, suggesting that in the latter two only a single-crossover recombination event had occurred or that a mixed mycelial population was present (Figure 7.7A). These genotypes were further confirmed by testing the growth of the seven clones in the presence of 50µg/ml kanamycin. The kanamycin resistance marker lies on the backbone of pIJ12125 and will be present in the genome if pIJ12125 has been incorporated by single-crossover recombination. However if a double-crossover event has taken place (completely removing the wild type copy of *mibA*) the kanamycin resistance marker would be lost. Clones 1, 2 and 4 were susceptible to 50 µg/ml kanamycin suggesting that these clones had resulted from a double-crossover recombination event, correlating with the PCR results (Figure 7.7B). The remaining clones showed some growth on kanamycin, generally corresponding to the PCR results e.g. clone 3 did not amplify a wild type band but showed some growth on kanamycin, whereas clones 5, 6 and 7 clearly amplified wild type bands and grew well on kanamycin (Figure 7.7B). Growth of the remaining clones on kanamycin indicated that they had resulted from homologous recombination of pIJ12125 into the chromosome by a single-crossover and not from spontaneous mutation to apramycin resistance. Finally all seven clones were tested for their ability to produce microbisporicin by growing on V0.1 agar medium for 11 days and overlaying plates with *M. luteus* in SNA. Like the wild type control, clones 3, 5 and 7 (the plate on which clone 6 grew was contaminated) produced a bioactive compound that inhibited the growth of *M. luteus* (the wild type in fact clearing the entire plate). The levels of bioactivity from these clones reflected the results of the PCR and kanamycin resistance studies. Clones 1, 2 and 4 by contrast produced no bioactive compounds (Figure 7.7C). The replacement of *mibA* with the apramycin resistance cassette in these clones abolished bioactivity.

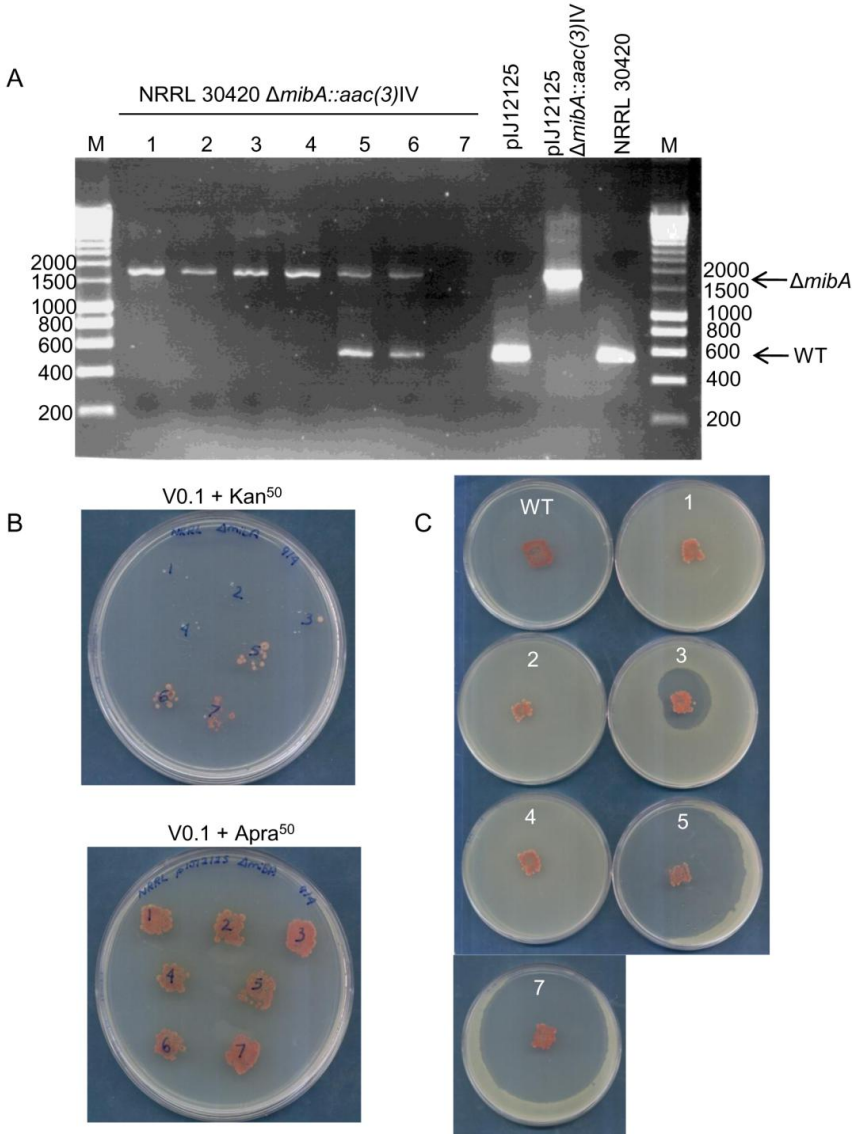

Figure 7.7 NRRL 30420 Δ*mibA*::*aac(3)*IV generated by the transfer of pIJ12125 Δ*mibA*::*aac(3)*IV from *E. coli* ET12567/pUZ8002. **A** Colony PCR using primers LF023F and LF023R2 that flank *mibA* in the NRRL 30420 genome. Mycelium from the seven clones of NRRL 30420 Δ*mibA*::*aac(3)*IV was used as a source of DNA template and pIJ12125, pIJ12125 Δ*mibA*::*aac(3)*IV and NRRL 30420 wild type gDNA were used as controls. The marker (M) was hyperladder (Bioline). Sizes are shown on the side of the gel. The PCR products amplified from wild type *mibA* (WT) and from Δ*mibA*::*aac(3)*IV (Δ*mibA*) should be 545 bp and 1776 bp, respectively (indicated by arrows on the right of the gel image). **B** The growth of NRRL 30420 Δ*mibA*::*aac(3)*IV clones on V0.1 containing 50 µg/ml kanamycin or 50 µg/ml apramycin. **C** Bioactivity from wild type NRRL 30420 (WT) and NRRL 30420 Δ*mibA*::*aac(3)*IV clones against *M. luteus*. *M. corallina* was grown for 11 d at 30°C on V0.1 and overlaid with *M. luteus* in SNA. Plates were incubated overnight at 30°C.

7.3 Gene Inactivation Mutants in *M. corallina*.

7.3.1 *mibA*

The three NRRL 30420 Δ*mibA*::*aac(3)*IV clones were analysed further by Southern blot hybridisation analysis using the wild type cosmid as a probe. Each of the three clones exhibited the band shift expected for deletion of *mibA* and no additional deletions or rearrangements were observed (Figure 7.8).

The NRRL 30420 Δ*mibA*::*aac(3)*IV clones along with the wild type strain were grown in VSPA liquid medium for 7 days. Supernatants were then tested for bioactivity against *M. luteus* (Figure 7.9). Unlike supernatant from wild type NRRL 30420, supernatants from the clones in which *mibA* had been inactivated showed no inhibitory activity against *M. luteus*. Supernatants were further investigated by MALDI-ToF mass spectrometry (Figure 7.10). In the wild type sample, ions were identified corresponding to the known variants of microbisporicin and the GPA-variants but no such ions were apparent in the spectra of supernatants from the three Δ*mibA* clones (Table 7.1). Along with heterologous expression in *Nonomuraea*, this provides further evidence that the *mib* cluster is responsible for the formation of compounds with these masses. It also confirms that the observed GPA-variants are likely to be an alternative form of microbisporicin. The *mibA* gene is essential for the production of bioactive compound and ions associated with microbisporicin variants. In combination with the amino acid sequence encoded by *mibA*, this indicates that MibA is extremely likely to be the prepropeptide for microbisporicin.

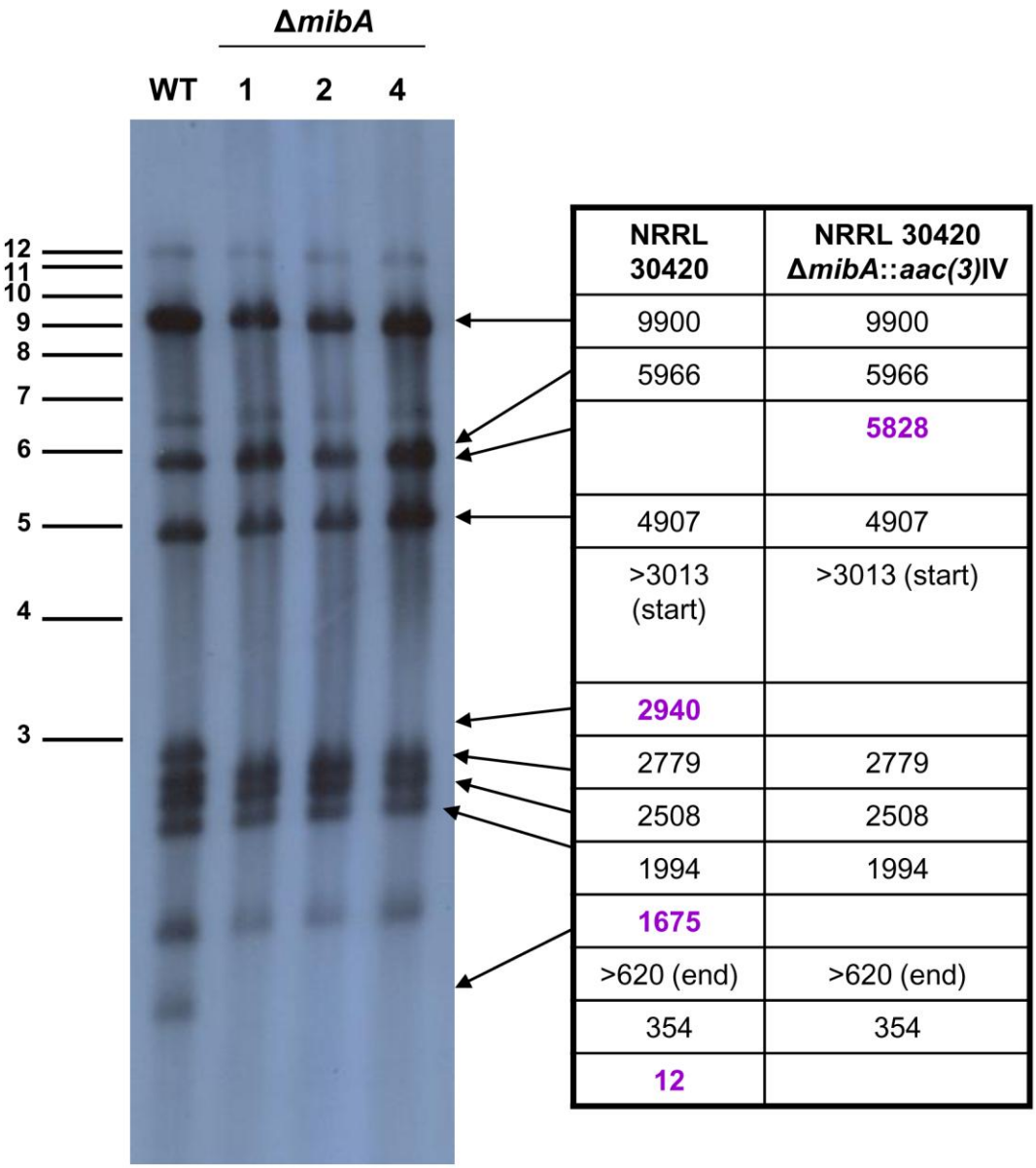

NRRL 30420	NRRL 30420 Δ*mibA*::*aac(3)*IV
9900	9900
5966	5966
	5828
4907	4907
>3013 (start)	>3013 (start)
2940	
2779	2779
2508	2508
1994	1994
1675	
>620 (end)	>620 (end)
354	354
12	

Figure 7.8 Southern blot hybridisation analysis of NRRL 30420 Δ*mibA*::*aac(3)*IV clones 1, 2 and 4 compared to the wild type using DIG-labelled pIJ12125 as a probe. Genomic DNA isolated from the wild type and the three clones was digested with *Apa*LI and the resulting fragments separated on a 1% agarose gel by electrophoresis. DNA was transferred to a nylon membrane by Southern transfer and the blot probed with DIG-labelled pIJ12125. The molecular weights of the size markers (Invitrogen 1 kb ladder) are given on the right in kb. The expected *Apa*LI restriction fragments from the known sequence of the insert of pIJ12125 are given to the right for the wild type and Δ*mibA* strains. Replacement of *mibA* with the *aac(3)*IV cassette results in the loss of bands at 2940 bp and 1675 bp, and the appearance of a band at 5828 bp (highlighted in purple), as predicted from the sequence.

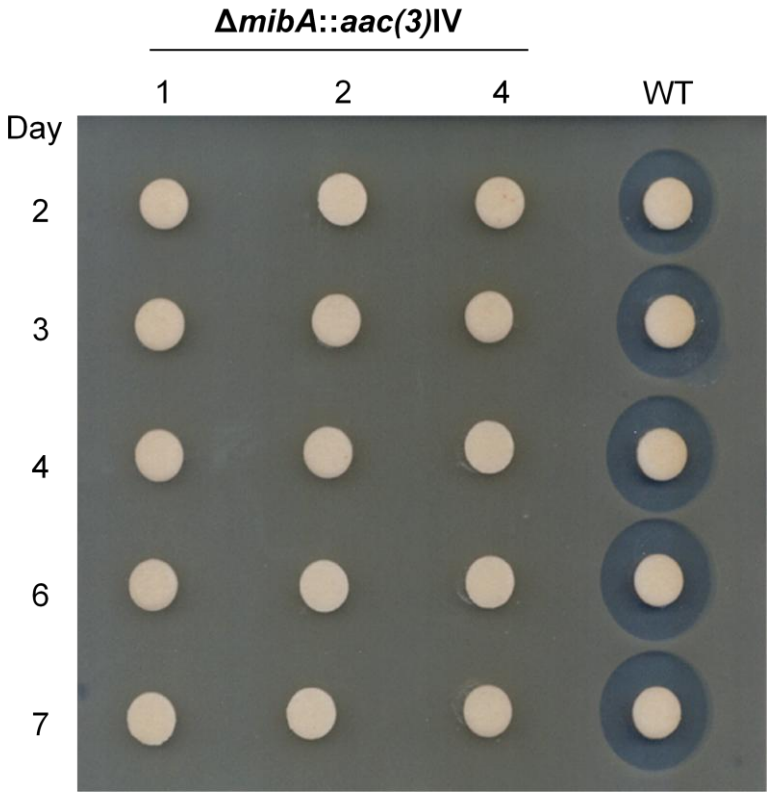

Figure 7.9 Bioassay of supernatants from NRRL 30420 wild type (WT) and Δ*mibA::aac(3)*IV mutants. Strains were grown in VSPA at 30°C and supernatant samples taken after 2, 3, 4, 6 and 7 days of fermentation. 40 µl supernatant was applied to each disc and discs placed on a lawn of *M. luteus*. The plate was incubated overnight at 30°C before zones of inhibition were visualised.

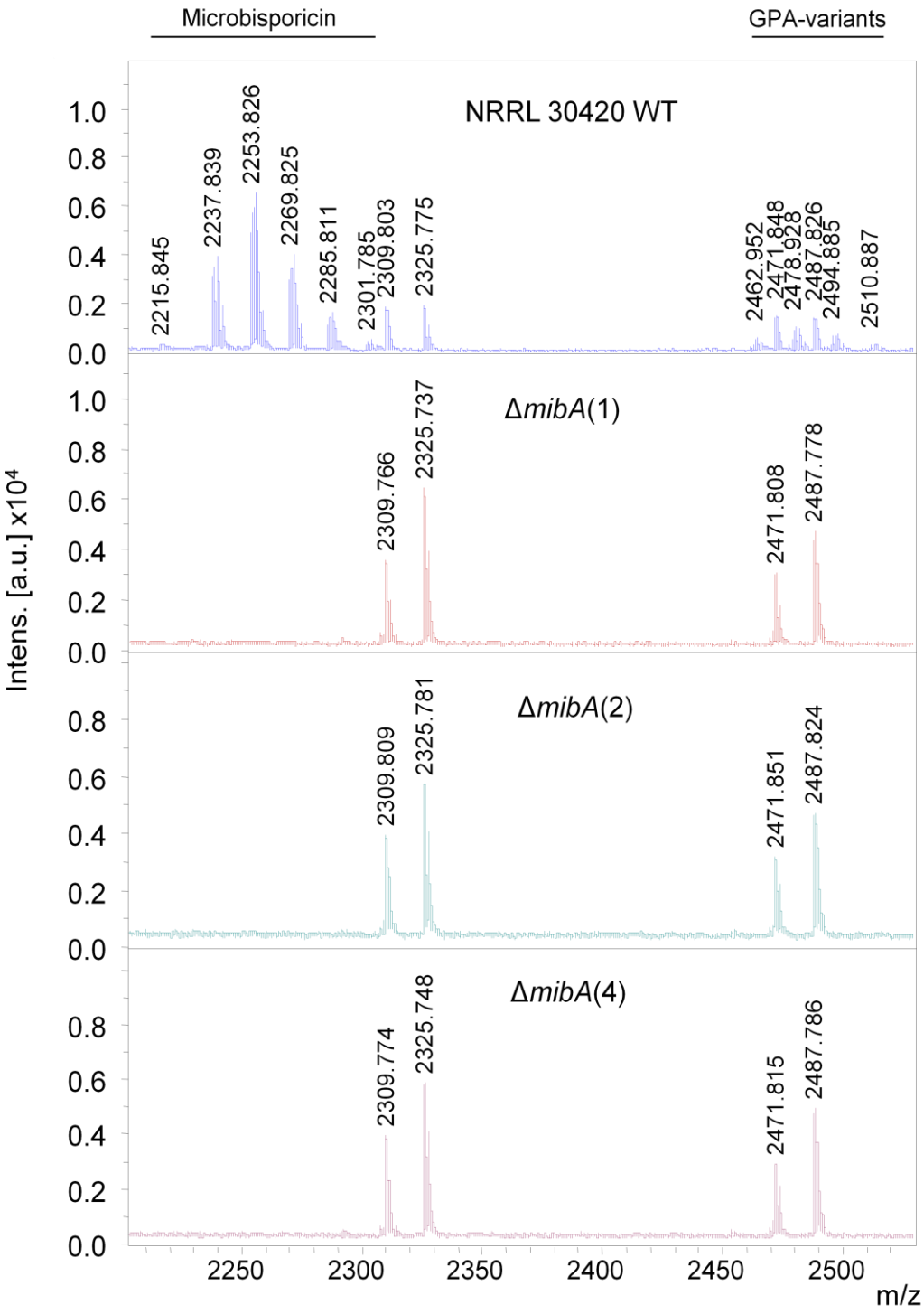

Figure 7.10 MALDI-ToF mass spectrum of supernatants from NRRL 30420 wild type (WT) and Δ*mibA::aac(3)*IV mutants. Strains were grown in VSPA at 30°C and a supernatant sample removed after 7 days of fermentation. The supernatants were subjected to MALDI-ToF analysis. m/z peaks at 2309.8, 2325.7, 2471.8 and 2487.8 correspond to medium components and serve as internal controls.

Table 7.1 Ions detected in supernatant samples from NRRL 30420 wild type and Δ*mibA* mutants (clones 1, 2 and 4) grown in VSPA for 7d. The possible identity of the compound generating a peak at that m/z value is given. Rows which relate to compounds which are likely variants of microbisporicin are highlighted in light purple and rows which relate to compounds which are likely variants of GPA-microbisporicin in light blue.

Possible Compound	NRRL 30420 WT	Δ*mibA*_1	Δ*mibA*_2	Δ*mibA*_4
Media	2147.75	2147.72	2147.77	2147.73
Media	2163.73	2163.69	2163.73	2163.70
1768α_1 Na	2237.83			
107891 A2 Na	2253.81			
107891 A1 Na	2269.80			
107891 A1 Na + 1O	2285.79			
107891 A1 Na+ 2O	2301.78			
Media	2309.81	2309.77	2309.81	2309.77
107891 A1 Na+ 3O	2317.78			
Media	2325.78	2325.74	2325.78	2325.75
Media	2471.85	2471.81	2471.85	2471.82
107891 A2 GPA Na	2478.92			
Media	2487.83	2487.78	2487.82	2487.79
107891 A1 GPA Na	2494.90			
107891 A1 GPA Na +1O	2510.88			
107891 A1 GPA Na +2O	2526.89			
Media	2633.90	2633.85	2633.90	2633.85

Interestingly, NRRL 30420 Δ*mibA*::*aac(3)*IV grown on V0.1 agar medium appeared visually different than the wild type strain, often with a more “fluffy” surface suggesting the formation of more aerial mycelium. The two strains were then grown on OBM agar medium, which had previously promoted the formation of aerial mycelium and a few associated spores by the NRRL 30420 wild type strain (chapter 3). After 5 days growth at 30°C a glass cover slip was carefully placed on to the lawn of each strain, removed and visualised by phase contrast microscopy. While only mycelial fragments were observed with the wild type strain, inspection of the Δ*mibA* mutant revealed, in addition, small spheres, often in pairs, either free or sometimes associated with the mycelium (Figure 7.11A). Using a cotton pad, free material on the surface of the two plates was collected in 20% glycerol and transferred to cryotubes. The material collected from the Δ*mibA* mutant was much more viscous and a very deep pink colour compared to that from the wild type (Figure 7.11A). 5 µl of the collected material was observed by phase contrast microscopy. Only a few refractive spherical objects were seen in the sample from the wild type strain, whereas in that from the Δ*mibA* mutant, these objects completely filled the microscopic field. These objects are likely to be spores.

To confirm that the Δ*mibA* mutant produced spores much more efficiently than the wild type strain, both were grown on OBM agar for 21 d (to promote spore formation by the wild type strain) and single colonies and confluent areas of growth were observed by cryo-scanning electron microscopy (performed by Kim Findlay, JIC). On the wild type plate, some poorly formed spores were observed attached to aerial mycelium in confluent areas of growth but none could be identified on single colonies. Many of the spores appeared deflated or mis-shapen (Figure 7.11B). On the Δ*mibA* mutant plate, while some spores could be observed on single colonies, many were present in confluent areas where they were attached to aerial mycelium, most often in pairs. The spores appeared to be well-formed and were reminiscent of those observed for DSM 44681 and DSM 44682 (chapter 3). The long incubation time resulted in the germination of some of the Δ*mibA* spores on top of the aerial mycelium; this was not seen in the wild type strain. This indicates that the Δ*mibA* spores, at least, are viable. Thus the Δ*mibA* mutant of NRRL 30420 appears to sporulate more efficiently than the wild type strain, both in terms of spore number and quality.

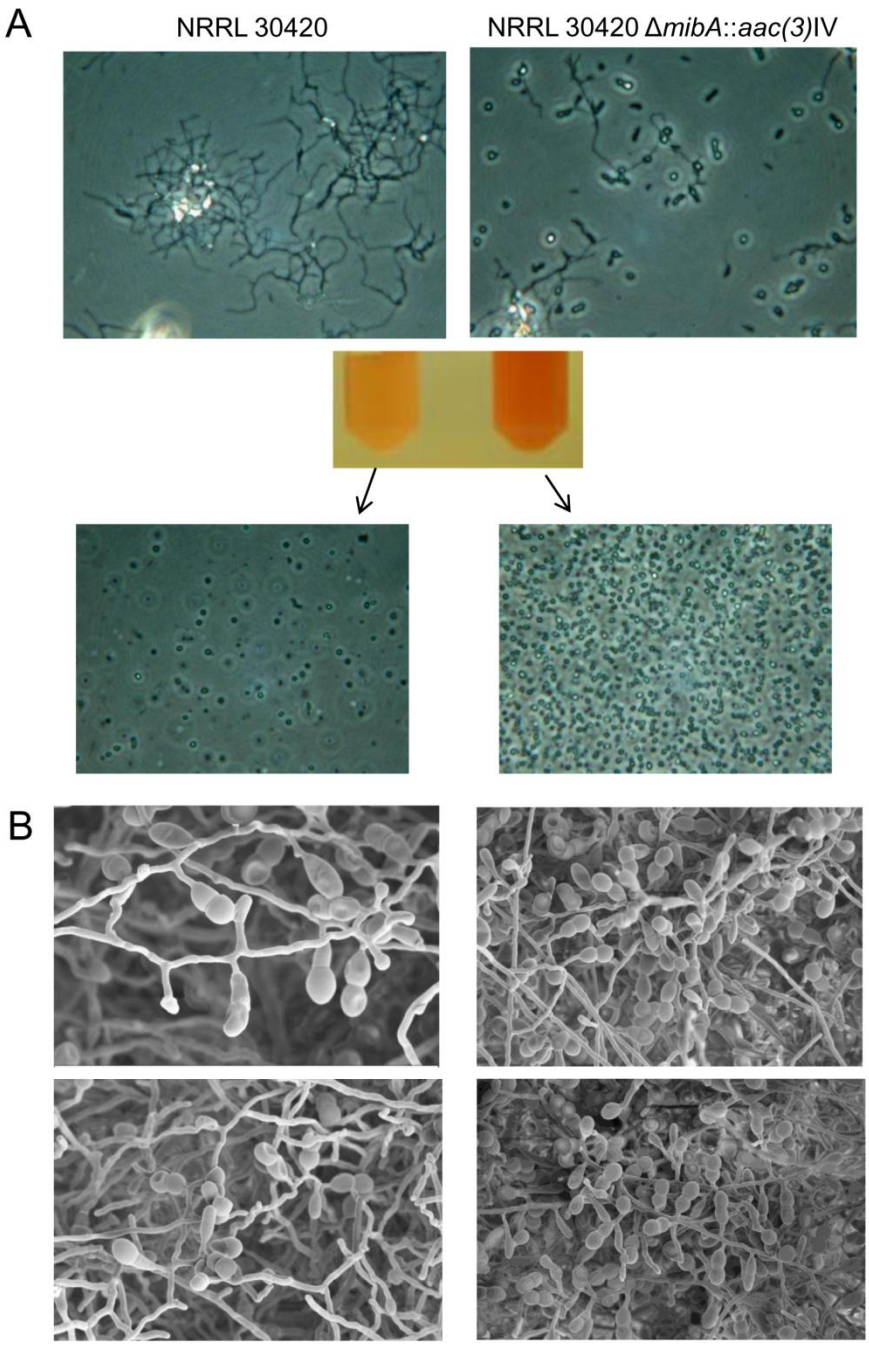

Figure 7.11 NRRL 30420 wild type and NRRL 30420 Δ*mibA* exhibit different sporulation phenotypes. **A** NRRL 30420 wild type and Δ*mibA* (clone 1) were grown on OBM for 5 d and loose surface material collected and visualised on a glass cover slip (top panel). Loose material from the plates was collected in cryotubes (middle image) and 5 µl observed by phase contrast microscopy (lower panel). **B** NRRL 30420 wild type (left-hand images) and Δ*mibA* (clone 1; right-hand images) were grown on OBM for 21 d and confluent areas of growth visualised by cryo-SEM.

7.3.2 Inactivation of other mib genes

Following the protocol described for the deletion of *mibA* from *M. corallina*, further deletion mutants were made in NRRL 30420. Due to the large number of open-reading frames in the *mib* gene cluster and the difficulties associated with working with *M. corallina*, only 10 further mutants were constructed. Furthermore due to the location of the *mib* cluster near one end of the pIJ12125 insert and the resulting lack of sufficient flanking sequence for efficient homologous recombination, (approximately 2-3 kb is required in *Streptomyces* (Kieser *et al.* 2000)) some genes could not be replaced using this cosmid. For this reason *mibJ* and *mibY* were not deleted. Genes encoding proteins for which functions could be quite confidently assigned, such as *mibB* and *mibC*, were not deleted. Unless stated, at least two independent clones for each mutant were studied for phenotypic changes. Mutants were confirmed initially by PCR analysis using primers that flanked the cassette insertion and primers lying internal to the deleted gene (to confirm that no wild type copies remained). Mutations were further confirmed in most cases by Southern blot analysis.

mibZ-mibR

MibZ, MibO, MibQ and MibR possess very low levels of similarity to proteins of known function and no homologs have been shown to be associated with lantibiotic biosynthesis. Consequently, it was necessary to delete *mibZOQR* to determine whether these genes were essential for microbisporicin production. This would also help to define the minimum gene set required for microbisporicin biosynthesis and to more clearly define the boundaries of the *mib* cluster. *mibZ* to *mibR* (about 3.6 kb) were replaced in pIJ12125 by the apramycin cassette leaving the stop codon of *mibY* intact. This left approximately 3 kb of flanking homologous sequence at the left hand end of the cosmid insert for double-crossover recombination. This construct was mobilised into NRRL 30420 by conjugation from *E. coli* ET12567/pUZ8002 yielding three independent apramycin resistant clones. Despite numerous attempts to identify double-crossover recombinants, no kanamycin sensitive colonies were obtained. This suggests that, unlike *Streptomyces*, 3 kb of flanking homologous sequence is not sufficient for gene replacement in *M. corallina*.

pIJ12126 (originally cosmid 7C22) was not fully sequenced but through end-sequencing and restriction digest mapping was thought to possess at least 4-5 kb more sequence upstream of *orf1* than pIJ12125. The end-sequence of the insert was extended using primer LF041F2, the sequence from which matched a large contig from the 454 database. This was used to extend the end-sequence by approximately 1500 nucleotides. This sequence was found to encode part of a xylosidase/arabinosidase homolog sharing 50-60% amino acid sequence identity with a protein from *Mycobacterium smegmatis*. This

extended end-sequence from the insert of pIJ12126 was used to design a primer that could be linked by long-range PCR to a primer in the 5' end of the insert of pIJ12125, generating an approximately 5 kb product from both pIJ12126 DNA and NRRL 30420 gDNA (Figure 7.12). The product amplified from gDNA was end-sequenced to confirm that it did indeed link these two sequences and was not a non-specific PCR product. These sequences are therefore contiguous in the genome of *M. corallina*. pIJ12126 therefore provided a much larger region of homology for the second recombination event than pIJ12125. The end-sequence of the insert of pIJ12126 (up to the 5' end of the pIJ12125 insert) was largely determined (using primers LF041F3, LF041F4, LF041R and LF041R2) through repeated PCR and sequence reactions, although due to the presence of sequence gaps it was not fully assembled.

pIJ12126 with the apramycin cassette replacing *mibZ-mibR* was mobilised into NRRL 30420 by conjugation. This transfer appeared to be somewhat less efficient than that of pIJ12125 and several conjugation attempts were made before nine putative mutant clones were identified. After three rounds of growth as single colonies on 50 µg/ml apramycin, 11 colonies of each mutant were tested for growth on 50 µg/ml kanamycin. Two clones were identified (10 and 12) that gave rise to single colonies (two from each clone were taken forward) that were sensitive to kanamycin. These clones were confirmed by PCR as double-crossover recombinants in which *mibZ-mibR* had been replaced by the apramycin cassette. The two clones (two single colonies from each) were grown in VSPA for 7 days along with the wild type strain. Unlike the wild type control, supernatants from the mutant strains did not generate a zone of inhibition in a lawn of *M. luteus* (Figure 7.13). One or more of *mibZ-mibR* thus appear to be essential for microbisporicin biosynthesis.

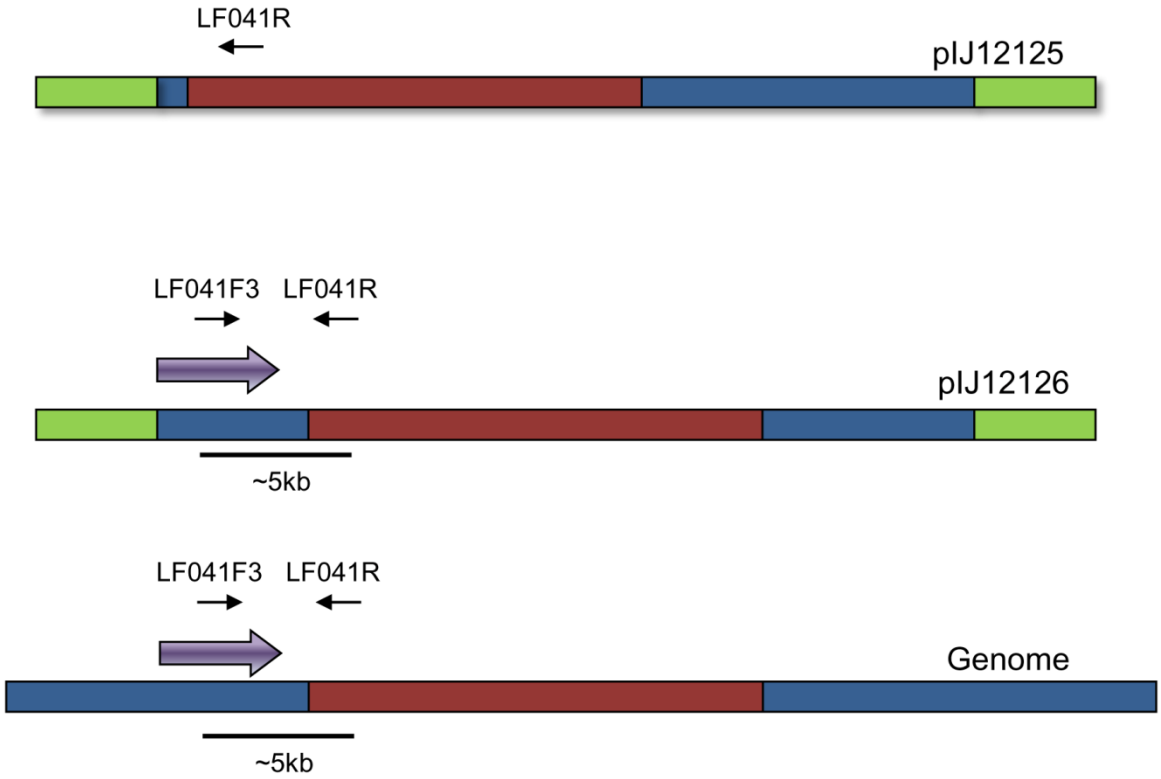

Figure 7.12 Further analysis of the insert of pIJ12126 (7C22). The cosmids pIJ12125 and pIJ12126 are represented along with the likely arrangement of the corresponding region of the *M. corallina* genome. The red boxes represent the defined *mib* gene cluster and blue boxes other flanking sequences. Green boxes represent the flanking Supercos1 vector sequences common to pIJ12125 and pIJ12126. A purple arrow represents a xylosidase/arabinosidase homolog (sharing 50-60% amino acid sequence identity with a protein from *Mycobacterium smegmatis*) identified by end-sequencing of the insert of pIJ12126. End-sequence from pIJ12126 and the complete insert sequence of pIJ12125 were used to design primers LF041F3 and LF041R, respectively. These primers could be linked by PCR when the template was pIJ12126 DNA or *M. corallina* NRRL 30420 gDNA, generating an approximately 5 kb product. This product was confirmed by end-sequencing to have originated from this region and was not a non-specific amplification product.

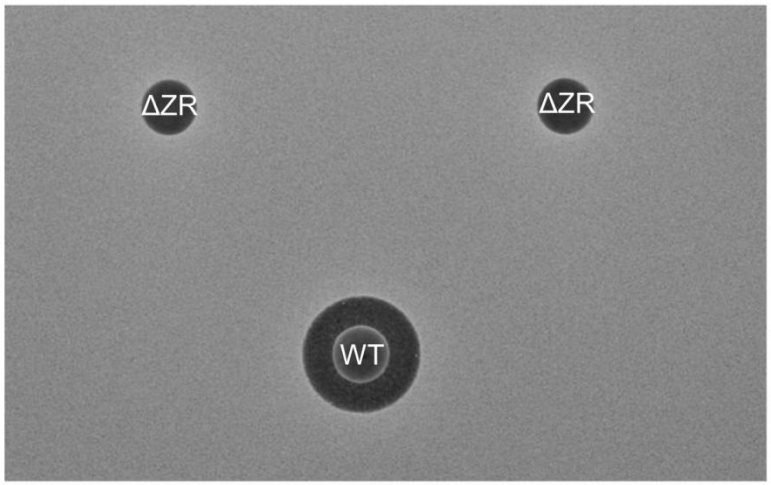

Figure 7.13 Bioassay of supernatants from NRRL 30420 wild type (WT) and Δ*mibZ-mibR::aac(3)*IV mutants (ΔZR; two clones). Strains were grown in VSPA at 30°C and supernatant samples taken after 7 days of fermentation. 40 µl supernatant was applied to each disc and discs placed on a lawn of *M. luteus*. The plate was incubated overnight at 30°C before zones of inhibition were visualised.

mibX

Deletion of *mibX,* encoding the ECF sigma factor, by double-crossover recombination was only identified in one clone and abolished activity against *M. luteus* (Figure 7.14). When analysed by mass spectrometry, the supernatant from a 7 day fermentation did not contain any peaks associated with microbisporicin (Figure 7.15). The putative ECF sigma factor appears to be essential for production of microbisporicin in *M. corallina*.

mibD

Deletion of *mibD* also abolished activity against *M. luteus* (Figure 7.14). When analysed by mass spectrometry, the supernatant from a 7 day fermentation again failed to show peaks corresponding to microbisporicin (Figure 7.15). *mibD* also appears to be essential for microbisporicin production.

mibTU

Deletion of *mibTU* had no significant effect on bioactivity (Figure 7.14), and when analysed by mass spectrometry the supernatant of a 7 day fermentation contained peaks associated with microbisporicin identical to those of the wild type strain (Figure 7.16). Only one clone of this particular mutant was isolated and characterised.

mibV

Deletion of *mibV* appeared to result in an increase in bioactivity against *M. luteus* compared to the wild type strain (Figure 7.14). When analysed by mass spectrometry, the supernatant from a 7 day culture of the *mibV* mutant contained peaks different from those in the wild type sample after the same length of fermentation (Figure 7.17). The ions detected in the supernatant of the *mibV* mutant were highly similar to those observed for the *mibH* mutant (described below). Unlike in the wild type strain, where variants appear to be based only on the chlorinated form of microbisporicin (see chapter 3), the *mibV* mutant appeared to produce only deschloromicrobisporicin. None of the ions associated with microbisporicin in the wild type strain were observed in the supernatant of the *mibV* mutant. Interestingly, the supernatant of the *mibV* mutant, but not the *mibH* mutant or the wild type strain, contained a number of compounds yielding m/z values lower than that of MF-BA-1768β_1 ([M+H$^+$]=2181.8 Da; peaks large enough to be annotated were 2122.8, 2138.8, 2129.8 and 2154/5/6.8 Da). Although seen at only low levels compared to the other peaks in the spectrum, these ions were observed reproducibly in supernatants from three independent clones of the *mibV* mutant. These m/z values could not be attributed to any specific species but since they are likely to be of lower mass than MF-BA-1768β_1 (the variant with the lowest mass described previously) they may represent degradation products of MF-BA-1768β_1.

Since *mibV* lies downstream from *mibTU,* a polar effect of the deletion of *mibTU* on *mibV* expression might have been expected. However, as described above, deletion of *mibTU* had no effect on bioactivity or on the MALDI-ToF spectra, suggesting lack of polarity.

mibEF

Deletion of *mibEF* resulted in an interesting phenotype. While supernatant from a 3-5 day culture failed to inhibit *M. luteus*, that from a 7 day fermentation gave a very small zone of inhibition (Figure 7.14). When analysed by mass spectrometry, the latter supernatant contained a few very small peaks associated with some microbisporicin variants (Figure 7.15). *mibEF* appear to be essential for wild type levels of microbisporicin biosynthesis, with deletion resulting in delayed and much reduced production.

mibH

Deletion of *mibH,* like *mibV,* appeared to result in an increase in bioactivity against *M. luteus* compared to the wild type strain (Figure 7.14). When analysed by mass spectrometry, supernatant from a 7 day culture of the *mibH* mutant contained peaks that were different from those in the wild type sample after the same length of fermentation (Figure 7.17). The spectrum of ions seen typically in supernatants from the wild type strain were described in chapter 3, and are believed to correspond to the chlorinated forms of microbisporicin. These ions were not observed in the supernatant from the *mibH* mutant. Instead a different spectrum of peaks was seen that can be attributed to compound BA-1768β_1 ([M+H$^+$] = 2181.88 Da) (Lee 2003) and its associated sodium/potassium adducts, oxidation products and GPA variants. These ions were never observed in wild type supernatant samples under the fermentation conditions used. BA-1768β_1 differs from BA-1768α_1 by 34/36 Da, which can be attributed to the lack of chlorination of tryptophan at position 4 (removal of a chlorine atom (35/37 Da) and addition of a proton (1 Da)). Thus only deschloromicrobisporicin and its derivatives were produced by the *mibH* mutant.

In addition to the mass difference of 34/36 Da, further evidence that the observed species are non-chlorinated forms of microbisporicin was obtained from the isotope distribution for peaks in the wild type sample and that of the *mibH* mutant. Due to the relative natural abundance of its two common isotopes, ^{35}Cl (75.77%) and ^{37}Cl (24.23%), chlorine provides a unique isotopic signature in mass spectrometry (Goodlett *et al.* 2000). Since chlorine is not normally found in proteins and peptides, this signature can be recognised in mass spectrometry and chlorine has been used as a molecular tag for protein identification (Goodlett *et al.* 2000). Using the theoretical molecular formulae for the microbisporicin compounds containing chlorine (such as MF-BA-1768α_1) the relative abundance of the first three isotopomers was predicted to be third>second>first (using Chemputer (University of Sheffield; http://winter.group.shef.ac.uk/chemputer/)). This was the observed isotope distribution of ions attributed to microbisporicin in wild type supernatants (Figure 7.18). When the isotope distribution was calculated for the predicted molecular formulae of MF-BA-1768β_1, which is not expected to contain chlorine (deschloromicrobisporicin), the isotope pattern shifted such that the relative abundance of the first three isotopomers was second>first>third. This predicted pattern was exactly that observed for the ions identified in the Δ*mibH* and Δ*mibV* mutants (Figure 7.18). This provides further evidence for the lack of incorporation of chlorine into compounds produced by the Δ*mibH* and Δ*mibV* mutants.

mibH is essential for production of the wild type spectrum of peaks attributed to microbisporicin, and is required for tryptophan chlorination. The compounds produced by the *mibH* mutant appear to be efficiently exported from the cell and show anti-bacterial activity against *M. luteus*. *mibH* and *mibV* mutants reproducibly exhibited higher than wild type levels of activity against *M. luteus* (Figure 7.14), suggesting that the non-chlorinated form of microbisporicin might be more active.

mibN

Deletion of *mibN* had no effect on bioactivity against *M. luteus* (Figure 7.14), and mass spectrometry of 7 day supernatants revealed a spectrum of peaks very similar to that of the wild type strain (Figure 7.16). The only notable difference was in the occurrence of sodium adducts. In the wild type supernatant, the majority of observed peaks were solely of microbisporicin in complex with sodium ions (2237.88, 2253.88, 2269.88, 2285.88, 2301.88) rather than the protonated species (2215.88, 2231.88, 2247.88, 2263.88, 2279.88). In contrast, in both clones of the *mibN* mutant, as well as sodium adduct peaks, a number of prominent peaks attributed to the protonated species were observed. *mibN* is not essential for production and export of microbisporicin in *M. corallina,* but for some reason its deletion alters the ratio of sodium:proton adducts in the supernatant.

Deletion of 7 kb downstream of the putative gene cluster

To confirm that the genes downstream from the defined *mib* cluster were not essential for microbisporicin biosynthesis, 7 kb of cosmid pIJ12125 lying downstream from *mibN* were replaced with the apramycin cassette. Deletion of this region had no effect on bioactivity against *M. luteus* (Figure 7.14), and mass spectrometry of the supernatant from a 7 day culture revealed a spectrum of peaks associated with microbisporicin that was identical to that found in the wild type strain (Figure 7.16). This segment of the genome does not appear to be involved in the production of microbisporicin.

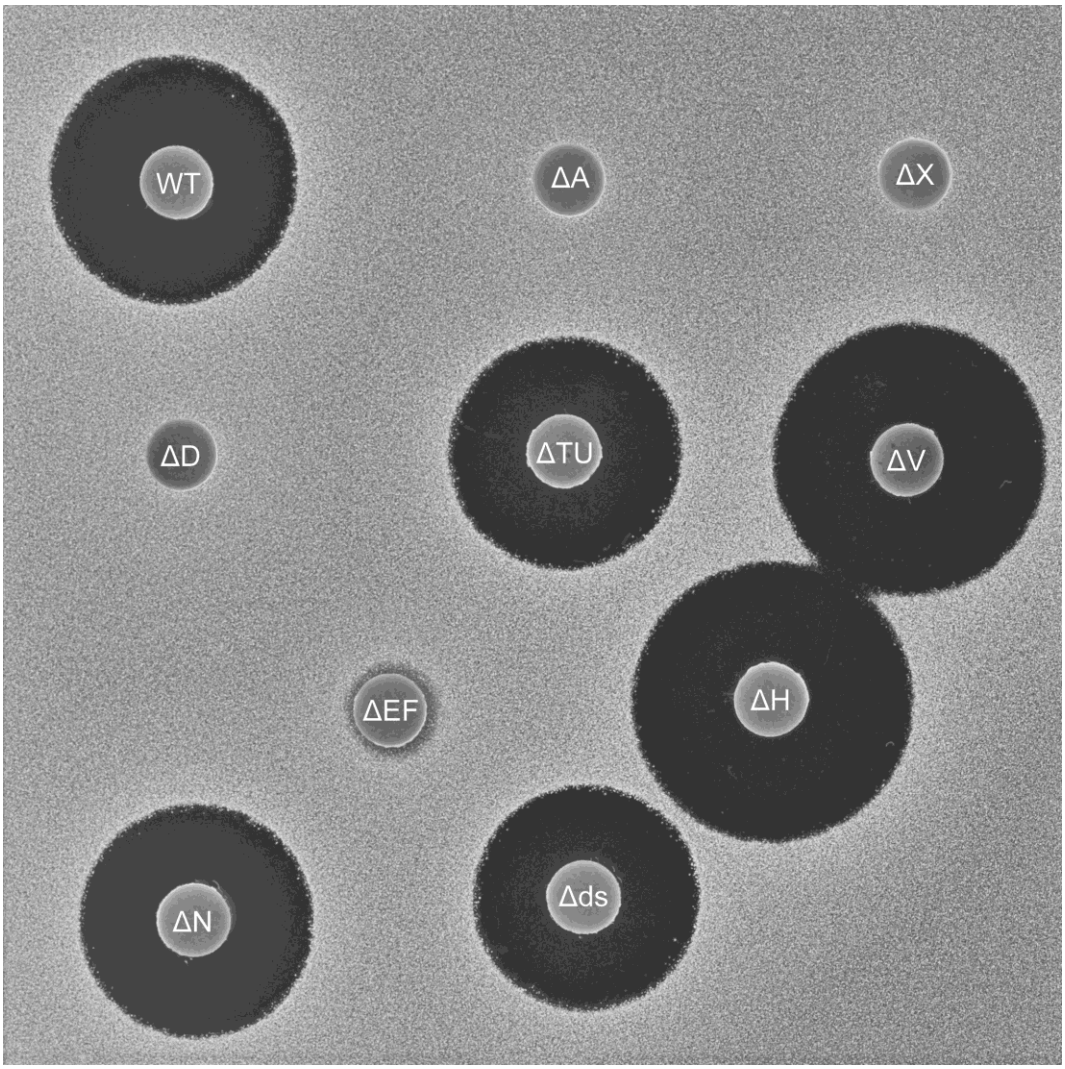

Figure 7.14 Analysis of bioactivity from deletion mutants of *M. corallina* NRRL30420. *M. corallina* NRRL 30420wild type (WT), Δ*mibA::aac(3)IV* (ΔA), Δ*mibX::aac(3)IV* (ΔX) Δ*mibD::aac(3)IV* (ΔD), Δ*mibTU::aac(3)IV* (ΔTU), Δ*mibV::aac(3)IV* (ΔV), Δ*mibEF::aac(3)IV* (ΔEF), Δ*mibH::aac(3)IV* (ΔH), Δ*mibN::aac(3)IV* (ΔN) and Δ*downstream::aac(3)IV* (Δds) were grown for 7 d in VSPA and culture supernatants assayed for bioactivity as in Figure 7.13.

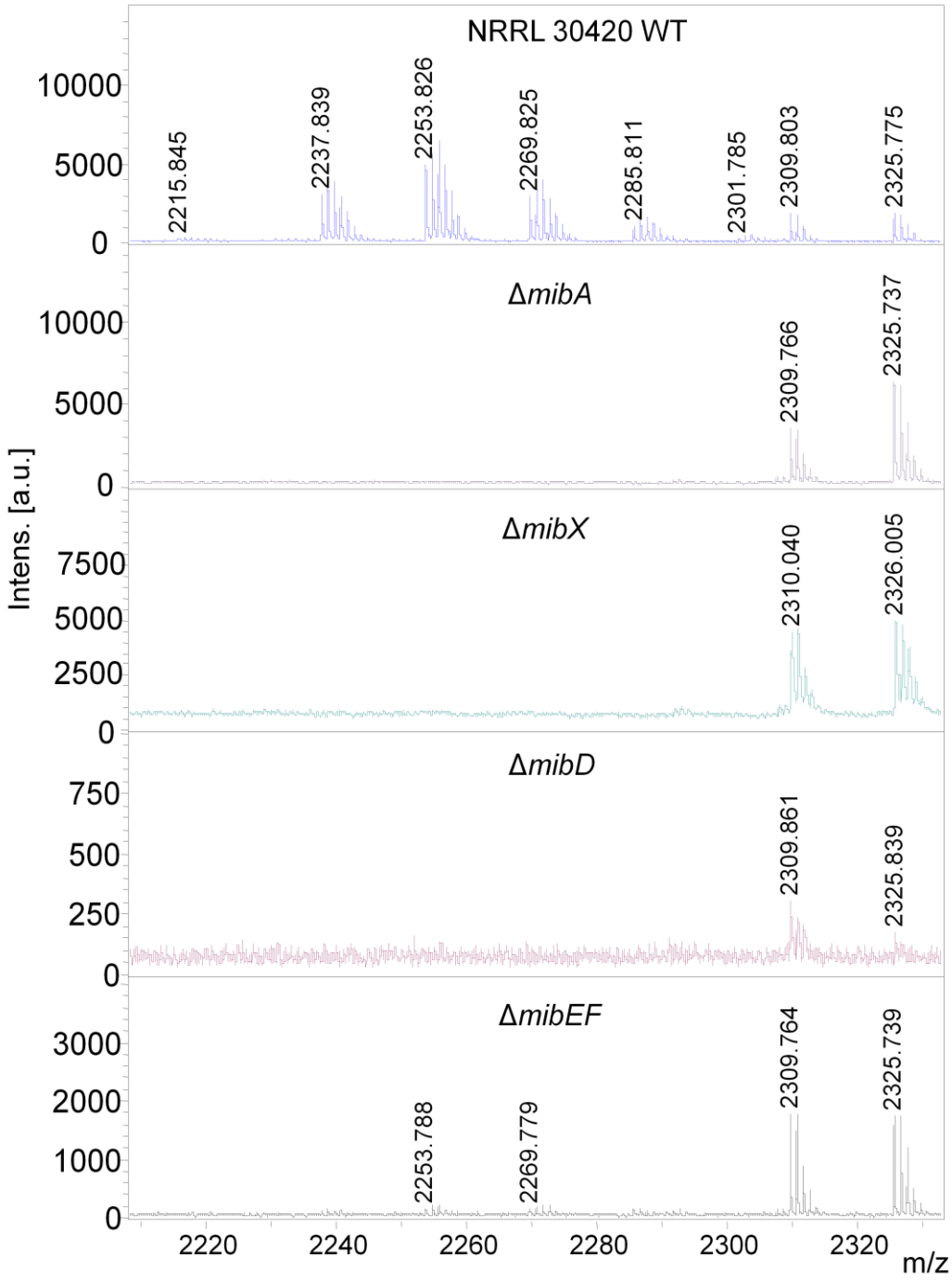

Figure 7.15 MALDI-ToF mass spectrometry of supernatants from NRRL 30420 wild type (WT) and representative clones of Δ*mibA::aac(3)*IV, Δ*mibX::aac(3)*IV, Δ*mibD::aac(3)*IV and Δ*mibEF::aac(3)*IV mutants. Strains were grown in VSPA at 30°C and a supernatant sample removed after 7 days of fermentation. The supernatants were subjected to MALDI-ToF analysis. Ions with m/z 2309.7 and 2325.7 correspond to medium components and serve as internal controls.

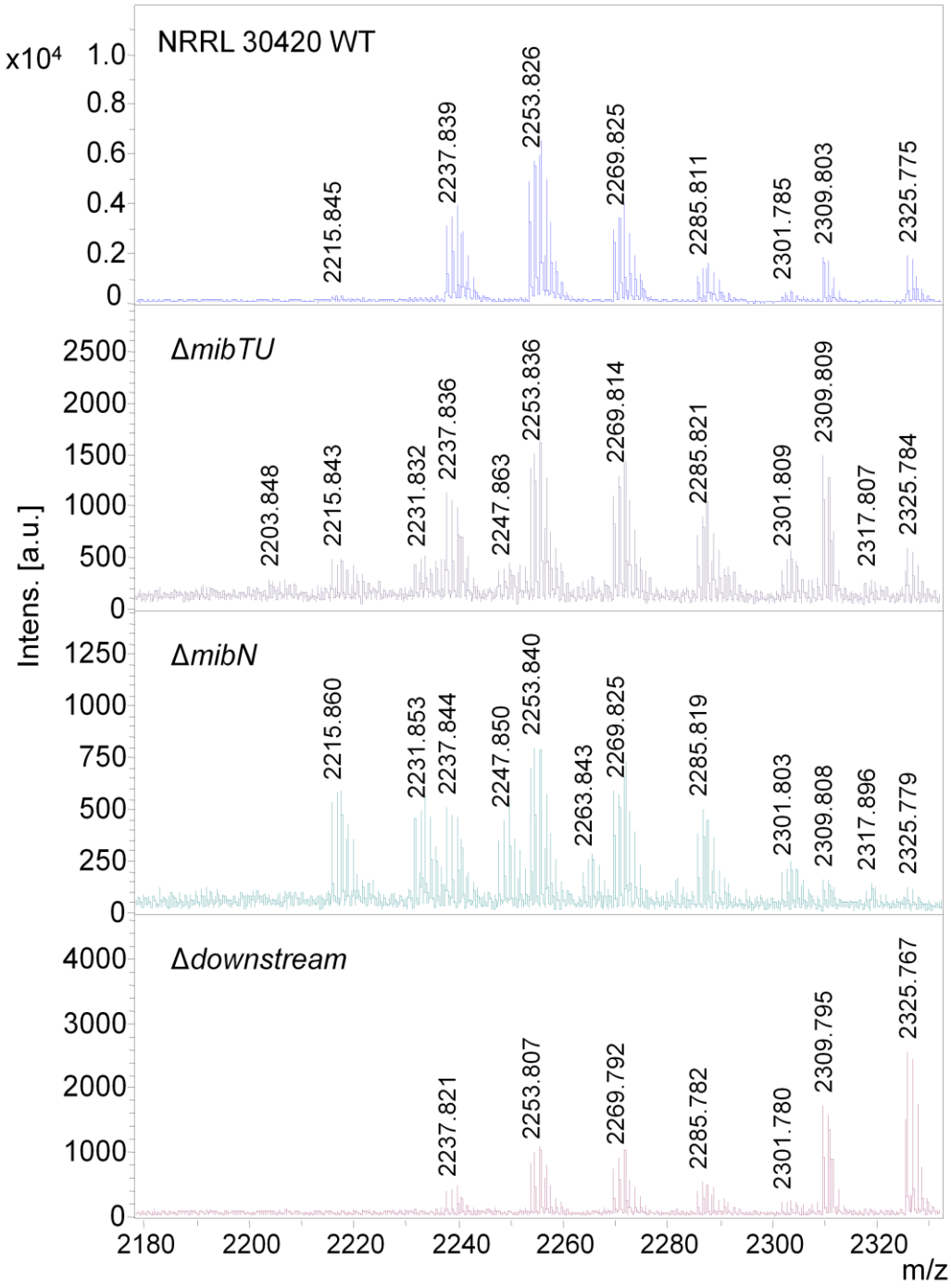

Figure 7.16 MALDI-ToF mass spectrometry of supernatants from NRRL 30420 wild type (WT) and representative clones of Δ*mibTU::aac(3)*IV, Δ*mibN::aac(3)*IV and Δ*downstream::aac(3)*IV mutants. Strains were grown in VSPA at 30°C and a supernatant sample removed after 7 days of fermentation. The supernatants were subjected to MALDI-ToF analysis. Ions with m/z 2309.7 and 2325.7 correspond to medium components and serve as internal controls.

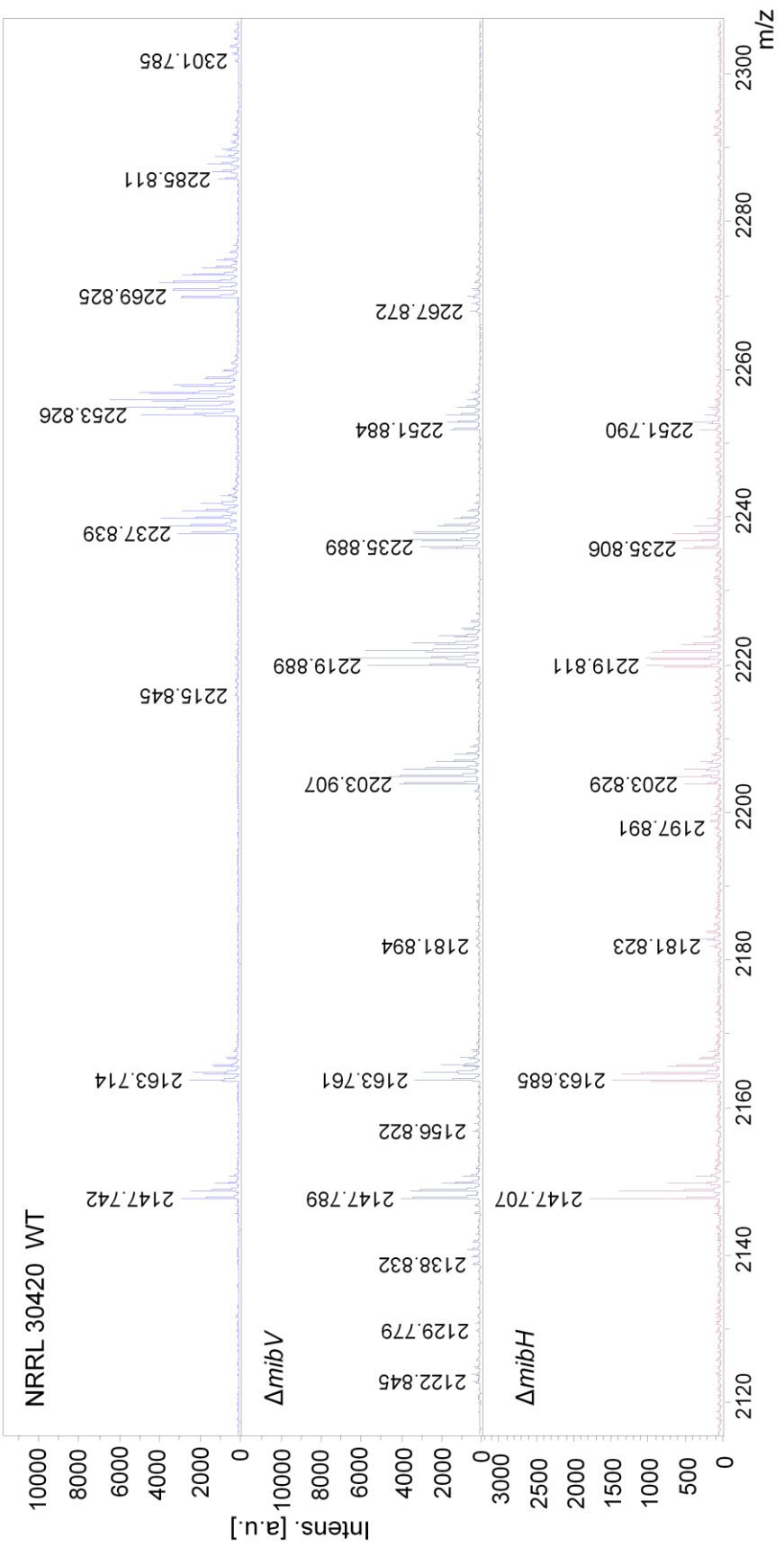

Figure 7.17 MALDI-ToF mass spectrometry of supernatants from NRRL 30420 wild type (WT) and representative clones of Δ*mibV::aac(3)*IV and Δ*mibH::aac(3)*IV mutants. Strains were grown in VSPA at 30°C and a supernatant sample removed after 7 days of fermentation. The supernatants were subjected to MALDI-ToF analysis. m/z peaks at Ions with m/z 2147.7 and 2163.7 correspond to medium components and serve as internal controls.

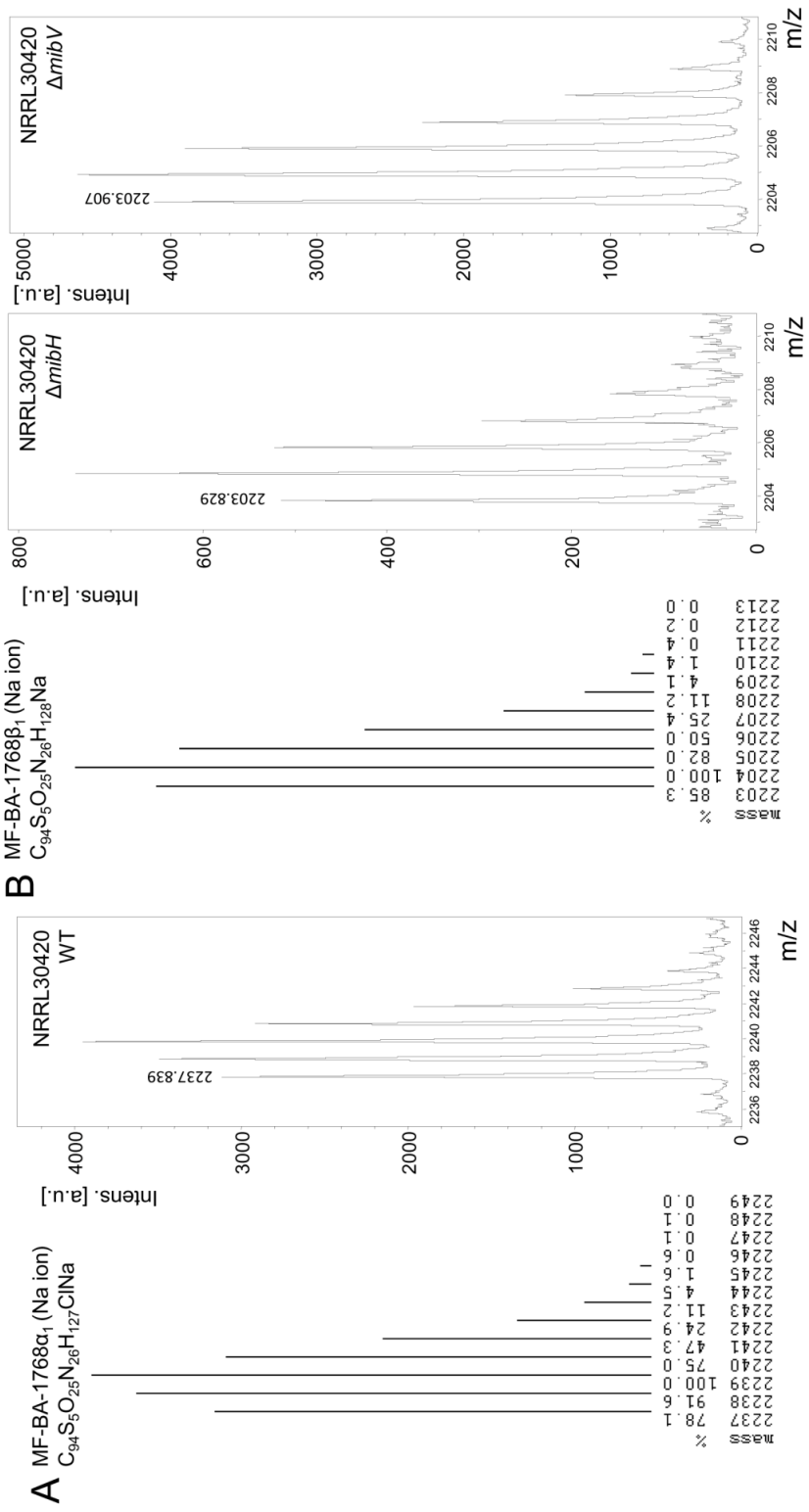

Figure 7.18 A comparison of the predicted and observed isotope patterns for microbisporicin (A) and deschloromicrobisporicin (B). The predicted theoretical molecular formulae of the sodium adducts of microbisporicin (MF-BA-1768α_1) and deschloromicrobisporicin (MF-BA-1768β_1) were used to predict the distribution of the isotopomers in mass spectrometry using Chemputer (University of Sheffield; http://winter.group.shef.ac.uk/chemputer/). These patterns were compared to those of the ions expected to correspond to these compounds from NRRL 30420 wild type, Δ*mibH* and Δ*mibV* supernatants.

7.4 Complementation of Mutant Phenotypes

Complementation of mutant phenotypes was carried out by introducing the deleted coding sequence *in trans* with expression from the native gene promoter. The vector used was pIJ10706, a variant of pSET152 that contains the selectable hygromycin resistance gene and integrates at the ΦC31 integration site in *M. corallina.* pSET152 had already been shown to transfer efficiently into *M. corallina* by conjugation from *E. coli* (section 7.2.4).

mibA

To complement the deletion of *mibA*, the region between *mibX* and *mibA* (defined as the *mibA* promoter; P_{mibA}) and the open-reading frame of *mibA* were cloned into pIJ10706 to generate pIJ12138. This construct was mobilised by conjugal transfer into one clone chosen as the representative NRRL 30420 Δ*mibA*::*aac(3)*IV mutant. Ex-conjugants were selected with 40 µg/ml hygromycin and were efficiently acquired. Four clones were chosen and confirmed to contain pIJ12138 by PCR. The clones were tested for production of bioactive compound along with the control strains NRRL 30420 Δ*mibA*::*aac(3)*IV pIJ10706 and NRRL 30420 pIJ10706. Four representative clones of each strain were grown for 8 days in VSPA liquid medium and 40 µl of supernatant applied to antibiotic assay discs that were placed on a lawn of *M. luteus*. Introduction of the vector pIJ10706 into NRRL 30420 wild type by conjugal transfer from *E. coli* had no effect on the production of bioactive compound (Figure 7.19A). However, neither the vector only control of the *mibA* mutant nor the mutant carrying the complementation construct pIJ12138 restored bioactivity (Figure 7.19A). The most likely explanation for the lack of complementation is a polar effect of *mibA* substitution on the expression of downstream genes. *mibABCDTUV* are likely to constitute one operon, with expression driven from the *mibA* promoter. Thus, replacement of *mibA* with the apramycin cassette likely interferes with expression of *mibBCDTUV*. Earlier deletional analysis (section 7.3.2) revealed that *mibD* is essential for microbisporicin biosynthesis and since the proteins encoded by *mibBC* are likely to be involved in lanthionine bridge formation, they are very likely to be essential. However, as described previously, *mibTU* and *mibV* were found not to be essential for microbisporicin production and so the phenotype of the *mibA* mutant would not be expected to be influenced by a polar effect on the expression of these genes (although if microbisporicin had been produced in the complemented *mibA* mutant, the spectrum of ions observed in MALDI-ToF analysis would have been influenced by a polar effect on *mibV* expression (see above)).

To determine whether the deletion of *mibA* caused a polar effect on the expression of essential downstream genes, the *mibA* mutation was complemented with *mibABCD*. This fragment, of about 5 kb, is too large to confidently amplify by PCR without the incorporation of mutations and would be difficult and resource-consuming to verify by sequencing. An *Xba*I site conveniently positioned within the FRT site of the apramycin cassette used to replace *mibTU* in pIJ12125 Δ*mibTU*::*aac(3)*IV could be used to liberate the 3' end of the required fragment. Similarly, a unique *Spe*I site within the *mibX-mibA* intergenic region could be used to liberate the 5' end. As described below, pIJ12139 was constructed (for the *in trans* expression of other *mib* genes) and consists of pIJ10706 with the *mibX-mibA* intergenic region cloned into the multiple-cloning site between *BamH*I and *Xba*I sites. Since this region includes the unique *Spe*I site, the excised *mibABCD* fragment could be cloned into this vector, cut with *Spe*I and *Xba*I, to reform the *mibA* promoter region followed by the *mibABCD* genes, generating pIJ12362 (Figure 7.20). This large construct was confirmed by restriction digest analysis and was transferred into NRRL 30420 Δ*mibA*::*aac(3)*IV by conjugation from *E. coli* ET12567/pUZ8002. Four ex-conjugants, selected with 40 µg/ml hygromycin, were grown on V0.1 agar medium and overlaid with *M. luteus* in SNA. None of the clones was able to produce a zone of clearing in the lawn of *M. luteus*. The clones were further tested by growing in VSPA for 7 days along with the control strains NRRL 30420 wild type and NRRL 30420 Δ*mibA*::*aac(3)*IV pIJ10706. Supernatant from the *mibABCD* clones was unable to inhibit the growth of *M. luteus*, unlike the wild type control (Figure 7.19B), and MALDI-ToF mass spectrometry failed to reveal ions associated with the production of microbisporicin. The representative clones were confirmed to contain pIJ12362 by PCR.

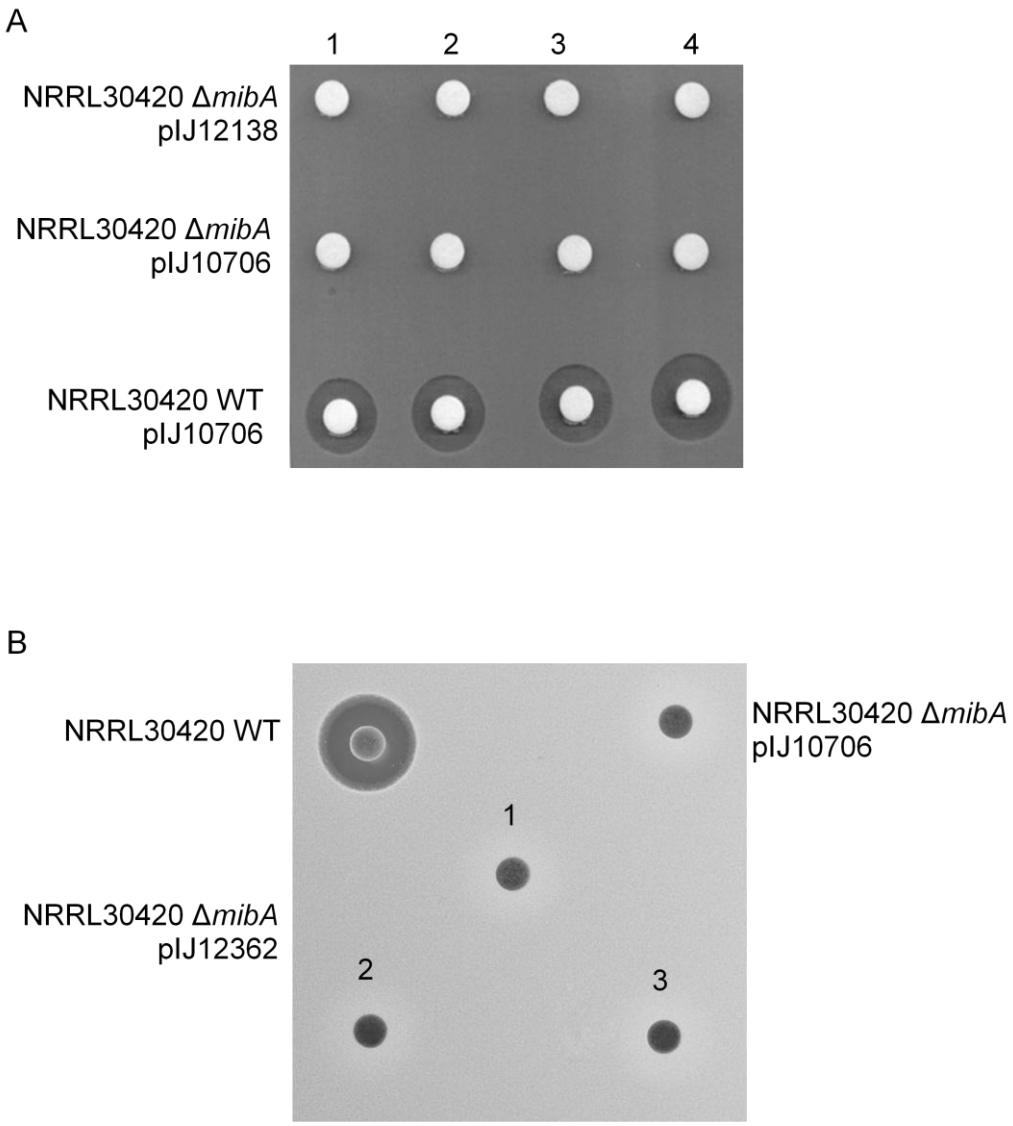

Figure 7.19 Analysis of bioactivity from the *mibA* deletion mutant of *M. corallina* NRRL 30420 with *in trans* provision of *mibA* and *mibABCD*.

A Four clones (1-4) of NRRL 30420 Δ*mibA*::*aac(3)*IV pIJ12138, NRRL 30420 Δ*mibA*::*aac(3)*IV pIJ10706 and NRRL 30420 pIJ10706 were grown for 8 d in VSPA. 40 µl of supernatant was applied to antibiotic assay discs that were placed on a lawn of *M. luteus*. The plate was incubated overnight at 30°C before zones of inhibition were recorded.

B Three clones (1-3) of NRRL 30420 Δ*mibA*::*aac(3)*IV pIJ12362, one clone of NRRL 30420 Δ*mibA*::*aac(3)*IV pIJ10706 and NRRL 30420 wild type were grown for 7 d in VSPA. 40 µl of supernatant was applied to antibiotic assay discs that were placed on a lawn of *M. luteus*. The plate was incubated overnight at 30°C before zones of inhibition were recorded.

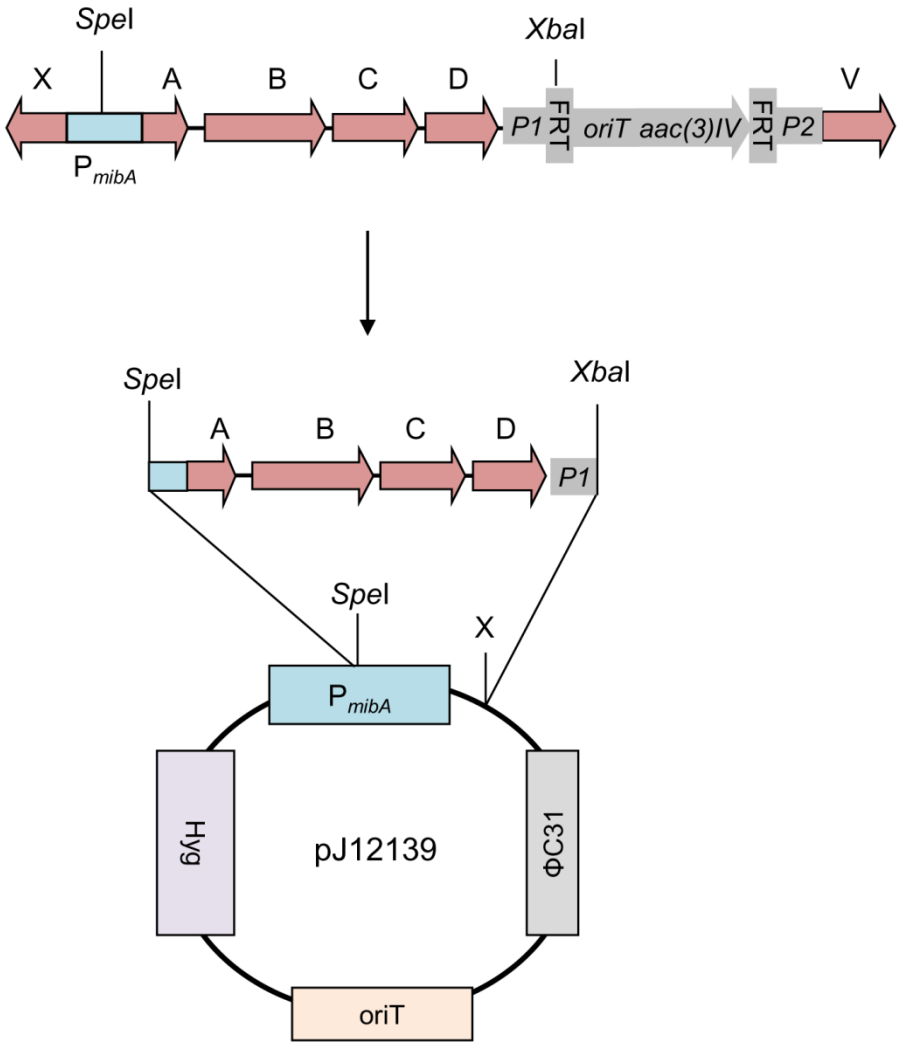

Figure 7.20 Schematic illustrating the cloning strategy used to generate a complementation construct pIJ12362 containing *mibABCD*. The top panel illustrates a section of pIJ12125 Δ*mibTU*::*aac(3)*IV. The genes of the *mib* cluster are shown in red. The intergenic region between *mibX* and *mibA,* thought to include the *mibA* promoter (P_{mibA}), is shown in light blue. The apramycin cassette from pIJ773 used to replace Δ*mibTU* is shown in grey (Gust, *et al.* 2003). A unique *Spe*I site in P_{mibA} and an *Xba*I site in the FRT sequence of the apramycin cassette were used to remove this *mibABCD* fragment and introduce it into pIJ12139 (see also figure 7.23). Ligation into the *Spe*I site in this vector restores the *mibA* promoter upstream of *mibABCD*. The vector pIJ12139 contains the hygromycin resistance marker (Hyg), the origin of transfer (oriT) and ΦC31 attachment site and integrase (ΦC31) (Kieser *et al.* 2000).

mibX

Deletion of *mibX* may have had a polar effect on expression of *mibW*, which lies downstream of *mibX* and is likely translationally coupled to it (although the start codon of *mibW* was left intact by the deletion). To determine whether the observed phenotype was caused by the absence of MibX or MibXW, both *mibX* and *mibXW* were expressed *in trans* from their own promoter region in the *mibX* mutant. The intergenic region between *mibA*-*mibX* along with *mibX* or *mibXW* was introduced into pIJ10706 to generate pIJ12349 and pIJ12350, respectively. The intergenic region *mibA*-*mibX* is present in pIJ12139 (see below) and this construct was used to generate a negative control strain. The three constructs were transferred into NRRL 30420 Δ*mibX::aac(3)*IV by conjugation from *E. coli* ET12567/pUZ8002. Three representative clones of each resulting strain were confirmed to contain the appropriate construct by PCR.

When grown on V0.1 agar medium, the strain carrying pIJ12139 did not produce compounds with bioactivity against *M. luteus* (Figure 7.21A). In contrast, strains carrying pIJ12349 produced large zones of clearing in an overlay of *M. luteus*, and strains carrying pIJ12350 gave small zones of clearing. The wild type strain was also grown in this assay but was patched at a very low starting density such that the production of microbisporicin would be limited and would not clear a large region of the plate in the overlay assay (as is common with the wild type strain) thus obscuring the other results. For this reason it is not possible to determine whether the level of bioactivity from the Δ*mibX* mutant complemented with *mibX* was higher than that of the wild type strain. Nevertheless, the *in trans* expression of *mibX* alone was sufficient to restore bioactivity to the mutant strain. MibW is proposed to negatively regulate MibX, which is presumed to be a positive regulator of microbisporicin production. Thus the absence or reduced levels of MibW would likely cause over-production of microbisporicin. This could explain the large halos produced by the Δ*mibX* mutant when complemented with *mibX* alone, assuming a polar effect on *mibW* expression of replacement of the chromosomal copy of *mibX* with the apramycin cassette. When both *mibX* and *mibW* were present in the complementing plasmid (pIJ12350), the halos were much smaller, suggesting either that regulation of MibX is restored to wild type levels (if the mutation was polar on *mibW*) or that two functional copies of *mibW* decrease MibX activity below wild type levels and thus decrease microbisporicin production.

To further investigate the complementation of the *mibX* mutant, the strains were grown in VSPA liquid medium for 7 d along with the wild type strain. Under these conditions supernatant from the wild type strain generated a large zone of inhibition in a lawn of *M.*

luteus. The Δ*mibX* mutant carrying pIJ12139 and pIJ12350 failed to produce any bioactive compound. Strains harbouring pIJ12349, which gave large zones of bioactivity on agar medium, produced only small zones of inhibition in this assay (Figure 7.21B). Thus complementation of the *mibX* deletion with *mibX* does not appear to be as efficient in liquid culture as it is on agar medium. The presence of microbisporicin in these samples was investigated by MALDI-ToF mass spectrometry. Ions associated with microbisporicin could not be detected in any of the supernatants despite bioactivity from Δ*mibX* pIJ12349. Since the level of bioactivity was very low, it is possible that the microbisporicin ions were obscured by other signals. To resolve this potential problem, microbisporicin was extracted from 5 ml supernatant samples from Δ*mibX* pIJ12139, Δ*mibX* pIJ12349 (three independent clones) and NRRL 30420 wild type using Diaion HP20 polystyrene resin (as described in chapter 2.15.1). The extracted compounds were eluted with methanol:butanol:water (9:1:1) and the solvents evaporated to concentrate the samples, which were analysed by MALDI-ToF mass spectrometry and by bioassay against *M. luteus*. This method extracted bioactive compounds from the wild type and Δ*mibX* pIJ12349 supernatants but not from the vector-only control supernatant (Figure 7.22). Furthermore, ions attributable to microbisporicin variants could be detected from both the wild type and Δ*mibX* pIJ12349 extracts (Figure 7.22). Interestingly the GPA variants of microbisporicin were present in a higher ratio compared to the non-GPA variants in the Δ*mibX* pIJ12349 extracts than in the wild type supernatant (Figure 7.22). This might explain the difference in the levels of bioactivity between the complemented and wild type strains, for example if the GPA variants are not as active as the non-GPA variants (although this has not been explored experimentally). The reason why these would accumulate at greater levels than the non-GPA form in this strain is not clear.

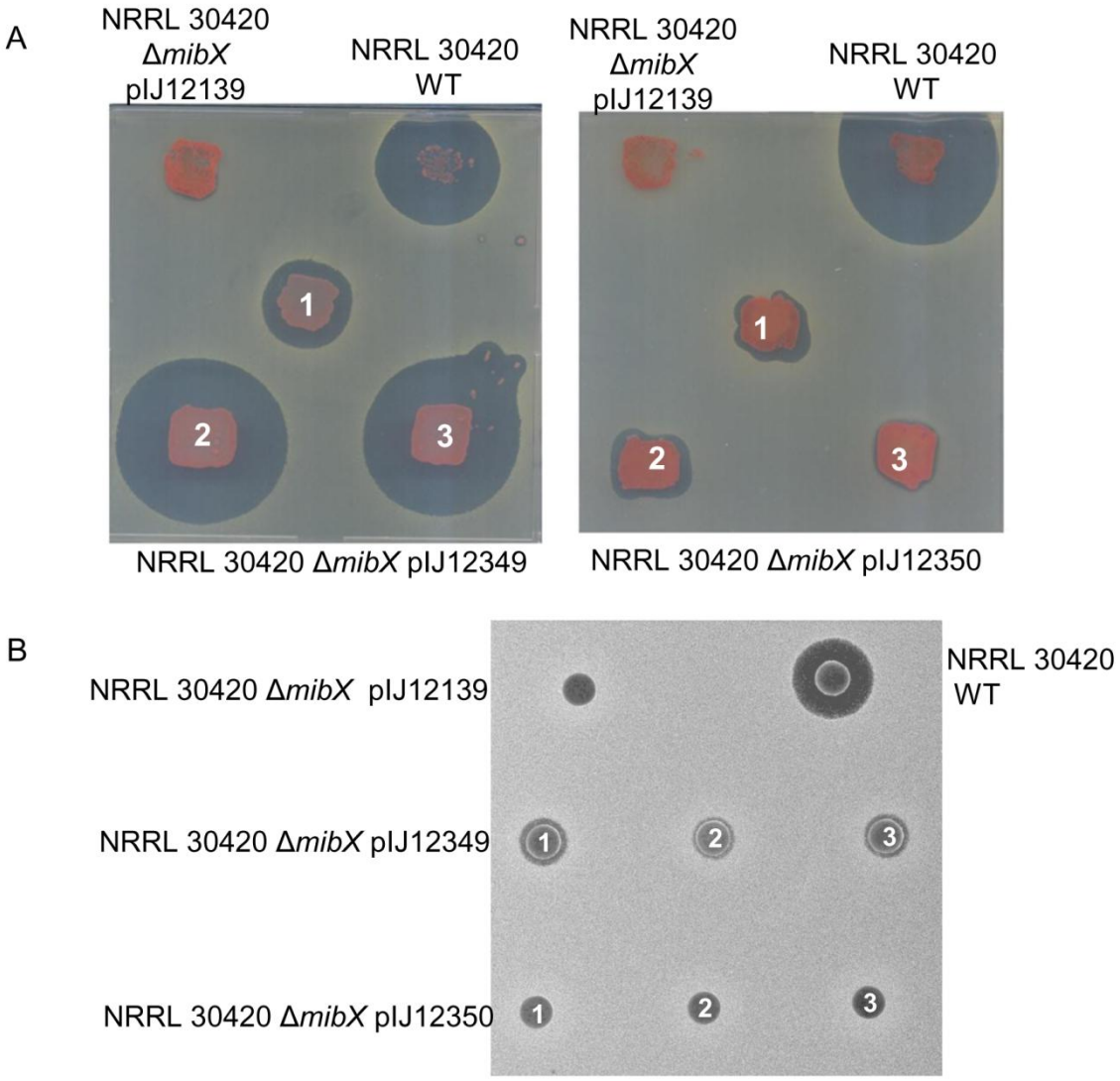

Figure 7.21 Analysis of bioactivity from the *mibX* deletion mutant of *M. corallina* NRRL 30420 with *in trans* expression of *mibX* and *mibXW*. **A** Three clones (1-3) of NRRL 30420 Δ*mibX*::*aac(3)*IV pIJ12349 (*mibX*) and NRRL 30420 Δ*mibX*::*aac(3)*IV pIJ12350 (*mibXW*), NRRL 30420 Δ*mibX*::*aac(3)*IV pIJ12139 and NRRL 30420 wild type were grown for 5 d on V0.1. The plates were overlaid with *M. luteus in* SNA. The plates were incubated overnight at 30°C before zones of inhibition were recorded. **B** Three clones (1-3) of NRRL 30420 Δ*mibX*::*aac(3)*IV pIJ12349 (*mibX*) and NRRL 30420 Δ*mibX*::*aac(3)*IV pIJ12350 (*mibX*), NRRL 30420 Δ*mibX*::*aac(3)*IV pIJ12139 and NRRL 30420 wild type were grown for 7 d in VSPA. 40 µl of supernatant was applied to antibiotic assay discs that were placed on a lawn of *M. luteus*. The plate was incubated overnight at 30°C before zones of inhibition were recorded.

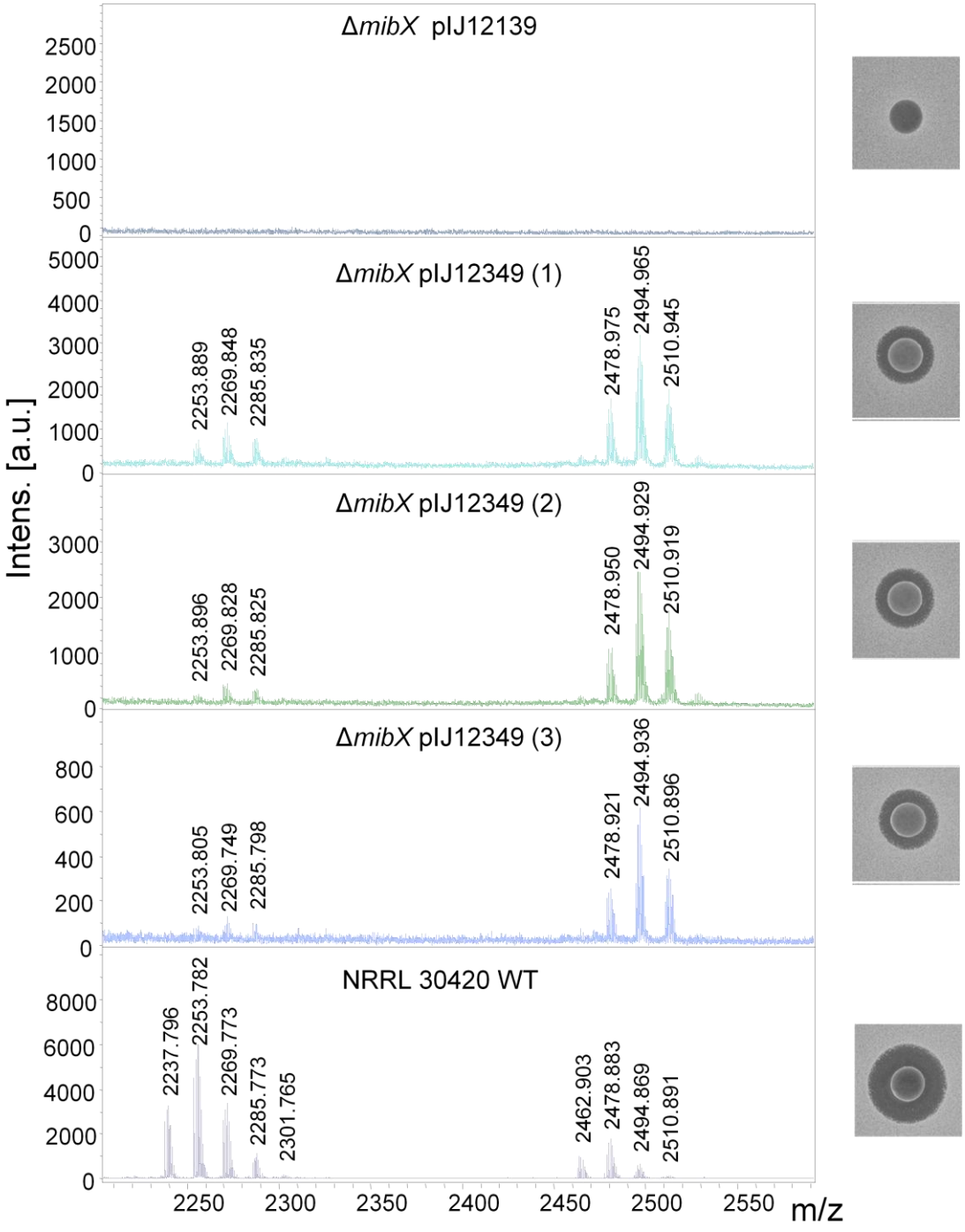

Figure 7.22 Analysis of Diaion HP20 resin extracts from supernatants from the *mibX* deletion mutant of *M. corallina* NRRL 30420 with *in trans* expression of *mibX*. Microbisporicin was extracted from 5 ml supernatant samples from Δ*mibX* pIJ12139, pIJ12349 (three independent clones) and NRRL 30420 wild type using Diaion HP20 polystyrene resin (as described in chapter 2.15.1). The extracted compounds were eluted with methanol:butanol:water (9:1:1) and the solvents evaporated to concentrate samples. These samples were investigated by MALDI-ToF mass spectrometry and by bioassay against *M. luteus* (Images shown on the right of the respective spectrum).

Complementation vectors pIJ12139 and pIJ12140

The other genes of the *mib* gene cluster for which complementation experiments were to be carried out are largely separated from their putative promoter regions. To express these genes from their native promoters (and since no constitutive promoters have been explored as tools in *M. corallina*) a set of complementation vectors was constructed. pIJ12139 was designed to allow expression of genes of the *mibA* operon from the *mibA* promoter likely located within the *mibX-mibA* intergenic region (Figure 7.23). pIJ12140 was designed to allow expression of genes of the *mibE* operon from the *mibE* promoter likely located within the *mibV-mibE* intergenic region (Figure 7.23). The two vectors were based on pIJ10706 and were constructed to allow the introduction of the gene of interest downstream of the appropriate promoter (Figure 7.23). Each gene was cloned with its own ribosome-binding site to promote wild type levels of translation initiation at the *in trans* location.

mibD

The phenotype of the *mibD* mutant was complemented to wild type by the *in trans* expression of the *mibD* ORF from the *mibA* promoter (likely its native promoter) (Figure 7.24). The bioactivity of this strain was restored to approximately wild type levels (estimated by bioassay) and the spectrum of ions visible by MALDI-ToF mass spectrometry was as seen in wild type NRRL 30420 supernatants. This indicated that there were no detrimental polar effects caused by replacement of *mibD* with the apramycin cassette and that the loss of *mibD* was solely responsible for the lack of microbisporicin production in the *mibD* mutant.

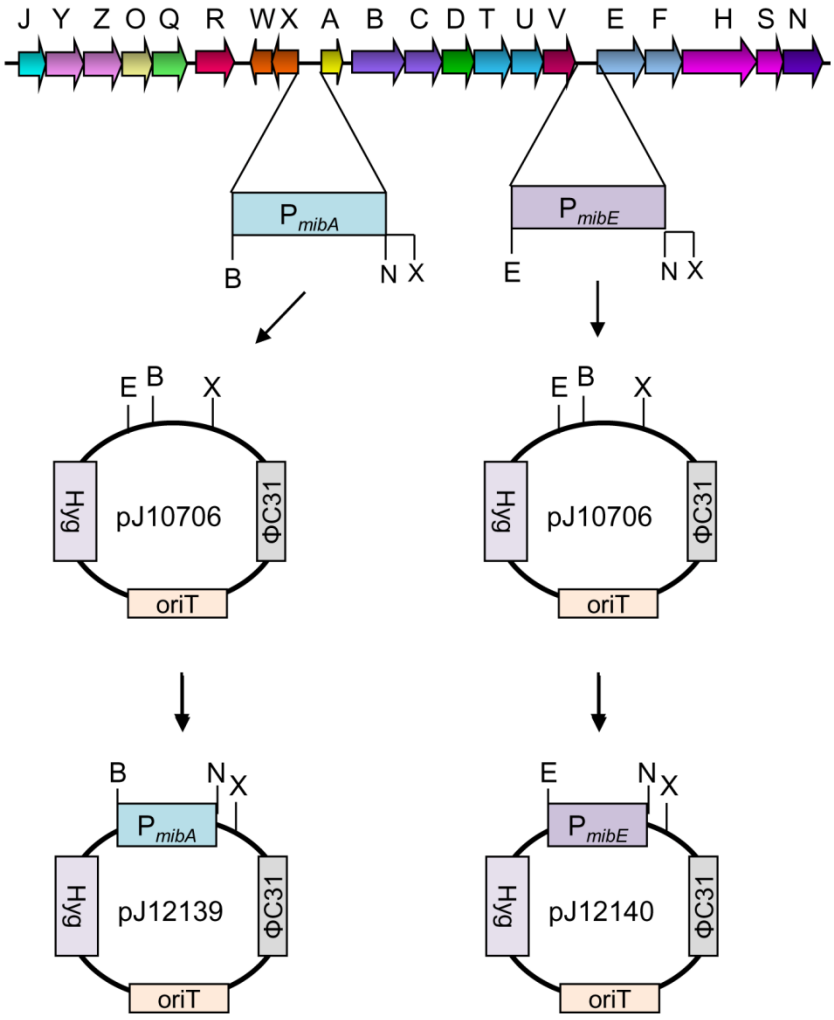

Figure 7.23 Schematic illustrating the cloning strategy used to generate the complementation constructs pIJ12139 and pIJ12140. The top panel illustrates the *mib* gene cluster. The intergenic region between *mibX* and *mibA,* thought to include the *mibA* promoter (P_{mibA}), is shown in light blue and was amplified by PCR using primers which introduce a *Bam*HI (B) site at the 5' end and *Nde*I (N) and *Xba*I (X) sites at the 3' end. The intergenic region between *mibV* and *mibE,* thought to include the *mibE* promoter (P_{mibE}), is shown in light purple and was amplified by PCR using primers which introduce an *Eco*RV (E) site at the 5' end and *Nde*I (N) and *Xba*I (X) sites at the 3' end. These fragments were cloned into pIJ10706 in the *Bam*HI/*Xba*I and *Eco*RV/*Xba*I sites respectively. The vector pIJ10706 is based on pSET152 and contains the hygromycin resistance maker (Hyg), the origin of transfer (OriT) and ΦC31 attachment site and integrase (ΦC31) (Kieser *et al.* 2000). Genes to be expressed from these promoters were introduced between the *Nde*I and *Xba*I sites such that they lie immediately downstream of the respective promoter (see also chapter 2.24).

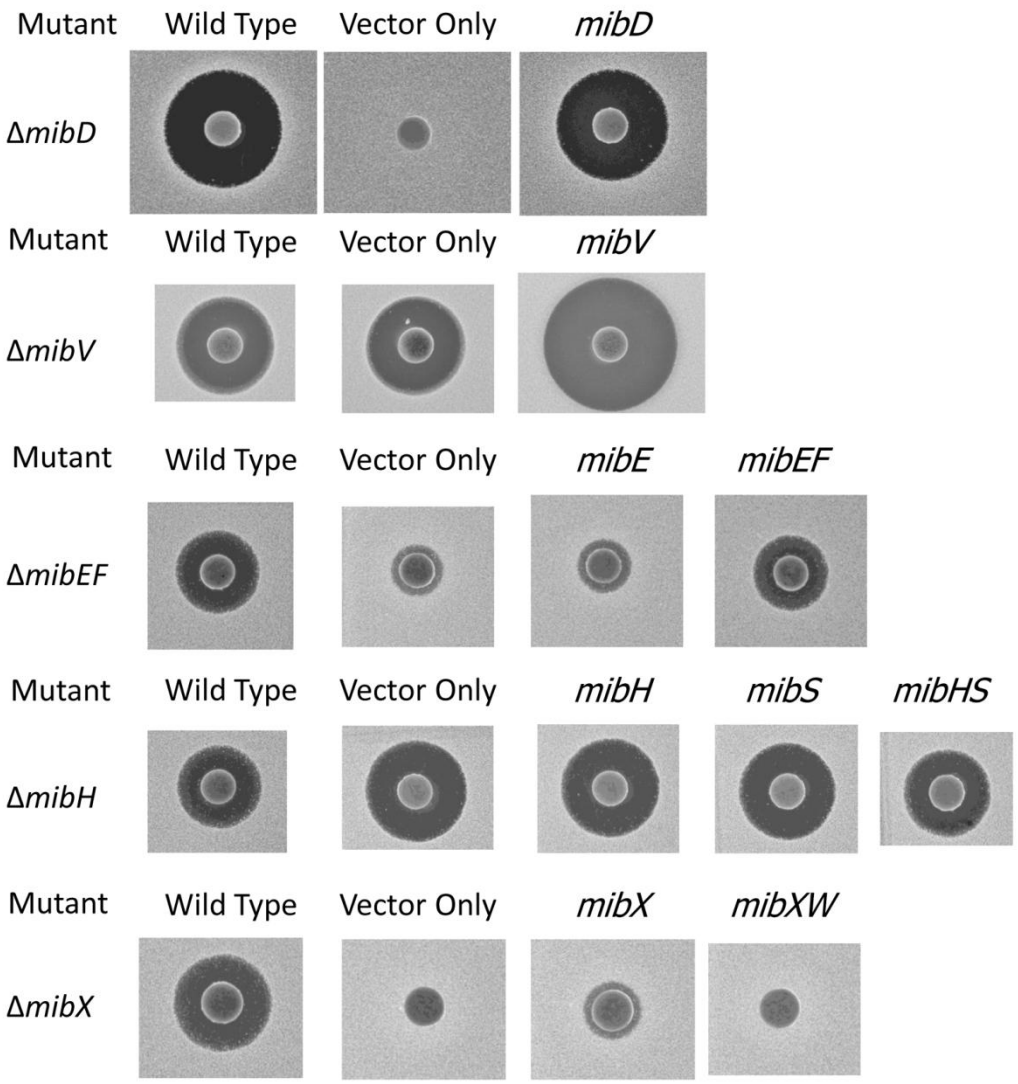

Figure 7.24 Analysis of bioactivity from deletion mutants of *M. corallina* NRRL 30420 with *in trans* expression of different *mib* genes from their cognate promoters. The mutant under study in each case is listed on the left. In each assay NRRL 30420 wild type was grown as a positive control ("Wild Type" in column 1). The mutant strain carrying the empty complementation vector (either pIJ12139 (*mibD*, *mibV* and *mibX*) or pIJ12140 (*mibEF*, *mibH*) were grown as negative controls (one representative clone selected; "Vector Only" in column 2). The *mib* genes expressed *in trans* in each mutant are given above each image in columns 3-4. All strains were grown for 7 d in VSPA and 40 µl supernatant tested for bioactivity against *M. luteus*. Zones of inhibition are shown for one representative clone for each strain (at least 2 clones were assayed in each case). Note that the Δ*mibV* mutant control strain grew poorly on this occasion and thus shows a reduced zone of inhibition than that seen previously.

mibV

mibV lies at the end of the likely *mibA* operon and thus replacement of *mibV* with the apramycin cassette would not be expected to have a polar effect on downstream genes. To determine whether the phenotype of the Δ*mibV* mutant was solely due to the loss of *mibV*, the gene was expressed *in trans* from the *mibA* promoter (likely its native promoter). The *mibV* mutant retains bioactivity but was also consistently found to give higher levels of bioactivity. When *mibV* was expressed in the Δ*mibV::aac(3)*IV mutant, the strain retained this higher level of bioactivity (Figure 7.24). The supernatant from Δ*mibV::aac(3)*IV pIJ12139-*mibV* was further investigated by MALDI-ToF mass spectrometry and compared to the profile of ions from the mutant strain carrying only pIJ12139. The *in trans* provision of *mibV* did not restore the Δ*mibV* mutant to a wild type phenotype since only ions corresponding to deschloromicrobisporicin production were observed in both strains (Figure 7.25). Additionally, the unidentified smaller ions identified in the Δ*mibV* mutant were also present in the supernatants from three Δ*mibV::aac(3)*IV pIJ12139-*mibV* clones (although they were not as obvious in the control strain in this particular experiment; this strain grew poorly on this occasion and also gave a reduced zone of inhibition by bioassay; Figures 7.24 and 7.25).

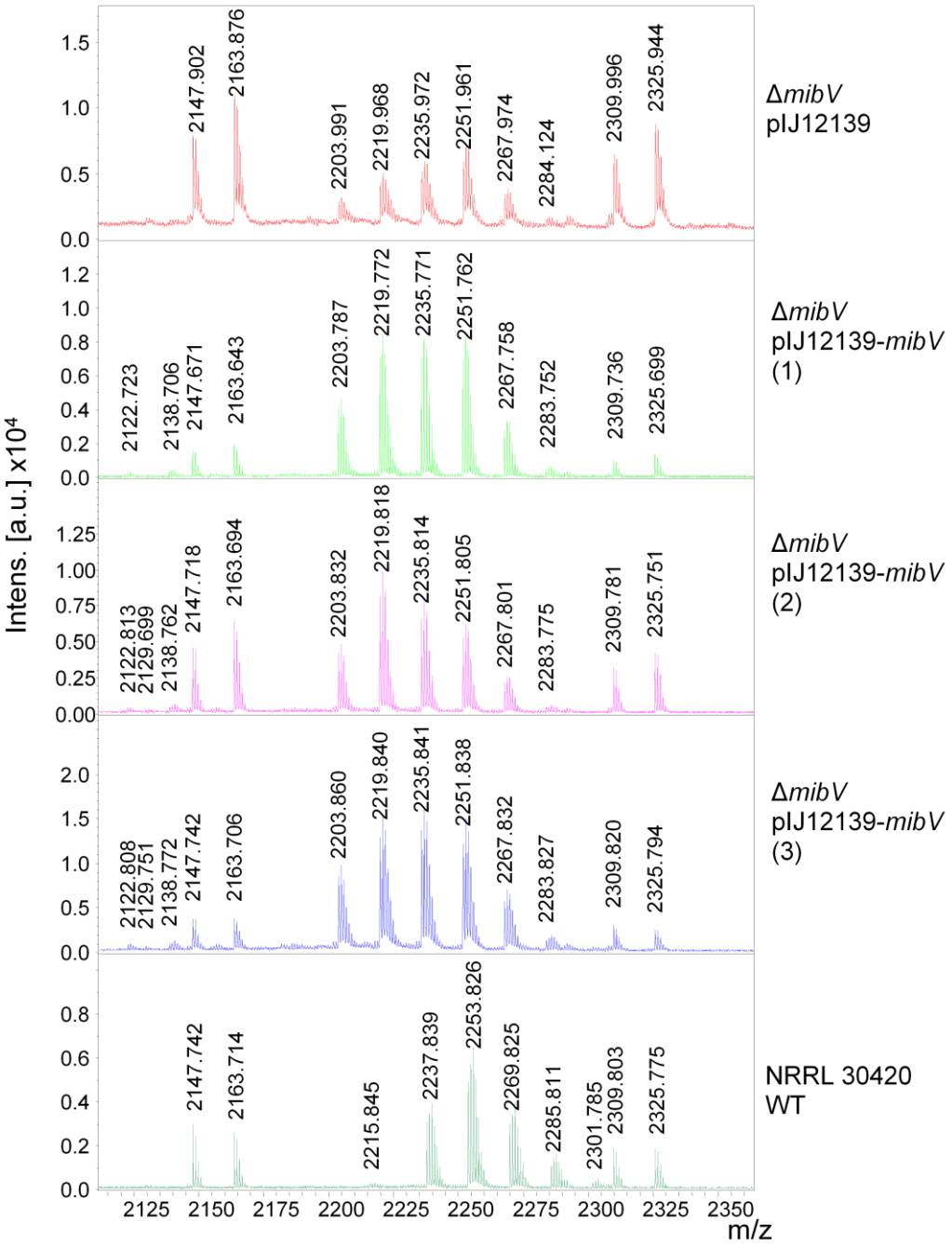

Figure 7.25 Analysis of supernatants from the *mibV* deletion mutant of *M. corallina* NRRL 30420 with *in trans* provision of *mibV*. NRRL 30420 Δ*mibV::aac(3)*IV pIJ12139, NRRL 30420 Δ*mibV::aac(3)*IV pIJ12139-*mibV* (3 independent clones) and NRRL 30420 wild type (WT) were grown in VSPA for 7 days at 30°C. Supernatant samples were investigated by MALDI-ToF mass spectrometry.

mibEF

The very marked reduction in bioactivity and microbisporicin production in the Δ*mibEF* mutant is likely due to the loss of both proteins since they are predicted to function as a two-component ABC transporter. To test whether this was the case, *mibE*, *mibF* and *mibEF* were to be expressed *in trans* to determine whether the phenotype could be restored. Deletion of the downstream genes *mibH and mibN* had no detrimental effect on bioactivity and so the phenotype of the *mibEF* mutant is unlikely to result from a polar effect on their expression, but this could also be assessed in the complementation experiment. *mibE*, *mibF* and *mibEF* were cloned in pIJ12140 such that expression was driven by the native *mibE* promoter. The construct carrying *mibF* alone was detrimental to the growth of *E. coli* DH5α (used in cloning) and was lethal in *E. coli* ET12567/pUZ8002. The reason for this is not clear, but it is possible that the protein is expressed (perhaps due to read-through expression from the *lacZ* promoter in pIJ12140) and that the ATPase activity of *mibF* is not well-tolerated by *E. coli.* For this reason, only *mibE*- and *mibEF*-containing constructs were transferred into NRRL 30420 Δ*mibEF*::*aac(3)*IV by conjugation from *E. coli*. Four independent clones of each resulting strain were grown along with a pIJ12140 only control strain on V0.1 agar medium at 30°C for 7 d before being overlaid with *M. luteus*. Under these conditions, Δ*mibEF* pIJ12140 and pIJ12140-*mibE* failed to generate zones of inhibition in a lawn of *M. luteus* (Figure 7.26). By contrast clones of Δ*mibEF* pIJ12140-*mibEF* produced large zones of inhibition, indicating that the *in trans* provision of *mibEF* was sufficient to complement the loss of *mibEF* from the *mib* gene cluster (Figure 7.26). The strains were further analysed by growing for 7 d in VSPA liquid medium and supernatant samples applied to antibiotic assay discs on a lawn of *M. luteus*. Unlike the pIJ12140 and pIJ12140-*mibE* strains, which failed to generate large zones of inhibition under these conditions, pIJ12140-*mibEF* supernatant generated a clear zone of inhibition (Figure 7.24). These supernatants were also analysed by MALDI-ToF mass spectrometry and found to contain wild type microbisporicin. This indicates that there is no severe polar effect on *mibH* expression in the Δ*mibEF* mutant. Thus, *mibF* is essential for microbisporicin biosynthesis in *M. corallina* and it is very likely that *mibE* is also required with MibEF functioning as a two-component ABC-transporter.

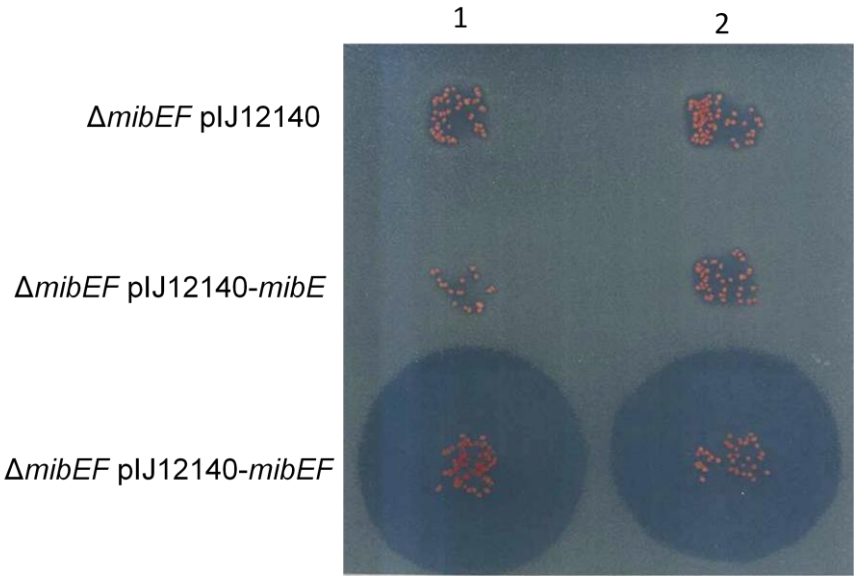

Figure 7.26 Clones of Δ*mibEF* pIJ12140, Δ*mibEF* pIJ12140-*mibE* and Δ*mibEF* pIJ12140-*mibEF* were grown on V0.1 agar at 30°C for 7 d before being overlaid with *M. luteus* in SNA. Plates were incubated overnight at 30°C before zones of inhibition were recorded. The result from two representative clones for each stain is shown.

mibH

mibH is translationally-coupled to the downstream gene *mibS*, which likely encodes the flavin reductase required for tryptophan halogenase (MibH) activity. Replacement of *mibH* with the apramycin cassette is therefore likely to have a polar effect on *mibS* expression. For this reason, *mibH*, *mibS* and *mibHS* were all assessed for their ability to complement the Δ*mibH* mutant. The genes were cloned in pIJ12140 such that expression was driven by the *mibE* promoter (likely the native promoter). The resulting constructs, along with pIJ12140, were transferred into the *mibH* mutant by conjugation from *E. coli*. The resulting strains were grown for 7 days in VSPA liquid medium and bioactivity against *M. luteus* assessed (Figure 7.24). Since the Δ*mibH* mutant retains bioactivity, this assay was unable to definitively show whether these genes could complement the mutation. However the *mibH* mutant was found to reproducibly generate larger zones of inhibition in a lawn of *M. luteus* compared to the wild type. These larger zones were apparent around discs of supernatant from the vector-only control, pIJ12140-*mibH* and pIJ12140-*mibS* strains, however the zone of clearing around a disc of supernatant from pIJ12140-*mibHS* was smaller in diameter and similar to that produced by the wild type strain (Figure 7.24). The supernatants were further analysed by MALDI-ToF mass spectrometry (Figures 7.27 and 7.28). Supernatants from the vector-only control, pIJ12140-*mibH* and pIJ12140-*mibS* strains gave ions corresponding only to the deschloro-form of microbisporicin, as described for the Δ*mibH* mutant (Figure 7.27). In contrast, expression of *mibHS* in the Δ*mibH* mutant resulted in ions relating to both the deschloro- and chloro- forms of microbisporicin (Figure 7.27). When compared to a wild type spectrum of ions, it is apparent that the spectral phenotype of Δ*mibH* expressing *mibHS* is intermediate between that of the mutant and the wild type strain (Figure 7.28). It was also possible to discern a shift in the ratios of isotopomers in this strain back to that typically seen in wild type supernatants. This suggests the incorporation of chlorine into the compounds. Thus both *mibH* and *mibS* are required for the chlorination of microbisporicin. This suggests that reduced flavin provided by MibS is essential for the chlorinating activity of MibH *in vivo* and its absence is not complemented by the presence of another flavin reductase in *M. corallina*.

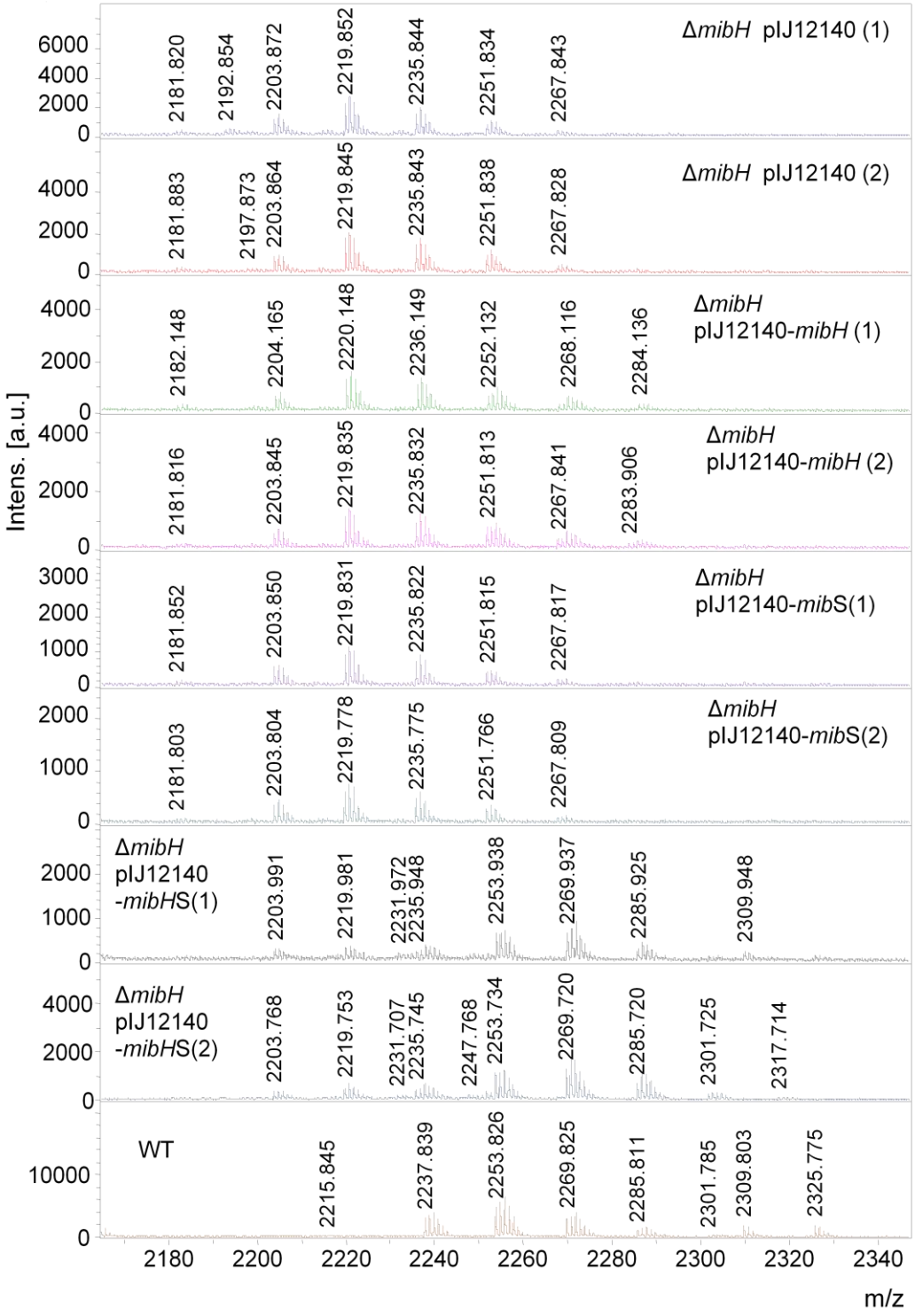

Figure 7.27 Analysis of supernatants from the *mibH* deletion mutant of *M. corallina* NRRL 30420 with *in trans* provision of *mibH, mibS* or *mibHS*. Two independent clones of NRRL 30420 Δ*mibH::aac(3)*IV pIJ12140, NRRL 30420 Δ*mibH::aac(3)*IV pIJ12140-*mibH,* NRRL 30420 Δ*mibH::aac(3)*IV pIJ12140-*mibS,* NRRL 30420 Δ*mibH::aac(3)*IV pIJ12140-*mibHS* and NRRL 30420 wild type (WT) were grown in VSPA for 7 days at 30°C. Supernatant samples were investigated by MALDI-ToF mass spectrometry.

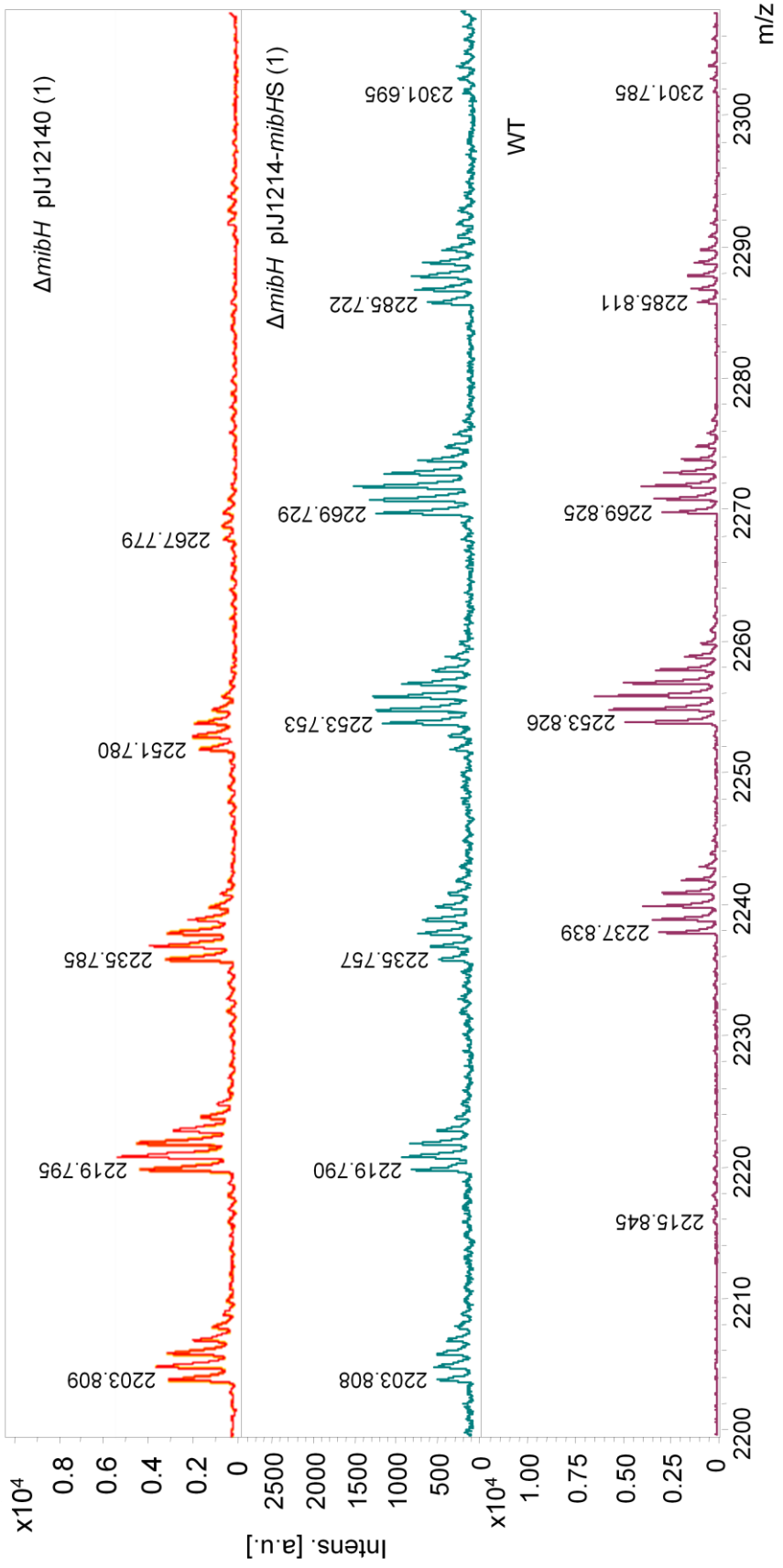

Figure 7.28 Zoomed-spectra from MALDI-ToF mass spectrometry of supernatants from NRRL 30420 wild type (WT) and representative clones of Δ*mibH*::*aac(3)*IV plJ12140 and Δ*mibH*::*aac(3)*IV plJ12140-*mibHS* from Figure 7.24.

7.5 Microbisporicin Resistance

Microorganisms that produce bioactive compounds often require a mechanism of self-resistance to prevent growth inhibition and potentially suicide. In the microbisporicin biosynthetic gene cluster, self-resistance is proposed to be conferred by MibEF, an ABC-transporter with homology to resistance proteins from other lantibiotic gene clusters. Furthermore, deletion of *mibEF* resulted in very low and much delayed levels of microbisporicin biosynthesis, potentially a consequence of negative feedback on production resulting from the lack of an effective self-resistance mechanism. To determine whether *mibEF* contribute to the resistance of *M. corallina* to microbisporicin, the following experiments were carried out.

During initial characterisation of the *M. corallina* strains and their ability to produce microbisporicin (see chapter 3) attempts were made to determine the sensitivity of the strains to microbisporicin. In the absence of purified compound, this was carried out using co-culture. The non-producer strain DSM 44681 and the producer strain NRRL 30420 were grown in a patch across one side of V0.1 agar plates for 11 d at 30°C. NRRL 30420 mycelium was then streaked perpendicular to each of the patches and its growth monitored for several days. After 5 d it was clear that NRRL 30420 was able to grow right up to the patch of DSM 44681 but would not grow near the NRRL 30420 patch (Figure 7.29A). This suggests that NRRL 30420 may not be resistant to its own compound at the stage of mycelial outgrowth. However, this was not too surprising since the genes for microbisporicin resistance may only be induced at the onset of production, which in liquid culture occurs during mid-late exponential phase. DSM 44681 and DSM 44682 showed similar responses to growth in the vicinity of NRRL 30420 (data not shown).

This assay was further extended by analysing the resistance of NRRL 30420 to microbisporicin produced in the supernatant of the same strain grown in liquid culture for six days. To determine the time point at which the wild type strain became resistant to its own compound, either through intrinsic resistance (e.g. mycelial out-growth has ceased) or through induction of a specific resistance mechanism (e.g. MibEF), the resistance of the strain was assessed at multiple stages of growth. The wild type strain was grown for 0, 24, 48, 72 and 96 hours on V0.1 agar medium before adding supernatant from NRRL 30420 into wells made in each of the lawns (Figure 7.29B). After 72 hours or more of growth, the wild type strain appeared to be completely resistant to microbisporicin. However, after 48 hours of growth, a small zone of inhibition was observed around the edge of the well into which the supernatant had been added. When added immediately

after inoculation (zero time point), the supernatant generated a sizable zone of inhibition. This is consistent with the results of the earlier experiment that suggested that early mycelial growth is inhibited by a compound or compounds produced by NRRL 30420. The Δ*mibA* mutant of NRRL 30420 was also grown and treated in exactly the same way as the wild type strain (Figure 7.29B). The Δ*mibA* mutant showed a more severe response to the presence of NRRL 30420 wild type supernatant, with growth inhibition up to 72h of growth. By 96h however, the strain showed the same level of resistance as the wild type. The zones of inhibition seen at earlier time points were much larger in the Δ*mibA* mutant. This phenotype might reflect differences in the starting inoculum or in the growth rates of the two strains, although in regions of the lawns not subjected to growth inhibiton, growth density of the two strains appeared to be similar. Additionally, it is not possible in this experiment to be confident that this is a response to microbisporicin and not another compound present in the supernatant of NRRL 30420. However, it would appear that the Δ*mibA* mutant is significantly less resistant to a compound produced by the wild type, and it is interesting to speculate that expression of *mibEF*, and hence microbisporicin resistance, is triggered by microbisporicin itself.

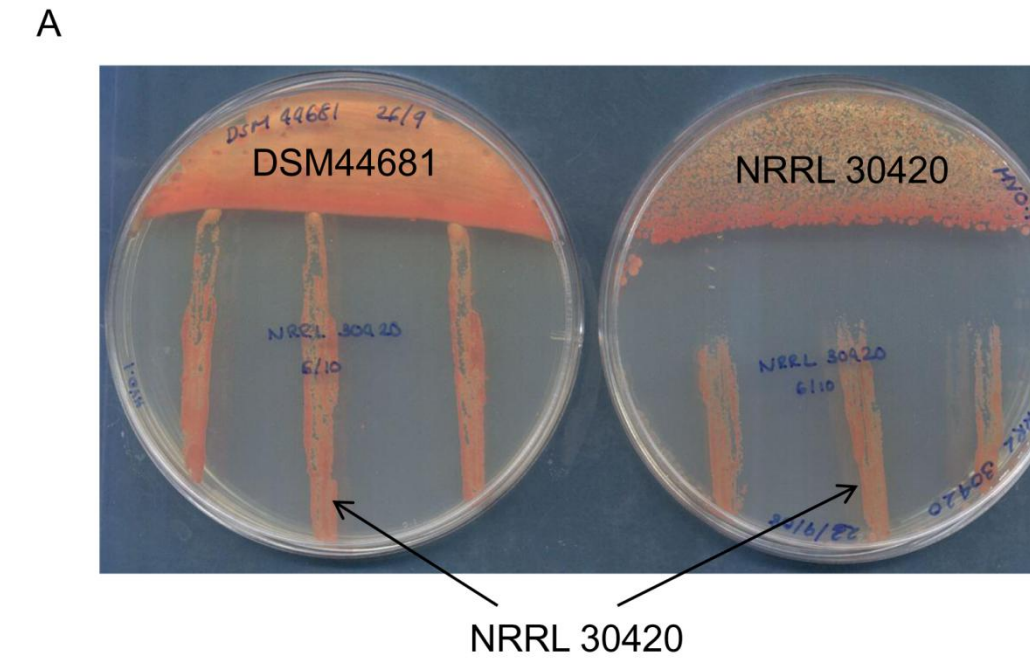

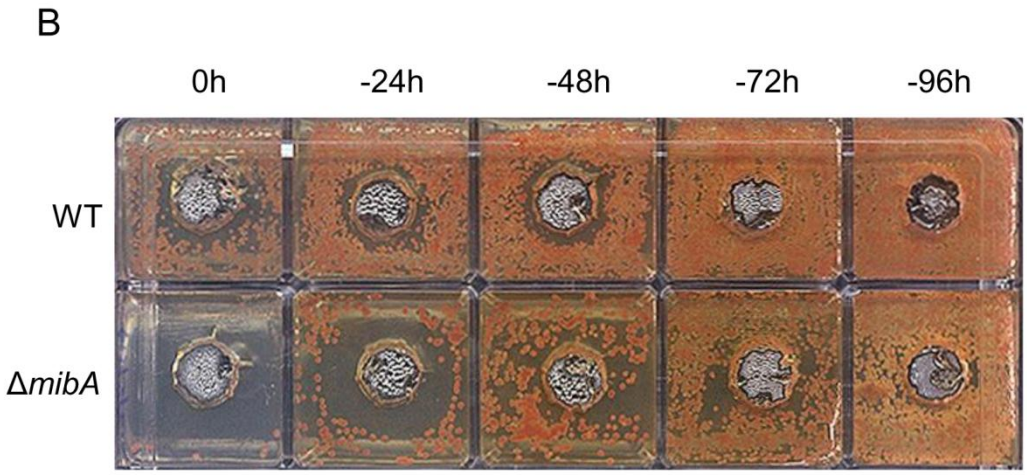

Figure 7.29 Analysis of the resistance of *M. corallina* to microbisporicin. **A** The non-producer strain DSM 44681 and the producer strain NRRL 30420 were grown in a patch across one side of V0.1 agar plates for 11 d at 30°C. NRRL 30420 was then streaked perpendicular to each of the patches and its growth monitored for several days. These images were recorded after 5 d. **B** NRRL 30420 wild type (WT) and Δ*mibA* strains were applied to V0.1 agar in wells of a square petri dish at the time points indicated above each well and were incubated at 30°C. At the zero time point wells were created in each agar plug using an inverted 200 µl Gilson pipette tip (Starlab). 40 µl of supernatant from NRRL 30420 wild type grown for 6 d in VSPA was added to each well. The plate was incubated at 30°C for several days and this image recorded after 5 d.

To narrow this effect to microbisporicin and not some other component of *M. corallina* supernatant, the above experiment was repeated but using duplicate wells of growth of each strain and applying to one wild type supernatant and to the other supernatant from the Δ*mibA* mutant grown under the same conditions. In this experiment, the wild type strain showed lower levels of sensitivity to supernatant from the wild type and did not give the clear zones of inhibition previously observed (Figure 7.30). The reason for this is not clear, but could relate to the starting inoculum used or the concentration of microbisporicin in the wild type supernatant (which was different to one used in the previous experiment, since it was prepared in parallel with the Δ*mibA* supernatant), especially as production levels have been observed to vary. There was no difference in the response of wild type growth to the wild type or Δ*mibA* supernatants (Figure 7.30). In contrast, while the *mibA* mutant was not prevented from growing at all by the Δ*mibA* supernatant, clear zones of inhibition were observed at 0 and 24 hours growth in response to the wild type supernatant (Figure 7.30). The reduced response in this experiment compared to the previous one is probably for the same reasons outlined above for the wild type strain. However, the clear difference in response to wild type and Δ*mibA* supernatant suggests that inhibition is due to the presence of microbisporicin (assuming that deletion of *mibA* doesn't affect the production of other compounds that are active against *M. corallina* and not *M. luteus*). This reinforces the notion that *mibA* influences the level of resistance of the strain.

To investigate the involvement of *mibEF* in resistance, the Δ*mibEF* mutant and the strain complemented by the *in trans* expression of *mibEF* (section 7.4) were also assessed for resistance in exactly the same manner. These two strains did not grow as well as the wild type and Δ*mibA* strains, making a direct comparison difficult. However, the two strains grew at similar densities to each other and the difference in the response to wild type and *mibA* supernatants could be compared (Figure 7.30). The Δ*mibEF* strain was able to grow at all time points in the vicinity of wells containing the Δ*mibA* supernatant but at early time points (0-48h) showed a severe growth inhibition when exposed to wild type supernatant. This suggests that, like *mibA*, *mibEF* play a role in conferring resistance to microbisporicin. The complemented strain, restored to almost wild type levels of production by the *in trans* expression of *mibEF*, similarly showed no growth response to Δ*mibA* supernatant but showed a much less severe response to the wild type supernatant than either the *mibEF* mutant (similar growth density) or the *mibA* mutant (higher growth density), and was only slightly inhibited in growth in the vicinity of the well at the earliest time point (0h). This suggests that as well as restoring microbisporicin production to the strain, *mibEF* are also capable of complementing the resistance phenotype of the *mibEF*

mutant. This analysis strongly suggests the involvement of *mibEF* in providing self-resistance to microbisporicin.

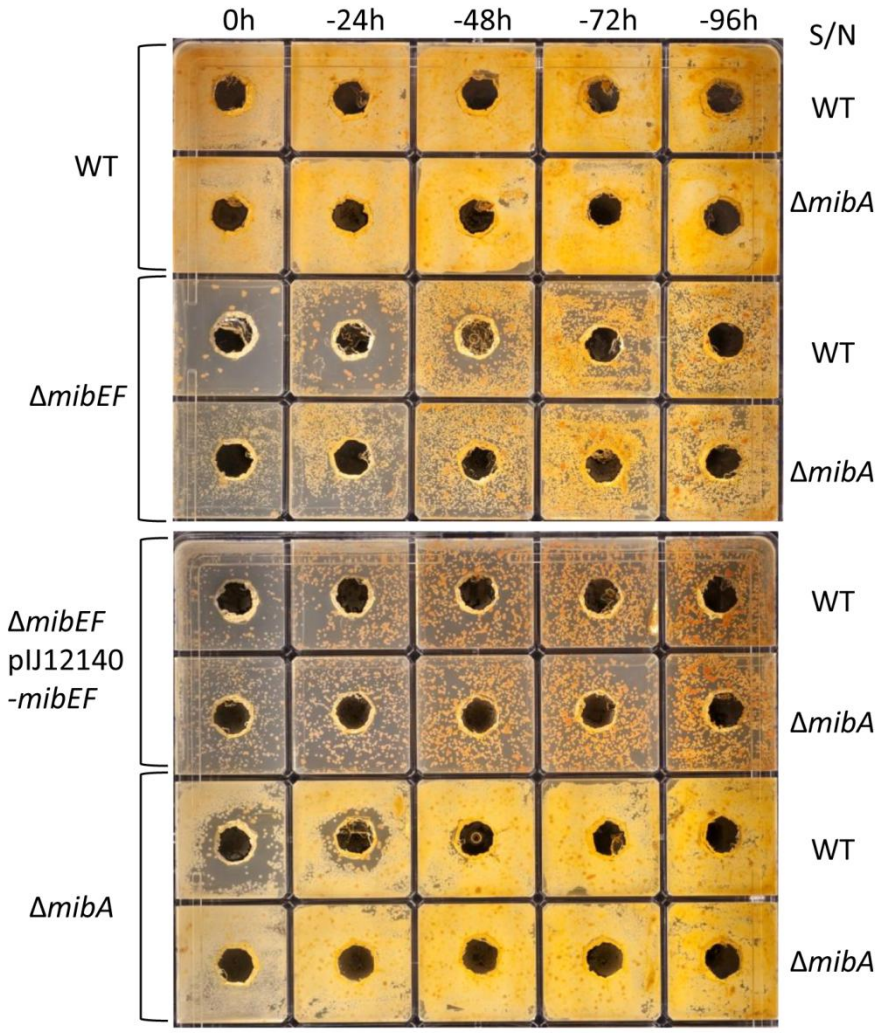

Figure 7.30 NRRL 30420 wild type (WT), Δ*mibEF*, Δ*mibEF* pIJ12140-*mibEF* and Δ*mibA* strains (as indicated on the left of the image) were applied in duplicate to V0.1 agar in wells of square petri dishes at the time points indicated above each well and were incubated at 30°C. At the zero time point wells were created in each agar plug using an inverted 200 µl Gilson pipette tip (Starlab). 50 µl of supernatant from NRRL 30420 wild type or Δ*mibA* grown for 7 d in VSPA was added to each well, as indicated on the right of the image. The plate was incubated at 30°C for several days and this image recorded after 4 d.

7.6 Regulation of *mib* gene cluster expression

The ECF sigma factor encoded by *mibX* was proposed as a potential regulator of *mib* gene expression in chapter 4 and furthermore microbisporicin was proposed to regulate its own production. Moreover, lack of microbisporicin production in the *mibX* mutant demonstrated an essential role for MibX in microbisporicin biosynthesis (section 7.3.2). To investigate the involvement of MibX in regulating expression of the *mib* gene cluster, the following experiments were carried out.

7.6.1 Analysis of *mib* gene expression in *M. corallina*

Transcription from the microbisporicin gene cluster was investigated through a reverse-transcriptase PCR approach. Wild type NRRL 30420 was previously found to grow with a lag phase of approximately 8-12 h followed by exponential growth until approximately 72 h (chapter 3). Microbisporicin production was first observed at around 46-50 h, equating to mid-exponential growth phase (chapter 3). Time points of 48 h (mid-exponential growth phase and onset of production) and 72 h (transition to stationary phase and maximum microbisporicin detection) were thus selected as appropriate time points at which to sample the mycelium for the preparation of RNA.

mib gene expression in the wild type strain was compared to that of the *mibA* and *mibX* mutants. The *mibA* deletion strain grew at approximately the same rate as the wild type strain (when compared across several growth analyses), whereas the *mibX* deletion mutant reproducibly grew at a slower rate and showed a tendency to reach a lower final optical density (at stationary phase) than the wild type and *mibA* mutant strains (Figure 7.31). Nevertheless, the same time points of 48 h and 72 h were selected for the comparison of gene expression and microbisporicin production in all three strains.

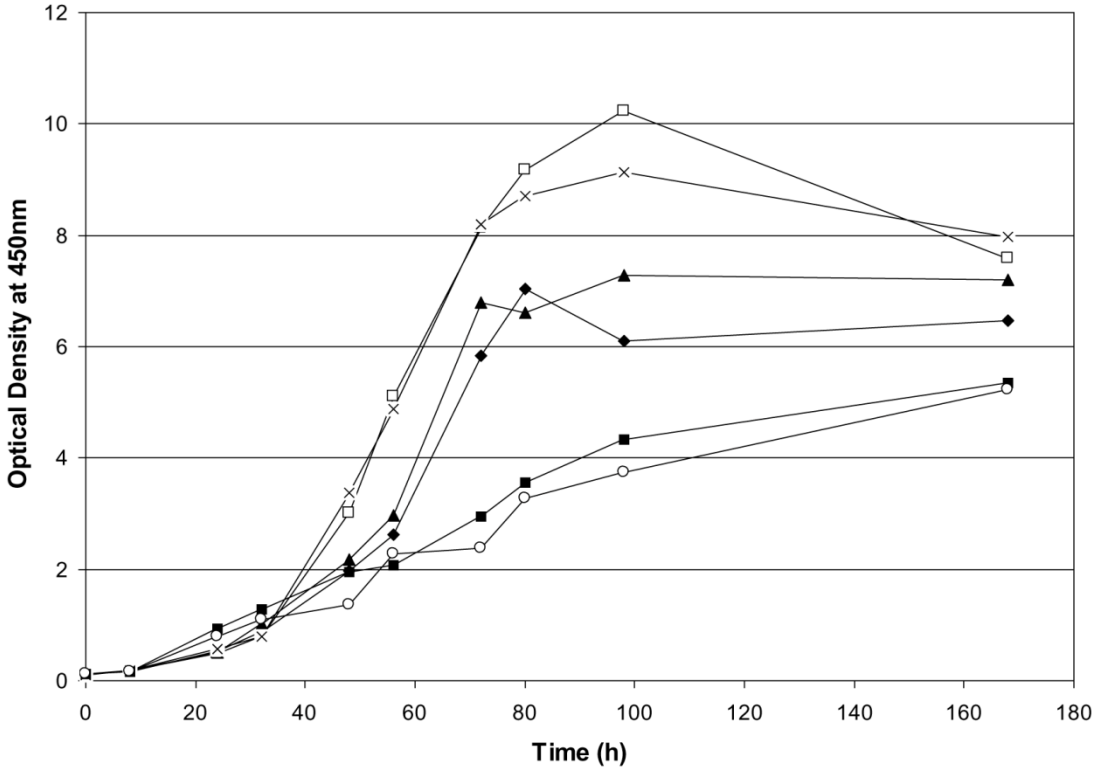

Figure 7.31 Analysis of the growth rates of *M. corallina* NRRL 30420 strains used for the collection of RNA for RT-PCR experiments at 48 h and 72 h. Optical density at 450 nm was measured for two independent cultures of each strain at each time point; *M. corallina* NRRL 30420 wild type (closed diamond ♦ and triangle ▲), Δ*mibA::aac(3)IV* (open square □ and cross ×*)* and Δ*mibX::aac(3)IV* (closed square ■ and open circle ○). While the *mibA* mutant grew at approximately the same rate as the wild type strain, the *mibX* mutant grew at a slower rate and reached a lower final optical density at stationary phase.

To provide an internal control for the amount of starting cDNA and RNA/cDNA quality, a homolog of *hrdB* from *S. coelicolor* was identified in the 454 sequence data from *M. corallina* (91% nucleotide identity across 509 nucleotides of available sequence at the 3' end of the gene). *hrdB* is commonly used as a control in RT-PCR and quantitative RT-PCR (qRT-PCR) experiments in *Streptomyces* sp. since it encodes the vegetative sigma factor σ^{70} (Hesketh *et al.* 2009). Primers LF106F and LF106R (chapter 2) were designed to amplify a 131 bp fragment from the transcript of *M. corallina hrdB.* This gene was expressed at roughly equal levels in all three strains (two replicates for each strain at both time points) at both 48 h and 72 h (Figure 7.32). Expression was somewhat higher at 48 h although this might have been expected since transcription levels would generally be expected to decrease during stationary growth (72 h). The *hrdB* homolog thus provides a useful control for RT-PCR experiments in *M. corallina*.

Expression of *mib* genes and of genes elsewhere on the sequenced cosmid pIJ12125 was analysed by RT-PCR using primers designed to lie internal to ORFs and by amplifying products typically less than 200 bp to ensure efficient amplification (Table 2.9). Of all the ORFs analysed, only one was expressed at approximately equivalent levels in all three strains at both time points (matching the result for *hrdB* expression); this was *orf1* which appears to belong to a separate transcriptional unit at one end of the insert present in pIJ12125 (Figure 7.32). For every other gene analysed (from *mibJ* to *mibN*), transcript levels were reduced in both the Δ*mibA* and Δ*mibX* mutants compared to the wild type strain at both 48 h and 72 h (Figure 7.32). As expected, the *mibA* transcript could not be detected in the *mibA* deletion strain, and was markedly reduced in amount in the *mibX* mutant when compared to the wild type strain. Similarly the *mibX* transcript was absent from the *mibX* mutant, as expected, and markedly reduced in the *mibA* mutant. Thus both *mibA* and *mibX* are required for wild type *mib* gene expression. Additionally, the similar expression patterns observed for *mibJ-mibR* suggests that these genes are co-regulated with the rest of the *mib* gene cluster and further indicates, along with the mutational studies, their involvement in microbisporicin biosynthesis.

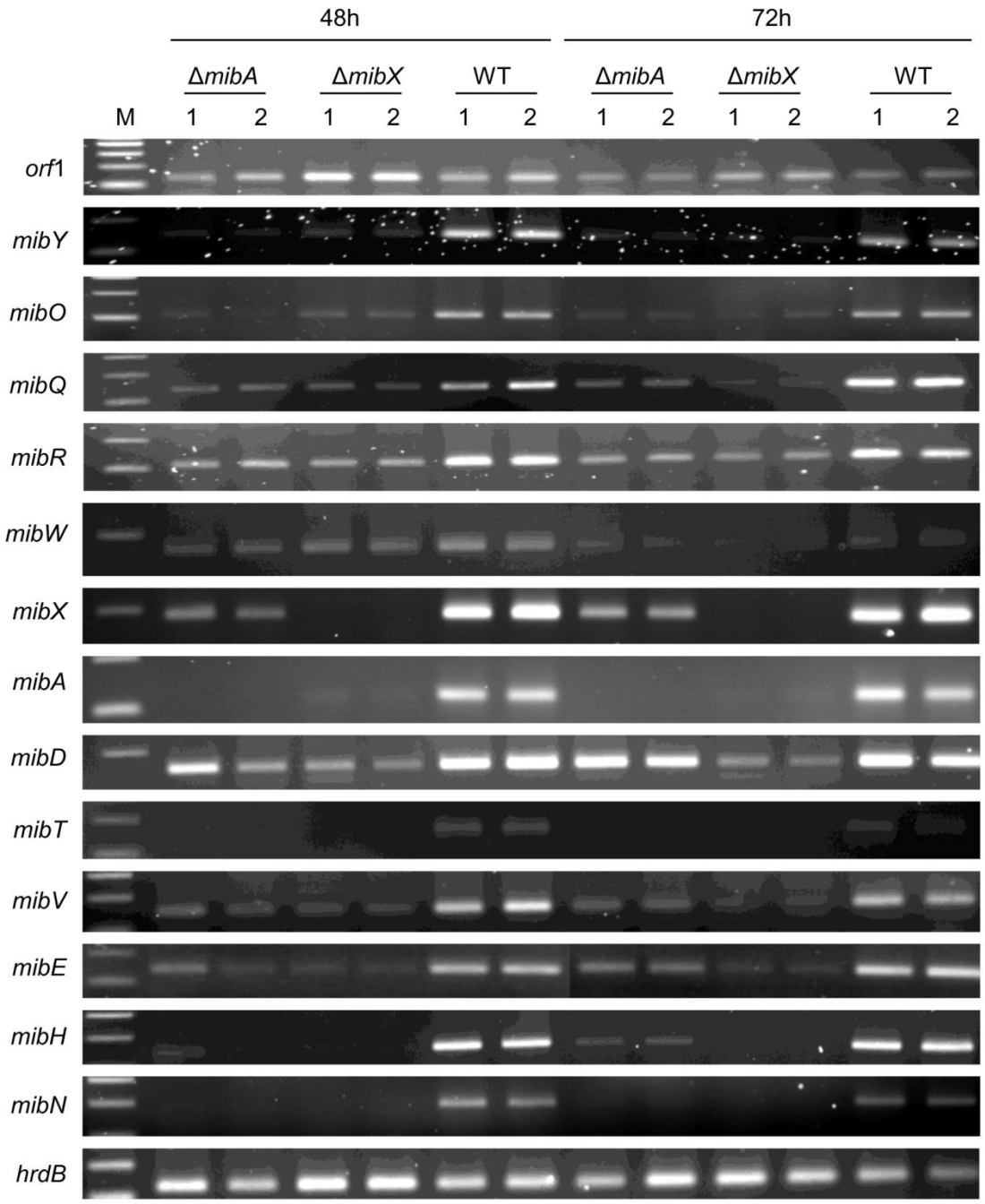

Figure 7.32 Reverse-transcriptase PCR analysis of *mib* gene expression during mid-exponential growth (48 h) and transition growth phase (72 h) in *M. corallina* NRRL 30420 wild type (WT), Δ*mibA::aac(3)IV* (Δ*mibA)* and Δ*mibX::aac(3)IV* (Δ*mibX*). Two samples of RNA were isolated from each strain (1&2) and converted into cDNA for use as the template in each reaction. Primers were designed lying internal to the open-reading frames shown on the left (primer pairs are listed in Table 2.9). Primers internal to *hrdB* from the *M. corallina* genome were used as a control (lowest panel). The marker (M) was 100 bp ladder (NEB).

7.6.2 A possible MibX consensus binding sequence

The apparent coordinate regulation of all of the analysed *mib* genes (from *mibJ* to *mibN*) suggested that it might be possible to identify a putative MibX binding motif in the intergenic regions present in the *mib* gene cluster. All possible intergenic sequences (*mibJ-mibY*, *mibO-mibQ*, *mibQ-mibR*, *mibX-mibA* and *mibV-mibE*) were thus submitted for analysis using MEME (Bailey *et al.* 1994), revealing a consensus motif of GAACC-N15-GCTAC for all five submitted sequences and present in the expected orientation in each case (Table 7.2 and Figure 7.33). Only for the transcriptional unit starting with *mibA* was this consensus not clearly identified (By manual searching a possible motif was identified 89 nucleotides upstream of *mibA* that shows homology to the consensus sequence in the -35 region but less so in the -10 region (Figure 7.33C). This motif was not identified at any other locations in the sequence of pIJ12125). The consensus sequence bears the hallmark of those identified for well-characterised ECF sigma factors in other systems (the AAC motif in the -35 region and the clustering of CGT nucleotides in the -10 region) (Staron *et al.* 2009). Taken together, these results suggest that these transcriptional units are co-regulated by the ECF sigma factor MibX.

Intergenic Region	Strand	Start	P-Value	Consensus Sequence
orf1-mibJ	+	41	$3.93e^{-11}$	GGGACGCACT GAACCGATCCGGCGTCTTCTGCTACAGCC CTGGTGTGGA
mibO-mibQ	+	35	$4.37e^{-12}$	TTCTCCACGT GAACCGGCGGGTGGCCGGACGCTACGTAC AGGGC
mibQ-mibR	+	216	$6.33e^{-12}$	GCTCCTGCGT GAACCTTCGTACGCCATCCCGCTACGTAC ACCTCCGAAA
mibX-mibA	-	93	$1.91e^{-12}$	AGATCCCCCC GAACCGGTACGGCAGCCGACGCTACATAC GAACGTGTGC
mibV-mibE	+	185	$4.73e^{-12}$	GCACGGCCGC GAACCGCCCACTCCCCACCCGCTACGTAC GGCGGGAAGG

Table 7.2 Table of MEME output data. Intergenic regions used for the input of the analysis were *orf1-mibJ*, *mibO-mibQ*, *mibQ-mibR*, *mibX-mibA* and *mibV-mibE.* "Start" indicates the position (in nucleotides) of the first nucleotide in the given consensus sequence (purple) before the annotated start codon of the open-reading frame. The consensus sequence is given in purple and the flanking sequences in green.

A

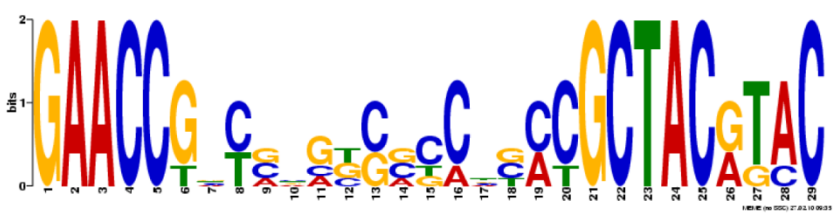

B

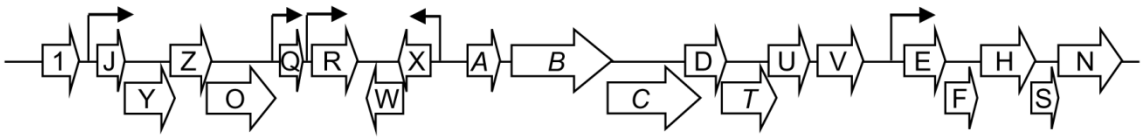

C

```
mibE      GAACCGCCCACTCCCCACCCGCTACGTAC
mibQ      GAACCGGCGGGTGGCCGGACGCTACGTAC
mibR      GAACCTTCGTACGCCATCCCGCTACGTAC
mibX      GAACCGGTACGGCAGCCGACGCTACATAC
mibJ      GAACCGATCCGGCGTCTTCTGCTACAGCC
mibA      GAACCATTATTGACACTAGTAGTCCGAAA
          *****           * *
```

Figure 7.33 A MEME output graphic for the analysis of the intergenic regions of the microbisporicin gene cluster showing the consensus sequence. **B** Positions of predicted consensus sequences (arrows) in the microbisporicin gene cluster. See also Table 7.2. **C** An alignment of the consensus sequences identified upstream of the listed open-reading frames. A potential consensus motif was manually identified 89 nucleotides upstream of *mibA* but only shares close homology at the -35 consensus region (yellow) and not the -10 (blue).

7.6.3 Analysis of the interaction between MibW and MibX

MibW was proposed in chapter 4 as an anti-sigma factor that regulated the activity of MibX. In this model MibW would bind to MibX, possibly through its predicted N-terminal cytoplasmic extension, and thus tether it to the membrane where MibW would be embedded via its predicted transmembrane helices. To determine if an interaction occurred between MibW and MibX, a bacterial-two-hybrid (BACTH) experiment was carried out.

The bacterial-two-hybrid system involves the use of two fragments of the adenylate cyclase enzyme from *Bordetella pertussis* which, when brought into close proximity, can reform a functional enzyme, the activity of which can be monitored through a variety of assays (Karimova *et al.* 1998). The adenylate cyclase fragments (T18 and T25) are attached separately to the two potentially interacting proteins, the two fusion proteins expressed in *E. coli* and adenylate cyclase activity monitored. The BACTH is particularly useful since it functions even when protein partners are tethered at the membrane (as is predicted to be the case for MibW) and, unlike other methods, does not depend upon reconstitution of transcription factors at their DNA binding sites.

mibX was fused to the gene encoding the T18 fragment of adenylate cyclase in two vectors; pUT18 in which MibX would be at the N-terminus of the fusion protein (pIJ12367) and pUT18C in which MibX would be at the C-terminus of the fusion protein (pIJ12368) (Figure 7.34). Thus each terminal region of MibX would be free to interact with MibW in one or other of the two fusion proteins. *mibW* was used to produce three different fusion constructs, all based on pT25 (also called XP458). The transmembrane helix prediction for MibW (TMHMM; see chapter 4; Figure 4.12) indicated that the N-terminus would extend into the cytoplasm and create a possible binding site for the ECF sigma factor. By contrast the C-terminus of MibW was predicted not to extend into the cytoplasm and would be very close to the membrane. Attaching the T25 fragment at the C-terminus might prevent possible interactions due to steric hindrance with the membrane and transmembrane fold of the protein. In all cases, MibW was therefore located at the C-terminus of the fusion protein (Figure 7.34). pIJ12369 contains the full-length *mibW* ORF, pIJ12370 encodes only the N-terminal portion of the protein that is expected to project into the cytoplasm (amino acids 1-73) and pIJ12371 encodes only the C-terminal transmembrane portion of MibW (amino acids 74-255). This was to determine whether only one segment of the protein could elicit an interaction or whether the overall structure of the protein was important. As a positive control for the interaction, pT25, pUT18 and pUT18C containing the leucine zipper fragment (zip) from GCN4 (yeast protein) were

used. This domain has been shown to interact strongly with itself and to provide a reliable positive control for bacterial-two hybrid studies (Karimova *et al.* 1998). Negative controls were the empty vectors.

The constructs were introduced by transformation into *E. coli* BTH101, a strain specifically developed for BACTH experiments in which the adenylate cyclase gene, *cya*, has been inactivated. The plasmids were transferred in pairs (Table 7.3). In the initial experiment, designed to determine whether an interaction could be detected and whether the attachment of the T18 fragment at the N- or C-terminus of MibX was important, positive control and test strains were plated on MacConkey-Maltose indicator agar and plates were incubated at 30°C for 4 d. MacConkey agar contains a pH indicator that turns red/purple under acidic conditions. In BTH101, the absence of adenylate cyclase activity means that cyclic AMP cannot be synthesised and therefore the catabolite activator protein CAP is unable to activate expression of maltose catabolic enzymes (Karimova *et al.* 1998). BTH101 is thus unable to utilise the maltose in this medium. If adenylate cyclase activity is restored by a protein-protein interaction, maltose can be utilised as a substrate. The fermentation of maltose acidifies the medium, allowing the interaction to be observed as a colour-change from white/pale pink to deep red/purple. After 4 days, a clear interaction could be seen on the positive control plate using T25-zip and T18-zip, but not with T18C-zip (Figure 7.35). The reason for this is unknown but the T18C-zip construct might be defective. A clear interaction was also apparent between T25-full length MibW and either T18-MibX or T18C-MibX (Figure 7.35). This suggests that MibX and MibW interact strongly in *E. coli* and that the position of the T18 fragment does not affect the ability of MibX to interact. In contrast there was no indication of a clear interaction from either the N-terminus or C-terminus of MibW alone, although the N-terminal constructs gave slightly more colouration than the C-terminal, suggesting that the N-terminus of MibW might be involved in the interaction (Figure 7.35).

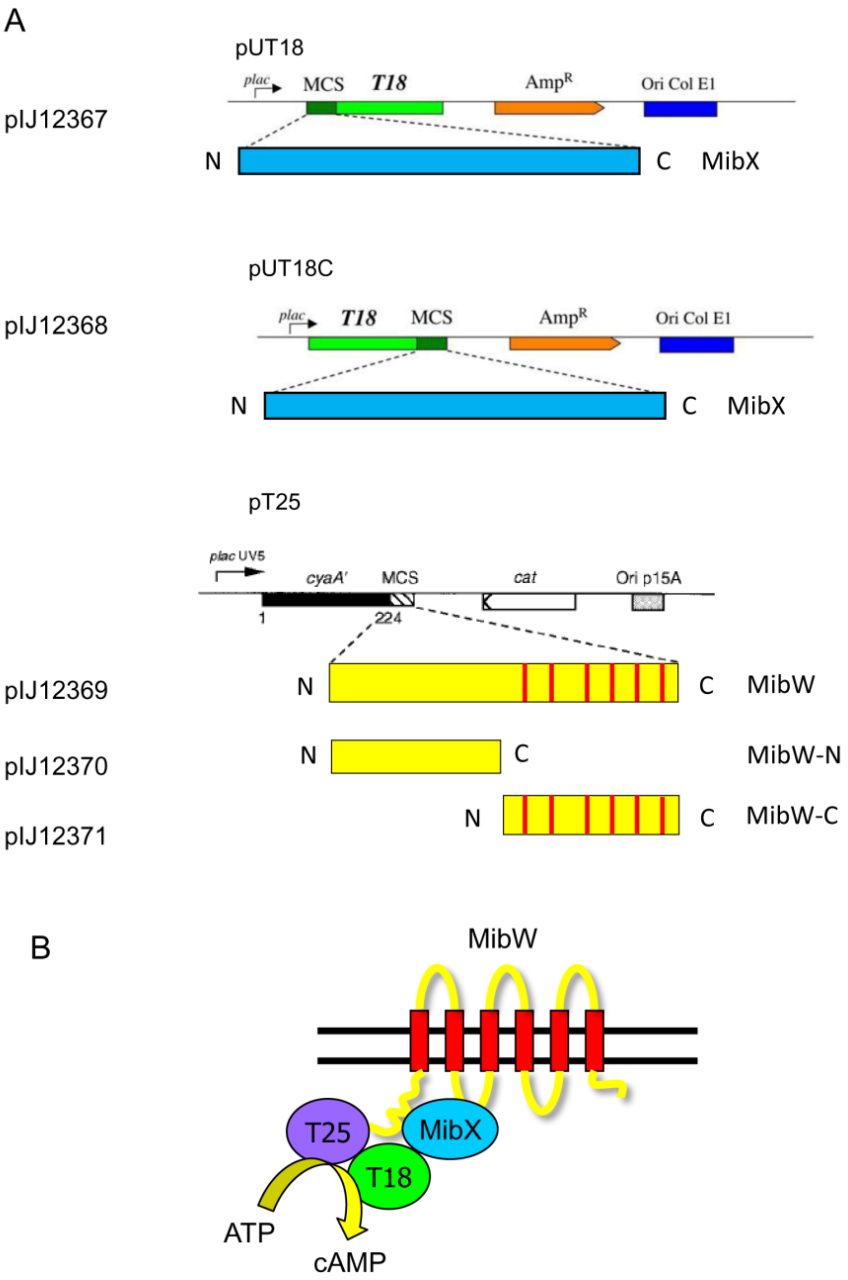

Figure 7.34 A The constructs used for bacterial-two hybrid analysis of the interaction between MibX and MibW. Construct names are shown on the right. The map of each vector is displayed (taken from Euromedex BACTH kit manual (pUT18 and pUT18C) and Karimova *et al.* 1998 (pT25)). Transmembrane helices of MibW are shown as red lines. **B** A model for the interaction between MibW and MibX in the bacterial-two hybrid experiment. MibW is embedded in the membrane by six transmembrane helices (red). MibW was attached to T25 at the N-terminus. MibX was attached to the T18 fragment at both the N- and C-terminus (not shown). Interaction between the T25 and T18 fragments of adenylate cyclase results in the synthesis of cyclic AMP (cAMP) from ATP (Karimova, *et al.* 1998).

Table 7.3 Combination of constructs transferred to BTH101 for bacterial-two hybrid experiments.

Name	Type	T25 plasmid	T18 plasmid	Selection
T25-zip T18-zip	positive	pKT25-zip (XP461)	pUT18-zip	Carb Chl
T25-zip T18C-zip	positive	pKT25-zip (XP461)	pUT18C-zip	Carb Chl
T25-MibW T18-MibX	test	pIJ12369 (pKT25-*mibW*)	pIJ12367 (pUT18-*mibX*)	Carb Chl
T25-MibW-N T18-MibX	test	pIJ12370 (pKT25-*mibW-N*)	pIJ12367 (pUT18-*mibX*)	Carb Chl
T25-MibW-C T18-MibX	test	pIJ12371 (pKT25-*mibW-C*)	pIJ12367 (pUT18-*mibX*)	Carb Chl
T25-MibW T18C-MibX	test	pIJ12369 (pKT25-*mibW*)	pIJ12368 (pUT18C-*mibX*)	Carb Chl
T25-MibW-N T18C-MibX	test	pIJ12370 (pKT25-*mibW-N*)	pIJ12368 (pUT18C-*mibX*)	Carb Chl
T25-MibW-C T18C-MibX	test	pIJ12371 (pKT25-*mibW-C*)	pIJ12368 (pUT18C-*mibX*)	Carb Chl
T25 T18-MibX	negative	pKT25	pIJ12367 (pUT18-*mibX*)	Carb Chl
T25-MibW T18	negative	pIJ12369 (pKT25-*mibW*)	pUT18	Carb Chl
T25-MibW-N T18	negative	pIJ12370 (pKT25-*mibW-N*)	pUT18	Carb Chl
T25-MibW-C T18	negative	pIJ12371 (pKT25-*mibW-C*)	pUT18	Carb Chl
T25 T18	negative	pKT25	pUT18	Carb Chl

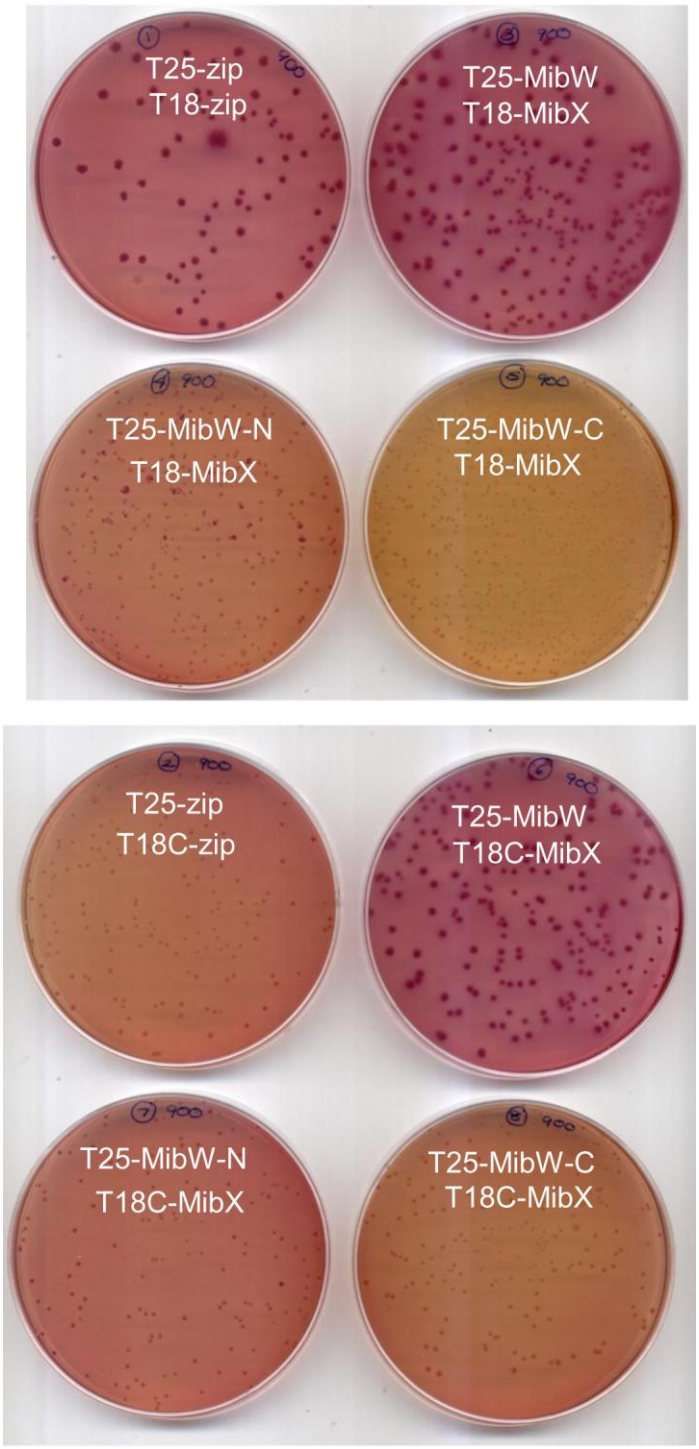

Figure 7.35 A bacterial-two hybrid experiment to investigate the interaction between MibW and MibX. The listed pairs of constructs (see also Table 7.3) were transferred into the BACTH reporter strain *of E. coli* BTH101 by transformation. The resulting transformants were selected on MacConkey/Maltose agar containing 100 µg/ml carbenicillin and 25 µg/ml chloramphenicol and incubated at 30°C for several days before phenotypes were recorded.

To further characterise the interaction, the experiment was repeated. Only the pUT18-*mibX* construct, and not the pUT18C-*mibX* construct, was used since the positive control plasmid pUT18C-zip gave a poor result and the location of MibX in the fusion protein appeared not to matter for the interaction. The negative controls listed in Table 7.3 were also carried out. The same result was obtained, and the negative controls confirmed that the interaction was specific to the presence of both MibW and MibX. To quantify the extent of the interaction, two clones from each interaction plate were sampled and assayed for β-galactosidase activity as described in chapter 2. β-galactosidase activity was plotted as the average value from the two independent clones and error bars were generated for each clone (Figure 7.36). This analysis revealed an extremely strong interaction between MibW and MibX, with β-galactosidase activity above that of the leucine-zipper control fragments. It furthermore reinforced the earlier conclusion that neither the N-terminus or C-terminus of MibW alone are capable of interacting strongly with MibX, the latter yielding no more than background levels of β-galactosidase activity. Consistent with the plate assays, the N-terminal segment of MibW gave slightly higher activity than the C-terminal segment, but this is unlikely to be significantly above background levels and may not have biological relevance.

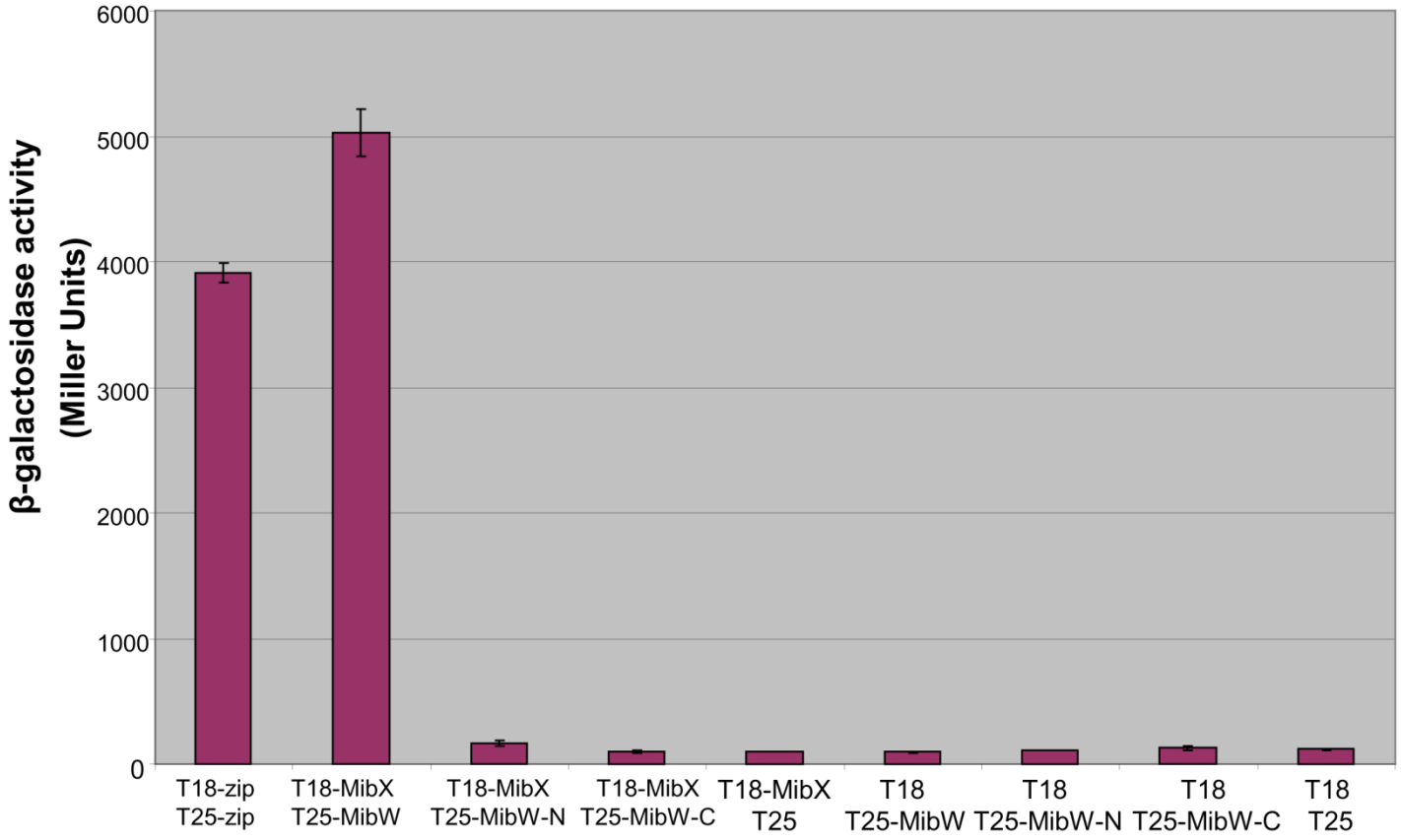

Figure 7.36 A bacterial-two hybrid experiment to investigate the interaction between MibW and MibX. The listed pairs of constructs (see also Table 7.3) were transferred into the BACTH reporter strain *of E. coli* BTH101 by transformation. The resulting transformants were selected on MacConkey/Maltose agar containing 100 µg/ml carbenicillin and 25 µg/ml chloramphenicol and incubated at 30°C for several days before two independent clones were picked and subjected to a β-galactosidase assay. The graph was plotted with the average activity in Miller units of the two clones and the error bars show the two individual values.

7.6.4 Reporter assays to investigate MibX activity

Analysis of *mib* gene expression by RT-PCR indicated a dependence of *mib* gene expression on *mibX*, but did not indicate whether this reflected direct interaction of MibX with the promoter regions of the *mib* genes. Furthermore, the lack of a clear consensus motif upstream of *mibA* suggested that MibX might not be responsible for direct activation of expression of the *mibA* operon. Finally many ECF sigma factors auto-regulate their own high level expression (Staron *et al.* 2009). An indication that this might be the case is clear from RT-PCR results for *mibW* (in the same operon as *mibX*), the expression of which appears to be decreased in the absence of *mibX* (Figure 7.32). To investigate these features of MibX activity, a reporter system based on the production of light by *luxAB* genes was employed.

Reporter plasmids pIJ12341, pIJ12342, pIJ12343 and pIJ12344 were constructed based on pIJ5972, which integrates into the ΦC31 attachment site and contains a promoterless *luxAB* cassette which encodes the enzyme luciferase (Figure 7.37). Luciferase expression is detectable by the application of the substrate N-decanal, the degradation of which results in light production, observable with a NightOwl camera. pIJ12341 contains the intergenic region between *mibX-mibA* (with the putative *mibA* promoter upstream of *luxAB*) as well as the *mibX* open-reading frame (with expression driven from its own promoter), whereas pIJ12342 contains only the intergenic region. pIJ12343 contains the intergenic region between *mibX-mibA* (with the putative promoter of *mibX* upstream of *luxAB*) and the *mibX* gene itself whereas pIJ12344 contains only the putative promoter (Figure 7.37). These constructs, along with pIJ5972, were introduced into the heterologous host *S. coelicolor* M1146. Three independent clones were selected for each strain and grown in duplicate for 2 d on Difco Nutrient Agar (where *S. coelicolor* does not sporulate, since spore formation can interfere with the assay; Figure 7.37)). Light production was assessed by exposing the mycelium to N-decanal on filter discs for 5 minutes before detecting light production using a NightOwl Camera. No light production was detected from the vector only control strain or from strains containing pIJ12341 or pIJ12342. Very low level light production was observed from strains containing pIJ12344, suggesting that the *mibX* promoter region possesses a low level of constitutive activity, at least in *S. coelicolor*. In contrast, high levels of light production were observed from clones containing pIJ12343, suggesting that the presence of the ECF sigma factor increases expression from the *mibX* promoter. This suggests that *mibX* can positively auto-regulate its own expression.

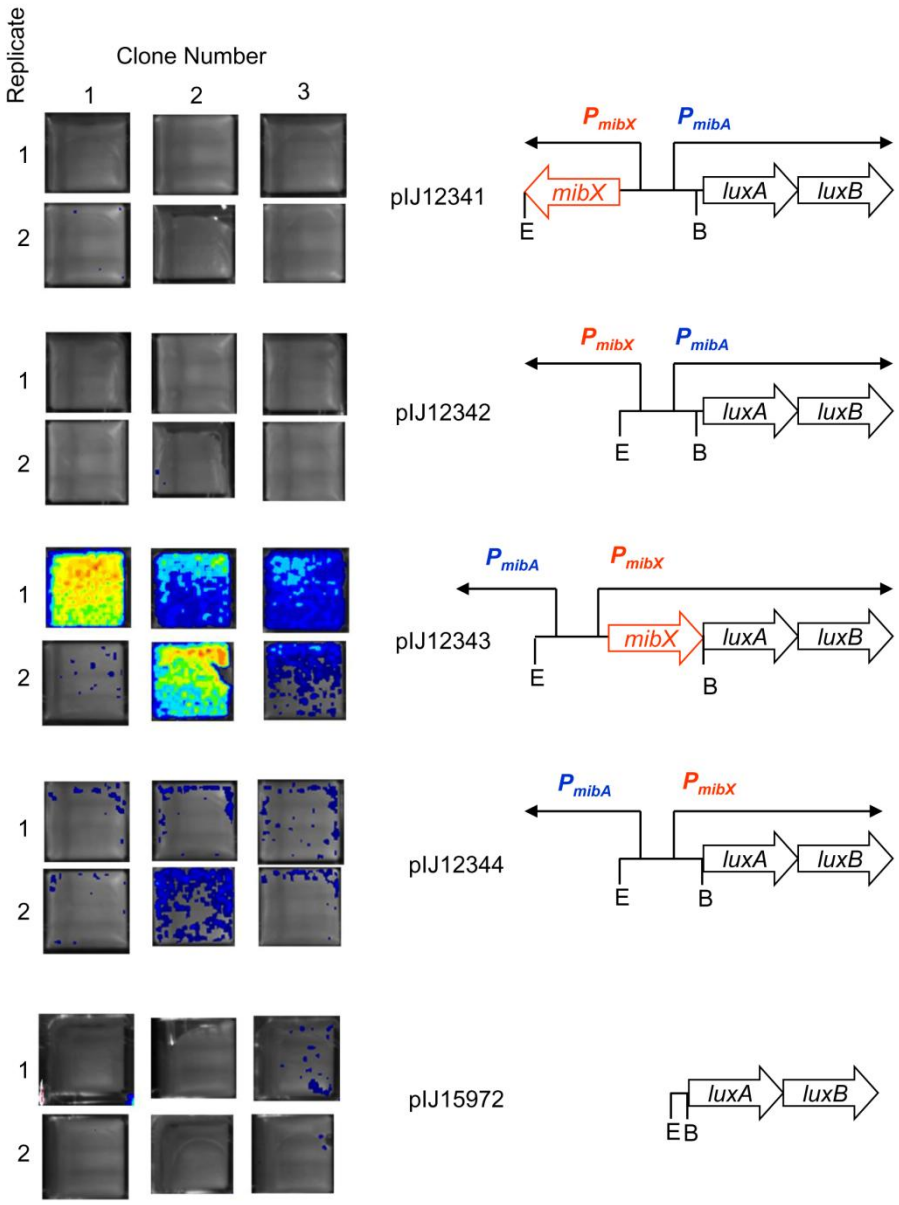

Figure 7.37 Luciferase-reporter analysis of MibX activity in *S. coelicolor* M1146. The vector pIJ5972 (bottom panel) contains promoterless *luxAB*. pIJ12341 contains the assumed promoter of *mibA* (P_{mibA}) and the *mibX* open-reading frame as shown. pIJ12342 contains only the assumed promoter of *mibA* (P_{mibA}). pIJ12343 contains the assumed promoter of *mibX* (P_{mibX}) and the *mibX* open-reading frame as shown. pIJ12344 contains only the assumed promoter of *mibX* (P_{mibX}). Three independent clones of *S. coelicolor* M1146 (shown side by side) containing these constructs were grown in duplicate (indicated by numbers on the left of the images) for 2 d on Difco nutrient agar and light production visualised using a NightOwl Camera (Berthold) after applying the substrate N-decanal on filter paper discs for 5 minutes. The images shown are representatives chosen from three independent experiments.

7.7 Discussion and Summary Points

7.7.1 Discussion

The development of a method for the transfer of DNA (of up to 50 kb) into *M. corallina* represents a milestone for the *Streptosporangiceae* family, members of which had proved largely refractory to genetic manipulation. Using a similar method, developed in conjunction with this work, *Nonomuraea*, another member of this family and the producer of the glycopeptide antibiotic A40926, has also been genetically manipulated (Marcone *et al.* 2010a). Interspecies conjugation thus presents a useful tool for the manipulation of these rare actinomycetes, many of which are important secondary metabolite producers.

The use of ΦC31 integrating vectors such as pSET152 in *M. corallina* provides a useful tool for the introduction of DNA into these organisms. Other vectors, commonly used in *Streptomyces* genetics, might be adapted for use in these strains, for example the ΦBT1 integrating vectors (Gregory *et al.* 2003) and those carrying constitutive promoters such as *ermE** (Bibb *et al.* 1994). Unfortunately such tools may need to be developed individually for different genera. For example, a study of a number of promoters, commonly used in *Streptomyces,* in *Actinoplanes friuliensis* indicated that promoters which showed high level expression in *Streptomyces,* such as *ermE**, had poor expression levels in *A. friuliensis* and vice versa (Wagner *et al.* 2009). In fact, in *A. friuliensis*, the *aac3*(IV) promoter, which drives the expression of the apramycin resistance gene, gave the highest expression levels (Wagner *et al.* 2009). However, the availability of genome sequence data for *M. corallina* should facilitate this process by allowing the identification of promoter sequences for *M. corallina* genes likely to show high or constitutive activity, such as that of the ribosomal proteins or elongation factors (Kieser *et al.* 2000).

The transfer of DNA into *M. corallina* by conjugation from *E. coli* could be further optimised. The method utilised in this study could be improved particularly in efficiency of transfer and in the time for ex-conjugants to appear. There was a high failure rate for conjugations, mostly when transferring large cosmids for homologous recombination, but also for some other vectors, and in some cases certain constructs could not be transferred at all. For example, several attempts were made to transfer pIJ12131, the integrative vector carrying the *mib* gene cluster for heterologous expression, into the non-producer strain DSM 44682, but this never resulted in the growth of ex-conjugants. When constructing gene inactivation mutants by homologous recombination, very often multiple attempts at cosmid transfer were carried out before mutant clones could be obtained and in some cases only one or two clones were isolated, for example Δ*mibTU*. This might be

improved by decreasing the size of the delivery vector to improve transfer efficiency whilst retaining sufficient homologous sequence for recombination (Flett *et al.* 1997). This was attempted for the Δ*mibTU* deletion construct where 7 kb of sequence downstream of *mibN* was also deleted from the cosmid. When making the Δdownstream deletion mutant, this improved conjugation efficiency compared to the full length cosmid, but this was not found to be the case for the *mibTU* mutant. The reason for this is not clear, but there are clearly aspects of the conjugation process between *M. corallina* and *E. coli* that should be explored further in order to improve the method.

There was also a significant difference in the amount of time required for the growth of clones resulting from the transfer of a small integrating vector, like pSET152 (about 10-14 days), and a cosmid by homologous recombination (from 3-8 weeks). This is likely to be a product of the efficiency of transfer into mycelial fragments. In the case of pSET152, a small vector, transfer efficiency would be expected to be high, and in addition integration at the ΦC31 attachment site should also be highly efficient (Flett *et al.* 1997). This means that a large proportion of compartments in each recipient mycelial fragment may have the resistance marker and thus the starting inoculum for growth in the presence of selection will be high. In the case of transferring a cosmid, the size of the DNA fragment will decrease the transfer rate but also the efficiency of integration into the genome will be lower since it relies on homologous recombination (Flett *et al.* 1997). This means that many fewer mycelial compartments will carry the resistance marker and so the starting inoculum for growth in the presence of selection will be much lower. The intrinsically slow rate of growth of *M. corallina* means that these differences in inoculum size will have a significant effect on the rate of appearance of clones. The length of time required to acquire clones for the acquisition of mutants made gene inactivation very time consuming. Furthermore, even when clones had been identified, their selection through several rounds of growth (requiring at least 7-14 days for each round of growth) and the slow growth of *M. corallina* upon transfer to liquid culture (about 6 days) meant that construction of each mutant took on average 3-4 months. With further optimisation of the method this might be improved. Further exploration of the metabolism and nutritional requirements of *M. corallina* may help to improve growth rates under laboratory conditions.

The replacement of *mibA* with the apramycin resistance cassette by homologous recombination in *M. corallina* NRRL 30420 provided further evidence that the *mib* gene cluster is responsible for the production of microbisporicin but also acted as a proof-of-principle for the deletion of other genes from the *mib* gene cluster. The translated amino acid sequence of *mibA* provides very good evidence that this gene encodes the

prepropeptide of microbisporicin since its primary sequence exactly matches that predicted from the structure of microbisporicin (see chapter 4). Deletion of *mibA* thus gave the expected phenotype, i.e. lack of microbisporicin biosynthesis.

In addition to abolishing microbisporicin biosynthesis, deletion of *mibA* also led to more efficient production of spores compared to the wild type. To date there are no reports of a negative effect of a lantibiotic upon sporulation by a producing species. Nisin and subtilin have been well-documented to prevent spore outgrowth in strains of *Bacillus sp.* but have not been described to inhibit the formation of spores (Liu *et al.* 1992; Chan *et al.* 1996). SapB, a lanthionine-containing peptide produced as a surfactant by *S. coelicolor*, is involved in promoting the formation of aerial mycelium and therefore sporulation (Kodani *et al.* 2004). A non-lantibiotic surfactant produced by *Bacillus subtilis,* surfactin, can however inhibit aerial mycelium formation in *S. coelicolor* (Straight *et al.* 2006). It is possible that, like SapB, microbisporicin can function as a surfactant, but like surfactin, has a negative rather than positive effect upon sporulation. The formation of aerial mycelium was not obviously different in the wild type and *mibA* mutant strains and so unlike these other compounds the effect of microbisporicin appears to be only on spore formation. However, there does appear to be a link between the production of microbisporicin and the inability of NRRL 30420 to produce spores efficiently under laboratory conditions. Interestingly, other strains of *M. corallina,* such as DSM 44681 and DSM 44682, appear not to produce microbisporicin but do sporulate under laboratory conditions (chapter 3).

The inability of *mibA,* provided *in trans* and expressed from its assumed native promoter, to complement the *mibA* deletion is interesting. Lack of complementation by *mibABCD* suggests that this was not due to a polar effect on *mibBCD* expression. However it is possible that a mutation was introduced during construction of the *mibABCD* plasmid that prevented complementation. Since the *mibA* promoter allowed expression of *mibD in* pIJ12139-*mibD*, it is clearly capable of driving *in trans* gene expression, apparently ruling out any positional effect on its functionality. Alternatively, deletion of *mibA* may have resulted in a second site mutation that was not detectable by Southern blot or PCR analysis. This could be determined by transferring the complementation constructs into the two other clones of the *mibA* mutant. Another possibility is that *mibA*, *mibB, mibC* and *mibD* need to be expressed in a specific ratio with other genes in the *mib* gene cluster and that this is disrupted by *in trans* expression. Alternatively the placement of the construct within the genomic context of the ΦC31 attachment site might affect expression levels of some genes. These hypotheses might be tested by restoring the wild type *mibA* gene at its own locus by homologous recombination. However this method could mask the

involvement of a second site mutation which, if present near to the *mibA* gene, would also be replaced by the recombination event. The ability to complement the deletion of *mibA in trans* would provide a useful system for the production of microbisporicin variants (Boakes *et al.* 2009).

Attempts to delete *mibZ-mibR* highlighted the need for more than 3 kb of homologous flanking sequence for efficient recombination in *M. corallina*. It also demonstrated the utility of pIJ12126 as an alternative cosmid for the construction of mutations in the left hand end of the *mib* gene cluster. Deletion of *mibZ-mibR*, a 3.6 kb region containing several genes of unknown function, resulted in a non-producing strain of *M. corallina*. This deletion is unlikely to have had a polar effect on downstream genes since *mibXW* are transcribed in the opposite orientation. At least one of *mibZ*, *mibO*, *mibQ* or *mibR* are therefore essential for microbisporicin biosynthesis. This might be further investigated by the *in trans* provision of each of these genes, individually and in combinations. This could be less time-consuming than making each mutant individually but assumes that these genes can be complemented *in trans*. These results give weight to the inclusion of these genes of unknown function within the *mib* gene cluster.

Deletion of *mibX* abolished detectable production of microbisporicin and suggested a role for the ECF sigma factor in the regulation of *mib* gene expression. The phenotype of the mutant was complemented by the *in trans* expression of *mibX* from its own promoter. Interestingly, complementation was more pronounced on agar medium than in liquid fermentation (discussed further below). As with several of the other *mib* genes, *in trans* expression of *mibX* did not restore the mutant to wild type levels of production, at least in liquid culture. This might reflect an altered level of gene expression at the ΦC31 integration site. Furthermore, in the case of an ECF sigma factor, which is normally expressed at a defined ratio with its cognate anti-sigma factor, separating the sigma factor and anti-sigma factor genes might have uncoupled the regulatory machinery with an adverse effect on production levels.

mibD was predicted to be a flavin-dependent decarboxylase involved in the formation of the *S*-[(*Z*)-2-aminovinyl]-D-cysteine at the C-terminus of microbisporicin. The function of this modification in the lantibiotics that possess it is not known. Deletion of *mibD* from the microbisporicin gene cluster abolished bioactivity, as did mutation of *epiD* involved in epidermin production in *S. epidermis*, suggesting similar roles for the two genes in lantibiotic maturation (Augustin *et al.* 1992). Moreover no microbisporicin variants, even those with the mass predicted for the unmodified compound, were detected in the supernatant of the Δ*mibD* strain. The absence of *mibD* may result in the production of a

compound that is either not able to exit the cell or that is rapidly degraded in the extracellular environment. Interestingly, many lantibiotics possess (methyl-)lanthionine bridges or *S*-[(*Z*)-2-aminovinyl]-D-cysteines at their C-termini (Chatterjee *et al.* 2005) that might serve to prevent carboxypeptidase degradation in the external environment.

mibTU appear to encode a two-component ABC-transporter which, on the basis of similarity to CinTH, are predicted to be involved in the export of microbisporicin. Deletion of *cinTH* in *S. cinnamoneus* resulted in a strain that did not show antimicrobial activity suggesting that *cinTH* are essential (S. O'Rourke, personal communication). Deletion of *mibTU* by contrast did not result in a non-producing strain of *M. corallina*. Since only one clone of this mutant was obtained it is possible that a second site mutation in this strain overcomes the block caused by the mutation. However, pIJ12131 Δ*mibTU* in two independent clones of *Nonomuraea* was also found to produce microbisporicin (chapter 6). This suggests that *mibTU* are not essential for microbisporicin biosynthesis. *spaT,* encoding a transport protein in the subtilin biosynthetic gene cluster, was also found to be non-essential for subtilin production although other phenotypic changes were noted that may have reflected accumulation of the compound inside the cells (Klein *et al.* 1992). This suggests that other host-encoded transporters can partially complement the absence of the specific lantibiotic transport system. This was also true for PepT, the transporter for Pep5 (Meyer *et al.* 1995), and in the epicidin 280 gene cluster that does not encode a LanT homolog (Heidrich *et al.* 1998). Finally like the cinnamycin gene cluster, the actagardine gene cluster also encodes a two-component ABC transporter thought to be involved in lantibiotic export (*garTH*) (Boakes *et al.* 2009). These genes were not essential for heterologous production of actagardine in *S. lividans* (Robert Bell, personal communication). It is possible that one of the other transporters encoded by the *mib* gene cluster (MibYZ, MibEF and/or MibN) can compensate for deletion of *mibTU*. Double and triple mutants of the transporters in the *mib* gene cluster would be required to determine this although due to the absence of production in a *mibEF* mutant it would be difficult to determine whether *mibEF* can complement a *mibTU* deletion in this way. It is also possible that microbisporicin could be exported by host transport systems.

The function of MibV could not be predicted on the basis of sequence similarity and thus deletion of *mibV* was crucial to the assessment of its role in microbisporicin biosynthesis. Interestingly Δ*mibV* exhibits a very similar phenotype to Δ*mibH*; the production of only deschloromicrbisporicin, suggesting a role for MibV in tryptophan chlorination. It is very unlikely that the deletion of *mibV* has a polar effect on the expression of *mibH* since inactivation of the intervening *mibEF* genes prevents high level microbisporicin production and this is not seen in the *mibV* mutant. Furthermore, the *mibV* and *mibEFH* genes

appear to lie within separate operons. It is possible that MibV acts as a transcriptional activator of *mibH* expression and thus in its absence prevents *mibH* transcription. However, MibV is not predicted to be a DNA-binding protein and RT-PCR experiments/motif searches suggest that the putative *mibEFHSN* operon is regulated by MibX. MibV could also function post-translationally to positively regulate MibH activity. This has not been previously documented for tryptophan halogenase enzymes and it is not clear why such regulation would be necessary.

MibV could play a direct role in tryptophan chlorination. This would not be entirely novel for tryptophan halogenase activity since many halogenases act on substrates bound to carrier proteins, some of which contribute to the specificity of the reaction (van Pee *et al.* 2006). Such proteins may be required for the correct presentation of the substrate to the enzyme, as apparently occurs in the chlorination of non-ribosomally synthesised peptides (Dorrestein *et al.* 2005; Rachid *et al.* 2009). This could be particularly important for a large substrate such as a peptide. However the homolog of MibV encoded by *Nocardiopsis dassonvillei* is in a lantibiotic gene cluster that does not include a tryptophan halogenase. This suggests a broader role for MibV beyond halogenation.

The identification of ions in the MALDI-ToF spectra of Δ*mibV* mutant clones with m/z values lower than those typically seen for deschloromicrobisporicin might suggest a stabilising or protective role for MibV. Should MibV function as a chaperone for MibA modification it might protect the prepropeptide from degradation (perhaps the cause of these lower molecular weight compounds) and present the MibA substrate to the tryptophan halogenase. This is not without precedent since *cinorf7* from the cinnamycin biosynthetic gene cluster has also been postulated to act as a chaperone, although it is essential for cinnamycin biosynthesis (S. O'Rourke personal communication). The inability of *mibV,* expressed *in trans,* to complement deletion of *mibV* might indicate that a specific ratio of MibV to MibA is important for the function of MibV.

MibEF were predicted to confer microbisporicin resistance in *M. corallina* based on homology to the LanFEG systems of other lantibiotics. Deletion of *mibEF* resulted in markedly reduced and delayed production of microbisporicin. In other well-characterised lantibiotic gene clusters it is not clear whether a link exists between resistance and compound production. In *B. subtilis*, where *spaEFG* confer resistance to subtilin, deletion of these genes does not render the strain incapable of subtilin biosynthesis, although susceptibility was slightly increased (Klein *et al.* 1994). However, this likely reflects the presence of a second contributing immunity system, SpaI. The effect of disrupting both systems on subtilin biosynthesis has not been reported. Similarly, deletion of *nisF*, *nisE*

and *nisG* in *L. lactis* 6F3, although affecting sensitivity to nisin, did not affect nisin production (Siegers *et al.* 1995). However, deletion of *nisI* decreased production to 20-40% of wild type levels (Ra *et al.* 1999). The epidermin biosynthetic gene cluster of *S. epidermis* encodes only one resistance mechanism, EpiFEG, although it has not been reported whether mutation of these genes affects biosynthesis. In a heterologous host, co-expression of *epiFEG* along with the biosynthetic genes did increase levels of production (Peschel *et al.* 1996). Finally, in the cinnamycin biosynthetic gene cluster of *S. cinnamoneus*, deletion of the resistance gene *cinL* resulted in the complete absence of bioactivity (S. O'Rourke personal communication). Deletion of *mibEF* gave a phenotype similar to that of Δ*cinL*. At early time points there was no indication of bioactivity suggesting a complete block in biosynthesis or compound export. At later time points very low levels of bioactivity were detected that might be explained by release of the compound through cell lysis. This suggests that *mibEF,* although not absolutely required for the biosynthesis of the compound, may in some way regulate its export from the cell or indeed its biosynthesis. MibEF may provide a mechanism of self-resistance and in the latter's absence the organism may respond by blocking microbisporcin export or production, suggesting the presence of a mechanism for sensing resistance levels. Alternatively, MibEF might themselves provide the only mechanism for export of microbisporicin.

MibH was predicted to be a tryptophan halogenase responsible for chlorination of the tryptophan at position 4 of microbisporicin, likely in collaboration with the flavin reductase MibS. The *mibH* mutant produced only the non-chlorinated form of the compound, corroborating this hypothesis. The mutant strain retains the ability to inhibit the growth of *M. luteus,* suggesting that chlorination is not essential for bioactivity of microbisporicin. In fact, in most cases both the Δ*mibH* and Δ*mibV* mutants exhibited higher than wild type levels of bioactivity, suggesting that deschloromicrobisporicin might be more active against *M. luteus*. Alternatively the absence of chlorine on this molecule could influence the diffusion rate of the antibiotic. Further analysis of these non-chlorinated variants may reveal differences in properties such as solubility, or differences in activity against other bacterial species. Results of previously reported MIC measurements suggest that the non-chlorinated MF-BA-1768β_1 exhibited higher MICs than the chlorinated MF-BA-1768α_1 against certain species of *Staphylococcus* and *Enterrococcus* (Lazzarini *et al.* 2005). Another study reported MICs for MF-BA-1768β_1 that were lower than MF-BA-1768α_1 for some species and higher for others (Lee 2003). Microbisporicin exhibits increased activity against Gram-negative pathogens when compared with many other lantibiotics (Lazzarini *et al.* 2005; Castiglione *et al.* 2008). It is possible that by increasing the polarity of the molecule, chlorination may increase the ability of the compound to permeate the Gram-

negative outer membrane. This could be assessed by comparing the activities of the chlorinated and non-chlorinated forms against Gram-negative bacteria.

Both *mibH* and *mibS* were required to complement the deletion of *mibH in trans*. This may be due to an uncoupling of *mibHS* expression or due to a polar effect on *mibS* expression in the *mibH* mutant. MibH and MibS are very likely to be working together to chlorinate microbisporicin *in vivo*. *In trans* expression of *mibHS* was unable to complement the phenotype of the mutant fully back to wild type, despite being expressed from what is likely to be their native promoter, suggesting that removing the genes from their natural location in the *mib* cluster may impact the efficiency with which microbisporicin is processed and modified. Additionally, the transcript is likely to differ from that of the natural locus which would also likely include *mibEF* and possibly *mibN*. This could influence the stability of the transcript and affect the expression level of *mibHS*.

MibN has homology to members of the sodium/proton antiporter family, particularly those associated with NRPS and glycopeptide biosynthetic gene clusters. To determine whether *mibN* plays a role in the biosynthesis of microbisporicin it was deleted from the gene cluster. The resulting strain has an essentially wild type phenotype suggesting that MibN is not involved in microbisporicin biosynthesis and could be a remnant of the horizontal transfer of *mibHS* into the *mib* gene cluster (as discussed in chapter 4). The phenotype of the *mibN* mutant could however be masked by redundancy with other transporters in the *mib* gene cluster or other sodium/proton antiporters encoded within the *M. corallina* genome. One possible clue to a role for MibN in microbisporicin biosynthesis was seen in MALDI-ToF mass spectra from both clones of the Δ*mibN* mutant which showed higher ratios of the non-sodium adduct variants to sodium adduct variants compared to the wild type strain. This might suggest that MibN influences the balance of intra- and extra-cellular sodium. Whether this is associated with the production of microbisporicin is not clear. The genes in the 7 kb segment of the genome which follows *mibN* are unlikely to be part of the *mib* gene cluster since their deletion had no effect on microbisporicin production and resulted in a spectrum of compounds identical to that of the wild type strain.

Complementation of deletions in *mib* genes was largely accomplished through the *in trans* expression of the respective gene or genes from their predicted native promoters at the ΦC31 integration site. The construction of pIJ12139 and pIJ12140 provides expression vectors for use in *M. corallina* although it is likely that these promoters are highly regulated and they are not likely to be suitable for constitutive expression. Nevertheless, the successful use of pIJ12139 and pIJ12140 for *in trans* complementation indicates that

promoter regions do indeed lie within the intergenic regions *mibX-mibA* and *mibV-mibE*. These promoter sequences could be further characterised by S1 nuclease protection studies.

Some deletions in the *mib* gene cluster could not be complemented *in trans*, namely Δ*mibA* and Δ*mibV*. As discussed this is unlikely to reflect polarity and does not appear to be due to lack of activity of the *mibA* promoter region, which was able to drive *mibD* expression. However transcription at a different site in the genome could be inhibited or impaired for other reasons, such as local genome structure. Many of the other constructs were unable to fully complement the mutant phenotypes suggesting that this may be a general issue when attempting to complement mutations *in trans*. Interestingly, deletion of *pepI* from the Pep5 gene cluster of *S. epidermis* could similarly not be complemented *in trans* by provision of *pepI* alone but only when *pepA* was also present (Pag *et al.* 1999). This was shown to be due to the presence of RNA secondary structure between the *pepI* and *pepA* open-reading frames which was required to stabilise the *pepI* transcript (Pag *et al.* 1999). Although this is unlikely to be the case for *mibA*, where both the up- and downstream regions were supplied in the complementation experiments, it indicates that other factors can impede *in trans* complementation. The inability to fully complement these deletions *in trans* might be an indication of interesting regulatory features of the *mib* gene cluster. Alternatively, differential mRNA stability of the *in trans* transcripts compared to the wild type transcripts might be playing a role.

Wild type *M. corallina* exhibited some sensitivity to microbisporicin during early stages of vegetative growth, and *mibA* was shown to be essential for wild type levels of resistance to microbisporicin in NRRL 30420. This has commonly been seen in other lantibiotic-producer species in which the lantibiotic auto-regulates the expression of the gene cluster (Draper *et al.* 2008). For example, disruption of *nisA* was found to increase nisin sensitivity in *L. lactis* (Ra *et al.* 1999). Furthermore, near wild type levels of resistance could be conferred on non-producer strains of *L. lactis* by *nisI* but only when *nisA* and the genes essential for nisin biosynthesis were also provided (Kuipers *et al.* 1993a). This was later found to be due to a requirement for mature nisin for the expression of the *nisI* and *nisFEG* resistance genes (Ra *et al.* 1999). However the involvement of the prepropeptide gene in resistance is not always due to auto-regulation, as described for Pep5 above

In an auto-regulatory model for microbisporicin production, in the wild type strain sub-inhibitory concentrations of microbisporicin would be expected to induce expression of other genes of the *mib* gene cluster, including the resistance genes, before the organism is exposed to inhibitory levels. Therefore, at very early time points even the wild type is

likely to be somewhat affected by the exogenous addition of microbisporicin. In the *mibA* mutant, the absence of low-level microbisporicin biosynthesis would prevent expression of the resistance genes resulting in microbisporicin sensitivity. Non-susceptibility would only occur once mycelial growth had already occurred or ceased.

mibEF were also required for wild type levels of resistance and the mutant phenotype was complemented by the *in trans* expression of *mibEF*. Since deletion of *mibA* also reduced the level of microbisporicin resistance, *mibEF* may mediate their effect by influencing microbisporicin biosynthesis. Further analysis will be required to determine whether there is a specific role of *mibEF* in resistance.

It would be interesting to look at the resistance phenotypes of other *mib* mutants as well. The assay design could also be improved by inoculating strains at a similar density by first determining the colony forming units of each inoculum. A further test of the role of *mibEF* in resistance would be through constitutive expression in a heterologous host. These experiments would be further improved by the acquisition of purified microbisporicin, allowing resistance levels to be quantified.

The pattern of gene expression observed in the *mibA* and *mibX* deletion mutants when compared to the wild type strain indicates a strong reliance on the products of both genes for efficient transcription from promoters in the gene cluster. A consensus binding motif, with similarity to those identified at other ECF sigma factor-controlled promoters, in several operons of the *mib* gene cluster adds further weight to the predicted role of MibX. MibW, a putative anti-sigma factor, interacted very strongly with MibX in *E. coli* providing experimental evidence for its predicted role in inhibiting MibX activity. Luciferase reporter experiments in *S. coelicolor* indicated that MibX likely auto-regulates its own expression but it does not appear to directly induce expression from the putative *mibA* promoter. The sensitivity of the luciferase reporter assay in *Streptomyces* is not known and it is possible that expression from the *mibA* promoter is too low to be detected by this method. This could be determined by quantitative RT-PCR. Since a heterologous host was used for these experiments it will be interesting to use similar constructs in wild type NRRL 30420 strain and some of the deletion mutants to see whether similar results are obtained in the natural producer.

Taken together the results presented in this chapter suggest a model in which MibX is required for high level expression of the microbisporicin gene cluster (including its own gene) and in which its activity depends on low levels of production of microbisporicin. In such a model, low levels of microbisporicin (potentially produced by expression from a starvation-induced promoter) or cell envelope stress (induced by the likely interaction of

microbisporicin with Lipid II) prevents MibW from interacting with MibX, thus releasing the ECF σ factor and resulting in high-level expression of the entire microbisporicin gene cluster.

The proposed mechanism by which MibXW function to regulate *mib* gene expression might also explain the difference between the level of bioactivity of the Δ*mibX* mutant complemented with *mibX* on agar medium, where bioactivity was high, with that observed in liquid fermentation, where only very low levels of bioactivity were detected. A higher local concentration of microbisporicin is likely to build up around mycelium grown on agar medium than in liquid culture. If the regulatory mechanism is already uncoupled through *in trans* expression of *mibX* at a separate locus from *mibW,* the lower level of microbisporicin in liquid culture may not be sufficient to induce high level expression of the biosynthetic genes.

Interestingly, the operon beginning with *mibA* does not have the identified ECF sigma factor consensus binding motif, suggesting that regulation by MibX may be mediated through a gene in one of the other MibX-regulated operons. A likely candidate for this is *mibR*, which encodes a protein with a helix-turn-helix DNA binding domain. Such a scenario would also explain the absence of expression from the *mibA* promoter in the luciferase reporter assay since even in the presence of MibX another component would be required for high level expression. Other *mib* genes of unknown function could also play a role in the proposed regulatory model. As discussed in chapter 4 it is possible that the release of MibX by MibW is mediated via regulated-intramembrane proteolysis. If this is the case, other components would be required and proteins such as MibJ, MibY and MibZ might fulfil these roles. It will be interesting to explore this mechanism of regulation in more detail in future.

7.7.2 Summary Points

- A method for the genetic manipulation of *M. corallina* was developed.
- Several *mib* genes were inactivated in *M. corallina* and the resulting phenotypes were assessed.
- *mibA* was essential for microbisporicin biosynthesis and its deletion increased the sensitivity of *M. corallina* to microbisporicin.
- *mibZ-mibR, mibX* and *mibD* were essential for microbisporicin biosynthesis.
- Deletion of *mibV* and *mibH* resulted in the production of deschloromicrobisporicin.
- *mibTU*, *mibN* and genes downstream of the *mib* gene cluster were not essential for microbisporicin biosynthesis.
- Deletion of *mibEF* resulted in a severe decrease in microbisporicin production and increased the sensitivity of *M. corallina* to microbisporicin.
- MibHS were essential for chlorination of microbisporicin.
- Wild type expression of the *mib* gene cluster was dependent on both *mibA* and *mibX*.
- An ECF sigma factor consensus binding motif was identified in all *mib* operons except that starting with *mibA*.
- MibW and MibX interact strongly in *E. coli*.
- MibX increased expression from the *mibX* promoter in *S. coelicolor*.
- MibX did not increase expression from the *mibA* promoter in *S. coelicolor*.

Chapter 8 – Discussion

8.1 A Model for Microbisporicin Biosynthesis

The results presented in this work, including both the bioinformatic and genetic analyses of the microbisporicin gene cluster, suggest a model for the biosynthesis of biosynthesis of microbisporicin and its regulation in *M. corallina*. This model provides a framework for the development of future research goals and will be presented in this section.

Microbisporicin likely auto-regulates its own biosynthesis. This is a common regulatory strategy for lantibiotic biosynthesis. As described in Chapter 7, deletion of *mibA* resulted in a decrease in the level of transcription of *mib* genes. In a quorum-sensing model low-level constitutive transcription of the *mib* genes would be expected to occur throughout growth, allowing the slow accumulation of microbisporicin, at sub-inhibitory levels, in the extracellular environment. Alternatively, low level production of microbisporicin might be induced, for example in response to starvation. For example, in *S. coelicolor* antibiotic biosynthesis in response to nutrient limitation was shown to be regulated by the stringent factor ppGpp (Hesketh *et al.* 2001; Hesketh *et al.* 2007). Through either mechanism, at a certain threshold concentration, microbisporicin would trigger an induction of *mib* gene expression leading to high level production. The extracellular level of microbisporicin must be sensed at the cell surface and relayed to result in a change in gene expression. An ECF sigma factor-anti-sigma factor pair, encoded by the *mib* gene cluster, were suggested to fulfil this function.

The ECF sigma factor MibX was essential for microbisporicin biosynthesis and transcription of the *mib* genes was dependent on the presence of MibX. This suggests that MibX is a positive regulator of *mib* gene expression either through a direct or indirect mechanism. The identification of ECF sigma factor consensus binding sequences within five intergenic regions in the *mib* gene cluster implies that MibX directly regulates the expression of these operons through interaction with RNA polymerase. The operons proposed to be regulated by MibX are *mibJYZO*, *mibQ, mibR, mibXW* and *mibEFHSN*. MibX was capable of inducing its own transcription, as shown by lux reporter assays. The *mibA* operon does not possess the ECF sigma factor consensus binding motif, and expression from the *mibA* intergenic region was not induced in the presence of MibX in a reporter assay, suggesting that MibX does not directly regulate *mibA* transcription.

MibW was predicted on a bioinformatic basis to be a putative anti-sigma factor for MibX. The location of *mibW* downstream of *mibX* is reminiscent of the transcriptional coupling of other ECF sigma factor-anti-sigma factor pairs (Staron *et al.* 2009). This gene arrangement is conserved in a range of actinomycetes that encode homologs of MibX and MibW (Chapter 4). The predicted transmembrane profile of MibW suggests a membrane-embedded location with an N-terminal cytoplasmic tail. Bacterial-two-hybrid analysis revealed a strong interaction between MibW and MibX in *E. coli* reinforcing the model of MibW as an anti-sigma factor for MibX. By comparison to other such systems, MibW would anchor MibX at the cell membrane in the absence of an activating signal. In the presence of the signal, MibX would be released allowing it to interact with RNA polymerase at target promoters (Figure 8.1).

This model for the regulation of *mib* gene expression by MibXW is reminiscent of the two-component regulatory systems employed by other lantibiotic gene clusters. For example, the presence of extracellular nisin is thought to activate NisK, a membrane embedded histidine kinase, which subsequently phosphorylates the response regulator, NisR, conferring the ability to interact with promoter binding sites in the nisin gene cluster. The exact signal detected by the histidine kinases involved in lantibiotic auto-regulation have not been deduced but is possibly through the direct interaction of the lantibiotic with the extracellular face of the kinase or through an indirect effect of the lantibiotic action on the cell envelope through Lipid II binding (i.e. cell envelope stress). A similar situation could be postulated for microbisporicin. In the simplest model, microbisporicin outside the cell membrane either interacts directly with MibW or induces a structural change in MibW through the induction of cell envelope stress, possibly through an interaction with Lipid II. A structural change in MibW would disrupt the binding interaction with MibX, releasing it to the cytoplasm (Figure 8.1).

A more complex regulatory model for the release of MibX can also be hypothesised. This model must be considered for two reasons. Firstly, it is common for ECF sigma factors to be released from membrane embedded anti-sigma factors through regulated intramembrane proteolysis (RIP); such is the case for RsiW (see Chapter 4) (Heinrich *et al.* 2009b). Secondly, the conservation of *mibJ*, *mibY* and *mibZ* homologs with the homologs of *mibXW* in all the actinomycete genomes in which they have been identified so far (see Chapter 4) strongly suggests a functional linkage. The conservation of these five genes together in the absence of lantibiotic biosynthetic genes in some bacterial genomes (*Streptosporangium roseum* and *Frankia* sp.) suggests that their function concerns MibXW and not lantibiotic biosynthesis *per se*. In the well-studied RsiW model, sigma factor release is brought about by the action of two proteases (PrsW and RasP)

that cleave RsiW, and an ABC-transporter, EcsAB, although the exact function of the transporter is not known. Both the site-1 and site-2 proteases are membrane-embedded proteins, the site-1 protease PrsW cleaving RsiW outside the membrane and the site-2 protease RasP within the membrane. MibJ is a transmembrane protein that could fulfil the role of a protease for the intramembrane cleavage of MibW. However, a two-step cleavage is normally observed for RIP in other systems and there is no clear candidate for a second protease, although it could possibly be encoded elsewhere in the genome (Heinrich *et al.* 2009b). This might provide an explaination for the lack of heterologous expression in *Streptomyces* sp. MibYZ are predicted on the basis of amino acid similarity to be a two-component ABC transporter.

A model can be envisaged in which one or both of these components (MibJ and/or MibYZ) is involved in "sensing" the presence of microbisporicin at the cell surface and subsequently relaying this signal, resulting in the cleavage of MibW and release of MibX. Possibly the ABC-transporter MibYZ is required to transport microbisporicin inside cells in order for it to be detected. For RsiW, it has been suggested that in the absence of EcsAB the protease RasP is inactive and that EcsAB might be responsible for removing a compound that inactivates RasP, and lantibiotics were suggested as a possibility (Heinrich *et al.* 2008). The function of MibYZ may therefore be to remove microbisporicin from the cell membrane (where it likely binds Lipid II and would somehow interfere with MibJ activity) and in so doing releases the protease activity of MibJ. With the available experimental evidence it is not possible to conclude whether MibJYZ are essential for microbisporicin biosynthesis but there is some indication that they could function in the regulation of the release of MibX from MibW (Figure 8.1).

The release of MibX from MibW by either model would increase the level of transcription from each of the *mib* operons. This would create a feed-forward mechanism for *mibXW* expression. In addition, *mibJYZ* would also be transcribed at a higher level and, if involved in regulation, would also contribute to this feed-forward mechanism. Additionally several other genes would be expressed. *mibQ* expression is likely MibX-dependent and the ECF sigma factor consensus sequence was found upstream of *mibQ*. Although conserved in gene clusters from other organisms that have *mibXWJYZ* genes, *mibQ* homologs mainly appear to be present when lantibiotic genes are also encoded nearby (see Figure 4.10). This might argue that MibQ is not part of the MibX regulatory pathway. MibQ is predicted to be a lipoprotein (Chapter 4). Since many lantibiotic gene clusters encode lipoproteins involved in resistance (*lanI*) this could be a possible function for MibQ. The involvement of MibQ in resistance might explain why NRRL 30420 Δ*mibEF* shows some residual level of microbisporicin production. It would thus follow that MibQ would be expressed, in a MibX

dependent manner, to prepare the cell for the production of high levels of microbisporicin. The same is likely true of MibEF, which are also encoded within an operon with an upstream ECF sigma factor consensus motif and are predicted to provide resistance to microbisporicin (Figure 8.1).

mibR expression is also predicted to be directly MibX-dependent. MibR is predicted to be a DNA-binding protein which might function as a transcriptional regulator. The absence of a clear ECF sigma factor consensus motif upstream of *mibA* might be explained by the presence of MibR. The indirect activation of high level *mibA* transcription by MibX through the induction of *mibR* would introduce a slight delay in high level biosynthesis of microbisporicin. This would allow the establishment of resistance before the accumulation of toxic levels of the compound (Figure 8.1). This delay may be enhanced by the requirement of an activation step for MibR binding to its DNA target site. For example a signal may be involved which communicates the resistant status of the cell prior to high level biosynthesis.

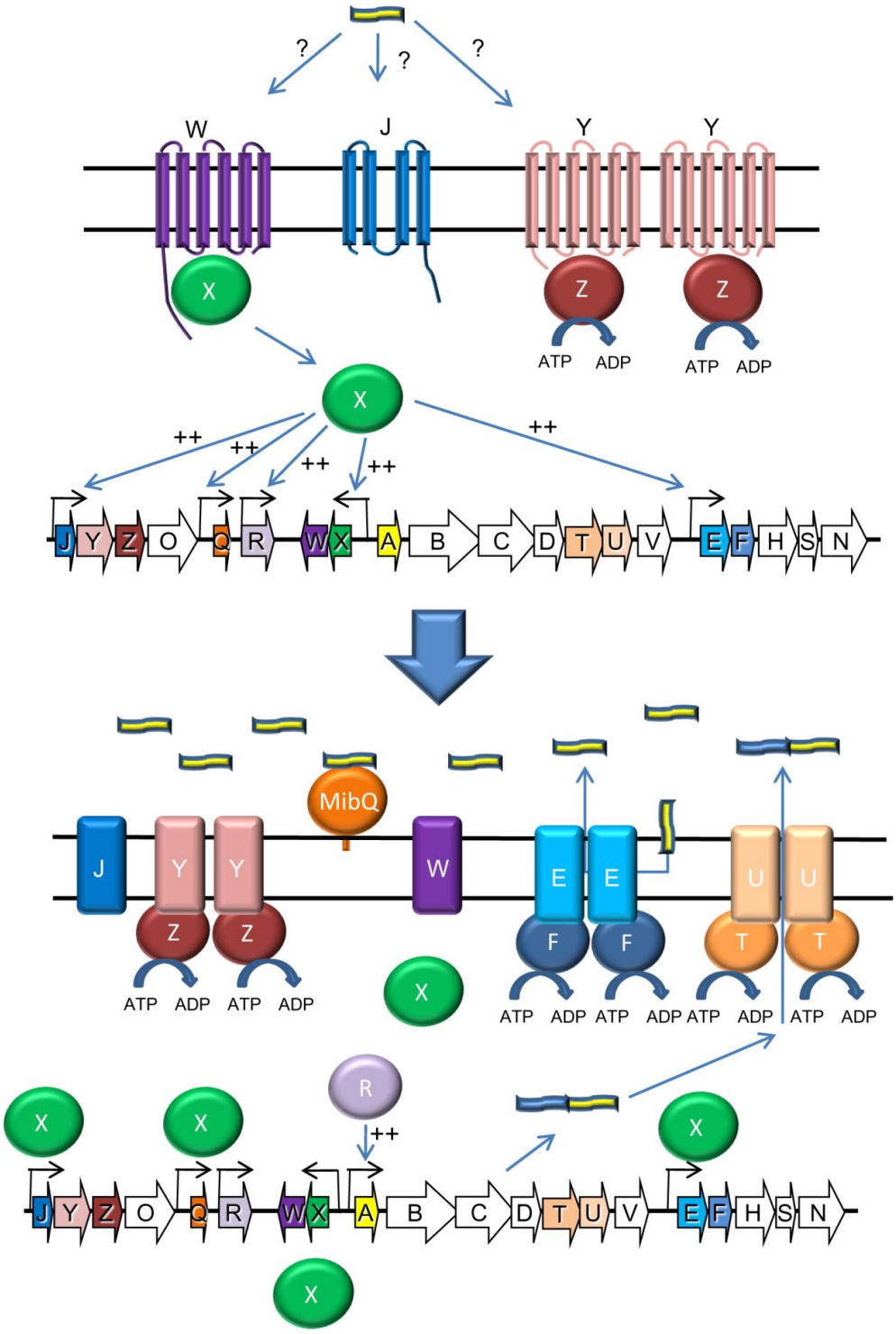

Figure 8.1 A model for the mechanism of regulation of the biosynthesis of microbisporicin by *M. corallina* as described in the text. The upper panel represents the status of the cell at early time points before the high level induction of microbisporicin biosynthesis. The lower panel represents the status of the cell at mid-late exponential phase at the transition to high level microbisporicin production.

The above proposed model for regulation is supported by a recently sequenced genome from *Thermobispora bispora*. This organism is a thermophilic actinomycete isolated from manure, the genome sequence of which was recently released to the public database. Amino acid sequence similarity searches revealed the presence of a group of genes in this organism encoding proteins with extremely high level amino acid sequence similarity (between 69-88% identity) to the proteins encoded by *mibXWJYZ* (the proposed "regulatory module") and to *mibQ* and *mibEF* (Figure 8.2). However, no lantibiotic genes homologous to any of the *mib* biosynthetic genes could be identified either near this gene cluster or in the rest of the genome of this organism. This suggests that *Thermobispora* may have acquired, likely by horizontal transfer, the genes required for resistance to a microbisporicin-like compound (*mibQ* and *mibEF*), as well as the genes required to express them in response to the presence of that compound (*mibXWJYZ*). Furthermore the same ECF sigma factor consensus motif could be identified upstream of the respective operons encoding these homologs in *T. bispora* using MEME (Figure 8.2).

The induction of high level expression of the *mibA* operon would result in the production of active microbisporicin. The MibA prepropeptide would be modified by MibB, MibC and MibD to introduce the lanthionine, methyl-lanthionine and AviCys bridges (Figure 8.3). It is likely that the prepropeptide will be supported by the action of the chaperone MibV. MibV is likely involved in directing the chlorination of tryptophan through the concerted action of MibH and MibS, and may also direct proline hydroxylation by MibO (Figure 8.3). MibV may also prevent degradation of the prepropeptide during maturation and export. MibTU likely constitute the major, but not exclusive, route of export of microbisporicin from the cell (Figure 8.1).

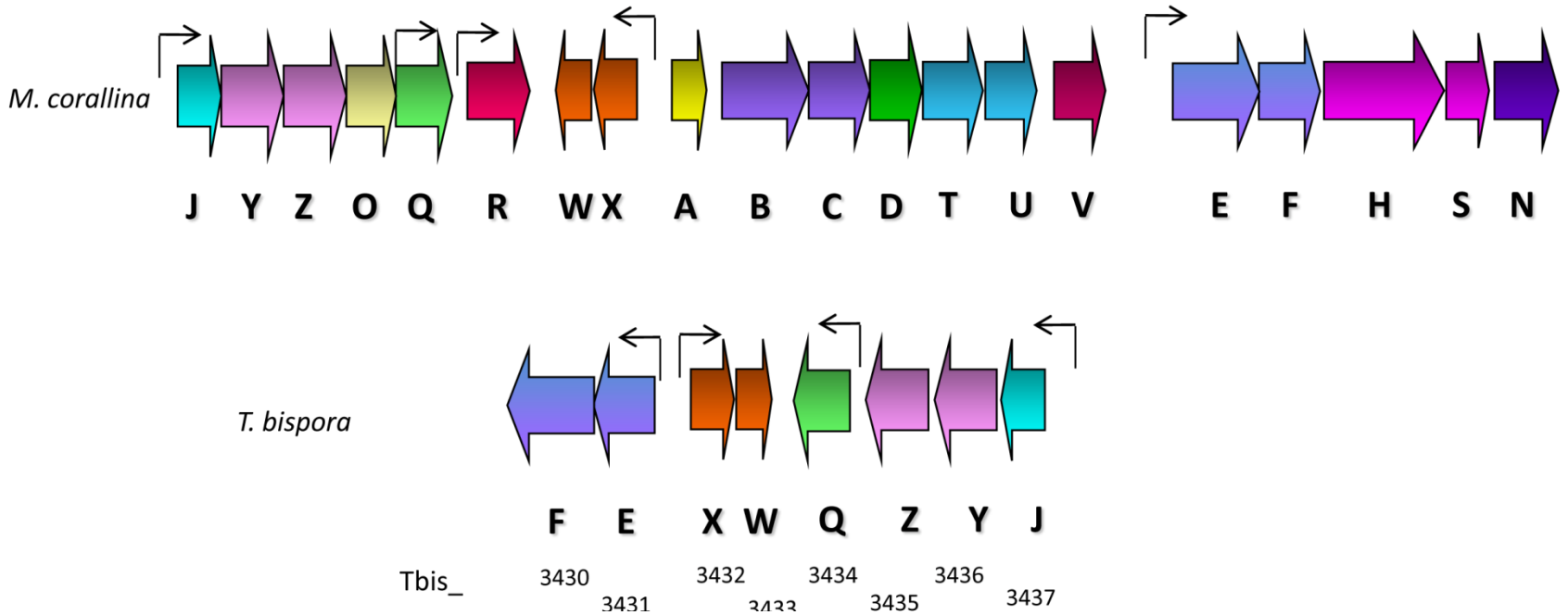

Figure 8.2 A comparison of the *mib* gene cluster from *M. corallina* (top) and the gene cluster from *Thermobsispora bispora* as described in the text. The number for each gene from *T. bispora* is given (Tbis_). The percentage amino acid (aa) sequence identity of the predicted protein encoded by each Tbis gene to the respective Mib homolog protein homolog is shown, as determined by NCBI BLAST (Altshul, 1990). The positions of the predicted MibX binding sites identified in both gene clusters are shown by black arrows.

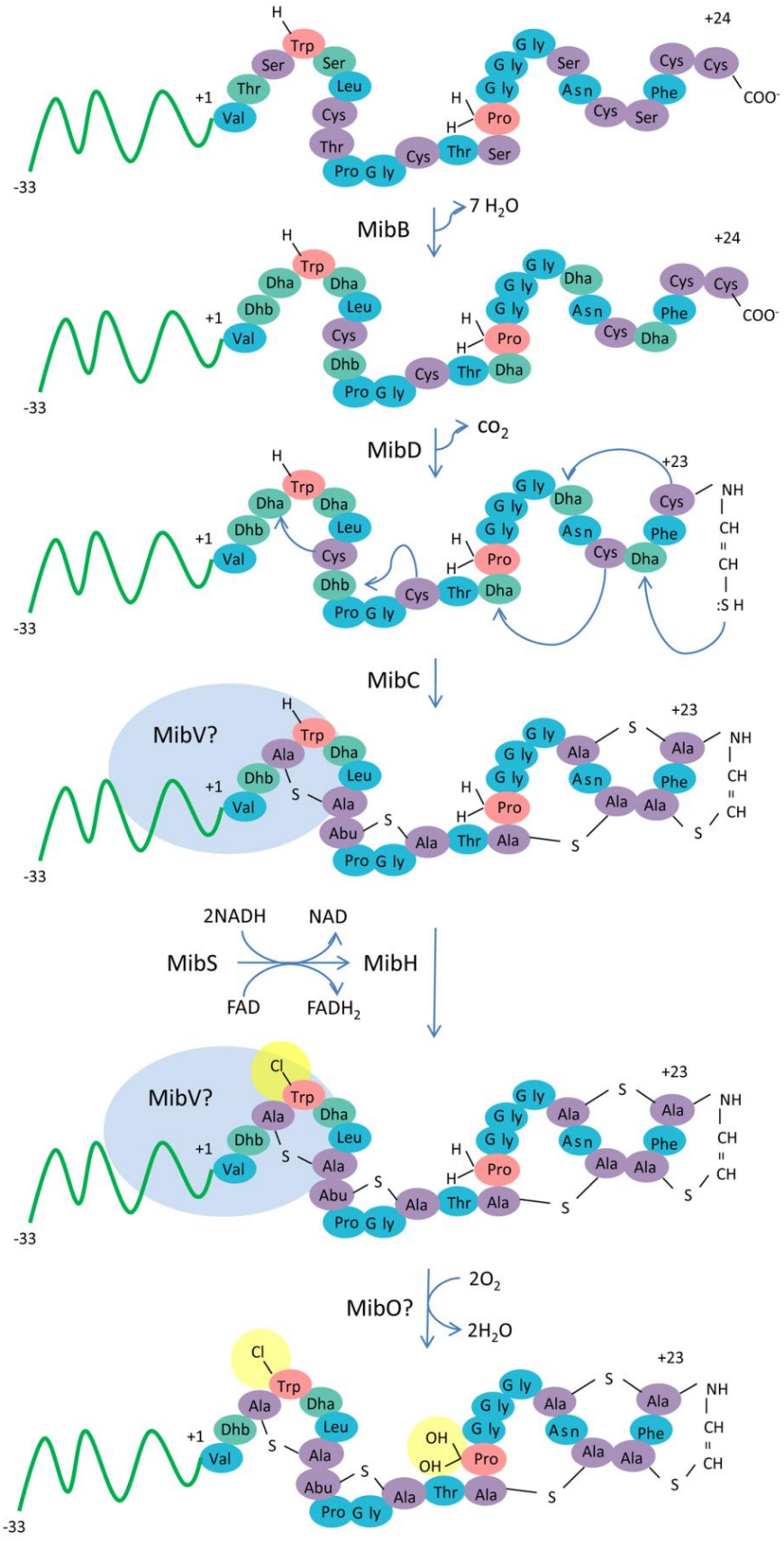

Figure 8.3 (legend over page)

Figure 8.3 A model for the mechanism of biosynthesis of microbisporicin by *M. corallina*. The exact order of modification of the prepropeptide is not known. The translated MibA prepropeptide shown in the top panel (leader peptide modelled by a green line) would be dehydrated by MibB. MibD would decarboxylate the C-terminal cysteine residue. Didehydroalanine (Dha) and didehydrobutyrine (Dhb) undergo nucleophilic attack from the thiol groups of cysteine residues, catalysed by MibC, to yield lanthionine, methyl-lanthionine and S-[(*Z*)-2-aminovinyl]-cysteine] bridges. MibS supplies reduced FAD to MibH to promote the chlorination of tryptophan to yield 5-chlorotryptophan. MibV might function as a chaperone in this process and may protect the peptide from degradation (modelled as a blue sphere). The cytochrome P450 MibO might be responsible for the dihydroxylation of proline to yield 3,4-dihydroxyproline.

8.2. Future Work

8.2.1 Short Term Aims

In the short term it will be important to refine the regulatory model presented for microbisporicin biosynthesis. The experimental evidence collected to date provides only indications of how regulation is mediated. The first aim would thus be to confirm the postulated model for the function of the two regulators MibX and MibR. Mapping the transcriptional start sites for each operon in the *mib* gene cluster would indicate whether the identified ECF sigma factor consensus sequences are likely to be important for transcription of those operons. *In vitro* run-off transcription assays could be carried out using purified MibX in conjunction with *E. coli* RNA polymerase to determine whether MibX interacts directly with these sites to recruit RNAP. A similar approach could be used to ascertain whether either MibX or purified MibR interacts with the *mibA* promoter region. This *in vitro* analysis could be complemented by an in-frame deletion of *mibR* to assess the importance of MibR for biosynthesis. The *lux*-reporter experiments described in Chapter 7 could be extended to provide further *in vivo* evidence.

The mechanism by which MibX activity is constrained by MibW should be investigated. In particular the signal to which MibW responds and how this signal is relayed to MibW to initiate the release of MibX should be resolved. Bacterial-two-hybrid experiments could indicate an interaction between MibW and MibJ/MibYZ which would provide further evidence for the involvement of these proteins. In-frame knock-out mutants of *mibJ* and *mibYZ* would indicate whether the corresponding proteins are essential for microbisporicin biosynthesis. The adaptation of the vectors used for *lux*-reporter analysis in *S. coelicolor* for use in *M. corallina* might allow the auto-regulatory model for microbisporicin biosynthesis to be further investigated. For example the effect of providing extracellular microbisporicin on *lux* reporter expression in the Δ*mibA* mutant could be assessed.

8.2.2 Long Term Aims

In the long term there are a number of areas of microbisporicin biosynthesis to address. Furthering the understanding of these areas is likely to provide tools for the improvement of microbisporicin yields and potency for use in a clinical context. The microbisporicin gene cluster also possesses a number of unusual and novel features, the investigation of which could provide interesting biological insights.

It will be interesting to look for other lantibiotic and antibiotic gene clusters which use ECF sigma factors as a mechanism of regulation and to determine whether they are more commonly used as pathway-specific regulators of antibiotic production in actinomycetes and other bacteria. The particular class of ECF sigma factors to which MibX appears to belong have not been studied in any detail to date but appear to be widespread in bacteria (see Chapter 4). The mechanism by which MibX activity is regulated might form a paradigm for this class. It will be interesting to determine the role of the homologs of MibX that do not appear to be linked to lantibiotic biosynthetic genes and how these are evolutionarily linked to MibX.

The function of the enzymes involved in the unique modifications of microbisporicin should be investigated. The tryptophan halogenase MibH was found to be involved in the chlorination of microbisporicin. The activity of this enzyme could be studied *in vitro*. Of particular interest is the substrate selectivity of this enzyme and whether MibH might be used to chlorinate other lantibiotics. The high degree of potency of microbisporicin suggests that chlorination might contribute to its mechanism of action. This should be confirmed by comparing the activity of the chloro- and deschloro- forms of the compound. Structural studies of MibH would provide information about the interaction of the enzyme with the prepropeptide substrate. The function of MibV should be investigated. The provision of MibV appears to influence chlorination and could be important for the transfer of chlorine to other lantibiotics.

The cytochrome P450 MibO was predicted to be involved in hydroxylating microbisporicin. This might be confirmed through the in-frame deletion of *mibO*. To assess the phenotype of such a mutant would require the use of methods to distinguish between proline hydroxylation and oxidation of lanthionine bridges. This might be achieved by the chemical removal of the lanthionine bridges (Martin *et al.* 2004). The *in vitro* activity and substrate specificity of MibO could be assessed. The importance of proline hydroxylation for microbisporicin activity could be explored.

A variant-generation system for microbisporicin could be established (Boakes *et al.* 2009). This would provide a method for the improvement of the pharmacokinetic properties of microbisporicin for use in the treatment of bacterial infections in humans. Variant-generation would likely be achieved in *M. corallina* since the heterologous production of microbisporicin was problematic. To achieve this aim however the inability of *mibA* to complement a *mibA* deletion *in trans* must first be addressed. A greater understanding of the mechanisms regulating gene expression in the *mib* gene cluster may contribute to this.

The self-resistance mechanism of *M. corallina* should be investigated in further detail. Over-expression of resistance determinants could provide a method for increased compound yields which are naturally very low for microbisporicin. The heterologous expression of *mibEF* and *mibQ* in hosts susceptible to microbisporicin would enable the determination of the contribution of each to resistance. Understanding the mode of regulation and timing of the expression of resistance genes may enable improvements to be made in the natural self-immunity of *M. corallina*. Further investigation of the mode of action of microbisporicin would enable a greater understanding of how these proteins provide resistance to the host. Furthermore, it may indicate possible routes for the development of resistance in target organisms and allow modifications in the structure of microbisporicin to avoid them in future.

Microbisporicin is a highly potent antibiotic which has activity against both Gram-positive and Gram-negative pathogens. If the basis of these qualities can be elucidated they might be transferred to other lantibiotics suggested for clinical use, such as mersacidin and actagardine. For example, generation of mersacidin variants revealed enhanced activity for the variant F3W (Appleyard *et al.* 2009). If this tryptophan residue could be chlorinated using MibH, the resulting variant might be improved even further. Several other lantibiotics (e.g. actagardine, DAB, michiganin A and the mutacins) have tryptophan near the N-terminus and might also be subject to such modification. Additionally, in the course of this study a number of microbisporicin-like compounds and gene clusters were identified. These compounds could be of similar potency to microbisporicin or, if not, could help to indicate what elements of microbisporicin make it so potent. Hybrid molecules could be constructed with improved properties.

8.3 Concluding Remarks

Microbisporicin is a highly promising candidate antibiotic for clinical development and as a gene-encoded peptide has significant potential for rational design. The identification and characterisation of the genes responsible for microbisporicin biosynthesis, and the development of methods for the genetic manipulation of the producing organism, provide the foundation for knowledge-based increases in strain productivity and the generation of variants with potentially improved pharmacological properties. Consequently, the work described here may represent a key milestone in the future clinical use of this novel and potent antibiotic.

References

Altena, K., A. Guder, *et al.* (2000). "Biosynthesis of the lantibiotic mersacidin: organization of a type B lantibiotic gene cluster." Appl Environ Microbiol **66**(6): 2565-71.

Altschul, S. F., W. Gish, *et al.* (1990). "Basic local alignment search tool." J Mol Biol **215**(3): 403-10.

Appelbaum, P. C. (2006a). "The emergence of vancomycin-intermediate and vancomycin-resistant Staphylococcus aureus." Clin Microbiol Infect **12 Suppl 1**: 16-23.

Appelbaum, P. C. (2006b). "MRSA--the tip of the iceberg." Clin Microbiol Infect **12 Suppl 2**: 3-10.

Appleyard, A. N., S. Choi, *et al.* (2009). "Dissecting structural and functional diversity of the lantibiotic mersacidin." Chem Biol **16**(5): 490-8.

Aso, Y., J. Nagao, *et al.* (2004). "Heterologous expression and functional analysis of the gene cluster for the biosynthesis of and immunity to the lantibiotic, nukacin ISK-1." J Biosci Bioeng **98**(6): 429-36.

Aso, Y., K. Okuda, *et al.* (2005). "A novel type of immunity protein, NukH, for the lantibiotic nukacin ISK-1 produced by Staphylococcus warneri ISK-1." Biosci Biotechnol Biochem **69**(7): 1403-10.

Augustin, J., R. Rosenstein, *et al.* (1992). "Genetic analysis of epidermin biosynthetic genes and epidermin-negative mutants of Staphylococcus epidermidis." Eur J Biochem **204**(3): 1149-54.

Bailey, T. L. and C. Elkan (1994). "Fitting a mixture model by expectation maximization to discover motifs in biopolymers." Proc Int Conf Intell Syst Mol Biol **2**: 28-36.

Bauer, R. and L. M. Dicks (2005). "Mode of action of lipid II-targeting lantibiotics." Int J Food Microbiol **101**(2): 201-16.

Beltrametti, F., D. Barucco, *et al.* (2007). "Protoplast fusion and gene recombination in the uncommon Actinomycete Planobispora rosea producing GE2270." J Antibiot (Tokyo) **60**(7): 447-54.

Bentley, S. D., K. F. Chater, *et al.* (2002). "Complete genome sequence of the model actinomycete Streptomyces coelicolor A3(2)." Nature **417**(6885): 141-7.

Berg, J., Tymoczko, J., & Stryer, L. (2002). Biochemistry., New York: W.H. Freeman & Co.

Bibb, M. J., P. R. Findlay, *et al.* (1984). "The relationship between base composition and codon usage in bacterial genes and its use for the simple and reliable identification of protein-coding sequences." Gene **30**(1-3): 157-66.

Bibb, M. J., J. White, *et al.* (1994). "The mRNA for the 23S rRNA methylase encoded by the ermE gene of Saccharopolyspora erythraea is translated in the absence of a conventional ribosome-binding site." Mol Microbiol **14**(3): 533-45.

Bierman, M., R. Logan, *et al.* (1992). "Plasmid cloning vectors for the conjugal transfer of DNA from Escherichia coli to Streptomyces spp." Gene **116**(1): 43-9.

Birmingham, V. A., K. L. Cox, *et al.* (1986). "Cloning and expression of a tylosin resistance gene from a tylosin-producing strain of Streptomyces fradiae." Mol Gen Genet **204**(3): 532-9.

Blaesse, M., T. Kupke, *et al.* (2000). "Crystal structure of the peptidyl-cysteine decarboxylase EpiD complexed with a pentapeptide substrate." EMBO J **19**(23): 6299-310.

Blaesse, M., T. Kupke, *et al.* (2003). "Structure of MrsD, an FAD-binding protein of the HFCD family." Acta Crystallogr D Biol Crystallogr **59**(Pt 8): 1414-21.

Boakes, S., A. N. Appleyard, *et al.* (2010). "Organization of the biosynthetic genes encoding deoxyactagardine B (DAB), a new lantibiotic produced by Actinoplanes liguriae NCIMB41362." J Antibiot (Tokyo).

Boakes, S., J. Cortes, *et al.* (2009). "Organization of the genes encoding the biosynthesis of actagardine and engineering of a variant generation system." Mol Microbiol **72**(5): 1126-36.

Bonelli, R. R., T. Schneider, *et al.* (2006). "Insights into in vivo activities of lantibiotics from gallidermin and epidermin mode-of-action studies." Antimicrob Agents Chemother **50**(4): 1449-57.

Bouhss, A., B. Al-Dabbagh, *et al.* (2009). "Specific interactions of clausin, a new lantibiotic, with lipid precursors of the bacterial cell wall." Biophys J **97**(5): 1390-7.

Bressollier, P., M. A. Brugo, *et al.* (2009). "Peptide Compound with Biological Activity, its Preparation and its Applications." US 20090312262 (10/06/2008).

Breukink, E. and B. de Kruijff (2006). "Lipid II as a target for antibiotics." Nat Rev Drug Discov **5**(4): 321-32.

Browning, D. F., D. E. Whitworth, *et al.* (2003). "Light-induced carotenogenesis in Myxococcus xanthus: functional characterization of the ECF sigma factor CarQ and antisigma factor CarR." Mol Microbiol **48**(1): 237-51.

Buedenbender, S., S. Rachid, *et al.* (2008). "Structure and Action of the Myxobacterial Chondrochloren Halogenase CndH: A New Variant of FAD-dependent Halogenases." J Mol Biol.

Butcher, B. G. and J. D. Helmann (2006). "Identification of Bacillus subtilis sigma-dependent genes that provide intrinsic resistance to antimicrobial compounds produced by Bacilli." Mol Microbiol **60**(3): 765-82.

Campbell, E. A., R. Greenwell, *et al.* (2007). "A conserved structural module regulates transcriptional responses to diverse stress signals in bacteria." Mol Cell **27**(5): 793-805.

Cao, M. and J. D. Helmann (2002a). "Regulation of the Bacillus subtilis bcrC bacitracin resistance gene by two extracytoplasmic function sigma factors." J Bacteriol **184**(22): 6123-9.

Cao, M. and J. D. Helmann (2004). "The Bacillus subtilis extracytoplasmic-function sigmaX factor regulates modification of the cell envelope and resistance to cationic antimicrobial peptides." J Bacteriol **186**(4): 1136-46.

Cao, M., T. Wang, *et al.* (2002b). "Antibiotics that inhibit cell wall biosynthesis induce expression of the Bacillus subtilis sigma(W) and sigma(M) regulons." Mol Microbiol **45**(5): 1267-76.

Castiglione, F., L. Cavaletti, *et al.* (2007). "A novel lantibiotic acting on bacterial cell wall synthesis produced by the uncommon actinomycete Planomonospora sp." Biochemistry **46**(20): 5884-95.

Castiglione, F., A. Lazzarini, *et al.* (2008). "Determining the structure and mode of action of microbisporicin, a potent lantibiotic active against multiresistant pathogens." Chem Biol **15**(1): 22-31.

Chakicherla, A. and J. N. Hansen (1995). "Role of the leader and structural regions of prelantibiotic peptides as assessed by expressing nisin-subtilin chimeras in Bacillus subtilis 168, and characterization of their physical, chemical, and antimicrobial properties." J Biol Chem **270**(40): 23533-9.

Chan, W. C., H. M. Dodd, *et al.* (1996). "Structure-activity relationships in the peptide antibiotic nisin: role of dehydroalanine 5." Appl Environ Microbiol **62**(8): 2966-9.

Chatterjee, C., M. Paul, *et al.* (2005). "Biosynthesis and mode of action of lantibiotics." Chem Rev **105**(2): 633-84.

Chen, P., F. X. Qi, *et al.* (2001). "Effect of amino acid substitutions in conserved residues in the leader peptide on biosynthesis of the lantibiotic mutacin II." FEMS Microbiol Lett **195**(2): 139-44.

Cheng, F., T. M. Takala, *et al.* (2007). "Nisin biosynthesis in vitro." J Mol Microbiol Biotechnol **13**(4): 248-54.

Cheng, J., K. Baldwin, *et al.* (1996a). "Na+/H+ antiport activity conferred by Bacillus subtilis tetA(L), a 5' truncation product of tetA(L), and related plasmid genes upon Escherichia coli." Antimicrob Agents Chemother **40**(4): 852-7.

Cheng, J., A. A. Guffanti, *et al.* (1996b). "Chromosomal tetA(L) gene of Bacillus subtilis: regulation of expression and physiology of a tetA(L) deletion strain." J Bacteriol **178**(10): 2853-60.

Cheng, J., D. B. Hicks, *et al.* (1996c). "The purified Bacillus subtilis tetracycline efflux protein TetA(L) reconstitutes both tetracycline-cobalt/H+ and Na+(K+)/H+ exchange." Proc Natl Acad Sci U S A **93**(25): 14446-51.

Chenna, R., H. Sugawara, *et al.* (2003). "Multiple sequence alignment with the Clustal series of programs." Nucleic Acids Res **31**(13): 3497-500.

Cherepanov, P. P. and W. Wackernagel (1995). "Gene disruption in Escherichia coli: TcR and KmR cassettes with the option of Flp-catalyzed excision of the antibiotic-resistance determinant." Gene **158**(1): 9-14.

Chiu, H. T., B. K. Hubbard, *et al.* (2001). "Molecular cloning and sequence analysis of the complestatin biosynthetic gene cluster." Proc Natl Acad Sci U S A **98**(15): 8548-53.

Chun, Y. J., T. Shimada, *et al.* (2006). "Understanding electron transport systems of Streptomyces cytochrome P450." Biochem Soc Trans **34**(Pt 6): 1183-5.

Circello, B. T., A. C. Eliot, *et al.* (2010). "Molecular cloning and heterologous expression of the dehydrophos biosynthetic gene cluster." Chem Biol **17**(4): 402-11.

Claesen, J. and M. Bibb (2010). "Genome mining and genetic analysis of cypemycin biosynthesis reveal an unusual class of posttranslationally modified peptides." Proc Natl Acad Sci U S A **107**(37): 16297-302.

Combes, P., R. Till, *et al.* (2002). "The streptomyces genome contains multiple pseudo-attB sites for the (phi)C31-encoded site-specific recombination system." J Bacteriol **184**(20): 5746-52.

Cooper, L. E., A. L. McClerren, *et al.* (2008). "Structure-activity relationship studies of the two-component lantibiotic haloduracin." Chem Biol **15**(10): 1035-45.

Cortes, J., S. F. Haydock, *et al.* (1990). "An unusually large multifunctional polypeptide in the erythromycin-producing polyketide synthase of Saccharopolyspora erythraea." Nature **348**(6297): 176-8.

Corvey, C., T. Stein, *et al.* (2003). "Activation of subtilin precursors by Bacillus subtilis extracellular serine proteases subtilisin (AprE), WprA, and Vpr." Biochem Biophys Res Commun **304**(1): 48-54.

Covello, P. S., K. H. Teoh, *et al.* (2007). "Functional genomics and the biosynthesis of artemisinin." Phytochemistry **68**(14): 1864-71.

Culpepper, M. A., E. E. Scott, *et al.* (2010). "Crystal structure of prolyl 4-hydroxylase from Bacillus anthracis." Biochemistry **49**(1): 124-33.

Dairi, T., T. Ohta, *et al.* (1992). "Organization and nature of fortimicin A (astromicin) biosynthetic genes studied using a cosmid library of Micromonospora olivasterospora DNA." Mol Gen Genet **236**(1): 39-48.

Datsenko, K. A. and B. L. Wanner (2000). "One-step inactivation of chromosomal genes in *Escherichia coli* K-12 using PCR products." Proc Natl Acad Sci U S A **97**(12): 6640-5.

de Kruijff, B., V. van Dam, *et al.* (2008). "Lipid II: a central component in bacterial cell wall synthesis and a target for antibiotics." Prostaglandins Leukot Essent Fatty Acids **79**(3-5): 117-21.

de Ruyter, P. G., O. P. Kuipers, *et al.* (1996). "Functional analysis of promoters in the nisin gene cluster of Lactococcus lactis." J Bacteriol **178**(12): 3434-9.

de Vos, W. M., O. P. Kuipers, *et al.* (1995). "Maturation pathway of nisin and other lantibiotics: post-translationally modified antimicrobial peptides exported by gram-positive bacteria." Mol Microbiol **17**(3): 427-37.

Donadio, S., M. J. Staver, *et al.* (1991). "Modular organization of genes required for complex polyketide biosynthesis." Science **252**(5006): 675-9.

Dong, C., S. Flecks, *et al.* (2005). "Tryptophan 7-halogenase (PrnA) structure suggests a mechanism for regioselective chlorination." Science **309**(5744): 2216-9.

Dorrestein, P. C., E. Yeh, *et al.* (2005). "Dichlorination of a pyrrolyl-S-carrier protein by $FADH_2$-dependent halogenase PltA during pyoluteorin biosynthesis." Proc Natl Acad Sci U S A **102**(39): 13843-8.

Draper, L. A., K. Grainger, *et al.* (2009). "Cross-immunity and immune mimicry as mechanisms of resistance to the lantibiotic lacticin 3147." Mol Microbiol **71**(4): 1043-54.

Draper, L. A., R. P. Ross, *et al.* (2008). "Lantibiotic immunity." Curr Protein Pept Sci **9**(1): 39-49.

Du, L., C. Sanchez, *et al.* (2000). "The biosynthetic gene cluster for the antitumor drug bleomycin from Streptomyces verticillus ATCC15003 supporting functional interactions between nonribosomal peptide synthetases and a polyketide synthase." Chem Biol **7**(8): 623-42.

Dupuy, B. and S. Matamouros (2006). "Regulation of toxin and bacteriocin synthesis in Clostridium species by a new subgroup of RNA polymerase sigma-factors." Res Microbiol **157**(3): 201-5.

Ellermeier, C. D. and R. Losick (2006). "Evidence for a novel protease governing regulated intramembrane proteolysis and resistance to antimicrobial peptides in Bacillus subtilis." Genes Dev **20**(14): 1911-22.

Elliot, M. A., M. J. Buttner, *et al.* (2008). Multicellular development in Streptomyces. Myxobacteria: Multicellularity and Differentiation. D. E. Whitworth. Washington D.C., ASM Press**:** 419-438.

Emanuelsson, O., S. Brunak, *et al.* (2007). "Locating proteins in the cell using TargetP, SignalP and related tools." Nat Protoc **2**(4): 953-71.

Engelke, G., Z. Gutowski-Eckel, *et al.* (1994). "Regulation of nisin biosynthesis and immunity in Lactococcus lactis 6F3." Appl Environ Microbiol **60**(3): 814-25.

Farrer, R. A., E. Kemen, *et al.* (2009). "De novo assembly of the Pseudomonas syringae pv. syringae B728a genome using Illumina/Solexa short sequence reads." FEMS Microbiol Lett **291**(1): 103-11.

Finn, R. D., J. Tate, *et al.* (2008). "The Pfam protein families database." Nucleic Acids Res **36**(Database issue): D281-8.

Flecks, S., E. P. Patallo, *et al.* (2008). "New insights into the mechanism of enzymatic chlorination of tryptophan." Angew Chem Int Ed Engl **47**(49): 9533-6.

Flett, F., V. Mersinias, *et al.* (1997). "High efficiency intergeneric conjugal transfer of plasmid DNA from Escherichia coli to methyl DNA-restricting streptomycetes." FEMS Microbiol Lett **155**(2): 223-9.

Franke, C. M., J. Tiemersma, *et al.* (1999). "Membrane topology of the lactococcal bacteriocin ATP-binding cassette transporter protein LcnC. Involvement of LcnC in lactococcin a maturation." J Biol Chem **274**(13): 8484-90.

Fujimori, D. G., S. Hrvatin, *et al.* (2007). "Cloning and characterization of the biosynthetic gene cluster for kutznerides." Proc Natl Acad Sci U S A **104**(42): 16498-503.

Furgerson Ihnken, L. A., C. Chatterjee, *et al.* (2008). "In vitro reconstitution and substrate specificity of a lantibiotic protease." Biochemistry **47**(28): 7352-63.

Furuya, T. and K. Kino (2010). "Regioselective oxidation of indole- and quinolinecarboxylic acids by cytochrome P450 CYP199A2." Appl Microbiol Biotechnol **85**(6): 1861-8.

Gartemann, K. H., B. Abt, *et al.* (2008). "The genome sequence of the tomato-pathogenic actinomycete Clavibacter michiganensis subsp. michiganensis NCPPB382 reveals a large island involved in pathogenicity." J Bacteriol **190**(6): 2138-49.

Gomez-Escribano, J. P. and M. J. Bibb (2010). " Engineering Streptomyces coelicolor for heterologous expression of secondary metabolite gene clusters." Microbial Biotechnology **doi: 10.1111/j.1751-7915.2010.00219.x**.

Goodlett, D. R., J. E. Bruce, *et al.* (2000). "Protein identification with a single accurate mass of a cysteine-containing peptide and constrained database searching." Anal Chem **72**(6): 1112-8.

Goto, Y., B. Li, *et al.* (2010). "Discovery of unique lanthionine synthetases reveals new mechanistic and evolutionary insights." PLoS Biol **8**(3): e1000339.

Grass, G., B. Fricke, *et al.* (2005). "Control of expression of a periplasmic nickel efflux pump by periplasmic nickel concentrations." Biometals **18**(4): 437-48.

Grass, G., C. Grosse, *et al.* (2000). "Regulation of the cnr cobalt and nickel resistance determinant from Ralstonia sp. strain CH34." J Bacteriol **182**(5): 1390-8.
Gregory, M. A., R. Till, *et al.* (2003). "Integration site for Streptomyces phage phiBT1 and development of site-specific integrating vectors." J Bacteriol **185**(17): 5320-3.
Gribble, G. W. (2003). "The diversity of naturally produced organohalogens." Chemosphere **52**(2): 289-97.
Guder, A., T. Schmitter, *et al.* (2002). "Role of the single regulator MrsR1 and the two-component system MrsR2/K2 in the regulation of mersacidin production and immunity." Appl Environ Microbiol **68**(1): 106-13.
Guder, A., I. Wiedemann, *et al.* (2000). "Posttranslationally modified bacteriocins--the lantibiotics." Biopolymers **55**(1): 62-73.
Gust, B., G. L. Challis, *et al.* (2003). "PCR-targeted Streptomyces gene replacement identifies a protein domain needed for biosynthesis of the sesquiterpene soil odor geosmin." Proc Natl Acad Sci U S A **100**(4): 1541-6.
Hammer, P. E., D. S. Hill, *et al.* (1997). "Four genes from Pseudomonas fluorescens that encode the biosynthesis of pyrrolnitrin." Appl Environ Microbiol **63**(6): 2147-54.
Harris, C. M., R. Kannan, *et al.* (1985). "The role of the chlorine substituents in the antibiotic vancomycin: preparation and characterization of mono- and didechlorovancomycin." J. Am. Chem. Soc. **107**(23): 6652-6658.
Hasper, H. E., B. de Kruijff, *et al.* (2004). "Assembly and stability of nisin-lipid II pores." Biochemistry **43**(36): 11567-75.
Hasper, H. E., N. E. Kramer, *et al.* (2006). "An alternative bactericidal mechanism of action for lantibiotic peptides that target lipid II." Science **313**(5793): 1636-7.
Heemstra, J. R., Jr. and C. T. Walsh (2008). "Tandem action of the O2- and FADH2-dependent halogenases KtzQ and KtzR produce 6,7-dichlorotryptophan for kutzneride assembly." J Am Chem Soc **130**(43): 14024-5.
Heidrich, C., U. Pag, *et al.* (1998). "Isolation, characterization, and heterologous expression of the novel lantibiotic epicidin 280 and analysis of its biosynthetic gene cluster." Appl Environ Microbiol **64**(9): 3140-6.
Heinrich, J., K. Hein, *et al.* (2009a). "Two proteolytic modules are involved in regulated intramembrane proteolysis of Bacillus subtilis RsiW." Mol Microbiol **74**(6): 1412-26.
Heinrich, J., T. Lunden, *et al.* (2008). "The Bacillus subtilis ABC transporter EcsAB influences intramembrane proteolysis through RasP." Microbiology **154**(Pt 7): 1989-97.
Heinrich, J. and T. Wiegert (2009b). "Regulated intramembrane proteolysis in the control of extracytoplasmic function sigma factors." Res Microbiol **160**(9): 696-703.
Helfrich, M., K. D. Entian, *et al.* (2007). "Structure-function relationships of the lanthionine cyclase SpaC involved in biosynthesis of the Bacillus subtilis peptide antibiotic subtilin." Biochemistry **46**(11): 3224-33.
Helmann, J. D. (2002). "The extracytoplasmic function (ECF) sigma factors." Adv Microb Physiol **46**: 47-110.
Hesketh, A., W. J. Chen, *et al.* (2007). "The global role of ppGpp synthesis in morphological differentiation and antibiotic production in Streptomyces coelicolor A3(2)." Genome Biol **8**(8): R161.
Hesketh, A., H. Kock, *et al.* (2009). "The role of absC, a novel regulatory gene for secondary metabolism, in zinc-dependent antibiotic production in Streptomyces coelicolor A3(2)." Mol Microbiol **74**(6): 1427-44.
Hesketh, A., J. Sun, *et al.* (2001). "Induction of ppGpp synthesis in Streptomyces coelicolor A3(2) grown under conditions of nutritional sufficiency elicits actII-ORF4 transcription and actinorhodin biosynthesis." Mol Microbiol **39**(1): 136-44.
Hibbing, M. E., C. Fuqua, *et al.* (2010). "Bacterial competition: surviving and thriving in the microbial jungle." Nat Rev Microbiol **8**(1): 15-25.
Hille, M., S. Kies, *et al.* (2001). "Dual role of GdmH in producer immunity and secretion of the Staphylococcal lantibiotics gallidermin and epidermin." Appl Environ Microbiol **67**(3): 1380-3.

Hillman, J. D. (2002). "Genetically modified Streptococcus mutans for the prevention of dental caries." Antonie Van Leeuwenhoek **82**(1-4): 361-6.

Hindre, T., J. P. Le Pennec*, et al.* (2004). "Regulation of lantibiotic lacticin 481 production at the transcriptional level by acid pH." FEMS Microbiol Lett **231**(2): 291-8.

Hoang, K. C., M. Tseng*, et al.* (2007). "Degradation of polyethylene succinate (PES) by a new thermophilic Microbispora strain." Biodegradation **18**(3): 333-42.

Hoffmann, A., T. Schneider*, et al.* (2004). "Localization and functional analysis of PepI, the immunity peptide of Pep5-producing Staphylococcus epidermidis strain 5." Appl Environ Microbiol **70**(6): 3263-71.

Holtsmark, I., D. Mantzilas*, et al.* (2006). "Purification, characterization, and gene sequence of michiganin A, an actagardine-like lantibiotic produced by the tomato pathogen Clavibacter michiganensis subsp. michiganensis." Appl Environ Microbiol **72**(9): 5814-21.

Hsu, S. T., E. Breukink*, et al.* (2003). "NMR study of mersacidin and lipid II interaction in dodecylphosphocholine micelles. Conformational changes are a key to antimicrobial activity." J Biol Chem **278**(15): 13110-7.

Hsu, S. T., E. Breukink*, et al.* (2004). "The nisin-lipid II complex reveals a pyrophosphate cage that provides a blueprint for novel antibiotics." Nat Struct Mol Biol **11**(10): 963-7.

Hu, H. and K. Ochi (2001). "Novel approach for improving the productivity of antibiotic-producing strains by inducing combined resistant mutations." Appl Environ Microbiol **67**(4): 1885-92.

Hutchings, M. I., H. J. Hong*, et al.* (2006). "The sigma(E) cell envelope stress response of Streptomyces coelicolor is influenced by a novel lipoprotein, CseA." J Bacteriol **188**(20): 7222-9.

Hutchings, M. I., T. Palmer*, et al.* (2009). "Lipoprotein biogenesis in Gram-positive bacteria: knowing when to hold 'em, knowing when to fold 'em." Trends Microbiol **17**(1): 13-21.

Ivanova, V., M. Kolarova*, et al.* (2007). "Microbiaeratin, a new natural indole alkaloid from a Microbispora aerata strain, isolated from Livingston Island, Antarctica." Prep Biochem Biotechnol **37**(2): 161-8.

Jabes, D., C. Brunati*, et al.* (2009a). *In vitro* Antibacterial Profile of the new Lantibiotic NAI-107. 49th Annual ICAAC, San Francisco.

Jabes, D., G. Candiani*, et al.* (2009b). NAI-107: Superior Efficacy in Animal Models of MDR Gram Positive Infections. 49th Annual ICAAC, San Francisco.

Jordan, S., M. I. Hutchings*, et al.* (2008). "Cell envelope stress response in Gram-positive bacteria." FEMS Microbiol Rev **32**(1): 107-46.

Juncker, A. S., H. Willenbrock*, et al.* (2003). "Prediction of lipoprotein signal peptides in Gram-negative bacteria." Protein Sci **12**(8): 1652-62.

Kall, L., A. Krogh*, et al.* (2007). "Advantages of combined transmembrane topology and signal peptide prediction--the Phobius web server." Nucleic Acids Res **35**(Web Server issue): W429-32.

Karimova, G., J. Pidoux*, et al.* (1998). "A bacterial two-hybrid system based on a reconstituted signal transduction pathway." Proc Natl Acad Sci U S A **95**(10): 5752-6.

Kaur, P. (1997). "Expression and characterization of DrrA and DrrB proteins of Streptomyces peucetius in Escherichia coli: DrrA is an ATP binding protein." J Bacteriol **179**(3): 569-75.

Keller, S., T. Wage*, et al.* (2000). "Purification and Partial Characterization of Tryptophan 7-Halogenase (PrnA) from Pseudomonas fluorescens " Angew Chem Int Ed Engl **39**(13): 2300-2302.

Kies, S., C. Vuong*, et al.* (2003). "Control of antimicrobial peptide synthesis by the agr quorum sensing system in Staphylococcus epidermidis: activity of the lantibiotic epidermin is regulated at the level of precursor peptide processing." Peptides **24**(3): 329-38.

Kieser, T., M. J. Bibb*, et al.* (2000). Practical Streptomyces Genetics Norwich, John Innes Foundation.

Kleerebezem, M. and L. E. Quadri (2001). "Peptide pheromone-dependent regulation of antimicrobial peptide production in Gram-positive bacteria: a case of multicellular behavior." Peptides **22**(10): 1579-96.

Kleerebezem, M., L. E. Quadri*, et al.* (1997). "Quorum sensing by peptide pheromones and two-component signal-transduction systems in Gram-positive bacteria." Mol Microbiol **24**(5): 895-904.

Klein, C. and K. D. Entian (1994). "Genes involved in self-protection against the lantibiotic subtilin produced by Bacillus subtilis ATCC 6633." Appl Environ Microbiol **60**(8): 2793-801.

Klein, C., C. Kaletta*, et al.* (1992). "Analysis of genes involved in biosynthesis of the lantibiotic subtilin." Appl Environ Microbiol **58**(1): 132-42.

Kluskens, L. D., A. Kuipers*, et al.* (2005). "Post-translational modification of therapeutic peptides by NisB, the dehydratase of the lantibiotic nisin." Biochemistry **44**(38): 12827-34.

Kodani, S., M. E. Hudson*, et al.* (2004). "The SapB morphogen is a lantibiotic-like peptide derived from the product of the developmental gene ramS in Streptomyces coelicolor." Proc Natl Acad Sci U S A **101**(31): 11448-53.

Kodani, S., M. A. Lodato*, et al.* (2005). "SapT, a lanthionine-containing peptide involved in aerial hyphae formation in the streptomycetes." Mol Microbiol **58**(5): 1368-80.

Komiyama, K., K. Otoguro*, et al.* (1993). "A new antibiotic, cypemycin. Taxonomy, fermentation, isolation and biological characteristics." J Antibiot (Tokyo) **46**(11): 1666-71.

Koponen, O., M. Tolonen*, et al.* (2002). "NisB is required for the dehydration and NisC for the lanthionine formation in the post-translational modification of nisin." Microbiology **148**(Pt 11): 3561-8.

Krulwich, T. A., O. Lewinson*, et al.* (2005). "Do physiological roles foster persistence of drug/multidrug-efflux transporters? A case study." Nat Rev Microbiol **3**(7): 566-72.

Kuipers, A., E. de Boef*, et al.* (2004). "NisT, the transporter of the lantibiotic nisin, can transport fully modified, dehydrated, and unmodified prenisin and fusions of the leader peptide with non-lantibiotic peptides." J Biol Chem **279**(21): 22176-82.

Kuipers, O. P., M. M. Beerthuyzen*, et al.* (1995). "Autoregulation of nisin biosynthesis in Lactococcus lactis by signal transduction." J Biol Chem **270**(45): 27299-304.

Kuipers, O. P., M. M. Beerthuyzen*, et al.* (1993a). "Characterization of the nisin gene cluster nisABTCIPR of Lactococcus lactis. Requirement of expression of the nisA and nisI genes for development of immunity." Eur J Biochem **216**(1): 281-91.

Kuipers, O. P., H. S. Rollema*, et al.* (1993b). "Biosynthesis and secretion of a precursor of nisin Z by Lactococcus lactis, directed by the leader peptide of the homologous lantibiotic subtilin from Bacillus subtilis." FEBS Lett **330**(1): 23-7.

Kupke, T., C. Kempter*, et al.* (1994). "Mass spectroscopic analysis of a novel enzymatic reaction. Oxidative decarboxylation of the lantibiotic precursor peptide EpiA catalyzed by the flavoprotein EpiD." J Biol Chem **269**(8): 5653-9.

Kupke, T., C. Kempter*, et al.* (1995). "Oxidative decarboxylation of peptides catalyzed by flavoprotein EpiD. Determination of substrate specificity using peptide libraries and neutral loss mass spectrometry." J Biol Chem **270**(19): 11282-9.

Kupke, T., S. Stevanovic*, et al.* (1992). "Purification and characterization of EpiD, a flavoprotein involved in the biosynthesis of the lantibiotic epidermin." J Bacteriol **174**(16): 5354-61.

Ladant, D. and A. Ullmann (1999). "Bordatella pertussis adenylate cyclase: a toxin with multiple talents." Trends Microbiol **7**(4): 172-6.

Lakey, J. H., E. J. Lea*, et al.* (1983). "A new channel-forming antibiotic from Streptomyces coelicolor A3(2) which requires calcium for its activity." J Gen Microbiol **129**(12): 3565-73.

Lane, W. J. and S. A. Darst (2006). "The structural basis for promoter -35 element recognition by the group IV sigma factors." PLoS Biol **4**(9): e269.
Lautru, S. and G. L. Challis (2004). "Substrate recognition by nonribosomal peptide synthetase multi-enzymes." Microbiology **150**(Pt 6): 1629-36.
Lautru, S., R. J. Deeth*, et al.* (2005). "Discovery of a new peptide natural product by Streptomyces coelicolor genome mining." Nat Chem Biol **1**(5): 265-9.
Lawton, E. M., P. D. Cotter*, et al.* (2007). "Identification of a novel two-peptide lantibiotic, haloduracin, produced by the alkaliphile Bacillus halodurans C-125." FEMS Microbiol Lett **267**(1): 64-71.
Lazzarini, A., L. Cavaletti*, et al.* (2000). "Rare genera of actinomycetes as potential producers of new antibiotics." Antonie Van Leeuwenhoek **78**(3-4): 399-405.
Lazzarini, A., L. Gastaldo*, et al.* (2005). "Antibiotic 107891, its factors A1 and A2, pharmaceutically acceptable salts and compositions, and use thereof." WO/2005/014628 (17.02.2005).
Le, T. B., H. P. Fiedler*, et al.* (2009). "Coupling of the biosynthesis and export of the DNA gyrase inhibitor simocyclinone in Streptomyces antibioticus." Mol Microbiol **72**(6): 1462-74.
Lechevalier, H. A. and M. P. Lechevalier (1970). "Chemical composition as a criterion in the classification of aerobic actinomycetes." Int. J. Syst. Bacteriol. **20**: 435-443.
Lee, M. D. (2003). "Antibiotics from Microbispora." US 6551591 (Apr. 22, 2003).
Lee, M. V., L. A. Ihnken*, et al.* (2009). "Distributive and directional behavior of lantibiotic synthetases revealed by high-resolution tandem mass spectrometry." J Am Chem Soc **131**(34): 12258-64.
Levengood, M. R., G. C. Patton*, et al.* (2007). "The leader peptide is not required for post-translational modification by lacticin 481 synthetase." J Am Chem Soc **129**(34): 10314-5.
Li, B. and W. A. van der Donk (2007). "Identification of Essential Catalytic Residues of the Cyclase NisC Involved in the Biosynthesis of Nisin." J Biol Chem **282**(29): 21169-75.
Li, B., J. P. Yu*, et al.* (2006a). "Structure and mechanism of the lantibiotic cyclase involved in nisin biosynthesis." Science **311**(5766): 1464-7.
Li, H. and D. J. O'Sullivan (2002). "Heterologous expression of the Lactococcus lactis bacteriocin, nisin, in a dairy Enterococcus strain." Appl Environ Microbiol **68**(7): 3392-400.
Li, H. and D. J. O'Sullivan (2006b). "Identification of a nisI promoter within the nisABCTIP operon that may enable establishment of nisin immunity prior to induction of the operon via signal transduction." J Bacteriol **188**(24): 8496-503.
Li, M., T. J. Kim*, et al.* (2008). "Effects of extracellular ATP on the physiology of Streptomyces coelicolor A3(2)." FEMS Microbiol Lett **286**(1): 24-31.
Linares, J. F., I. Gustafsson*, et al.* (2006). "Antibiotics as intermicrobial signaling agents instead of weapons." Proc Natl Acad Sci U S A **103**(51): 19484-9.
Liu, G., J. Zhong*, et al.* (2009). "Characteristics of the bovicin HJ50 gene cluster in Streptococcus bovis HJ50." Microbiology **155**(Pt 2): 584-93.
Liu, W. and J. N. Hansen (1992). "Enhancement of the chemical and antimicrobial properties of subtilin by site-directed mutagenesis." J Biol Chem **267**(35): 25078-85.
Livermore, D. M. (2009). "Has the era of untreatable infections arrived?" J Antimicrob Chemother **64 Suppl 1**: i29-36.
Lonetto, M. A., K. L. Brown*, et al.* (1994). "Analysis of the Streptomyces coelicolor sigE gene reveals the existence of a subfamily of eubacterial RNA polymerase sigma factors involved in the regulation of extracytoplasmic functions." Proc Natl Acad Sci U S A **91**(16): 7573-7.
Lopez, D., M. A. Fischbach*, et al.* (2008). "Structurally diverse natural products that cause potassium leakage trigger multicellularity in Bacillus subtilis." Proc Natl Acad Sci U S A.

Loria, R., D. R. Bignell, *et al.* (2008). "Thaxtomin biosynthesis: the path to plant pathogenicity in the genus Streptomyces." Antonie Van Leeuwenhoek **94**(1): 3-10.

Louie, T. M., X. S. Xie, *et al.* (2003). "Coordinated production and utilization of FADH2 by NAD(P)H-flavin oxidoreductase and 4-hydroxyphenylacetate 3-monooxygenase." Biochemistry **42**(24): 7509-17.

Lubelski, J., R. Rink, *et al.* (2008). "Biosynthesis, immunity, regulation, mode of action and engineering of the model lantibiotic nisin." Cell Mol Life Sci **65**(3): 455-76.

Luo, Y. and J. D. Helmann (2009). "Extracytoplasmic function sigma factors with overlapping promoter specificity regulate sublancin production in Bacillus subtilis." J Bacteriol **191**(15): 4951-8.

MacNeil, D. J. (1988). "Characterization of a unique methyl-specific restriction system in Streptomyces avermitilis." J Bacteriol **170**(12): 5607-12.

MacNeil, D. J., K. M. Gewain, *et al.* (1992). "Analysis of Streptomyces avermitilis genes required for avermectin biosynthesis utilizing a novel integration vector." Gene **111**(1): 61-8.

Maffioli, S. I., D. Potenza, *et al.* (2009). "Structure revision of the lantibiotic 97518." J Nat Prod **72**(4): 605-7.

Majer, F., D. G. Schmid, *et al.* (2002). "The flavoprotein MrsD catalyzes the oxidative decarboxylation reaction involved in formation of the peptidoglycan biosynthesis inhibitor mersacidin." J Bacteriol **184**(5): 1234-43.

Makino, A., T. Baba, *et al.* (2003). "Cinnamycin (Ro 09-0198) promotes cell binding and toxicity by inducing transbilayer lipid movement." J Biol Chem **278**(5): 3204-9.

Makino, M., H. Sugimoto, *et al.* (2007). "Crystal structures and catalytic mechanism of cytochrome P450 StaP that produces the indolocarbazole skeleton." Proc Natl Acad Sci U S A **104**(28): 11591-6.

Malabarba, A., F. Spreafico, *et al.* (1989). "Dechloro teicoplanin antibiotics." J Antibiot (Tokyo) **42**(11): 1684-97.

Marcone, G. L., F. Beltrametti, *et al.* (2010a). "Novel mechanism of glycopeptide resistance in the A40926 producer Nonomuraea sp. ATCC 39727." Antimicrob Agents Chemother **54**(6): 2465-72.

Marcone, G. L., L. Carrano, *et al.* (2010b). "Protoplast preparation and reversion to the normal filamentous growth in antibiotic-producing uncommon actinomycetes." J Antibiot (Tokyo) **63**(2): 83-8.

Marcone, G. L., L. Foulston, *et al.* (2010c). "Methods for the genetic manipulation of Nonomuraea sp. ATCC 39727." J Ind Microbiol and Biotech **In press**.

Martin, N. I., T. Sprules, *et al.* (2004). "Structural characterization of lacticin 3147, a two-peptide lantibiotic with synergistic activity." Biochemistry **43**(11): 3049-56.

Mauger, A. B. (1996). "Naturally occurring proline analogues." J Nat Prod **59**(12): 1205-11.

McArthur, M. and M. Bibb (2006). "In vivo DNase I sensitivity of the Streptomyces coelicolor chromosome correlates with gene expression: implications for bacterial chromosome structure." Nucleic Acids Res **34**(19): 5395-401.

McAuliffe, O., T. O'Keeffe, *et al.* (2001). "Regulation of immunity to the two-component lantibiotic, lacticin 3147, by the transcriptional repressor LtnR." Mol Microbiol **39**(4): 982-93.

McClerren, A. L., L. E. Cooper, *et al.* (2006). "Discovery and in vitro biosynthesis of haloduracin, a two-component lantibiotic." Proc Natl Acad Sci U S A **103**(46): 17243-8.

McLean, K. J., M. Sabri, *et al.* (2005). "Biodiversity of cytochrome P450 redox systems." Biochem Soc Trans **33**(Pt 4): 796-801.

Meyer, C., G. Bierbaum, *et al.* (1995). "Nucleotide sequence of the lantibiotic Pep5 biosynthetic gene cluster and functional analysis of PepP and PepC. Evidence for a role of PepC in thioether formation." Eur J Biochem **232**(2): 478-89.

Meyer, H. E., M. Heber, *et al.* (1994). "Sequence Analysis of Lantibiotics: Chemical Derivatization Procedures Allow a Fast Access to Complete Edman Degradation." Analytical Biochemistry **223**(2): 185-190.
Miao, V. and J. Davies (2010). "Actinobacteria: the good, the bad, and the ugly." Antonie Van Leeuwenhoek.
Minami, Y., K.-I. Yoshida, *et al.* (1994). "Structure of Cypemycin, a New Peptide Antibiotic." Tetrahedron Letters **35**(43): 8001-8004.
Mlot, C. (2009). "Microbiology. Antibiotics in nature: beyond biological warfare." Science **324**(5935): 1637-9.
Murphy, C. D. (2006). "Recent developments in enzymatic chlorination." Nat Prod Rep **23**(2): 147-52.
Nakajima, T. and B. E. Volcani (1969). "3,4-dihydroxyproline: a new amino acid in diatom cell walls." Science **164**(886): 1400-1.
Nakajima, Y., V. Kitpreechavanich, *et al.* (1999). "*Microbispora corallina* sp. nov., a new species of the genus *Microbispora* isolated from Thai soil." Int J Syst Bacteriol **49 Pt 4**: 1761-7.
Neis, S., G. Bierbaum, *et al.* (1997). "Effect of leader peptide mutations on biosynthesis of the lantibiotic Pep5." FEMS Microbiol Lett **149**(2): 249-55.
Nes, I. F. and H. Holo (2000). "Class II antimicrobial peptides from lactic acid bacteria." Biopolymers **55**(1): 50-61.
Neumann, C. S., C. T. Walsh, *et al.* (2010). "A flavin-dependent halogenase catalyzes the chlorination step in the biosynthesis of Dictyostelium differentiation-inducing factor 1." Proc Natl Acad Sci U S A **107**(13): 5798-803.
Newman, D. J., G. M. Cragg, *et al.* (2000). "The influence of natural products upon drug discovery." Nat Prod Rep **17**(3): 215-34.
Nonomura, H. and Y. Ohara (1957). "Distribution of Actinomycetes in the soil. II. Microbispora, a new genus of the Streptomycetaceae." Journal of Fermentation Technology **35**: 307-311.
O'Rourke, S. (unpublished).
Oh, D. C., M. Poulsen, *et al.* (2009). "Dentigerumycin: a bacterial mediator of an ant-fungus symbiosis." Nat Chem Biol **5**(6): 391-3.
Ohi, N., B. Aoki, *et al.* (1987). "Semisynthetic beta-lactam antibiotics. III. Effect on antibacterial activity and comt-susceptibility of chlorine-introduction into the catechol nucleus of 6-[(R)-2-[3-(3,4-dihydroxybenzoyl)-3-(3-hydroxypropyl)-1-ureido]-2- phenylacetamido]penicillanic acid." J Antibiot (Tokyo) **40**(1): 22-8.
Ohnishi, Y., H. Yamazaki, *et al.* (2005). "AdpA, a central transcriptional regulator in the A-factor regulatory cascade that leads to morphological development and secondary metabolism in Streptomyces griseus." Biosci Biotechnol Biochem **69**(3): 431-9.
Okuda, K., Y. Aso, *et al.* (2005). "Characterization of functional domains of lantibiotic-binding immunity protein, NukH, from Staphylococcus warneri ISK-1." FEMS Microbiol Lett **250**(1): 19-25.
Okuda, K., Y. Aso, *et al.* (2008). "Cooperative transport between NukFEG and NukH in immunity against the lantibiotic nukacin ISK-1 produced by Staphylococcus warneri ISK-1." J Bacteriol **190**(1): 356-62.
Okuda, K. I., S. Yanagihara, *et al.* (2010). "Functional significance of the E-loop, a novel motif conserved in the lantibiotic-immunity ABC transport systems." J Bacteriol.
Okujo, N., H. Iinuma, *et al.* (2007). "Bispolides, novel 20-membered ring macrodiolide antibiotics from microbispora." J Antibiot (Tokyo) **60**(3): 216-9.
Oman, T. J. and W. A. van der Donk (2010). "Follow the leader: the use of leader peptides to guide natural product biosynthesis." Nat Chem Biol **6**(1): 9-18.
Otto, M., A. Peschel, *et al.* (1998). "Producer self-protection against the lantibiotic epidermin by the ABC transporter EpiFEG of Staphylococcus epidermidis Tu3298." FEMS Microbiol Lett **166**(2): 203-11.

Ouellet, H., L. M. Podust*, et al.* (2008). "Mycobacterium tuberculosis CYP130: crystal structure, biophysical characterization, and interactions with antifungal azole drugs." J Biol Chem **283**(8): 5069-80.

Pag, U., C. Heidrich*, et al.* (1999). "Molecular analysis of expression of the lantibiotic pep5 immunity phenotype." Appl Environ Microbiol **65**(2): 591-8.

Paget, M. S. B., H.-J. Hong*, et al.* (2002). The ECF sigma factors of Streptomyces coelicolor A3(2). Signals, Switches, Regulons and Cascades: Control of Bacterial Gene Expression. D. A. Hodgson and C. M. Thomas, Cambridge University Press**:** 105-125.

Papadelli, M., A. Karsioti*, et al.* (2007). "Characterization of the gene cluster involved in the biosynthesis of macedocin, the lantibiotic produced by Streptococcus macedonicus." FEMS Microbiol Lett **272**(1): 75-82.

Park, S. H., S. S. Choi*, et al.* (2009). "Functional expression of SCO7832 stimulates tautomycetin production via pathway-specific regulatory gene overexpression in Streptomyces sp. CK4412." J Ind Microbiol Biotechnol **36**(7): 993-8.

Paul, M., G. C. Patton*, et al.* (2007). "Mutants of the zinc ligands of lacticin 481 synthetase retain dehydration activity but have impaired cyclization activity." Biochemistry **46**(21): 6268-76.

Peschel, A., J. Augustin*, et al.* (1993). "Regulation of epidermin biosynthetic genes by EpiQ." Mol Microbiol **9**(1): 31-9.

Peschel, A. and F. Gotz (1996). "Analysis of the Staphylococcus epidermidis genes epiF, -E, and -G involved in epidermin immunity." J Bacteriol **178**(2): 531-6.

Peschel, A., N. Schnell*, et al.* (1997). "Secretion of the lantibiotics epidermin and gallidermin: sequence analysis of the genes gdmT and gdmH, their influence on epidermin production and their regulation by EpiQ." Mol Gen Genet **254**(3): 312-8.

Pootoolal, J., M. G. Thomas*, et al.* (2002). "Assembling the glycopeptide antibiotic scaffold: The biosynthesis of A47934 from Streptomyces toyocaensis NRRL15009." Proc Natl Acad Sci U S A **99**(13): 8962-7.

Qi, F., P. Chen*, et al.* (1999a). "Functional analyses of the promoters in the lantibiotic mutacin II biosynthetic locus in Streptococcus mutans." Appl Environ Microbiol **65**(2): 652-8.

Qi, F., P. Chen*, et al.* (1999b). "Purification of mutacin III from group III Streptococcus mutans UA787 and genetic analyses of mutacin III biosynthesis genes." Appl Environ Microbiol **65**(9): 3880-7.

Qiao, M., T. Immonen*, et al.* (1995). "The cellular location and effect on nisin immunity of the NisI protein from Lactococcus lactis N8 expressed in Escherichia coli and L. lactis." FEMS Microbiol Lett **131**(1): 75-80.

Qiao, M. and P. E. Saris (1996). "Evidence for a role of NisT in transport of the lantibiotic nisin produced by Lactococcus lactis N8." FEMS Microbiol Lett **144**(1): 89-93.

Ra, R., M. M. Beerthuyzen*, et al.* (1999). "Effects of gene disruptions in the nisin gene cluster of Lactococcus lactis on nisin production and producer immunity." Microbiology **145 (Pt 5)**: 1227-33.

Rachid, S., M. Scharfe*, et al.* (2009). "Unusual chemistry in the biosynthesis of the antibiotic chondrochlorens." Chem Biol **16**(1): 70-81.

Rao, D. K. and P. Kaur (2008). "The Q-loop of DrrA is involved in producing the closed conformation of the nucleotide binding domains and in transduction of conformational changes between DrrA and DrrB." Biochemistry **47**(9): 3038-50.

Rawlinson, E. L., I. F. Nes*, et al.* (2002). "LasX, a transcriptional regulator of the lactocin S biosynthetic genes in Lactobacillus sakei L45, acts both as an activator and a repressor." Biochimie **84**(5-6): 559-67.

Rawlinson, E. L., I. F. Nes*, et al.* (2005). "Identification of the DNA-binding site of the Rgg-like regulator LasX within the lactocin S promoter region." Microbiology **151**(Pt 3): 813-23.

Redenbach, M., H. M. Kieser, *et al.* (1996). "A set of ordered cosmids and a detailed genetic and physical map for the 8 Mb Streptomyces coelicolor A3(2) chromosome." Mol Microbiol **21**(1): 77-96.

Rhodes, P. M., N. Winksell, *et al.* (1981). "Biochemical and Genetic Characterization of Streptomyces rimosus Mutants Impaired in Oxytetracycline Biosynthesis." J Gen Microbiol **124**: 329-338.

Rietkotter, E., D. Hoyer, *et al.* (2008). "Bacitracin sensing in Bacillus subtilis." Mol Microbiol **68**(3): 768-85.

Rigali, S., F. Titgemeyer, *et al.* (2008). "Feast or famine: the global regulator DasR links nutrient stress to antibiotic production by Streptomyces." EMBO Rep **9**(7): 670-5.

Rince, A., A. Dufour, *et al.* (1997). "Characterization of the lacticin 481 operon: the Lactococcus lactis genes lctF, lctE, and lctG encode a putative ABC transporter involved in bacteriocin immunity." Appl Environ Microbiol **63**(11): 4252-60.

Rink, R., A. Kuipers, *et al.* (2005). "Lantibiotic structures as guidelines for the design of peptides that can be modified by lantibiotic enzymes." Biochemistry **44**(24): 8873-82.

Rink, R., J. Wierenga, *et al.* (2007). "Dissection and modulation of the four distinct activities of nisin by mutagenesis of rings A and B and by C-terminal truncation." Appl Environ Microbiol **73**(18): 5809-16.

Ro, D. K., G. Arimura, *et al.* (2005). "Loblolly pine abietadienol/abietadienal oxidase PtAO (CYP720B1) is a multifunctional, multisubstrate cytochrome P450 monooxygenase." Proc Natl Acad Sci U S A **102**(22): 8060-5.

Roes, M. and P. R. Meyers (2008). "Nonomuraea candida sp. nov., a new species from South African soil." Antonie Van Leeuwenhoek **93**(1-2): 133-9.

Rudd, B. A. and D. A. Hopwood (1980). "A pigmented mycelial antibiotic in Streptomyces coelicolor: control by a chromosomal gene cluster." J Gen Microbiol **119**(2): 333-40.

Rutherford, K., J. Parkhill, *et al.* (2000). "Artemis: sequence visualization and annotation." Bioinformatics **16**(10): 944-5.

Sambrook, J., E. F. Fritch, *et al.* (2001). Molecular Cloning: A Laboratory Manual, Cold Spring Harbor Laboratory Press.

Sanchez, C., I. A. Butovich, *et al.* (2002). "The biosynthetic gene cluster for the antitumor rebeccamycin: characterization and generation of indolocarbazole derivatives." Chem Biol **9**(4): 519-31.

Sanchez, C., L. Zhu, *et al.* (2005). "Combinatorial biosynthesis of antitumor indolocarbazole compounds." Proc Natl Acad Sci U S A **102**(2): 461-6.

Schleifer, K. H. and O. Kandler (1972). "Peptidoglycan types of bacterial cell walls and their taxonomic implications." Bacteriol Rev **36**(4): 407-77.

Schmid, D. G., F. Majer, *et al.* (2002). "Electrospray ionization Fourier transform ion cyclotron resonance mass spectrometry to reveal the substrate specificity of the peptidyl-cysteine decarboxylase EpiD." Rapid Commun Mass Spectrom **16**(18): 1779-84.

Schmitz, S., A. Hoffmann, *et al.* (2006). "The lantibiotic mersacidin is an autoinducing peptide." Appl Environ Microbiol **72**(11): 7270-7.

Schobel, S., S. Zellmeier, *et al.* (2004). "The Bacillus subtilis sigmaW anti-sigma factor RsiW is degraded by intramembrane proteolysis through YluC." Mol Microbiol **52**(4): 1091-105.

Scott, J. J., D. C. Oh, *et al.* (2008). "Bacterial protection of beetle-fungus mutualism." Science **322**(5898): 63.

Shimizu, K. and T. Masaki (2004). "Peptidic Antibiotic."

Siegers, K. and K. D. Entian (1995). "Genes involved in immunity to the lantibiotic nisin produced by Lactococcus lactis 6F3." Appl Environ Microbiol **61**(3): 1082-9.

Siegers, K., S. Heinzmann, *et al.* (1996). "Biosynthesis of lantibiotic nisin. Posttranslational modification of its prepeptide occurs at a multimeric membrane-associated lanthionine synthetase complex." J Biol Chem **271**(21): 12294-301.

Simon, R., U. Priefer, *et al.* (1983). "A Broad Host Range Mobilization System for In Vivo Genetic Engineering: Transposon Mutagenesis in Gram Negative Bacteria." Nat Biotech **1**(9): 784-791.

Slavny, P., R. Little, *et al.* (2010). "Quaternary structure changes in a second Per-Arnt-Sim domain mediate intramolecular redox signal relay in the NifL regulatory protein." Mol Microbiol **75**(1): 61-75.

Smith, L., H. Hasper, *et al.* (2008). "Elucidation of the antimicrobial mechanism of mutacin 1140." Biochemistry **47**(10): 3308-14.

Smith, L., J. Novak, *et al.* (2000). "Covalent structure of mutacin 1140 and a novel method for the rapid identification of lantibiotics
doi:10.1046/j.1432-1033.2000.01777.x." European Journal of Biochemistry **267**(23): 6810-6816.

Sosio, M., S. Stinchi, *et al.* (2003). "The gene cluster for the biosynthesis of the glycopeptide antibiotic A40926 by nonomuraea species." Chem Biol **10**(6): 541-9.

Staron, A., H. J. Sofia, *et al.* (2009). "The third pillar of bacterial signal transduction: classification of the extracytoplasmic function (ECF) sigma factor protein family." Mol Microbiol **74**(3): 557-81.

Stein, T., S. Borchert, *et al.* (2002). "Dual control of subtilin biosynthesis and immunity in Bacillus subtilis." Mol Microbiol **44**(2): 403-16.

Stein, T., S. Heinzmann, *et al.* (2003). "Function of Lactococcus lactis nisin immunity genes nisI and nisFEG after coordinated expression in the surrogate host Bacillus subtilis." J Biol Chem **278**(1): 89-94.

Stinchi, S., S. Azimonti, *et al.* (2003). "A gene transfer system for the glycopeptide producer Nonomuraea sp. ATCC39727." FEMS Microbiol Lett **225**(1): 53-7.

Straight, P. D. and R. Kolter (2009). "Interspecies chemical communication in bacterial development." Annu Rev Microbiol **63**: 99-118.

Straight, P. D., J. M. Willey, *et al.* (2006). "Interactions between Streptomyces coelicolor and Bacillus subtilis: Role of surfactants in raising aerial structures." J Bacteriol **188**(13): 4918-25.

Sutcliffe, I. C. and D. J. Harrington (2002). "Pattern searches for the identification of putative lipoprotein genes in Gram-positive bacterial genomes." Microbiology **148**(Pt 7): 2065-77.

Takala, T. M. and P. E. Saris (2006). "C terminus of NisI provides specificity to nisin." Microbiology **152**(Pt 12): 3543-9.

Tang, L., S. Shah, *et al.* (2000). "Cloning and heterologous expression of the epothilone gene cluster." Science **287**(5453): 640-2.

Tibazarwa, C., S. Wuertz, *et al.* (2000). "Regulation of the cnr cobalt and nickel resistance determinant of Ralstonia eutropha (Alcaligenes eutrophus) CH34." J Bacteriol **182**(5): 1399-409.

Unversucht, S., F. Hollmann, *et al.* (2005). "$FADH_2$-Dependence of Tryptophan 7-Halogenase." Advanced Synthesis & Catalysis **347**(7-8): 1163-1167.

van den Berg van Saparoea, H. B., P. J. Bakkes, *et al.* (2008). "Distinct contributions of the nisin biosynthesis enzymes NisB and NisC and transporter NisT to prenisin production by Lactococcus lactis." Appl Environ Microbiol **74**(17): 5541-8.

van der Meer, J. R., J. Polman, *et al.* (1993). "Characterization of the Lactococcus lactis nisin A operon genes nisP, encoding a subtilisin-like serine protease involved in precursor processing, and nisR, encoding a regulatory protein involved in nisin biosynthesis." J Bacteriol **175**(9): 2578-88.

van der Meer, J. R., H. S. Rollema, *et al.* (1994). "Influence of amino acid substitutions in the nisin leader peptide on biosynthesis and secretion of nisin by Lactococcus lactis." J Biol Chem **269**(5): 3555-62.

van Pee, K. H. and E. P. Patallo (2006). "Flavin-dependent halogenases involved in secondary metabolism in bacteria." Appl Microbiol Biotechnol **70**(6): 631-41.

van Wageningen, A. M., P. N. Kirkpatrick, *et al.* (1998). "Sequencing and analysis of genes involved in the biosynthesis of a vancomycin group antibiotic." Chem Biol **5**(3): 155-62.

van Wezel, G. P., J. White, *et al.* (2000). "Application of redD, the transcriptional activator gene of the undecylprodigiosin biosynthetic pathway, as a reporter for transcriptional activity in Streptomyces coelicolor A3(2) and Streptomyces lividans." J Mol Microbiol Biotechnol **2**(4): 551-6.

Vollmer, W., D. Blanot, *et al.* (2008). "Peptidoglycan structure and architecture." FEMS Microbiol Rev **32**(2): 149-67.

Wagner, N., C. Osswald, *et al.* (2009). "Comparative analysis of transcriptional activities of heterologous promoters in the rare actinomycete Actinoplanes friuliensis." J Biotechnol **142**(3-4): 200-4.

Walsh, C. T., H. Chen, *et al.* (2001). "Tailoring enzymes that modify nonribosomal peptides during and after chain elongation on NRPS assembly lines." Curr Opin Chem Biol **5**(5): 525-34.

Wendt-Pienkowski, E., Y. Huang, *et al.* (2005). "Cloning, sequencing, analysis, and heterologous expression of the fredericamycin biosynthetic gene cluster from Streptomyces griseus." J Am Chem Soc **127**(47): 16442-52.

Widdick, D. A., H. M. Dodd, *et al.* (2003). "Cloning and engineering of the cinnamycin biosynthetic gene cluster from Streptomyces cinnamoneus cinnamoneus DSM 40005." Proc Natl Acad Sci U S A **100**(7): 4316-21.

Wiedemann, I., T. Bottiger, *et al.* (2006). "Lipid II-based antimicrobial activity of the lantibiotic plantaricin C." Appl Environ Microbiol **72**(4): 2809-14.

Willey, J. M. and W. A. van der Donk (2007). "Lantibiotics: Peptides of Diverse Structure and Function." Annu Rev Microbiol.

Wilson-Stanford, S., A. Kalli, *et al.* (2009). "Oxidation of lanthionines renders the lantibiotic nisin inactive." Appl Environ Microbiol **75**(5): 1381-7.

Winter, J. M., M. C. Moffitt, *et al.* (2007). "Molecular basis for chloronium-mediated meroterpene cyclization: cloning, sequencing, and heterologous expression of the napyradiomycin biosynthetic gene cluster." J Biol Chem **282**(22): 16362-8.

Woodford, N. and D. M. Livermore (2009). "Infections caused by Gram-positive bacteria: a review of the global challenge." J Infect **59 Suppl 1**: S4-16.

Wright, L. F. and D. A. Hopwood (1976a). "Actinorhodin is a chromosomally-determined antibiotic in Streptomyces coelicolar A3(2)." J Gen Microbiol **96**(2): 289-97.

Wright, L. F. and D. A. Hopwood (1976b). "Identification of the antibiotic determined by the SCP1 plasmid of Streptomyces coelicolor A3(2)." J Gen Microbiol **95**(1): 96-106.

Xie, L., C. Chatterjee, *et al.* (2002). "Heterologous expression and purification of SpaB involved in subtilin biosynthesis." Biochem Biophys Res Commun **295**(4): 952-7.

Xie, L., L. M. Miller, *et al.* (2004). "Lacticin 481: in vitro reconstitution of lantibiotic synthetase activity." Science **303**(5658): 679-81.

Yanai, K., T. Murakami, *et al.* (2006). "Amplification of the entire kanamycin biosynthetic gene cluster during empirical strain improvement of Streptomyces kanamyceticus." Proc Natl Acad Sci U S A **103**(25): 9661-6.

Yeh, E., S. Garneau, *et al.* (2005). "Robust in vitro activity of RebF and RebH, a two-component reductase/halogenase, generating 7-chlorotryptophan during rebeccamycin biosynthesis." Proc Natl Acad Sci U S A **102**(11): 3960-5.

Yim, G., H. H. Wang, *et al.* (2006). "The truth about antibiotics." Int J Med Microbiol **296**(2-3): 163-70.

You, Y. O., M. R. Levengood, *et al.* (2009). "Lacticin 481 Synthetase as a General Serine/Threonine Kinase." ACS Chem Biol.

You, Y. O. and W. A. van der Donk (2007). "Mechanistic investigations of the dehydration reaction of lacticin 481 synthetase using site-directed mutagenesis." Biochemistry **46**(20): 5991-6000.

Young, J. and I. B. Holland (1999). "ABC transporters: bacterial exporters-revisited five years on." Biochim Biophys Acta **1461**(2): 177-200.

Yuksel, S. and J. N. Hansen (2007). "Transfer of nisin gene cluster from Lactococcus lactis ATCC 11454 into the chromosome of Bacillus subtilis 168." Appl Microbiol Biotechnol **74**(3): 640-9.

Zehner, S., A. Kotzsch*, et al.* (2005). "A regioselective tryptophan 5-halogenase is involved in pyrroindomycin biosynthesis in Streptomyces rugosporus LL-42D005." Chem Biol **12**(4): 445-52.

Zellmeier, S., W. Schumann*, et al.* (2006). "Involvement of Clp protease activity in modulating the Bacillus subtilissigmaw stress response." Mol Microbiol **61**(6): 1569-82.

Zerbino, D. R. and E. Birney (2008). "Velvet: algorithms for de novo short read assembly using de Bruijn graphs." Genome Res **18**(5): 821-9.

Zhang, H., Y. Wang*, et al.* (2008). "Bacterial hosts for natural product production." Mol Pharm **5**(2): 212-25.

Zhao, B., X. Lin*, et al.* (2008). "Biosynthesis of the sesquiterpene antibiotic albaflavenone in Streptomyces coelicolor A3(2)." J Biol Chem **283**(13): 8183-9.

Zhao, C., J. Ju*, et al.* (2006). "Utilization of the methoxymalonyl-acyl carrier protein biosynthesis locus for cloning the oxazolomycin biosynthetic gene cluster from Streptomyces albus JA3453." J Bacteriol **188**(11): 4142-7.